



UNIVERSITY COLLEGE LONDON

***Stachybotrys chartarum: its
identification and response to
antimicrobial treatment and prevention***

By

Zuraifah Asrah Binti Mohamad

A thesis submitted to the University College London for the award of the degree
of Doctor of Philosophy

In the

Faculty of Engineering Sciences

Department of Civil, Environmental and Geomatic Engineering

2018

DECLARATION OF AUTHORSHIP

'I, Zuraifah Asrah binti Mohamad, confirm that the work presented in this thesis is my own. Where information has been derived from other sources, I confirm that this has been indicated in the thesis.'

Signed:

Zuraifah Asrah binti Mohamad

Date:

ACKNOWLEDGEMENTS

This thesis is dedicated to my late grandmother, Chek Rejab, who raised me up from the first day I was born, for her unconditional love and her philosophy that taught me how to be a better human every single day.

My deepest appreciation to my first supervisor, Dr Lena Ciric for having me as her first PhD student and for her tireless support and positive vibes to keep me going; and to my secondary supervisor, Professor Christopher Kibbler for his enormous contribution by sharing his expertise in mycology and providing research direction when I needed it the most. Not forgotten, Dr Manni Bhatti for her kind supervision during my first year of my PhD.

Special thanks to Dr Rebecca Gorton at the Regional Mycology Unit, Royal Free London for kindly sharing her skills in mycology; Dr Elaine Cloutman-Green at Infection Control, Great Ormond Street Hospital for kindly providing the MALDI-TOF platform; and Dr John Timms at UCL Institute for Women's Health for his valuable guidance and assistance in proteomic work. Dr Nicola Mordan for her kind assistance and lesson on the electron microscopy and Dr Saba Ferdous at Computational Biology, UCL for her kind assistance in bioinformatics. My heartfelt gratitude to all staff at CEGE/UCL who have helped me during my studies especially to Dr Melisa Canales, Dr Judith Zhou, Ian Seaton and Catherine Unsworth.

To Dr Claire, Like, Stacey, Fan and Cecilia at HIRG/EE, and fellow PhD students for their kind help and motivational support. My sincere appreciation goes to all Malaysian students at UCL especially Sophia, Sharila, Umaima, Zahirah, Asyura, and Shireen for being part of my journey as a student in the UK.

To both my beloved parents, Mohamad and Noor Siah, for their patience, hardship and sacrifice. Without them, I would not be who I am right now. To all family members for standing by me through thick and thin especially to my uncle, Ehsan and Roslan; my

aunt, Epah; my brothers, Nizam and Zaman; sisters-in-law, Imah and Zy, my cousins, Fiza and Dikwan, my lovely nieces, Amanina, Damia and Aimi and my nephew, Adam.

To my mentors and other fellow researchers in Malaysia, especially to Datuk Dr Lokman Hakim for his endless support throughout my career and self-development, to Dr Amir Kamaluddin for paving a career pathway for me into indoor environmental health research, and to Dr Sumitra Sithamparam for sharing her positive values and experiences.

Last but not least, I am deeply grateful to the Ministry of Health, Malaysia for its generous human capital investment by providing me financial support to pursue my studies at UCL. Hopefully, this PhD will be a stepping-stone for my career as a successful and an independent researcher.

ABSTRACT

BACKGROUND: *Stachybotrys chartarum* is mostly associated with water intrusion in the indoor environment. It is known as a species complex fungus and it can often be misidentified with its closely related species. Fungal resilience is a challenging problem when attempting to eradicate it from the environment and several studies have documented the ineffectiveness of antimicrobials when applied in real-life settings.

OBJECTIVES: This study aims to: a) evaluate various identification methods to characterise *Stachybotrys* species; and b) determine the effects of antimicrobial agents on *S. chartarum*.

METHODS: Current identification methods; a) Culture characteristics and microscopy; b) Polymerase chain reaction (PCR); and c) Matrix assisted desorption ionisation- time of flight (MALDI-TOF), were employed. The effects of antimicrobial agents consisting of bleach, aerosolised hydrogen peroxide, peracetic acid and organosilane (OS) on *S. chartarum* were evaluated a) *in vitro*; b) On building material and; c) By using a proteomic approach.

RESULTS: The methods of culture and microscopy are useful for early stage screening. A universal PCR primer set is suitable for identification at the genus level. However, tri5 primers provide a quick and specific method for identifying *S. chartarum* and *S. chlorohalonata*. MALDI-TOF could differentiate both species but could not provide reliable identification for other *Stachybotrys* species. The *in vitro* and environmental studies of antimicrobial agents show that bleach and OS appeared to be effective as treatment and prevention strategies, respectively. Differences in protein changes towards bleach and OS suggest that a combination of antimicrobial agents with different modes of action might provide a more effective way to eliminate fungal growth.

CONCLUSION: Confirmatory methods are important to obtain the correct identification especially for less commonly studied moulds such as *S. chartarum*. More research with regard to an effective application strategy or delivery method is required to complement the antimicrobial agents that are currently available on the market.

IMPACT STATEMENT

Indoor environmental health is an interdisciplinary field which involves the association between the built environment and its health impact on the occupants. Nowadays, urbanisation and development is taking place globally with many more indoor spaces being built. Most people spend their time indoors where maintaining a healthy indoor environment is crucial.

Although dampness and high humidity are common problems in the tropics and the Southeast Asian region, research on indoor mould contamination derives mainly from America and European countries. The issue may also be underreported due to limited resources and skills in the field. A recent survey conducted from 7 Asian countries with 241 participating laboratories has reported that only 16.9% and 12.3% of identification methods for fungal diagnoses used DNA sequencing and MALDI-TOF, respectively ⁽¹⁾. It is timely to apply the recent advances in fungal identification in this area, particularly in the field of environmental engineering.

It is anticipated that this study will significantly facilitate the assessment and remediation of mould-infested buildings by public health practitioners and environmental hygienists. In addition to the basic indoor air quality assessment of total bacteria or fungi, specific identification techniques investigated in this project would provide more insight into the association of this fungus with disease and overall health complaints or occupant perceived indoor environmental quality ^(2, 3).

The knowledge and skills acquired during this project can be used to facilitate the Malaysian government and related agencies in dealing with health problems associated with mould infestation by providing laboratory support and developing expertise in the field. Expertise and skills help in creating a research niche in this area by keeping personnel up-to-date with current methods as well as developing new ones. Local short courses can be organised to significantly improve both routine fungal diagnosis and investigation of building-related illness.

The studies on the efficacy of antimicrobial agents which can be used environmentally, has emphasized the importance of preventative measures in the pre-construction phase by the building developers and building owners. Replacing contaminated materials often costs considerable effort and money, particularly in public buildings,

such as healthcare facilities. Furthermore, application or delivery methods of antimicrobial agents need to be improved to achieve their optimal efficacy. Given the impact of inoculum demonstrated in these studies, it is clear that cleaning and maintenance should also be standard practice in homes and facilities. It is of the utmost importance to create awareness of the importance of a healthy indoor environment for a better quality of life.

Last but not least, this study is a stepping stone for other research as *S. chartarum* itself produces many molecules that can be manipulated for potential human therapeutic application such as antifungal, antiviral and anticancer compounds ⁽⁴⁾. This opens up the possibility of future collaborations with other researchers to widen the scope of research on this fungal species.

CONTENTS

Declaration of authorship	2
Acknowledgements	3
Abstract	5
Impact statement	6
Contents	8
Figures	15
Tables	24
Abbreviations	26
Units	27
CHAPTER 1	28
Research background and motivation	28
1.1 Research background and its significance.....	28
1.2 Research motivation.....	29
1.3 Research objectives	31
CHAPTER 2	33
Literature review	33
2.1 Mould as an indoor contaminant	33
2.2 The role of fungi in indoor-related illness	37
2.2.1 Spores	38
2.2.2 β -(1,3)-D-glucan	38
2.2.3 Stachylysin	38
2.2.4 Microbial volatile organic compounds	38
2.2.5 Mycotoxins.....	39
2.3 Fungal resilience in the indoor environment	43
2.4 <i>Stachybotrys chartarum</i> and its related species	45
2.4.1 Identification, taxonomy and nomenclature	45
2.4.2 Indoor environment as a habitat.....	53
2.4.3 Toxicity and public health concern	55
2.5 Methods of fungal identification.....	59
2.5.1 Culture characteristics and light microscopy examination	59
2.5.2 Sequence-based identification using Internal transcribed spacer (ITS)- Polymerase Chain Reaction (PCR).....	61

2.5.3	Matrix-assisted laser desorption ionization- time of flight (MALDI-TOF) - mass spectrometry.....	63
2.6	Proteomics.....	66
2.7	Antimicrobial control agents	69
2.7.1	Sodium hypochlorite	69
2.7.2	Organosilane	71
2.7.3	Hydrogen peroxide	72
2.7.4	Peracetic acid	73
CHAPTER 3		74
Culture-based identification and microscopy of <i>Stachybotrys</i> species		74
3.1	Introduction.....	74
3.2	Materials and methods	75
3.2.1	<i>Stachybotrys</i> spp. isolates.....	75
3.2.2	Optimisation of growth on different media.....	76
3.2.3	Haemolytic activity on blood sheep agar.....	77
3.2.4	Microscopic examination	77
3.3	Results.....	77
3.3.1	Optimisation of growth on different media.....	77
3.3.1.1	<i>S. chartarum</i> , NCPF 7587	77
3.3.1.2	<i>S. chartarum</i> , ATCC® 16026™	78
3.3.1.3	<i>S. chartarum</i> , Stachy CU.....	78
3.3.1.4	Other <i>Stachybotrys</i> spp. isolates.....	81
3.3.2	Effects of temperature on fungal growth	87
3.3.3	Haemolytic activity of <i>Stachybotrys</i> spp. on blood agar.....	88
3.3.4	Microscopic examination of <i>Stachybotrys</i> spp.	88
3.3.4.1	<i>S. chartarum</i> , NCPF 7587	89
3.3.4.2	<i>S. chartarum</i> , ATCC 16026	90
3.3.4.3	<i>S. chartarum</i> , Stachy CU.....	90
3.3.4.4	Other <i>Stachybotrys</i> spp. isolates.....	91
3.4	Discussion	93
3.5	Conclusions	95
CHAPTER 4		96
Identification of <i>Stachybotrys</i> species using DNA-based methods.....		96
4.1	Introduction.....	96
4.2	Materials and methods	97
4.2.1	<i>Stachybotrys</i> spp. isolates.....	97
4.2.2	Preparation of spore suspension.....	98
4.2.3	Optimization of DNA extraction	98
4.2.3.1	Internal transcribed spacer/restriction fragment length polymorphism (ITS/RFLP-PCR).....	98

4.2.3.2	Trichodiene synthase gene (tri5) as a specific target for PCR.....	98
4.2.4	Development of a novel trichodiene synthase gene (tri5)-based primer.....	99
4.2.5	DNA sequencing and sequence alignment	101
4.2.6	<i>In-silico</i> PCR.....	102
4.3	Results.....	102
4.3.1	Optimisation of DNA extraction	102
4.3.2	Universal primer internal transcribed spacer PCR (ITS-PCR)	104
4.3.3	Internal transcribed spacer-restriction fragment length polymorphism PCR (ITS/RFLP-PCR).....	106
4.3.4	Trichodiene synthase genes (tri5)-based primers.....	108
4.3.5	<i>In-silico</i> PCR.....	118
4.4	Discussion	119
4.4.1	Optimisation of DNA extraction	120
4.4.2	Internal transcribed spacer- restriction fragment length polymorphism (ITS/RFLP-PCR).....	120
4.4.3	Tri5-based primers	122
4.4.4	Sequence alignment and phylogenetics analysis	123
4.4.5	<i>In-silico</i> PCR.....	124
4.5	Conclusions	125
CHAPTER 5		126
Identification of <i>Stachybotrys chartarum</i> using Matrix Assisted Laser Desorption Ionisation – Time of Flight (MALDI-TOF).....		126
5.1	Introduction.....	126
5.2	Materials and methods	127
5.2.1	Reference strains and fungal isolates	127
5.2.2	Fungal culture.....	127
5.2.3	Protein extraction.....	128
5.2.3.1	Protein extraction from liquid media	128
5.2.3.2	Protein extraction from solid media	129
5.2.4	Preparation of Bruker Matrix HCCA, portioned	129
5.2.5	Preparation of Bacterial Test Standard (BTS).....	130
5.2.6	MALDI-TOF	130
5.2.6.1	Calibration.....	131
5.2.6.2	Spectral acquisition and data analysis.	131
5.2.6.3	Generation of MSPs	132
5.3	Results.....	133
5.3.1	Optimisation of fungal growth conditions.....	133
5.3.1.1	The effects of different broth media on protein profiles.....	133
5.3.1.2	The effects of liquid versus solid media	135
5.3.1.3	The effects of temperature on protein profiles.....	136

5.3.1.4	The effects of incubation period on protein profiles	139
5.3.2	Control of masses and calibration	140
5.3.3	Development of Mass Spectrum Profiles (MSPs)	142
5.3.4	Identification of fungi using Biotyper© Bruker database	145
5.3.4.1	<i>Aspergillus niger van Tieghem</i> (ATCC® 16888™).....	145
5.3.4.2	Identification of <i>Stachybotrys</i> spp. isolates	148
5.3.4.2.1	<i>S. chartarum</i>	149
5.3.4.2.2	<i>S. chlorohalonata</i>	151
5.3.4.2.3	Other <i>Stachybotrys</i> spp.....	153
5.3.5	Summary of score values of <i>Stachybotrys</i> spp.	155
5.4	Discussion	156
5.4.1	Protein extraction optimisation	157
5.4.2	Development of MSPs in-house database	160
5.4.3	Identification of <i>Stachybotrys</i> spp.....	161
5.5	Conclusions	163
CHAPTER 6		164
Inhibitory effects of selected antimicrobial agents on <i>Stachybotrys chartarum</i>		164
6.1	Introduction.....	164
6.2	Materials and methods	165
6.2.1	Experimental set-up.....	165
6.2.1.1	Direct treatment of antimicrobial agents on fungal inoculum grown on solid media (method 1)	165
6.2.1.2	Fungal growth in liquid suspension containing antimicrobial agents using microdilution plates (method 2)	166
6.2.1.3	Fungal spores grown on solid media containing antimicrobial agents (method 3)	167
6.2.2	Preparation of fungal inocula.....	167
6.2.2.1	Preparation of isolates.....	167
6.2.2.2	Preparation of spore suspension.....	167
6.2.3	Antimicrobial experiments	168
6.2.3.1	Sodium hypochlorite (bleach).....	168
6.2.3.2	Aerosolised hydrogen peroxide (AHP).....	169
6.2.3.3	Peracetic acid (PAA)	170
6.2.3.4	Organosilane (OS).....	172
6.3	Results.....	173
6.3.1	Inhibitory effects of antimicrobial agents using direct treatment	173
6.3.1.1	Sodium hypochlorite (bleach).....	173
6.3.1.2	Aerosolised hydrogen peroxide (AHP)	178
6.3.1.3	Peracetic acid (PAA)	180
6.3.1.4	Organosilane (OS).....	184

6.3.2	Inhibitory effects of antimicrobial agents using liquid media assays	188
6.3.2.1	Sodium hypochlorite (bleach)	188
6.3.2.2	Peracetic acid (PAA)	190
6.3.2.3	Organosilane (OS).....	191
6.3.3	Inhibitory effects of antimicrobial agents using agar dilution methods	193
6.3.3.1	Sodium hypochlorite (bleach)	193
6.3.3.2	Organosilane (OS).....	195
6.3.4	Summary	197
6.4	Discussion	198
6.4.1	Sodium hypochlorite (bleach)	198
6.4.2	Aerosolised hydrogen peroxide (AHP)	200
6.4.3	Peracetic acid (PAA)	201
6.4.4	Organosilane (OS).....	202
6.5	Conclusions	203
CHAPTER 7		204
Efficacy of antimicrobial treatment and prevention on <i>S. chartarum</i> infested building material		204
7.1	Introduction.....	204
7.2	Materials and methods	205
7.2.1	Experimental set-up.....	205
7.2.2	Optimization of chamber conditions	205
7.2.3	Antimicrobial agents	206
7.2.4	Mycology	207
7.2.4.1	Inoculation of fungi	207
7.2.4.2	Fungal viability following antimicrobial application	207
7.2.5	Microscopy	207
7.2.5.1	Preparation of samples for light microscopy	207
7.2.5.2	Preparation of samples for scanning electron microscopy (SEM)	208
7.3	Results.....	209
7.3.1	Optimization of chamber condition	209
7.3.2	Gypsum board without fungal inoculation and application of antimicrobial agents 211	
7.3.3	<i>S. chartarum</i> -infested gypsum board with or without application of antimicrobial agents.....	215
7.3.3.1	Without treatment	215
7.3.3.2	Effect of sodium hypochlorite (bleach)	219
7.3.3.3	The effect of aerosolised hydrogen peroxide (AHP)	228
7.3.3.4	The effect of peracetic acid (PAA).....	231
7.3.3.5	The effect of organosilane (OS)	237
7.4	Discussion	243

7.4.1	The effects of environmental condition and building materials on <i>S. chartarum</i> .	243
7.4.2	Effectiveness of antimicrobial agents on <i>S. chartarum</i> -infested gypsum board	244
7.4.2.1	Sodium hypochlorite (bleach)	244
7.4.2.2	Aerosolised hydrogen peroxide (AHP)	245
7.4.2.3	Peracetic acid (PAA)	246
7.4.2.4	Organosilane (OS)	248
7.5	Conclusions	249
CHAPTER 8		250
Proteomic profiles of <i>Stachybotrys chartarum</i> in response to antimicrobial agents		250
8.1	Introduction	250
8.2	Materials and methods	251
8.2.1	Preparation of fungal samples	251
8.2.2	Protein extraction	252
8.2.2.1	Sample disruption	252
8.2.2.2	TCA/acetone precipitation	252
8.2.2.3	Phenol extraction	252
8.2.3	Buffer exchange and concentrate	253
8.2.4	Determination of protein concentration using the Bradford assay	253
8.2.5	NuPAGE® Bis-Tris Mini Gel electrophoresis	254
8.2.6	Preparing and labelling peptides for mass spectrometry analysis	254
8.2.6.1	Protein reduction	254
8.2.6.2	Protein alkylation	255
8.2.6.3	Protein digestion	256
8.2.6.4	Peptide labelling	256
8.2.7	Sample clean-up	257
8.2.8	Sample fractionation	257
8.2.9	Sample clean- up with Zip-tip® U-18	257
8.2.10	Mass spectrometry and data acquisition	257
8.2.10.1	Data analysis and bioinformatic analysis	258
8.3	Results	260
8.3.1	Optimization of protein extraction from <i>S. chartarum</i> , NCPF 7587	260
8.3.2	Descriptive data and quality control on proteomic analysis of <i>S. chartarum</i> , NCPF 7587	260
8.3.3	PANTHER classification of protein profiles of untreated <i>S. chartarum</i> , NCPF 7587	264
8.3.3.1	Protein classes in untreated <i>S. chartarum</i> , NCPF 7587	264
8.3.3.2	Molecular functions in untreated <i>S. chartarum</i> , NCPF 7587	266

8.3.3.3	Biological processes in untreated <i>S. chartarum</i> , NCPF 7587	267
8.3.3.4	Cellular components in <i>S. chartarum</i> , NCPF 7587	269
8.3.3.5	PANTHER pathway in <i>S. chartarum</i> , NCPF 7587	270
8.3.4	Changes in protein abundance in <i>S. chartarum</i> , NCPF 7587, exposed to antimicrobial agents.....	275
8.3.4.1	Changes in protein abundance in <i>S. chartarum</i> , NCPF 7587, exposed to bleach	275
8.3.4.2	Changes in protein abundance in <i>S. chartarum</i> , NCPF 7587, exposed to organosilane	277
8.3.5	Heatmap of the changes in protein abundance patterns	278
8.3.6	PANTHER analysis of the different proteomes in response to different chemical treatment methods	281
8.3.6.1	PANTHER classification based on protein classes	281
8.3.6.2	PANTHER classification based on molecular functions.....	283
8.3.6.3	PANTHER classification based on biological processes	285
8.3.6.4	PANTHER classification based on biochemical pathways.....	287
8.4	Discussion	289
8.4.1	Method optimisation	289
8.4.2	Proteomic searches and databases of <i>S. chartarum</i> , NCPF 7587	290
8.4.3	Heatmap of changes in protein abundance patterns in <i>S. chartarum</i> following treatment with bleach and organosilane.....	292
8.4.4	PANTHER biological function classification of treated <i>S. chartarum</i> proteins	294
8.5	Conclusions	295
CHAPTER 9		296
General discussion and future direction.....		296
9.1	Limitations of the study.....	296
9.2	Summary of the main findings.....	298
9.3	Discussion of the main findings.....	301
9.3.1	To evaluate various fungal identification methods to characterise <i>Stachybotrys</i> species with confidence (and be able to distinguish between its closely-related species)	302
9.3.2	To determine the effects of different antimicrobial agents on <i>S. chartarum</i> ..	305
9.4	Recommendation and future research	308
References		311
Appendices		332

FIGURES

Figure 2-1: A mould requires a suitable substrate in the presence of moisture to grow.....	37
Figure 2-2: The pathway showing mechanism of action of several mycotoxins affecting major sites in RNA and protein synthesis.	40
Figure 2-3: Basic structure of trichothecenes and four types of trichothecenes (type A, B, C and D) based on substitution pattern at C-8 position.....	41
Figure 2-4: Trichothecenes and atronones produced by <i>Stachybotrys</i> spp..	42
Figure 2-5: The degradation of cellulose by fungi to produce glucose as the nutrient source. ..	44
Figure 2-6: The cultural characteristics of <i>Stachybotrys chartarum</i> grown on potato dextrose agar at 30 °C for 7 days.	46
Figure 2-7: Microscopic appearances of <i>Stachybotrys chartarum</i> , NCPF 7587.....	46
Figure 2-8: Morphological characteristics of conidia, phialide arrangement and conidiophore structures of <i>Stachybotrys</i> spp. grown on MEA and incubated for 7 days at 25 °C.	48
Figure 2-9: The Corda's first figures of a <i>Stachybotrys</i> sp. (known as <i>S. atra</i>).	49
Figure 2-10: The morphological difference in the arrangement of the conidia of a. <i>Stachybotrys chartarum</i> and b. <i>Memnoniella echinata</i>	50
Figure 2-11: Proposed mechanisms of stachybotryotoxicosis.	56
Figure 2-12: Shapes and surface types of fungal spores found in air samples.	60
Figure 2-13: The 3 primary steps in a basic PCR reaction consist of denaturation, annealing and extension or elongation.....	62
Figure 2-14: Ribosomal DNA (rDNA) gene complex consisting of 18S rDNA (Small subunit rDNA), 5.8S rDNA and 28S rDNA (Large subunit rDNA).	63
Figure 2-15: Schematic diagram of sample analysis by MALDI-TOF as shown by a single spot on the metal plate.	65
Figure 2-16: The chemical structure of TMT-label consisting of 3 functional regions of mass reporter mass reporter, mass normalizer and reactive regions.	67
Figure 2-17: Schematic diagram of TMT- labelling gel free proteomic analysis.	68
Figure 2-18: Mechanisms of action of sodium hypochlorite.....	70
Figure 2-19: General structure and mechanism of action of organosilane.	71

Figure 3-1: The surface and reverse morphology of <i>S. chartarum</i> type strains NCPF 7587 and ATCC 16026 grown on 4 different media.	80
Figure 3-2: Surface and reverse morphologies of NCPF 7587 and CU Stachy grown on ESA and incubated at 25 °C or 30 °C for 7 days.	87
Figure 3-3: BSA cultured with <i>Stachybotrys</i> spp. (ATCC 16026, NCPF 7587 and Stachy CU) and <i>Penicillium</i> spp. (negative control) incubated at 25 °C	88
Figure 3-4: The microscopic images a. 20x (taken using Nikon DS-Fi1-L2), b. 40x (taken using Nikon DS-Fi1-L2) and c. 100x (taken using Brunel digicam) showing the microscopic structures of <i>S. chartarum</i> , NCPF 7589 grown on ESA.	89
Figure 3-5: The microscopic images a. 40x (taken using Nikon DS-Fi1-L2) and b. 100x (taken using Brunel digicam) showing the microscopic structures <i>S. chartarum</i> , ATCC 16026 grown on ESA.	90
Figure 3-6: The microscopic images a. 40x (taken using Nikon DS-Fi1-L2) and b. 100x (taken using Nikon DS-Fi1-L2) showing the microscopic structures of Stachy CU grown on ESA.	90
Figure 3-7: Microscopic images (40x) of <i>Stachybotrys</i> spp. (taken using 5.0 MP Moticam)	92
Figure 4-1: Agarose gel run PCR products of different bead-milling and incubation times.	102
Figure 4-2: PCR results of different types of beads shown on 2% agarose gel.	103
Figure 4-3: Real-time PCR graph of <i>S. chartarum</i> NCPF 7589 using ITS primers showing average CT values of 11.37 ± 0.14 and 13.05 ± 0.17 using glass beads and silica beads, respectively.	103
Figure 4-4: Standard curve using concentrations of amplicons produced with different types of beads showing slightly higher concentrations using glass beads compared to silica beads.	104
Figure 4-5: The output sequence for the CU Stachy isolate was obtained by using ITS4 primer. The <i>Hae</i> III cut sites are marked in red.....	106
Figure 4-6: Restriction analysis of <i>S. chartarum</i> (**), <i>S. chlorohalonata</i> (*), other <i>Stachybotrys</i> spp., <i>S. cerevisiae</i> and <i>Ulocladium</i> spp.....	107
Figure 4-7: PCR products using designed tri5 primer sets on 3 isolates of <i>S. chartarum</i> (ATCC 16026, NCPF 7587 and CU) shown on 4% agarose gel.	108
Figure 4-8: PCR products using designed tri5 primer sets on 3 isolates of <i>S. chartarum</i> (ATCC 16026, NCPF 7587 and CU) shown on 4% agarose gel. a) SC1, b) SC2, c) SC3, d) SC4 and e) SC5.	109
Figure 4-9: Amplification using designed tri5 primers, a) SC1 and b) SC3 on 13 isolates of <i>Stachybotrys</i> spp. (4% agarose gel).	110

Figure 4-10: Nucleotide differences in <i>S. chartarum</i> and <i>S. chlorohalonata</i> isolates constructed from the longest sequence to the left, Cruse <i>et al.</i> and the longest sequence to the right, SC1.	115
Figure 4-11: Differences in phylogenetic tree of Cruse <i>et al.</i> , Black <i>et al.</i> and SC1 built with published sequences from <i>S. chartarum</i> and <i>S. chlorohalonata</i>	117
Figure 4-12: Phylogenetic tree of the nucleotide consensus Cruse <i>et al.</i> , Black <i>et al.</i> and SC1 built with published sequences from <i>S. chartarum</i> and <i>S. chlorohalonata</i>	118
Figure 5-1: A Biotarget adapter was required to fit in the Biotarget plate into the MALDI-TOF Microflex instrument.	129
Figure 5-2: A disposable MALDI Biotarget 48 spotted with samples and BTS (Bacterial Test Standard) (as shown in white circles) was kept in a transport box.	130
Figure 5-3: Parameters used for calibration from the BTS manual as provided by Bruker.	131
Figure 5-4: Representation of growth characteristics of a. <i>A. niger</i> , ATCC 16888 and b. <i>S. chartarum</i> , NCPF 7587 grown in SDB and PDB for 24 hours at 25 °C.	133
Figure 5-5: Representation of the protein profiles of <i>S. chartarum</i> , NCPF 7587 grown in a. SDB and b. PDB for 24 hours at 25 °C.	134
Figure 5-6: Representation of the protein profiles of <i>A. niger</i> , ATCC 16888 grown in a. SDB and b. PDB for 24 hours at 25 °C. Consistent peaks were observed in <i>A. niger</i> grown in both media.	134
Figure 5-7: Representation of protein spectra of <i>S. chartarum</i> , a. NCPF 7587, b. ATCC 16026 and c. CBS 182.80 grown in ESA for 7 days and incubated at 25 °C.	135
Figure 5-8: Representation of protein spectra of <i>S. chartarum</i> , NCPF 7587 grown in SDB for 24 hours and incubated at 30 °C.	136
Figure 5-9: Representation of protein spectra of <i>S. chartarum</i> , NCPF 7587 grown in PDB for 24 hours and incubated at 30 °C.	137
Figure 5-10: Representation of protein spectra of <i>A. niger</i> , ATCC 16888 grown in SDB for 24 hours and incubated at 30 °C.	138
Figure 5-11: Representation of protein spectra of <i>A. niger</i> , ATCC 16888 grown in PDB for 24 hours and incubated at 30 °C.	138
Figure 5-12: Representation of protein spectra of <i>S. chartarum</i> , NCPF 7587 grown in a. SDB and b. PDB for 48 hours and incubated at 25 °C.	139
Figure 5-13: Representation of protein spectra of <i>S. chartarum</i> , NCPF 7587 grown in SDB for 48 hours and incubated at 25 °C.	139
Figure 5-14: Representation of protein spectra of <i>S. chartarum</i> , NCPF 7587 grown in PDB for 48 hours and incubated at 25 °C.	140

Figure 5-15: The spectra obtained from Flex Analysis shows masses produced by BTS used for internal calibration	141
Figure 5-16: Representatives of raw spectra obtained from 2 biological replicates of <i>S. chartarum</i> grown on ESA for 24 hours.	142
Figure 5-17: Examples of normalised spectra obtained from 2 biological replicates of <i>S. chartarum</i> grown on ESA for 24 hours.	142
Figure 5-18: Representation of the result obtained from one of the replicates showing the peaks before and after analysis.....	144
Figure 5-19: Identification by Biotyper© Bruker database showing aligned protein profiles from the Bruker's database and <i>A. niger</i> (ATCC 16888) grown in SDB.	145
Figure 5-20: Both replicates were identified as <i>Aspergillus niger</i> grown in SDB with the highest log (score) values of 2.075 and 2.223 obtained from the existing Bruker's Library for Filamentous fungi.....	146
Figure 5-21: Identification by Biotyper© Bruker database showing aligned protein profiles from the Bruker's database and <i>A. niger</i> (ATCC 16888) grown in PDB.	147
Figure 5-22: Both replicates were identified as <i>Aspergillus niger</i> grown in PDB with the highest log (score) values of 2.265 and 2.160 obtained from the existing Bruker's Library for Filamentous fungi.....	148
Figure 5-23: Identification by Biotyper© Bruker database showing aligned protein profiles from the MSP using <i>S. chartarum</i> , NCPF 7587 and another <i>S. chartarum</i> , ATCC 16026 treated as a sample , both grown in SDB.	149
Figure 5-24: Sample was identified as the highest log (score) values obtained from newly created MSPs and existing Bruker's Library for Filamentous fungi.	149
Figure 5-25: Representation of the protein profiles of <i>S. chartarum</i> strains NCPF 7587, ATCC 16026, CBS 324.65 and CBS 182.80 grown in a. SDB and b. PDB.	150
Figure 5-26: Representation of the protein profiles of <i>S. chlorohalonata</i> strains; CBS 109286, CBS 109283, Stachy CU and, d. CBS 328.37 grown in a. SDB and b. PDB.	152
Figure 5-27: Representation of protein profiles of other <i>Stachybotrys</i> spp. a. <i>S. oenanthes</i> (CBS 252.76), b. <i>S. oenanthes</i> (CBS 463.74); c. <i>S. bisbyi</i> (CBS 363.58), d. <i>S. bisbyi</i> (CBS 399.65); and d. <i>S. dichroa</i> (CBS 949.72) grown in a. SDB and b.PDB.....	154
Figure 6-1: Sodium hypochlorite (bleach, Evans Vanodine International PLC).	168
Figure 6-2: Aerosolised hydrogen peroxide (AHP) machine (ASP GLOSAIR™).	169
Figure 6-3: The experimental set up with the AHP machine located approximately 180 cm away from the plates containing fungal samples opened prior to treatment placed on top of the smaller chamber.	170

Figure 6-4: Peracide PAA <i>in situ</i> (Peracide™).....	170
Figure 6-5: The preparation of peracetic acid at concentration 16000 ppm showed the colour indicator from activation stage (purple) to sporicidal stage (pink).	171
Figure 6-6: Organosilane (Biosafe®).	172
Figure 6-7: Effects of a single application of 500 µl sodium hypochlorite on <i>Stachybotrys chartarum</i> shown on ESA and PDA media and microscopy.	174
Figure 6-8: Effects of two applications (on consecutive days) of 500 µl sodium hypochlorite on <i>Stachybotrys chartarum</i> shown on ESA and PDA media, with accompanying microscopy.....	176
Figure 6-9: Samples from the repeat application plates were inserted into new plates of ESA and PDA and showed no visible new growth after a further 14 days incubation.....	177
Figure 6-10: Samples from the repeat application experiment plates were vortexed in PBS to produce a suspension and dropped onto the centre of the plate showed no growth after 14 days of incubation.....	177
Figure 6-11: Plates treated with a single application of AHP on PDA and ESA compared to control (untreated).....	178
Figure 6-12: Plates treated with two applications of AHP on PDA and ESA compared to control (untreated).....	179
Figure 6-13: Effects of a single application of 500 µl PAA on <i>S. chartarum</i> grown on ESA and PDA media with accompanying microscopy.....	181
Figure 6-14: Effects of two applications PAA on <i>S. chartarum</i> grown on ESA and PDA media with accompanying microscopy.	183
Figure 6-15: Effects of a single treatment at day-1 with OS on <i>S. chartarum</i> grown on ESA and PDA media with accompanying microscopy.....	185
Figure 6-16: Effects of repeated treatment with OS on <i>S. chartarum</i> grown on ESA and PDA media with accompanying microscopy.	187
Figure 6-17: The intermediate concentration (before 1:1 dilution with spore suspension) of bleach mixed with RPMI 1640 - 2% G- buffered with MOPS in 2 ml well plates.....	188
Figure 6-18: Bleach inhibits fungal spore germination at concentrations of 1000 ppm and above assessed by OD _{650nm} after 24 hours.	189
Figure 6-19: PAA inhibits fungal spore germination assessed by OD _{650nm} after 24 hours.....	190
Figure 6-20: The intermediate concentrations (before 1:1 dilution with spore suspension) of organosilane mixed with RPMI 1640 - 2% G- buffered with MOPS in 2 ml well plates.	191

Figure 6-21: Inconsistency of organosilane/ RPMI mixture dilutions prior to addition of spores assessed by OD _{650nm} after 24 hours.	192
Figure 6-22: Agar dilution plates showing the effects of bleach on the growth of <i>S. chartarum</i> after 7 days incubation at 25 °C.....	194
Figure 6-23: Agar dilution plates showing the effects of OS on the growth of <i>S. chartarum</i> after 7 days incubation at 25 °C.	196
Figure 7-1: Optimisation of experimental condition using potassium sulphate	206
Figure 7-2: RH and temperature test with 30 g salt in 10 ml of water showed temperature ranged from 21- 22°C and 94 - 95% RH.....	209
Figure 7-3: RH and temperature was compared using different amount of salt dissolved in equal amount of water recorded for 4 hours.....	210
Figure 7-4: RH in the small chamber test with plates containing 60 g potassium sulphate dissolved in 20 ml water remained constant for 3 weeks.	211
Figure 7-5: Gypsum board with no antimicrobial treatment or fungal growth (uninoculated control).	211
Figure 7-6: Sections of uninoculated gypsum board.....	212
Figure 7-7: Fungal growth on tested materials sampled after 11 weeks growth using tape-mounts, stained with lactophenol blue and observed under light microscopy at 40x magnification.....	213
Figure 7-8: The SEM images of <i>S. chartarum</i> -infested gypsum board after 11 weeks incubation.	214
Figure 7-9: Fungal growth on gypsum board without any antimicrobial treatment shown in duplicate.....	215
Figure 7-10: Fungal infested gypsum were cut into 1 cm ² pieces and placed on ESA for 10 days at 25 °C.	216
Figure 7-11: Fungal growth on gypsum board without any antimicrobial treatment using SEM images at 250x magnification.	217
Figure 7-12: Fungal growth on gypsum without any antimicrobial treatment using SEM images at 1000x magnification.	218
Figure 7-13: Fungal growth on gypsum before and after treatment with a single application of bleach at concentrations of 20000 ppm and 25000 ppm bleach shown in duplicates.	219
Figure 7-14: The materials were cut into 1 cm ² pieces and placed onto ESA on the same day of bleach application. The materials were incubated on ESA where growth recovery was documented after 10 days.	220

Figure 7-15: Fungal growth on gypsum treated with 20000 ppm bleach.	221
Figure 7-16: Fungal growth on gypsum treated with 25000 ppm bleach. a. Surface, b. Cross-section SEM images at 1000x magnification. The red coloured arrows indicate fungal structure coated with bleach.	222
Figure 7-17: Mould-infested gypsum boards before and after 1 to 5 applications of 25000 ppm bleach at 24-hours interval.....	224
Figure 7-18: Mould-infested gypsum boards before and after 1 to 5 applications of 45000 ppm bleach at 24-hours interval.....	225
Figure 7-19: Fungal recovery after 10 days from mould-infested gypsum treated with 1 to 5 applications of 25000 ppm and 45000 ppm bleach at 24-hour interval grown on ESA at 25 °C.	226
Figure 7-20: Fungal growth on gypsum board following 45000 ppm bleach treatment.	227
Figure 7-21: Mould-infested gypsum board before and after 1 cycle of AHP treatment.	228
Figure 7-22: Fungal growth recovered from mould-infested gypsum boards after treatment with 1 cycle AHP shown in duplicates incubated at 25 °C on ESA for 10 days.	228
Figure 7-23: Representation of fungal growth on gypsum. a. Surface; b. Cross-section (fungi) with one cycle of AHP treatment using SEM images at 250x magnification.	229
Figure 7-24: Representation of fungal growth on gypsum. a. Surface; b. Cross-section (fungi) with one cycle AHP treatment using SEM images at 1000x magnification.	230
Figure 7-25: Fungal growth on gypsum before and after treatment with PAA at concentrations of 4000 ppm and 8000 ppm shown in duplicate.	231
Figure 7-26: The PAA-treated materials were cut into 1 cm ² and placed onto ESA on the same day of PAA application. The materials were incubated on ESA at 25 °C where growth recovery was documented after 10 days.	232
Figure 7-27: Representation of fungal growth on gypsum following PAA treatment at 4000 ppm. a. Surface; b. Cross-section using SEM images at 250x magnification.	233
Figure 7-28: Fungal growth on gypsum board following PAA treatment at 8000 ppm. a. Surface; b. cross-section SEM images at 250x magnification.	234
Figure 7-29: Fungal growth on gypsum board following PAA treatment at 4000 ppm. a. Surface; b. Cross-section SEM images at 1000x magnification.	235
Figure 7-30: Fungal growth on gypsum board following PAA treatment at 8000 ppm. a. Surface; b. Cross-section SEM images at 1000x magnification.	236
Figure 7-31: Gypsum board pre-treated with and without OS coating at concentrations 2500 ppm and 5000 ppm prior to inoculation with <i>S. chartarum</i> shown in duplicates.....	237

Figure 7-32: The OS-treated materials grown inoculated with <i>S. chartarum</i> were cut into 1 cm ² after 5 weeks incubation.	238
Figure 7-33: Fungal growth on gypsum board following OS pre-inoculation treatment at 2500 ppm.	239
Figure 7-34: Representation of fungal growth on gypsum board following OS treatment at 5000 ppm.	240
Figure 7-35: Fungal growth on gypsum board following pre-inoculation OS treatment at 2500 ppm.	241
Figure 7-36: Fungal growth on gypsum board following pre-inoculation OS treatment at 5000 ppm.	242
Figure 8-1: Diagram of samples preparation of fungal plugs or suspension with antimicrobial agents' treatment or prevention.	251
Figure 8-2: Diagram showing the reduction process by TCEP, breaking disulphide bonds to maintain activity and stability and prevent the formation of aggregates.	255
Figure 8-3: Diagram showing the alkylation process by iodoacetamide, adding alkyl groups to cysteine thiol moieties to prevent formation of disulphide bonds.	255
Figure 8-4: The diagram illustrates the relationships between different data types in PANTHER.	259
Figure 8-5: Optimisation of protein extraction was performed by comparing phenol extraction alone or in combination with TCA/acetone precipitation in the first step.	260
Figure 8-6: Pie chart represents total number and percentage of protein obtained from LC MS/MS and proteins that were quantified in all groups.	261
Figure 8-7: Pie chart showing the total number and percentage of proteins obtained from LC MS/MS that were quantified in all groups.	261
Figure 8-8: Pie chart showing the total number and percentage of identified proteins from the TrEMBL database.	262
Figure 8-9: Pie chart represents the total number and percentage of homologous proteins obtained from NCBI database.	262
Figure 8-10: PANTHER classification of proteins identified in <i>S. chartarum</i> , NCPF 7587 with no contact with antimicrobial agents.	265
Figure 8-11: PANTHER classification of proteins identified in <i>S. chartarum</i> , NCPF 7587 with no contact with antimicrobial agents based on molecular function.	267
Figure 8-12: PANTHER classification of proteins identified in <i>S. chartarum</i> , NCPF 7587 with no contact with antimicrobial agents based on biological processes.	268

Figure 8-13: PANTHER classification of proteins identified in <i>S. chartarum</i> , NCPF 7587 with no contact with antimicrobial agents based on cellular components.....	269
Figure 8-14: The diagram illustrates biosynthesis of the amino acid valine which is critical to protein biosynthesis identified by PANTHER ⁽³²⁰⁾ in <i>S. chartarum</i>	270
Figure 8-15: The diagram illustrates biosynthesis of the amino acid isoleucine, critical to protein synthesis identified by PANTHER ⁽³²⁰⁾ in <i>S. chartarum</i>	271
Figure 8-16: The diagram shows the ubiquitin proteasome pathway	272
Figure 8-17: PANTHER classification of proteins identified in <i>S. chartarum</i> , NCPF 7587 with no contact with antimicrobial agents.....	274
Figure 8-18: Heatmap of significant proteins with changes in abundance in <i>S. chartarum</i> after 7 days' growth following the exposure to bleach and OS.....	280
Figure 8-19: PANTHER classification of proteins with increased in abundance based on protein classes of 7 days-old <i>S. chartarum</i> following the treatment of bleach and organosilane on Day-1.....	281
Figure 8-20: PANTHER classification of proteins with decrease in abundance based on protein classes of 7 days-old <i>S. chartarum</i> following treatment with bleach and organosilane on Day-1.....	282
Figure 8-21: PANTHER classification of proteins with increase in abundance based on molecular functions of 7 days-old <i>S. chartarum</i> following treatment with bleach and organosilane on Day-1.....	283
Figure 8-22: PANTHER classification of proteins with decrease in abundance based on molecular functions of 7 days-old <i>S. chartarum</i> following treatment with bleach and organosilane on Day-1.....	284
Figure 8-23: PANTHER classification of proteins with increase in abundance based on biological processes of 7 days-old <i>S. chartarum</i> following treatment with bleach and organosilane on Day-1.....	285
Figure 8-24: PANTHER classification of proteins with decrease in abundance based on biological processes of 7 days-old <i>S. chartarum</i> following treatment with bleach and organosilane on Day-1.....	286
Figure 8-25: The protein levels in the GABA signalling pathway ⁽³²⁰⁾ were decreased following 7 days after exposure to bleach.....	287
Figure 8-26: The protein levels in the toll receptor signalling pathway were increased in abundance in the OS group.	288

TABLES

Table 2-1: Key taxonomic history of <i>Stachybotrys chartarum</i>	51
Table 3-1: <i>Stachybotrys</i> spp. strains used in this study designated with strain numbers, species and origins.....	76
Table 3-2: Comparison of mean diameter growth of point inoculated <i>S. chartarum</i> (ATCC 16026) on different media compared to PDA as the control using unpaired t-test.....	80
Table 3-3: Comparison of mean diameter growth of point inoculated <i>S. chartarum</i> (NCPF 7589) on different media compared to PDA as the control using unpaired t-test.	80
Table 3-4: Comparison of mean diameter growth of point inoculated <i>S. chartarum</i> (Stachy CU) on ESA compared to PDA as the control using unpaired t-test.....	81
Table 3-5: Colony characteristics of <i>S. chartarum</i> (CBS 324.65, CBS 328.37), <i>S. chlorohalonata</i> (CBS 109286, CBS 109283), <i>S. bisbyi</i> (CBS 363.58, CBS 399.65), <i>S. oenantes</i> (CBS 252.76, CBS 463.74) and <i>S. dichroa</i> , (CBS 949.72, CBS 182.80) grown on ESA and PDA followed by incubation at 25 °C	81
Table 4-1: 13 strains of <i>Stachybotrys</i> spp. representing 5 different species as identified from the original source.....	97
Table 4-2: Primer data provided by Primer3Plus and Sigma.....	100
Table 4-3: Reference sequences from the whole genome sequence published by Semeik <i>et al.</i> ⁽⁸¹⁾ used to align all the sequences from Cruse <i>et al.</i> , Black <i>et al.</i> , and SC1.....	101
Table 4-4: <i>Stachybotrys</i> spp. strains and ITS primer sequence BLAST.....	105
Table 4-5: Tri5 primers sequence BLAST (<i>S. chartarum</i>).....	111
Table 4-6: Tri5 primers sequence BLAST (<i>S. chlorohalonata</i>).	113
Table 4-7: Summary of nucleotides differences in <i>S. chartarum</i> and its cryptic species, <i>S. chlorohalonata</i> from consensus sequences of Cruse <i>et al.</i> and SC1.....	116
Table 4-8: <i>In-silico</i> PCR using 2 sets of whole genome sequences of <i>S. chartarum</i> (KL652499.1) and <i>S. chlorohalonata</i> (*KL659704.1) ⁽⁸¹⁾	119
Table 5-1: Allowable peak shift from mass 3000-12000 Da as recommended by Bruker.	132
Table 5-2: Score values as suggested by Bruker.	132
Table 5-3: Calibration points for representing 8 known reference masses of peptides and additional protein in BTS solution.	141

Table 5-4: Score values of <i>Stachybotrys</i> spp. grown in SDB for 24 hours against MSPs generated from 2 biological replicates of <i>S. chartarum</i> , NCPF 7587.	155
Table 5-5: Score values of <i>Stachybotrys</i> spp. grown in PDB for 24 hours against MSPs generated from 2 biological replicates of <i>S. chartarum</i> , NCPF 7587.	156
Table 5-6: Summary of cut-off point obtained from this study and previous studies.	162
Table 6-1: Recommended concentrations of antimicrobial agents by the manufacturers and the effective concentrations tested from this study.	197
Table 8-1: BSA standards used in Bradford assay for the quantification of protein concentration.	254
Table 8-2: TMT reagents of different isobaric mass tags used to label each sample in replicates	256
Table 8-3: Summary of filtering process and number of proteins in each step.	263
Table 8-4: The differential protein expression of replicates used in each condition measured as mean average and median ratio.	263
Table 8-5: Number of proteins with changes in abundance in <i>S. chartarum</i> treated with bleach and organosilane compared to no exposure to antimicrobial agents.	275
Table 8-6: Examples of proteins which decreased in abundance in <i>S. chartarum</i> treated with bleach and their functions.	276
Table 8-7: Examples of proteins which increased in abundance in <i>S. chartarum</i> treated with bleach and their functions.	276
Table 8-8: Examples of proteins which decreased in abundance in <i>S. chartarum</i> treated with organosilane and their functions.	277
Table 8-9: Examples of proteins which increased in abundance in <i>S. chartarum</i> treated with organosilane and their functions.	278
Table 9-1: Contribution to the identification of <i>Stachybotrys chartarum</i>	298
Table 9-2: The effects of antimicrobial agents used for treatment and prevention on the growth and the changes in protein abundance of <i>S. chartarum</i>	300

ABBREVIATIONS

α-CHCA	alpha-cyano-4-hydroxycinnamic acid
ACDP	Advisory Committee on Dangerous Pathogens
bp	base pairs
BSA	Bovine serum albumin
BTS	Bruker bacterial test standard
CDC	U.S. Centers for Disease Control and Prevention
DHB	2, 5-dihydroxybenzoic acid
DMSO	Dimethyl sulfoxide
DNA	Deoxyribonucleic acid
ESA	Sabouraud dextrose agar, Emmons
H+	Protons
H₂O₂	Hydrogen peroxide
HOCl	Hypochlorous acid
MALDI-TOF	Matrix-assisted laser desorption ionisation-time of flight
MS/MS	Tandem mass spectrometry
MSPs	Mass spectral profiles
NaOCl	Sodium hypochlorite
NaOH	Sodium hydroxide
-OCl	Hypochlorite ions
PCR	Polymerase chain reaction
PDA	Potato dextrose agar
sinapinic acid	3, 5-dimethoxy-4-hydroxycinnamic acid
spp.	species
SDA	Sabouraud dextrose agar
SDB	Sabouraud dextrose broth
TFA	Trifluoroacetic acid
TMT	Tandem mass tags

UNITS

°C	degree Celsius
μl	microliter
x g	times gravity
Da	Dalton
m/z	mass-to-charge ratio
mg/L	milligram per litre
nm	nanometer
pH	potential of hydrogen
rpm	rotation per minute
m/s	meters per second

CHAPTER 1

RESEARCH BACKGROUND AND MOTIVATION

This chapter introduces the research background and its significance, research motivation, aims and objectives and overall thesis framework.

1.1 RESEARCH BACKGROUND AND ITS SIGNIFICANCE

Stachybotrys chartarum, often referred to as 'black mould', is a dematiaceous mould present in both outdoor and indoor environments ^(5, 6). It is mostly associated with poor indoor environmental quality caused by severe water intrusion problems and has been proposed as an indicator of mould contamination related to moisture problems in buildings alongside *Chaetomium* spp. and *Ulocladium* spp. ⁽⁷⁻¹⁰⁾.

Stachybotrys chartarum produces a variety of secondary metabolites including mycotoxins which can be highly toxic to human and other organisms as well. However, the toxicity depends on the mycotoxin classes derived from different metabolic pathways. The well-documented mycotoxins produced by *Stachybotrys* spp. are the highly toxic macrocyclic trichothecenes. The production of mycotoxins and other toxic by-products are influenced by biotic and abiotic stresses, such as relative humidity, temperature and chemical exposure.

Previously, *Stachybotrys* spp. have been characterised based on their culture characteristics and morphology. However, since the 2000s, in addition to the newly discovered species, *S. chlorohalonata*, there have been further taxonomic revisions due to the variability in toxicity of two different chemotypes A and S, produced by *S. chartarum* ^(11, 12). Several other methods have been developed which offer more rapid and reliable identification such as mycotoxin gene-based polymerase chain reaction (PCR) and matrix assisted laser desorption ionisation-time of flight (MALDI-TOF).

These methods have their own advantages and disadvantages. In the case of the *Stachybotrys chartarum* species complex, it is important to assess and compare all the methods available.

Fungal resilience and adaptation poses another huge challenge to building owners and related authorities. The root problem has always been due to excessive moisture which is unavoidable in many cases such as a climate catastrophe or geographical layout. In the indoor environment, *Stachybotrys* spp. cause problems by inhabiting cellulose-based building materials particularly gypsum board. Several remediation strategies have been implemented, from engineering control to antimicrobial application. Although there is a wide range of antimicrobial agents available in the market, the problem of fungal infestation still persists.

Various concentrations of chemicals have been recommended by the manufacturers, but higher concentrations are often required to kill or inhibit fungal growth. The efficacy of antimicrobial agents is very much dependant on the half-life of the chemicals and types of target materials infested with mould. Most of the microbial inhibitory testing to determine the efficacy of antimicrobial agents is performed *in vitro* or on non-soiled surfaces which makes the results less comparable to the real environment. Changes in the expression of certain antioxidative proteins may lead to fungal adaptation and eventually antifungal resistance. Protein and gene expression studies enable researchers to understand fungal adaptation which contributes to the failure of antimicrobial agents.

1.2 RESEARCH MOTIVATION

Research on mould infestation in the indoor environment involves a multidisciplinary approach encompassing molecular biology, chemistry, public health and engineering control which requires a concerted effort of different skills and expertise for it to function holistically.

Most studies on the relationship between dampness and moulds are widely reported from European countries, Canada and the United States. Different tools and techniques have been developed that might be the main contributors to the growing output of research in this area. Although most of the developing or under-developed countries are in the tropics where high precipitation and humidity is found, fewer

studies have been performed there, probably due to limited skills and expertise in the area of indoor environmental moulds.

The author of this thesis is currently employed as a researcher at the Environmental Health Research Centre, Institute for Medical Research, Malaysia and has been previously been involved in a series of indoor environmental investigations in Malaysia, particularly in collaboration with the Engineering Department or the State Health Department. One of the issues studied was the incidence of microbial contamination associated with respiratory tract infection due to severe and prolonged water intrusion initiated from leaking air-conditioners. Airborne microbial samples were taken, however, *Stachybotrys* spp. were only recovered using swabs from visible mould growth behind damp wallpaper ⁽¹³⁾. The identification was performed solely based on microscopy and culture characteristics with the help of an external mycologist due to a lack of knowledge and skills about *Stachybotrys* spp. in that particular time. The process of identification was time consuming since no rapid and reliable method for environmental moulds, in particular *Stachybotrys* spp., had been established. Moreover, there was no local understanding of the complexity of the species or the different chemotypes to assist future investigation.

The other demanding issue is fungal growth recurrence following remediation particularly after the application of antimicrobial agents. Many studies have investigated and compared different antimicrobial agents only to find a lack of efficacy in the real environment for many possible reasons. Amongst the reasons are ineffective mode of application and types of mould-infested materials. However, the efficacy of antimicrobial agents is often determined by log reduction or recovery of viable microorganisms in culture media. Therefore, it is important to evaluate the effects of respective chemicals on mould inhibition using different ways of application in different types of media. Proteome changes can be unique depending on the conditions to which the organism is exposed. It would be helpful to elicit more information on the response of *Stachybotrys* spp. to adaptation following the exposure to antimicrobial treatment and prevention. Since proteomic profiles for *Stachybotrys* spp. have not been established, this study will also provide information on the protein changes under different antimicrobial treatments. Furthermore, *Stachybotrys* spp. are among the moulds associated with the indoor environment but have not convincingly been associated with human disease, compared to other fungi such as *Aspergillus* spp. and *Fusarium* spp., suggesting they are a good model to be safely manipulated in an engineering setting.

1.3 RESEARCH OBJECTIVES

The two main objectives of this study were:

1. To assess various identification methods to characterise *Stachybotrys* species, and
2. To determine the effects of different antimicrobial agents on *S. chartarum* in response to antimicrobial agents.

This thesis is organised into 9 chapters consisting of an introduction, a literature review, 6 experimental chapters and general discussions and conclusions. The experimental chapters are divided into two main sections to answer the main and specific objectives as follows:

Section 1- Identification: To assess various identification methods to characterise *Stachybotrys* species

Chapter 3: To identify and characterise *S. chartarum* by culture characteristics and microscopy

Chapter 4: To identify *S. chartarum* using molecular techniques using universal primers, ITS-PCR (ITS 1 and ITS 4), and restriction fragment length polymorphism (RFLP) patterns and specific primers for the trichodiene synthase genes (*tri5*)

Chapter 5: To identify *S. chartarum* based on protein profiling using matrix assisted laser desorption ionisation-time of flight (MALDI-TOF) mass spectrometry

Section 2- Response to antimicrobial agents: To determine the effects of different antimicrobial agents on *S. chartarum*

Chapter 6: To evaluate the effects of antifungal agents (minimum inhibitory concentrations) of selected antimicrobial agents on *S. chartarum* growth using liquid media, solid media and plate dilution bioassays

Chapter 7: To study the inhibitory effects of antifungal agents on *S. chartarum* grown on gypsum board in a controlled environment using culture viability and electron microscopy

Chapter 8: To characterise changes in protein abundance in *S. chartarum* in response to antimicrobial agents using gel-free quantitative proteomics consisting of tandem mass spectrometry (TMT) labelling and mass spectrometry

CHAPTER 2

LITERATURE REVIEW

This chapter provides the background information on moulds and their significant role in indoor environmental contamination, as well as the special attributes of fungi that contribute to their resilience and resistance. It then focusses on *Stachybotrys chartarum* and its related species as our subject of interest. Finally, previous work on the identification methods and remedial strategies used in this study is discussed.

2.1 MOULD AS AN INDOOR CONTAMINANT

According to the World Health Organisation (WHO, 2009), “microbial pollution is a key element of indoor air pollution” ⁽⁵⁾. The indoor environment contains a complex mixture of microbiological contaminants such as fungi and bacteria. Microbial agents can be circulated in the air, attach to various surfaces and continue to replicate if optimum temperature, humidity and substrates are present. Since most people spend almost 90% of their time indoors, this escalates the risk of exposure to indoor environmental contaminants ⁽¹⁴⁾. Furthermore, pollution in indoor environments can be up to two to five-fold higher than in the outdoor environment ⁽¹⁵⁾.

A mould, commonly a term used interchangeably with fungus, refers to a filamentous fungus such as *Aspergillus* spp., *Alternaria* spp., *Penicillium* spp., *Cladosporium* spp. and *Stachybotrys* spp.. In general, a fungus (plural: fungi) is defined as any group of unicellular or multicellular spore-producing organism comprised of mushrooms, moulds, mildews, smuts, rusts and yeasts. Fungi are heterotrophic which means they lack chlorophyll and obtain their energy by using the organic matter from plants and animals ⁽¹⁶⁾. They are phylogenetically closer to animals than plants, protists and bacteria. Multiple proteins involved in glycolysis, protein synthesis, and other pathways

are shared by animals and fungi ⁽¹⁷⁾. They can be found in natural environments such as in soil and plants or in the indoor environment ⁽¹⁸⁾.

Building construction materials such as plaster, wood, wallpaper, gypsum board and fibrous glass insulation are frequently contaminated by moulds and have been shown to greatly affect indoor fungal levels ^(2, 19). Mould infestation normally occurs in places with water intrusion issues, high humidity, poor ventilation and a lack of maintenance or sanitation ^(20, 21). Cellulose based walls or furniture are the most suitable environments and substrates to promote the growth of indoor moulds ⁽²²⁾. Gravesen *et al.*⁽²³⁾ have reported *Penicillium* spp. (68%), *Aspergillus* spp. (56%), *Chaetomium* spp. (22%), *Ulocladium* spp. (21%), *Stachybotrys* spp. (19%) and *Cladosporium* spp. (15%) with *Penicillium chrysogenum*, *Aspergillus versicolor* and *S. chartarum* as the most frequently occurring species in water-damaged houses.

The prevalence of indoor dampness and mould varies between studies and is influenced by geographical layout and environmental factors such as continents, climates and surroundings such as riverside and coastal areas. In tropical or subtropical climates, high precipitation and humidity occur normally throughout the year which contribute to quick mould growth ⁽⁵⁾. In 'Dampness and Mould' by the WHO (2009), there were approximately 20 - 45% mould occurrences in buildings reported in the United Kingdom, the Netherlands, USA and Canada between 1988 to 1999 ⁽⁵⁾. In a review, Havarinen *et al.*⁽²⁴⁾ reported prevalence estimates of 12.1% for dampness, 10.3% for mould and 10.0% for water damage in homes from 31 European countries. In the United States, Mudarri and Fisk ⁽²⁵⁾ estimated prevalences of up to 50% for dampness and mould in US houses based on previous studies between 1989 to 2003.

Although there is no conclusive evidence of a causal relationship between mould exposure in the indoor environment and toxin-mediated ill-health, several epidemiological studies have shown a strong association between dampness, mould and health ⁽²⁶⁻²⁹⁾. Airborne fungal particles and their secondary metabolites, particularly mycotoxins have been indicated as the possible causes of illness among the occupants ^(30, 31). Indoor moulds such as *Stachybotrys*, *Cladosporium* and *Aspergillus* species produce spores, secondary metabolites and other components such as microbial volatile organic compounds (MVOCs), mycotoxins and β -(1,3)-D-glucans during development. Most of these by-products are highly toxic and have the potential to cause numerous adverse effects to humans.

Exposure to indoor mould has been associated with significant respiratory illnesses such as asthma, hypersensitivity pneumonitis, rhinosinusitis, wheezing, cough, eczema and upper respiratory symptoms to exposed individuals ^(26, 32). People living or working in mouldy and damp buildings exhibit a higher prevalence and incidence of respiratory symptoms and diseases than people in non-problem buildings ⁽³³⁻³⁵⁾.

The European Community Respiratory Health Survey (ECRHS) was a multicentre study consisting of 48 centres in 23 countries which began in 1990 to assess the prevalence of asthma and allergic disease in the European community ⁽³⁶⁾. Several publications have been produced including those related to the association of mould, dampness and respiratory diseases. Norback *et al.*⁽³⁷⁾ reported 50.1% dampness, 41.3% mould occurrence and significant lung function decline among women. In another publication, Norback *et al.*⁽³⁸⁾ reported 24.8% mould occurrence, 27.9% water damage and 5% new-onset asthma among healthy young subjects.

In a tropical climate, Tham *et al.*⁽³⁹⁾ reported home dampness and mould exposure to be significantly associated with rhinoconjunctivitis and rhinitis among children in Singapore. In Malaysia, Norback *et al.*⁽⁴⁰⁾ found associations between fungal DNA from *A. versicolor* and the mycotoxin verrucarol produced by *S. chartarum* collected from classroom dust samples, which were associated with rhinitis and sick building symptoms (SBS) among school pupils. Since mycotoxins are not readily volatile, the pathway of exposure was possibly via inhalation of dust containing mycotoxin. In another investigation, an outbreak of respiratory symptoms was reported among secondary school students living in a fully air conditioner hostel with severe water intrusion in Malaysia, which might also be due to inhalation of fungal materials. Pathogenic fungi such as *A. niger*, *A. versicolor* and *Penicillium* spp. were isolated from air samples and *Stachybotrys* spp. was sampled from contaminated walls under leaking air conditioner units ⁽¹³⁾.

Indoor moulds also increase the risk of opportunistic infections among immune-compromised individuals and susceptible groups including children and the elderly ⁽⁵⁾. The allergenic moulds were found to trigger asthmatic symptoms in asthma patients such as shortness of breath, wheezing, and coughing ⁽⁴¹⁾. In Finnish homes, mould odour increased the risk of developing asthma among children by 2.4 times in 6 years after exposure compared to the non-exposed children ⁽⁴²⁾. In another study conducted in New Zealand homes, new-onset wheezing in children has been strongly associated with the occurrence of visible moulds and mould odour ⁽⁴³⁾.

In the workplace, it is critically important to address the issues on indoor microbial contaminants as these lead to productivity loss and medical burden to the employers and healthcare providers ^(44, 45). Approximately 15% of known asthma cases are caused by or worsen due to exposure in the workplace ⁽⁴⁶⁾. An increased incidence of sick building syndrome (SBS), hypersensitivity pneumonitis, sarcoidosis, increased bronchial responsiveness and eosinophilic inflammation was also associated with dampness and moulds in the workplace building ^(10, 47).

Concerning the health effects of certain pathogenic moulds, the World Health Organization (WHO, 2009) has published the most comprehensive guideline for indoor air quality and health problems, the 'Guidelines for Indoor Air Quality: Dampness and Moulds'. The guideline serves as a key document which summarises epidemiological and clinical evidence associated with damp and mouldy buildings; and lists intervention strategies and control measures, primarily controlling moisture and improving ventilation ⁽⁵⁾.

Several other guidelines and standards on indoor microbial contaminants have been established for various indoor settings including schools, workplaces, non-industrial buildings ^(21, 48) , and hospitals ⁽⁴⁹⁻⁵¹⁾. In cases of mould infestation, remediation strategies such as cleaning and antimicrobial treatment or removal of mould contaminated materials are considered crucial to kill or stop fungal growth from spreading ⁽⁵²⁻⁵⁴⁾.

2.2 THE ROLE OF FUNGI IN INDOOR-RELATED ILLNESS

The pathogenesis of indoor mould related health problems is not clearly understood. Terms such as sick building syndrome (SBS) is commonly used to indicate the health effects derived from exposure to indoor contaminants with slightly different definitions in terms of diagnosis ⁽⁵⁵⁾. The SBS is a complex spectrum of ill-health symptoms consists of acute and non-specific symptoms such as headache, eye, nose or throat irritation, dry cough, scaly or itchy skin, dizziness, nausea, vomiting, difficulty in concentrating and fatigue ^(56, 57).

Indoor moulds such as *S. chartarum* produce spores, secondary metabolites and other components such as microbial volatile organic compounds (MVOCs), mycotoxins and other fungal components such as β -(1,3)-D-glucans and stachylysin which have been associated with adverse health effects in animals and humans (Figure 2-1). Non-specific symptoms such as fever, general malaise, headache, cough, and shortness of breath in humans have been associated with the presence of 10^3 - 10^7 spores per cubic metre of air presence in the environment ⁽⁵⁷⁾.

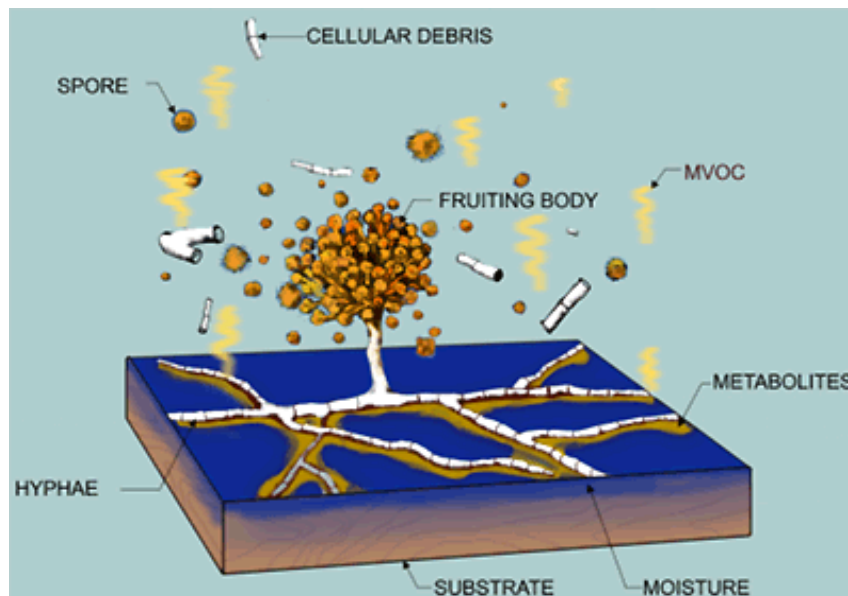


Figure 2-1: A mould requires a suitable substrate in the presence of moisture to grow. It releases spores, MVOC and other debris during development. The diagram was adapted from the Whole Buildings Design Guide, “Indoor Air Quality and Mold Prevention of the Building Envelope (www.wbdg.org, last updated 22 February 2017)⁽⁵⁸⁾. Used with permission from the National Institute of Building Science.

2.2.1 Spores

In the United Kingdom, a temporal relationship between fungal sensitization and asthma severity has been demonstrated during the period of July to September when numbers of mould spore concentrations in the air peak. The study showed a 2.16-fold increased risk of asthmatic death among the young adults exposed to more than 1000 spores per cubic metre ⁽⁵⁹⁾. This increased risk of fungal allergy is considered low, but it may provide an insight into the health burden should the population be exposed to allergenic moulds, especially during certain seasonal variations and concentrations of spores in the air. In another study conducted in the United States, almost 2% of the general population had been estimated to develop fungal allergy regardless of the season ⁽²²⁾.

2.2.2 β -(1,3)-D-glucan

β -(1,3)-D-glucan is one of the cell wall components in most fungi and has been used as a surrogate for mould exposure ⁽⁶⁰⁾. In indoor environments, exposure to β -(1,3)-D-glucan has been associated with respiratory health problems and other allergic responses such as airway inflammation, nasal and throat irritation, cough, wheezing, and skin rashes ⁽⁶¹⁾. However, Douwes *et al.*⁽⁶⁰⁾ found no clear evidence of specific adverse health effects associated with the exposure to β -(1,3)-D-glucan in adults. In children, Tischer *et al.*⁽⁶²⁾ have reported an inverse association of extracellular polysaccharides (EPS) and endotoxin from children's mattresses with doctor-diagnosed asthma and rhinitis in Germany, but no association with β -(1,3)-D-glucan.

2.2.3 Stachylysin

Stachylysin is a haemolysin isolated from *Stachybotrys* isolates obtained from mould-infested homes in Cleveland. In *S. chartarum*, it is localised in the inner cell wall of the spore, based on immunohistochemical staining. In an *in vivo* mouse model, stachylysin was observed in mouse lung tissues with a higher level at 72 hours than at 24 hours, suggesting slow release from the spores ⁽⁶³⁾. Stachylysin has the ability to lyse red blood cells and has been proposed as a cause of pulmonary haemorrhage in humans ⁽⁶⁴⁻⁶⁶⁾.

2.2.4 Microbial volatile organic compounds

Fungi emit MVOCs (in the gas phase) that are responsible for the characteristic mouldy odours associated with damp indoor spaces. Volatile organic compounds are defined as organic compounds that vaporize (become a gas) at room temperature. A great

number of MVOCs are produced by fungi including certain alcohols, aliphatic C8 compounds, alkanes, alkenes, esters, ketones, lactones, pyrazines and terpenes. Some of them are unique MVOCs to certain fungi and bacteria which are referred to as UMVOCs ⁽⁶⁷⁾. In a study comparing MVOCs produced by three strains of *S. chartarum*, four unique MVOCs, namely 1-butanol, 3-methyl-1-butanol, 3-methyl-2-butanol and thujopsene, were detected on rice cultures, and only 1-butanol was detected on gypsum board cultures ⁽⁶⁸⁾.

MVOCs have been identified as the leading cause of ground level ozone (a major constituent of smog). In sufficient quantities, MVOCs can cause eye, nose, and throat irritations, headaches, dizziness, visual disorders and memory impairment and are possibly be carcinogenic to humans ⁽⁶⁹⁾.

2.2.5 Mycotoxins

The term mycotoxin refers to the fungal compounds that have harmful effects on health at low concentrations ⁽⁷⁰⁾. The word mycotoxin is derived from the Greek words 'mykes' which means "fungi" and 'toxikon' which means "poison" ⁽⁷¹⁾. Mycotoxins are also defined as a low-molecular weight product produced as a secondary metabolite by filamentous fungi ⁽⁷²⁾.

The term mycotoxin was first introduced in 1962 after the death of approximately 100,000 turkeys in England linked to aflatoxin contaminated Brazilian peanut meal which had been improperly stored ^(73, 74). Since then, researchers have become aware of the risks mycotoxins pose to humans and have begun to characterise them from various sources, such as food commodities and the environment ⁽⁷²⁾. Mycotoxins are known to affect major sites of RNA and protein synthesis in animals and humans. The interaction of mycotoxins with functional molecules and subcellular organelles results in the symptoms of mycotoxicosis. The mechanism of action of a mycotoxin may be the modification of the DNA template, impairment of the transcription or inhibition of the translation in protein synthesis or interaction with the protein molecules themselves ⁽⁷⁵⁾ (Figure 2-2).

Trichothecenes are sesquiterpenoid metabolites produced by some fungi such as *Fusarium*, *Myrothecium*, *Trichoderma* and *Stachybotrys* spp. ⁽²²⁾. Trichothecenes comprise of a tetracyclic core with an epoxy ring at C-12 and C-13 (12,13-epoxytrichothec-9-ene) (EPT) that plays a role in toxicity. Trichothecenes inhibit DNA, RNA, and protein synthesis and eventually affect downstream metabolic reactions. They can cause feed refusal, immunological problems, vomiting, skin dermatitis, and

haemorrhagic lesions in humans ⁽⁷⁶⁾. Trichothecenes can be classified into 4 types (A, B, C and D) according to the substitution pattern at the C-8 position (Figure 2-3). They are further grouped into either non-macrocytic or macrocytic compounds based on the presence or absence of a macrocytic ring at C-4 and C-15 ⁽⁷⁷⁾. Of these, type D trichothecenes, or the macrocytic trichothecenes produced by *Stachybotrys* spp. have gained much attention in relation to potential disease associated with the indoor environment ^(78, 79).

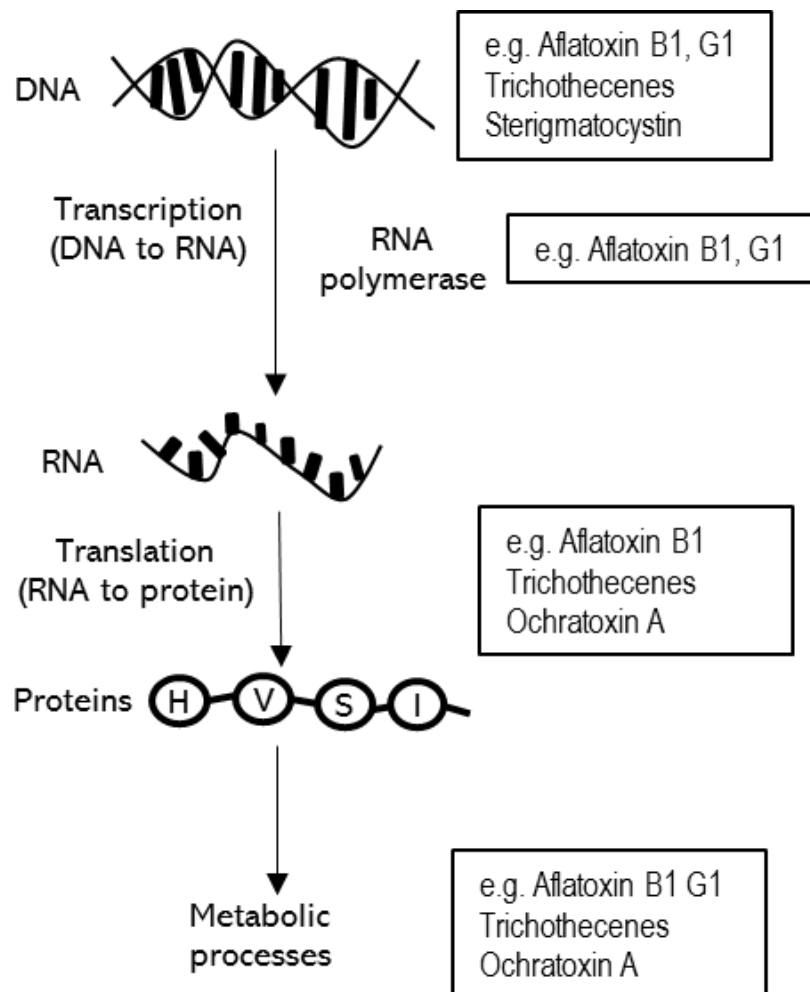


Figure 2-2: The pathway showing mechanism of action of several mycotoxins affecting major sites in RNA and protein synthesis.

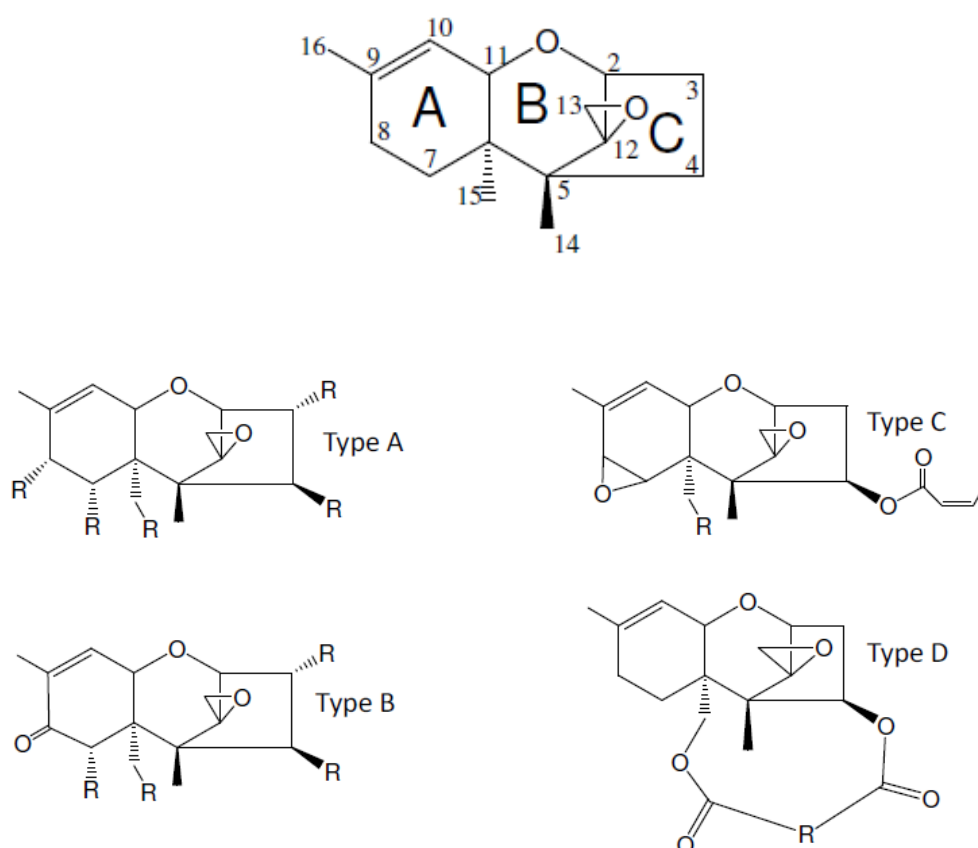


Figure 2-3: Basic structure of trichothecenes and four types of trichothecenes (type A, B, C and D) based on substitution pattern at C-8 position. Diagram adapted from McCormick *et al.*⁽⁷⁷⁾. Licensed under Creative Commons Attribution (<http://creativecommons.org/licenses/by/3.0/>).

Several trichothecenes have been detected in commonly used building materials, heavily contaminated with *S. chartarum*⁽²³⁾. *S. chartarum* produces either macrocyclic trichothecenes consisting of roridins, verrucarins, satratoxins F, G and H, isosatratoxins F, G, and H or less toxic simple non-macrocyclic trichothecenes consisting of verrucarol, trichodermol and trichodermin⁽⁸⁰⁾. In addition, two chemotypes of *S. chartarum* have been identified: chemotype S that produces highly toxic macrocyclic trichothecenes and chemotype A that produces less toxic atronones which can be distinguished phylogenetically, based on tri5 sequences⁽¹¹⁾ (Figure 2-4).

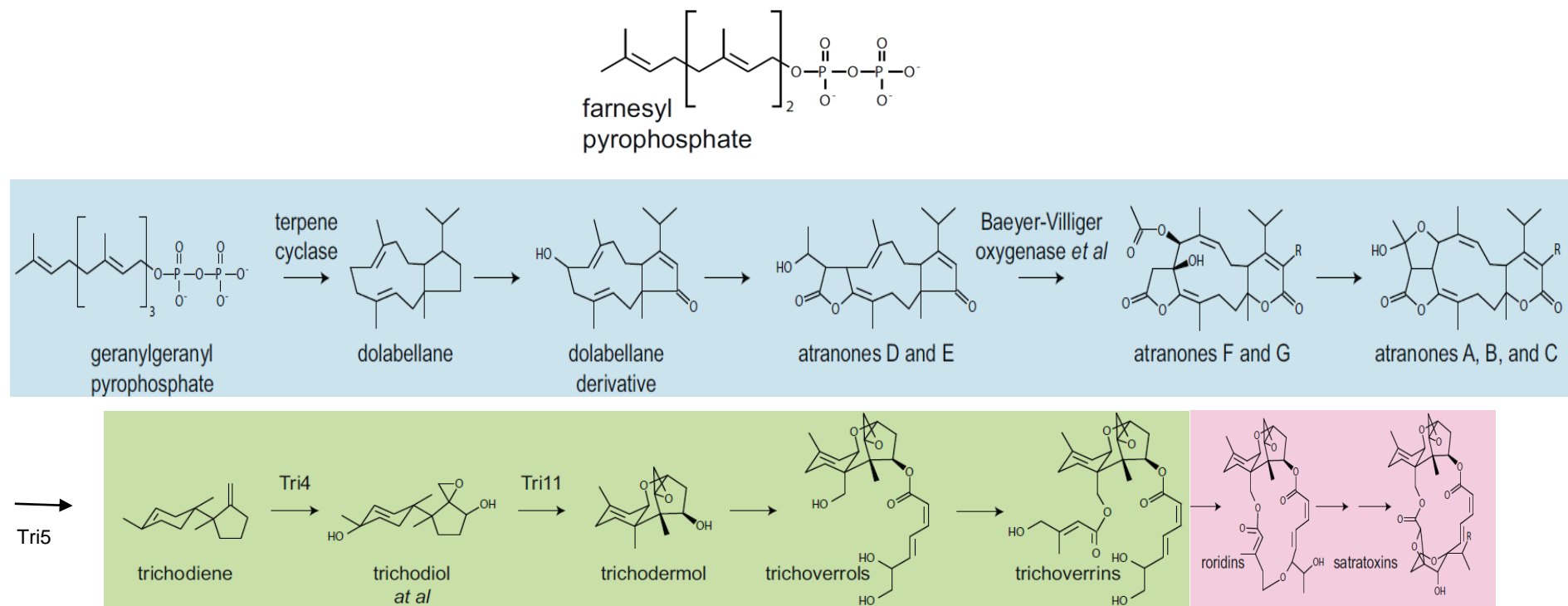


Figure 2-4: Trichothecenes and atranones produced by *Stachybotrys* spp.. Metabolites are derived from the primary metabolite farnesyl pyrophosphate (FPP) as shown in blue for atranones, green for simple trichothecenes, and pink for macrocyclic trichothecenes. Enzymes shown were characterised from *Fusarium* (tri5) and *Trichoderma* (tri4 and tri11). Diagram adapted from Semeiks *et al.*⁽⁸¹⁾. Licensed under Creative Commons Attribution (<http://creativecommons.org/licenses/by/2.0>).

2.3 FUNGAL RESILIENCE IN THE INDOOR ENVIRONMENT

Fungal infestation poses many challenges to building owners and has been associated with numerous factors. The major problems that have been identified are related to climatic factors (e.g. humidity and temperature), human factors (e.g. poor maintenance and cleanliness) and building structure and engineering (e.g. building materials and ventilation systems) ^(20, 21). However, biological adaptation by the fungus is another important factor that contribute to its resilience in the indoor environment.

Most building materials are rich in cellulose and are capable of being degraded by most fungi, and thus, are prone to mould infestations. Fungi, in general, require organic carbon for growth and development in the form of carbohydrates such as cellulose. Fungi secrete certain enzymes such as cellulases and β -1,4-glucosidase that are capable of degrading cellulose materials into glucose as a source of energy ⁽⁸²⁾. Water-damaged buildings, high humidity indoor environments and cellulose based walls or furniture are the most suitable environments and substrates to promote the growth of indoor moulds (Figure 2-5).

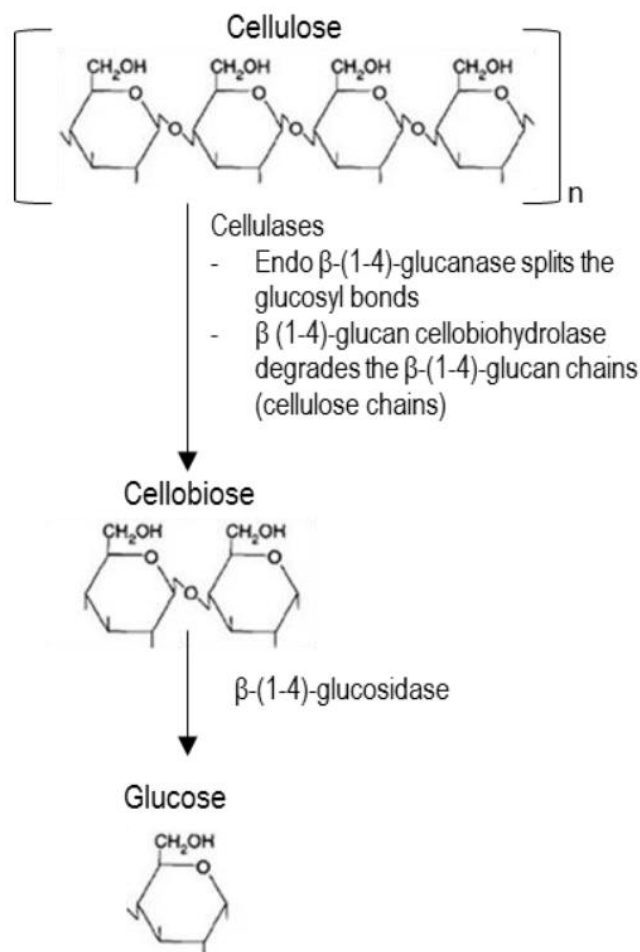


Figure 2-5: The degradation of cellulose by fungi to produce glucose as the nutrient source. Enzyme endo β -(1-4)-glucanase splits the glucosyl bonds yielding single β -(1-4)-glucan chains. A second enzyme, β (1-4)-glucan cellobiohydrolase degrades the β -(1-4)-glucan chains (cellulose chains) to give cellobiose. The cellobiose is finally converted to glucose by β -(1-4)-glucosidase.

Most filamentous fungi grow by extension at the tip (apex) of the hyphae which later form a network of hyphae called the mycelium. This structure plays a vital role in nutrient uptake in fungi which is required for growth and reproduction. Fungi are heterotrophic (require organic carbon compounds for growth) and therefore grow on cellulose-rich surfaces such as wood and gypsum boards ⁽⁸³⁾. Hyphae penetrate into the substrate and release cellulolytic enzymes to break down the complex substrate into simple glucose. Fungal growth may be visible on surfaces; however, hyphae may also penetrate through the porous materials and grow inside the material cavity. These will weaken the building material or may eventually cause the contaminated materials to be discarded ⁽⁸⁴⁾. Furthermore, hard to reach areas make cleaning of fungal contaminated materials a difficult task.

On the other hand, fungal spores are dormant structures in a resting state in the fungal life cycle. Spores may be harmful to humans whether in a dormant, viable or non-viable state, especially via inhalation. In the indoor environment, spores can be dispersed and circulated in indoor air and attach to other surfaces when proper ventilation is not available. Spores are able to withstand unfavourable environmental conditions such as changes in pH and temperature or deficiency in water and nutrients ^(84, 85). The dormant spores are able to retain their genomic material for a long period of time and are ready to germinate when environmental conditions are favourable for growth ⁽⁸⁶⁾. Moreover, improper cleaning can lead to the production of mycotoxins and spore dispersion.

Even worse, Murtoniemi *et al.* ⁽⁸⁷⁾ reported incomplete remediation of mould growth by antifungal agents increases the toxicity of spores in certain fungi. In the study, *S. chartarum* was grown on plasterboards with modifications in the composition of board core or liner including the addition of a biocide. The study demonstrates that the bioactivity of spores in mouse macrophages were affected by changes to the composition. Moreover, the addition of a biocide was only partially effective to prevent fungal growth on the modified plasterboards.

There is also the possibility of the development of resistance ^(88, 89). The uncontrolled use of fungicides in the environment has led to mutations in fungi that cause resistance to said fungicides, which is a cause of concern to clinical mycologists. It has been proposed that human pathogenic fungi resistant to the antifungal agents used in the clinical settings may have origins in the environment based on identical isolates found both in environmental and patient samples ⁽⁸⁸⁾. Changes in certain genes or proteins serve as a part of fungal defence and survival mechanisms. However, these genetic adaptations reduce sensitivity to antifungal agents which later develops into resistance. The upregulation or downregulation of certain genes or proteins is produced in response to biotic or abiotic stresses ⁽⁹⁰⁾.

2.4 STACHYBOTRYS CHARTARUM AND ITS RELATED SPECIES

2.4.1 Identification, taxonomy and nomenclature

Stachybotrys chartarum is a slow to moderately fast growing fungus, usually maturing after 7-14 days on medium with a high cellulose content ⁽⁹¹⁾. It requires a temperature range from 22.2 to 27.8 °C and an optimum pH of 5.6-6.0. The American Type Culture Collection (ATCC) suggests ATCC strains should be cultured on cornmeal medium

(CMA), potato dextrose medium (PDA) or Emmon's modified Sabouraud's medium (ESA). *S. chartarum* has a white surface which later becomes dark grey to black effuse, with a cottony or powdery bloom of conidial masses (Figure 2-6). The reverse morphology is colourless, turning black with age ^(91, 92).

Microscopically, *S. chartarum* has septate and colourless to dark hyphae, which are simple, straight or flexuous, branched or unbranched. Its conidiophores are usually about 100 µm to 1000 µm long and 3-6 µm wide, bearing clusters of 3-10 phialides. The conidia are dark, ellipsoidal, smooth or rough walled, aggregated in slimy masses at the tip of the phialides (Figure 2-7) ⁽⁹¹⁾. The phialides are colourless or pigmented, non-septate and cylindrical with a swollen upper portion ^(92, 93).

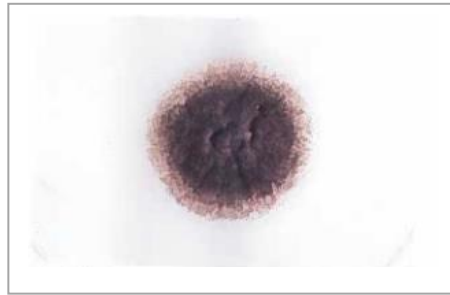


Figure 2-6: The cultural characteristics of *Stachybotrys chartarum* grown on potato dextrose agar at 30 °C for 7 days. Image adapted from Larone DH ⁽⁹¹⁾. ©2011 American Society for Microbiology. Used with permission. No further reproduction or distribution is permitted without the prior written permission of American Society for Microbiology.

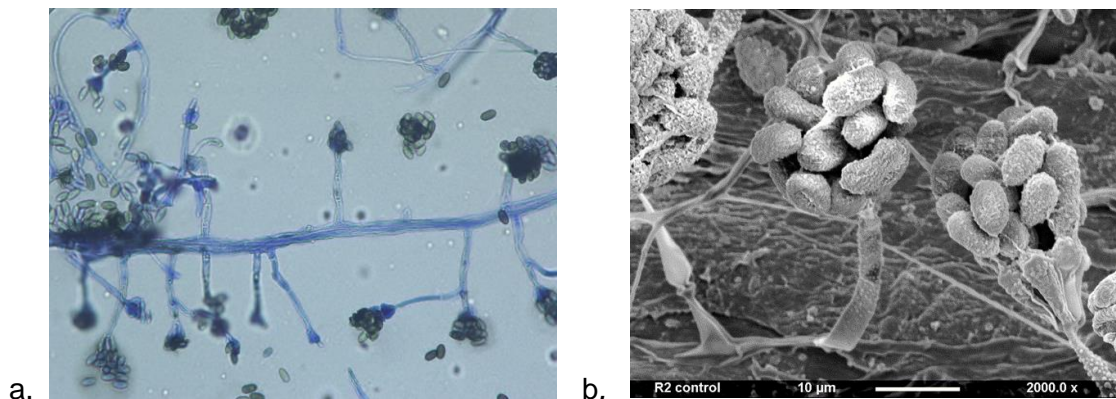


Figure 2-7: Microscopic appearances of *Stachybotrys chartarum*, NCPF 7587. a. Conidiophores 100x, and b. SEM micrographs 2000x.

Most *Stachybotrys* isolates from water-damaged buildings have been referred to as *S. chartarum*, but they have varied in toxicity profiles and consequently have led to taxonomic confusion due to *S. chartarum* species complexity⁽⁹⁴⁾. A 'species complex' is a group of species that are morphologically (or phenotypically) indistinguishable. It is only with the advent of phylogenetic (or molecular) analysis that it has become possible to detect novel cryptic species within *S. chartarum*. A 'cryptic species' is a species recognised by nucleic acid variation that had not been recognised as distinct on the basis of its morphological characteristics. Using three polymorphic protein loci (chitin synthase 1, beta tubulin 2, and trichodiene synthase 5) to search for cryptic species, Cruse *et al.*⁽¹²⁾ have reported two distinct phylogenetic species within a single described morphological of *S. chartarum*.

Subsequently, Andersen *et al.*^(11, 94) have characterised and identified 122 *Stachybotrys* isolates using 3 different methods: morphology and culture characteristics and metabolite production and found 2 different taxa; *S. chartarum* and a new species; which was later described as *S. chlorohalonata* based on different *tri5*, *chs1* and *tub1* gene sequences, different growth characteristics and green pigment production on potato sucrose agar and Czapek yeast agar. *S. chartarum* chemotypes, S and A share the same morphology, but differ in some of the metabolites they produce using LC-MS.

However, other researchers have remarked on the difficulty of distinguishing between *S. chartarum* isolates and its cryptic species, *S. chlorohalonata* based on morphological characteristics alone^(95, 96). Li and Yang⁽⁹⁵⁾ have reported the risk of misidentification due to the great variation in size and shape of conidia that change with age and development (Figure 2-8).

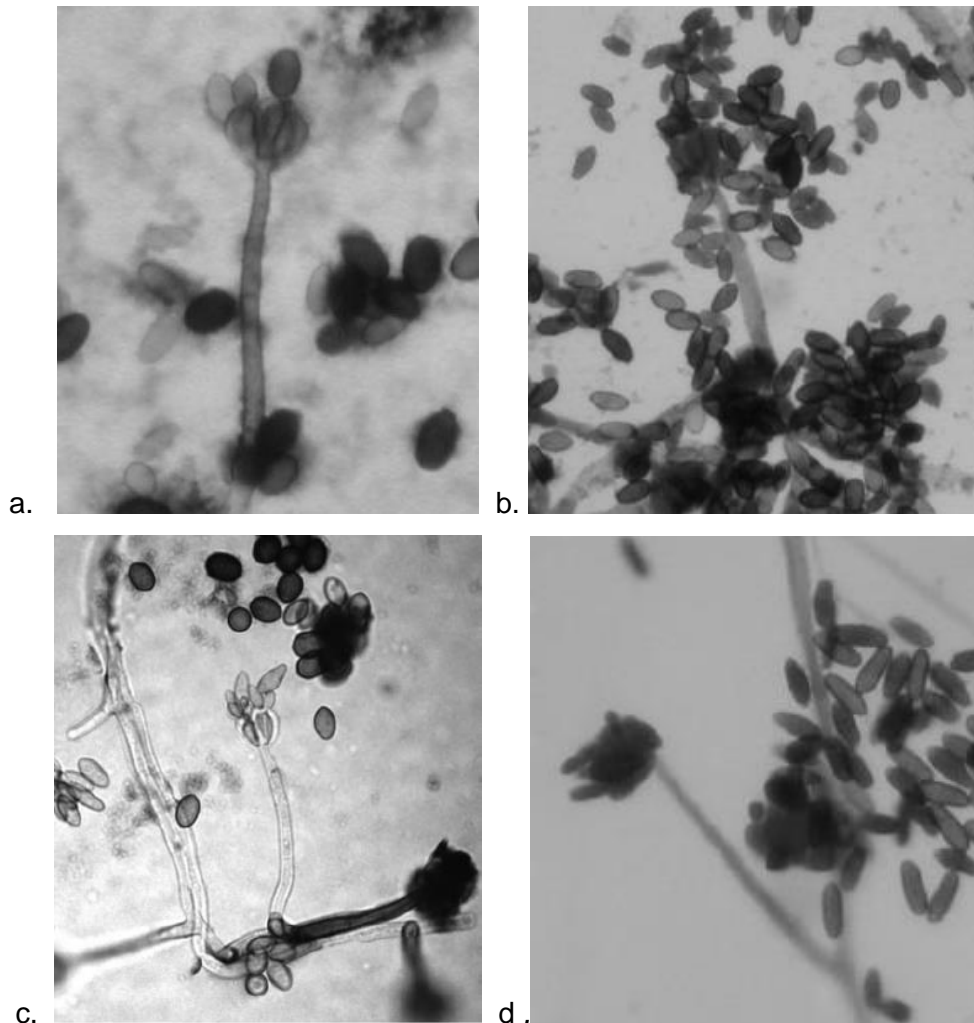


Figure 2-8: Morphological characteristics of conidia, phialide arrangement and conidiophore structures of *Stachybotrys* spp. grown on MEA and incubated for 7 days at 25 °C. a & b. *S. chartarum*, c. *S. chlorohalonata* and d. *S. yunanensis*. Images adapted from Li and Yang ⁽⁹⁵⁾. ©2005 John Wiley and Sons. Used with permission from John Wiley and Sons and Copyright Clearance Center.

Stachybotrys chartarum (Ehrenb. Ex Link) Hughes, also previously known as *S. atra*, *S. alternans*, *Stilbospora chartarum*, *Oidium chartarum*, *Oospora chartarum* or black mould has commonly been associated with contaminated indoor air in the 20th century ⁽⁹⁷⁾. The genus has been continuously revised since it was proposed due to developments in identification methodology ⁽⁹⁵⁾. The nomenclature of *Stachybotrys* sp. has been unclear until recently with three species names, *S. chartarum*, *S. alternans* and *S. atra* used interchangeably in the literature ⁽⁹¹⁾.

The genus *Stachybotrys* was originally described by a Czech mycologist, August Carl Joseph Corda in 1837 (Figure 2-9). The mould was first isolated from a wall of a house

in Prague during winter and was initially identified as *Stachybotrys atra* ⁽⁹⁸⁾. The genus name of *Stachybotrys* was derived from the Greek word ‘stakhus’ which means “ear of grain” or ‘stachy’ which means progeny and ‘botrys’ which means “bunch of grapes” which very much resembles its morphology (Merriam Webster Online, 2014). Since then, till the 1940s, *Stachybotrys* spp. was classified by a few mycologists including Berkeley (1841), Bonorden (1851), Grove (1886) and others with regards to its taxonomy and nomenclature, which were summarised as follows:

“Hyphae, phialophores, and phialides hyaline, brightly coloured, or dark;
Strands or ropes of hyphae may be produced. Conidia (slime-spores) one celled, normally dark and accumulating into a cluster. The distinctive characteristic of the genus is the septate phialophore or simple conidiophore bearing a crown of phialides and generally becoming dark. A phialophore arises directly from a hypha or, frequently, from another phialophore. Perfect stage unknown.” ⁽⁹⁸⁾

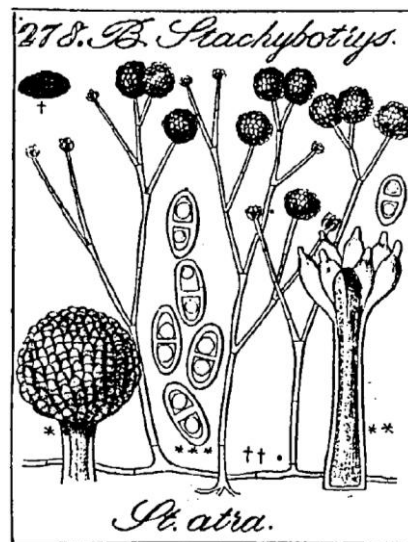


Figure 2-9: The Corda’s first figures of a *Stachybotrys* sp. (known as *S. atra*). Image adapted from Bisby (1942)⁽⁹⁸⁾. ©1943 Elsevier. Used with permission from Elsevier and Copyright Clearance Center.

Corda described *Stachybotrys* as having a two-celled conidia, which was later disputed ⁽⁹⁹⁾. Hughes (1958) found Corda’s description to be inaccurate which led to the re-examination of *Stachybotrys atra* as described by Bisby (1942). Hughes (1958) identified *S. atra* as *Stachybotrys chartarum* (Ehrenb.) Hughes. Eventually, in accordance with the International Code of Botanical Nomenclature, Jong and Davis⁽⁹⁹⁾ proposed the scientific name of *Stachybotrys chartarum* (Ehrenb. Ex Link) Hughes (see Table 2-1).

In 1976, Jong and Davies⁽⁹⁹⁾ also published an extensive report on the identification of *Stachybotrys* spp. and *Memnoniella* spp. obtained from the American Type Culture Collection (ATCC). These two genera have been compared in many studies due to their economic relevance and closely related morphology and physiology ⁽⁹⁸⁻¹⁰⁰⁾. *S. chartarum* and *M. echinata* were used for fungal resistance tests by the United States and British military as they were capable of utilizing cellulose-based materials such as fabrics ⁽⁹⁹⁾.

Morphologically, *Stachybotrys* resembles *Memnoniella* in the production of conidiophores with an apical cluster of unicellular conidiogenous cells. However, the genera are distinguished from each other by the arrangement of conidia (Figure 2-10). The conidia of *Stachybotrys* spp. are segregated in a slimy head while in *Memnoniella* spp., the conidia exist as long persistent chains with the youngest conidium at the basal end of the chain ⁽⁹⁹⁾.

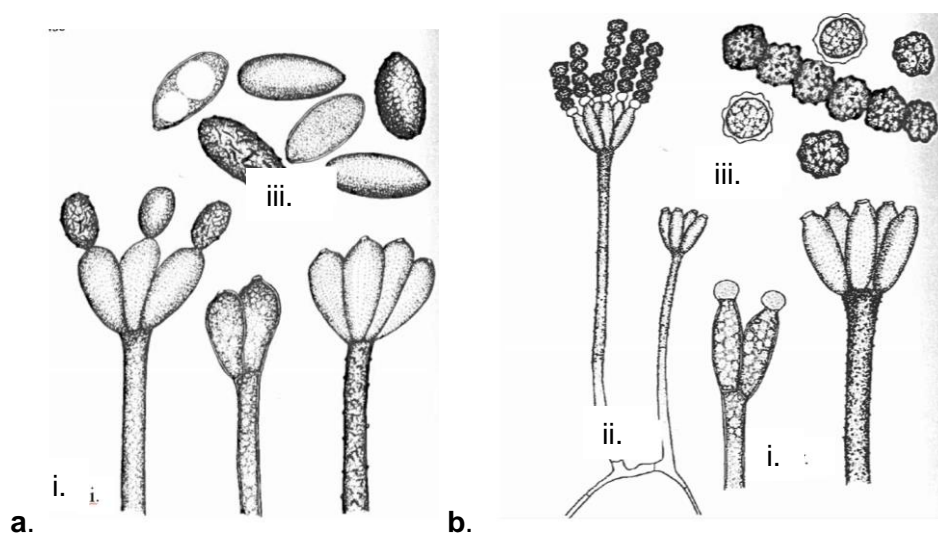


Figure 2-10: The morphological difference in the arrangement of the conidia of a. *Stachybotrys chartarum* and b. *Memnoniella echinata*. (i) Phialides. (ii) Conidiophores with phialides and phialoconidia. (iii) Phialoconidia. Images adapted from Jong *et al.*⁽⁹⁹⁾. Used with permission from Mycotaxon.

Table 2-1: Key taxonomic history of *Stachybotrys chartarum*

Year	Descriptions	References
1837	The first characterisation as <i>Stachybotrys atra</i> Corda as septate, branched hyphae, conidiophore terminate in a whirl of phialide and two-celled conidia	Corda, 1837 ⁽⁹⁸⁾
1943	Total of 20 <i>Stachybotrys</i> spp. (12 new taxa, unispore), revised into 2 species: <i>S. atra</i> Corda and <i>S. subsimplex</i>	Bisby, 1943 ⁽⁹⁸⁾
1958	<i>Stilbospora chartarum</i> Ehrenb. 1818, <i>Oidium chartarum</i> Ehrenb. Ex Link 1824, <i>Oospora chartarum</i> (Ehrenb. ex Link) Wallr. 1833. all classified as <i>S. chartarum</i> (Ehrenb) Hughes	Hughes, 1958 ^(95, 99)
1962	<i>Memnoniella echinata</i> classified as <i>Stachybotrys</i> sp.	Smith, 1962 ⁽⁹⁹⁾
1945-1971	<i>Memnoniella</i> described as distinctive from <i>Stachybotrys</i> spp.	Padwick (1945), Deighton (1960), Matsushima (1971) and Ellis (1971) ⁽⁹⁹⁾
1966	Proposed new variant of <i>S. atra</i> with smaller conidia (6-8 x 4-5 µm), elliptical to globose named <i>S. atra</i> Corda var. <i>microspora</i> Mathur and Sankhla	Manthur and Sankhla, 1966 ⁽⁹⁵⁾
1976	All <i>Stachybotrys</i> spp. described as having unicellular conidia Proposed a standardised and proper nomenclature as <i>S. chartarum</i> (Ehrenberg ex Link) Hughes Re-examined <i>S. atra microspora</i> and found the deposit mixed with <i>S. chartarum</i> . Renamed <i>S. atra microspora</i> into <i>S. microspora</i> (Mathur & Sankhla) Jong & Davis <i>Stachybotrys</i> spp. and <i>Memnoniella</i> spp. were considered as physiologically and morphologically closely related but the main difference is in the conidia	Jong and Davis, 1976 ⁽⁹⁹⁾
1980	No valid generic distinction between <i>Stachybotrys</i> spp. and <i>Memnoniella</i> spp. as proposed by Jong & Davis, 1976 Suggested both genera to be classified under <i>Stachybotrys</i> spp.	Carmichael, 1980 ⁽¹⁰¹⁾
1997	<i>S. yunanensis</i> as a new species (but no new report since 1997), most likely to have been <i>S. chartarum</i>	Kong, 1997 ⁽⁹⁵⁾
2001	<i>Memnoniella echinata</i> (Rivolta) Galloway renamed as	Haugland, 2001 ⁽¹⁰⁰⁾

	<i>Stachybotrys echinata</i> (Rivolta) G. Sm and <i>M. subsimplex</i> (Cooke) Deighton as <i>S. subsimplex</i> Cooke following phylogenetic and morphological analysis using 18S, 28S, 5.8S rDNA genes and ITS1 and ITS2 regions	
2002	Examined 30 isolates of <i>S. chartarum</i> using three genetic markers (chitin-synthase 1, beta tubulin 2 and trichodiene synthase 5), and found two distinct cryptic species exist within the single morphological species	Cruse, 2002 ⁽¹²⁾
2002	Found 2 chemotypes produced by <i>S. chartarum</i> : atronones producing isolates and macrocyclic trichothecenes isolates and one undescribed taxon. Identification was based on morphology, colony characteristics on culture media and metabolite production using LC-MS	Anderson, 2002 ⁽⁹⁴⁾
2003	Examined 25 isolates of <i>Stachybotrys</i> spp. using morphological, chemical and phylogenetic methods. The isolates could be segregated into two chemotypes of <i>S. chartarum</i> , and a novel species, <i>S. chlorohalonata</i> . The new species showed some morphological differences from <i>S. chartarum</i> and possessed different tri5, chs1 and tub1 gene sequences. There was no difference between the two chemotypes of <i>S. chartarum</i> in the tub1 gene, and only a single nucleotide difference in each of the tri5 and chs1 genes.	Anderson, 2003 ⁽¹¹⁾

Molecular DNA-based approaches have been developed as an alternative choice for the identification of *Stachybotrys* spp.. Haugland *et al.*⁽¹⁰²⁾ developed 2 primer pairs, StacR4 and StacR3 from the Internal Transcribed Spacers (ITS) regions for the detection of *S. chartarum* and tested them against a representative isolate of *S. chartarum* and its related species. One of the primer sets, StacR3, showed a DNA band specific to *S. chartarum*, but not other *Stachybotrys* spp.. The findings were later confirmed by Li and Yang ⁽⁹⁵⁾ , who found no products for *S. elegans*, *S. microspora* and *S. nephrospora* but failed to differentiate *S. chlorohalonata* and *S. yunanensis* from *S. chartarum*. In another study, Dean *et al.*⁽¹⁰³⁾ utilised ITS primers (ITS1 and ITS4) combined with restriction fragment length polymorphism (PCR/RFLP) to identify fungi at the species level based on the banding patterns seen on agarose gels. However, this study was performed using only *S. chartarum*, but not with other *Stachybotrys* spp. which provides limited evidence on its suitability for this fungal genus.

Other species-specific molecular primers for use in PCR assays have been designed for the purpose of identifying *S. chartarum* from indoor samples, including those targeting 18S ribosomal RNA, ribosomal RNA, trichodiene synthase (*tri5*), beta-tubulin and chitin synthase 1 regions ^(12, 104, 105). Black *et al.*⁽¹⁰⁵⁾ have reported inconsistencies in rRNA primers to detect *S. chartarum* and other indoor air moulds consist of *Alternaria alternate*, *A. fumigatus*, *A. versicolor*, *C. cladosporioides* and *Penicillium brevicompactum*. However, more conclusive results were obtained using the *tri5* primer set. In an earlier study, Cruse *et al.*⁽¹²⁾ found two distinct phylogenetic groups within isolates from the apparently single species of *S. chartarum* using primers from *tri5*, beta-tubulin and chitin synthase 1 regions which was documented as a cryptic species within *S. chartarum* complex. Using the same primer set, Andersen *et al.*⁽¹¹⁾ later segregated *S. chartarum* into two chemotypes and a new species, *S. chlorohalonata*. Of the three regions described above, the *tri5* gene showed the most consistent results by separating the *S. chartarum* chemotypes by a single nucleotide substitution.

Currently, MALDI-TOF proves to be a rapid and reliable alternative to the identification of fungi by culture characteristics, microscopy and PCR. Gruenwald *et al.*⁽¹⁰⁶⁾ reported the use of MALDI-TOF to differentiate dematiaceous fungi, including *S. chartarum* and its closely related species, *S. chlorohalonata*. Although a previous study has reported signal suppression caused by melanin, good spectra were obtained by doubling the volume of matrix. However, lower log(score) values (<2.0) were obtained for more than 50% of the isolates. In a more comprehensive study, Ulrich *et al.*⁽¹⁰⁷⁾ identified *Stachybotrys* spp. by using additional washing in the protein extraction phase to remove unspecific low molecular weight mass proteins. Cut off points of 2.509 to 2.739 and from 2.148 to 2.622 were obtained for *S. chartarum* and for *S. chlorohalonata*, respectively. Both studies offer ways to identify *S. chartarum* and *S. chlorohalonata* although neither study provided distinct cut off points between 'highly probable species' and 'secure genus' level identification.

2.4.2 Indoor environment as a habitat

In the natural environment, *Stachybotrys* spp. are ubiquitous, however they prefer damp and highly cellulolytic substrates such as soil, plant materials such as wood, and plant-based animal feed such as hays and grains. *S. chartarum* often exists together with other fungi such as *Penicillium* spp., *Alternaria* spp. and *Cladosporium* spp. which require low to moderate moisture ⁽¹⁰⁸⁾. Whereas, in indoor environments, it is generally found on cellulose-based materials such as fibreboard, gypsum board, and wallpaper

particularly in places with damp or water-damaged materials saturated with water such as leaking roofs or plumbing, air-conditioner condensation or flooding ⁽¹⁰⁹⁾.

S. chartarum requires a high water activity (water available in a material) between 0.91-0.93 for growth and sporulation and is characterized as hydrophilic ^(10, 80). *S. chartarum* grows at 86% to 95% relative humidity but requires a lower minimum water activity when grown at higher temperatures ⁽¹¹⁰⁾. *Stachybotrys* spp. require long-term wetness or high humidity for at least 48 hours but ideally lasting for days or weeks to germinate and grow. The presence of hydrophilic fungi has been proposed as an indicator of dampness or water-damaged buildings ⁽¹⁰⁾. Other moulds such as *Trichoderma* spp., *Chaetomium* spp. and *Aspergillus niger* require water activity of more than 0.9 and can also grow well in moisture damaged and cellulose-based materials ^(57, 111, 112).

The presence of *Stachybotrys* spp. is thought to be infrequent in the air compared to other moulds. *Stachybotrys* spp. spores form a relatively heavy mucilaginous mass compared to *Aspergillus* spp., *Penicillium* spp. and *Cladosporium* spp. which produce dry spores that can be easily dispersed in the air. However, dry *Stachybotrys* spores may become airborne and attached to settled dust particles and this has been linked to mycotoxin detection on contaminated surfaces ⁽¹¹³⁾. A cohort study conducted among 3193 French dwellings reported detection of *S. chartarum* in 27% of dwellings compared to 88% for *A. alternata* using qPCR ⁽¹¹⁴⁾. However, in general, *Stachybotrys* spp. have often been isolated from swabs or lift tape samples rather than air sampling ⁽¹⁰⁸⁾. Therefore, an association between *Stachybotrys* spp. and health risks is difficult to establish because the true extent of contamination is largely unknown.

The occurrence of *S. chartarum* and its interactions with other indoor moulds in the indoor environment is not well studied ⁽¹¹⁵⁾. Nevertheless, a study has documented that *S. chartarum*, together with other fungi including *Aspergillus* spp., *Mucor* spp. and *Penicillium* spp. were present as fungal biofilm in a water distribution system ⁽¹¹⁶⁾. *S. chartarum* is known as relatively slow or moderately fast grower depending on the substrate and does not compete well with other fast growing moulds such as *Aspergillus* spp. and *Penicillium* spp. ⁽¹¹⁷⁾.

Its closely related species, *Stachybotrys chlorohalonata* was found even more rarely than *S. chartarum*. This species was only recently recognized and has been found indoors in conjunction with *S. chartarum*. Initial studies have shown that *S. chlorohalonata* is found less commonly than *S. chartarum* indoors ^(11, 12, 118).

Previous studies that have used DNA sequencing to identify *S. chlorohalonata* and chemotypes of *S. chartarum* have looked primarily at indoor isolates from diverse geographic origins. Andersen *et al.*⁽⁹⁴⁾ examined isolates the majority of which were collected from buildings in Europe and the United States. Approximately 20% of the 122 isolates were identified as *S. chlorohalonata*, 49% as *S. chartarum* chemotype A, and 31% as *S. chartarum* chemotype S. Cruse *et al.*⁽¹²⁾ examined 30 isolates collected primarily in northern California; approximately 23% were *S. chlorohalonata*, 47% were *S. chartarum* chemotype S and 30% were *S. chartarum* chemotype A. While the exact distribution of isolates among the three taxa varied between these studies, as well as another by Koster *et al.*⁽⁹⁶⁾ found no correlation between gene sequence and geographical location.

2.4.3 Toxicity and public health concern

S. chartarum produces harmful secondary metabolites such as mycotoxins, MVOCs and other biologically active products including the haemolysin stachylysin, proteinases, glucans and spirocyclic drimanes ^(22, 30, 119) (Figure 2-11). Although *Stachybotrys* sp. was first isolated in the 1800s, pathogenicity was first documented in the 1930s. The first report of stachybotryotoxicosis dates back to the 1930s in Siberia, when thousands of horses became ill after ingesting contaminated hay ⁽¹²⁰⁾. The symptoms of stachybotryotoxicosis were characterized as haemorrhages and ulceration of the mucosal membranes, followed by leucopenia, anaemia and eventually death. Since then, stachybotryotoxicosis has been reported in chicks, sheep, calves, dogs and cattle ⁽¹²¹⁻¹²⁵⁾.

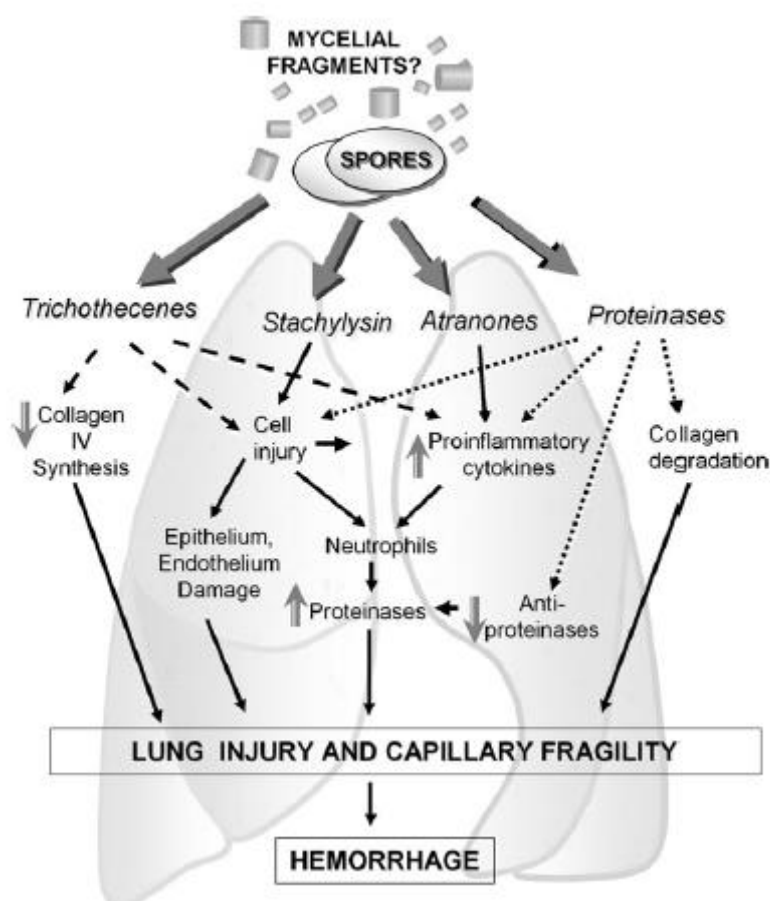


Figure 2-11: Proposed mechanisms of stachybotryotoxicosis. Diagram adapted from Pestka *et al.* ⁽¹²⁶⁾. ©2007 Oxford University Press. Used with permission from Oxford University Press and Copyright Clearance Centre.

In an animal model, Yike *et al.*^(127, 128) reported extensive lung haemorrhages in dead rats and impaired growth in surviving 4 day old Sprague-Dawley rat pups which were instilled intratracheally with intact *S. chartarum* spores. However, the toxicity decreased significantly with spores pre-washed with alcohol, which probably reduced mycotoxin exposure. Lichtenstein *et al.*⁽¹²⁹⁾ found immune responses shifted from type 1 to type 2 after multiple intratracheal instillation in BALB/c mice.

This finding was in line with other studies showing direct toxicity of mycotoxins. Sam *et al.*⁽¹³⁰⁾ has reported induction of apoptosis of olfactory sensory neurons in mice caused by satratoxin G, a type of macrocyclic trichothecene produced by *S. chartarum*. This was supported by Carey *et al.*⁽¹³¹⁾ who showed induction of rhinitis and apoptosis of olfactory sensory neurons in the nasal airways of rhesus monkeys by the same mycotoxin class.

In an *in vivo* study, the inflammatory responses of mouse RAW264.7 macrophages were investigated after exposure to *S. chartarum* and a few other moulds, alone and combined with *Streptomyces californicus*. The findings showed a synergistic interaction between *S. chartarum* and *Streptomyces californicus* by inducing the production of IL-6 involved in the inflammatory response ⁽¹³²⁾.

Epidemiological studies have shown that exposure to *Stachybotrys* spp. can occur through inhalation and ingestion. In relation to the incidence in horses, Drobotko ⁽¹²⁰⁾ also reported symptoms of skin eruption, sweating and chest congestion among the human volunteers in contact with mouldy hay contaminated with *S. alternans*. The author also suggested that a previous outbreak of similar disease in horses that occurred earlier in Siberia caused by ingestion of contaminated stored grain was stachybotryotoxicosis based on similar symptoms. Occupation-related stachybotryotoxicosis has also been documented among farmers, cottonseed, grain processing workers, textile and binder twine factory workers, and those involved with the reprocessing of mouldy grain. The health symptoms reported are chest and upper respiratory tract symptoms, dermatitis, fever and in some cases, leukopenia ⁽⁷⁸⁾.

The concentration of mycotoxins produced by *S. chartarum* are relatively high compared to other fungi prevalent in indoor environments such as *Aspergillus* spp. and *Penicillium* spp. ⁽¹³³⁾. The macrocyclic trichothecenes produced by *Stachybotrys* spp. are present in the spores and in mycelium fragments ⁽¹³⁴⁾. In the 1980s, *S. chartarum* spores were isolated from interior ducts and ceiling materials in a heavily infested residence in Chicago, associated with a flu-like illness, dermatitis, and malaise in a family of five for more than 5 years until the contaminated materials were removed. Samples taken from ceiling fibre board were shown to contain the macrocyclic trichothecenes verrucarin J and satratoxin H as well as the precursors trichoverrins A and B ⁽¹³⁵⁾. Yet, this was believed to be a rare case until the mid-1990s ⁽¹¹⁹⁾.

Between January 1993 and December 1994, an apparent outbreak of stachybotryotoxicosis occurred in homes contaminated with *S. chartarum* (previously known as *S. atra*) and other moulds in Cleveland, Ohio. Etzel *et al.* ⁽¹³⁶⁾ reported a high incidence of acute pulmonary haemorrhage among children living in the contaminated homes. The development of idiopathic pulmonary hemosiderosis (IPH) was thought to be due to exposure to mycotoxins produced by *S. chartarum* ⁽¹³⁷⁾ and other indoor environmental contaminants ⁽¹³⁸⁾. However, following reviews by the Centers for Disease Control and Prevention (CDC) and external experts (2000), the causal relationship was later found not scientifically proven due to statistical errors, biases in

sampling and little evidence of culturable airborne *S. chartarum* ⁽¹³⁹⁾. In addition, there was no direct evidence of fungal or mycotoxin exposure. The study was also confounded by exposure to environmental tobacco smoke (ETS) ⁽¹⁴⁰⁾. Although this study did not prove an association with IPH, evidence continues to accumulate with regards to *S. chartarum* and ill-health.

The health effects among the occupants living in water-damaged homes have been associated with the presence of mycotoxins produced by *Stachybotrys* spp. found in environmental samples. In Finland, satratoxins G and H were identified in the houses of 26 residents with respiratory illness and other symptoms including irritation of eyes and skin and lymphocytosis in half of the patients ⁽¹⁴¹⁾. In another episode, Thrasher *et al.* ⁽¹⁴²⁾ have reported the development of asthma and other health symptoms including nose bleeds among a family of six including new born twins who lived in a water-damaged house. Several indoor moulds, including *Stachybotrys* spp., and the presence of mycotoxins including satratoxin G and H, roridin E, and isosatratoxin F were identified from environmental samples. One of twins died due to pulmonary haemorrhage with the autopsy confirming the presence of trichothecenes in his lungs, liver and brain. However, both studies have documented the health threat only among the susceptible groups such as infants and people with existing respiratory problems.

For many decades, many reviews of SBS have suggested that there is little to no evidence suggesting that indoor moulds pose a threat to healthy individuals ^(9, 55, 143). It has generally been believed that most mycotoxins are not volatile ⁽⁷⁰⁾, and therefore widespread exposure is unlikely to occur unless the fungal mass are disturbed ⁽¹⁴⁴⁾. Aleksic *et al.* ⁽¹⁴⁵⁾ have investigated the mycotoxin production from *S. chartarum*, *P. brevicompactum* and *A. versicolor* during their growth on wallpaper to elucidate the probable exposure of mycotoxin by inhalation following fungal aerosolisation. The study showed that mycotoxins were detected at substantial concentrations in the air when air velocity was applied to the wallpaper and the toxic load was detected from fungal particles corresponded to spores or mycelium fragments. Owing to its heavy spores and slimy mass, *Stachybotrys chartarum* required the highest air velocity of 5.9 m/s compared to *P. brevicompactum* (0.3 m/s) and *A. versicolor* (2 m/s).

Although most fungal growth in indoor environment occurs at water activity near 0.8, significant quantities of mycotoxin are produced only when the water activity reaches 0.95 ⁽¹³³⁾. This suggests that the conditions that are conducive for mould growth are not necessarily optimal for mycotoxin production. However, it is important to prevent direct contact with fungi such as by inhalation of aerosolised fungal particles which possibly

increase the risks to health. In a guideline “Mould prevention strategies and possible health effects in the aftermath of hurricanes and major flood”, the CDC has outlined several recommendations to prevent exposure from severely mould-contaminated houses such as by avoiding areas with visible mould, the use of protective equipment, and by keeping hands and clothes clean from mould-contaminated dust ⁽¹⁴⁴⁾.

Potential effects on health from other metabolites of *Stachybotrys* spp. includes those of spirocyclic drimanes which cause enzyme inhibition, cytotoxicity, neurotoxicity and potent immunosuppression ⁽¹⁴⁶⁾; stachylysin causes leakage or rupturing of red blood cells ⁽⁶⁶⁾ and MVOCs are associated with the discomfort of mould odour and respiratory problems ⁽¹⁴⁷⁾.

2.5 METHODS OF FUNGAL IDENTIFICATION

Laboratory methods play an important role in fungal identification for clinical diagnosis or environmental research. In addition to conventional microscopy identification, more sensitive and specific methods have been developed to identify moulds with more confidence, such as polymerase chain reaction (PCR)⁽¹⁰³⁾ and mass spectrometry ⁽¹⁴⁸⁾ .

2.5.1 Culture characteristics and light microscopy examination

The conventional methods of fungal identification are based on cultural, morphological and physiological characteristics which involve culturing, staining and examination with the light microscope ^(149, 150). Key features of fungal cultures are their surface textures and the colours of both surface and reverse aspects. Their morphologies may vary depending on types of media used, temperature for incubation and growth rate ⁽¹⁵⁰⁾.

The culture process involves plating samples on suitable agar media followed by incubation at optimal temperature for a given period of time where the colonies will grow as the hyphae elongate and finally sporulate. The choice of culture medium is important to guarantee the reliability of the analysis. The medium should allow the fast recovery of fungi but not be too thick to avoid hyphal growth in the agar and at the same time avoid bacterial contamination. Different growth rates of fungi are seen as some fungi appear macroscopically after 2-3 days, whereas some are slow growers and cultures need to be kept for 2 weeks or longer ⁽⁹¹⁾. Important colonial characteristics include colour, pigmentation, texture, edge/margin, elevation, size and degree of growth. However, colonial morphology alone may not provide a confident

identification due to variation between isolates and type of media used, thus it needs to be supplemented with microscopic examination.

Fungi can be observed microscopically by looking at their shape and the arrangement of conidia or spores, presence of hyphae with or without branching, and size. Chemical staining is needed to enhance the contrast depending on the type of fungal structure to be observed and the type of sample. Lactophenol cotton blue is the most widely used staining method for fungi as it is easy to prepare. This dye contains phenol as a fungicide and lactic acid, which acts as a preservative to preserve the fungi structures (151).

Observation at 100x magnification with immersion oil yields good clear images of the conidia structures. Conidia are one of the most important fungal elements for identification. They may be present as clusters and are distinguished by their shapes (ellipsoidal, globose) surface (ridged, smooth) and colours (pigmented, hyaline)⁽¹⁵²⁾ (Figure 2-12). Other structures observed under the microscopes are the hyphae, conidiophores and presence of phialides. Fungal hyphae can be identified as septate or aseptate and with conidiophores either simple or branched⁽⁹¹⁾.

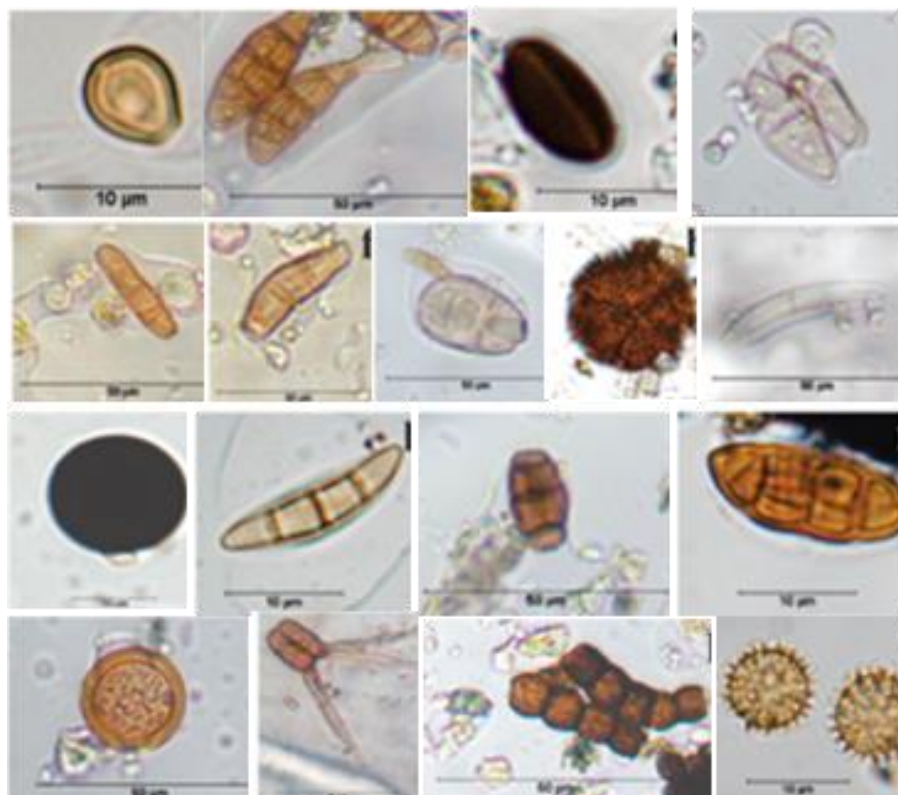


Figure 2-12: Shapes and surface types of fungal spores found in air samples. Diagram adapted from Guarin *et al.*⁽¹⁵²⁾. Licensed under Creative Commons Attribution (<https://creativecommons.org/licenses/by-nc/3.0/deed.en>).

Although this method is widely available in most laboratories, the macroscopic and microscopic examination of the culture relies on well trained and experienced mycologists. The method is also time consuming due to the long culture incubation time. Moreover, the morphological characteristics of many fungi can be similar, which leads to incorrect identification. In addition to conventional microscopy, more sensitive and specific methods to identify moulds such as PCR and mass spectrometry have been developed.

2.5.2 Sequence-based identification using Internal transcribed spacer (ITS)-Polymerase Chain Reaction (PCR)

PCR is an *in vitro* method that allows exponential amplification from a single gene or nucleic acid sequence (DNA) to generate thousands to millions of copies of the DNA sequence ⁽¹⁵³⁾. PCR has been widely used in many fields including medical diagnostics, forensics and environmental research ⁽¹⁵⁴⁻¹⁵⁶⁾.

Basic PCR involves repetitive cycles of denaturation, annealing and extension or elongation ⁽¹⁵³⁾ (Figure 2-13). This method requires the presence of several other components including a thermostable DNA polymerase, reaction buffer solution suitable for activity and stability of DNA polymerase, deoxynucleotide triphosphates (dNTPs) and DNA forward and reverse primers.

The primer pairs should be designed to uniquely hybridise with the target sequence. Several primer design tools are available such as NCBI and Primer3Plus ^(157, 158). Primers can be designed by searching the possible regions where the DNA target can bind from a nucleotide database such as the NCBI followed by aligning the sequences available to find the sequence with the best nucleotide match.

The use of the ribosomal DNA (rDNA) complex has long been the favoured choice of gene target in fungal molecular identification. The ribosomal DNA complex is a collection of genes encoding for the ribosomal RNA. In eukaryotes, such as fungi, this gene complex comprises of the 18S (small-subunit rDNA), a 5.8S subunit and the 28S (large-subunit rDNA) genes. There are interspaces between these three genes, called the Internal Transcribed Spacers (ITS) (Figure 2-14). The region between the 18S and 5.8S subunits and the region between the 5.8S and 28S subunits are known as ITS1 and ITS2, respectively ⁽¹⁵⁹⁾.

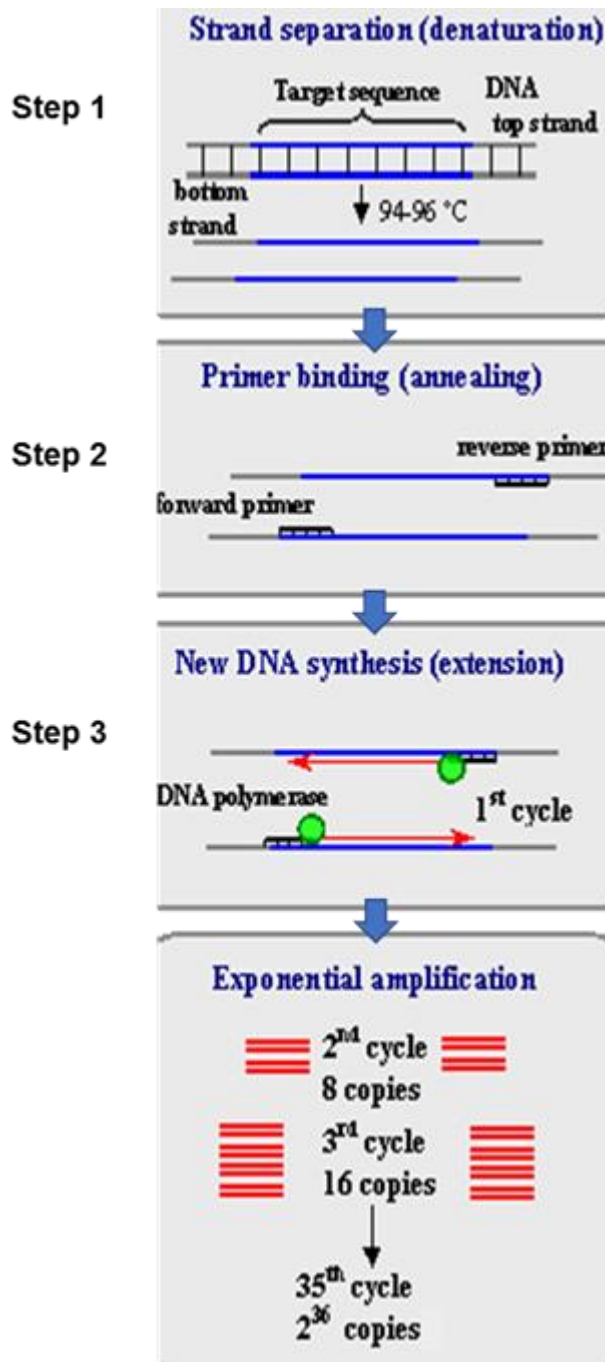


Figure 2-13: The 3 primary steps in a basic PCR reaction consist of denaturation, annealing and extension or elongation. Step 1) Denaturation: DNA strand containing target sequence is separated at high temperature (94 to 96 °C); Step 2) Annealing: Forward and reverse primer anneal to target sequence at lower temperature (e.g. 54 to 60 °C), and Step 3: Extension/elongation: After the primers are attached, the DNA polymerase enzyme begins to add the dNTPs which act as building blocks to form new complementary strands at 72 °C. Diagram adapted from <https://www.ncbi.nlm.nih.gov/probe/docs/techpcr/>. Information is within the public domain (<https://www.ncbi.nlm.nih.gov/pubmed/29140470>).

The ITS-PCR provides mycologist with a quick and accurate fungal identification compared to conventional methods. The ITS1 and ITS2 regions are relatively variable between species, therefore making them good targets for species identification. This method has been used to distinguish closely related fungal species, especially those from different environments ⁽¹⁶⁰⁾. In addition to the ITS regions, other highly conserved regions are used as target sequences, such as beta-tubulin, chitin synthase and trichodiene synthase 5 gene (*tri5*) in *Stachybotrys* spp. ⁽¹²⁾. The *tri5* gene, for instance, is the gene present in trichothecene producing fungi such as *Stachybotrys* spp., *Fusarium* spp. and *Trichoderma* spp. ^(81, 161).

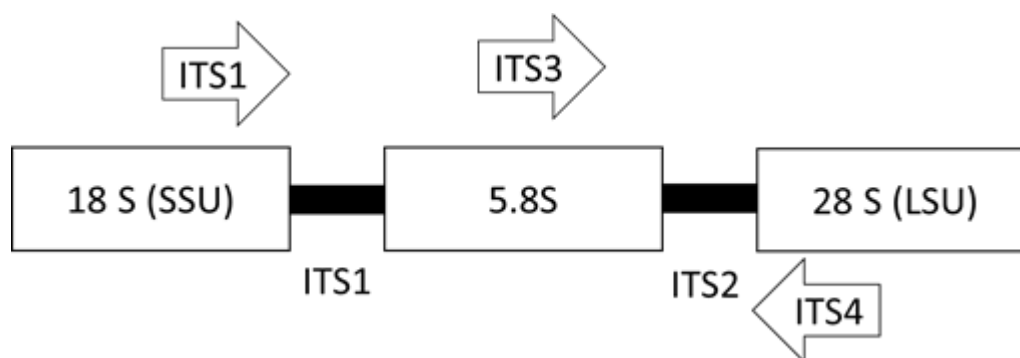


Figure 2-14: Ribosomal DNA (rDNA) gene complex consisting of 18S rDNA (Small subunit rDNA), 5.8S rDNA and 28S rDNA (Large subunit rDNA). ITS PCR sequences are constructed from the ITS regions which are relatively conserved.

Although PCR is widely used in most laboratories, it can potentially lead to biases depending on target regions amplified and primer combinations ⁽¹⁶²⁾. In addition, DNA extraction from fungal sample is often a challenge due to the thick cell wall structure and the presence of PCR inhibitors such as melanin ^(163, 164).

2.5.3 Matrix-assisted laser desorption ionization- time of flight (MALDI-TOF) - mass spectrometry

MALDI-TOF is an ionisation technique which has become a powerful tool for microbial identification in routine clinical microbiology laboratories based on their protein profiles ⁽¹⁴⁸⁾. MALDI-TOF is less laborious, less time-consuming and has low operational costs compared to conventional methods and PCR ⁽¹⁶⁵⁾. Sample preparation is the key step required to generate a good quality database for accurate identification. In yeasts, protein extraction involves sample inactivation in 75% ethanol and suspension in 70% formic acid and acetonitrile to produce a supernatant suitable for analysis ⁽¹⁶⁶⁾. Due to their more rigid cell wall, filamentous fungi require more extensive protein extraction

methods such as the use of mechanical disruption through bead-beating and additional treatment to get rid of contaminants such as melanin. Fungi are grown in liquid or solid media, although liquid media give more uniform growth with less risk of aerosolised materials and contamination ^(167, 168) .

Analysis using MALDI-TOF involves three main stages consisting of co-crystallisation sample and matrix, ionisation and laser desorption and generation of mass spectra based on mass-to-charge ratio (m/z) (Figure 2-15). In the first stage, co-crystallisation of samples and matrix involves spotting samples on a metallic target plate followed by the application of a thin layer of matrix over the samples. The most commonly used matrices are 3,5-dimethoxy-4-hydroxycinnamic acid (sinapinic acid), α -cyano-4-hydroxycinnamic acid (α -CHCA) and 2,5-dihydroxybenzoic acid (DHB) depending on the peptide mass. The matrix needs to be prepared fresh by adding highly purified water, organic solvents (such as acetonitrile or ethanol) to allow both hydrophobic and water-soluble molecules to dissolve into the solution; and trifluoroacetic acid (TFA) to enhance ionisation ⁽¹⁶⁹⁾. In the second stage, a pulsed laser beam at a wavelength of 337 nm irradiates the sample-matrix mixture which triggers desorption or ionisation of analyte molecules into the gas phase to generate singly protonated ions.

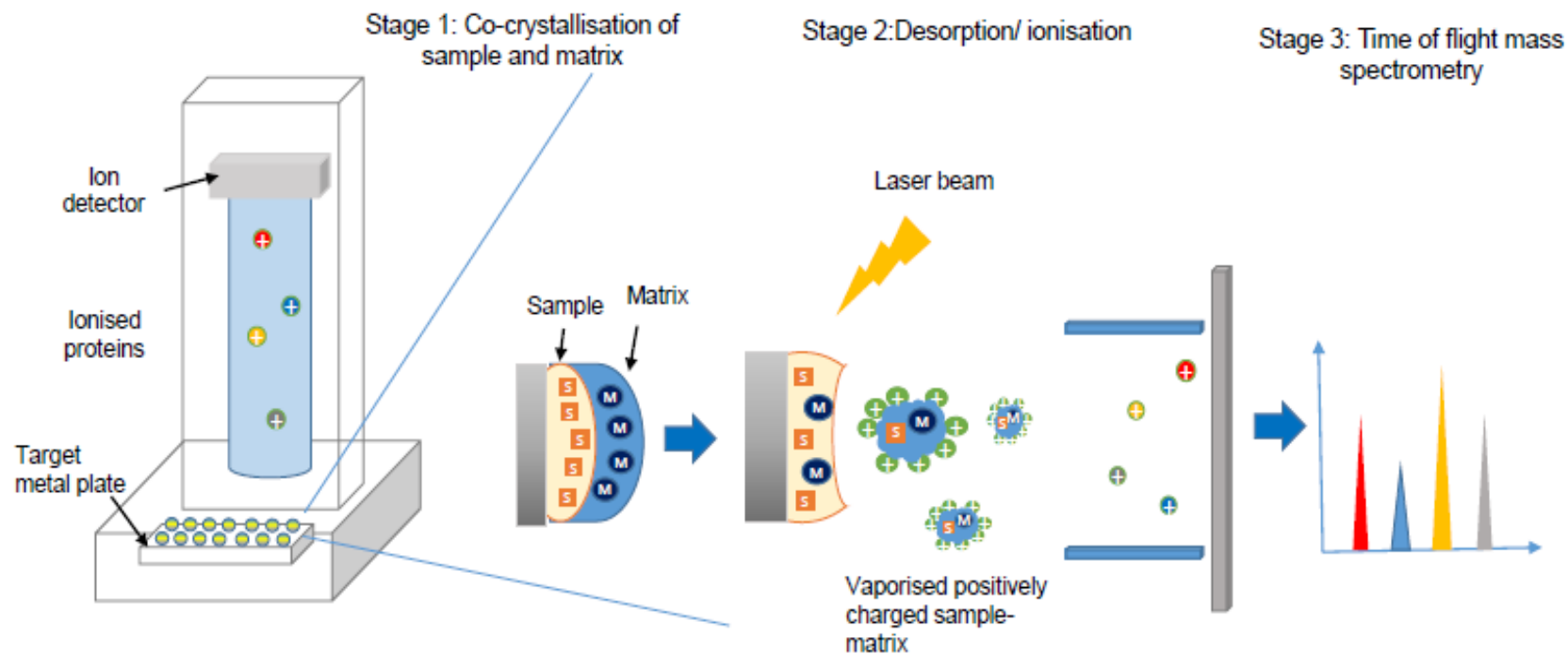


Figure 2-15: Schematic diagram of sample analysis by MALDI-TOF as shown by a single spot on the metal plate. The process involves 3 main stages; Stage 1: Co-crystallisation of sample and matrix; Stage 2: Desorption/ ionisation of analytes by pulsed laser beam; and Stage 3: Separation of analytes by time of flight mass spectrometry on the basis of mass-to-charge ratio.

In the final stage, the ions pass through a mass analyser flight tube (TOF) where they are separated on the basis of mass-to-charge ratio (m/z). The m/z ratio governs the velocity or time required for the ions to travel the length of the flight tube. In the time-of-flight (TOF), ions travel a specified distance, which depends on their mass and energy, to reach the detector to produce a signal. Therefore, ions with smaller m/z value and more highly charged ions move faster through the mass analyser flight tube. Subsequently, a peptide mass fingerprints will be produced which can be matched with the mass spectra profiles (MSPs) in the protein database provided by the manufacturer or developed in-house.

Although MALDI-TOF has emerged as a useful tool in fungal identification, its effectiveness is restricted by poor reproducibility of spectra. MALDI-TOF requires an extensive database when dealing with highly heterogeneous phenotypes ⁽¹⁷⁰⁾. Moreover, MSPs of some fungal species are not available and need to be constructed. In order to construct the MSPs, sufficient and good quality peaks with high abundance mass signals above the background noise need to be generated ⁽¹⁷¹⁾. Differences in growing conditions, which include media type, incubation temperature and time as well as the extraction methods have been shown to affect mass spectra profiling by MALDI-TOF and need careful consideration when this is done. ^(172, 173).

2.6 PROTEOMICS

Proteomics is the large-scale study of proteins which allows qualitative and quantitative measurements of proteins in a sample. The term proteome refers to the entire set of proteins produced by an organism or system which varies by time or exposure to certain stresses ⁽¹⁷⁴⁾. Proteome changes affect cellular biochemistry in a biological system and since mRNA is not always translated into protein, proteomics provides a direct measure of gene expression. ^(175, 176).

Proteomics technology has evolved from the separation and isolation of proteins using 2-dimensional gel electrophoresis to gel-free quantification which allows a greater number of proteins to be represented and avoids the problems of running gel electrophoresis which are more labour-intensive and time-consuming ⁽¹⁷⁷⁾. Tandem mass tags (TMT) labelling, also known as isobaric mass tagging is one of the gel-free quantitative proteomic methods using stable isotope labels with their capability of multiplexing up to 10 samples ⁽¹⁷⁸⁾. Peptides are labelled with reporter ions of different

mass consisting of mass reporter, mass normalizer and reactive regions which are assigned to each sample so that they can be distinguished (Figure 2-16). TMT requires a mass spectrometry system capable of MS/MS fragmentation such as ion trap or time-of flight (TOF-TOF). In the MS/MS mode, samples are fragmented into peptides and mass reporter ions which give rise to sequence information and quantification, respectively.

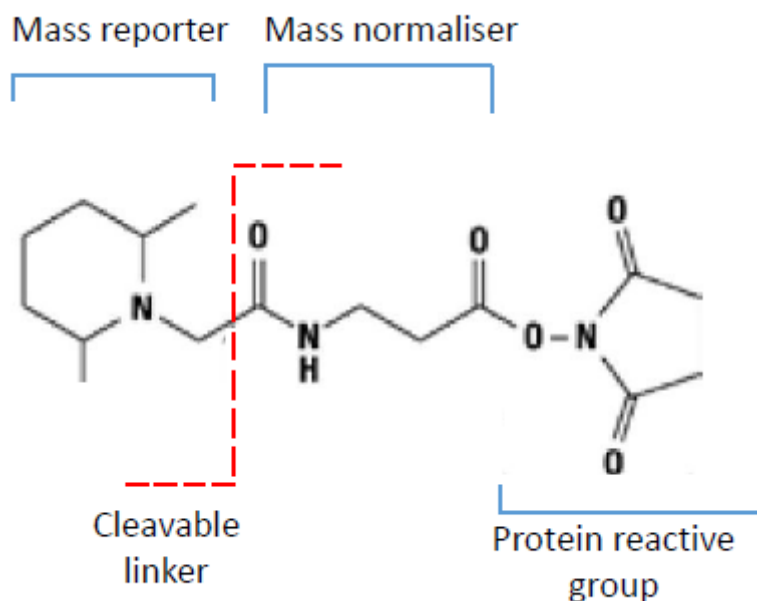


Figure 2-16: The chemical structure of TMT-label consisting of 3 functional regions of mass reporter mass reporter, mass normalizer and reactive regions. Used with permission from ©2018 Thermo Fisher Scientific.

The whole process involves protein extraction, digestion into peptides and labelling with isobaric stable isotope tags (Figure 2-17). Protein extraction and clean-up is essential to obtain good quality and yield suitable for TMT-labelling and to get rid of possible contaminants that may interfere with the mass spectrometry. Samples are fractionated to isolate multiple proteins from the complex mixture prior to LC MS/MS. Finally, the list of peptide mass values are submitted to a protein database such as Mascot or TrEMBL (TRanslation of EMBL) for identification.

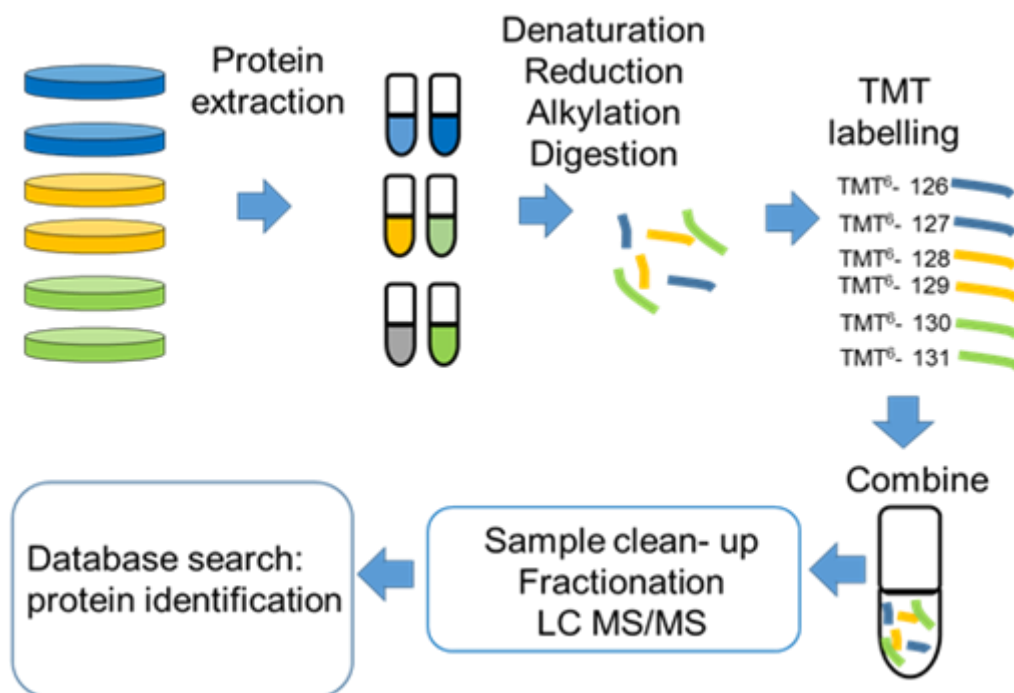


Figure 2-17: Schematic diagram of TMT- labelling gel free proteomic analysis. Proteins were extracted and digested into small peptides. The peptides were labelled and combined into single tube followed by LC MS/MS and protein identification.

Proteomic studies offer the detection and identification of expressed proteins leading to the discovery of genes and pathways involved in stress response and tolerance. In clinical settings, proteomics has been used to study the failure of antifungal agents such as the mechanism of *C. albicans* azole resistance resulting from alterations in the proteins involved in the ergosterol synthetic pathway ⁽¹⁷⁹⁾. Similarly, *A. fumigatus* has shown differential expression of proteins involved in the ergosterol pathway, stress responses, cell wall structure and transport in response to an antifungal drug, Amphotericin B ⁽¹⁸⁰⁾.

Proteomics is also useful in the study microbial responses to environmental stressors. Exposure of *Trichoderma* spp. to dichlorvos, an organophosphate pesticide, has shown to induce changes in proteins linked with energy metabolism, transport, signal transduction and stress tolerance which were considered to be associated with fungal adaptation to stress ⁽¹⁸¹⁾. Nevertheless, proteomic studies of indoor moulds, in particular *Stachybotrys* spp., is lacking. Such information may provide a better understanding of protein changes which occur as a stress response due to the exposure to antimicrobial agents commonly used in bioremediation of indoor environments.

2.7 ANTIMICROBIAL CONTROL AGENTS

Antimicrobial agents inhibit or to prevent microbial growth. The term 'biocide' is also used interchangeably to describe a wide variety of antimicrobial agents used for disinfection, sterilisation and preservation ⁽¹⁸²⁾. There is a wide range of biocides with various targets of action, such as oxidising agents (e.g. sodium hypochlorite, hydrogen peroxide) and cell membrane damage agents (e.g. quaternary ammonium compounds) ⁽¹⁸³⁾.

2.7.1 Sodium hypochlorite

Sodium hypochlorite (NaOCl) is the main active ingredient in bleach which is commercially available as 3–6% solution in water. Since it has a broad antimicrobial spectrum, is cost-effective and easy to use, it is widely used for bleaching, cleaning and disinfection in households and public places.

The effectiveness depends on the concentration of free chlorine and the pH of the solution. NaOCl works by adding the hypochlorite to water to form hypochlorous acid (HOCl) and sodium hydroxide (NaOH) which are very strong oxidising agents. HOCl is a weak acid and dissociates to hypochlorite ions (OCl^-) and protons (H^+). The mechanism of action of NaOCl depends on the ions ability to penetrate microbial cells. Hypochlorous acid (HOCl) is able to penetrate through the cell lipid bilayer producing antimicrobial activity both outside and inside the microbial cell. On the other hand, the hypochlorite ion (OCl^-) has poor germicidal activity due to its inability to diffuse through the membranes and is only able to act from outside the cell ⁽¹⁸⁴⁾ (Figure 2-18).

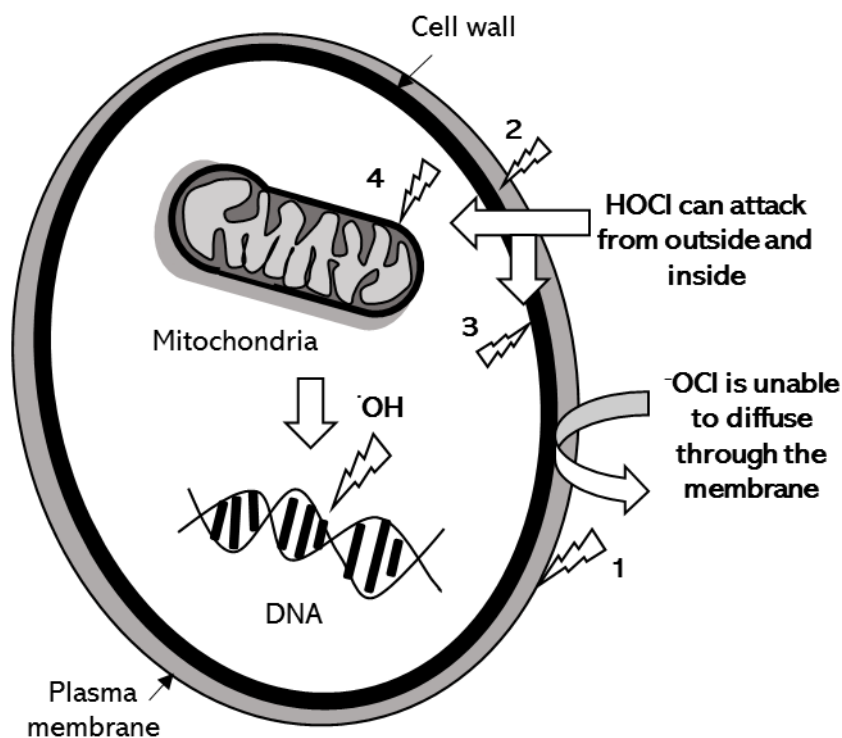


Figure 2-18: Mechanisms of action of sodium hypochlorite. The numbered circles indicate sites of action based on membrane permeability; 1: hypochlorite ion (OCl^-) acts only outside the cell; and 2 to 4: hypochlorous acid (HOCl) acts both outside and inside the cell.

The World Health Organisation recommend a solution containing 0.05% or 500 ppm NaOCl for disinfecting tools, equipment or other non-porous surfaces at healthcare facilities ⁽¹⁸⁵⁾. However, a higher concentration of 2.4% NaOCl was reported to be able to kill spores of *S. chartarum* and other fungi including *Aspergillus niger*, *Penicillium chrysogenum* and *Trichophyton mentagrophytes* grown on ceramic tiles ⁽¹⁸⁶⁾.

Despite its effectiveness in cleaning and disinfection, NaOCl is a corrosive substance and harmful to humans and the environment. It produces a toxic gas and a strong odour as well as being an irritant. Safety precautions need to be taken when handling NaOCl, especially by avoiding inhalation and dermal contact.

2.7.2 Organosilane

Organosilane (OS) is an antimicrobial agent in the form of a solution which can be applied on soft or hard solid surfaces such as construction materials, textiles and touch surfaces. It is hydrophobic and has UV and thermal stability, chemical resistance and does not require light activation. OS acts against viruses, bacteria and fungi by forming a nanocoating on the surface which prevents the attachment of microbes and eventually leads to a failure to colonize.

OS prevents microbial attachment on the surface by puncturing the outer membrane of the microbes that come in contact with it. It is comprised of 3 components of a silane base, a positively charged nitrogen atom and long molecular chain (Figure 2-19). The silane base acts as an antimicrobial anchor by binding covalently to the surface. The positively charged nitrogen atom attracts the negatively charged microbial membranes resulting in their puncture by the long chain molecules.

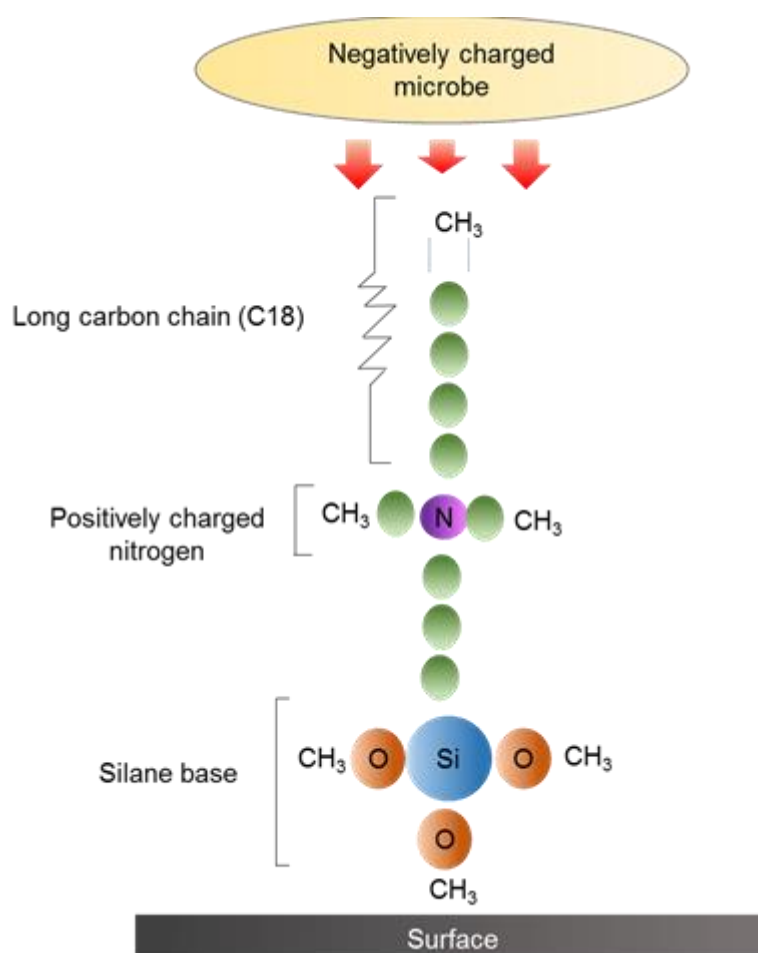


Figure 2-19: General structure and mechanism of action of organosilane.

Studies have also shown significant reductions of yeast and bacteria on silicone rubber (187, 188). However, no significant antimicrobial activity was observed with gram negative bacilli and yeast on cotton-polyester fabric coated with OS (189).

Although there is lack of evidence to support the effectiveness of OS in real-life settings, it could be a useful complementary tool to prevent microbial transmission and reduce the amount of surface cleaning time needed to maintain clean environments (190). OS is considered less harmful to humans and the environment compared to other biocides in the market.

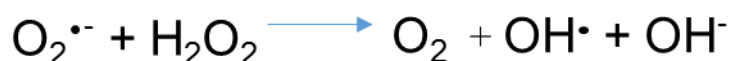
2.7.3 Hydrogen peroxide

Hydrogen peroxide (H₂O₂) is a broad-spectrum oxidising agent which is widely used for disinfection and sterilization in medical, food and industrial applications, as well as in water treatment. H₂O₂ in the form of vapour or mist has been proven to be more effective by causing greater interaction with and oxidation of microbial macromolecules than in its liquid form (191). It is considered environmentally friendly as it is rapidly degraded into non-toxic by-products consisting of water and oxygen (192) (Equation 2-1).



Equation 2-1.

In the enclosed environment, aerosolised hydrogen peroxide (AHP) has been widely used for surface disinfection or room fumigation. H₂O₂ acts by reacting with oxygen radicals present in the microbial cell to produce highly reactive hydroxyl free radicals. These hydroxyl radicals can cause damage to the microbial cell membrane and important cellular components including lipids, proteins, and DNA which eventually lead to cell death (192) (Equation 2-2).



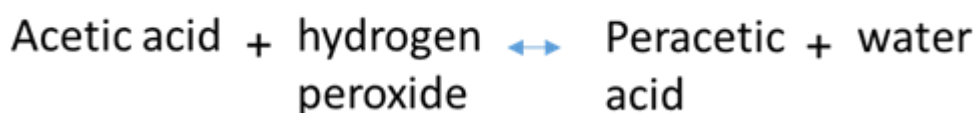
Equation 2-2

Concentrations of hydrogen peroxide solution between 6% and 25% have been demonstrated to sporicidal, mycobactericidal, fungicidal and viricidal. However, no studies have been reported on the effect of AHP on *S. chartarum*.

Although AHP is effective for disinfection and easy to disperse, the whole operation requires at least 2 hours with exclusion of occupants throughout the treatment ⁽¹⁹³⁾.

2.7.4 Peracetic acid

Peracetic acid (PAA) ($\text{CH}_3\text{CO}_3\text{H}$) is a broad spectrum biocide made up of an equilibrium mixture of acetic acid and hydrogen peroxide in aqueous solution (Equation 2-3) ⁽¹⁹⁴⁾. Acetic acid is the main component of vinegar that gives a strong pungent odour to PAA. PAA is environmentally safe as it decomposes by chemical oxidation into the non-toxic by-products acetic acid and oxygen.



Equation 2-3

Although hydrogen peroxide alone is a strong oxidising agent, the combination of acetic acid and hydrogen peroxide has been found to work synergistically. A lower concentration of hydrogen peroxide is needed in the presence of acetic acid to give the same level of antimicrobial effect ⁽¹⁹⁵⁾. PAA is considered more potent than hydrogen peroxide alone due to its water and fat solubility. Also, unlike hydrogen peroxide, PAA remains active in the presence of organic matter ⁽¹⁹⁶⁾. Similar to hydrogen peroxide, the mechanism of action probably involves disruption of cell wall permeability and denaturation of cell proteins, DNA and other metabolites.

PAA has been shown to inhibit the growth of bacteria, fungi and yeasts at a concentration of 100 ppm for 5 minutes contact time, and concentrations between 200 and 500 ppm in the presence of organic matter ⁽⁵¹⁾.

Similar to other oxidising agents, PAA can be very corrosive to instruments and cause irritation. The health hazards associated with 12% PAA are similar to the health hazards of 50% hydrogen peroxide ⁽¹⁹⁴⁾. Occupational exposure to PAA and hydrogen peroxide contribute to asthma development with symptoms of coughing, wheezing and shortness of breath⁽¹⁹⁷⁾.

CHAPTER 3

CULTURE-BASED IDENTIFICATION AND MICROSCOPY OF *STACHYBOTRYS* SPECIES

This chapter presents the work on the identification of *Stachybotrys* species using culture-based methods and microscopy technique. In this chapter, we have tested various media to determine the optimal recovery of *Stachybotrys* spp. and to observe the differences in morphology and pigmentation between species and strains. This was followed by the characterisation of *Stachybotrys* spp. using conventional macroscopic and microscopic methods.

3.1 INTRODUCTION

Classical methods of culture based identification and microscopic characterisation have always been the standard in most laboratories. Culture characteristics includes colony surface colour, texture, margin, growth patterns and pigment exudates. Fungal growth is known to be influenced by many factors such as nutrients, temperature, water activity and pH ⁽¹⁹⁸⁻²⁰⁰⁾.

A wide range of culture media have been developed for either general purpose or specific needs. Media choice can affect fungal growth and characteristics which play a vital role in fungi identification such as colony size, morphology and sporulation ⁽⁹¹⁾. Hence, suitable media for cultivation is crucial to aid the identification process. Generally, culture media contains sources of nutrients for the fungi, often carbon sources such as dextrose and nitrogen sources such as peptone or yeast extract. For instance, potato dextrose agar (PDA) is a relatively rich plant-based medium containing potatoes and dextrose to support the growth of most fungi and is widely used for general recovery of fungi *S. chartarum* ⁽²⁰¹⁻²⁰³⁾.

Dematiaceous, or dark-pigmented fungi grow well in less rich media such as cornmeal agar (CMA), which contains more complex carbohydrate sources compared to PDA. Cellulose-degrading fungi, such as *Stachybotrys chartarum*, can reproduce even in water agar supplemented with sources of cellulose such as filter paper, by releasing cellulotic enzymes to breakdown the complex cellulose into a carbon source ^(12, 82).

Another generic medium, Sabouraud dextrose agar (SDA) was formulated and named after Raymond Sabouraud in 1892. It is acidic (pH 6.5) to slightly inhibit bacterial growth and is normally used for clinical samples. The medium also contains dextrose and peptones which are sufficient for the recovery of dermatophytes ^(204, 205). Another formulation of SDA is Emmons modified formula of Sabouraud dextrose agar (ESA), created by Chester W. Emmons. Emmons modified SDA contains half of the dextrose concentration and a neutral pH of 7 to enhance recovery of some pathogenic fungi. However, it need to be supplemented with antibiotics, such as chloramphenicol to inhibit the growth of bacteria in the culture ⁽²⁰⁶⁾.

In this chapter, the efficacy of 4 different media, namely PDA, ESA, CMA and SDA to produce sufficient fungal biomass recovery and growth were evaluated. The plates were assessed for colony characteristics followed by microscopic examination. A differential medium, blood sheep agar was also used to assess haemolysis patterns from two reference *S. chartarum* strains, ATCC 16026 and NCPF 7587 and an environmentally isolated strain, Stachy CU.

3.2 MATERIALS AND METHODS

3.2.1 *Stachybotrys* spp. isolates

Stachybotrys spp. strains were obtained from various sources as shown in Table 3-1. Two isolates, namely ATCC 16026 and NCPF 7587, used as reference organisms were purchased from the American Type Culture Collection and Public Health England, respectively. One isolate, was obtained from Cranfield University (courtesy of Dr Dave Alfred) which had been characterised as *S. chartarum* based on its morphology, macroscopically and microscopically ⁽²⁰⁷⁾. Other isolates were purchased from The Centraalbureau voor Schimmelcultures (CBS) Fungal Biodiversity Centre.

Table 3-1: *Stachybotrys* spp. strains used in this study designated with strain numbers, species and origins.

No	Strain number	Species	Origin
1	ATCC 16026	<i>Stachybotrys chartarum</i> (Ehrenb.) S. Hughes	England
2	NCPF 7587	<i>Stachybotrys chartarum</i>	England
3	CBS 324.65	<i>Stachybotrys chartarum</i> (Ehrenb.) S. Hughes	Netherlands
4	CBS 328.37	<i>Stachybotrys chartarum</i> (Ehrenb.) S. Hughes	Italy
5	Stachy CU	<i>Stachybotrys chartarum</i>	England
6	CBS 109286	<i>Stachybotrys chlorohalonata</i> B. Andersen & Thrane	Finland
7	CBS 109283	<i>Stachybotrys chlorohalonata</i> B. Andersen & Thrane	Denmark
8	CBS 252.76	<i>Stachybotrys oenantes</i> M.B. Ellis	Cuba
9	CBS 463.74	<i>Stachybotrys oenantes</i> M.B. Ellis	Suriname
10	CBS 363.58	<i>Stachybotrys bisbyi</i> (Sriniv.) G.L. Barron	Mozambique
11	CBS 399.65	<i>Stachybotrys bisbyi</i> (Sriniv.) G.L. Barron	Germany
12	CBS 949.72	<i>Stachybotrys dichroa</i> Grove	Turkey
13	CBS 182.80	<i>Stachybotrys dichroa</i> Grove	Netherlands

3.2.2 Optimisation of growth on different media

The two *S. chartarum* type strains obtained ATCC 16026 and NCPF 7587 were grown on four different media:

- i. Potato dextrose medium (PDA) (Cat. No CM0139, Oxoid TM)
- ii. Sabouraud medium, Emmons Modified (ESA) (Cat. No 274710, BD Difco TM)
- iii. Cornmeal medium (CMA) (Cat. No 42347, Sigma Aldrich [®])
- iv. Sabouraud Dextrose with Cholaramphenicol medium (SDA) (Cat. No 11933672, Thermo Fisher Scientific TM Oxoid TM)

Stachybotrys chartarum, CU Stachy and the other *Stachybotrys* spp. were grown on PDA and ESA. All plates tested were incubated at 25 °C under aerobic atmospheric conditions. The surface and reverse morphologies were documented after 7 days or until fully matured based on the pigmentation. The adhesive tape mount method was used for microscopic examination. PDA, ESA and CMA were prepared in the laboratory according to manufacturers' instructions. Prepared media plates of SDA plates

(containing chloramphenicol) were purchased from Thermo Fisher Scientific™ Oxoid™ and stored in 4 °C until use.

3.2.3 Haemolytic activity on blood sheep agar

Blood sheep agar (Columbia agar + 5% sheep blood) (Cat. no 100253ZFMP, VWR ®) was used to determine the haemolytic activity of *Stachybotrys* spp.. The plates were observed and classified based on the clearance zones patterns.

3.2.4 Microscopic examination

The adhesive tape mount method was used to collect fungal structures grown on ESA medium for microscopic examination. The fungi specimens were stained with lactophenol blue to produce more distinct structural characteristics and to aid with the microscopic observation. Images were taken using Nikon Model DS-Fi1-L2, Brunel Digicam or 5.0 MP Moticam as stated in each figures.

3.3 RESULTS

3.3.1 Optimisation of growth on different media

We have compared *S. chartarum* growth on different media based on the Product Information Sheet for type strain ATCC 16026™. PDA was used as a standard comparison against CMA, SDA and ESA.

3.3.1.1 *S. chartarum*, NCPF 7587

S. chartarum, NCPF 7587 was originally isolated from cotton fabric in Birmingham, England in 1960. This isolate was obtained in a form of agar slope from the National Collection of Pathogenic Fungi operated by the Mycology Reference Laboratory, Public Health England and is categorised under ACDP Hazard group 2. It also holds the synonyms of *Stachybotrys alterans* and *Stachybotrys atra*.

After incubation at 25 °C at 7 days, the NCPF 7587 isolate showed maximum colony growth on ESA and restricted growths on both CMA and SDA (Figure 3-1). There was slightly smaller colony diameter growths of *S. chartarum* on PDA as compared to ESA this strain (and indeed all three *S. chartarum* strains), although the differences are not statistically significant (Table 3-2). The smallest colony was on CMA which appeared to be brown to greenish and powdery with a filamentous edge. On SDA, the surface

colony was white in colour, not uniform, dense with a distinct margin due to lack of sporulation while the reverse was dark brown.

3.3.1.2 *S. chartarum*, ATCC® 16026™

S. chartarum, ATCC ® 16026™ is also designated as IMI 82021 and deposited as *Stachybotrys atra Corda*. It is classified as Biosafety Level 1 by the US Centers for Disease Control and Prevention (CDC) and has been used in many studies including a fungus resistance test for adhesives by the British Standard Institution Specification BS 3046:1981 and phylogenetic studies⁽⁹⁹⁾. After incubation at 25 °C for 7 days, ATCC 16026 showed similar colony growth to NCPF 7587 and restricted growth on both CMA and SDA as also observed with NCPF 7587 (Figure 3-1). There were slightly smaller colony diameter on PDA as compared to ESA for all three *S. chartarum* strains, although the differences are not statistically significant (Table 3-3).

3.3.1.3 *S. chartarum*, Stachy CU

The strain was originally isolated from a severely damaged indoor environment and was cultivated on Malt Extract Agar (MEA) at 25 °C for 7 days by Cranfield Health. The given isolate was then reconstituted on PDA and ESA in our laboratory (Figure 3-1). Similar result was obtained as in NCPF 7587 and ATCC 16026 (Table 3-4).

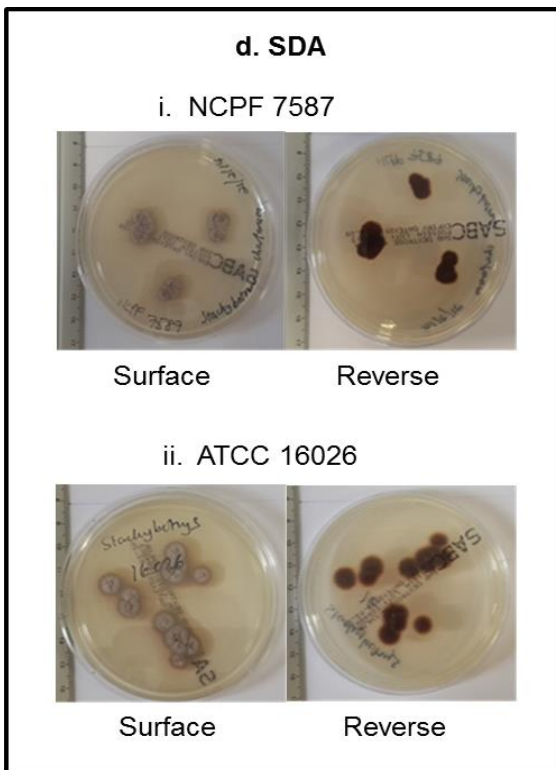
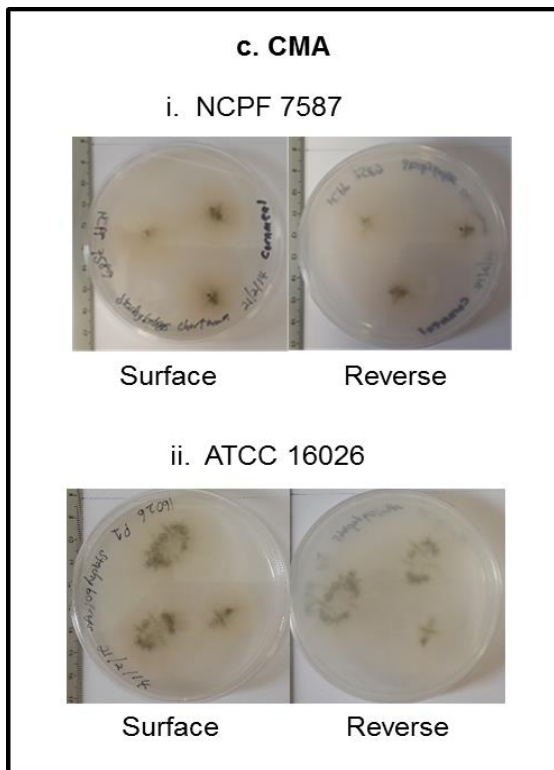
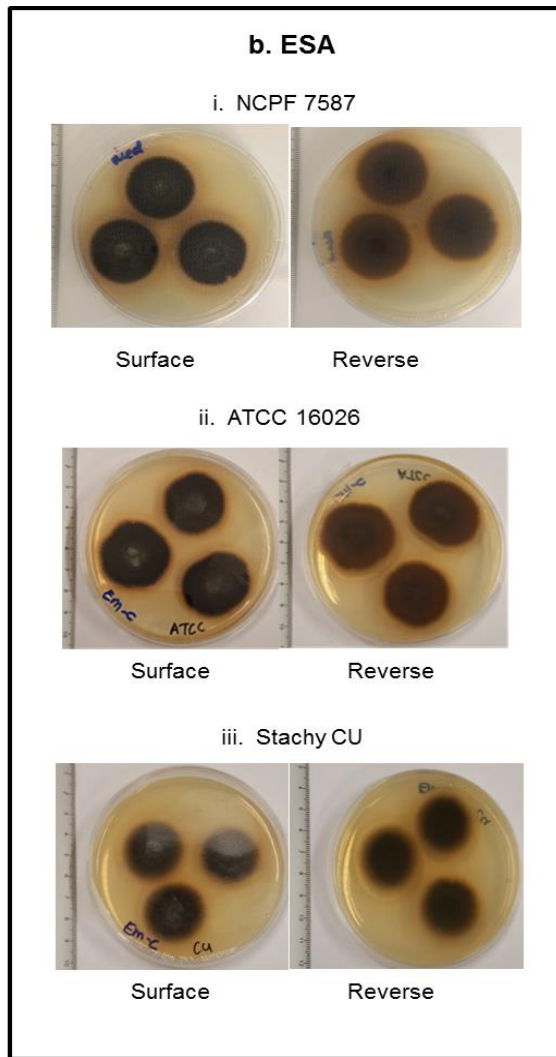
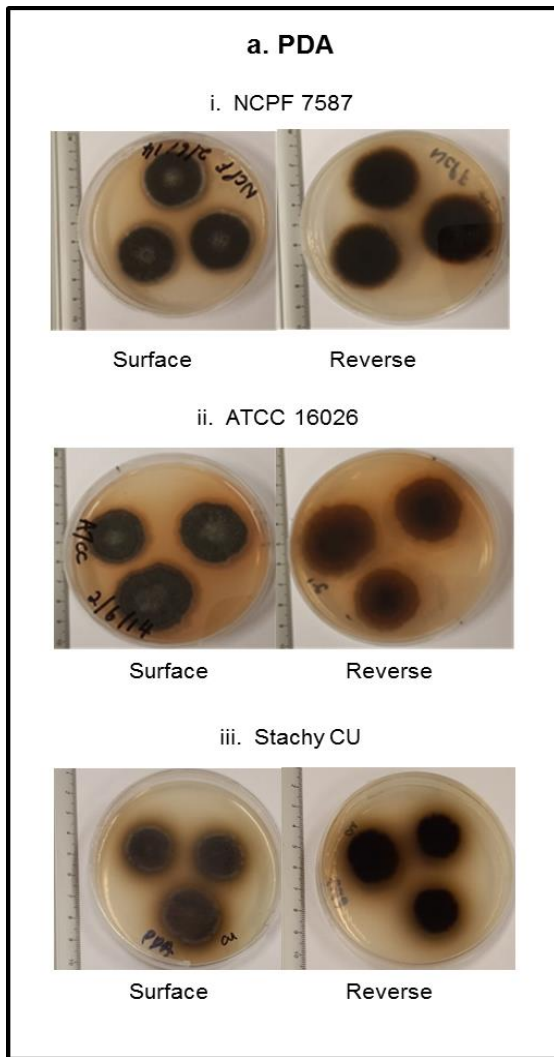


Figure 3-1: The surface and reverse morphology of *S. chartarum* type strains NCPF 7587 and ATCC 16026 grown on 4 different media. a. PDA, b. ESA, c. CMA, and d. SDA incubated at 25 °C for 7 days. Stachy CU isolate was not grown on CMA and SDA, as both media showed poor recovery for both *S. chartarum* type strains, ATCC 16026 and NCPF 7587.

Table 3-2: Comparison of mean diameter growth of point inoculated *S. chartarum* (ATCC 16026) on different media compared to PDA as the control using unpaired t-test. Mean diameter growth of *S. chartarum* with p-value ≤ 0.05 indicates statistically significant differences. Symbol meaning: NS = $P > 0.05$, * = ($p \leq 0.05$), ** = ($p \leq 0.01$), * = ($p \leq 0.001$), **** = $p \leq 0.0001$.**

Types of media	Mean diameter (cm)	SD	SE	Mean difference 95% CI	p-value
Potato dextrose agar	3.467	0.462	0.267		
Emmons Modified	3.600	0.265	0.153	-0.133 (-0.987, 0.720)	0.6868 ^{NS}
Cornmeal agar	1.567	0.513	0.296	1.900 (0.793,3.007)	0.0089 ^{**}
Sabouraud dextrose	1.117	0.397	0.162	2.350 (1.653, 3.047)	0.0001 ^{****}

Table 3-3: Comparison of mean diameter growth of point inoculated *S. chartarum* (NCPF 7589) on different media compared to PDA as the control using unpaired t-test. Mean diameter growth of *S. chartarum* with p-value ≤ 0.05 indicates statistically significant differences. Symbol meaning: NS = $P > 0.05$, * = ($p \leq 0.05$), ** = ($p \leq 0.01$), * = ($p \leq 0.001$), **** = $p \leq 0.0001$.**

Types of media	Mean diameter (cm)	SD	SE	Mean difference 95% CI	p-value
Potato dextrose agar	3.600	0.100	0.058		
Emmons Modified	3.833	0.153	0.088	-0.100 (-0.526,0.059)	0.0913 ^{NS}
Cornmeal agar	0.633	0.115	0.067	2.967 (2.722, 3.212)	0.0001 ^{****}
Sabouraud dextrose	1.500	0.200	0.115	1.333 (0.930,1.737)	0.0008 ^{***}

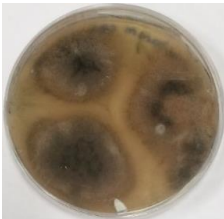
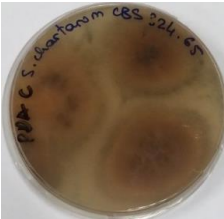
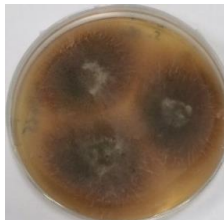
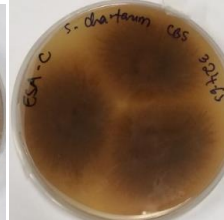
Table 3-4: Comparison of mean diameter growth of point inoculated *S. chartarum* (Stachy CU) on ESA compared to PDA as the control using unpaired t-test. Mean diameter growth of *S. chartarum* with p-value ≤ 0.05 indicates statistically significant differences. Symbol meaning: NS = $P > 0.05$, * = ($p \leq 0.05$), ** = ($p \leq 0.01$), * = ($p \leq 0.001$), **** = $p \leq 0.0001$.**


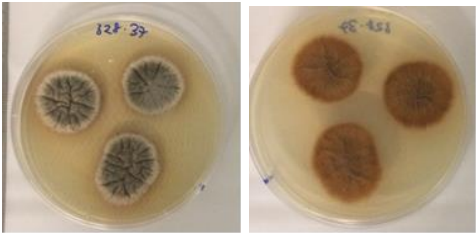
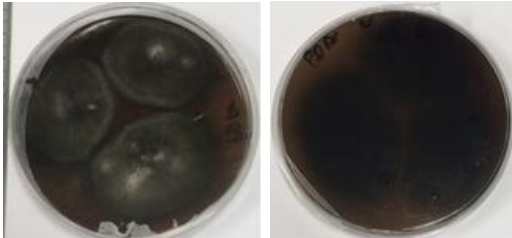
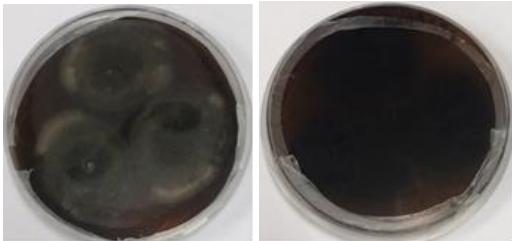
Types of media	Mean diameter (cm)	SD	SE	Mean difference 95% CI	p-value
Potato dextrose agar	2.267	0.115	0.067		
Emmons Modified	2.400	0.100	0.058	-0.133 (-0.378, 0.112)	0.2051 ^{NS}

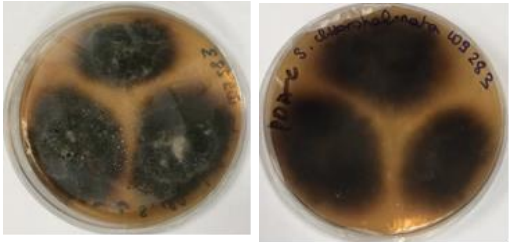
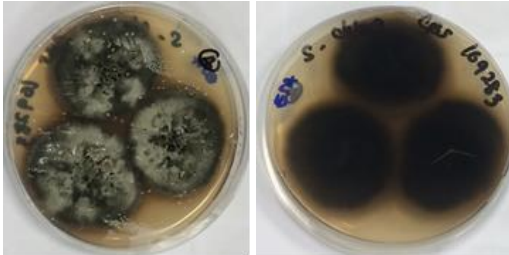


3.3.1.4 Other *Stachybotrys* spp. isolates

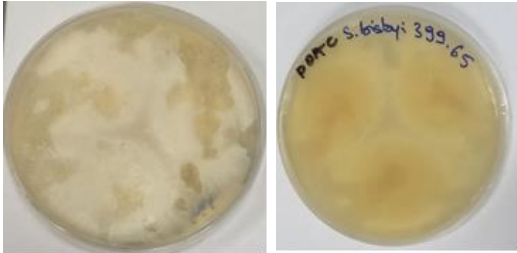

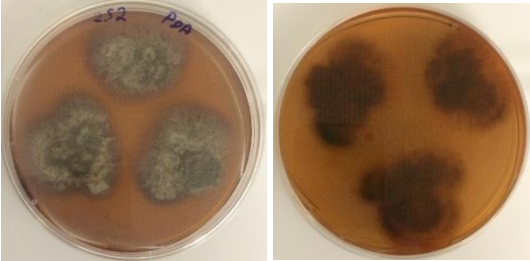
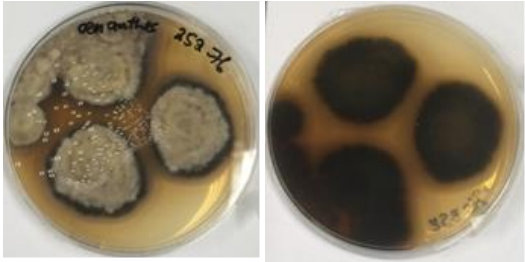
Colonies ranged from white to dark brown or black. All strains (except *S. bisbyi*) turned to brown when mature (up to 4 weeks). The plates were incubated at 25 °C for at least 7 days or until fully matured for further experiments (Table 3-5).


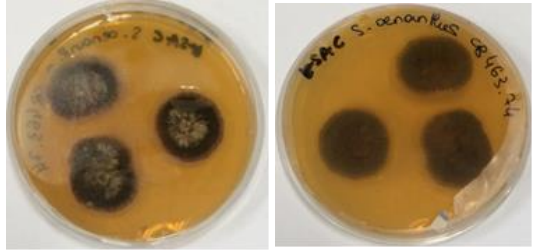
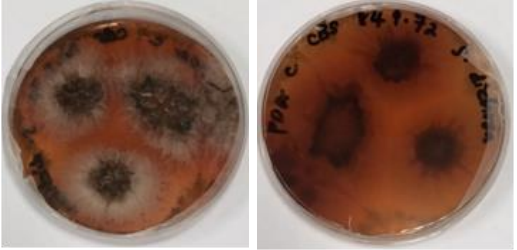
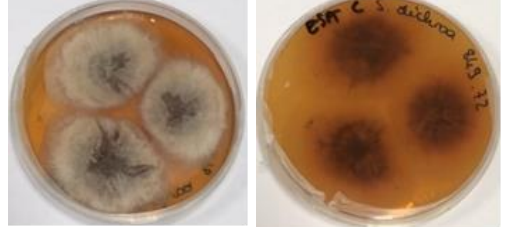
Table 3-5: Colony characteristics of *S. chartarum* (CBS 324.65, CBS 328.37), *S. chlorohalonata* (CBS 109286, CBS 109283), *S. bisbyi* (CBS 363.58, CBS 399.65, *S. oenantes* (CBS 252.76, CBS 463.74) and *S. dichroa*, (CBS 949.72, CBS 182.80) grown on ESA and PDA followed by incubation at 25 °C


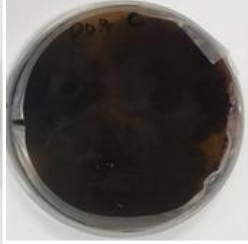

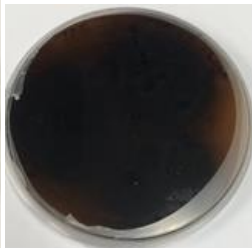
Species	Colony	Description	
<i>S. chartarum</i> CBS 324.65	i. PDA		
			Surface and reverse were dark brown in both media. Less sporulation compared to other <i>S. chartarum</i> strains, ATCC 16026 and NCPF 7587.
	Surface	Reverse	
	ii. ESA		
			
	Surface	Reverse	Surface and reverse were more pigmented on ESA compared to PDA.

Species	Colony	Description
<p><i>S. chartarum</i> CBS 328.37</p>	<p>i. PDA</p>  <p>Surface Reverse</p> <p>ii. ESA</p>  <p>Surface Reverse</p>	<p>Surface was white in the middle and black at the edge. Reverse was dark brown on PDA.</p> <p>Surface was dense and black in the middle but with white edge, but lighter brown on reverse on ESA.</p>
<p><i>S. chlorohalonata</i> CBS 109286</p>	<p>i. PDA</p>  <p>Surface Reverse</p> <p>ii. ESA</p>  <p>Surface Reverse</p>	<p>Heavy sporulation and intense black on both media.</p>

Species	Colony	Description
<p><i>S. chlorohalonata</i> CBS 109283</p>	<p>i. PDA</p>  <p>Surface Reverse</p> <p>ii. ESA</p>  <p>Surface Reverse</p>	<p>Colonies were dark brown on both surface and reverse on PDA.</p> <p>On ESA, colonies were black with white mass on surface and black to greenish on reverse.</p>
<p><i>S. bisbyi</i> CBS 363.58</p>	<p>i. PDA</p>  <p>Surface Reverse</p> <p>ii. ESA</p>  <p>Surface Reverse</p>	<p>Surface was white to yellow in both surface and reverse on PDA.</p> <p>Surface was white but black on reverse on ESA.</p>

Species	Colony	Description
<p><i>S. bisbyi</i> CBS 399.65</p>	<p>i. PDA</p>  <p>Surface Reverse</p> <p>ii. ESA</p>  <p>Surface Reverse</p>	<p>Surface and reverse were white to yellow on both PDA and ESA.</p>
<p><i>S. oenanthae</i> CBS 252.76</p>	<p>i. PDA</p>  <p>Surface Reverse</p> <p>ii. ESA</p>  <p>Surface Reverse</p>	<p>Surface was dark brown with white mass on surface and dark brown on reverse on PDA.</p> <p>Surface was white with black margin and reverse was black-greenish.</p>

Species	Colony	Description
<p><i>S. oenantes</i> CBS 463.74</p>	<p>i. PDA</p>  <p>Surface Reverse</p> <p>ii. ESA</p>  <p>Surface Reverse</p>	<p>Surface and reverse were white to light brown on PDA.</p> <p>Both surface and reverse were dark brown on ESA.</p>
<p><i>S. dichroa</i>, CBS 949.72</p>	<p>i. PDA</p>  <p>Surface Reverse</p> <p>ii. ESA</p>  <p>Surface Reverse</p>	<p>On PDA, surface was black in the middle with white hyphae growing outwards. Surface was dark brown.</p> <p>On ESA, surface was white with black mass submerged into agar. Reverse was dark brown.</p>

Species	Colony	Description
<p><i>S. dichroa</i>, CBS 182.80</p>	<p style="text-align: center;">i. PDA</p> <div style="display: flex; justify-content: space-around;">   </div> <p style="text-align: center;">Surface Reverse</p> <p style="text-align: center;">ii. ESA</p> <div style="display: flex; justify-content: space-around;">   </div> <p style="text-align: center;">Surface Reverse</p>	<p>Heavy sporulation and intense black in both media.</p>

3.3.2 Effects of temperature on fungal growth

Two strains of *S. chartarum*, NCPF 7587 and Stachy CU were grown on ESA and were incubated at 25 °C or 30 °C to determine the effects of temperature on growth. Both isolates produced dark brown to black pigmented surface and reverse when incubated at 30 °C compared to greenish-dark brown with yellowish margin when incubated at 25 °C (Figure 3-2). Radial growth was slightly smaller on plates incubated at 25 °C compared to 30 °C, but with more a flatter surface and less sporulation. The results showed that, in addition to the media types, incubation temperature can also induce more pigmentation and different colony morphologies in *S. chartarum*.

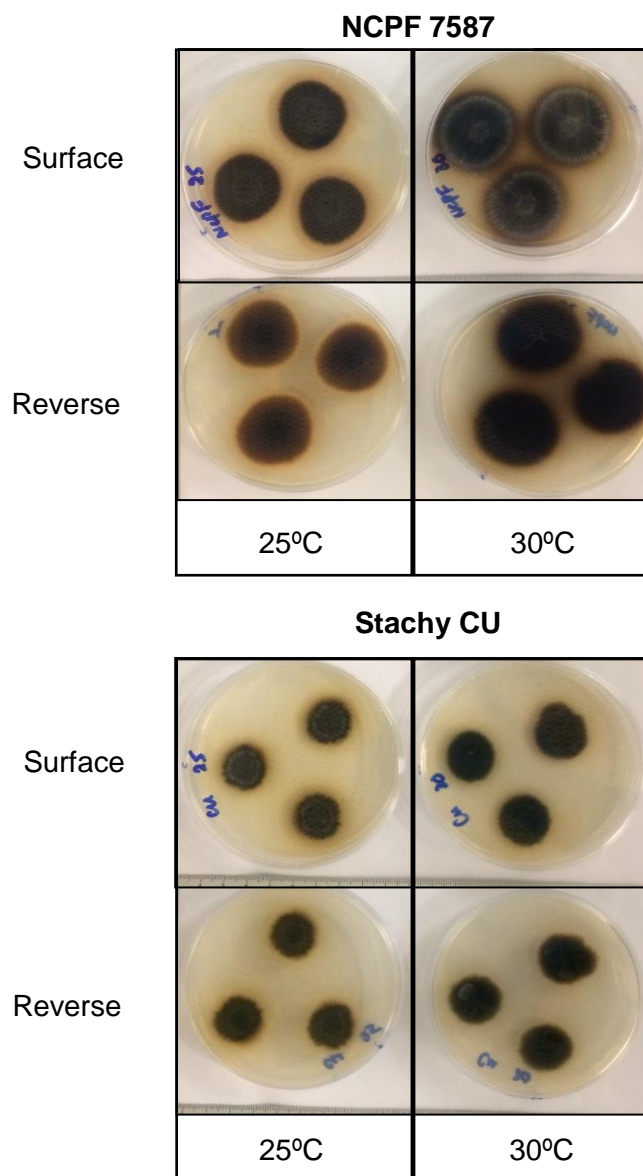


Figure 3-2: Surface and reverse morphologies of NCPF 7587 and CU Stachy grown on ESA and incubated at 25 °C or 30 °C for 7 days.

3.3.3 Haemolytic activity of *Stachybotrys* spp. on blood agar

In this study, 3 strains of *Stachybotrys chartarum* (ATCC 16026, NCPF 7587 and Stachy CU) were grown on a differential medium, blood sheep agar (BSA) to determine their abilities to induce haemolysis, *in vitro*. An environmentally isolated *Penicillium* spp. was used as a comparison that represent other commonly found indoor environmental fungi. On day-3, all tested *Stachybotrys* spp. strains showed a zone clearing around the colonies on the BSA plates which indicates β -haemolysis, while the *Penicillium* sp. showed no change in the BSA which indicates γ - haemolysis (Figure 3-3). The incubation was extended to day 7 to assess further cell lysis caused by the fungi. However, the haemolysis patterns remain the same from day 3 to day 7.

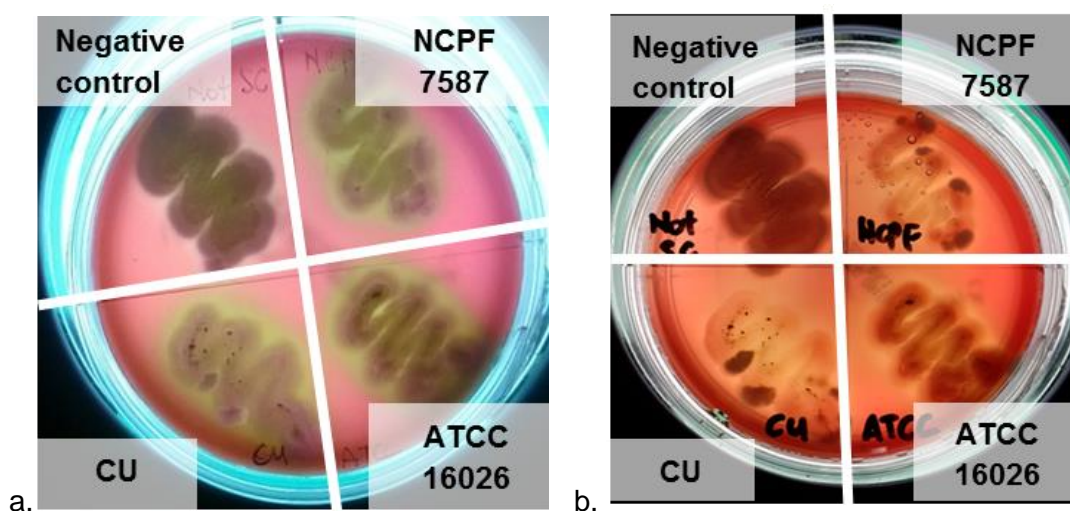


Figure 3-3: BSA cultured with *Stachybotrys* spp. (ATCC 16026, NCPF 7587 and Stachy CU) and *Penicillium* spp. (negative control) incubated at 25 °C after a) 3 days and b) 7 days showed clearance on the BSA plate for all 3 tested *Stachybotrys* spp..

3.3.4 Microscopic examination of *Stachybotrys* spp.

In this study, structures of *S. chartarum* were observed for the characteristics described in published guidelines. It has been documented in many studies that *S. chartarum* appears as septate and colourless to dark hyphae which are, with simple, straight or flexous, branched or unbranched. Its conidiphores are about 100-1000 μm long and 3-6 μm wide and bear clusters of 3-10 phialides. The conidia maybe dark, round to ellipsoidal, smooth or rough walled and aggregated in slimy masses of phialides⁽⁹¹⁾. While, the phialides are colourless or pigmented, non-septate and cylindrical with swollen upper portion which produces monophaialidic, terminal, discrete, determinate (stable), clavate and smooth conidiogenous cells^(92, 93)

3.3.4.1 *S. chartarum*, NCPF 7587

From the microscopic observation, NCPF 7587 produced a huge number of spores as shown in the 20x magnification image. Phialides and septate hyphae structures were clearly observed as dark blue, with simple straight conidiophores. Conidia were dark and ellipsoidal to semi-ellipsoidal and formed aggregates on the phialides as shown in 40x and 100x magnification (Figure 3-4).

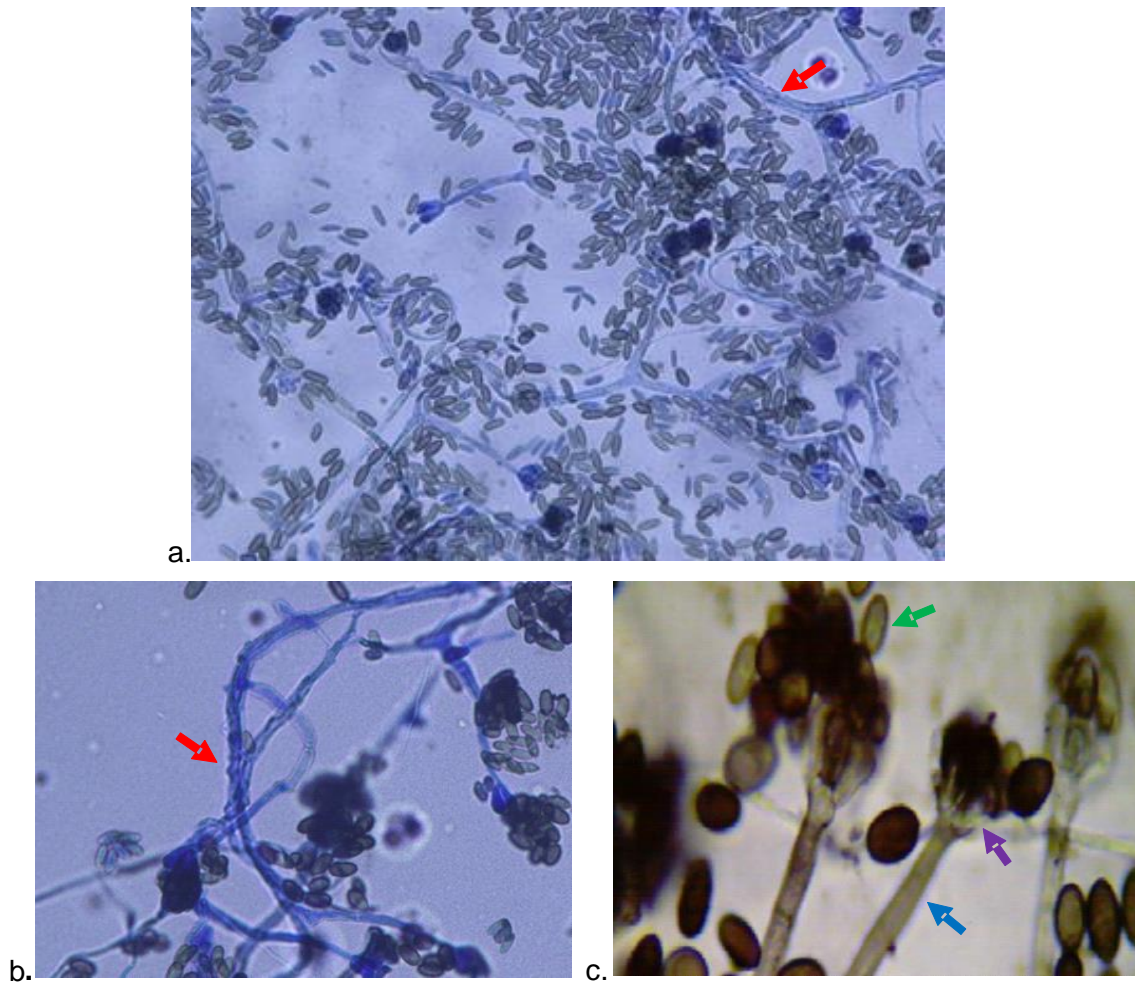


Figure 3-4: The microscopic images a. 20x (taken using Nikon DS-Fi1-L2), b. 40x (taken using Nikon DS-Fi1-L2) and c. 100x (taken using Brunel digicam) showing the microscopic structures of *S. chartarum*, NCPF 7589 grown on ESA. Coloured arrows indicate different structures; Red: Hyphae, Green: Spores/conidia, Blue: Conidiophore and Purple: Phialides.

3.3.4.2 *S. chartarum*, ATCC 16026

The structure of ATCC 16026 was close to NCPF 7587 (Figure 3-5). However, the rough surface of the conidiophores was more distinct in ATCC 16026.

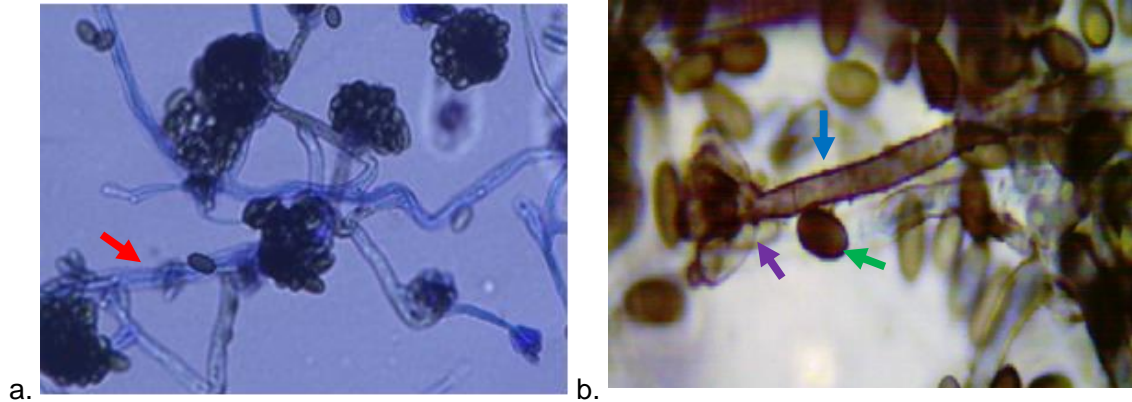


Figure 3-5: The microscopic images a. 40x (taken using Nikon DS-Fi1-L2) and b. 100x (taken using Brunel digicam) showing the microscopic structures *S. chartarum*, ATCC 16026 grown on ESA. Coloured arrows indicate different structures; Red: Hyphae, Green: Spores/ conidia, Blue: Conidiophore and Purple: Phialides.

3.3.4.3 *S. chartarum*, Stachy CU

The structure of the Cranfield isolate resembles ATCC 16026 and NCPF 7589 with the presence of conidiophores bearing several phialides (Figure 3-6). However, the conidia were semi-ellipsoidal to round under 100x magnification. This might be because the isolate needs a longer time to fully develop its structures or due to different strain characteristics.

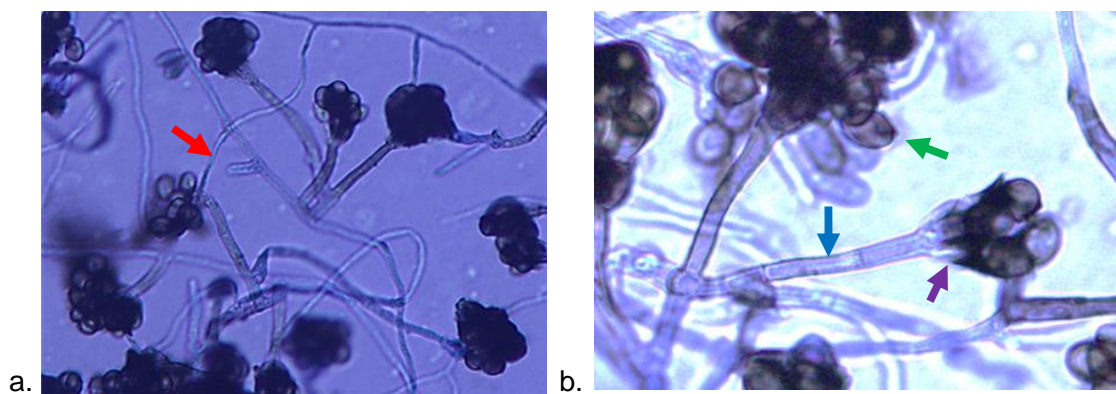


Figure 3-6: The microscopic images a. 40x (taken using Nikon DS-Fi1-L2) and b. 100x (taken using Nikon DS-Fi1-L2) showing the microscopic structures of Stachy CU grown on ESA. Coloured arrows indicate different structures; Red: Hyphae, Green: Spores/conidia, Blue: Conidiophore and Purple: Phialides.

3.3.4.4 Other *Stachybotrys* spp. isolates

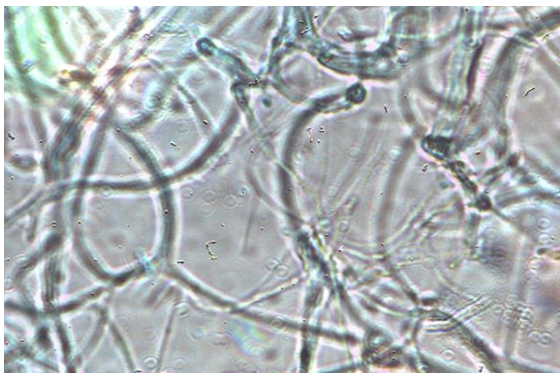
All the strains were observed under the microscope for their structural differences (Figure 3-7). However, not all strains were able to produce spores making it difficult to obtain a well-defined structure. The fungal structures were predominantly made up of hyphae and lack of distinct phialides and conidia arrangement particularly with *S. bisbyi* (CBS 399.65 and CBS 363.58), *S. dichroa* (CBS 949.72), *S. oenantes* (CBS 252.76 and CBS 463.74) making the identifications and comparisons were rather complicated. Only *S. chartarum*, *S. chlorohalonata* and *S. dichroa* (CBS 182.80) were able to produce complete structures.



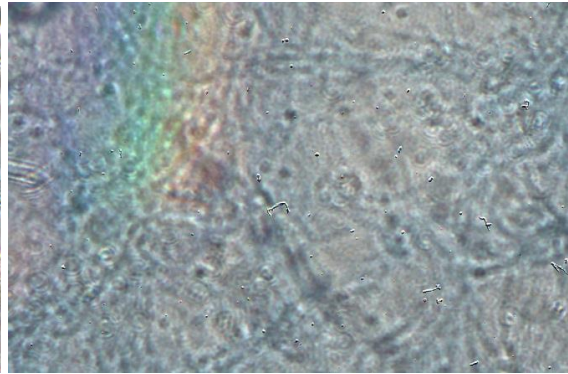
Stachybotrys chartarum, CBS 324.65



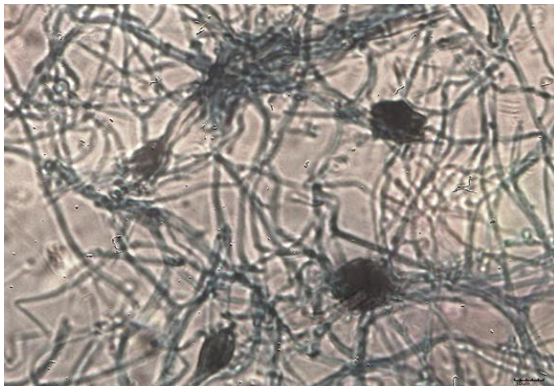
Stachybotrys chartarum, CBS 328.37



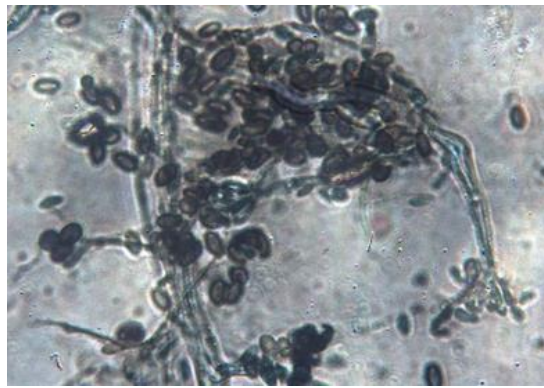
Stachybotrys bisbyi, CBS 399.65



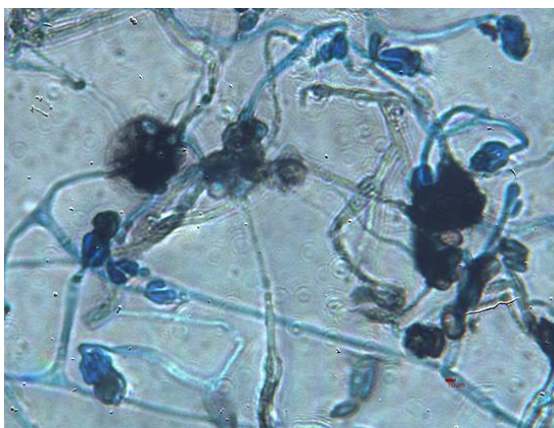
Stachybotrys bisbyi, CBS 363.58



Stachybotrys dichroa, CBS 949.72



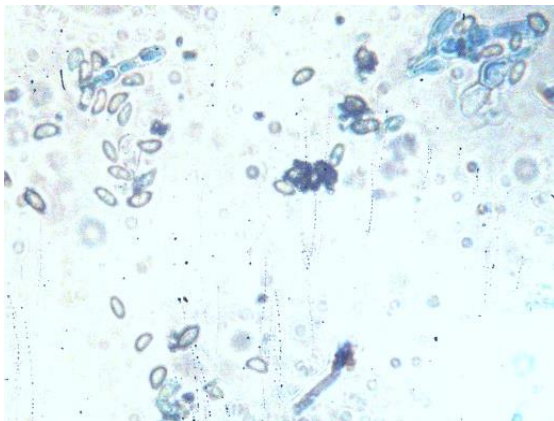
Stachybotrys dichroa, CBS 182.80



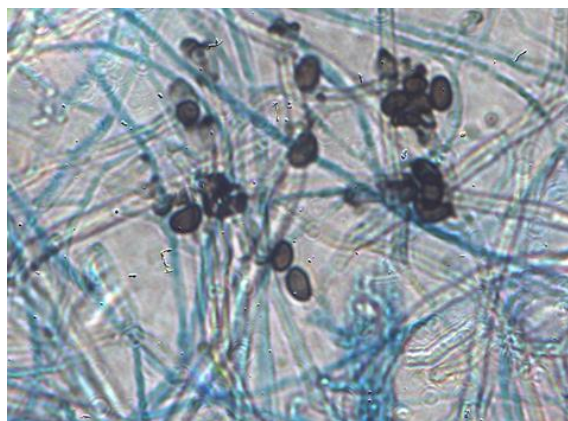
Stachybotrys chlorohalonata, CBS 109386



Stachybotrys chlorohalonata, CBS 109283



Stachybotrys oenantes, CBS 463.74



Stachybotrys oenantes, CBS 252.76

Figure 3-7: Microscopic images (40x) of *Stachybotrys* spp. (taken using 5.0 MP Moticam) of *S. chartarum* (CBS 324.65, CBS 328.37), *S. chlorohalonata* (CBS 109283, CBS 109286), *S. bisbyi* (CBS 399.65, CBS 363.58), *S. dichroa* (CBS 182.80, CBS 949.72) and *S. oenantes* (CBS 252.76, CBS 463.74).

3.4 DISCUSSION

Stachybotrys chartarum species are perceived by many to be a 'black mould'. However their colour ranges from black to black-green in appearance depending on the media used. In addition, other *Stachybotrys* spp. may appear similar to *S. chartarum* and difficult to distinguish from it. Although previous studies have recommended several media for cultivation of *Stachybotrys* spp., there is no standard medium used for *Stachybotrys* spp. due to variations in the outcomes between studies. *Stachybotrys* species are known to be slow or moderately fast growing fungi depending on the media used. Culture media contain mainly carbon or nitrogen sources and other elements to support growth and to enhance certain characteristics that have significant role in fungi identification. Hence, optimisation of the growth conditions would provide more evidence and better understanding on the growth of *Stachybotrys* spp. and their identifications.

Until now, the American Type Culture Collection (ATCC) has recommended yeast morphology agar (YMA), cornmeal agar (CMA) and potato dextrose agar (PDA) for the propagation of ATCC 16026⁽²⁰⁸⁾. Nonetheless, other media have also been used or recommended for *Stachybotrys* spp. including malt dextrose agar (MEA), DG-18 and cellulose agar (CA)^(12, 209, 210). In an earlier study, Anderson and Nissen⁽²¹¹⁾ evaluated 22 mycological media on the growth of nine *Stachybotrys* spp. isolates. Interestingly, they found that the recommended medium such as DG-18, MEA and water agar were not effective for sporulation and growth for most isolates compared to V8 media which contains plant-based ingredient. This was followed by Billups *et al.*⁽²¹²⁾ who proposed a novel *Stachybotrys* selective medium consisting of PDA, miconazole and chloramphenicol which is commercially available as a pre-poured medium. This was claimed to promote a more rapid growth of *Stachybotrys* spp. than CA, CMA and MEA and was able to restrict the growth of other fast-growing fungi. The medium also showed better recovery compared to MEA.

In this study, we have tested the effectiveness of PDA, ESA, CMA and SDA to produce the best growth and sporulation of *Stachybotrys* spp. to be used for identification and further experiments. From our findings, both PDA and ESA are suitable media for the isolation and recovery of *Stachybotrys* spp.. The pH of ESA is more neutral to enhance biomass recovery of fungi and this effect could be seen with all the isolates providing a better visualization of the fungal structures to be used in the identification. All other *Stachybotrys* spp. grown on both ESA and PDA showed that the pigmentation ranged

from white to dark brown and black depending on the media. We also found that the growth was either restricted or slower with CMA and SDA after 7 days at 25 °C. Larone⁽⁹¹⁾ had documented that *S. chartarum* is a moderately rapidly growing fungus, usually maturing after approximately 7 - 14 days on a medium with high cellulose content. This might indicate that longer incubation time is required at different incubation temperature for different media. The findings also reveal that not all *Stachybotrys* spp. produce black colonies, and thus, the term 'black mould' is misleading and inaccurate when applied to the entire genus.

Two isolates exhibited different morphological characteristics particularly in the production of pigment as seen in *Stachybotrys bisbyi* (CBS 363.58) and *S. oenantes* (CBS 463.74). *S. bisbyi* (CBS 363.58) was seen as white colonies on both media, but with a black reverse morphology on ESA. Whereas, *S. oenantes* (CBS 463.74) had white to light brown colonies on PDA but dark brown colonies on both surface and reverse on ESA. From the results, we conclude that the fungal growth and morphologies were influenced greatly by the choice of culture medium. Our finding was in accordance with Sharma *et al.*⁽¹⁹⁹⁾ who found that fungal growth, colony characteristics and sporulation were greatly influenced by the type of medium used. The melanin pigment in fungi plays an important role in the protective mechanisms against harsh environment and stress response and is associated with enhanced virulence in some pathogenic fungi⁽²¹³⁾. The pigmentation became more distinct in ESA which might be related to its lower dextrose content. However, the fungal mass increased compared to other *Stachybotrys* spp. grown on other media. This increase in the fungal mass is in contrast with findings by Babitha *et al.*⁽²¹⁴⁾ who demonstrated that environmental stress was capable of inducing pigmentation in fungi but decreasing the fungal biomass. The increase in biomass might be associated with other factors such as a more neutral pH which appears to enhance the growth and sporulation in some fungi⁽²⁰⁰⁾.

The capability of *S. chartarum* to produce haemolysis on blood sheep agar (BSA) indicates the production of hemolysin, a substance able to lyse red blood cells⁽⁶⁵⁾. We found that all three *S. chartarum* strains, ATCC 16026, NCPF 7587 and Stachy CU can cause haemolysis on BSA. Stachylisin, a fungal hemolysin, has been previously proposed as a potential biomarker of *S. chartarum*⁽⁶⁶⁾. However, this method cannot be a gold standard due to its lack of specificity to only *S. chartarum*. Haemolysis produced by Stachy CU (subsequently shown to be not a *S. chartarum* strain - see chapter 4) confirms this.

Microscopic examination showed a distinct structure of *Stachybotrys* spp. with clusters of slimy conidia that aggregate on the phialides. The structure of *S. chartarum* ATCC 16026 very closely resembles NCPF 7587. However, the rough surface of conidiophores was more distinct in ATCC 16026. The structure of the environmental *S. chartarum* isolate, Stachy CU resembles ATCC 16026 and NCPF 7587 with the presence of conidiophores bearing several phialides. However, the conidia were more semi-ellipsoidal to round compared to both reference strains. This might be because the isolate needs a longer time to fully develop its structure or due to different strain characteristics. Li & Yang ⁽⁹⁵⁾ have reported on the great variations in size and shapes of phialides and conidia of *S. chartarum*, leading to confusion in the identification process which has seen continuous revision of taxonomy since the genus was proposed in 1837 by Corda. Moreover, *Stachybotrys* spp. have undergone a series of reclassifications due to high similarities to its closely related genus, *Memnoniella* spp.. Recently, the latter has been re-evaluated and re-classified into the *Stachybotrys* genus ⁽⁹⁹⁻¹⁰¹⁾. The new species, *S. cholorohalonata* was previously classified as *S. chartarum* characterised by having smooth conidia, more restricted colonies and producing greenish pigment on Czapek yeast agar ⁽¹¹⁾.

Owing to the high similarity of characteristics within the genus, using classical identification and characterisation methods for *Stachybotrys* spp. can be a challenge when the isolate is not fully developed and in fact, 90% of the environmentally collected *S. chartarum* spores failed to fully germinate making identification more difficult ⁽¹⁰⁸⁾. Therefore, we found that ESA and PDA were most suitable to cultivate *Stachybotrys* spp. in all future experiments. These findings also challenge the concept that all *Stachybotrys* spp. are 'black mould'.

3.5 CONCLUSIONS

The results provide a basic understanding on the growth requirement and morphological characteristics of *Stachybotrys* spp. using different media. This strain needs to be further analysed with other more reliable methods such as polymerase chain reaction (PCR) and matrix assisted laser desorption ionisation (MALDI) to confirm its identity.

CHAPTER 4

IDENTIFICATION OF *STACHYBOTRYS* SPECIES USING DNA-BASED METHODS

This chapter presents the work on the identification of *Stachybotrys* species using DNA-based methods. PCR using different primers were compared and assessed for their specificities to characterise different *Stachybotrys* spp.. PCR was employed using the universal primer pair ITS 1 and ITS 4, restriction fragment length polymorphism (RFLP) and the mycotoxin-specific primer, trichodiene synthase 5 (tri5). *In-silico* PCR was used as a complementary method to examine primer specificity.

4.1 INTRODUCTION

Studies in the identification of *Stachybotrys* spp. are important due to the complexity in their morphology and physiology, especially their toxicity which is very much dependent on chemotype groups ⁽⁸¹⁾. Molecular methods, particularly PCR and mass spectrometry, are the best options to distinguish between species. Furthermore, *Stachybotrys chartarum* is a species complex fungus which is very similar to its closely related species, *S. chlorohalonata*. Therefore, discrimination between closely related species can prove challenging.

S. chartarum produces numerous compounds, however, the toxicity of *Stachybotrys* spp. is associated with the production of highly toxic macrocyclic trichothecenes ^(131, 215-217). Macrocyclic trichothecenes are known to be potent protein synthesis inhibitors in eukaryotes acting as translational inhibitors and stress kinase activators ^(76, 97). The types of mycotoxins produced have been used to identify *S. chartarum* of different chemotypes and with its closely related species, *S. chlorohalonata*. Several studies

have also reported on the assessment and application of *tri5* gene-based primers for the detection of toxic *S. chartarum* from various environmental sources (11, 12, 105, 108).

In this chapter, we report on the development of a high throughput molecular method to identify members of the *S. chartarum* species-complex and distinguish them from the other morphologically similar *Stachybotrys* spp.. We compared two different techniques: the universal primers ITS 1 and ITS 4 combined with RFLP and specific primers for the *tri5* gene. This has led to the development of a novel *tri5* primer set with the aim to develop a high throughput molecular method for identifying *S. chartarum* species complex with confidence.

4.2 MATERIALS AND METHODS

4.2.1 *Stachybotrys* spp. isolates

A total of 13 *Stachybotrys* strains representing 5 different species were tested (Table 4-1). *Stachybotrys* spp. strains were obtained from various sources as described previously. All isolates were grown on Sabouraud agar or Emmons modified medium (274720, Difco™) supplemented with 100 mg/l chloramphenicol (C0378, Sigma Aldrich, UK) and incubated at 25 °C under aerobic conditions.

Table 4-1: 13 strains of *Stachybotrys* spp. representing 5 different species as identified from the original source.

No	Species	Strains
1	<i>Stachybotrys chartarum</i>	ATCC 16026
2		NCPF 7587
3		CBS 324.65
4		CBS 328.37
5		CU Stachy
6	<i>Stachybotrys chlorohalonata</i>	CBS 109286
7		CBS 109283
8	<i>Stachybotrys oenantes</i>	CBS 252.76
9		CBS 463.74
10	<i>Stachybotrys bisbyi</i>	CBS 363.58
11		CBS 399.65
12	<i>Stachybotrys dichroa</i>	CBS 949.72
13		CBS 182.80

4.2.2 Preparation of spore suspension

Fungal spores were harvested by adding 3 ml of 0.01 M PBS with 0.1% (v/v) Tween-20. The spore suspension was transferred carefully into sterile Eppendorf tubes and spun down at 8000 rpm (4722 x g) for 5 minutes. The supernatant was removed, and the pellet was washed 3 times with 1 ml of 0.01 M PBS and resuspended in 500 µL of 0.01 M PBS.

4.2.3 Optimization of DNA extraction

Fungal DNA was extracted using DNeasy kit (Qiagen) as per the manufacturer's instructions. Briefly, 300 µL of spore suspension was disrupted using a TissueLyser LT (Qiagen) at the maximal rate (50 Hz) for 2 minutes and placed on ice for 10 minutes. The process was repeated three times. The suspension was then centrifuged and supernatant was transferred into new microtubes. The samples were further extracted following the DNeasy® Plant MiniKit (Qiagen) protocol.

4.2.3.1 Internal transcribed spacer/restriction fragment length polymorphism (ITS/RFLP-PCR)

We employed a PCR-based methods for the identification of *S. chartarum* using fungal universal primer set, ITS1 forward primer (5'-TCCGTAGGTGAACCTGCGG-3') and reverse primer ITS4 (5'-TCCTCCGCTTATTGATATGC-3') (Sigma-Aldrich) followed by restriction digestion by using *Hae*III (Promega) as described by Dean *et al.* ⁽¹⁰³⁾. Each 25 µl PCR reaction contained 12.5 µl of 2X SensiFast Sybr Lo-Rox Mix (Bioline), 0.8µl each of forward and reverse primers (320 nM in the reaction), and 2 µl of DNA. The PCR was performed by heating to 50 °C for 2 minutes followed by 95 °C for 10 minutes and 40 cycles consisting of 95 °C for 15 seconds and 60 °C for 1 minute. Restriction digests were performed by using 5 units of *Hae*III enzyme (Promega, USA) and 1 µg DNA and incubating for 3-4 hours at 37 °C. A custom digest performed *in silico* with *Hae*III using NEB cutter (New England BioLabs) was also performed in-parallel to determine the expected fragment sizes.

4.2.3.2 Trichodiene synthase gene (*tri5*) as a specific target for PCR

Two sets of *tri5*-based primers from previously published studies by Cruse *et al.* ⁽¹²⁾ and Black *et al.* ⁽¹⁰⁵⁾ were used. Prior to the experiment, both primer sets were subjected to NCBI nucleotide BLAST to check for their specificity. The PCR reagents were used at the same concentrations as in the ITS-PCR (section 4.2.3.1). The PCR was performed

by heating the reagents to 50 °C for 2 minutes followed by 95 °C for 10 minutes and then 35 cycles at 95 °C for 15 seconds and 65 °C for 1 minute.

4.2.4 Development of a novel trichodiene synthase gene (*tri5*)-based primer

A total of 48 sequences of *S. chartarum* available from NCBI were aligned using DNASTar Lasergene V7.1 software (Appendix 4-A) and assessed for suitability in primer design using Primer3Plus software. The sequence selected for primer design had fewer nucleotide differences and better alignment in comparison to the published primers.

Using Primer3Plus software, 5 sets of primers (SC1F&R, SC2F&R, SC3F&R, SC4F&R and SC5F&R) were generated along with their estimates melting temperature (T_m), GC content and ability to form dimers and secondary binding determined (Table 4-2). All primers were within the optimal length of PCR primers (18-22 bp) with adequate specificity and short enough to bind to the template. All primers were in the range of ideal primers with melting temperatures (T_m) between 55 and 65 °C and within 5 °C of each other. The GC contents were ranged between 40.0-60%, unlikely to promote non-specific binding. All primers were checked for the presence of primer secondary structures such as hairpins and self-dimerization that would interfere with annealing to the template leading to poor product yield. All these primers have the possibility to form hairpins ranging from 3.0 to 6.0 hairpins and self-annealing potential ranging from 0.0 to 2.0, but were deemed acceptable. All the primers were purchased from Sigma©. The T_m s were slightly higher compared with Primer3Plus and there were differences in the likelihood of secondary structure formation and binding for primers SC4F&R and SC5F&R (Table 4-2).

Table 4-2: Primer data provided by Primer3Plus and Sigma.

Sequences (5'-3')			Length (bp)	Product size (bp)	Primer3Plus				Sigma		
					Tm (°C)	GC (%)	Hairpin	Self-annealing	Tm (°C)	Dimer	Secondary structure
SC1	Forward	TGAGACACTTTGGCCCTTTC	20	247	60.2	50.0	4.0	0.0	64.1	No	None
	Reverse	CACAAAGATCCTCCGACACA			59.7				63.8		
SC2	Forward	TGAGACACTTTGGCCCTTTC	20	248	60.2	50.0	4.0	0.0	64.1	No	None
	Reverse	CCACAAAGATCCTCCGACAC			60.5	55.0			64.5		
SC3	Forward	TCCCCCAAAATATTCCAAGA	20	202	59.2	40.0	6.0	2.0	62.9	No	None
	Reverse	ATGCTCCTGCTCGTTGAAGT			60.0	50.0	3.0	1.0	63.2		
SC4	Forward	TCCCCCAAAATATTCCAAGA	20	211	59.2	40.0	6.0	2.0	62.9	No	None
	Reverse	TTCCAAGAAATGCTCCTGCT			60.0	45.0	3.0	0.0	63.8		Weak
SC5	Forward	TCCCCCAAAATATTCCAAGA	20	197	59.2	40.0	6.0	2.0	59.2	No	None
	Reverse	CCTGCTCGTTGAAGTTTTCC			59.9	50.0	3.0	1.0	59.9		Weak
Tri 5 Black	Forward	GCACACTGGACTGTAAGTCT	20	136	Not available				56.8	No	Moderate
	Reverse	CCTGGGAAGCCATGGAAGT	19		66.3	Weak					
Tri 5 Cruse	Forward	CATCAATCCAACAGTTTCAC	20	641	Not available				57.9	No	None
	Reverse	GCAACCTTCAAAGACTATTG			56.5	None					

4.2.5 DNA sequencing and sequence alignment

PCR was performed as described above (Section 4.2.3). The PCR products were purified using a PCR purification kit (Bioscience) as per manufacturer's instructions. The purified PCR products were sequenced on an ABI Prism (Bioscience, Cambridge), edited and aligned using DNASTar Lasergene V7.1. Sequences were identified for similarities against the National Center for Biotechnology Information (NCBI) (<http://blast.ncbi.nlm.nih.gov>) GenBank database. Reference sequences of chemotypes A and S from the whole genome sequence published by Semeik *et al.*⁽⁸¹⁾ were used to align all the sequences from the 3 primer sets (Cruse *et al.*, Black *et al.*, and SC1) (Table 4-3). Only *Stachybotrys chlorohalonata* strain D13 trichodiene synthase (tri5) gene (AY095987.2) was used as the reference sequence for the reverse sequence of position of *S. chlorohalonata* IBT 40285 (KL659704.1) .

Table 4-3: Reference sequences from the whole genome sequence published by Semeik *et al.*⁽⁸¹⁾ used to align all the sequences from Cruse *et al.*, Black *et al.*, and SC1.

Trichothecenes classes	Reference sequences	Positions
Chemotype S	<i>Stachybotrys chartarum</i> IBT 7711 (KL648755.1) scaf 1385 whole genome	89373 to 90599
	<i>Stachybotrys chartarum</i> IBT 40293 (KL652499.1) scaf 1227 whole genome	98983 to 100209
Chemotype A	<i>Stachybotrys chartarum</i> IBT 40288 (KL658018.1) scaf 1227 whole genome	66591 to 67817
Atronones	<i>Stachybotrys chlorohalonata</i> D13 trichodiene synthase (tri5) gene (AY095987.2)	11497 to 12722
	* <i>S. chlorohalonata</i> IBT 40285 (KL659704.1) scaf 618 whole genome	nil

*used for *in silico* PCR (Section 4.2.4)

4.2.6 *In-silico* PCR

In-silico simulation of PCR (<http://insilico.ehu.eus/>) was carried out for the primer sets to predict the product size using whole genome sequences as described previously (Section 4.2.3).

4.3 RESULTS

4.3.1 Optimisation of DNA extraction

The effects of different bead milling and incubation times were studied. All samples were disrupted using silica beads except for the sample shown in lane 6. The results showed good DNA yields for bead milling times of both 2 and 30 minutes. In fact, bead milling times of 2 and 30 minutes with several short periods of cooling on ice gave very similar results compared to a bead milling time of 1 minute (Figure 4-1). Therefore, we have subsequently established bead milling for 2 minutes with incubation on ice for 10 minutes, repeated 3 times as the optimal method.

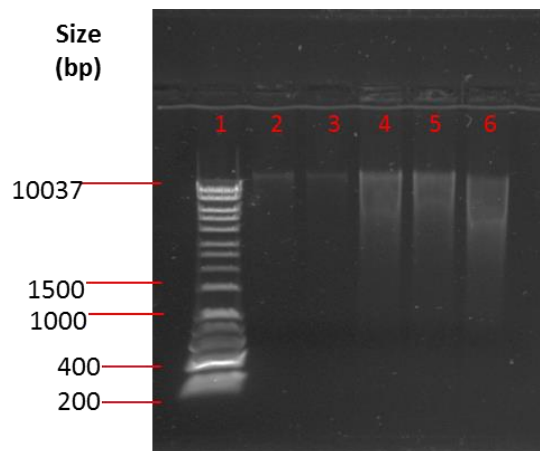


Figure 4-1: Agarose gel run PCR products of different bead-milling and incubation times. Lane 1: HyperLadder 1kb; lane 2: Beating for 1 min, incubated on ice for 1 min, repeated twice; lane 3: Beating for 1 min, incubated on ice for 1 min, repeated 4 times; lane 4: Beating for 2 mins, incubated on ice for 10 min, repeated three times; lane 5 & *6: Beating for 30 mins, incubated on ice every 5 mins. (*) indicates use of glass bead.

Good amounts of PCR products of more than 20 ng/ μ l were observed for both silica and glass beads as shown on 2% agarose gel (Figure 4-2), although, real-time PCR showed that glass beads yielded a slightly higher concentration of DNA compared to silica beads (Figure 4-3 and Figure 4-4).

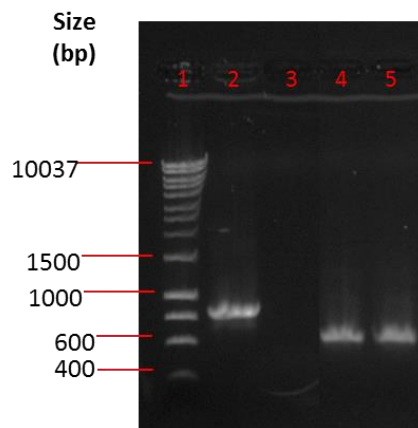


Figure 4-2: PCR results of different types of beads shown on 2% agarose gel. Samples were successfully amplified using fungal universal primers, ITS1 and ITS 4. Lane1: HyperLadder 1kb; lane 2: Positive control (*Saccharomyces cerevisiae*); lane 3: Negative control; lane 4: NCPF 7589 (Glass bead); lane 5: NCPF 7589 (Silica).

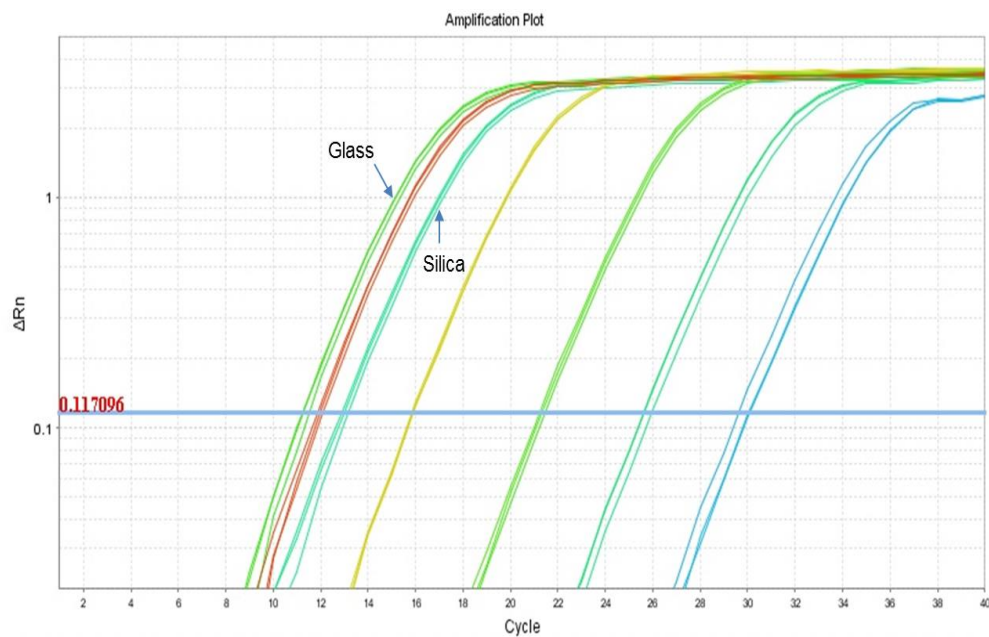


Figure 4-3: Real-time PCR graph of *S. chartarum* NCPF 7589 using ITS primers showing average CT values of 11.37 ± 0.14 and 13.05 ± 0.17 using glass beads and silica beads, respectively.

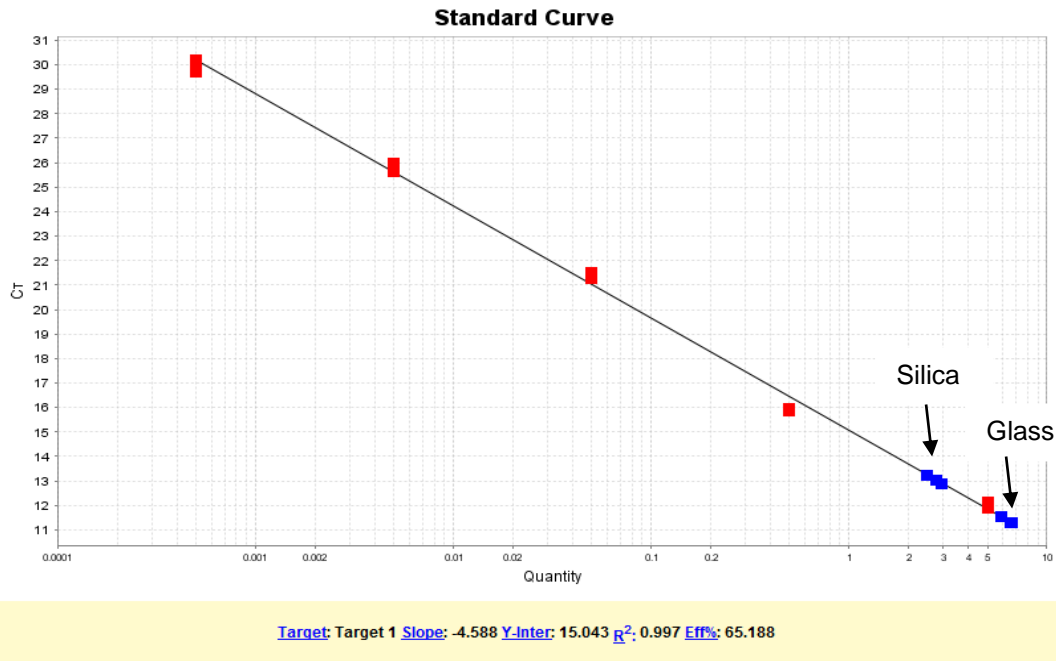


Figure 4-4: Standard curve using concentrations of amplicons produced with different types of beads showing slightly higher concentrations using glass beads compared to silica beads. The standard curve was plotted using an initial DNA concentration of 50 ng/ μ l and 10 fold serial dilutions performed in triplicate.

4.3.2 Universal primer internal transcribed spacer PCR (ITS-PCR)

For all the strains, ITS amplicons were sequenced and subjected to Basic Local Alignment Search Tool (BLAST) searches to re-confirm their identities (Table 4-4). The BLAST searches identified *S. chlorohalonata* strains (CBS 109286 and CBS 109283) as *S. chartarum*. However, both species gave high identity scores with different strains of *S. chartarum*. *S. chlorohalonata* and another 2 strains of *S. chartarum* (CU Stachy and CBS 328.37) were identified as having similarity with *S. chartarum* MUT: 5350, while *S. chartarum* (ATCC 16026, NCPF 758, CBS 324.65) and an *S. dichroa* strain (CBS 182.80) were similar to *S. chartarum* CBS 129.13.

Furthermore, some other species tested did not produce the same identity as provided in the reference strain catalogue such as *S. eonantes* (CBS 252.76) and *S. dichroa* (CBS 949.72). We also identified CBS 363.58 as *S. elegans* in this study, however it was identified as *S. bisbyi* (as catalogued by CBS) at a lower score (760) and lower percentage (97%).

Table 4-4: *Stachybotrys* spp. strains and ITS primer sequence BLAST.

Species	Strain number	BLAST ID	NCBI Accession	Max score	Total score	QC	ID
<i>S. chartarum</i>	ATCC 16026	<i>Stachybotrys chartarum</i> strain	KM231858.1	809	809	100	100
<i>S. chartarum</i>	NCPF 7587	CBS 129.13 18S ribosomal RNA gene					
<i>S. chartarum</i>	CBS 324.65						
<i>S. dichroa</i>	CBS 182.80						
<i>S. chartarum</i>	CU Stachy	<i>Stachybotrys chartarum</i> culture-collection	KU158160.1	809	809	100	100
<i>S. chlorohalonata</i>	CBS 328.37						
<i>S. chlorohalonata</i>	CBS 109286	MUT:5350 18S ribosomal RNA gene					
<i>S. chlorohalonata</i>	CBS 109283						
<i>S. oenanthes</i>	CBS 252.76	<i>Stachybotrys nephrospora</i> isolate Stanep1907; 5.8S ribosomal RNA gene	KF626486.1	877	877	100	100
<i>S. oenanthes</i>	CBS 463.74	<i>Stachybotrys oenanthes</i> 18S ribosomal RNA gene	AF081473.1	490	490	100	93
<i>S. bisbyi</i>	CBS 363.58	<i>Stachybotrys elegans</i> strain LAHC-LSPK-M15; 5.8S ribosomal RNA gene	KF815059.1	824	824	100	99
		<i>Stachybotrys bisbyi</i> 18S ribosomal RNA gene, partial sequence; internal transcribed spacer 1, 5.8S ribosomal RNA gene	AF081480.2	760	760	100	97
<i>S. bisbyi</i>	CBS 399.65	<i>Stachybotrys bisbyi</i> 18S ribosomal RNA gene	AF081480.2	944	944	100	98

<i>S. dichroa</i>	CBS 949.72	<i>Stachybotrys parvispora</i> isolate Stapar9707; 5.8S ribosomal RNA gene	KF626491.1	815	815	100	99
-------------------	------------	--	------------	-----	-----	-----	----

4.3.3 Internal transcribed spacer-restriction fragment length polymorphism PCR (ITS/RFLP-PCR)

A custom digest performed *in silico* with *HaeIII* using NEBcutter (New England BioLabs) showed the expected fragment sizes using the ITS-PCR/RFLP method. The sequences from the ITS amplicons digested with *HaeIII* enzyme were subjected to the custom digest NEBcutter (New England BioLabs). From the analysis, *HaeIII* cut at 2 sites at 'GC:CC' to produce 3 fragment sizes from *S. chartarum* or *S. chlorohalonata* amplified with ITS1 and ITS4 primers consisting of 16 bp, 96 bp and 381 bp (Figure 4-5).

```
GGGTTTTANGGCGTGG:CCGCGCTGAGCTCCGATGCGAGGTTGTA ACTACT
ACGCAGGGGAGGCTGCAGCGAGACCGCCACTGAATTTGGGGGACGGCGC
CGCACGGGGCGGG:CCGATCCCCAACACCAGGTTCCCCGCCGGAACGGGG
ACCCTGAGGGTTGAAATGACGCTCGGACAGGCATGCCCGCTAGAATGCTAA
CGGGCGCAATGTGCGTTCAAAGATTCGATGATTCACTGAATTCTGCAATTCA
CATTACTTATCGCATTTCGCTGCGTTCTTCATCGATGCCAGAGCCAAGAGAT
CCGTTGTTAAAAGTTTTGATTTATTTTTGCGTTTGCCACTCAGAGAATACTGA
AAAAACACAAGAGTTTGGGGTCTCCGGCGGGCGCCTGGATCCGGGGCGCA
GGGCGCCGGGGCGTTCCCGCCGAAGCAACGATAGGTACGGTTCACATAAG
GGTTTGGGAGTTGTAAACTCGGTAATGATCCCTCCGC
```

Figure 4-5: The output sequence for the CU Stachy isolate was obtained by using ITS4 primer. The *HaeIII* cut sites are marked in red.

The output sequence for the CU Stachy isolate was obtained by using ITS1 and ITS 4 primers. The sequence was subjected to Basic Local Alignment Search Tool (BLAST, NCBI) to produce significant alignments. Based on the search, 100 Blast hits were obtained, with identity values ranging from 96% to 99%. The isolate showed high similarity with *S. chartarum*, *S. subreniformis* and *S. chlorohalonata* (100% query cover and 99% identity). These results showed that the primers were not specific to *S. chartarum* and highlighted the need to test the strains with a more specific primer set.

The *in silico* digestion patterns were in accordance with the results obtained in this study. From the agarose gel, the largest fragments, approximately 96 bp and 381 bp, were observed for *S. chartarum* and *S. chlorohalonata*. However, the 16 bp fragments

were not shown on the gel due to the lowest marker ladder used being 25 bp. The results also indicate the same restriction patterns for all the strains of *S. chartarum* and *S. chlorohalonata* but different patterns when compared to other species (Figure 4-6).

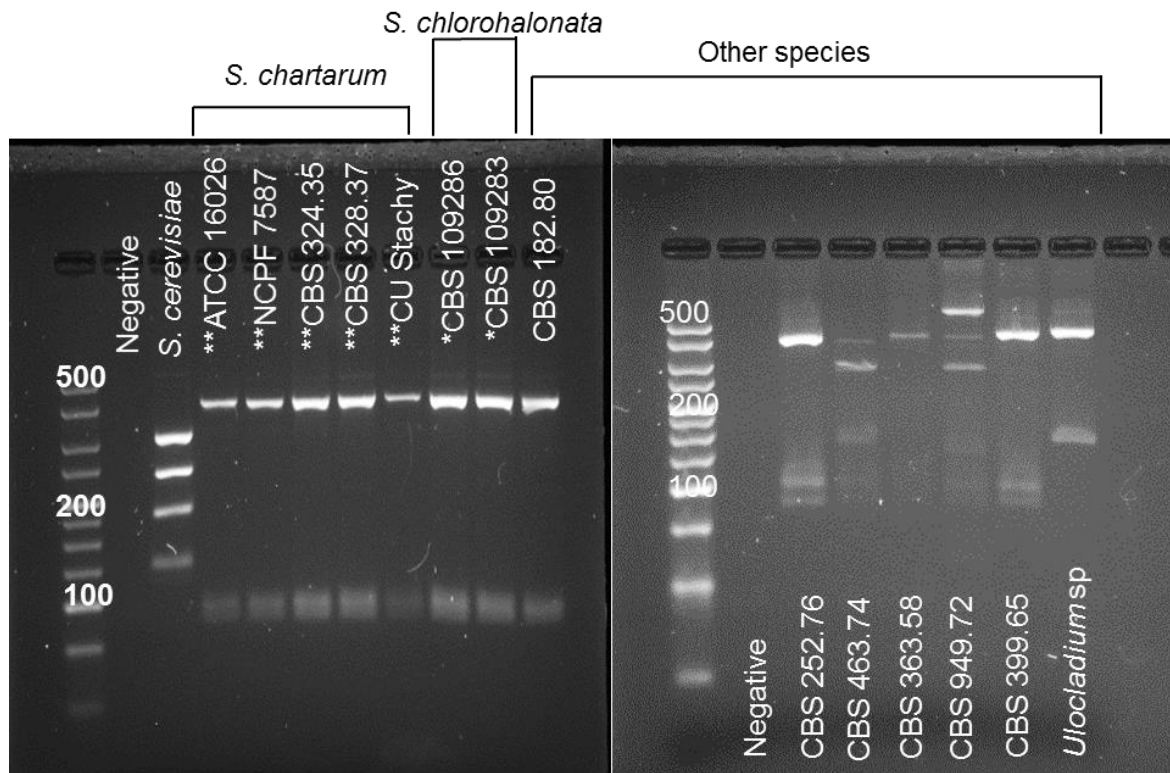


Figure 4-6: Restriction analysis of *S. chartarum* (**), *S. chlorohalonata* (*), other *Stachybotrys* spp., *S. cerevisiae* and *Ulocladium* spp. Five-microliters of PCR products digested using *Hae*III on 4% agarose gel loaded with 10 μ l samples. Different RFLP patterns were shown for species other than *S. chartarum* and *S. chlorohalonata*.

4.3.4 Trichodiene synthase genes (*tri5*)-based primers

To discriminate between *S. chartarum* and *S. chlorohalonata*, we have employed the *tri5*-based primer sets which was known to be more specific for *S. chartarum*. All of the primers tested were aligned to assess their similarity for both forward and reverse primers.

Two sets of published primers were tested and are referred to as Cruse *et al.* and Black *et al.* primers, respectively. Three strains (ATCC16026, NCPF 7587 and CU Stachy) which were identified as *S. chartarum* by the ITS primers produced similar product sizes with the individual primers (Cruse: 600 bp; Black: 130 bp, approximately) (Figure 4-7).

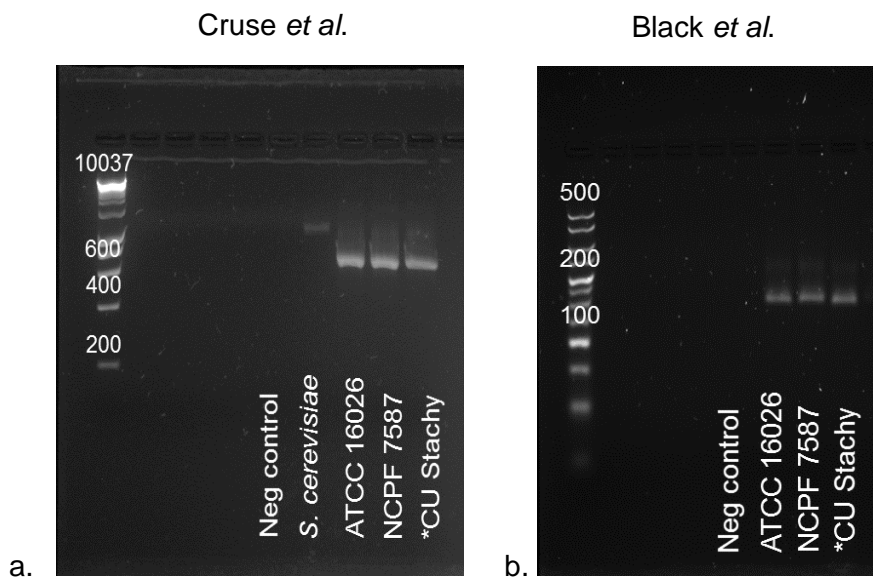


Figure 4-7: PCR products using designed *tri5* primer sets on 3 isolates of *S. chartarum* (ATCC 16026, NCPF 7587 and CU) shown on 4% agarose gel. a) Cruse *et al.*, and b) Black *et al.*

All the in-house primers were tested with the same 3 strains (Figure 4-8). All primers yielded products for all 3 strains except for SC3, which showed no product for CU Stachy.

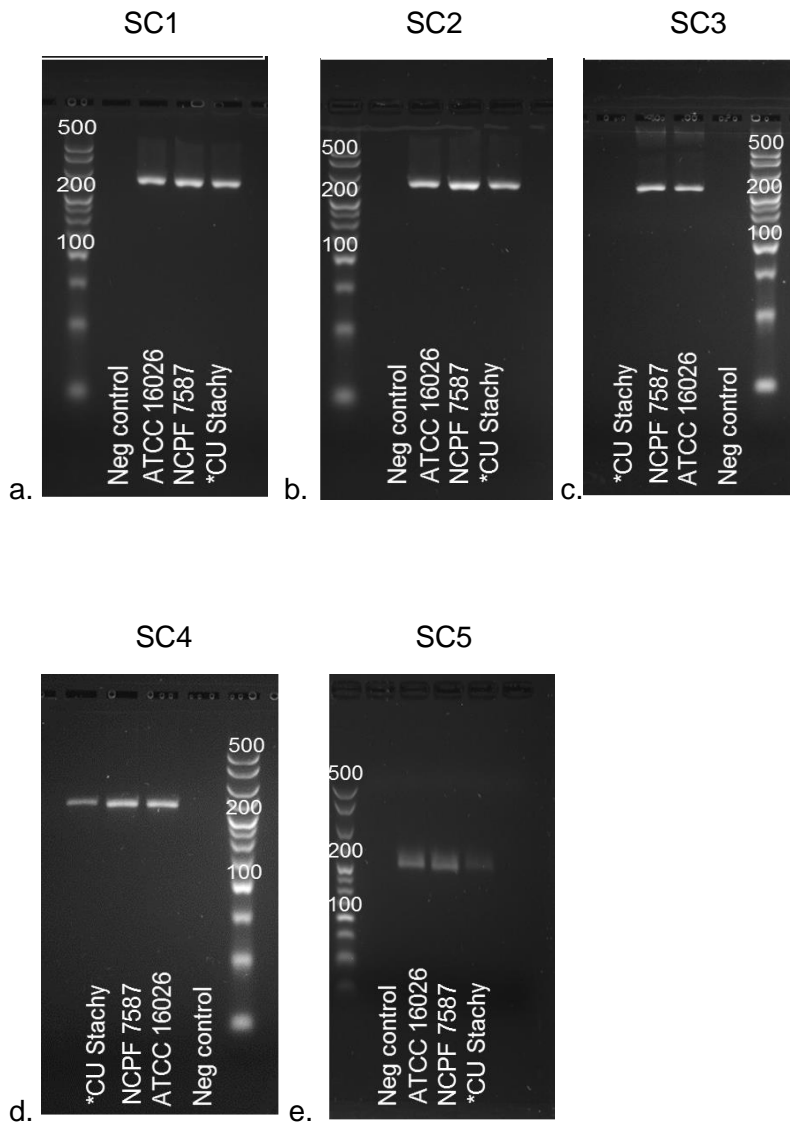


Figure 4-8: PCR products using designed tri5 primer sets on 3 isolates of *S. chartarum* (ATCC 16026, NCPF 7587 and CU) shown on 4% agarose gel. a) SC1, b) SC2, c) SC3, d) SC4 and e) SC5.

Further tests with 13 *Stachybotrys* strains showed similar results using SC1 and SC3. *S. chartarum* strains were amplified successfully using both primers, whereas SC3 showed low to no amplification of all *S. chlorohalonata* and other strains (Figure 4-9). The agarose gel showed PCR products of approximately 250 bp for SC1 and 200bp for SC3.

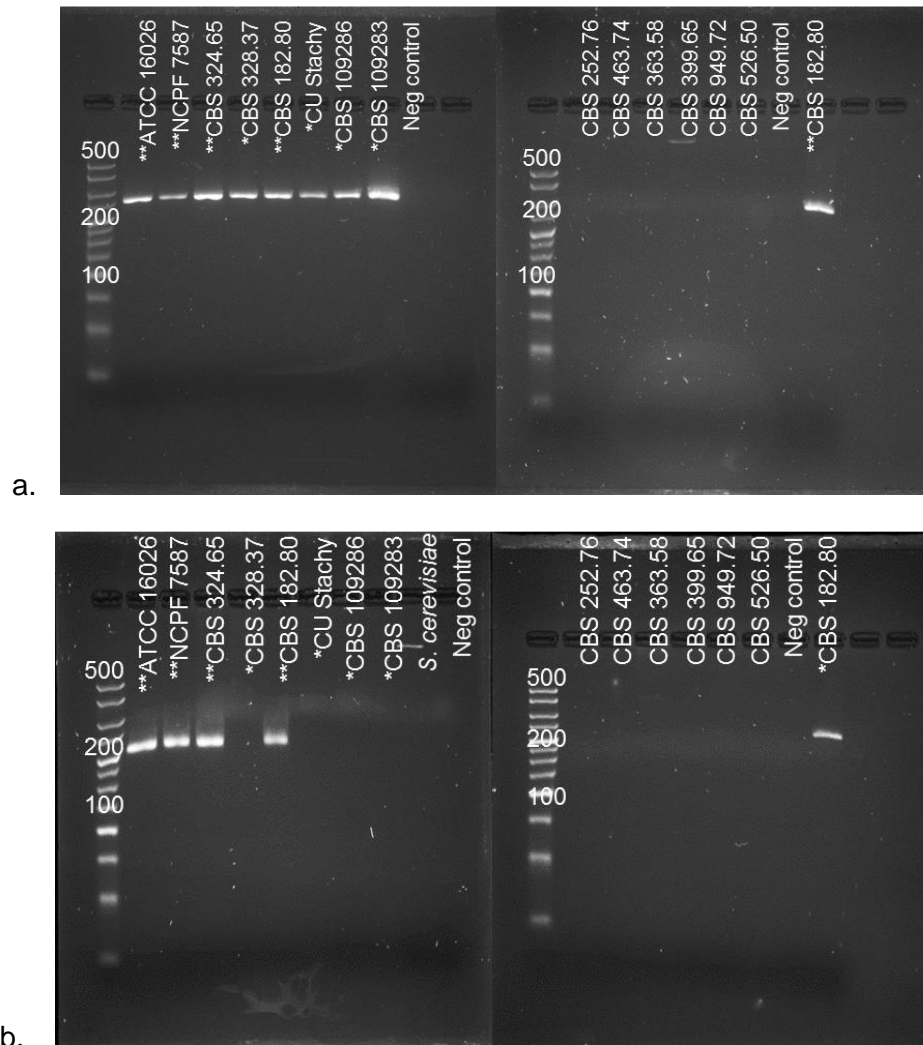


Figure 4-9: Amplification using designed tri5 primers, a) SC1 and b) SC3 on 13 isolates of *Stachybotrys* spp. (4% agarose gel). PCR products show discrimination between *S. chartarum* (), *S. chlorohalonata* (*) and other *Stachybotrys* sp.. *Saccharomyces cerevisiae* was used as a negative control.**

The PCR products were sequenced and identified using nucleotide BLAST search. Using the tri5 primers, Cruse *et al.*, Black *et al.*, and SC1, Sanger sequencing showed that CU Stachy was a *S. chlorohalonata* strain and not *S. chartarum*. The PCR products were sequenced and identified (Table 4-5 and Table 4-6). All the primers were further tested by using *in-silico* PCR. This is in line with previous results shown in figures 4.8 and 4.9.

Table 4-5: Tri5 primers sequence BLAST (*S. chartarum*). Sequences obtained from this study were identified for similarities against the GenBank database.

Strains/ Primer	Black <i>et al</i>	Cruse <i>et al</i>	SC1
ATCC 16026	<i>Stachybotrys chartarum</i> strain ATCC 16026 trichodiene synthase (tri5) gene AY180276.2 Max score:150 Total score:150 QC:100% ID:100%	<i>Stachybotrys chartarum</i> trichodiene synthase (TRI5) gene AF329103.1 Max score: 1007 Total score: 1007 QC:100% ID:100%	<i>Stachybotrys chartarum</i> strain ATCC 16026 trichodiene synthase (tri5) gene AY180276.2 Max score: 364 Total score: 364 QC:100% ID:100%
NCPF 7587	<i>Stachybotrys chartarum</i> strain ATCC 16026 trichodiene synthase (tri5) gene AY180276.2 Max score:150 Total score:150 QC:100% ID:100%	<i>Stachybotrys chartarum</i> trichodiene synthase (TRI5) gene AF329103.1 Max score: 1007 Total score:1007 QC:100% ID:100%	<i>Stachybotrys chartarum</i> strain ATCC 16026 trichodiene synthase (tri5) gene AY180276.2 Max score: 364 Total score: 364 QC:100% ID:100%
CBS 324.65	<i>Stachybotrys chartarum</i> strain ATCC 16026 trichodiene synthase (tri5) gene AY180276.2 Max score:150 Total score:150 QC:100% ID:100%	<i>Stachybotrys chartarum</i> trichodiene synthase (TRI5) gene AF329103.1 Max score:1002 Total score:1002 QC:100% ID:99%	<i>Stachybotrys chartarum</i> strain J1 trichodiene synthase (tri5) gene AY095982.1 Max score: 364 Total score: 364 QC:100% ID:100%

<p>CBS 182.80</p>	<p><i>Stachybotrys chartarum</i> strain ATCC 16026 trichodiene synthase (tri5) gene AY180276.2 Max score:150 Total score:150 QC:100% ID:100%</p>	<p><i>Stachybotrys chartarum</i> trichodiene synthase (TRI5) gene AF053926.1 Max score:1007 Max score:1007 QC:100% ID:100%</p>	<p><i>Stachybotrys chartarum</i> strain J1 trichodiene synthase (tri5) gene AY095982.1 Max score: 364 Total score: 364 QC:100% ID:100%</p>
-------------------------------------	---	--	---

Table 4-6: Tri5 primers sequence BLAST (*S. chlorohalonata*). Sequences obtained from this study were identified for similarities against the GenBank database.

Strains/ Primer	Black et al.	Cruse et al.	SC1
CU	<i>Stachybotrys chlorohalonata</i> strain D13 trichodiene synthase (tri5) gene AY095987.2 Max score:150 Total score:150 QC:100% ID:100%	<i>Stachybotrys chlorohalonata</i> strain D13 trichodiene synthase (tri5) gene AY095987.2 Max score:1000 Total score:1000 QC:100% ID:99%	<i>Stachybotrys chlorohalonata</i> strain D13 trichodiene synthase (tri5) gene AY095987.2 Max score:357 Total score:357 QC:100% ID:99%
CBS328.37	<i>Stachybotrys chlorohalonata</i> strain D13 trichodiene synthase (tri5) gene AY095987.2 Max score:150 Total score:150 QC:100% ID:100%	<i>Stachybotrys chlorohalonata</i> strain D13 trichodiene synthase (tri5) gene AY095987.2 Max score: 1000 Total score: 1000 QC: 100% ID: 99%	<i>Stachybotrys chlorohalonata</i> strain D13 trichodiene synthase (tri5) gene AY095987.2 Max score:357 Total score:357 QC:100% ID:99%
CBS 109286	<i>Stachybotrys chlorohalonata</i> strain D13 trichodiene synthase (tri5) gene, AY095987.2 Max score:150 Total score:150 QC:100% ID:100%	<i>Stachybotrys chlorohalonata</i> strain D13 trichodiene synthase (tri5) gene AY095987.2 Max score:1005 Max score:1005 QC: 100% ID:100%	<i>Stachybotrys chlorohalonata</i> strain D13 trichodiene synthase (tri5) gene AY095987.2 Max score:357 Total score:357 QC:100% ID:99%
CBS 109283	<i>Stachybotrys chlorohalonata</i> strain D13 trichodiene synthase (tri5) gene AY095987.2 Max score:150 Total score:150 QC:100% ID:100%	<i>Stachybotrys chlorohalonata</i> strain D13 trichodiene synthase (tri5) gene AY095987.2 Max score:1005 Max score:1005 QC: 100% ID:100%	<i>Stachybotrys chlorohalonata</i> strain D13 trichodiene synthase (tri5) gene AY095987.2 Max score:357 Total score:357 QC:100% ID:99%

These showed CU Stachy and CBS 328.37 to be *S. chlorohalonata* (previously identified as *S. chartarum*) and CBS 182.80 as *S. chartarum* (previously identified as *S. dichroa*).

Sequences from all the 3 primers were aligned with a *S. chartarum* (AF329103.1) sequence from NCBI (Appendix 4-B). Sequences from Cruse *et al.* amplified products showed consensus from nucleotide position 2 to 546, from SC1 products from nucleotide position 463 to 659 and from Black *et al.* products there was sequence overlapping with the other 2 primer products from nucleotide position 512 to 592 (Appendix 4-C).

Sequence alignments with individual primer sets produced a nucleotide consensus for *S. chartarum* and *S. chlorohalonata* (Cruse primers: 94.3% identity; SC1 primers: 90.8% identity and Black primers: 92.6% identity). The 2 primer sets, Cruse *et al.* and SC1 were combined and aligned with (AF329103.1) to standardise and to determine nucleotide differences in *S. chartarum* and *S. chlorohalonata* sequences. Consistent nucleotide differences were observed between both species (Figure 4-10).

Chapter 4: DNA-based methods

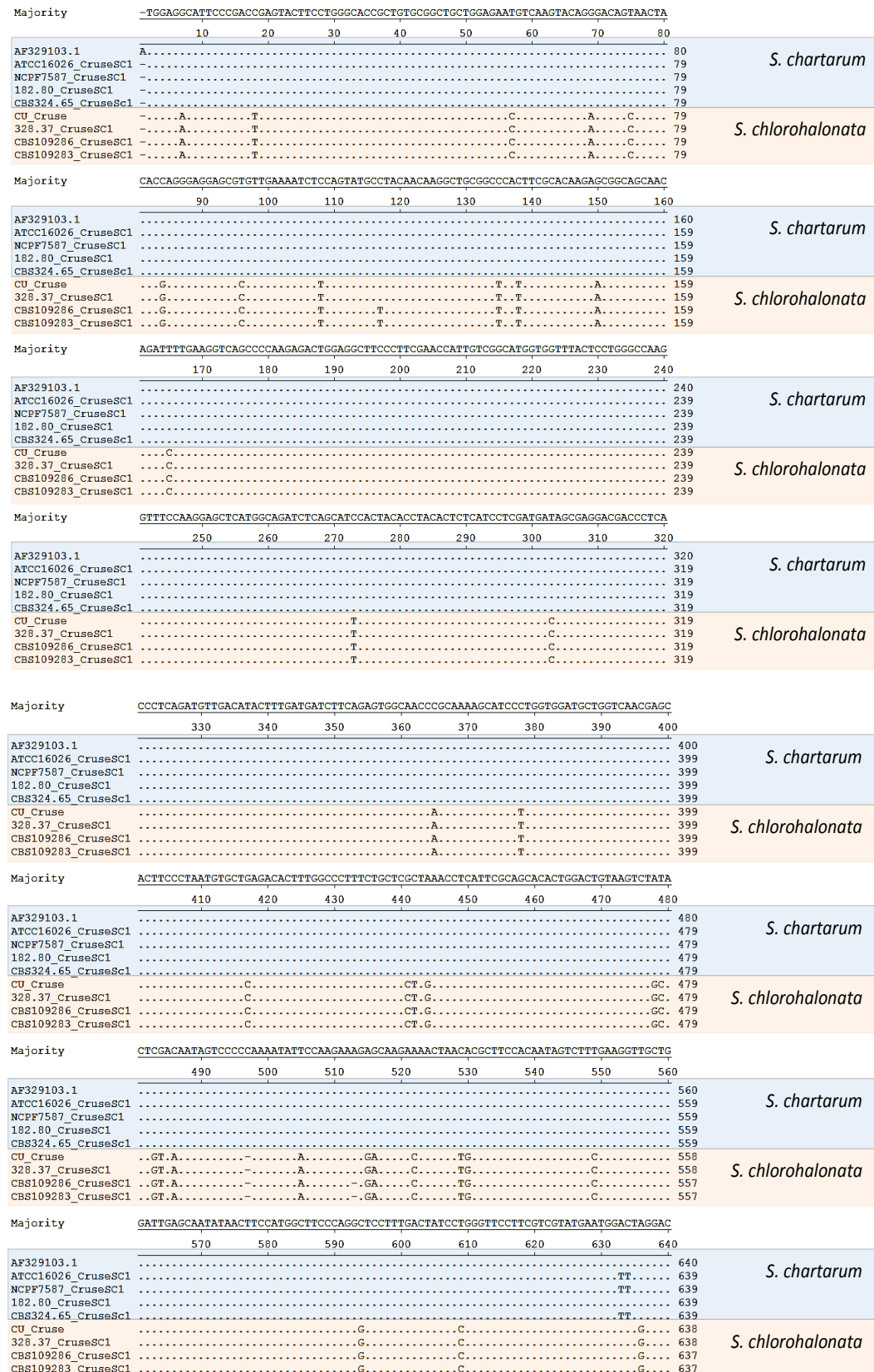


Figure 4-10: Nucleotide differences in *S. chartarum* and *S. chlorohalonata* isolates constructed from the longest sequence to the left, Cruse *et al.* and the longest sequence to the right, SC1. A known *Stachybotrys chartarum* sequence (NCBI Number AF 329103.1) was included in the sequence alignment to standardise the nucleotide position.

The nucleotide differences in *S. chartarum* and *S. chlorohalonata* are summarised in Table 4-7.

Table 4-7: Summary of nucleotides differences in *S. chartarum* and its cryptic species, *S. chlorohalonata* from consensus sequences of *Cruse et al.* and SC1.

	Nucleotide position	Nucleotide differences
<i>S. chartarum</i> versus <i>S. chlorohalonata</i>	478-79	AT → GC
	483-84	CG → GT
	486	C → A
	496	C → -
	505	T → A
	515-516	AG → GA
	522	A → C
	529-30	CA → TG
	549	T → C
	594	C → G
	609	T → C
635	T → G	

The sequences from all the 3 primer sets were aligned with whole genome sequences reference strain of *S. chlorohalonata* and *S. chartarum* chemotypes A and S to group them phylogenetically ⁽⁸¹⁾ (Figure 4-11). From the result, we have observed a distinct tree divergence between both species of *S. chartarum* and *S. chlorohalonata* as shown in the blue and green boxes for all 3 primer sets. The *S. chartarum* strains were closely grouped as chemotypes S by all the 3 primer sets. Therefore, it is concluded that *S. chlorohalonata* is best described as a cryptic species within the *S. chartarum* species complex.

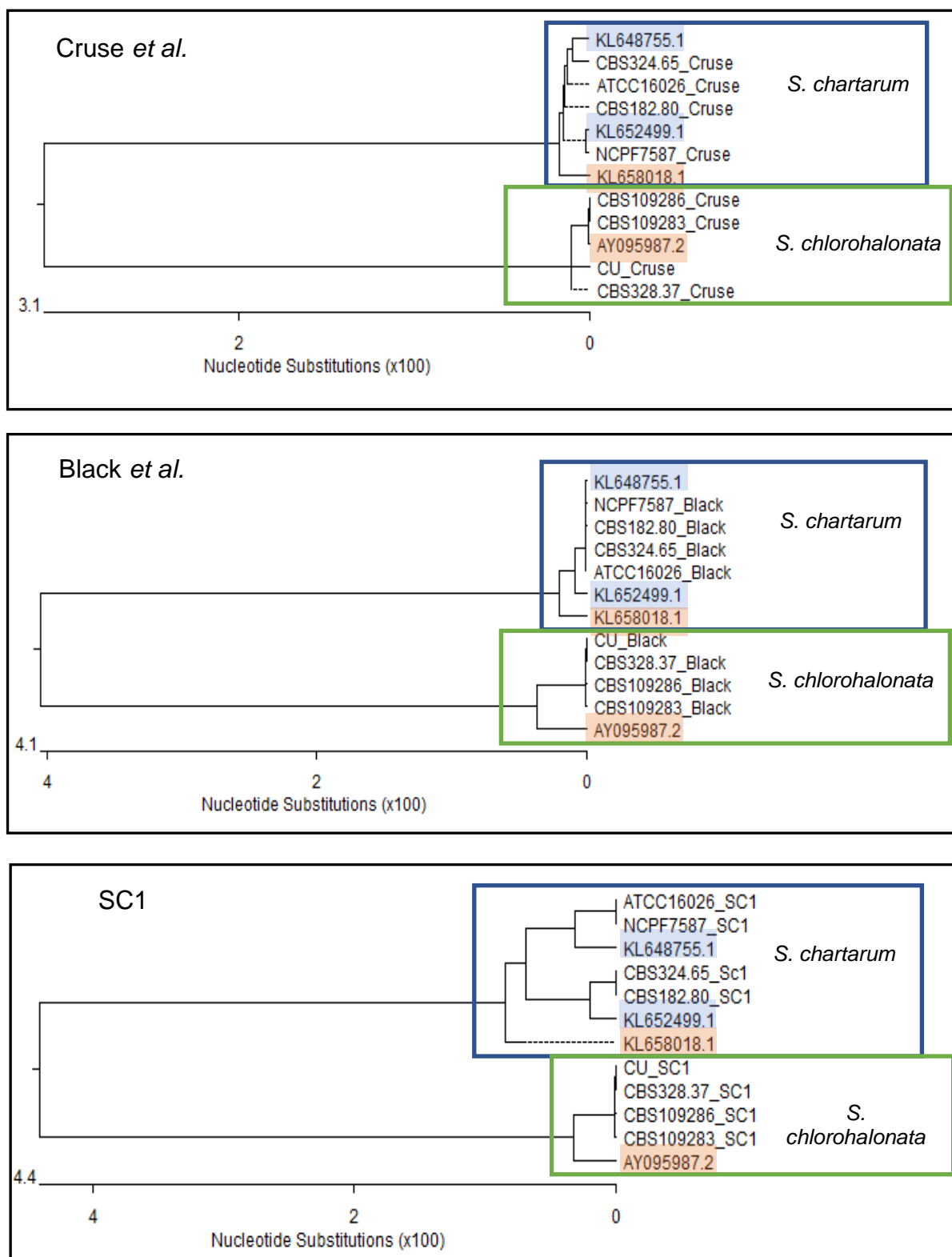


Figure 4-11: Differences in phylogenetic tree of Cruse *et al.*, Black *et al.* and SC1 built with published sequences from *S. chartarum* and *S. chlorohalonata*. Chemotypes S (blue) = *S. chartarum* IBT 7711 (KL648755.1) and *S. chartarum* IBT 40293 (KL652499.1), chemotypes A (orange) = *S. chartarum* IBT 40288 (KL658018.1) and *S. chlorohalonata* strain D13 trichodiene synthase (*tri5*) gene (AY095987.2).

The consensus sequences (with at least sequences from 2 primer sets overlapping) were generated and reanalysed with the reference strains. From the result, more distinct groups were observed compared to individual primer analysis (Figure 4-12).

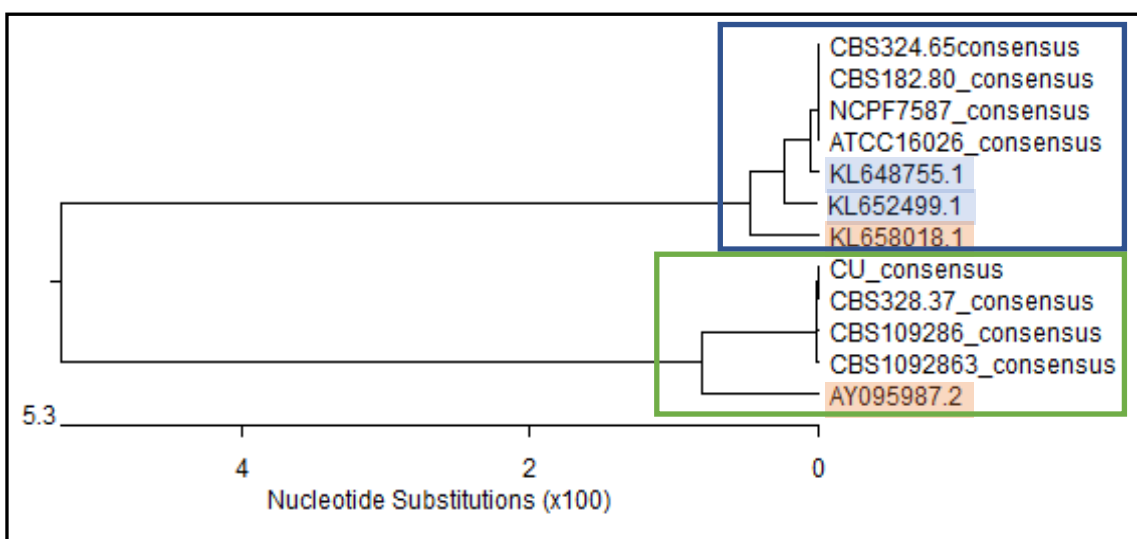


Figure 4-12: Phylogenetic tree of the nucleotide consensus Cruse *et al.*, Black *et al.* and SC1 built with published sequences from *S. chartarum* and *S. chlorohalonata*. Chemotypes S (blue) = *S. chartarum* IBT 7711 (KL648755.1) and *S. chartarum* IBT 40293 (KL652499.1), chemotypes A (orange) = *S. chartarum* IBT 40288 (KL658018.1) and *S. chlorohalonata* strain D13 trichodiene synthase (*tri5*) gene (AY095987.2).

4.3.5 *In-silico* PCR

The *in-silico* PCR was used to simulate the PCR reactions for all the isolates of *Stachybotrys* sp. using the 2 sets of published primers and SC1 and SC3 from this study and to predict product sizes (Table 4-8). *In-silico* PCR using all the *tri5* primers was also performed against 2 sets of whole genome sequences, *Stachybotrys chartarum* IBT 40293 (KL652499.1) and *Stachybotrys chlorohalonata* IBT 40285 (KL659704.1).

The results showed that all *S. chartarum* sequences generated the same product size using all the primer sets, with slightly lower size for *S. chlorohalonata*. Using the *in silico* PCR, the product sizes for the two species using the *tri5* primers and the Black *et al.* and Cruse *et al.* primers differed by only 1 bp and 3 bp, respectively but could be distinguished by Sanger sequencing. Primer SC3 *tri5* amplified all *S. chartarum* strains but not *S. chlorohalonata* (in accordance with the agarose gel - see figure 4.8).

Table 4-8: *In-silico* PCR using 2 sets of whole genome sequences of *S. chartarum* (KL652499.1) and *S. chlorohalonata* (*KL659704.1) ⁽⁸¹⁾.

Primer name	Species	NCBI Accession	Positions in whole genome sequences (bp)	<i>In-silico</i> product length (bp)
Tri5 [Black <i>et al.</i>]	<i>S. chartarum</i>	KL652499.1	99493	136
	<i>S. chlorohalonata</i>	*KL659704.1	12185	135
Tri5 [Cruse <i>et al.</i>]	<i>S. chartarum</i>	KL652499.1	98953	641
	<i>S. chlorohalonata</i>	*KL659704.1	12220	638
Primer SC1tri5	<i>S. chartarum</i>	KL652499.1	99451	247
	<i>S. chlorohalonata</i>	*KL659704.1	12116	246
Primer SC2tri5	<i>S. chartarum</i>	KL652499.1	99451	248
	<i>S. chlorohalonata</i>	*KL659704.1	12115	247
Primer SC3tri5	<i>S. chartarum</i>	KL652499.1	99527	202
	<i>S. chlorohalonata</i>	*KL659704.1	Not available	no amplification
Primer SC4tri5	<i>S. chartarum</i>	KL652499.1	99529	209
	<i>S. chlorohalonata</i>	*KL659704.1	12077	209
Primer SC5tri5	<i>S. chartarum</i>	KL652499.1	99527	197
	<i>S. chlorohalonata</i>	*KL659704.1	Not available	no amplification

4.4 DISCUSSION

Classical methods for fungal identification are based on conventional techniques such as culture, staining and microscopic examination. *Stachybotrys chartarum* is a slow to moderately rapid growing fungus, usually matured at approximately 7-14 days on medium with high cellulose content ⁽⁹¹⁾. Most *S. chartarum* strains have a white surface which later becomes dark grey to black effuse, and the reverse morphology is colourless then turning black when aged ^(91, 92). However, not all *S. chartarum* strains have the same appearance making macroscopic identification more difficult (as described previously in chapter 3). Their morphologies also vary depending on the types of media used, temperature and period of incubation period ⁽¹⁵⁰⁾. Culture based identification of *S. chartarum* can be a challenge when the isolate is not fully developed. In this study, a total of 13 *Stachybotrys* strains representing 5 different species were tested using universal primers, ITS-PCR/RFLP and specific primers based on the trichodiene synthase gene (tri5).

4.4.1 Optimisation of DNA extraction

Fungal spores are known to have higher resistance to harsh conditions, such as chemical and physical treatment. In the laboratory, fungal spores are known to resist lysis and DNA extraction ⁽¹⁶³⁾. There is also potential loss of DNA during extractions, due to the treatment required for cell wall breakdown. Furthermore, most *Stachybotrys* sp. are pigmented which makes extraction more difficult.

In this study, DNA extraction was optimised by combining mechanical treatments prior to extraction. Studies have compared various kits such as SV Genomics (Madison, WI), Qiagen Tissue (Qiagen, Valencia, CA) and Qiagen Plant (Qiagen, Valencia, Ca) ^(163, 218). The method using DNeasy® Plant MiniKit (Qiagen) is simple and quick. Moreover, it gives sufficient yields of DNA for PCR amplification and visualisation on agarose gels. To improve yield, we have incorporated bead milling for 2 minutes and incubation on ice for 10 minutes, repeated 3 times using glass beads. The freeze-thaw technique and bead milling has been shown to enhance fungal cell lysis ^(71, 218). The supernatant was further purified using DNeasy® Plant MiniKit (Qiagen). During the process, *S. chartarum* spores tended to clump in the buffer suspension and hinder the process of cell washing, breakage and DNA extraction. This is due to the unique cysteine-rich protein called hydrophobin present in filamentous fungi which forms a hydrophobic coating in fungal spores ⁽²¹⁹⁾. The addition of Tween 20 reduced the hydrophobicity of the spores and increased the surface area for cell washing and lysis with bead milling.

In other studies, the use of the phenol:chloroform method has been a common technique for DNA extraction ^(103, 220). However, we wanted to avoid using these toxic chemical in the laboratories.

4.4.2 Internal transcribed spacer- restriction fragment length polymorphism (ITS/RFLP-PCR)

In most laboratories, the use of the ribosomal DNA (rDNA) complex has been the gene target of choice in fungal molecular identification. ITS-PCR has been widely used in distinguishing closely related fungal species, especially in distinguishing fungal samples from different environments ^(102, 221). In this study, the universal primer pair, ITS1/ITS4 was employed and complemented with RFLP to try to generate species specific patterns ⁽¹⁰³⁾.

However, we have found that the ITS1/ITS4 primers were unable to properly distinguish between *S. chartarum* and *S. chlorohalonata*. This was shown by the same product sizes on agarose gel and the BLAST sequences which identified *S. chlorohalonata* strains as *S. chartarum*. These indicate non-specificity of the fungal universal primer and the *Hae*III restriction patterns in distinguishing both species within this closely-related and species complex fungi.

Furthermore, some other species tested such as *S. eonanthes* (CBS 252.76) and *S. dichroa* (CBS 949.72) did not produce the same identity as provided by the reference source. We also found that CBS 363.58 was identified as *S. elegans* in this study, however it was also matched with *S. bisbyi* (as catalogued by CBS) at a lower score (760) and lower percentage (97%).

Since ITS1/ITS4 primer pair is broad spectrum primers, they are able to identify *Stachybotrys* spp. other than *S. chartarum* and *S. chlorohalonata*. Several studies have developed or reviewed other primers in various ITS regions such as ITS1 region (ITS1F/ITS86R), ITS2 region (ITS86F/ITS4), or ITS 1 and 2 regions (ITS1F/ITS4B) for more specific identification in fungal community studies ^(222, 223).

The choice of primer pair certainly has an important role in accurate identification. Bellemain *et al.*⁽¹⁶²⁾ has reported potential biases in different parts of the ITS region and suggested that combinations of different primers should be used and analysed in parallel or for new ITS primers should be developed if they fail to provide correct identification.

Furthermore, the identification may vary depending on the sequences deposited in databases search. There are numerous public databases for organisms such as Genbank NCBI as well as curated specialty databases such as Mycobank for fungi ^(224, 225). In this study, Genbank NCBI was employed as the standard nomenclature and classification repository by current consensus in the systematic literature ⁽²²⁵⁾. The identification obtained very much depends on the sequences submitted by the depositors, or on genomic data being represented from different loci, or lack of sequence information on *Stachybotrys* spp. strains that require more research. To date, there are 11301 genome sequences of *Stachybotrys* spp. in Genbank NCBI compared to more than 200 000 sequences of the other indoor moulds, *Aspergillus* spp. and *Penicillium* spp. (last accessed 13/09/2016).

The misidentifications which occurred in this study highlighted the need for a more standardised method to identify *Stachybotrys* spp.. Although ITS1/ITS4 is considered

as a universal primer, they are not adequate to give accurate identification of *Stachybotrys* spp..

4.4.3 Tri5-based primers

Another distinct characteristic which can be used to classify *Stachybotrys* spp. are the mycotoxins they produce. *S. chartarum*, for example, is a known producer of a number of potent mycotoxins particularly those derived from the trichothecenes biosynthetic pathway⁽⁷⁷⁾. Thus far, the primers by Cruse *et al.* have been noted as the most reliable PCR-based method to differentiate *S. chartarum* chemotypes A and S as a result of a 1 bp difference; in addition to direct toxin identification using LC-MS/MS from spores suspension or guttation droplets^(226, 227). Other methods for direct toxin identification include the MTT and the ELISA assays⁽²⁰⁹⁾. In this study, we have limited the scope to using the PCR technique with the main aim of identifying the species and simultaneously classifying the chemotype using phylogenetics analysis.

Different primers have been compared in several studies. For example, Andersen *et al.*⁽¹¹⁾ reported that gene fragment sequences of tri5, chitin synthase 1 (chs1) and beta-tubulin 1 (tub1) can differentiate between *S. chartarum* and *S. chlorohalonata*. Further differentiation of *S. chartarum* chemotypes was shown by a one nucleotide difference in the tri5 and chs1 gene fragments, but no difference in the tub1 gene fragment. Black *et al.*⁽¹⁰⁵⁾ reported greater specificity for *S. chartarum* identification using primers from tri5 and beta-tubulin regions than for rRNA region primers (18S rRNA and 28 S, LSU rRNA) tested with other environmental fungi such as *Alternaria* sp., *Aspergillus fumigatus*, *A. versicolor*, *Cladosporium* spp. and *Penicillium* spp..

In this study, an environmental isolate, CU Stachy which was provided as a known strain of *S. chartarum* was compared to two *S. chartarum* reference strains. In the preliminary experiment, we had successfully amplified the NCPF 7587, ATCC 16026 and CU Stachy strains using the ITS primers. This was followed by product sequencing which identified all strains as *S. chartarum*. However, this was contradictory to the results from the tri5 primer, SC3 where one of the strains, CU Stachy, failed to amplify. Initially, CU Stachy was hypothesised to be a *S. chartarum* strain from a different clade since the strain was obtained from the environment and had not been characterised before. In a previous study, Peltola *et al.*⁽²²⁸⁾ reported that using their novel tri5 genes primers, only 22 out of 33 isolates of *S. chartarum* were tri5 positive (associated with the production of satratoxin or trichodermol).

In fact, despite finding similar product sizes between all the tri5 products across all the 3 strains, we were able to distinguish *S. chartarum* from *S. chlorohalonata* by Sanger sequencing. With the extended number of strains, the BLAST search showed CU Stachy (and CBS 328.37), identified as *S. chartarum*, were actually *S. chlorohalonata*. The result is in accordance with Lombart *et al.*⁽²²⁹⁾ who re-identified CBS 328.37 and CBS 182.80 as *S. chlorohalonata* and *S. chartarum*, respectively.

Following identification using universal primers ITS1/ITS4 for all *Stachybotrys* spp., further analysis of identified *S. chartarum* strains using tri5 primers, particularly with SC3, provides more discrimination of the closely related species *S. chlorohalonata*. Protein-based MALDI-TOF analysis has also been widely studied for the rapid microbiological identification of fungi, including *Stachybotrys* spp. ^(106, 107). Since this analysis is related to the detection of ribosomal proteins, it has been reported as not being able to distinguish species with no significant differences in their ribosomal gene sequences. This indicates that specific DNA-based methods, using alternative targets, are still required in some cases ⁽²³⁰⁾.

4.4.4 Sequence alignment and phylogenetics analysis

Sequence alignment showed the degree of nucleotide sequence similarity in *S. chartarum* and *S. chlorohalonata*. The sequence analysis was performed with a *Stachybotrys* sp. reference whole genome sequence.⁽⁸¹⁾ Alignment with other deposited chemotype sequences could lead to biases depending on the primer used for amplification and sequencing. The sequences obtained from all 3 primer sets showed agreement in nucleotide alignment between both species. Although there were only a few nucleotide differences seen between the species, they allowed classification into different chemotype classes. From the findings, we have observed a distinct tree divergence between the species *S. chartarum* and *S. chlorohalonata* in all 3 primer sets, respectively (Figure 4-11 and Figure 4-12). The SC1 primer in our study provides the lowest similarity (i.e. the greatest discrimination) between these 2 species compared to the previously published primers (Cruse primer: 94.3%, Black primer: 92.6% and SC1: 90.8% identities). There were some differences in the dendrogram distances for the different chemotypes of *S. chartarum*. However, the chemotype S *S. chartarum* strains were closely grouped by all 3 primers. However, the consensus sequences showed more distinct groups compared to individual primer analysis (Figure 4-12).

Previous studies have utilised *tri5* as a tool to explore morphologically closely related species using phylogenetic analyses. Cruse *et al.* revealed 2 phylogenetically distinct groups from strains of the single species *S. chartarum* using *tri5*, *tub2* and chitin synthase 1⁽¹²⁾. This was confirmed by Andersen *et al.* who segregated *S. chartarum sensu lato* into 2 chemotypes with only 1 nucleotide difference in *tri5* and *chs1*; and a new species, *S. chlorohalonata*⁽¹¹⁾. Semeiks *et al.*⁽⁸¹⁾ have also documented chemotype-specific gene clusters in *Stachybotrys* spp by using comparative genome sequencing. The chemotypes A or S are widely used to distinguished *S. chartarum*, either it is an atronones producer or a highly toxic macrocyclic trichothecene producer or an atronones producing *S. chlorohalonata*. The reason behind this is not clear, but generally, mycotoxin production is thought to be a defence mechanism and as adaptation to the environment⁽⁷⁷⁾.

Studies have also revealed different metabolite profiles of *Stachybotrys* spp. are produced on various substrates such as building materials, wood, fabric, plant or soil or even strains isolated from the same water-damaged environment^(94, 226). This suggests the toxicity of *Stachybotrys* spp. varies even within the same species and strain.

Using phylogenetic analysis, *tri5* genes in *Stachybotrys* spp. have been shown to be consistent with toxin production and that they are highly conserved at the amino acid level⁽¹¹⁸⁾. The phylogenetic analysis showed distinct tree divergence between *S. chartarum* and *S. chlorohalonata* using the Cruse *et al.*, Black *et al.* and the novel SC1 primer set. Although the chemotype patterns were not identical, consensus *tri5* sequences produced a more distinct correlation compared to individual primers, likely due to different nucleotide coverage and positions.

4.4.5 *In-silico* PCR

In addition to PCR, we have employed *in-silico* PCR with the *tri5* genes within the whole genome sequences of both *S. chartarum* and *S. chlorohalonata* to determine expected product sizes and positions amplified in the whole genome sequence. *In silico* PCR has been regarded as a complementary method to determine primer specificity using web-based tools prior to 'wet' laboratory experiments⁽²³¹⁾.

The findings predicted that the specificity of the primer SC3 compared to other primers would quickly discriminate *S. chartarum* and *S. chlorohalonata* using only PCR. This suggests that the SC3 primer set can be used as a fast screening method for distinguishing *S. chartarum* and *S. chlorohalonata* without the need for sequence analysis to identify both species.

4.5 CONCLUSIONS

In conclusion, the trichodiene synthase gene-based primers (tri5) are useful in aiding the specific identification of the *S. chartarum* complex and offer a solution to species misidentification by the standard ITS1/ITS4 primer method. Moreover, tri5-based primers provide information on chemotype classes and therefore could facilitate an assessment of health risk in *Stachybotrys* spp. infested buildings. This study also highlighted the needs to use highly discriminatory identification methods for *Stachybotrys* spp. in the future.

CHAPTER 5

IDENTIFICATION OF *STACHYBOTRYS* *CHARTARUM* USING MATRIX ASSISTED LASER DESORPTION IONISATION – TIME OF FLIGHT (MALDI-TOF)

This chapter presents the work on the construction of mass spectral profiles (MSPs) using MALDI-TOF and the Bruker database as the platform for a more rapid and reliable identification of *S. chartarum*.

5.1 INTRODUCTION

A rapid, reliable and low cost method has always been the goal in laboratories especially when dealing with routine mycological diagnostics. Apart from conventional methods and identification from DNA sequence using polymerase chain reaction (PCR) (as discussed in previous chapters), identification of fungi has expanded to include the utilisation of protein profiles generated by matrix- assisted laser desorption ionisation-time of flight (MALDI-TOF). With the advancement in mass spectrometry, fungal identification has become less laborious, less time-consuming, with a low operational cost and high specificity.

Several studies have been conducted in relation to the development of protein profiles of *Stachybotrys* spp. using MALDI-TOF particularly on the effects of pigment on the quality of spectra ^(106, 107, 172). MSPs for *Stachybotrys* spp. have been established in-house by many researchers resulting in different cut-off points for the score values. Various techniques and modifications were performed by different researchers with

regard to *Stachybotrys* spp. to obtain good spectra and this makes it difficult to apply consistent methods for all fungi encountered on the diagnostic laboratory. Furthermore, there was no available MSPs of *S. chartarum* in the existing Bruker database and therefore, it was a requirement to establish our own in-house MSPs to aid with the identification. This study aimed to establish and identify *S. chartarum* using the MALDI-TOF mass spectrometer by using the standardised protocol for filamentous fungi provided by Bruker Daltonics. We have also studied the effects of different growth conditions and media choices to determine the suitability of this standard method.

5.2 MATERIALS AND METHODS

5.2.1 Reference strains and fungal isolates

NCPF 7587 (Public Health England) was used as the reference isolate for *S. chartarum*, and *Aspergillus niger* (ATCC 16888) obtained from American Type Culture Collection was used as a control organism. In total, 13 *Stachybotrys* spp. isolates representing 5 different species were tested. Other *Stachybotrys* spp. strains were obtained from The Centraalbureau voor Schimmelcultures (CBS) Fungal Biodiversity Centre and Cranfield University.

5.2.2 Fungal culture

All isolates had been identified using ITS1/ITS4 and *S. chartarum* and *S. chorohalonata* were further identified using tri5-based primers by Black *et al.*, Cruse *et al.* and in-house developed primers, SC1 and SC3 (see chapter 4). ATCC 16888 was used as a control for the extraction process and MALDI-TOF identification. Initially, fungi were grown on Sabouraud dextrose, modified agar (ESA) (Cat No. 27420, BD Difco) at 25 °C under aerobic conditions. The plates were incubated for 7 days due to the characteristics of *Stachybotrys* spp. as slow-growing fungi and to achieve good sporulation. The 7-day old fungal spores were inoculated in 10 mL liquid medium containing either Sabouraud dextrose broth (SDB) (Cat No. 238230, BD Difco) or potato dextrose broth (PDB) (Cat no. P6685, Fluka Analytical) by using sterile swabs and further incubated using a SB2 rotator (Order no. Y552.1, Carl Roth GmbH & Co KG) at 20 rpm. A negative control of only medium without spores was included to rule out any environmental contamination.

5.2.3 Protein extraction

5.2.3.1 Protein extraction from liquid media

Tubes containing fungal mass were removed from the rotator after 24 hours or 48 hours. The tubes were placed on the bench for approximately 10 minutes to form sediment at the bottom of the tubes. The fungal sediment was transferred into microtubes up to 1.5 mL using a disposable pipette, followed by centrifugation at 13,000 rpm (12,470 x g) for 2 minutes. The resultant supernatant was discarded and the pellet was resuspended in 1 mL HPLC-grade water to wash out the liquid medium. The process of centrifugation and resuspension was repeated until no bubbles in the medium were present and a well-defined pellet was obtained. Presence of bubbles was used as an indication that liquid medium was still present in the tube. This process was repeated two or three times. Once a well-defined pellet was obtained, the pellet was resuspended again in HPLC-grade water, vortexed for 1 minute, and centrifuged again at 13,000 rpm (12,470 x g) for 2 minutes. The process was repeated once.

Next, the pellet was resuspended in 300 μ L HPLC-grade water and 900 μ L ethanol (Cat no. E7148, Sigma-Aldrich) followed by centrifugation at 13,000 rpm (12,470 x g) for 2 minutes. The supernatant was discarded and the pellet left to dry for about 30 minutes to completely remove the residual ethanol. The extraction efficiency could be reduced if residual ethanol was too high or the pellet was over-dried and could not be resuspended effectively. The dried pellet was resuspended in freshly prepared 70% formic acid (Cat no. 56302, Fluka) proportional to the size of the pellet and incubated for 5 minutes at room temperature. Then, the same volume of acetonitrile (Cat no.10660131, Fisher Scientific) was added and thoroughly mixed followed by centrifugation at 13,000 rpm (12,470 x g) for 2 minutes. A few additional steps of 30 s centrifugation at 13,000 rpm (12,470 x g) to obtain a supernatant free from floating debris, were performed followed by gentle mixing prior to spotting on the target plate.

One-microliter of sample was taken by gentle mixing of the top layer of the supernatant and was spotted carefully onto the disposable MALDI target plate (Cat no 8268711, Bruker). The sample spots were left to dry for approximately 5 minutes (not to over-dry) followed by layering with 1 μ L matrix. A minimum of 8 spots were loaded for each sample per extraction for the construction of MSPs. The MALDI target plate was transported in a MALDI Biotarget Transport box (Cat no. 8270006, Bruker) and was inserted in a MSP Biotarget Adapter (Cat no. 8267615, Bruker) before loading into the MALDI-TOF machine (Figure 5-1).



Figure 5-1: A Biotarget adapter was required to fit in the Biotarget plate into the MALDI-TOF Microflex instrument.

5.2.3.2 Protein extraction from solid media

Fungal colonies were swabbed with moistened cotton at the middle-ring part from the between the centre and edges. This was consistently done each time to minimise the difference of protein patterns due to different phases of growth on the solid media. The fungal samples were emulsified in HPLC-grade water, vortexed for 10 s and centrifuged for 30 s at 13,000 rpm (12,470 x g). The pellet was resuspended with 250 μ l ethanol and mixed thoroughly. The suspension was transferred into a new tube containing 50 μ l 0.1 mm diameter Zirconia/silica beads (Cat no 11079101Z, Biospec) and vortexed for 15 minutes. The suspension was transferred to a new tube avoiding beads, and was spun down at 12,000 rpm (10,625 x g) to obtain a strong pellet and to remove any floating debris followed by the protocol as recommended by Bruker. Samples were cleaned-up by washing thoroughly several times with ultrapure water to get rid of colours and possible contaminants that could affect the mass spectra.

5.2.4 Preparation of Bruker Matrix HCCA, portioned

HCCA (α -Cyano-4-hydroxycinnamic acid) matrix, portioned solution (Cat no. 8255344, Bruker) was used as the matrix following the standard protocol. The dried HCCA was kept at 4 $^{\circ}$ C prior to use. Briefly, HCCA was suspended in 250 μ l of standard solvent containing 50% acetonitrile, 47.5% water and 2.5% trifluoroacetic acid, which has been tested by Bruker Daltonik GmbH (Cat no. 19182, Sigma-Aldrich), mixed thoroughly and spun down at 13,000 rpm (12,470 x g) for 2 minutes. The dissolved HCCA was kept in the dark at room temperature and discarded after 7 days.

5.2.5 Preparation of Bacterial Test Standard (BTS)

Prior to every run, Bruker Bacterial Test Standard (BTS) (Cat no. 8255343, Bruker) was used as a quality control to calibrate the system. BTS contains the extract of *Escherichia coli* DH5 alpha peptides and protein profile plus additional proteins. The spiked proteins make the upper boundary of the mass range extended so that the overall mass range covered is from 3.6 to 17 kDa in the MALDI-TOF mass spectra. BTS aliquots were prepared by adding 50 μ L standard solvent (Cat no. 19182, Sigma-Aldrich) to the pellet. The solution was dissolved by pipetting up and down at least 20 times at room temperature followed by incubation for 5 minutes. The solution was mixed again by pipetting for another 20 times followed by centrifugation at 13,000 rpm (12,470 \times g) for 2 minutes at room temperature. The solution was transferred into several chemical resistant tubes (Cat no. E1415-1500, Starlab) containing 5 μ L of aliquots and stored at -20 $^{\circ}$ C prior to use. The frozen BTS was subsequently fully thawed at room temperature. One-microlitre of BTS solution was deposited on any position marked as (+) on the MALDI target plate and allowed to dry at room temperature followed by overlaying of 1 μ L HCCA to the BTS calibrant spot (Figure 5-2). The time between drying and spotting of the HCCA matrix was kept to a minimum (recommended to complete this step within 30 minutes by the manufacturer).

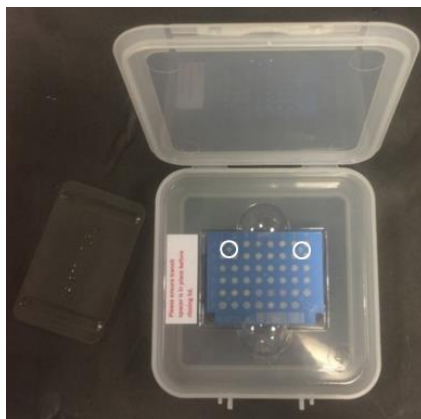


Figure 5-2: A disposable MALDI Biotarget 48 spotted with samples and BTS (Bacterial Test Standard) (as shown in white circles) was kept in a transport box.

5.2.6 MALDI-TOF

A Microflex LT MALDI-TOF mass spectrometer (Bruker) was used to generate the protein spectra. The geometry was set as MSP MALDI Biotyper 48. The measurement was performed in a linear positive mode (m/z 2000-20 000 Da) with the standard Bruker Daltonics GmbH AutoX method (MBT_AutoX) using the FlexControl software (Version 3.4 Build 105).

5.2.6.1 Calibration

The system was calibrated on a daily basis. In addition, calibration was included in each run using the bacterial standard (BTS) consisting of 8 known protein masses with the tolerance range of ± 300 ppm from the nominal value. The calibration points with the mass tolerance were provided by the manufacturer as shown in the results section (Table 5-3). The system was calibrated using the calibration parameters following the instruction manual for BTS by Bruker either by manual or automatic calibration (Figure 5-3). The system was successfully calibrated when the masses were within the tolerance range (manually) or shown in the system with the calibration information dialog opened after each calibration (automatically).

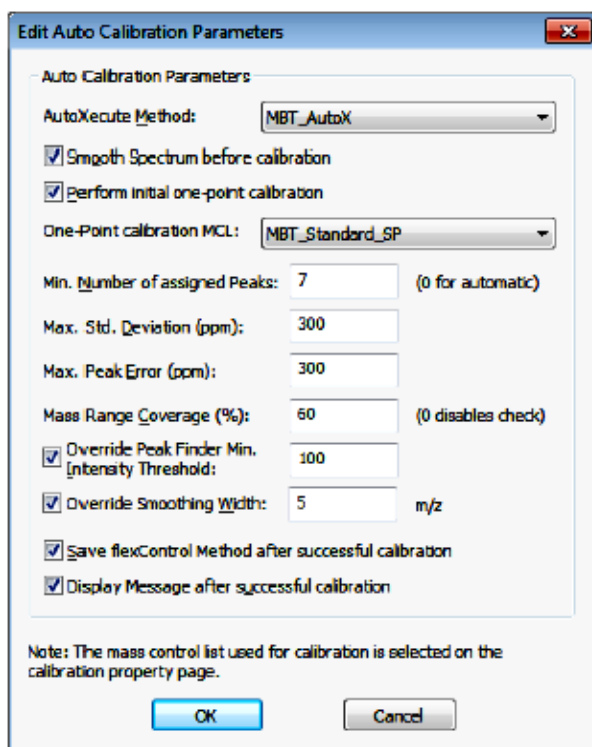


Figure 5-3: Parameters used for calibration from the BTS manual as provided by Bruker.

5.2.6.2 Spectral acquisition and data analysis.

The quality of all spectra generated was analysed using the Flex Analysis 3.4 Software in the Compass 1.4 Flex Series (Order no. 10240882, Bruker Daltonics). A total of 24 spectra were obtained from 8 spots with 3 measurements for each spot. The MBT_Standard.FAMS method was chosen to normalise the spectra. Spectra were normalised by using 'Smooth' and 'Baseline Subtraction' tools and observed for flat lines and outlier' peaks. The outlier' peaks were determined by a peak shift of individual masses from 3000 to 10000 Da. The acceptable peak shift between the smallest and

the largest spectra were set at 500 ppm range (Table 5-1). As recommended by Bruker, a minimum of 20 spectra needed to be included, otherwise new spectra has to be obtained for the mass spectral profiles (MSPs).

Table 5-1: Allowable peak shift from mass 3000-12000 Da as recommended by Bruker.

Mass(Da)	3000 to 4000	4000 to 5000	5000 to 6000	6000 to 7000	7000 to 8000	8000 to 9000	9000 to 10000	10000 to 11000	11000 to 12000
Tolerance	1.5	2	2.5	3	3.5	4	4.5	5	5.5

Differences in peak shift were analysed using Excel and the average of the means m/z for collected peaks from each replicate were calculated. The data was saved using the same file name. To prevent overwrite to the original file, the original file was given a suffix '_24' to indicate the original number of spectra before analysis. Prior to the peak shift analysis, the Student's t-test was performed to determine the reproducibility of both replicates (<http://www.socscistatistics.com/tests/studentttest/Default2.aspx>, last accessed September 2017). The peaks with a p-value of more than 0.05 were referred to as not statistically different and therefore considered reproducible in both replicates.

5.2.6.3 Generation of MSPs

The processed MSPs were loaded into the Biotyper OC followed by all the information regarding species, strain type and culture condition. The spectrum was selected and run against the replicate and finally, the MSP which produced the most reproducible and best scores was chosen. The database was subsequently challenged with *Stachybotrys* spp. isolates in replicates. Spectra were analysed by using Biotyper database V 3.1 © Bruker GmbH 2005-2012 against the Bruker Filamentous Fungi Library V1.0 database, our created MSPs alone, and then both combined. The recommended cut off scores for species-level identification is ≥ 2.0 and for genus-level is ≥ 1.7 . The scores below 1.7 are considered as unreliable (Table 5-2).

Table 5-2: Score values as suggested by Bruker.

Range	Description	Symbols	Colour
2.300 – 3.000	Highly probable species identification	+++	Green
2.000 – 2.299	Secure genus identification, probable species identification	++	Green
1.700 -1.999	probable genus identification	+	Yellow
0.000 – 1.699	Not reliable identification	-	Red

5.3 RESULTS

5.3.1 Optimisation of fungal growth conditions

5.3.1.1 The effects of different broth media on protein profiles

The effects of different media for cultivation, SDB and PDB on the protein profiles were investigated for *S. chartarum*, NCPF 7587 and *A. niger*, ATCC 16888. In this experiment, 2 isolates of *S. chartarum*, NCPF 7587 and *A. niger* (ATCC 16888) were previously grown on ESA and after 7 days, fungal mass was transferred into sterile tubes containing SDB or PDB.

We found that, both isolates produced sufficient biomass when grown in both PDB and SDB. More pigmentation was observed in SDB compared to PDB for both isolates, however, *A. niger* was less pigmented compared to *S. chartarum* in both media. Furthermore, a heavier fungal mass was produced by *A. niger* compared to *S. chartarum*. It was difficult to harvest *S. chartarum* and as a result, the fungal mass required several centrifugation steps to form a stronger sedimentation (pellet) to maximise the harvest (Figure 5-4)

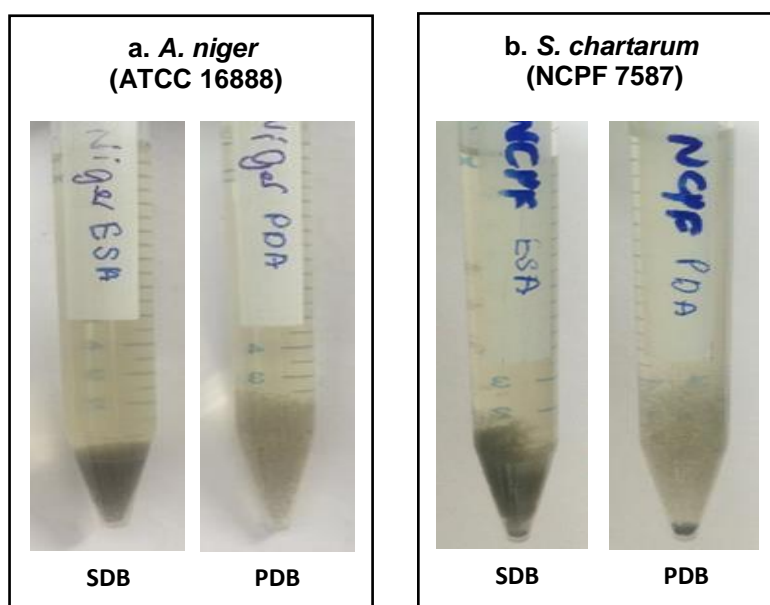


Figure 5-4: Representation of growth characteristics of a. *A. niger*, ATCC 16888 and b. *S. chartarum*, NCPF 7587 grown in SDB and PDB for 24 hours at 25 °C.

From the mass spectra, we observed that *S. chartarum*, NCPF 7587 grown on both SDB and PDB (Figure 5-5) showed some differences in profiles. Higher intensity of low molecular weight peaks was observed in SDB ranging from approximately 2000 to 3500 m/z. However, more consistent peaks were observed ranging from approximately 6000 to 9000 m/z in both media. The low MW proteins were probably associated with the pigment since they were present only in the fungi grown in SDB.

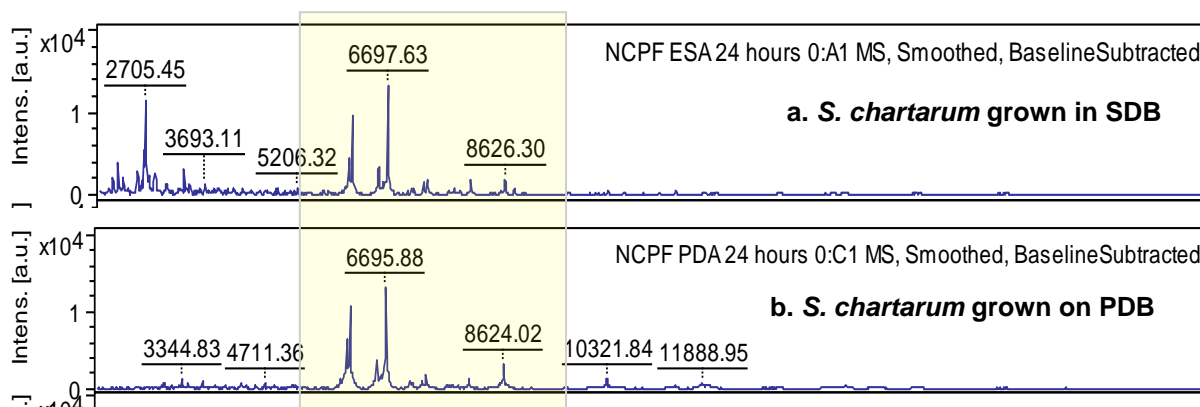


Figure 5-5: Representation of the protein profiles of *S. chartarum*, NCPF 7587 grown in a. SDB and b. PDB for 24 hours at 25 °C. Consistent peaks were observed ranging from approximately 6000 to 9000 m/z in both media are highlighted in yellow.

Whereas, *A. niger*, ATCC 16888 showed more consistent peaks in both SDB and PDB (Figure 5-6). High intensity peaks were observed ranging approximately from 3360 to 11830 m/z in both media. Although *A. niger* grown in SDB (Figure 5-4) gave darker coloured fungal mass compared to PDB, however, that did not affect the protein profiles of *A. niger* as observed in *S. chartarum* grown on SDB.

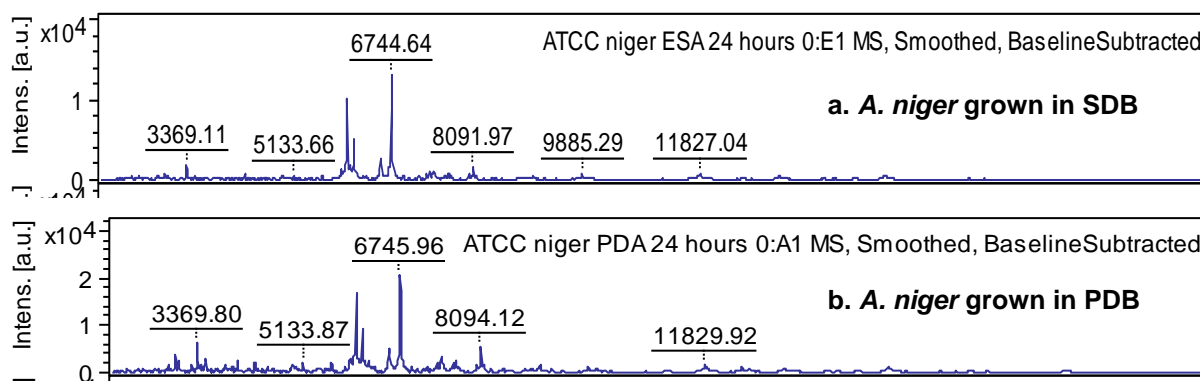


Figure 5-6: Representation of the protein profiles of *A. niger*, ATCC 16888 grown in a. SDB and b. PDB for 24 hours at 25 °C. Consistent peaks were observed in *A. niger* grown in both media.

5.3.1.2 The effects of liquid versus solid media

Protein extraction was also performed directly from original culture grown on ESA. Three *S. chartarum* strains, NCPF 7587, ATCC 16026 and CBS 182.80 were compared for differences in the protein profiles (Appendix 5-A). From the results, we observed some similarity of protein profiles patterns particularly at range 4470 m/z to 8680 m/z generated from all the tested *S. chartarum* strains, although the level of intensities varied between isolates (Figure 5-7).

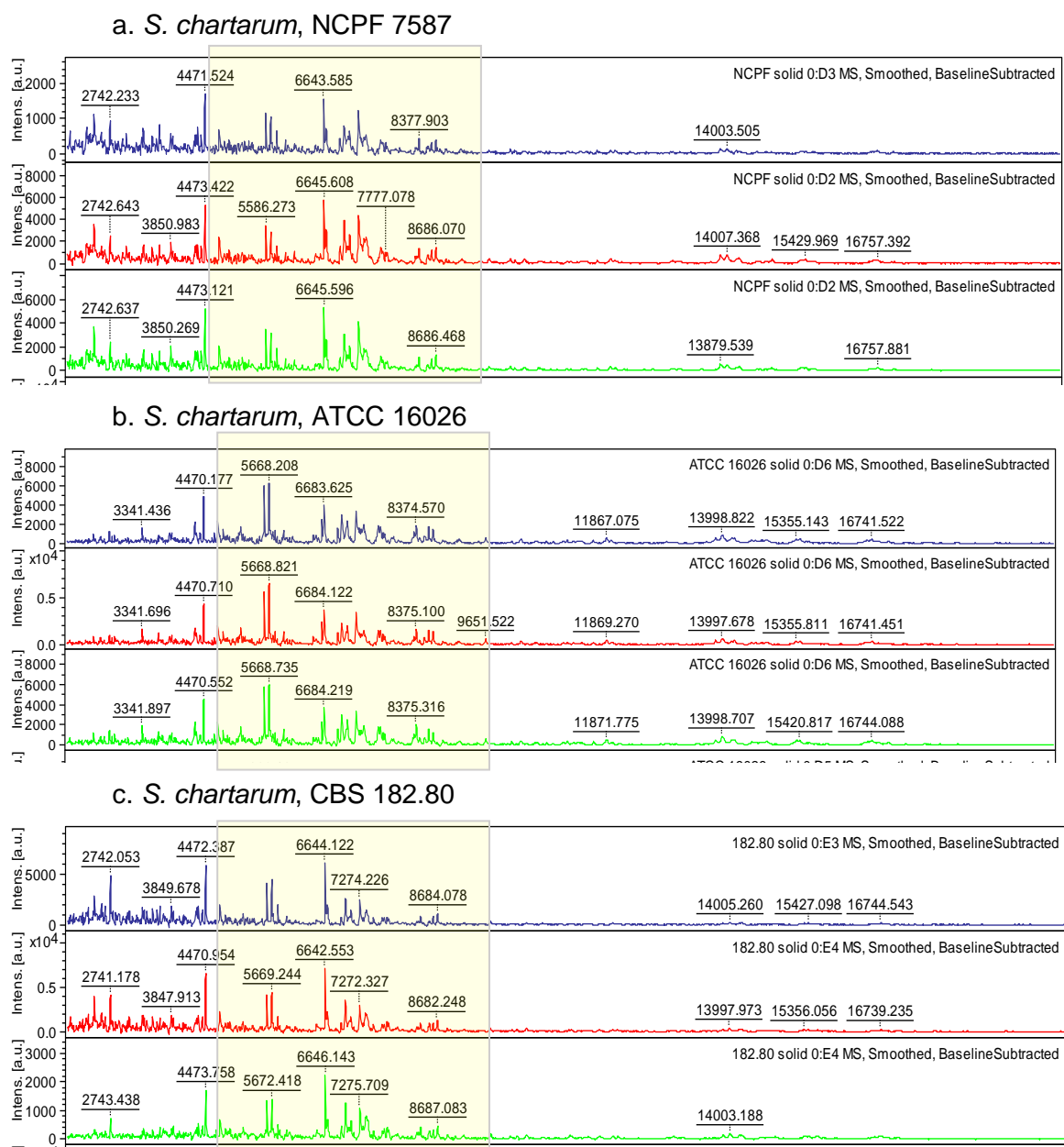


Figure 5-7: Representation of protein spectra of *S. chartarum*, a. NCPF 7587, b. ATCC 16026 and c. CBS 182.80 grown in ESA for 7 days and incubated at 25 °C. The spectra for each strain shown were generated from a single spot measured 3 times by the machine. Similarity of protein profiles patterns at range 4470 m/z to 8680 m/z are highlighted in yellow.

5.3.1.3 The effects of temperature on protein profiles

In addition to an incubation temperature of 25 °C (the optimum temperature for *S. chartarum*), we have also tested the incubation temperature commonly used in most laboratories (30 °C). This was performed in order to determine any effects on protein profiles in both isolates grown in both SDB (Appendix 5-B) and PDB (Appendix 5-C). From the results of *S. chartarum* grown in SDB, we found that most of the spectra were reproducible although there was a slight difference in one of the spots with the absence of low molecular weight peaks (Figure 5-8). Furthermore, peak intensities of less than 1×10^4 were observed in at least 3 out of 6 spots in both replicates with the possibility of flat lines or outliers in further analysis.

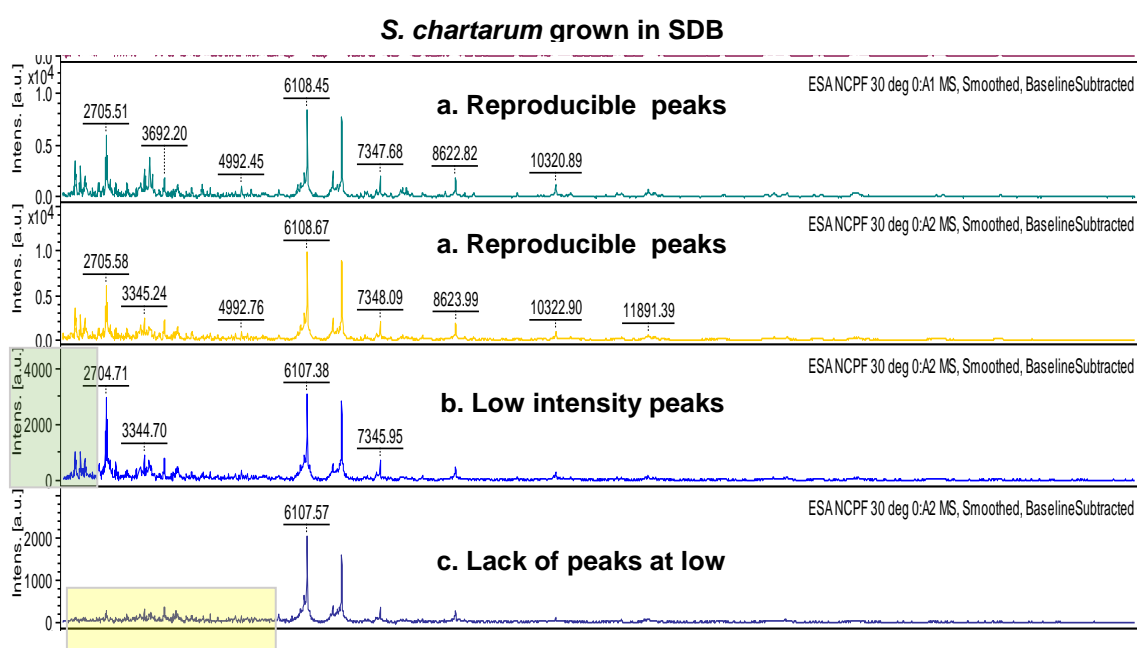


Figure 5-8: Representation of protein spectra of *S. chartarum*, NCPF 7587 grown in SDB for 24 hours and incubated at 30 °C. The spots with different quality of peaks shown as; a. Reproducible and good intensity peaks, b. Low intensity (scale highlighted in green) and c. Lack of low MW peaks (m/z range highlighted in yellow).

With *S. chartarum* grown in PDB, the results showed inconsistent mass spectra of very low intensity in both replicates to no signal in most of the spots in one of the replicates (Figure 5-9).

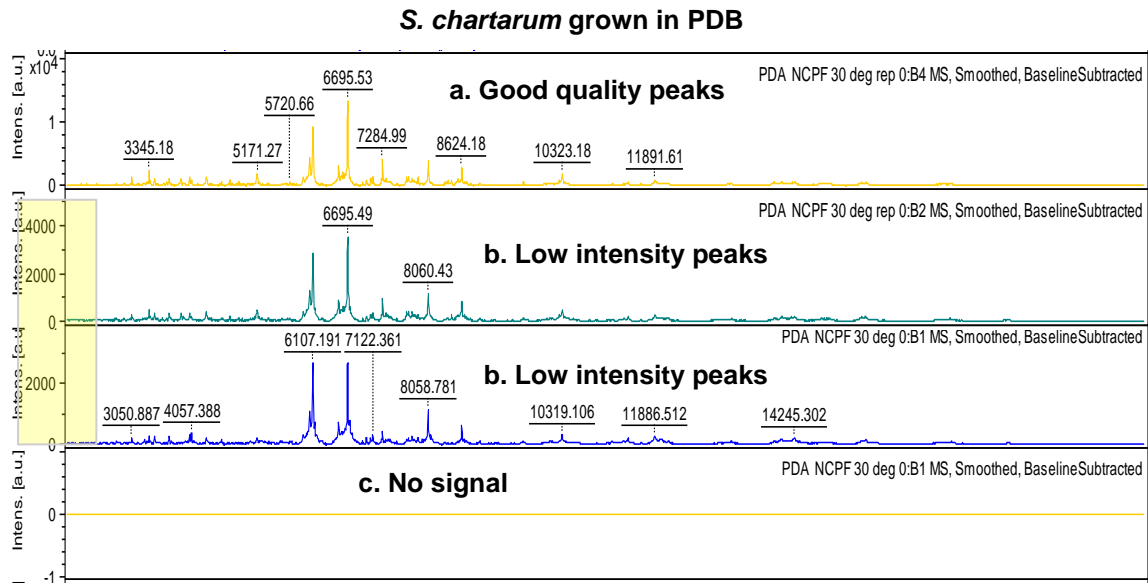


Figure 5-9: Representation of protein spectra of *S. chartarum*, NCPF 7587 grown in PDB for 24 hours and incubated at 30 °C. The spots with different quality of peaks are indicated with: a. Good quality peaks, b. Low intensity peaks (scale highlighted in yellow) and c. No signal peak.

The same experiment was conducted on *A. niger*, ATCC 16888 grown in SDB (Appendix 5-D) and PDB (Appendix 5-E). We found that *A. niger* grown in SDB at 30°C showed good spectral intensity of more than 1.0×10^4 in most of the spots (Figure 5-10). High intensity peaks are present in the low molecular weight range which were absent when the isolate was incubated at 25 °C (see figure 5-6).

A. niger grown in SDB at 30 °C

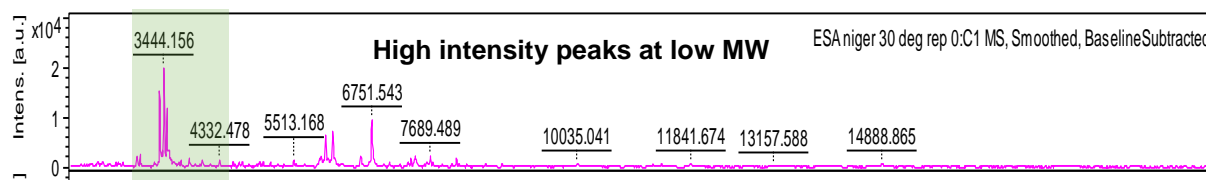


Figure 5-10: Representation of protein spectra of *A. niger*, ATCC 16888 grown in SDB for 24 hours and incubated at 30 °C. High intensity peaks are present in the low molecular weight range (highlighted in green), which were absent when the isolate was incubated at 25 °C

However, *A. niger* grown in PDB showed low intensity to no signal (Figure 5-11). We also observed that there were slightly different peaks intensities at the low molecular weight range in both SDB and PDB compared to the *A. niger* incubated for 24 hours.

A. niger grown in PDB at 30 °C

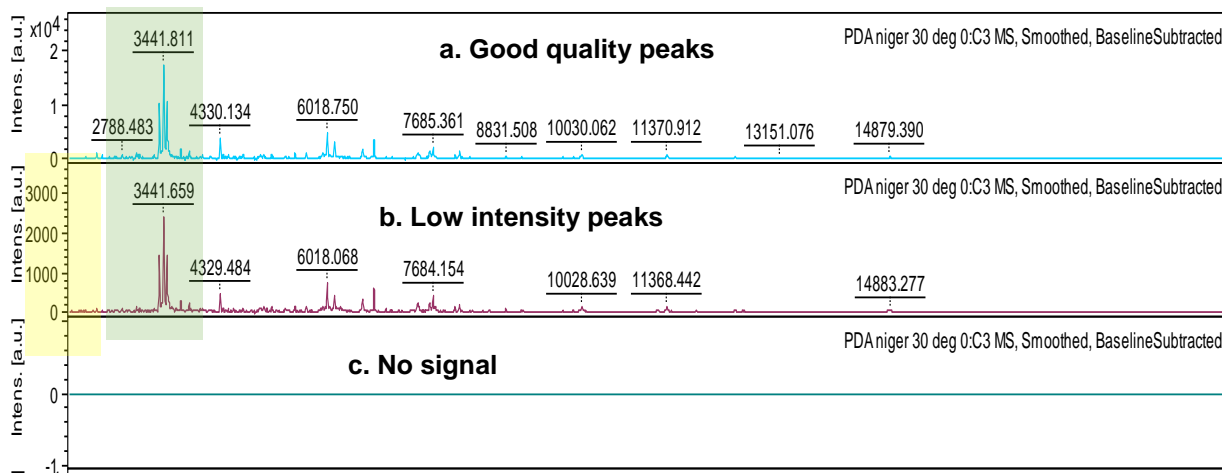


Figure 5-11: Representation of protein spectra of *A. niger*, ATCC 16888 grown in PDB for 24 hours and incubated at 30 °C. The spots with different quality peaks shown as a. Good quality peaks, b. Low intensity peaks (scale highlighted in yellow) and c. No signal. High intensity peaks are present in the low molecular weight range (highlighted in green), which were absent when the isolate was incubated at 25 °C.

5.3.1.4 The effects of incubation period on protein profiles

The effects of incubation period on protein profiles of *S. chartarum*, NCPF 7587 grown in SDB (Appendix 5-F) and PDB (Appendix 5-G). were investigated. Fungal mass was incubated for 48 hours before extraction. From the results, reproducible peaks that were also present in *S. chartarum* cultures incubated for 24 hours both in SDB and PDB (Figure 5-12). However, there were some noise in the signals and slightly higher signals at low MW in both replicates. These might indicate more interference compounds in the protein extract compared to incubation for 24 hours.

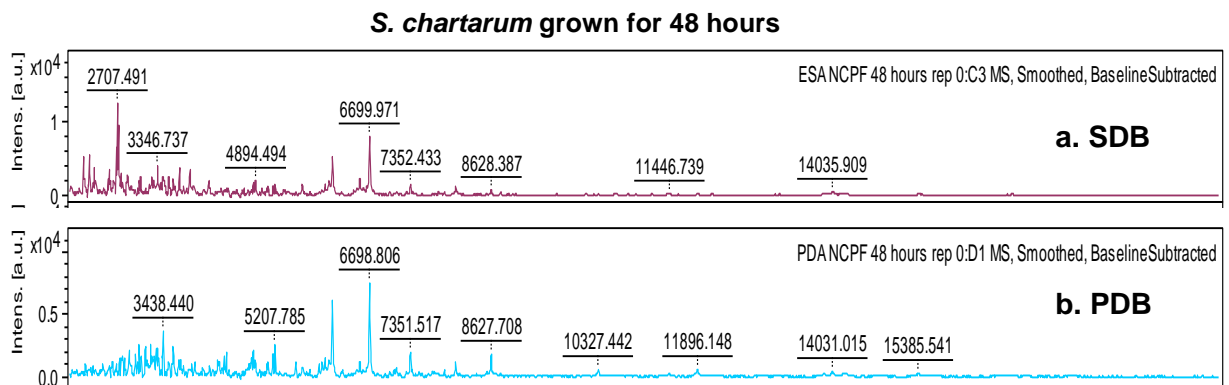


Figure 5-12: Representation of protein spectra of *S. chartarum*, NCPF 7587 grown in a. SDB and b. PDB for 48 hours and incubated at 25 °C.

In addition to the noise in the signals, some spots gave low intensity spectra or no signal in one of two of the biological replicates grown in SDB (Figure 5-13) and PDB (Figure 5-14).

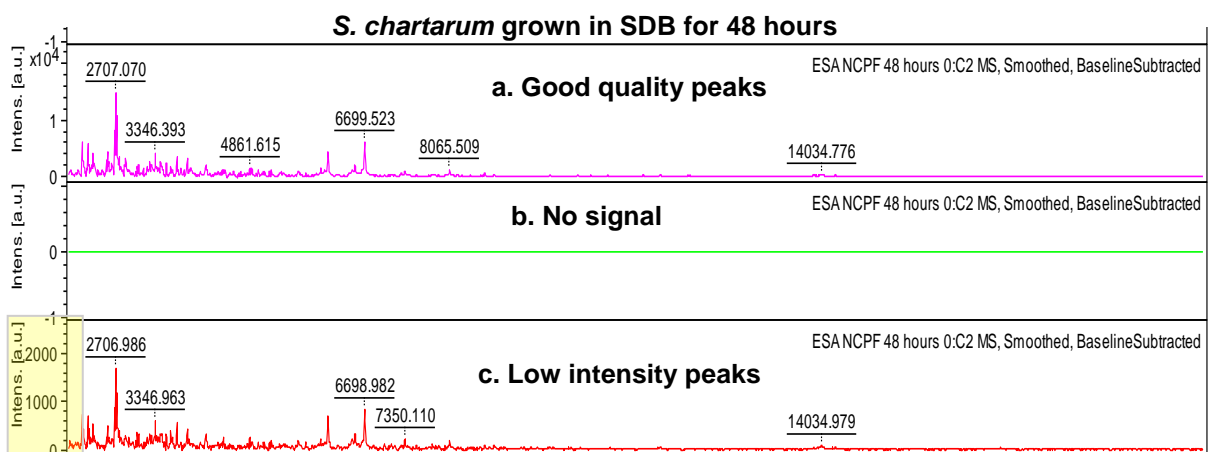


Figure 5-13: Representation of protein spectra of *S. chartarum*, NCPF 7587 grown in SDB for 48 hours and incubated at 25 °C. The spots with different quality peaks shown as a. Good quality peaks, b. No signal, and c. Low intensity peaks (scale highlighted in yellow).

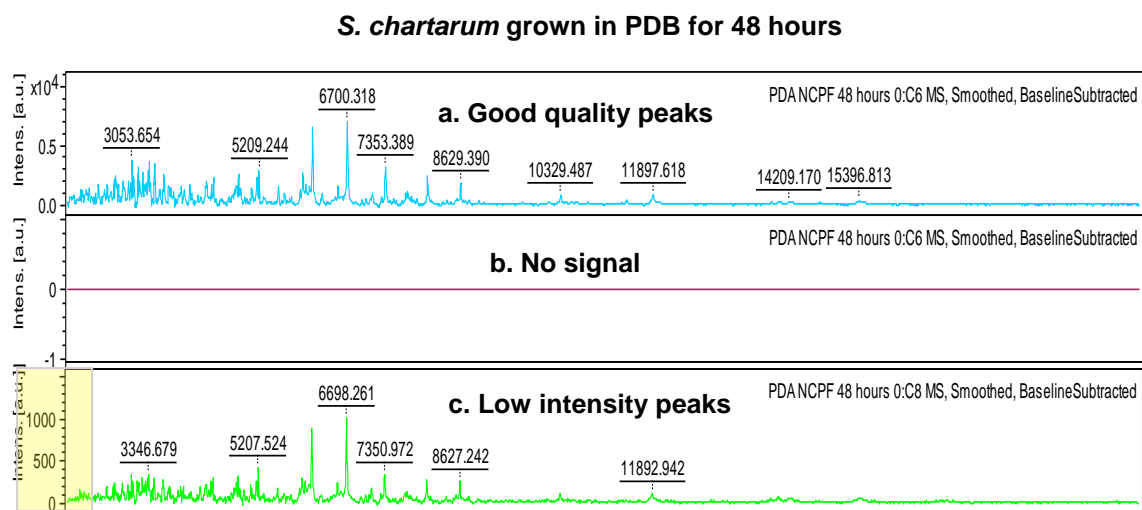


Figure 5-14: Representation of protein spectra of *S. chartarum*, NCPF 7587 grown in PDB for 48 hours and incubated at 25 °C. The spots with different quality peaks shown as a. Good quality peaks, b. No signal and c. Low intensity peaks (scale highlighted in yellow).

5.3.2 Control of masses and calibration

Calibration was performed using the both manual and automatic calibration procedure. Manual calibration could also be performed as shown in Figure 5-15. The experimental peaks were compared with the reference mass and should be within the tolerance range. From the result, the lowest mass of 3637.8 Dalton had low intensity as shown by manual observation, and the other 7 reference masses were within the tolerance range. This was acceptable according to the criterion requiring at least 7 peaks to be assigned (Figure 5-3). This was confirmed by using the automatic calibration procedure. Automatic calibration was performed by selecting the BTS followed by the 'calibrate' button. The system had been correctly calibrated when the masses were within the tolerance range.

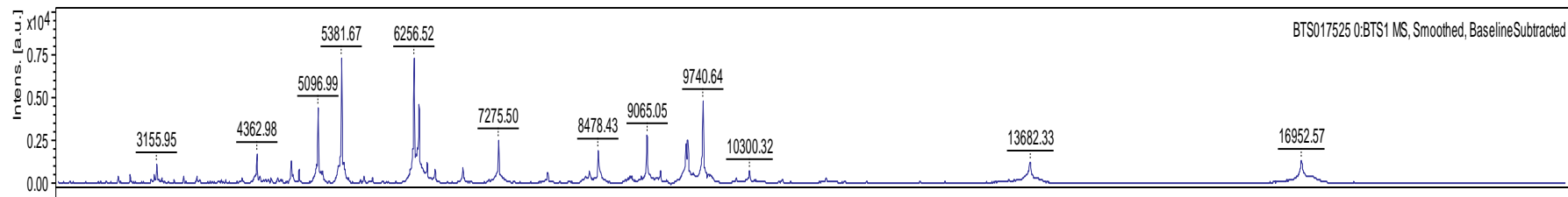


Figure 5-15: The spectra obtained from Flex Analysis shows masses produced by BTS used for internal calibration used in this study should be within the tolerance range as shown in Table 5-3.

Table 5-3: Calibration points for representing 8 known reference masses of peptides and additional protein in BTS solution.

Protein	Reference mass	± 300 ppm range (Dalton)	This study	Within range
RL29 [M+2H] 2+	3637.8 Da	3636.7 – 3638.8	Low intensity	NA
RS32 [M+H] +	5096.8 Da	5095.3 – 5098.3	5096.99	Yes
RS34 [M+H] +	5381.4 Da	5379.8 – 5383.0	5381.67	Yes
RS33meth [M+H] +	6255.4 Da	6253.5 – 6257.3	6256.52	Yes
RL29 [M+H] +	7274.5 Da	7272.3 – 7276.7	7275.50	Yes
RS19 [M+H] +	10300.1 Da	10297.0 – 10303.2	10300.32	Yes
RNAse A [M+H] +	13683.2 Da	13679.1 – 13687.3	13682.33	Yes
Myoglobin [M+H] +	16952.3 Da	16947.2 – 16957.4	16952.57	Yes

5.3.3 Development of Mass Spectrum Profiles (MSPs)

A total of 24 raw spectra was obtained from 8 spots with triplicate measurements per extraction and was carried out in 2 biological replicates (Figure 5-16). Both replicates recorded intensities of more than 1×10^4 . The raw spectra from both replicates were then subjected to spectra Flex Analysis 3.4 to produce normalised protein profiles (Figure 5-17).

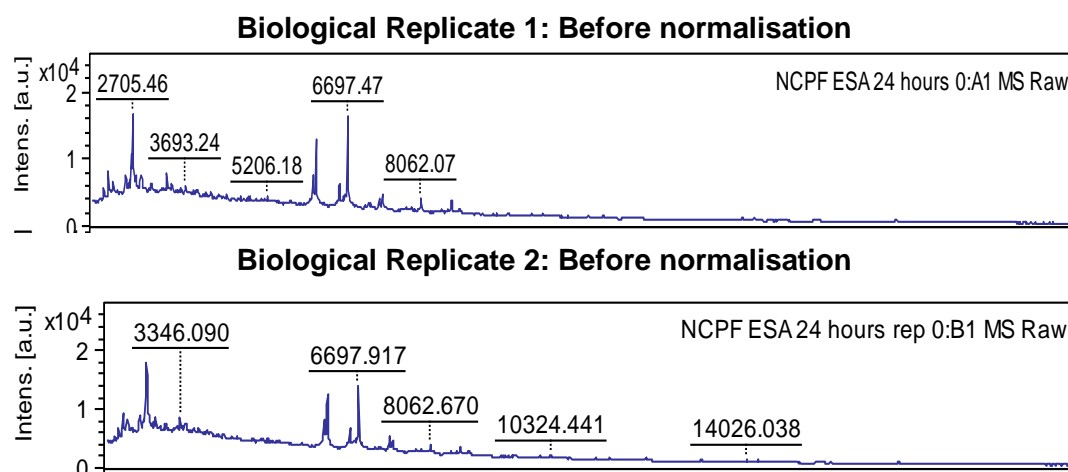


Figure 5-16: Representatives of raw spectra obtained from 2 biological replicates of *S. chartarum* grown on ESA for 24 hours.

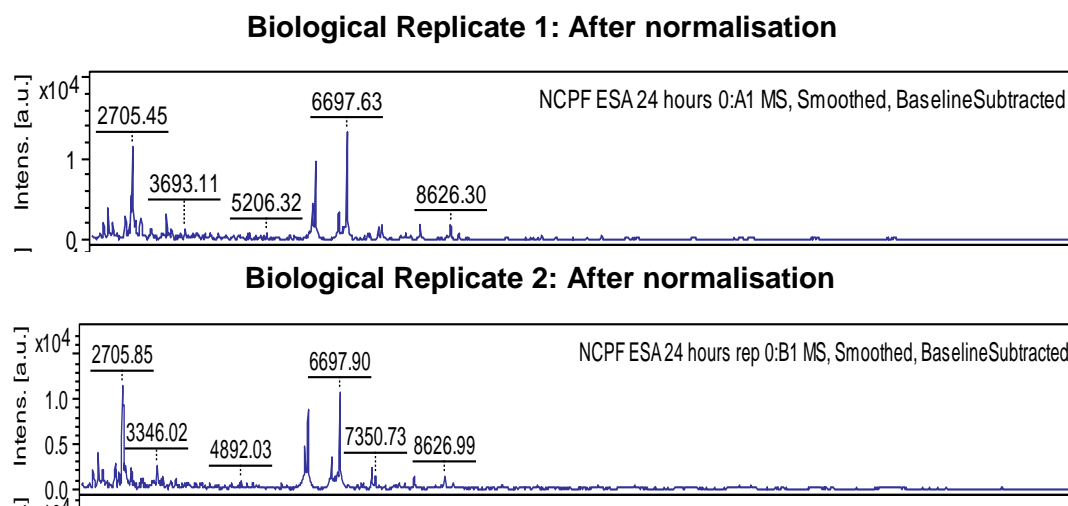


Figure 5-17: Examples of normalised spectra obtained from 2 biological replicates of *S. chartarum* grown on ESA for 24 hours.

The reproducibility of both replicates grown in SDB and PDB was assessed using the Student's t-test. The mass peaks for all 8 spots in triplicates of *Stachybotrys chartarum*, NCPF 7587 grown in SDB in replicates (Appendix 5-H and Appendix 5-I) and PDB in replicates (Appendix O and Appendix P) are shown in the appendices. We found that all the peaks from NCPF 7587 grown in SDB were not statistically different between replicates which indicated the reproducibility of all the spots in the biological replicates (Appendix 5-J). On the other hand, NCPF 7587 grown in PDB showed a statistically different peak between replicates at m/z 4000 (Appendix 5-Q). However, this was within the allowable peak range using the protocol provided by Bruker.

The normalised spectra from each replicate were analysed for flatlines and outliers according to the protocol as previously described in the method section (Figure 5-18). This was followed by the peak shift of individual peaks. The allowed peaks were calculated as the differences between the smallest and the largest mass for each peak. The analysis of the peaks shift showed the peaks that were outside the allowable range in *S. chartarum*, NCPF 7587 grown in SDB (Appendix 5-K, Appendix 5-L, Appendix 5-M, and Appendix 5-N) and PDB (Appendix 5-R, Appendix 5-S, Appendix 5-T and Appendix 5-U). The masses outside the allowable range were removed and a new set of spectra were used to generate the MSPs.

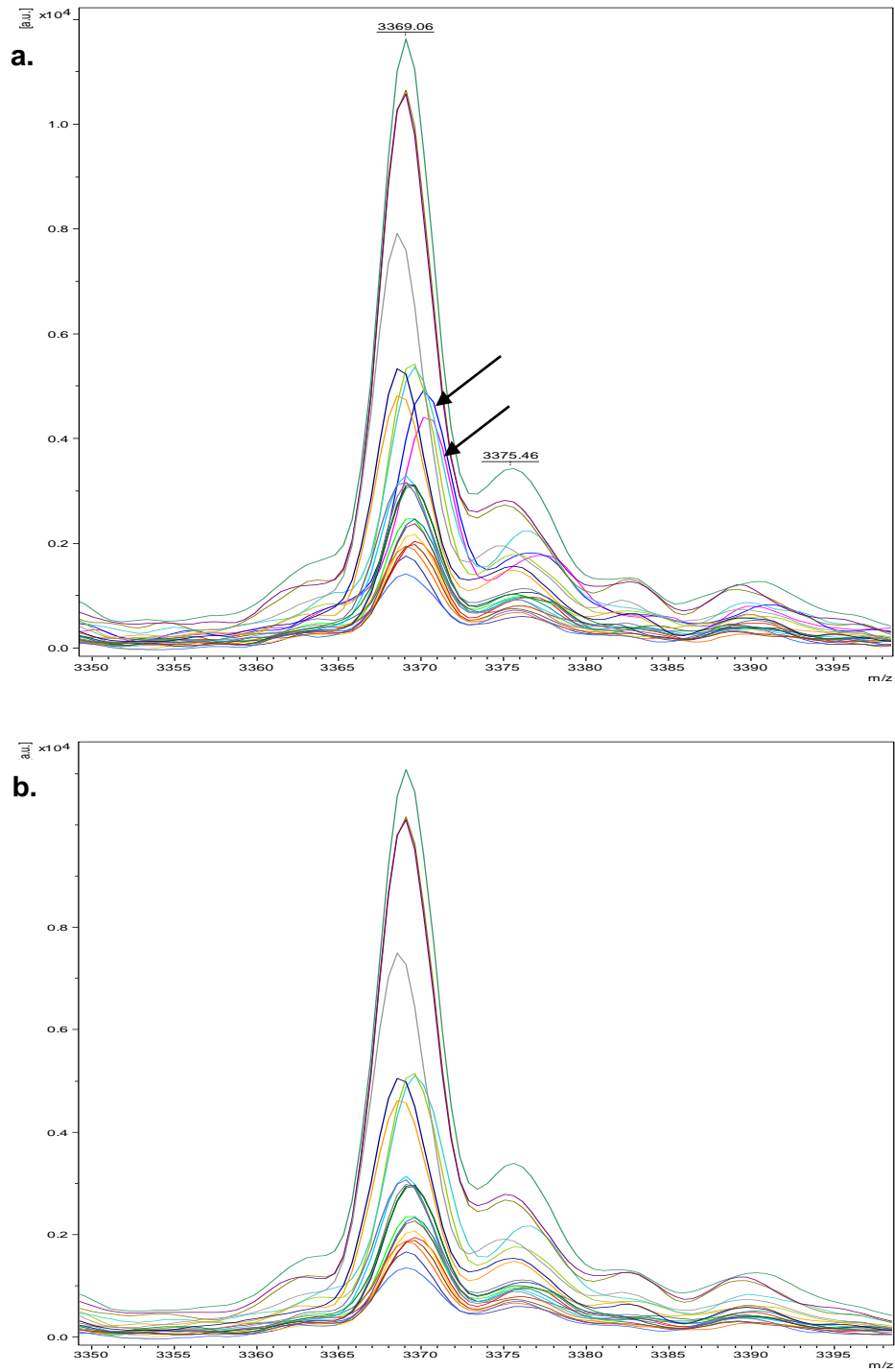


Figure 5-18: Representation of the result obtained from one of the replicates showing the peaks before and after analysis. a. Blue and purple lines were the outliers and therefore deleted from the spectra (as marked with arrows) and b. New spectra obtained for generation of MSP.

5.3.4 Identification of fungi using Biotyper® Bruker database

5.3.4.1 *Aspergillus niger* van Tieghem (ATCC® 16888™)

All the mass spectra obtained from *Aspergillus niger* (ATCC 16888) grown in both SDB (Appendix V and Appendix W) and PDB (Appendix X and Appendix Y) were included as a control to determine the efficacy of the extraction method and its accuracy against the existing Bruker database. From the Biotyper® Bruker software, peaks were generated from the samples grown in SDB and PDB in 2 replicates.

The MSPs generated from *A. niger* grown in SDB were aligned with *A. niger* from the Bruker database for similarities (Figure 5-19). The similarity was translated into scoring values to find the closest match against the database with green colour code as the highest match.

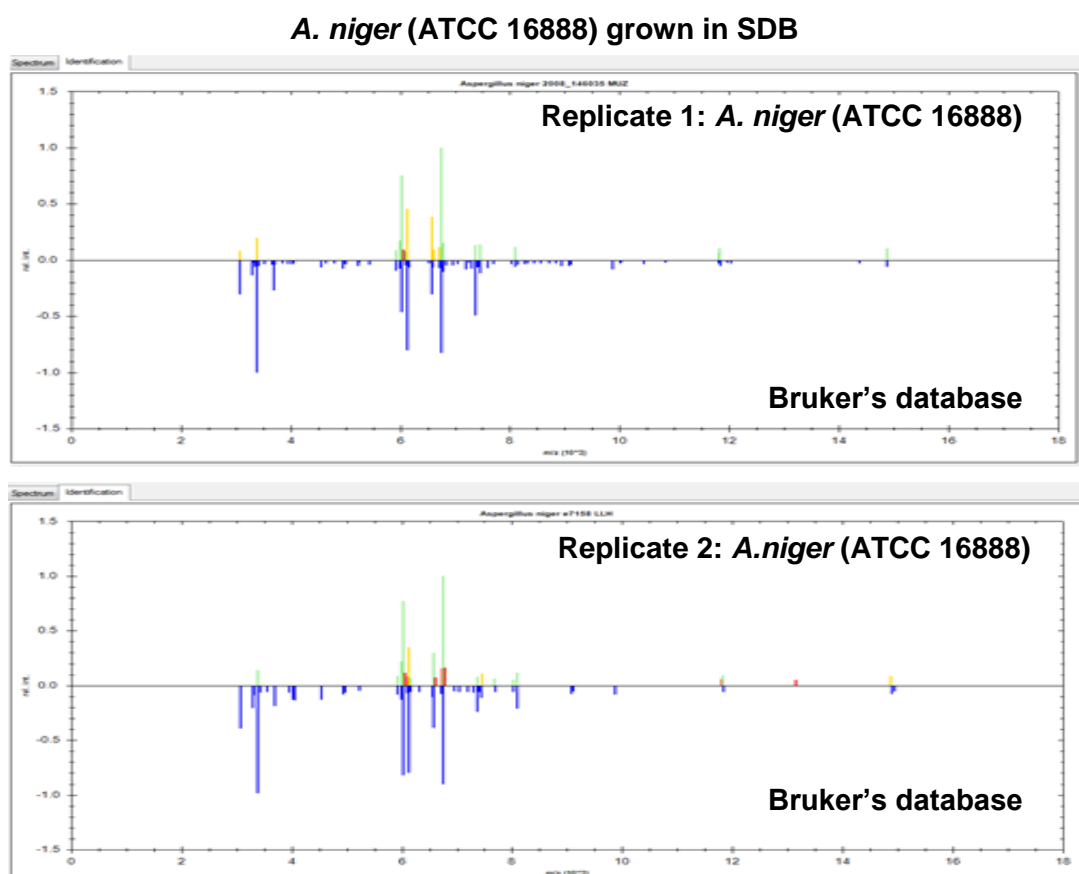


Figure 5-19: Identification by Biotyper® Bruker database showing aligned protein profiles from the Bruker's database and *A. niger* (ATCC 16888) grown in SDB.

Score values for both replicates grown in SDB showed the highest log (score) values of 2.075 and 2.223 (Figure 5-20) which indicate 'secure genus identification, probable species identification' according to Bruker's recommendation. Replicate 1 showed lower scores with 2 log scores lower than 1.7 which was regarded as an unreliable identification, while replicate 2 showed good identification of at least at genus level with log scores more than 1.7. However, overall scores showed that the extraction method was reproducible and could be used with Bruker's database, even though the scores were lower than the recommended cut-off point.

Replicate 1: *A. niger* (ATCC 16888) grown in SDB

Mx	Detected Species	Log(Score)
1	<i>Aspergillus niger</i> 2008 146035 MUZ	2.075
2	<i>Aspergillus niger</i> e7158 LLH	2.056
3	<i>Aspergillus niger</i> DSM 737 DSM	1.991
4	<i>Aspergillus niger</i> DSM 12634 DSM	1.952
5	<i>Aspergillus niger</i> DSM 11167 DSM	1.937
6	<i>Aspergillus niger</i> M10 RLH	1.860
7	<i>Aspergillus niger</i> DSM 22593 DSM	1.837
8	<i>Aspergillus niger</i> 01 MPA 1261 MPA	1.812
9	<i>Aspergillus niger</i> Asp Nr 2 UGB	1.666
10	<i>Aspergillus niger</i> M14 RLH	1.577

Replicate 2: *A. niger* (ATCC 16888) grown in SDB

Mx	Detected Species	Log(Score)
1	<i>Aspergillus niger</i> e7158 LLH	2.223
2	<i>Aspergillus niger</i> 01 MPA 1261 MPA	2.067
3	<i>Aspergillus niger</i> 2008 146035 MUZ	2.049
4	<i>Aspergillus niger</i> DSM 12634 DSM	1.923
5	<i>Aspergillus niger</i> DSM 11167 DSM	1.903
6	<i>Aspergillus niger</i> DSM 22593 DSM	1.891
7	<i>Aspergillus niger</i> M10 RLH	1.891
8	<i>Aspergillus niger</i> M16 RLH	1.765
9	<i>Aspergillus niger</i> M14 RLH	1.745
10	<i>Aspergillus niger</i> D 16 256 7 3 LLH	1.742

Figure 5-20: Both replicates were identified as *Aspergillus niger* grown in SDB with the highest log (score) values of 2.075 and 2.223 obtained from the existing Bruker's Library for Filamentous fungi.

Subsequently, the MSPs generated from *A. niger* grown in PDB were aligned for similarities (Figure 5-21).

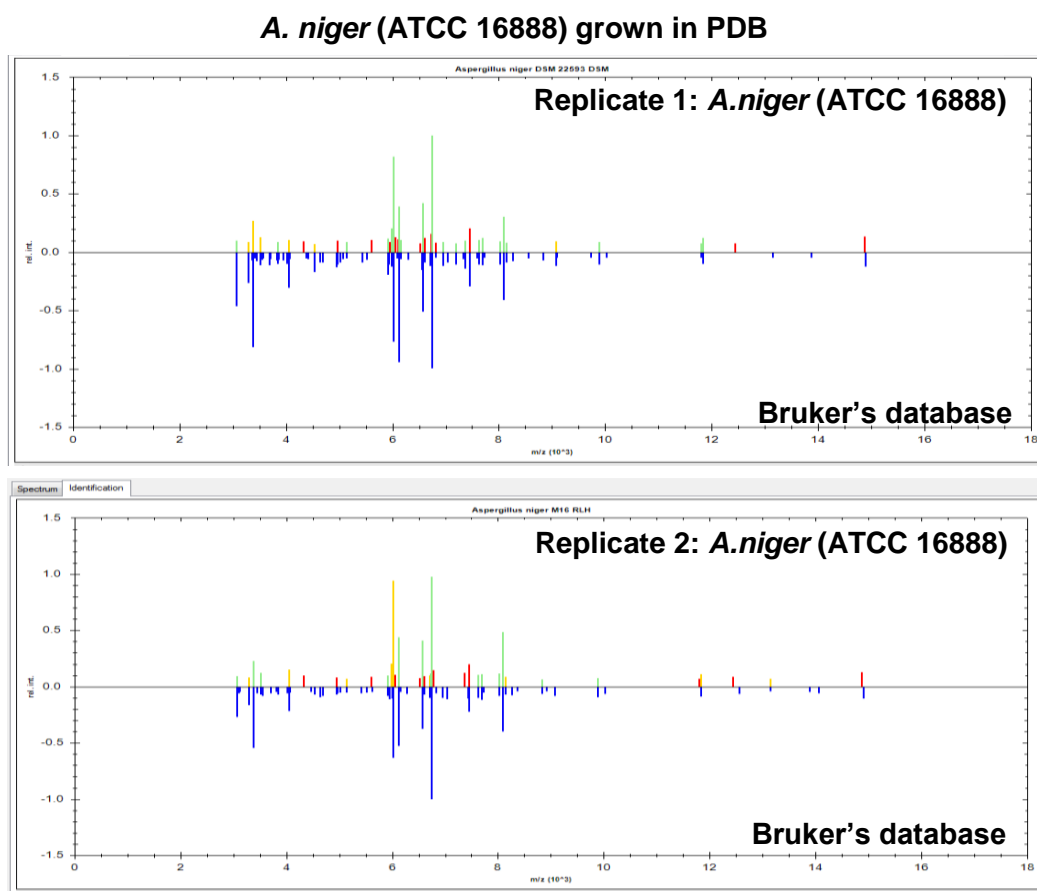


Figure 5-21: Identification by Biotyper© Bruker database showing aligned protein profiles from the Bruker's database and *A. niger* (ATCC 16888) grown in PDB.

The score values for both replicates grown in PDB showed the highest log (score) values of 2.265 and 2.160 (Figure 5-22) which indicate 'secure genus identification, probable species identification' according to Bruker's recommendation. The results were similar to the isolate grown in SDB, however, higher log scores were obtained in replicate 1 with all scores above 2.00 and for replicate 2 with all scores above 1.890.

Replicate 1: *A. niger* (ATCC 16888) grown in PDB

Mx	Detected Species	Log(Score)
1	<i>Aspergillus niger</i> DSM 22593 DSM	2.265
2	<i>Aspergillus niger</i> DSM 12634 DSM	2.255
3	<i>Aspergillus niger</i> M10 RLH	2.184
4	<i>Aspergillus niger</i> M16 RLH	2.178
5	<i>Aspergillus niger</i> e7158 LLH	2.172
6	<i>Aspergillus niger</i> Asp Nr 2 UGB	2.131
7	<i>Aspergillus niger</i> M14 RLH	2.066
8	<i>Aspergillus niger</i> 2008 146035 MUZ	2.028
9	<i>Aspergillus niger</i> DSM 11167 DSM	2.026
10	<i>Aspergillus niger</i> D 16 256 7 3 LLH	2.006

Replicate 2: *A. niger* (ATCC 16888) grown on PDB

Mx	Detected Species	Log(Score)
1	<i>Aspergillus niger</i> M16 RLH	2.160
2	<i>Aspergillus niger</i> DSM 22593 DSM	2.149
3	<i>Aspergillus niger</i> DSM 12634 DSM	2.067
4	<i>Aspergillus niger</i> M10 RLH	2.025
5	<i>Aspergillus niger</i> e7158 LLH	2.005
6	<i>Aspergillus niger</i> Asp Nr 2 UGB	2.004
7	<i>Aspergillus niger</i> DSM 11167 DSM	1.917
8	<i>Aspergillus niger</i> 2008 146035 MUZ	1.902
9	<i>Aspergillus niger</i> M14 RLH	1.902
10	<i>Aspergillus niger</i> 01 MPA 1261 MPA	1.890

Figure 5-22: Both replicates were identified as *Aspergillus niger* grown in PDB with the highest log (score) values of 2.265 and 2.160 obtained from the existing Bruker's Library for Filamentous fungi.

5.3.4.2 Identification of *Stachybotrys* spp. isolates

All isolates were subjected to protein extraction followed by spotting the protein extracts onto the MALDI metal plate. Spotting was done in triplicate with each spot producing 3 protein spectra making a total of 9 spectra per isolate. Of the 9 spectra, flatlines were excluded, and therefore, the remaining spectra of at least 6 spots were combined to make an average for further analysis. All spectra used for identification are shown in the appendices section (Appendix 5-Z and Appendix 5-AA). *Stachybotrys* spp. isolates were identified using the MSPs generated from *S. chartarum*, NCPF 7587 and Bruker's Library for Filamentous fungi.

5.3.4.2.1 *S. chartarum*

From the Biotyper© Bruker software, peaks generated from the samples and MSPs were aligned for similarities (Figure 5-23). Score values (Figure 5-24) were then compared with cut-off points as recommended by Bruker. Both figures represent *S. chartarum*, ATCC 16026 which was identified to be the closest with *S. chartarum*, NCPF 7587 grown in SDB for 24 hours with log (score) of 2.693 indicating 'highly probable species identification' based on the recommended cut-off points by Bruker as previously described in the method section (Table 5-2). This was followed by other fungal genera such as *Curvularia* spp., *Aspergillus* spp. and *Fusarium* spp. with scores of less than or equal to 1.077.

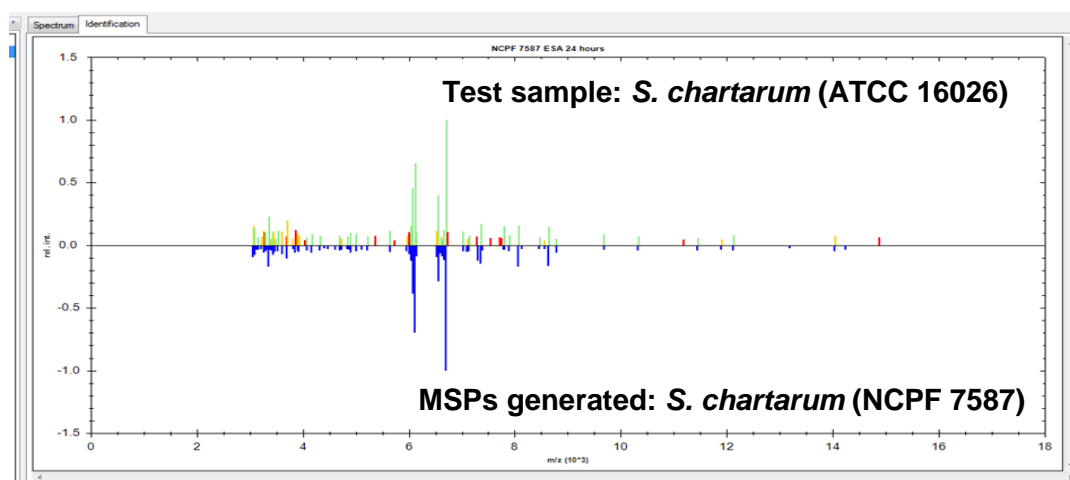


Figure 5-23: Identification by Biotyper© Bruker database showing aligned protein profiles from the MSP using *S. chartarum*, NCPF 7587 and another *S. chartarum*, ATCC 16026 treated as a sample, both grown in SDB.

Mix	Detected Species	Log(Score)
1	NCPF 7587 ESA 24 hours	2.693
2	NCPF ESA others	2.688
3	NCPF PDA 24 hours	2.333
4	NCPF PDA others	2.106
5	<i>Curvularia pallescens</i> CC2 DSM 62482 DSM	1.077
6	<i>Aspergillus flavus</i> CC1 MPA 1327 MPA	1.038
7	<i>Fusarium solani</i> D 16 256 6 1 LLH	0.980
8	<i>Aspergillus flavus</i> CC1 M19 RLH	0.965
9	<i>Aspergillus unguis</i> 614 UGB	0.951
10	<i>Aspergillus terreus</i> DSM 826 DSM	0.943

Figure 5-24: Sample was identified as the highest log (score) values obtained from newly created MSPs and existing Bruker's Library for Filamentous fungi.

Consistencies in protein profiles were observed in all *S. chartarum* strains within the same growth conditions. From the results, we found the same pattern of higher intensity peaks was observed in all *S. chartarum* grown in SDB which were absent in *S. chartarum* grown in PDB (Figure 5-25).

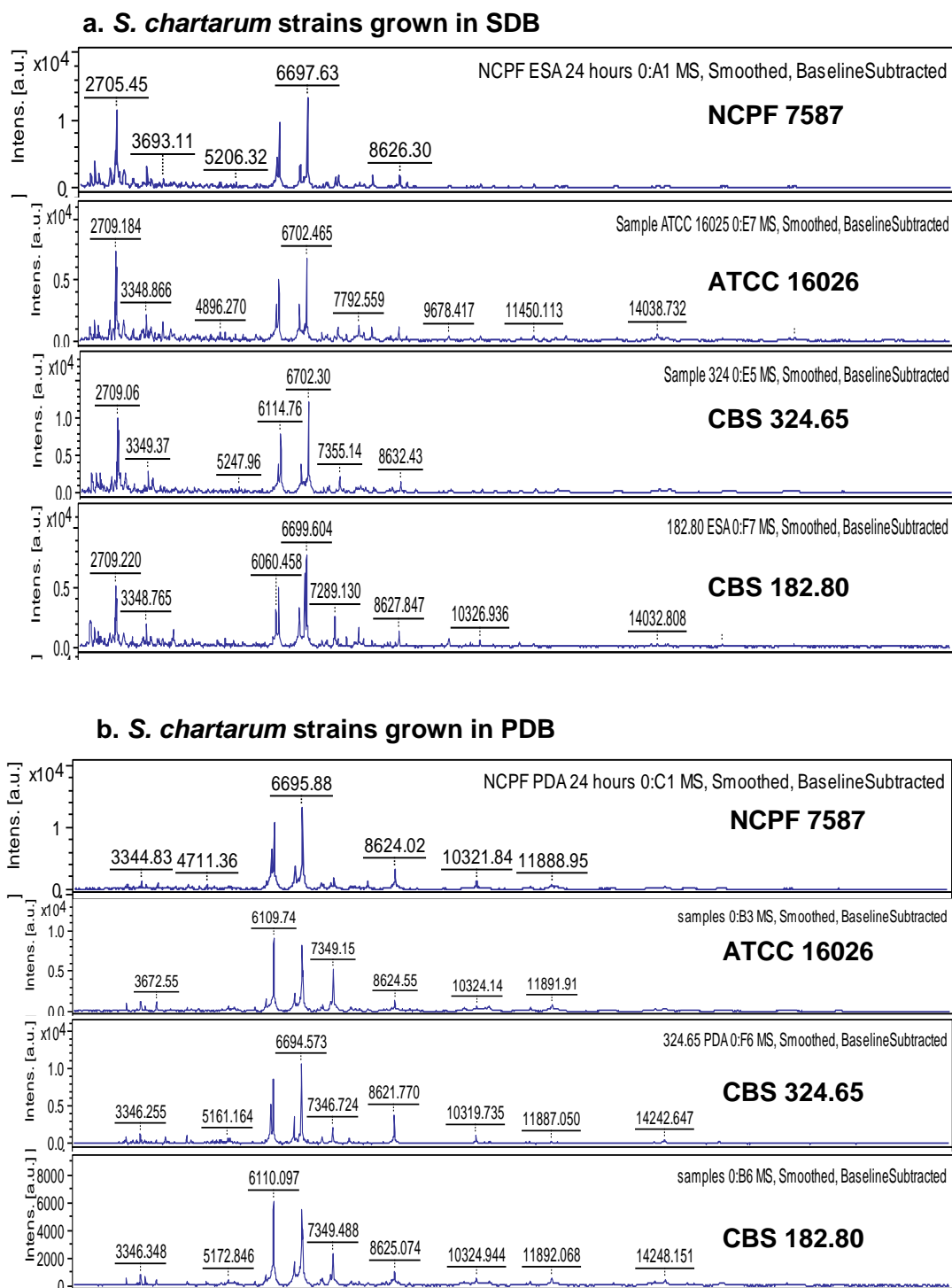
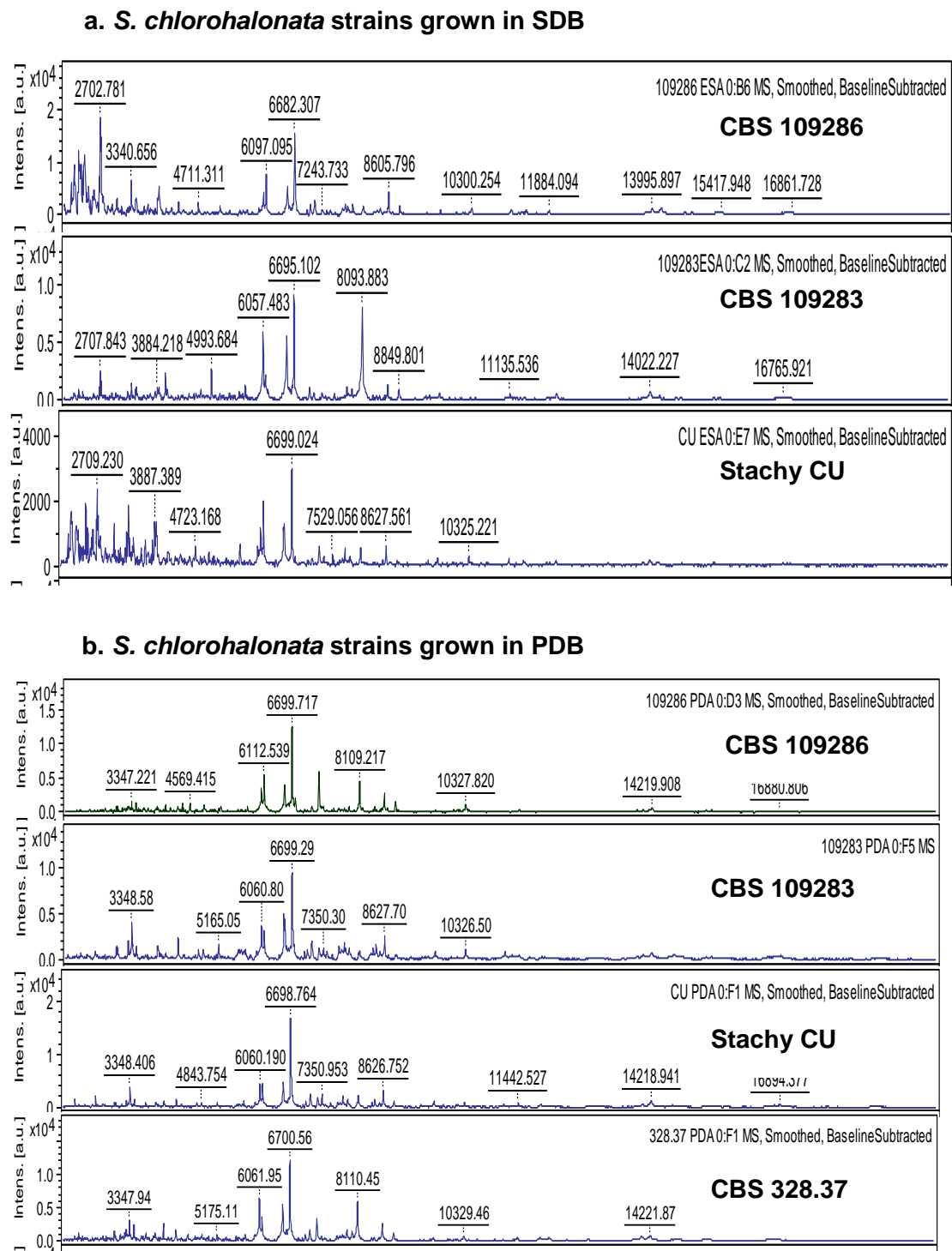


Figure 5-25: Representation of the protein profiles of *S. chartarum* strains NCPF 7587, ATCC 16026, CBS 324.65 and CBS 182.80 grown in a. SDB and b. PDB.

5.3.4.2.2 *S. chlorohalonata*

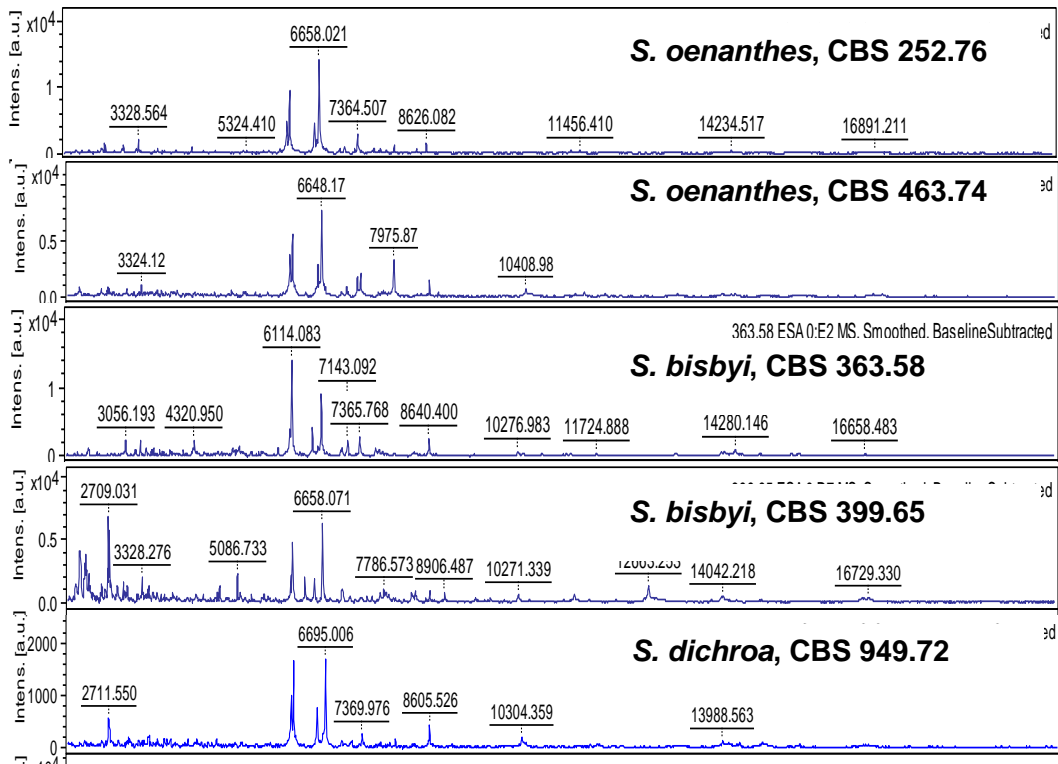
Four *S. chlorohalonata* strains were used for the validation of the MSPs (Figure 5-26). From the results, we observed some peak differences in the isolate grown on SDB, particularly CBS 108283, with less intensity at the lower m/z and one prominent peak at approximately 8093 m/z. All isolates produced more than 6 spectra except for CBS 328.37. The extraction had been repeated for CBS 328.37 grown in SDB, however, it was difficult to obtain produced poor spectra and were therefore this isolate was excluded from the study. The spectra generated from *S. chlorohalonata* grown in PDB showed a more consistent but fewer high intensity low molecular weight peaks compared with SDB. However, peaks ranging from 6000 – 6700 m/z were present in both conditions and appeared to be the most prominent peaks in most of the strains in both media.



5.3.4.2.3 Other *Stachybotrys* spp.

Five isolates of other *Stachybotrys* spp. grown in SDB (Appendix 5-Z) and PDB (Appendix 5-AA) also included in this study consisted of 3 species namely: *S. oenanthae* (CBS 252.76), *S. oenanthae* (CBS 463.74), *S. bisbyi* (CBS 363.58), *S. bisbyi* (CBS 399.65); and. *S. dichroa* (CBS 949.72) (Figure 5-27). However, by using PCR of universal and specific primers as presented in Chapter 4, we had re-identified some of the species including *S. oenanthae* (CBS 252.76) to *S. nephrospora*, *S. bisbyi* (CBS 363.58) to *S. elegans* and *S. dichroa* (CBS 949.72) to *S. parvispora*. Therefore, we would expect some differences in their protein patterns and not to be closely related to *S. chartarum* or *S. chlorohalonata*.

a. Other *Stachybotrys* spp. grown in SDB



b. Other *Stachybotrys* spp. grown in PDB

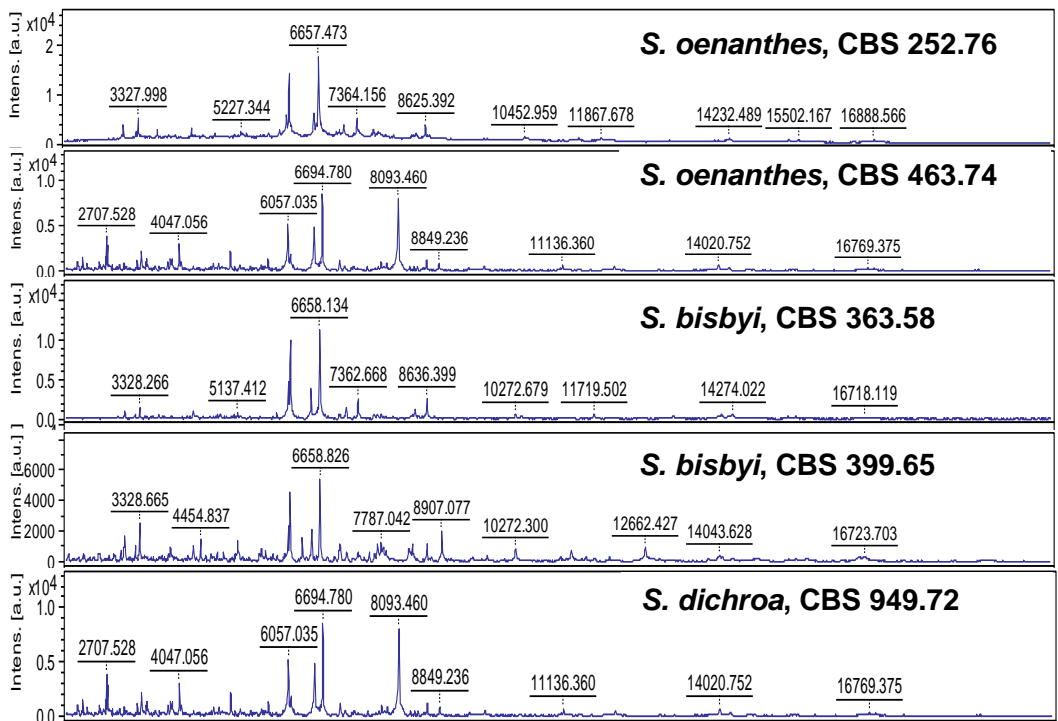


Figure 5-27: Representation of protein profiles of other *Stachybotrys* spp. a. *S. oenanthes* (CBS 252.76), b. *S. oenanthes* (CBS 463.74); c. *S. bisbyi* (CBS 363.58), d. *S. bisbyi* (CBS 399.65); and d. *S. dichroa* (CBS 949.72) grown in a. SDB and b.PDB.

5.3.5 Summary of score values of *Stachybotrys* spp.

All *Stachybotrys* spp. were compared with the MSP generated from *S. chartarum*, NCPF 7597 in replicates for SDB (Table 5-4) and PDB (Table 5-5). The cut-off points suggested by Bruker were applied as described in Table 5-2 (method section 5.2.6).

From the results, we found that fungi grown in SDB gave more consistent and higher scores compared to fungi grown in PDB. This might be due to the generation of more peaks in SDB which allowed for better comparison between samples. There was also more distinct range between species where the cut off point for *S. chartarum* was in the range was 2.3 – 2.7, *S. chlorohalonata* in the range of 1.8 to 2.1 and other *Stachybotrys* spp. below 1.6.

Table 5-4: Score values of *Stachybotrys* spp. grown in SDB for 24 hours against MSPs generated from 2 biological replicates of *S. chartarum*, NCPF 7587.

Species	Strains	NCPF 7587 (replicate 1)	NCPF 7587 (replicate 2)
<i>S. chartarum</i>	ATCC 16026	2.693	2.688
	NCPF 7587	3	2.933
	CBS 324.65	2.465	2.501
	CBS 182.80	2.392	2.387
<i>S. chlorohalonata</i>	CU Stach	2.034	2.116
	CBS 109286	1.737	1.807
	CBS 109283	1.857	1.916
<i>S. oenanthes</i>	CBS 252.76	1.504	1.212
	CBS 463.74	1.424	0.967
<i>S. bisbyi</i>	CBS 363.58	1.118	0.672
	CBS 399.65	0.877	0.914
<i>S. dichroa</i>	CBS 949.72	1.082	1.27

With the fungi grown in PDB, replicate 1 gave more consistent results compared to replicate 2 (Table 5-5). A low score was obtained for *S. chartarum*, CBS 182.80 against NCPF 7587 replicate 2. Two isolates, *S. chlorohalonata*, CBS 109283 and *S. dichroa*, CBS 949.72 gave different cut-off points against both replicates based on Bruker classification although the differences between replicates were only 0.084 and 0.114, respectively. However, the overall range was comparable to the MSPs generated from SDB, where the cut-off points for *S. chartarum* were between 2.2 – 2.6, *S. chlorohalonata* between 1.8 and 2.1 and other *Stachybotrys* spp. was below 1.8.

Table 5-5: Score values of *Stachybotrys* spp. grown in PDB for 24 hours against MSPs generated from 2 biological replicates of *S. chartarum*, NCPF 7587.

Species	Strains	NCPF 7587 (replicate 1)	NCPF 7587 (replicate 2)
<i>S. chartarum</i>	ATCC 16026	2.422	2.596
	NCPF 7587	3	2.774
	CBS 324.65	2.292	2.266
	CBS 182.80	2.273	0.35
<i>S. chlorohalonata</i>	CU Stach	2.098	2.02
	CBS 328.37	1.83	1.927
	CBS 109286	1.992	1.928
	CBS 109283	2.047	1.903
<i>S. oenanthes</i>	CBS 252.76	1.478	0.944
	CBS 463.74	1.138	1.117
<i>S. bisbyi</i>	CBS 363.58	0.601	0.671
	CBS 399.65	0.328	0.198
<i>S. dichroa</i>	CBS 949.72	1.704	1.62

5.4 DISCUSSION

This study demonstrates the application of MALDI-TOF for the identification of *S. chartarum* and its species using a standard, general protocol for filamentous fungal identification provided by Bruker. Many studies have demonstrated that filamentous fungi could be identified with MALDI-TOF using various platforms such as the Vitek MS (bioMérieux, Marcy l'Étoile, France), the Bruker Biotyper (Bruker Daltonics, Bremen, Germany), the Andromas (Andromas SAS, Paris, France) and the Axima/ Saramis (Shimadzu/AnagnosTec, Duisburg, Germany) ^(148, 232-234). We have opted to work with the Bruker platform as the machine was available and was properly maintained and calibrated. Although Vitek MS also integrates the open database SARAMIS (Spectral Archiving and Microbial Identification System) with its own database, most of the publications on MALDI-TOF referred to Bruker techniques which would allow us to make a better comparison. Furthermore and the Bruker Biotyper gave more accurate identification when compared side by side with the Vitek MS ⁽²³⁵⁾.

MALDI-TOF requires an effective protein extraction and extensive MSPs databases which play a central role in identifications ⁽²³⁶⁾. MALDI-TOF platform such as Bruker, not

only provides its own database but also allows addition of new MSPs into the system. Lau *et al.*⁽¹⁶⁷⁾ from the National Health Institute (NIH, USA), developed one of the most comprehensive clinically-relevant mould database for mould identification directly from fungi grown on solid media which includes 70 dematiaceous fungi from a total 294 isolates obtained from the CBS, ATCC and the NIH, USA. The in-house database outperformed Bruker database when challenged against 421 blinded clinical isolates from NIH, USA with 88.9% isolates were identified as accurate species level (score ≥ 2) compared to the Bruker's database with only 0.7% isolates. However, Singh A *et al.*⁽²³⁷⁾ reported a higher identifiable rate of 32% (23/72) of clinically melanised fungi isolates compared to the study by Lau *et al.*⁽¹⁶⁷⁾, probably due to the usage of liquid culture. Only 20% (6/29) of fungal species were identified by Bruker as accurate species level (score ≥ 2) but a 100% identification was achieved by using the in-house database.

Prior to identification, we had to construct the MSPs for *S. chartarum* since most of the fungi listed in the database are the common clinically important fungi. MALDI-TOF has been widely use in clinical laboratories and therefore most of the MSPs generated are mainly clinical isolates with a few environmental isolates. The same species derived from either clinical or environmental samples may have different protein profiles depending on the sources or changes due to environmental stress. The variations in protein profiles indicate the need to expand the library to environmental fungi and encompass both clinical and environmental isolates for the same species.

5.4.1 Protein extraction optimisation

Protein extraction from dematiaceous fungi has often been a problem due to the melanin which causes signal suppression in mass spectrometry ^(172, 238). Several modifications of standard protocols have been studied, such as the suppression of melanin, choosing a different medium and the additional chemical treatment to improve the mass spectrometry signals. The modifications include addition of a melanin suppressors such as tricyclazone ⁽¹⁷²⁾, and additional washing with a chemicals such as dimethyl sulfoxide (DMSO) ⁽¹⁰⁷⁾. The modifications makes it difficult to apply a standard protocol on routine laboratories for the identification of all fungi.

For method optimisation, the standard operating procedure for the cultivation and sample preparation for filamentous fungi supplied by Bruker was performed on *S. chartarum*, NCPF 7587 and *A. niger*, ATCC 16888. In this study, we have successfully generated good reproducible spectra for both *S. chartarum*, NCPF 7587 and *A. niger*, ATCC 16888 grown in SDB and PDB for 24 hours at 25 °C.

We found that the choice of media greatly influenced the quality of mass spectra. *S. chartarum* grown in PDB produced less melanised fungal mass which yielded good spectra with lower peaks. On the other hand, fungi grown in SDB produced a heavily melanised fungal mass but the mass spectra tended to be inconsistent with a high number of peaks detected at the lower molecular weight peaks. This was probably due to the presence of 'inhibitors' particularly melanin. Busbirk *et al.*⁽¹⁷²⁾ has reported on the inhibition of MALDI-TOF spectra by fungal pigment from *A. niger* and solved the problem by adding tricylazole to the growth media. However, melanin suppression might alter the protein profiles due to disturbances in the metabolic pathway and would not be suitable for protein expression studies. Ulrich *et al.*⁽¹⁰⁷⁾ claimed to achieve very good reproducibility and an extensive identification of 45 isolates of *Stachybotrys* spp. by the addition of dimethyl sulfoxide to remove non-specific low molecular weight compounds. However, the mean scores for *S. chartarum* and *S. chlorohalonata* were 2.509 to 2.739 and 2.148 to 2.622, respectively which means the cut-off points between 'highly probable species' and 'secure genus' identification were not clearly differentiated. Moreover, in this study, more peaks were observed in SDB compared to PDB and eventually led to a higher score which suggests that more peaks would provide more peaks matches and enhance the scores.

The types of media were shown to influence the protein profiles in *S. chartarum* as shown by growth in SDB and PDB. The differences were observed particularly in the low molecular weight proteins which were present only in *S. chartarum* grown in SDB. This might reflect the phenotypic characteristics of the more pigmented fungal mass compared to *S. chartarum* grown on PDB. The finding was in accordance with *S. chartarum* grown on ESA which produced more pigmentation compared to PDA (as discussed in Chapter 3). Although *A. niger* grown in SDB also gave darker coloured fungal mass compared to PDB (Figure 5-4), interestingly, that did not affect the protein profiles. This might be due to the characteristics and different type of pigment produced by *S. chartarum* in contrast to *A. niger* as a non-dematiaceous fungi. Dematiaceous fungi such as *S. chartarum* produce dark brown or black surface colonies like *A. niger*, but more importantly, it also has a black reverse that distinguishes the dematiaceous fungi from other black conidia producing fungi such as *A. niger*.

We have also performed direct identification using solid media as it was thought to be easier and quicker compared to cultivation in broth⁽¹⁶⁷⁾. We obtained different protein profiles from *S. chartarum* grown in broth, and inconsistencies between replicates. Compared to bacteria or yeasts, mould biomass is more heterogeneous which leads to

more variations, and therefore the protocol needs to be standardised ⁽²³⁹⁾. Due to the heterogeneity, the sampling technique needs to be optimised to obtain reproducible and reliable protein profiles each time, and we also need to take into account the differences in fungal morphology and growth on solid media when some fungi take longer to grow and produce a mature colony. Media affects sporulation and therefore, the choice of medium is crucial. Hettick *et al.* ⁽²³⁸⁾ demonstrated poor fingerprint mass spectra from *A. niger* grown in malt extract agar. In our study, the quality of spectra were also affected by temperature and the incubation period. Higher temperature (30 °C) and 48 hours incubation gave poor quality of mass spectra with spectral inhibition and higher low molecular weight peaks. Therefore, we conclude that *Stachybotrys* spp. grown in SDB or PDB incubated at 25 °C for 24 hours as most suitable for identification using MALDI-TOF.

Although we were following the Bruker method for protein extraction without the addition of chemicals, we have identified a few simple, critical, steps that have significantly influenced the success of generating good spectra by MALDI-TOF mass spectrometry without major modifications, as follows:

Firstly, the starting material needs to be obtained from a fresh and actively growing colony (before the edge and mainly spores) and this needs to be standardised each time.

Secondly, only a small amount of sample needs should be transferred into the liquid media to allow unsaturated growth of fungal mass. The fungal mass was mixed by using a swab or vortexing to avoid clumps, followed by incubation using a rotary shaker. Several tubes could be pooled together if the fungal mass obtained was too small as some fungal mass was lost during the washing steps.

Thirdly, it was important to thoroughly wash the samples by completely breaking up the pellet to eliminate of the potential inhibitors such as media proteins and fungal pigments. The presence of residual media could be seen by the occurrence of bubbles in the supernatant when vortexed. Additional washing steps with ultrapure water were required in addition to those recommended by Bruker.

Next, the choice of media played a vital role as some media, such as MEA, increased melanisation in *Stachybotrys* spp. leading to the inhibition of spectra. Although MEA was recommended as general detection media for indoor environmental fungi, it was unsuitable for MALDI-TOF ^(172, 211).

Finally, we spun down the final supernatant prior to loading onto the MALDI plates to obtain an even layer of protein on the plate without debris. This was left to dry before layering with HCCA matrix.

5.4.2 Development of MSPs in-house database

After the spectral normalisation, the peaks from both replicates were tested for reproducibility between replicates. Although this protocol is not included in the Bruker manual, we included this step to ensure the reproducibility of the extraction method, biological replicates and sample loading ('spotting') onto the MALDI plates.

We obtained reproducible peaks for both *S. chartarum*, 7587 replicates grown in SDB tested by using the Student's t-test. On the other hand, NCPF 7587 grown in PDB showed a peak different between 2 replicates at m/z 4000 which indicated that one of the replicate was slightly out of the normal range. The reliability of the MSPs were then tested with other isolates treated as test samples.

Both replicates were identified as *A. niger* grown in SDB with the log (score) values of 1.577 to 2.075 (replicate 1) and 1.890 to 2.223 (replicate 2) against the existing Bruker Library for Filamentous fungi (Figure 5-20 and Figure 5-22). Whereas, the score values for both replicates grown in PDB showed the log (score) values of 2.006 to 2.365 (replicate 1) and 1.890 to 2.160 (replicate 2). Even though the majority of the scores ranged from 'probable species' and 'probable genus' based on the Bruker classification, all of the identifications were given as *A. niger*.

We challenged *S. chartarum*, ATCC 16026 grown in SDB against the MSPs created and the existing Bruker database. Although the scores were lower against MSPs created from *S. chartarum* grown in PDB, the highest log (score) of 2.33 (replicate 1) and 2.106 (replicate 2) still indicated 'probable to highly probable species'. The other identifications given were other fungal genera such as *Culvularia* sp., *Aspergillus* sp. and *Fusarium* sp. with scores of no more than 1.077 which indicate unreliable identification (Table 5-2). Therefore, the MSPs created showed highly reliable identification of *S. chartarum* and needs to be further tested with more *Stachybotrys* isolates.

The score values obtained might not be applicable for filamentous fungi since the cut-offs were designed for bacterial identification, hence the lower score values might be appropriate ⁽²⁴⁰⁾. More reliable identification down to the species level has also been obtained with yeasts compared to moulds ⁽²³⁹⁾. Until now, there was no consensus on

the threshold for filamentous fungi. Different researchers have employed different approaches to increase the score values such as lowering the threshold to 1.7 or depositing more than one spot per extract to decrease the number of unidentified samples ^(240, 241). However, in this study, we have successfully identified *S. chartarum* to the species level according to Bruker's recommended log (scores) by depositing at least 3 spots per sample.

5.4.3 Identification of *Stachybotrys* spp.

We have successfully distinguished *S. chartarum* from other species, particularly *S. chlorohalonata* using the Bruker standard method. We compared our results with a previous studies on *Stachybotrys* spp. (Table 5-6). Clear cut-off points in the scores values were obtained for both *S. chartarum* and *S. chlorohalonata* compared to other studies by Gruenwald *et al.*⁽¹⁰⁶⁾ and Ulrich *et al.* ⁽¹⁰⁷⁾.

S. chartarum grown in SDB gave consistent and higher scores, probably because it produced more peaks in both replicates, and therefore increased the number of peak matches. The score values for 'highly probable species' *S. chartarum* grown in PDB was slightly lower compared to the Bruker recommendation which was 2.2 to 2.8. However, the range was higher compared to the study by Gruenwald *et al.* with 1.691 to 2.441 from *S. chartarum* grown on malt extract agar (MEA). This study also showed more distinct ranges between 'high probable species' and 'probable species' compared to both previous studies where score values overlapped for both species. Although Ulrich *et al.* demonstrated higher score values for *S. chartarum* grown in malt dextrose broth (MEB), *S. chlorohalonata* was also classified as a 'highly probable species' using both Bruker's recommendation and their created MSPs.

Other *Stachybotrys* spp. gave the score values of 'no reliable identification' when compared with our MSPs, although it was supposed to be at least within the range of 'probable genus' according to the Bruker classification. This study is in accordance with the result by Gruenwald *et al.* which showed log (scores) of *S. bisbyi* below 1.699. The small difference of log (scores) between *S. chartarum* and *S. chlorohalonata* showed that both isolates were very closely related not only in terms of DNA sequences but also protein profiles. However, the MSPs were not suitable to identify other *Stachybotrys* spp., and therefore, MSPs from other species need to be generated in the future.

Table 5-6: Summary of cut-off point obtained from this study and previous studies.

Bruker		Fungi	Gruenwald <i>et al.</i> (2015)	Ulrich <i>et al.</i> (2016)	This study (against <i>S. chartarum</i>)	
Description	Range		MEA	MEB	SDB	PDB
Highly probable species identification	2.3 to 3.00	<i>S. chartarum</i>	1.691 – 2.441	2.509 – 2.739	2.3 - 2.9	2.2 - 2.8
Secure genus identification, probable species identification	2.0 to 2.299	<i>S. chlorohalonata</i>	1.955 - 2.348	2.148 – 2.622	1.8 - 2.29	1.8 - 2.19
Probable genus identification	1.7 to 1.999	Other than <i>S. chartarum</i>	Refer to <i>S. chlorohalonata</i>			
Not reliable identification	below 1.699	Other than <i>S. chartarum</i> and <i>S. chlorohalonata</i>	1.594 (<i>S. bisbyi</i>)	NA	below 1.6	below 1.7

5.5 CONCLUSIONS

The standardised Bruker protocol can be applied to pigmented moulds provided several critical additional steps are taken. The standard Bruker method for protein extraction was successfully employed without chemical addition or melanin suppression. The choice of media for cultivation was crucial, such that media which promotes melanin production should not be used for MALDI-TOF when the standard protocol is applied. We have also identified critical steps that have significantly influenced the success of generating good spectra by MALDI-TOF mass spectrometry. Solid media is another way forward for dematiaceous fungi, but more studies and optimisation in the method are required to facilitate the reproducibility of the results.

CHAPTER 6

INHIBITORY EFFECTS OF SELECTED ANTIMICROBIAL AGENTS ON *STACHYBOTRYS CHARTARUM*

This chapter presents work on the inhibitory effects of selected antimicrobial agents commonly used for treatment and prevention of environmental microbial colonization, contamination or infestation. Bleach, hydrogen peroxide vapor and peracetic acid (treatment) and organosilane (prevention) were examined for their impact on *S. chartarum* grown on solid media or in liquid suspension, using laboratory assays. The term 'treatment' in this study refers to the chemicals used for cleaning or treating contaminated surfaces, while 'prevention' refers to the chemical used to prevent fungal growth on surfaces.

6.1 INTRODUCTION

Antifungal agents are designed specifically to inhibit or interfere with fungal growth, either clinically, where they are antifungal drugs, or as fungicides used in the environment. Antimicrobial agents with various modes of action have been developed, and their effectiveness against target organisms is often measured as the minimum inhibitory concentration (MIC). The MIC, determined either by agar or broth dilution methods, is the lowest concentration of a chemical which inhibits the growth of the microorganism but does not necessarily kill it. It has also been employed to evaluate the resistance of certain microorganisms to antimicrobial agents.

The aim of this study was to assess the efficacy of various commercially available antimicrobial agents for their fungistatic (inhibit the growth) or fungicidal (kill the fungus) effects ^(242, 243).

Here, we describe the effects of antimicrobial agents consisting of bleach (NaOCl), aerosolised hydrogen peroxide (AHP), peracetic acid (PAA) and organosilane (OS) on *S. chartarum* grown on solid media and liquid suspension using direct treatment, microdilution plates adapted from the EUCAST method and the agar dilution plate methods.

6.2 MATERIALS AND METHODS

6.2.1 Experimental set-up

Effects of antimicrobial activity were assessed by comparing the average hyphal growth on solid media plates and measuring the optical density which was directly proportional to fungal growth in liquid media by following the European Committee on Antimicrobial Susceptibility Testing (EUCAST) method. Four types of antimicrobial agents namely sodium hypochlorite (Bleach, Evans Vanodine International PLC), hydrogen peroxide (Glosair™, ASP Johnson & Johnson), peracetic acid (Peracide™, Sky Chemical UK Limited) and Organosilane (Biosafe®, Gelest Inc.) were tested on *S. chartarum* grown on solid media and in broth.

6.2.1.1 Direct treatment of antimicrobial agents on fungal inoculum grown on solid media (method 1)

This method was referred to as direct treatment, whereby chemicals were applied placed directly on top of the fungal inoculum grown on ESA and PDA. A 7-mm cork borer inoculum (from an established 7-days fungal colony) was placed in the exact centre of a solid media plate into a previously prepared 7-mm hole. The fungal inoculum was then treated with 500 µl concentrations of antimicrobial chemicals at various concentrations with a one-off application or single applications repeated for 2 consecutive days with the concentrations as described in section 6.2.3. The plates were incubated at 25 °C for 7 days. For double applications, the plates were incubated in between treatments for 24 hours and after the treatment for 7 days. Radial growth and microscopic appearances were observed for any significant changes. The test was carried out in replicate.

6.2.1.2 Fungal growth in liquid suspension containing antimicrobial agents using microdilution plates (method 2)

This method was performed following the EUCAST antifungal MIC method for moulds (EUCAST definitive document E. (Def. 9.3) with some modification. Since the antifungals used in this study are not stable once prepared, we did not prepare the stock solutions and store them according to EUCAST. This method was employed only for bleach and PAA.

Double strength RPMI 1640-2% Glucose-buffered with 3-(N-morpholino) propanesulfonic acid (MOPS) was prepared according to EUCAST (Appendix 6-A). Briefly, RPMI 1640 (with L-glutamine but without bicarbonate) (R6504, Sigma Aldrich) was supplemented with glucose to a final concentration of 2% and MOPS to a final concentration of 0.165 mol/ L (M1254, Sigma Aldrich). The solution was carefully mixed with a magnetic stirrer, and the pH was adjusted to 7.0 at 25°C using 1 M sodium hydroxide (NaOH) (S8045, Sigma Aldrich). The media was filter sterilised with a 0.22 µm pore size filter (Z290807, Merck) and stored at 4°C until use.

Each experiment was set up in two sets of Corning® 96-well plates with flat-bottom wells (CLS3595, Sigma Aldrich) with and without fungal spores. Wells without spores were used as a measure of background absorbance reading. To each of the wells were added 100 µl of the various antifungal agents, diluted with RPMI-2% G-MOPS, and 100 µl spore suspension. Control wells contained 100 µl of RPMI-2% G-MOPS only (without chemical) and 100 µl spore suspension. Blank wells served as negative control and contained 100 µl of RPMI-2% G- MOPS, and sterile deionised water supplemented with 0.1% Tween-20 to prepare the spore suspension. The plate was incubated without agitation at 25°C (instead of at 34 to 37 °C according to EUCAST) for 24 hours. The test was carried out in triplicate.

The absorbance was recorded at 650 nm. Statistical analysis was performed using one-way analysis of variance (ANOVA) with the Dunnett multiple comparison test where $p < 0.05$ denoted a significant difference compared to control.

6.2.1.3 Fungal spores grown on solid media containing antimicrobial agents (method 3)

The agar dilution method was used for OS due to insolubility of the compound in the RPMI 1640 medium, with bleach as a comparison. Each antimicrobial agents were mixed with each melted agar medium (ESA and PDA) accordingly, to make up a total volume of 20 mL medium containing the diluted chemical. Fungal conidia ($2-5 \times 10^4$ CFU/mL) were prepared in suspension containing 1:10 PBS-Tween in sterile water. 100 μ l of the spore suspension were applied onto the centre of the plates. Plates were incubated at 25 °C for 7 days. The MIC was determined from the lowest concentration of the agents with no visible growth. Each test was run in triplicate.

6.2.2 Preparation of fungal inocula

6.2.2.1 Preparation of isolates

S. chartarum (NCPF 7587) was grown on ESA at 25 °C for 7 days. The inoculum was prepared to be use directly for method 1 by removing a disc using a 7-mm cork borer.

6.2.2.2 Preparation of spore suspension

The inoculum was taken from 5-7 day-old culture and added to 10 ml of sterile deionized water supplemented with 0.1% Tween-20 (P1379, Sigma Aldrich). The suspension was filtered with an 11 μ m pore size sterile filter (NY1104700, EMD Milipore Merck) to remove hyphae and obtained a suspension of conidia.

The suspension was adjusted by counting in a 0.100 mm depth BRAND® haemocytometer chamber (717820, Sigma Aldrich). Briefly, a sample was diluted 1:1 with lactophenol blue before loading 10 μ l of the resultant solution in between glass coverslip and the chamber. The slide was observed under the microscope at 20X magnification. Cell density was calculated as described in Appendix 6-B. In method 2, $2-5 \times 10^6$ CFU/ml was used to achieve a final inoculum of $1-2 \times 10^5$ CFU/ml, whereas in method 3, the spore suspension was adjusted to $2-5 \times 10^4$ CFU/ml.

6.2.3 Antimicrobial experiments

6.2.3.1 Sodium hypochlorite (bleach)

Sodium hypochlorite (bleach, Evans Vanodine International PLC) was the main active ingredient which made up approximately 4.5% of NaOCl (Figure 6-1). Other ingredients were not disclosed in the product information sheet or the Material Safety Data Sheet (MSDS) provided by the manufacturer.



Figure 6-1: Sodium hypochlorite (bleach, Evans Vanodine International PLC).

For method 1, bleach was prepared by diluting 45000 ppm into 25000, 20000, 15000, 10000 and 5000 ppm NaOCl in sterile water. The solution was prepared in chemically resistant tubes and kept in the dark prior to use.

For method 2, bleach was prepared by diluting it with RPMI to obtain intermediate concentrations of 45000, 40000, 30000, 20000, 10000 and 5000. The final concentrations of 22500, 20000, 15000, 10000, 5000, and 2500 ppm were achieved after adding 1:1 (v/v) of fungal suspension into the wells.

For method 3, bleach was diluted and mixed with ESA and PDA to obtain the final concentrations of 200, 500, 1000, 1500, 2000 and 2500 ppm to make up a final volume of 20 ml in each plates.

6.2.3.2 Aerosolised hydrogen peroxide (AHP).

The aerosolised hydrogen peroxide (AHP) machine (ASP GLOSAIR™) was operated according to the manufacturer's protocol (Figure 6-2). The machine was sufficient to treat 10 m³ to 200 m³ room volume with a density of 6 ml / m³ and mist particle size of 8 to 12 µm.

An ASP Glosair™ 400 Cartridge containing 5% hydrogen peroxide was inserted into the machine. The “de-gas” sticker was removed to allow fluid from the cartridge to be emptied into the machine. The experiment was carried out in an environmental chamber (UniTemp) at 25°C. The quantity of the disinfectant sprayed was automatically calculated by the machine by filling in the volume of the room to be treated in cubic mm. The room volume was given as 4025 X 4025 X 2700 mm³ which was equal to approximately 43.74 m³, and therefore the spraying time was automatically set for 10 minutes with the mean misting rate of 30 ml per minute.



Figure 6-2: Aerosolised hydrogen peroxide (AHP) machine (ASP GLOSAIR™).

Prior to the experiment, plates containing fungal inocula were placed approximately 180 cm from the source (Figure 6.3). The machine was initiated and gave a countdown before the disinfectant began to spray. A safety sign was displayed at the door to avoid entry during the AHP operation. After the spraying completed, the contact time required for effective decontamination was 2 hours. After 2 hours, the plates were collected and transferred to an incubator, set at 25 °C, for 7 days.

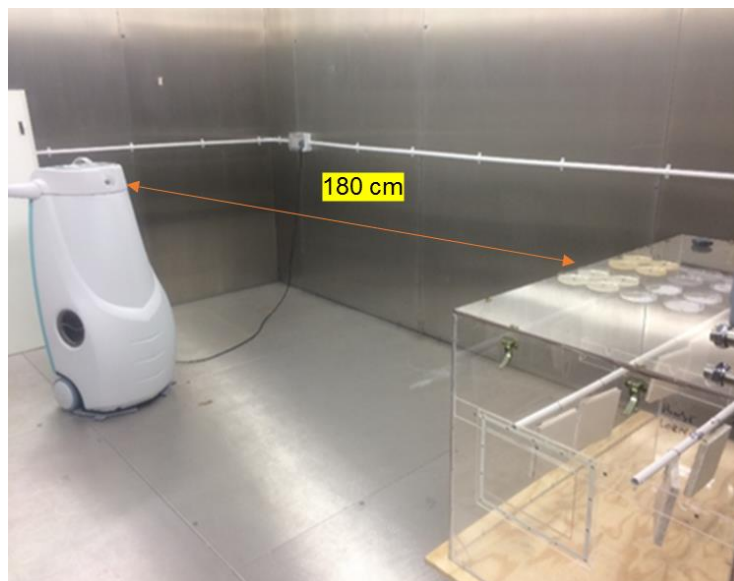


Figure 6-3: The experimental set up with the AHP machine located approximately 180 cm away from the plates containing fungal samples opened prior to treatment placed on top of the smaller chamber.

6.2.3.3 Peracetic acid (PAA)

Peracide PAA *in situ* (10-20% adipic acid, 30-50% sodium percarbonate, tetraacetythylenediamine (TAED) and apple acid perfume) was obtained in 6 g PAA tablets (Figure 6-4). Sodium percarbonate rapidly dissolves in water and breaks down into sodium carbonate and hydrogen peroxide. The reaction with acid produces peracetic acid *in situ* which eventually breaks down to water, carbon dioxide and oxygen.

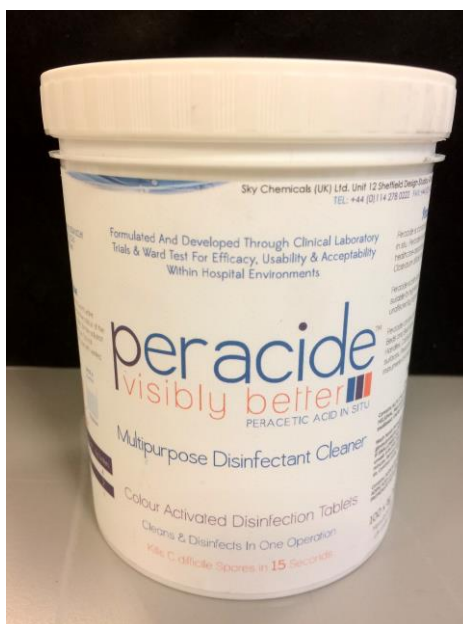


Figure 6-4: Peracide PAA *in situ* (Peracide™).

For method 1, peracetic acid was prepared according to the manufacturer's recommendation of 4 tablets of 6 g PAA tablets dissolved in 1000 ml sterile water. In this experiment, we dissolved 1 tablet in 125 ml sterile water to produce the highest concentration of 8000 ppm. The solution was prepared fresh for every experiment. A pink colour indicated it was ready for use, whereas a colourless solution should be discarded as inactive (Figure 6-5).

For method 2, PAA was prepared by dissolving two tablets in 125 ml sterile water to produce 16 000 ppm as the highest intermediate concentration and serially diluting to lower concentrations with RPMI. The final concentrations were obtained as half of the serial concentrations after adding 1:1 (v/v) spore suspension to obtain the final concentrations of 8000, 4000, 2000 and 1000 ppm.

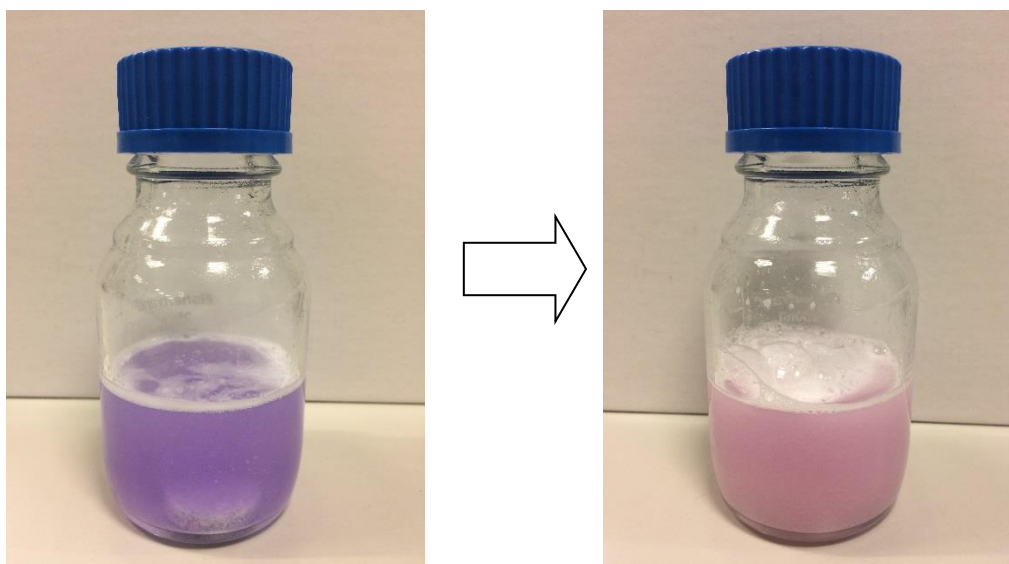


Figure 6-5: The preparation of peracetic acid at concentration 16000 ppm showed the colour indicator from activation stage (purple) to sporicidal stage (pink).

6.2.3.4 Organosilane (OS)

Organosilane (5% (3-trihydroxysilyl) propyldimethyloctadecyl ammonium chloride) was diluted to a 1% (10000 ppm) solution as recommended by the manufacturer and sprayed onto a surface until uniformly wet (Figure 6-6).

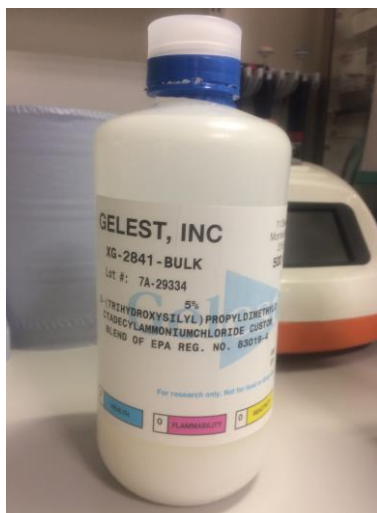


Figure 6-6: Organosilane (Biosafe®).

For method 1, OS was freshly prepared from 50000 ppm into 10000, 5000 and 1000 ppm in sterile water and kept in the dark until use. For method 2, OS was prepared by diluting 50000 ppm with RPMI to obtain intermediate concentrations of 40000, 20000, 10000, 5000 and 2000 ppm.

For method 3, OS was diluted and mixed with ESA and PDA to obtain the final concentrations of 1000, 2500, 5000, 10000 and 15000 ppm to make up a final volume of 20 ml in each plates.

6.3 RESULTS

6.3.1 Inhibitory effects of antimicrobial agents using direct treatment

6.3.1.1 Sodium hypochlorite (bleach)

The effect of bleach on the growth of *S. chartarum* was observed by measuring the diameter of growth on media plates and microscopic observation of fungal structures. Fungal inocula were grown on ESA and PDA and were treated with bleach concentrations ranging from 45000 ppm down to 5000 ppm with a volume of 500 μ l bleach dropped onto the biomass per treatment in a single or repeated (on two consecutive days).

The results from the single applications showed a decrease in growth diameter in both media as the bleach concentrations increased (Figure 6-7). Significant reduction in colony diameter was recorded starting from 10000 ppm in both media, with ESA (2.575 ± 0.050 cm, $p = 0.0014$) and PDA (2.175 ± 0.050 cm, $p = 0.0001$) (Appendix 6-C). There were no increase in colony diameter (0.700 ± 0.000 cm, p -value = 0.0001) on ESA at 45000 ppm and PDA at 25000 ppm and 45000 ppm.

The fungi were seen as dark brown to black from the centre and white at the edge. In ESA, the fungal inocula were covered by the newly formed growth of white mycelium. Microscopically, thicker hyphae were seen as the concentration of bleach increased. No new hyphal growth was observed at 45000 ppm of bleach on ESA and 25000 ppm on PDA and bleach at 25000 ppm appeared to inhibit the production of new spores in ESA. The microscopic images also indicated that the black mass was predominantly spores and the white mass consisted of fungal hyphae. The fungi showed no growth at 45000 ppm bleach on either media as shown in both macroscopic and microscopic images.

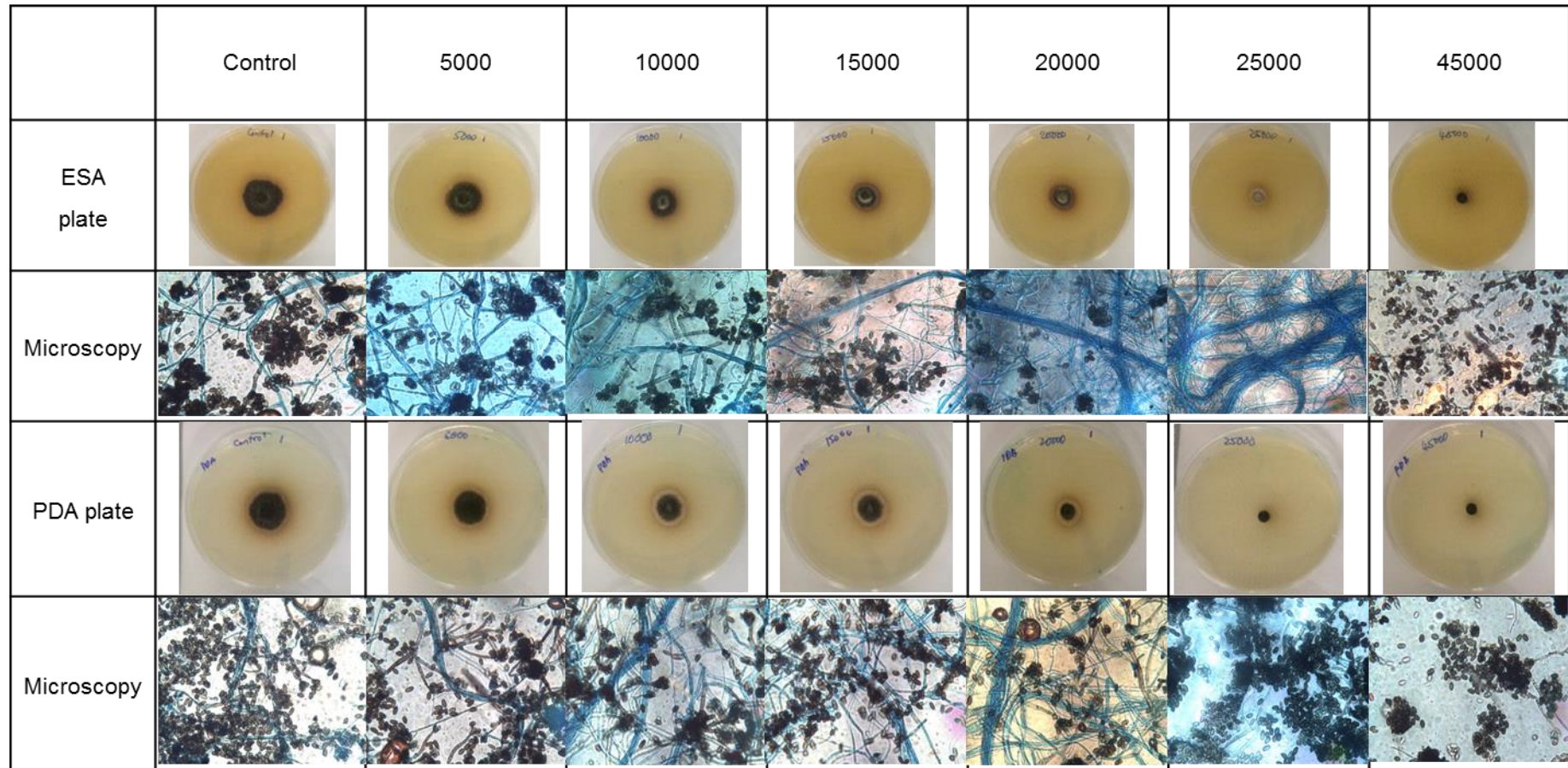


Figure 6-7: Effects of a single application of 500 µl sodium hypochlorite on *Stachybotrys chartarum* shown on ESA and PDA media and microscopy.

Since a high concentration of bleach was required to inhibit the growth of *S. chartarum*, we repeated the application of bleach on a second day to determine the effect of multiple applications on the fungal growth. The effects of two applications showed that a lower concentration of bleach is required to inhibit fungal growth in both media (Figure 6-8). Significant reduction in colony diameter was recorded starting from 10000 ppm in both media, with ESA (2.550 ± 0.100 cm, $p = 0.0175$) and PDA (1.900 ± 0.141 cm, $p = 0.0498$) (Appendix 6-D). There were no increase in colony diameter (0.700 ± 0.000 cm, p -value = 0.0001) on both media at 25000 ppm.

The fungus produced white masses on top of the original fungal mycelium in ESA even at the lowest concentration at 5000 ppm. No growth was observed at 25000 ppm in both media. Microscopically, thicker hyphae were observed particularly in the fungus grown on ESA correlated with the white masses at concentrations starting from 10000 ppm. In fact, the new growth comprised of mainly thick hyphae. Mainly spores were observed from both media at concentrations of 25000 ppm and 45000 ppm and it is thought these were derived from the original fungal inoculum.

From both applications using this direct method, we found that bleach was effective at inhibiting the growth of *S. chartarum*, but at higher than the concentration recommended by the manufacturer (1800 ppm) for cleaning and disinfecting. However, the manufacturer recommends an undiluted solution for sinks, toilets and drains.

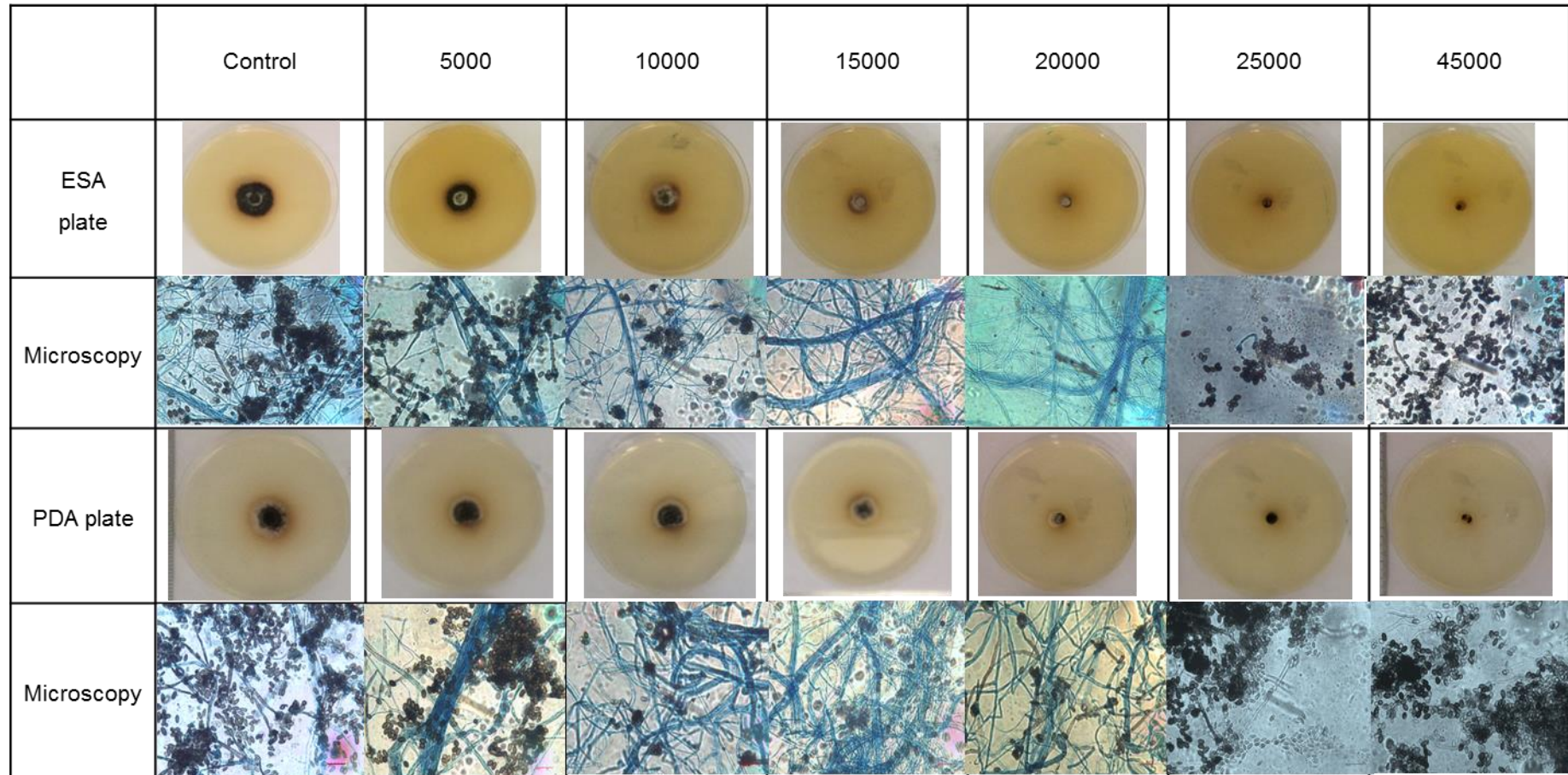


Figure 6-8: Effects of two applications (on consecutive days) of 500 μ l sodium hypochlorite on *Stachybotrys chartarum* shown on ESA and PDA media, with accompanying microscopy.

To determine whether bleach was fungistatic or fungicidal, the fungal inocula from the twice treated plates were directly transferred onto new plates or were mixed vigorously in PBS using a vortex to form a suspensions which were then dropped onto new plates. The plates were left for two weeks at 25 °C. No growth was observed on any of the plates which indicated that direct treatment with bleach at 25000 and 45000 ppm killed *S. chartarum* after two consecutive days treatment; measured either using direct insertion of fungal inoculum on solid media (Figure 6-9) or with spore suspensions (Figure 6-10).

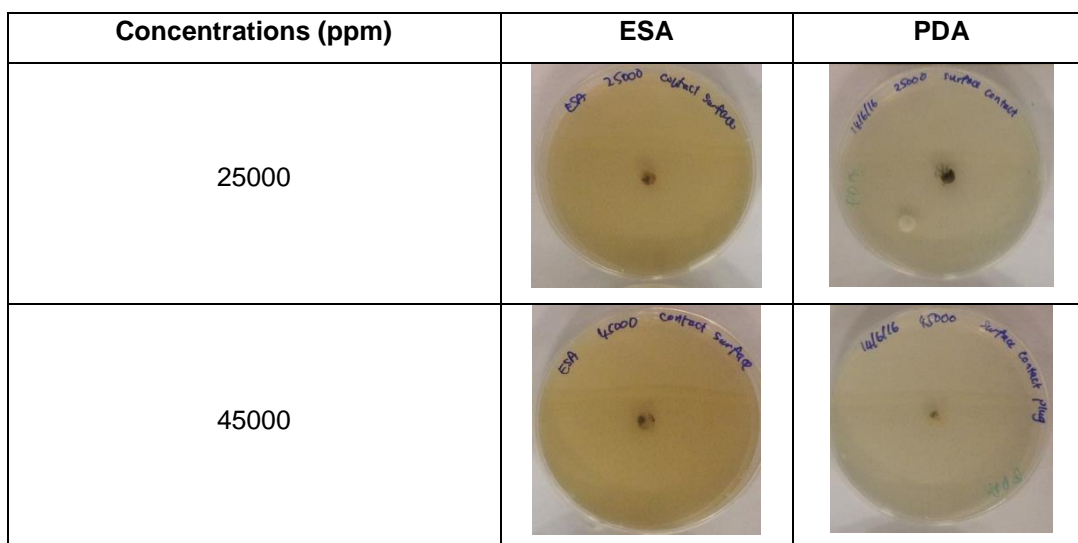


Figure 6-9: Samples from the repeat application plates were inserted into new plates of ESA and PDA and showed no visible new growth after a further 14 days incubation.

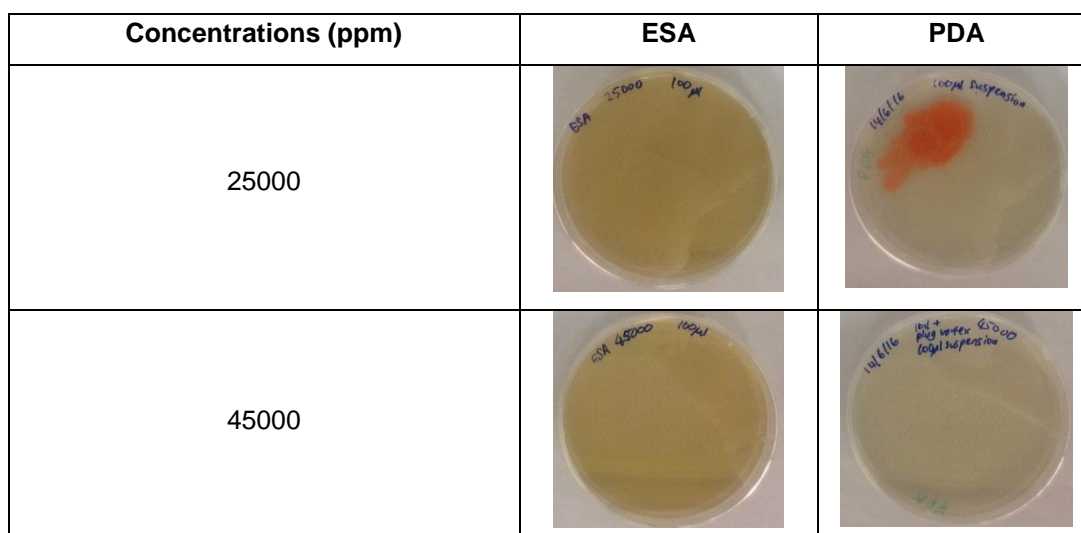


Figure 6-10: Samples from the repeat application experiment plates were vortexed in PBS to produce a suspension and dropped onto the centre of the plate showed no growth after 14 days of incubation. The red coloured colony on PDA at 25000 ppm was contamination from an unknown microorganism.

6.3.1.2 Aerosolised hydrogen peroxide (AHP)

The effects of one cycle of treatment with aerosolised hydrogen peroxide (AHP) on the growth of *S. chartarum* was determined from measurement of growth diameter on ESA and PDA (Figure 6-11). No significant reduction in colony diameter was recorded in both media, with ESA (3.275 ± 0.189 cm, $p = 0.0871$) and PDA (3.250 ± 0.058 cm, $p = 0.3202$) (Appendix 6-E). The results showed no complete inhibition on fungal growth and morphology on both media in all the replicates. This suggests that one cycle of AHP was not effective in killing or inhibiting the growth of *S. chartarum*.

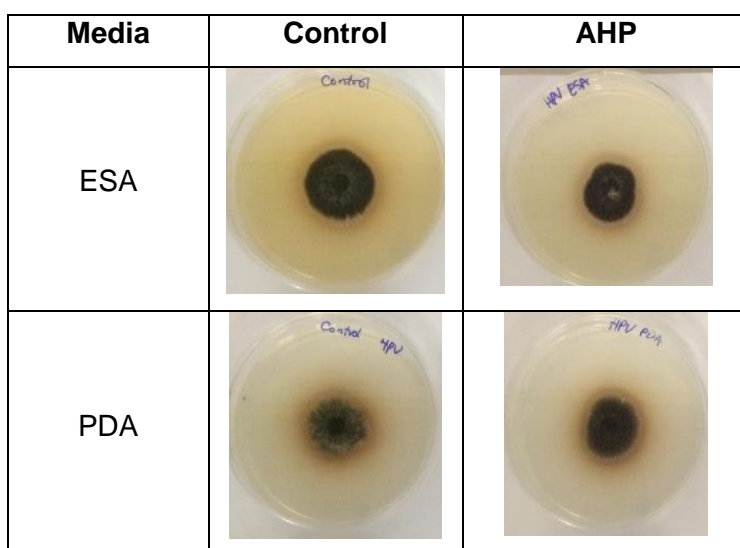


Figure 6-11: Plates treated with a single application of AHP on PDA and ESA compared to control (untreated).

We also performed two cycles of AHP treatment to determine the effects of multiple applications on the fungal growth. From the results, growth and sporulation still occurred on both media (Figure 6-12). However, the diameter of the colonies was significantly reduced following two cycles of AHP in both media, with ESA (1.000 ± 0.115 cm, $p = 0.0001$) and PDA (1.825 ± 0.171 cm, $p = 0.0001$) (Appendix 6-F). Although there was no complete inhibition of growth, it was shown that two cycles of AHP could inhibit the growth of *S. chartarum* more effectively compared to only one cycle.

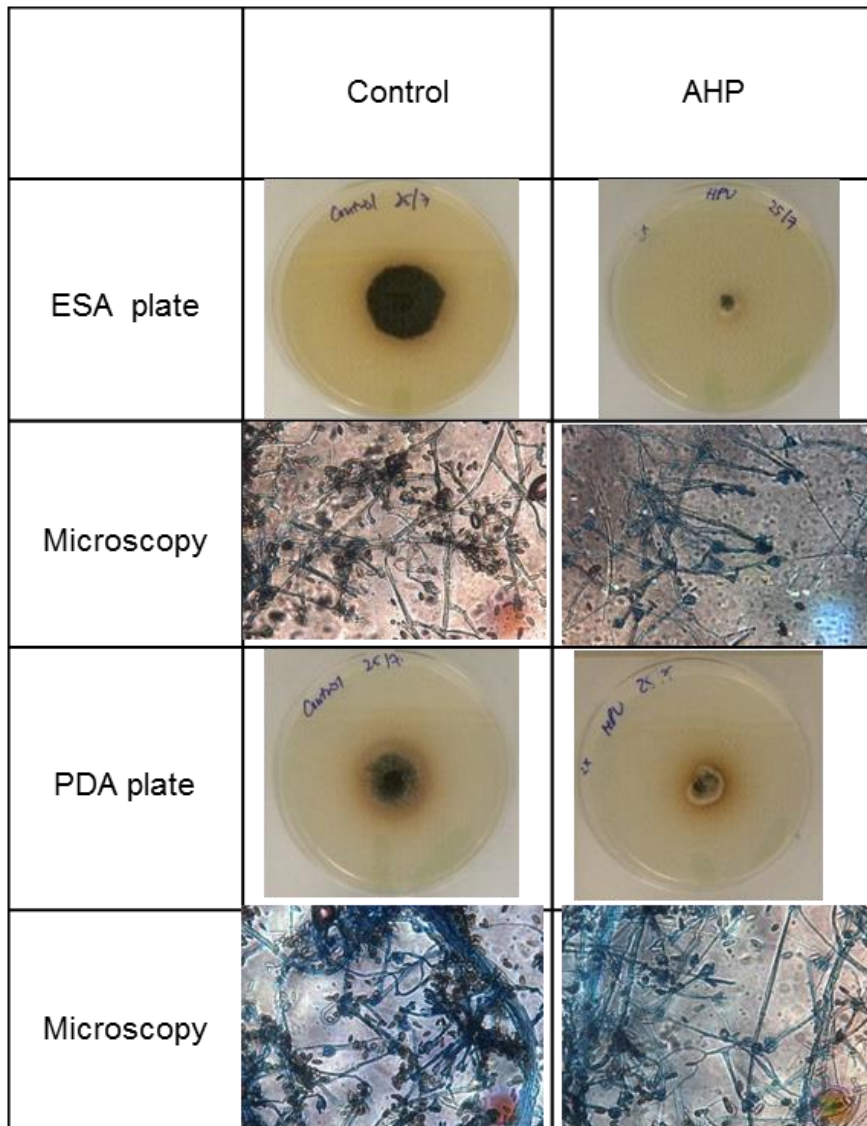


Figure 6-12: Plates treated with two applications of AHP on PDA and ESA compared to control (untreated).

6.3.1.3 Peracetic acid (PAA)

The effects of PAA treatment on the growth of *S. chartarum* grown on ESA and PDA were observed based on growth diameter and microscopic appearances. The fungal samples were treated with one or two applications of 500 µl peracetic acid per treatment with concentrations ranging from 1000 to 8000 ppm. The recommended concentration from the manufacturer is 4000 ppm. However, the concentration was doubled up to 8000 ppm by halving the amount of water used for dissolving the PAA tablet.

The single application of PAA did not show significant reduction in the diameter size in either media (Figure 6-13). Significant reduction in colony diameter was recorded in ESA starting from 1000 ppm (2.875 ± 0.158 cm, $p = 0.0115$) but no significant reduction in PDA at any concentrations (Appendix 6-G). Furthermore, secondary colonies were formed as a result of dispersion of PAA solution on the media (which failed to inhibit them). The microscopic images also showed evidence of fungal growth although less sporulation was observed compared to the control. This indicates that a single treatment of PAA was not effective against *S. chartarum*.

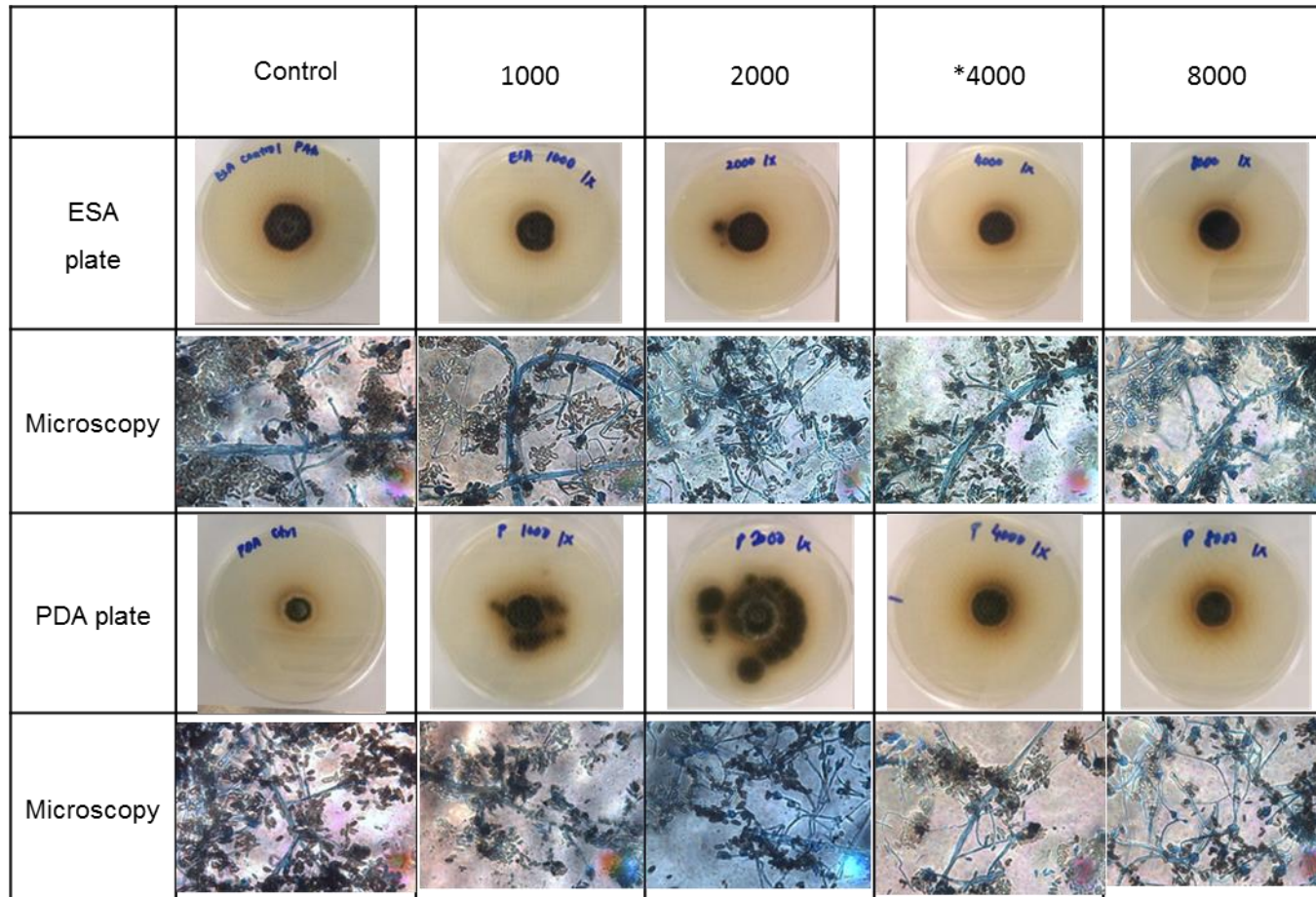


Figure 6-13: Effects of a single application of 500 μ l PAA on *S. chartarum* grown on ESA and PDA media with accompanying microscopy. (*) indicates the recommended concentration by the manufacturer = 4000 ppm.

The effect of two application of PAA was also studied (Figure 6-14). As observed in the single application experiment, lower concentrations of 1000 ppm and 2000 ppm of PPA led to formation of secondary colonies on the media. Significant reduction in colony diameter was recorded in ESA starting from 1000 ppm (2.750 ± 0.071 cm, $p = 0.0156$) but no significant reduction in PDA at any concentrations (Appendix 6-H). However, the diameter colonies was slightly smaller at concentrations of 4000 ppm and 8000 ppm PAA compared to the control in both media, although fungal growth still occurred at all concentrations regardless of multiple exposures to PAA. The fungal growth was also evident from the microscopic images at all concentrations on both media.

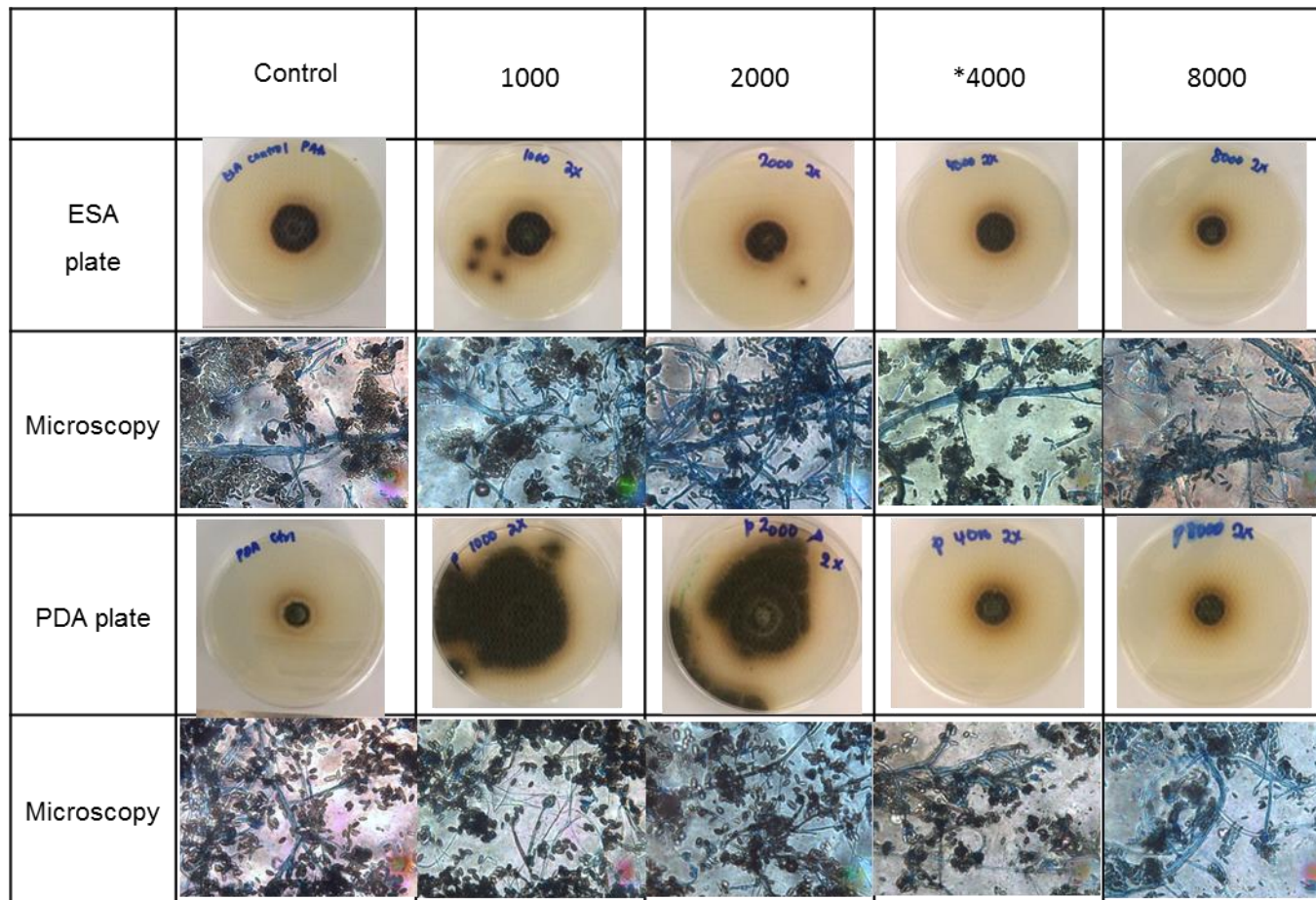


Figure 6-14: Effects of two applications PAA on *S. chartarum* grown on ESA and PDA media with accompanying microscopy. (*) indicates the recommended concentration by the manufacturer = 4000 ppm.

6.3.1.4 Organosilane (OS)

The effects of OS on the growth of *S. chartarum* was again assessed by measuring colony diameter on media plates and microscopic structures. Fungal cork borer inocula were grown on ESA and PDA and were treated with 500 µl OS per treatment in a single or repeated application (on 2 consecutive days) with OS concentrations ranging from 1000 to 10000 ppm.

The lower concentrations of OS at 1000 ppm led to spreading of fungal growth on plates. The single application of OS produced a reduction of colony diameter at concentrations of 10000 compared to control in both media, with ESA (1.050 ± 0.058 cm, p-value = 0.0001) and PDA (1.550 ± 0.058 , p-value = 0.0001) (Figure 6-15) (Appendix 6-l). However, fungal growth still occurred at all concentrations which was also evident from the microscopic images. OS formed a thick white to light brown coloured coating on top of the media at concentrations of 5000 ppm and 10000 ppm where it came in contact with the OS.

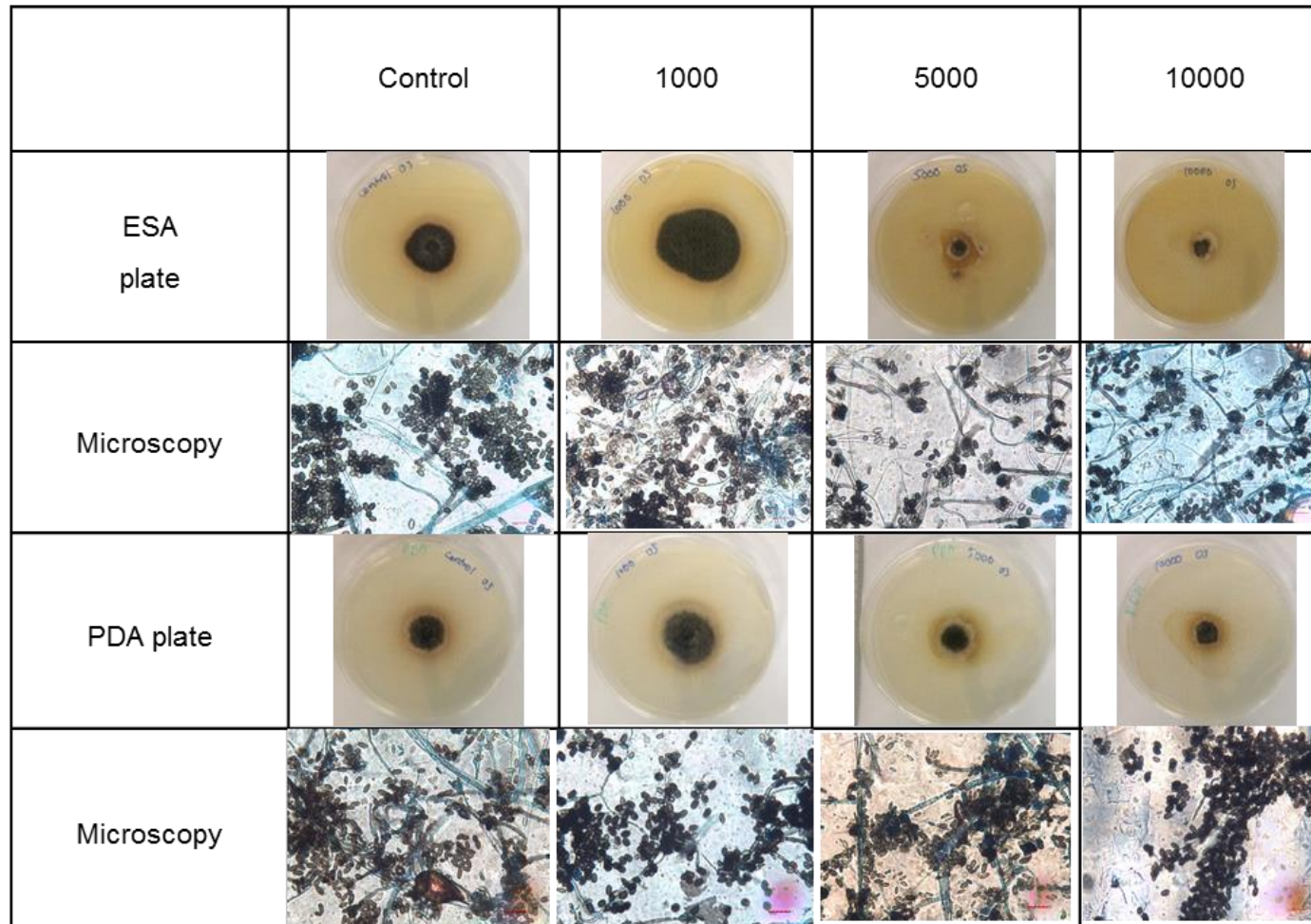


Figure 6-15: Effects of a single treatment at day-1 with OS on *S. chartarum* grown on ESA and PDA media with accompanying microscopy.

The effects of two applications of OS showed reduction in growth only at a concentration of 10000 ppm on both media, with ESA (1.233 ± 0.058 cm, p-value = 0.0001) and PDA (1.033 ± 0.153 cm, p-value = 0.0001) (Figure 6-16) (Appendix 6-J). Secondary colonies were formed at concentrations of 1000 ppm and 5000 ppm suggesting that multiple applications of solution led to dispersion of spores on the media plates (and failed to inhibit subsequent growth). There was no complete inhibition at any concentration on either media regardless of multiple exposures as is evident from both macroscopic and microscopic observations.

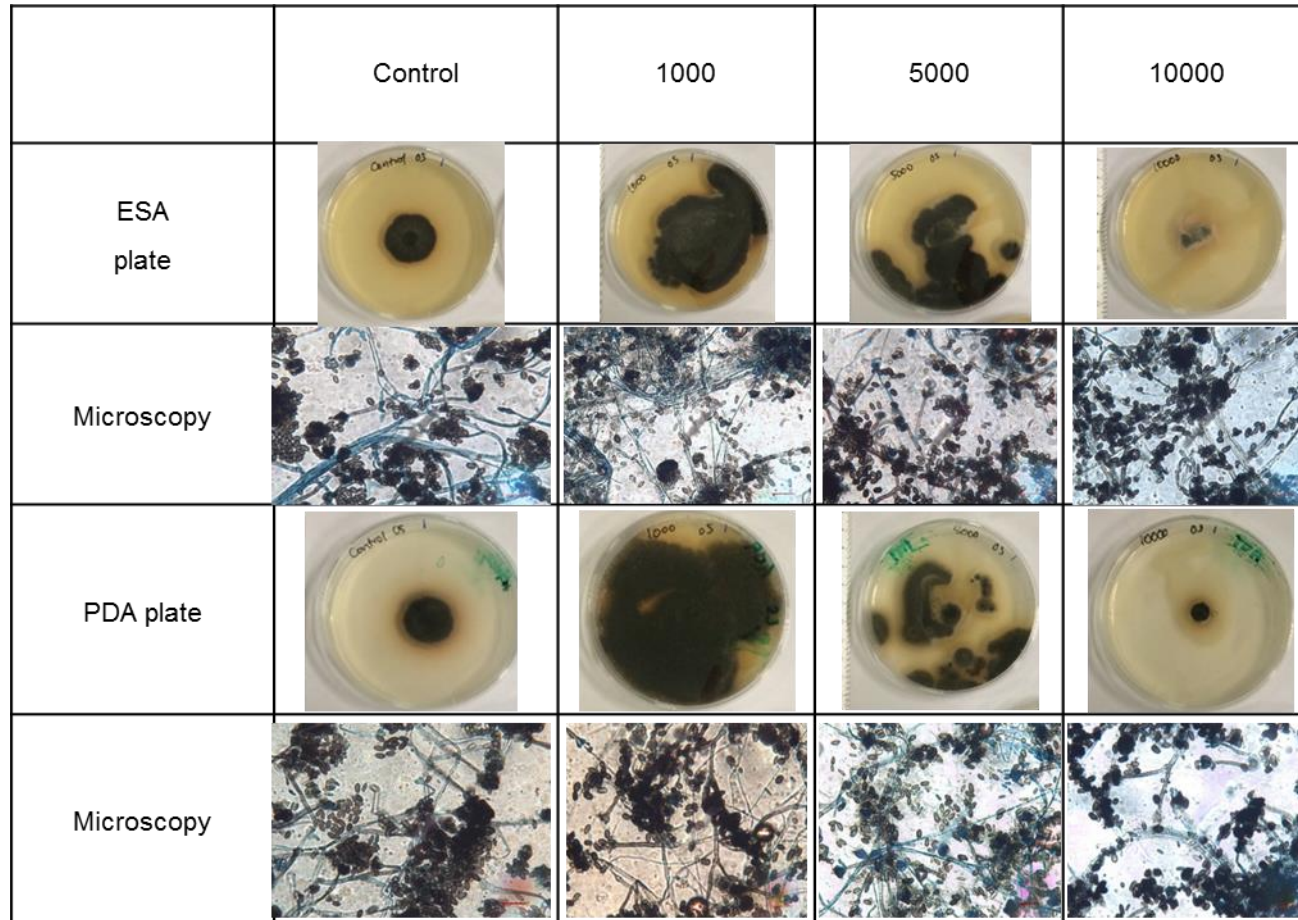


Figure 6-16: Effects of repeated treatment with OS on *S. chartarum* grown on ESA and PDA media with accompanying microscopy.

6.3.2 Inhibitory effects of antimicrobial agents using liquid media assays

6.3.2.1 Sodium hypochlorite (bleach)

It was observed that the addition of bleach changed the colour of the media at various concentrations (Figure 6-17). As a result, a similar plate without spores was prepared to be used as a background reading control for each concentration (Appendix 6-K).

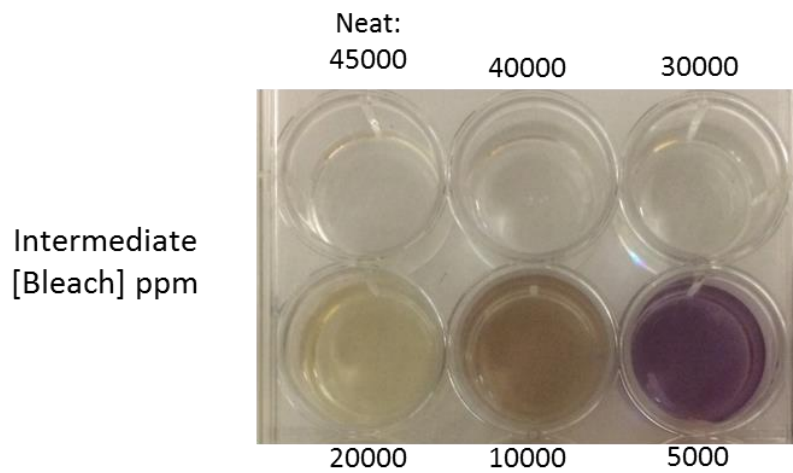


Figure 6-17: The intermediate concentration (before 1:1 dilution with spore suspension) of bleach mixed with RPMI 1640 - 2% G- buffered with MOPS in 2 ml well plates.

The final OD was obtained by subtracting the OD of plates with and without spores. From the results, a significant inhibition of growth was observed at concentrations higher than 1000 ppm compared to the control (Figure 6-18) (Appendix 6-L). The concentration of 22500 ppm marked the lowest absorbance which was almost equal to the blank (without bleach and spores).

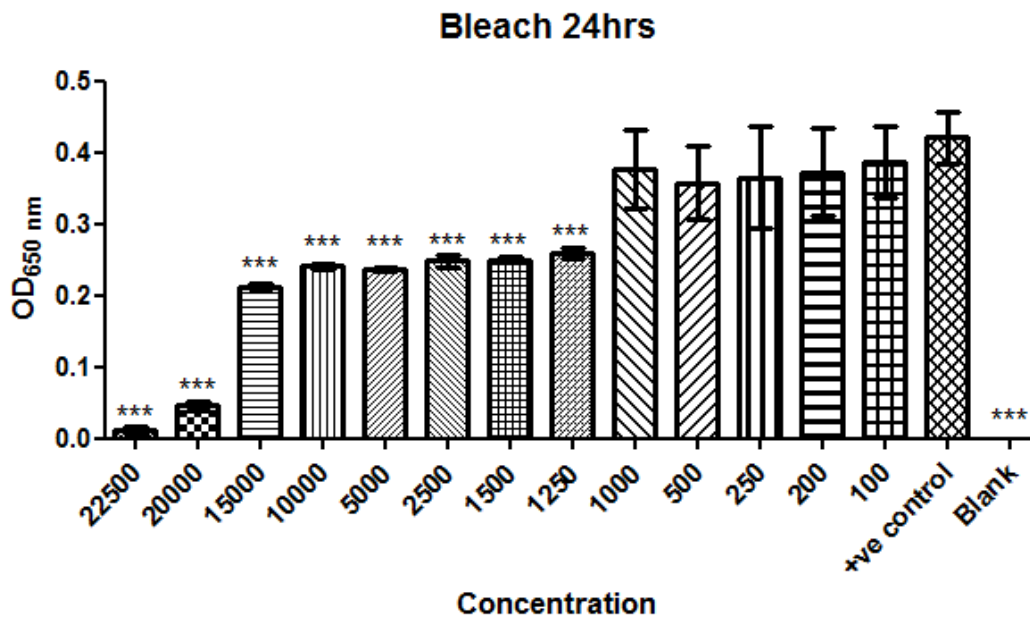


Figure 6-18: Bleach inhibits fungal spore germination at concentrations of 1000 ppm and above assessed by OD_{650nm} after 24 hours. Error bars represent standard deviations of 3 experimental replicates. Statistical analysis was performed using one-way analysis of variance (ANOVA) with Dunnett multiple comparison test, * p < 0.05 as significant.

6.3.2.2 Peracetic acid (PAA)

The inhibition of spore germination by PAA was assessed by growing the fungal spores in PAA concentrations ranging from 1000 ppm to 8000 ppm. A background reading was also included since PAA produced a colour change in the solution (Appendix 6-M). The result showed significant growth inhibition at all concentrations used compared to the control (Figure 6-19) (Appendix 6-N). The concentration of 8000 ppm gave the lowest absorbance which was almost equal to the blank (without bleach and spores).

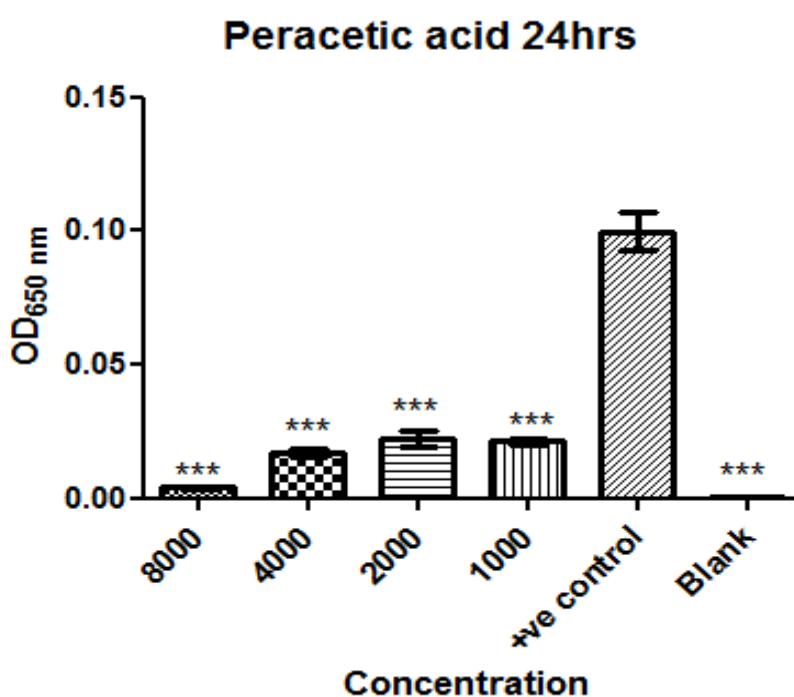


Figure 6-19: PAA inhibits fungal spore germination assessed by OD_{650nm} after 24 hours. Error bars represent standard deviations of 3 experimental replicates. Statistical analysis was performed using one-way analysis of variance (ANOVA) with Dunnett multiple comparison test, * $p < 0.05$ as significant.

6.3.2.3 Organosilane (OS)

We also attempted to use liquid media to study the effects of organosilane at concentrations ranging from 1000 ppm to 25000 ppm on *S. chartarum* spore germination. However, the mixture flocculated instead of producing a homogeneous solution (Figure 6-20).

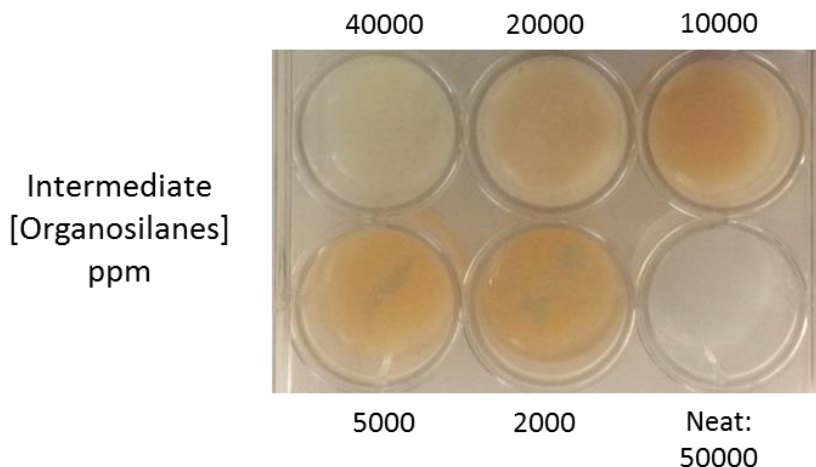


Figure 6-20: The intermediate concentrations (before 1:1 dilution with spore suspension) of organosilane mixed with RPMI 1640 - 2% G- buffered with MOPS in 2 ml well plates.

The absorbance of organosilane/RPMI mixture dilutions prior to addition of spores showed inconsistent readings when assessed by OD_{650nm} after 24 hours (Figure 6-21). Therefore, this method was not considered suitable for OS due to its insolubility in RPMI and it was replaced with method 3, the agar dilution method.

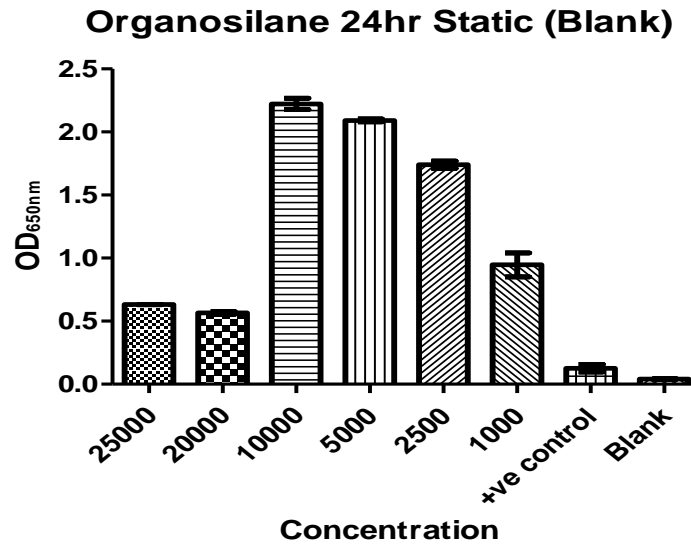


Figure 6-21: Inconsistency of organosilane/ RPMI mixture dilutions prior to addition of spores assessed by OD_{650nm} after 24 hours. Error bars represent standard deviations of 3 experimental replicates.

6.3.3 Inhibitory effects of antimicrobial agents using agar dilution methods

6.3.3.1 Sodium hypochlorite (bleach)

The effects of bleach on the inhibition of *S. chartarum* spore suspension was further assessed by using solid agar dilution techniques (Figure 6-22). The media was incorporated with various concentrations of bleach ranging from 200 ppm to 2500 ppm performed in triplicates for ESA (Appendix O) and PDA (Appendix P).

Complete inhibition of growth was seen at a 1500 ppm in ESA and 1000 ppm in PDA. A bleach concentration of 1000 ppm on ESA produced the same fungal diameter but more white mass indicating hyphal growth.

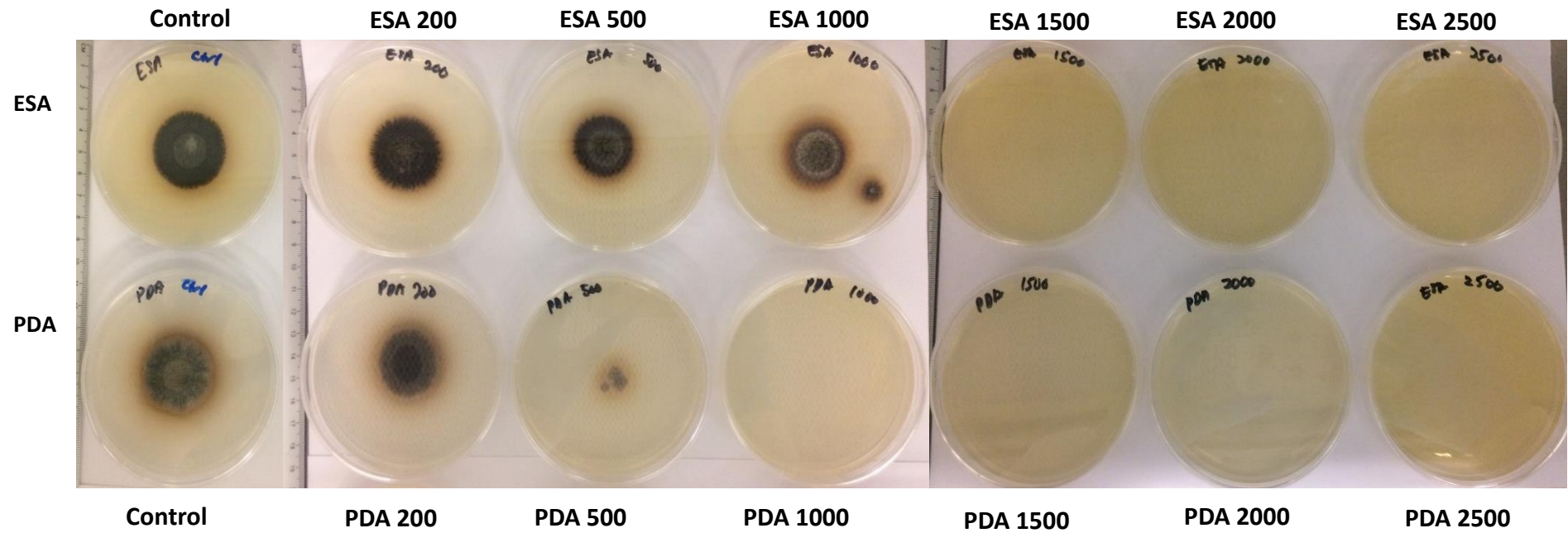


Figure 6-22: Agar dilution plates showing the effects of bleach on the growth of *S. chartarum* after 7 days incubation at 25 °C.

6.3.3.2 Organosilane (OS)

Due to the insolubility of OS in RPMI, the agar dilution method was performed by growing the spore suspension on various concentrations of OS ranging from 1000 ppm to 15000 ppm incorporated in ESA (Appendix Q) and PDA (Appendix R) and performed in replicates. From the results, complete inhibition of growth was seen at 5000 ppm in ESA and 2500 ppm in PDA (Figure 6-23).

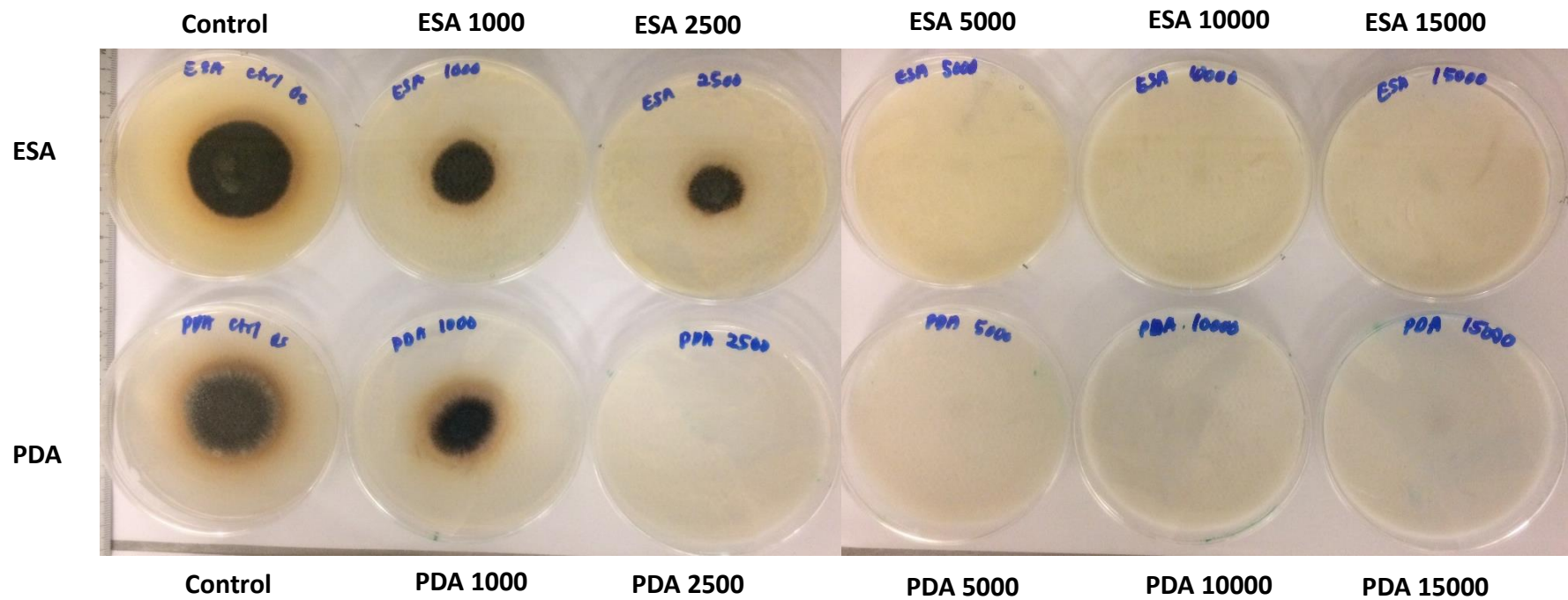


Figure 6-23: Agar dilution plates showing the effects of OS on the growth of *S. chartarum* after 7 days incubation at 25 °C.

6.3.4 Summary

Four antimicrobial agents consisting of bleach, AHP, OS and PAA were tested using different methods. The findings are summarised in Table 6-1. Only sodium hypochlorite showed fungicidal effects against *S. chartarum* using a direct method and agar dilution method. However, OS which is used as an antimicrobial coating, was effective in preventing the growth of *S. chartarum* using the agar dilution plate method at high concentrations.

Table 6-1: Recommended concentrations of antimicrobial agents by the manufacturers and the effective concentrations tested from this study.

Antimicrobial agents	Recommended concentration by manufacturer	Direct application (method 1)	Broth dilution (method 2)	Agar dilution (method 3)
Bleach (NaOCl)	360 ppm (40 ml of neat bleach per 5 litres) for cleaning and disinfecting use. 45000 ppm (undiluted concentration) for sinks, toilets and drains	Inhibitory effect: 10000 ppm in both media No increased in colony diameter after 2 times applications in both media: 25000 ppm, 45000 ppm	Inhibitory: 1250 ppm	No growth: 1500 ppm in both media
AHP	1 cycle, 6 ml / m ³ Approximately 5-6% H ₂ O ₂ (50000 to 60000 ppm)	Inhibitory effect in both media: At least 2 cycles	NA	NA
PAA	4000 ppm	Inhibitory effect: 1000 ppm in ESA	Inhibitory effect: 1000 ppm	NA
OS	1% (10000 ppm)	Inhibitory effect: 5000 ppm on ESA	NA	No growth: 5000 ppm in both media

6.4 DISCUSSION

This study demonstrates the effects of sodium hypochlorite (bleach), aerosolised hydrogen peroxide (AHP), peracetic acid (PAA) and organosilane (OS) on *S. chartarum* grown on solid media and in liquid suspension. Three methods were employed depending on the suitability of the methods in combination with the antimicrobial agents. The method of direct application (method 1) was applicable to all the antimicrobial agents and was used in an attempt to study the effects of these agents as they were intended to be used in the environment. The microdilution method following the EUCAST protocol (with some necessary modification) (method 2) could only be performed with bleach and PAA. The effects of OS could only be studied using agar dilution plates (method 3) as it is more likely that OS had an effect on the constituents of the RPMI causing them to coagulate or flocculate. This method was also applied to bleach so that it could be used as a comparison with other methods. AHP testing was only performed using the direct method since the application was by mist spraying in an enclosed room.

6.4.1 Sodium hypochlorite (bleach)

Sodium hypochlorite (NaOCl) is known as the active ingredient in bleach and is widely used as household bleach, for environmental decontamination, for healthcare disinfection, for water treatment and in dentistry^(51, 244-248). The concentration of NaOCl varies according to manufacturer and regular household bleach normally contains 3-6% NaOCl. Different concentrations of bleach are recommended by the manufacturer depending on the usage, by institutions government agencies or by the end-users.

The World Health Organisation recommend a solution containing 0.05% or 500 ppm NaOCl for disinfection with at least 10 minutes contact time for tools, equipment or other non-porous surfaces and 30 minutes for immersed items at healthcare facilities⁽¹⁸⁵⁾. In a guideline provided by the Advisory Committee on Dangerous Pathogens, UK (ACDP)⁽²⁴⁹⁾, a concentration of 1000 ppm (0.1%) was recommended for general environmental cleaning and 10000 ppm (1%) NaOCl for treating blood spillage. The recommended dilution provided by the manufacturer was 40 ml per 5 litres that produced approximately 360 ppm (0.03%) of NaOCl for cleaning and disinfecting use and an undiluted concentration - approximately 45000 ppm (4.5%) was recommended for sinks, toilets and drains⁽²⁵⁰⁾. We have carried out three different methods to determine the effects of NaOCl on *S. chartarum*.

Using direct application, we found that a single application was effective at inhibiting the growth of *S. chartarum* at 45000 ppm on both media (ESA and PDA) and no new growth was observed on PDA at 25000 ppm. Although there was still growth observed on ESA at 25000 ppm, the microscopic images showed mainly hyphal growth following the exposure to NaOCl which suggested that a lack of sporulation occurred at this stage. However, NaOCl at 25000 ppm (2.5%) and 45000 ppm (4.5%) showed fungicidal effects on *S. chartarum* grown on solid media after applications on 2 consecutive days. The concentration required was higher than the standard recommended concentration for surface disinfection and this might be due to the high numbers of fungal spores and the established fungal growth used in this method to reflect visible mould infestation in the environment. Reynolds *et al.*⁽¹⁸⁶⁾ documented that 1×10^6 spores of *S. chartarum* and other fungi including *Aspergillus niger*, *Penicillium chrysogenum* and *Trichopython mentagrophytes* inoculated on ceramic tiles were inactivated by spraying 2.4% NaOCl with 10 minutes contact time. The tiles were left to dry for more than 20 minutes and no growth was detected in potato dextrose broth after 10 days of incubation. Although a different approach was used, this suggests that a higher concentration of NaOCl is required for heavily contaminated surfaces or visible fungal growth.

In method 2, using standard EUCAST methodology to determine the MIC with bleach concentrations ranging from 100 ppm to 22500 ppm, significant growth inhibition was observed at concentrations higher than 1000 ppm (0.1%). This effect at a lower concentration might be due to greater surface contact of loose spores compared to an established fungal mass (as that used in method 1) as well as a likely lack of “consumption” or binding of the agent by the proteins and fatty acids of the mycelial mat. The MIC of 1000 ppm NaOCl is in accordance with the existing standards for disinfection, however it is slightly higher compared to the recommended concentration by the manufacturer 300 ppm (0.03%).

The agar dilution method assay (method 3) showed complete inhibition of growth at 1500 ppm (0.15%) in ESA and 1000 ppm (0.1%) in PDA. Although a similar growth diameter was observed at 1000 ppm on ESA, the colony was paler which might be due to the effect of discoloration by bleach. We also found that the concentration of 1000 ppm (0.1%) to 1500 ppm (0.15%) NaOCl completely prevented fungal growth which also correlates with the result from method 2.

From these findings, we suggest that the recommended concentration for disinfection of 1000 ppm (0.1%) NaOCl is effective against loose spores, as determined either by

liquid suspension or by agar dilution. However, a higher concentration of 25000 ppm (2.5%) NaOCl and above are required to inhibit established fungal mass.

6.4.2 Aerosolised hydrogen peroxide (AHP)

AHP machines produce hydrogen peroxide (H₂O₂) in the form of a liquid mist. In particular, AHP has been used as an airborne disinfectant to decontaminate enclosed and sealed environments such as those in hospitals, laboratories, animal houses and airline cabins, as well as in the food industry ⁽²⁵¹⁻²⁵⁴⁾. Concentrations of hydrogen peroxide between 6% and 25% have been demonstrated to sporicidal, mycobactericidal, fungicidal and viricidal ⁽⁵¹⁾. In this study, the machine used was sufficient to treat a 10 m³ to 200 m³ room volume with a density of 6 ml / m³ and a mist particle size of 8 to 12 µm giving a concentration of about 5-6% H₂O₂ (50000 to 60000 ppm) and 50 ppm silver cations according to the manufacturer. Previous study has demonstrated that combination of hydrogen peroxide and silver ions exhibited higher antimicrobial effects and acted synergistically in some cases ⁽²⁵⁵⁾.

Using the direct method, we found that one cycle of AHP was not effective at killing or inhibiting the growth of *S. chartarum*. However, the diameter of the colonies was significantly reduced following exposure to AHP on 2 consecutive days. Koburger *et al.* ⁽²⁵⁶⁾ demonstrated that Glosair™ had reduced *Aspergillus brasiliensis* spore counts (CFU/m³) by approximately 9-fold and the number of CFU of bacteria and fungi in room air 13-fold after one treatment cycle.

The data on the effectiveness of AHP on fungi is quite limited and rather difficult to compare. Studies on the effectiveness of AHP have mainly focused on *Staphylococcus aureus* (MRSA), and *Clostridium difficile* as both microbes are known healthcare-associated pathogens ^(251, 257, 258). Fu *et al.* ⁽¹⁹³⁾ have reported that a higher concentration of 30% hydrogen peroxide from a different manufacturer (Bioquell, UK) was more effective against *Staphylococcus aureus*, *Clostridium difficile* and *Acinetobacter baumannii* compared to Glosair™.

In contrast to AHP, the effects of hydrogen peroxide solution on fungi have been documented in several studies such as in water disinfection, dental unit waterlines, food sanitation and plant disease control ⁽²⁵⁹⁻²⁶²⁾. Venturini *et al.* ⁽²⁶³⁾ have reported that 5% and 10% hydrogen peroxide totally inhibited the growth of *Penicillium expansum* using an agar diffusion assay and found a minimum inhibitory concentration of 0.05% using an agar dilution assay. On the other hand, Cerioni *et al.* ⁽²⁶²⁾ showed a very low

minimum inhibitory concentrations of 300 mM (1020 ppm) of H₂O₂ against *Penicillium digitatum* when applied to a conidial suspension for 2 minutes.

From our findings, AHP was capable of inhibiting the growth of *S. chartarum* after 2 cycles but did not completely kill the fungus. This might be due to the high number of spores in the established fungal mass that limits contact with hydrogen peroxide, as well as the “consumption” effect of the proteins and fatty acids in the mycelial mat mentioned previously.

6.4.3 Peracetic acid (PAA)

Peracetic acid (PAA) functions as a strong oxidising and bleaching agent. It has been widely used as a disinfectant in the food and textile industries, healthcare facilities, and wastewater treatment ^(51, 264-266). The microbicidal activity of PAA has been documented in the inactivation of bacteria, fungi and yeasts at a concentration of 100 ppm for 5 minutes contact time. In the presence of organic matter, concentrations between 200 and 500 ppm were required ⁽⁵¹⁾.

Peracide™ PAA *in situ* tablets were dissolved in water according to the manufacturer's instructions to produce peracetic acid *in situ* at a concentration of 4000 ppm. This concentration is capable of killing *C. difficile* spores within 30 seconds contact time using a liquid suspension test following the modified BS EN 13704 method ^(267, 268). This preparation of peracetic acid against fungi has not yet been documented. In this study, we performed a direct method (method 1) and a liquid suspension method (method 2) to determine the effects of PAA on *S. chartarum*.

Using the direct method (method 1), we found that PAA concentrations of 1000 ppm to 8000 ppm was ineffective in inhibiting *S. chartarum* after a single application. On the other hand, colony diameters were reduced at concentrations of 4000 ppm and 8000 ppm PAA after two applications but growth was not completely inhibited. This showed that PAA was not effective against established fungal mass of *S. chartarum*. Moreover, secondary colonies were formed as a result of dispersion of the PAA solution on the media at lower concentrations, indicating that PAA is incapable of interrupting the fungal life cycle at these concentrations. No complete inhibition was observed after 7 days of incubation which might also be related to stability of PAA which is inactivated after 24 hours as stated by the manufacturer.

Method 2 showed significant inhibition in growth as observed at concentrations of 1000 ppm (0.1%) and above. This concentration was higher than the concentration shown to

be microbicidal (100 ppm). Various concentrations of 100 ppm and above have been reported from previous studies. Alla *et al.*⁽²⁶⁹⁾ used lower concentrations of up to 100 ppm PAA which achieved a reduction of up to 66.3% of *Botrytis cinerea*. In a previous study, Maria *et al.*⁽²⁷⁰⁾ tested higher concentrations of 500 ppm (0.05%), 1000 ppm (0.1%) and 3000 ppm (0.3%) PAA. Only the concentration of 3000 ppm (0.3%) was effective against *Alternaria alternata*, *Fusarium graminearum*, *Aspergillus ochraceus* but not against *A. niger*, *A. flavus*, *Penicillium roqueforti* and *P. expansum*. These results suggest that the effectiveness of PAA depend on the fungal species and its phenotype rather than concentration used.

Based on our findings, inhibition using both methods. PAA was effective at reducing fungal growth at higher concentrations of 4000 ppm and 8000 ppm after two direct applications. A lower concentrations of 1000 ppm and above significantly inhibited the fungal growth in liquid suspension. This difference might be related to the limited duration of activity of PAA, in addition to the higher fungal load and reduced surface contact of the mycelial growth compared to liquid suspension.

6.4.4 Organosilane (OS)

Organosilane has been used as an antimicrobial surface coating to prevent microorganisms from attaching to surfaces. Organosilane has been used on surfaces, fabrics, walls and for water treatment^(190, 271-273). The concentration recommended by the manufacturer is 10000 ppm (1%) OS produced by diluting the original 5% concentration.

Using direct application (method 1), we found that fungal growth still occurred at all concentrations with either one or two applications and this is also evident from the microscopic images. Secondary colonies were formed at lower concentrations (1000 ppm and 5000 ppm). However, the fungal growth decreased as the concentration increased above 10000 ppm in both media.

Due to the insolubility of OS in RPMI, method 2 was replaced with the agar dilution method (method 3). The complete inhibition of *S. chartarum* spores germination at 5000 ppm in ESA and 2500 ppm in PDA occurred at lower than the in-use concentration recommended by the manufacturer at 10000 ppm.

From previous studies, the antimicrobial effectiveness of OS is still unclear. Most studies in real-life settings have documented that there was no significant antimicrobial activity demonstrated by OS-containing products at concentrations recommended by

the manufacturers. Boyce *et al.*⁽¹⁹⁰⁾ reported a controlled trial of two OS-containing products applied to nine sites of pre-cleaned high touch surfaces in patient rooms and found no significant residual antimicrobial activity of the tested products. Furthermore, colony counts were higher at seven sites than in the control rooms. The method of application, such by as direct application (fogging) or indirectly using a cotton or microfibre cloth, might affect the amount of OS delivered to the surface. Baxa *et al.*⁽²⁷³⁾ suggest that the effectiveness of antimicrobial coatings depends on the organisms, composition of surfaces and the method of application.

We found that OS was only effective in the agar dilution method (method 3) at 5000 ppm in both media by and there was no complete inhibition using the direct application method (method 1). This suggests that OS should be as a preventative measure rather than as direct treatment of a contaminated surface and, indeed, this is how it is recommended to be used. However, the study was performed *in vitro* and used a completely different surface composition compared to real life settings.

6.5 CONCLUSIONS

The overall findings support previous evidence that high fungal load reduces the effectiveness of antimicrobial agents. The efficacy of the antimicrobial agents used was highly dependent on the frequency of treatment and the method of application and concentration. Furthermore, most antimicrobial agents (such as AHP) are used in combination with physical cleaning to reduce microbial load and increase surface contact which indicates the importance of a cleaning process preceding treatment with antimicrobial agents.

CHAPTER 7

EFFICACY OF ANTIMICROBIAL TREATMENT AND PREVENTION ON *S. CHARTARUM* INFESTED BUILDING MATERIAL

This chapter presents the work on the effectiveness of antimicrobial agents consisting of sodium hypochlorite or bleach, aerosolised hydrogen peroxide, peracetic acid and organosilane to kill or prevent *S. chartarum* growth on gypsum board. The antimicrobial concentrations derived from previous studies (chapter 6) were tested on *S. chartarum*-infested building materials in a controlled chamber to simulate a high humidity environment.

7.1 INTRODUCTION

Fungal infestation in the indoor environment has been associated with numerous factors such as excessive humidity, lack of maintenance and poor ventilation, as well as some types of building materials. Studies on antimicrobial agents have mostly been carried out *in vitro* to extrapolate their effectiveness in real life settings. Most building materials used were cellulose-based made up of paper fibres which could easily trap moisture. This makes them very vulnerable and likely to be adversely affected by prolonged exposure to water intrusion. Furthermore, building materials such as gypsum board are not stable and are highly porous which makes fungal infestation more difficult to remediate.

The aim of this study was to assess the efficacy of selected antimicrobial agents in the treatment of *S. chartarum*-infested gypsum board. Here, we assessed the effects of antimicrobial agents consisting of bleach, aerosolised hydrogen peroxide (AHP),

peracetic acid (PAA) and organosilane (OS) on *S. chartarum* by observing visible fungal growth on gypsum board, microscopic examination and growth recovery on culture media. Prior to selecting gypsum board, we carried out simple preliminary testing to investigate the best substrate for this study with the aim of achieving sufficient growth of fungus comparable with that seen in “mouldy” buildings.

7.2 MATERIALS AND METHODS

7.2.1 Experimental set-up

Initially, a preliminary study was performed in 5L- air-tight boxes (height: 11 cm, width: 22.5 cm). The aims were to determine the best substrate and to optimise the environmental conditions to achieve a relative humidity (RH) of more than 98%. Different building materials were selected as they are common substrates for mould in the indoor environment consisting of 7.5 cm x 7.5 cm gypsum board, mosaic grouting, shower curtain, ceramic tiles and wallpaper (Appendix 7-A).

The experiment was scaled up in 3 large containers with dimension of 50 cm X 50 cm X 50 cm for control and organosilane and 130 cm X 70 cm X 70 cm for sodium hypochlorite, peracetic acid and 100 cm X 100 cm X 100 cm for AHP. The AHP experiments were carried out over a different time course from the other treatments. All of the antimicrobial agents were tested only on 15 cm X 15 cm gypsum board based on the preliminary result; as it appeared to be the best substrate to support the growth of *S. chartarum* within a feasible time frame. The time frame of the experiments are shown in Appendix 7-B for bleach, aerosolised hydrogen peroxide and peracetic acid (treatment) and in Appendix 7-C for organosilane (prevention).

For both preliminary and larger-scale experiments, all materials (including the surface substrates) were sterilised by autoclaving and left to dry in the oven at 40 to 50 °C. Samples were pre-wetted by soaking with sterile water and left to slightly dry in the laminar hood for 30 minutes prior to fungal inoculation. All samples were tested in duplicate with positive controls included.

7.2.2 Optimization of chamber conditions

Prior to the application of antimicrobial agents, air-tight boxes were used to optimise the environmental conditions to support the growth of *Stachybotrys* sp. Building materials were placed in the boxes with sterile plates containing potassium sulphate

salt and sterile water. The temperature and RH were recorded using HOBO® temp/RH logger with the aim to achieve an optimum temperature within the range between 25 ± 5 °C with an RH of more than $98 \pm 5\%$ humidity to simulate a typical damp environment. Data were plotted using HOBOware® software Version 3.7.1. Subsequently, the experiment was tested in a larger container placed in an environmental chamber for the large-scale study (Figure 7-1).

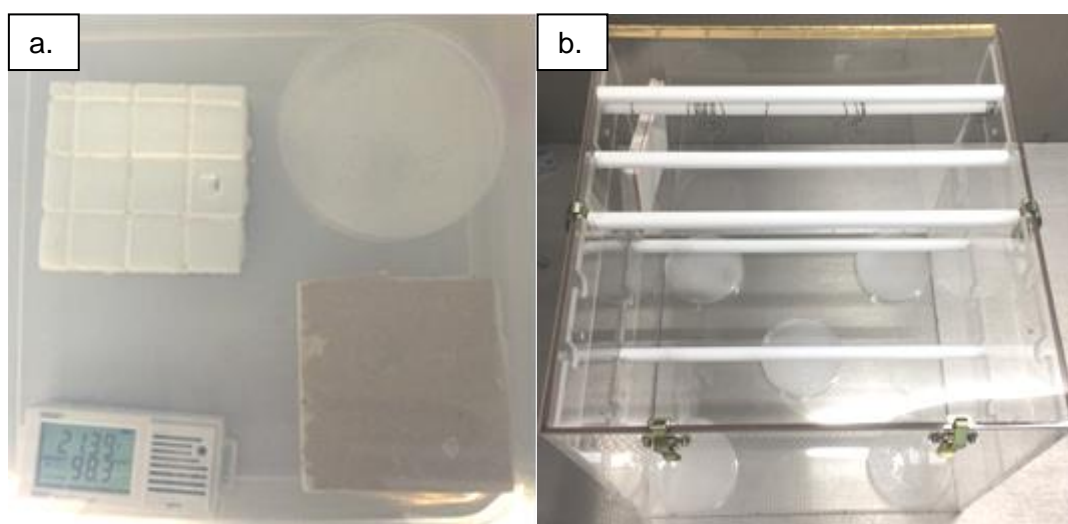


Figure 7-1: Optimisation of experimental condition using potassium sulphate a. Air-tight container (11 cm X 22.5 cm) containing materials (7.5 cm X 7.5 cm) for the preliminary study showing RH of 98.3% at 21.4 °C; b. Plates containing 30 g potassium sulphate dissolved in 20 ml sterilised water in the small chamber (50 cm X 50 cm X 50 cm).

The use of potassium salt in our experiment was optimised. Initially, 30 g of salt was dissolved in 10 ml of water and both RH and temperature were recorded for 17 hours. This was followed by testing different amounts of salt - 30 g and 60 g potassium sulphate with 20 ml of water, to determine whether this would affect the environmental conditions. In the larger scale study, the 30 g of salt in 20 ml of water was used to obtain the same results as in the preliminary study.

7.2.3 Antimicrobial agents

Four types of environmental antimicrobial agents, consisting of sodium hypochlorite (Bleach, Evans Vanodine International PLC), hydrogen peroxide (Glosair™, ASP Johnson & Johnson), peracetic acid (Peracide™, Sky Chemical UK Limited) and Organosilane (Biosafe®, Gelest Inc.) were used as previously described in Chapter 6. The antimicrobial agents were tested for the efficacy to remove or prevent the growth

of *S. chartarum* on gypsum board. Sodium hypochlorite, peracetic acid and aerosolised hydrogen peroxide were applied at subinhibitory and inhibitory concentrations obtained in chapter 6 on pre-incubated *S. chartarum*-infested gypsum board, while organosilane was pre-coated onto materials prior to fungal inoculation.

Following antimicrobial applications of 20000 ppm, 25000 ppm and 45000 ppm sodium hypochlorite and 4000 ppm and 8000 ppm peracetic acid, samples were left to dry for 5 hours in the chamber. Samples treated with 6 ml / m³ of 5 – 6% hydrogen peroxide per 1 cycle AHP and were left in contact for 2 hours as stated by the manufacturer. The gypsum boards was coated by soaking in 20 ml of OS at concentrations of 2500 ppm and 5000 ppm until they were sufficiently wet and evenly coated (approximately 5 minutes) and left overnight to fully dry in laminar flow.

7.2.4 Mycology

7.2.4.1 Inoculation of fungi

S. chartarum (NCPF 7587) was grown on ESA at 25 °C for 7 days. Fungal spores (1 – 5 X 10⁶) suspended in sterile water supplemented with 0.1% Tween-20 were evenly sprayed across the entire surface of the pre-wetted test materials. The volume of antimicrobial agents applied was approximately 500 µl for 7.5 cm X 7.5 cm materials for the preliminary test and 1800 µl for 15 cm X 15 cm for gypsum board in the larger-scale study. The treated materials were kept in controlled conditions of 25 ± 5 °C with RH 98 ± 5% humidity until sufficient fungal growth could be visibly observed.

7.2.4.2 Fungal viability following antimicrobial application

Following antimicrobial application (except for organosilane), samples were left to dry for 5 hours before cutting them into 1 cm² pieces and placed into the centre of plates containing ESA to determine fungal viability. Samples were wetted with 100 µl of sterile water and incubated for 7 days at 25 °C to provide sufficient moisture and time required for *S. chartarum* growth, respectively. Material coated with organosilane was harvested after fungal growth was observed at the end of the experiment.

7.2.5 Microscopy

7.2.5.1 Preparation of samples for light microscopy

In the preliminary study, materials (7.5 cm X 7.5 cm) were sampled using sellotape mounts prepared by pressing the adhesive tape onto the materials with visible growth.

The fungal mass was stained with lactophenol blue and observed under the light microscope at 40x magnification using a light microscope (Labomed™ Lx 400, Labomed America Inc.) and the images were taken using 5.0 Moticam (Motic®). The samples were evaluated as growth by the presence of complete fungal structures or no growth

7.2.5.2 Preparation of samples for scanning electron microscopy (SEM)

Samples were cut to approximately 1 cm X 1 cm X 0.5 cm. The materials were mounted onto an aluminium pin stub using adhesive monomer (in-house) and were then irradiated with UV light (DEMi™, Demetron/Kerr) for approximately 5 seconds. The mounted samples were coated with 95% gold / 5% palladium under vacuum for 1 minute 30 seconds using a sputter coater machine (SEM coating unit E5000, Polaron Equipment Limited). They were examined using SEM (XL30 FEG X Series, Philips™, the Netherlands) and Microscope Controller (XL Version 6.20, 17th Jan 2003, FEI Company™). The microscopy was conducted with a vacuum below 1.7×10^{-5} mBar and an electron beam setting of 5.0 kV. Images were viewed and taken using Saturn Imaging software (Saturn 1.17.0, 23rd April 2015).

7.3 RESULTS

7.3.1 Optimization of chamber condition

We have optimised the use of potassium salt in our experiment. Using 30 g of salt was dissolved in 10 ml of water recorded for 17 hours, the temperature ranged from 21.4 to 22 °C and the RH began to stabilize after 2 hours to achieve approximately 94 - 95% humidity. (Figure 7-2).

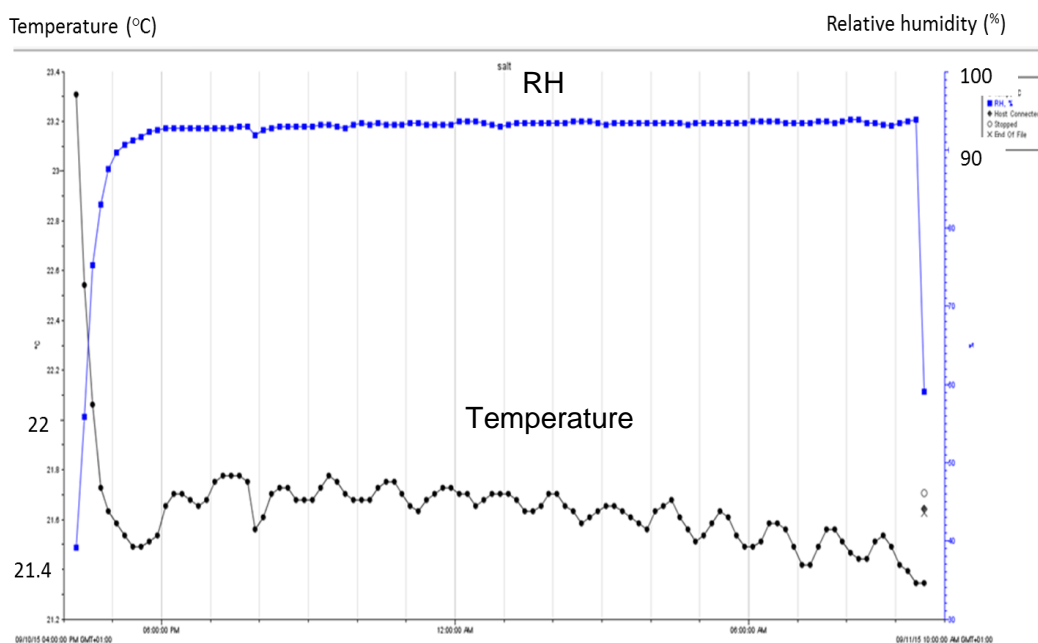


Figure 7-2: RH and temperature test with 30 g salt in 10 ml of water showed temperature ranged from 21- 22°C and 94 - 95% RH.

We observed a similar pattern of RH and temperature with both 30 g and 60 g potassium sulphate. The findings suggest that the amount of salt did not influence the RH but it was affected by amount of solvent (water) (Figure 7-3).

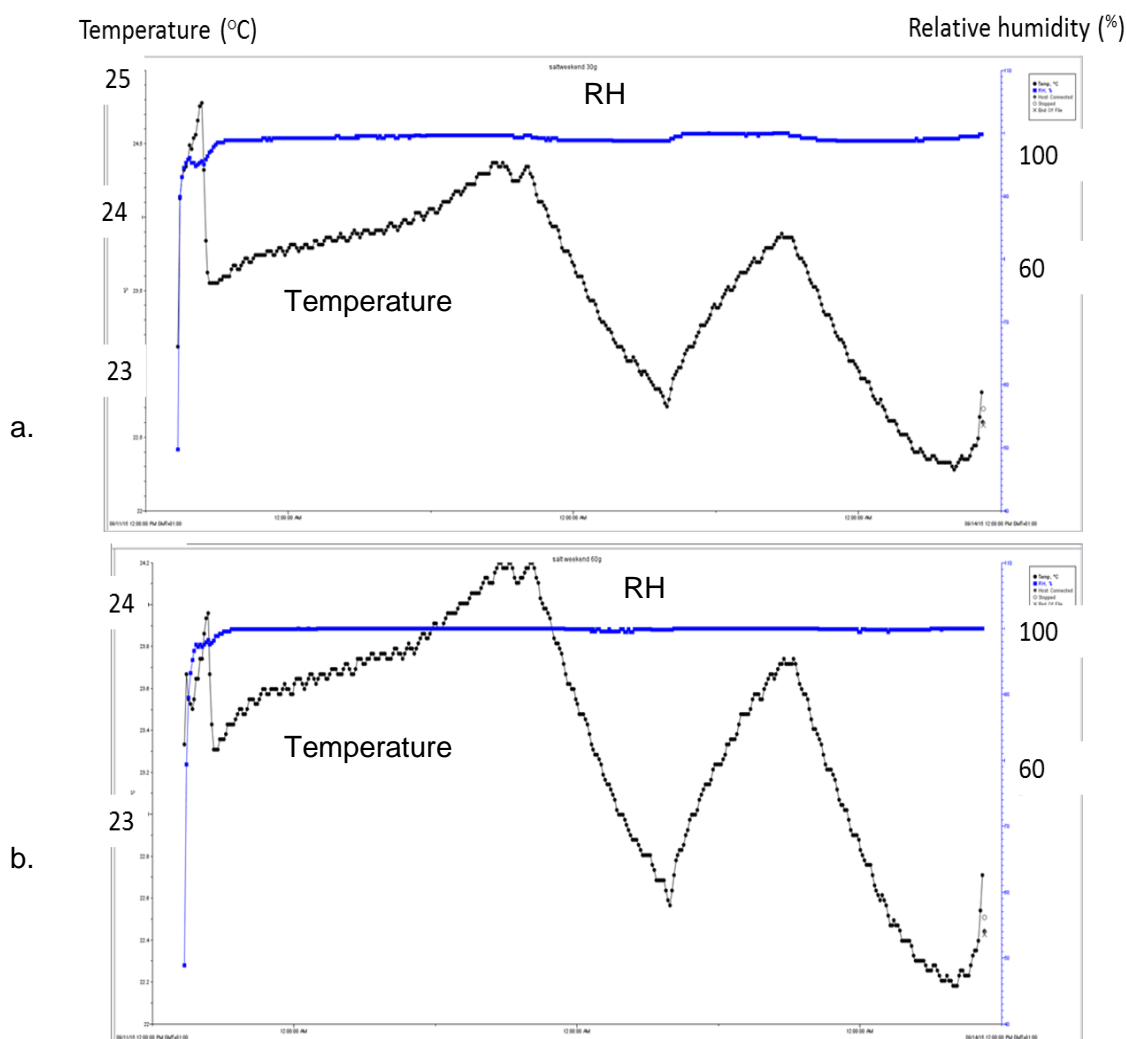


Figure 7-3: RH and temperature was compared using different amount of salt dissolved in equal amount of water recorded for 4 hours showed RH \pm 100% and temperature ranged from 22- 24 °C using a. 30 g and b. 60 g salt in 20 ml of water.

In the larger scale study, the 30 g of salt in 20 ml of water was used to obtain the same results as in the preliminary study. We found that 5 plates of salts containing 60 g salt in 20 ml water each were required to obtain RH of more than 98% humidity. The results remained constant after 3 weeks of monitoring (Figure 7-4). The RH was monitored throughout the whole experiment by adding more water when the RH started to drop to 95%.

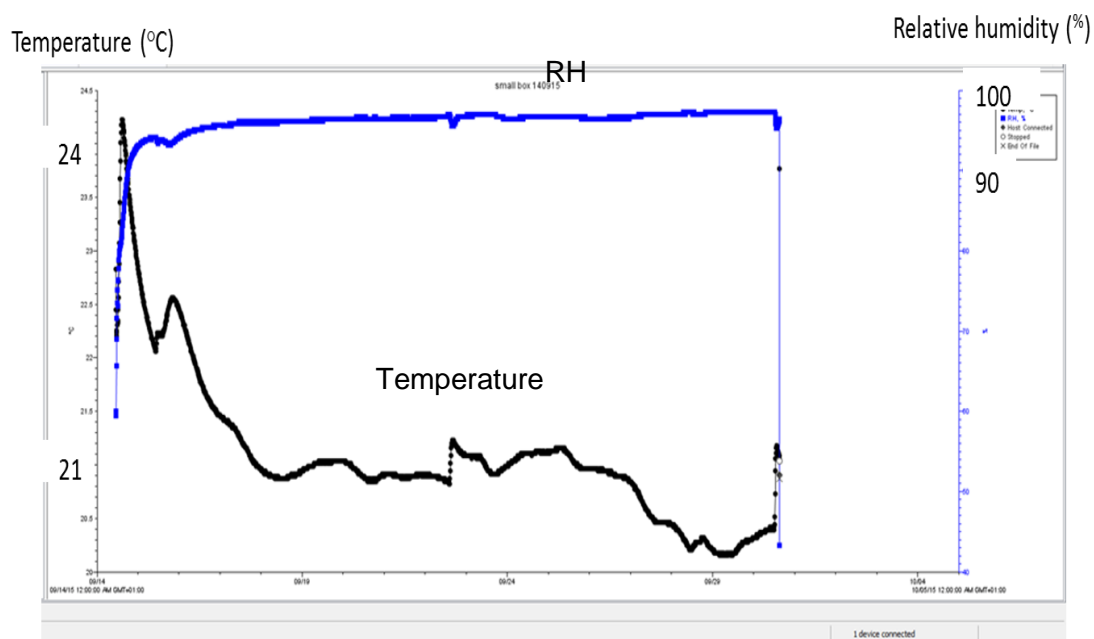


Figure 7-4: RH in the small chamber test with plates containing 60 g potassium sulphate dissolved in 20 ml water remained constant for 3 weeks.

7.3.2 Gypsum board without fungal inoculation and application of antimicrobial agents

The original gypsum board was obtained as brown coloured surface composed of paper layers attached to gypsum (Figure 7-5).



Figure 7-5: Gypsum board with no antimicrobial treatment or fungal growth (uninoculated control).

To compare the effects of before and after fungal infestation and treatment, gypsum board without both fungal inoculation and treatment was subjected to SEM. From the SEM, the surface of gypsum board was not flat and smooth but comprised of intertwined paper fibres which were strongly attached to the gypsum. The non-uniform arrangement of paper fibres also created some porous structures on the surface. From the cross-section, the paper layer on the surface was observed as a grey coloured

layer and it was strongly attached to gypsum shown as a white-coloured layer at the bottom (Figure 7-6).

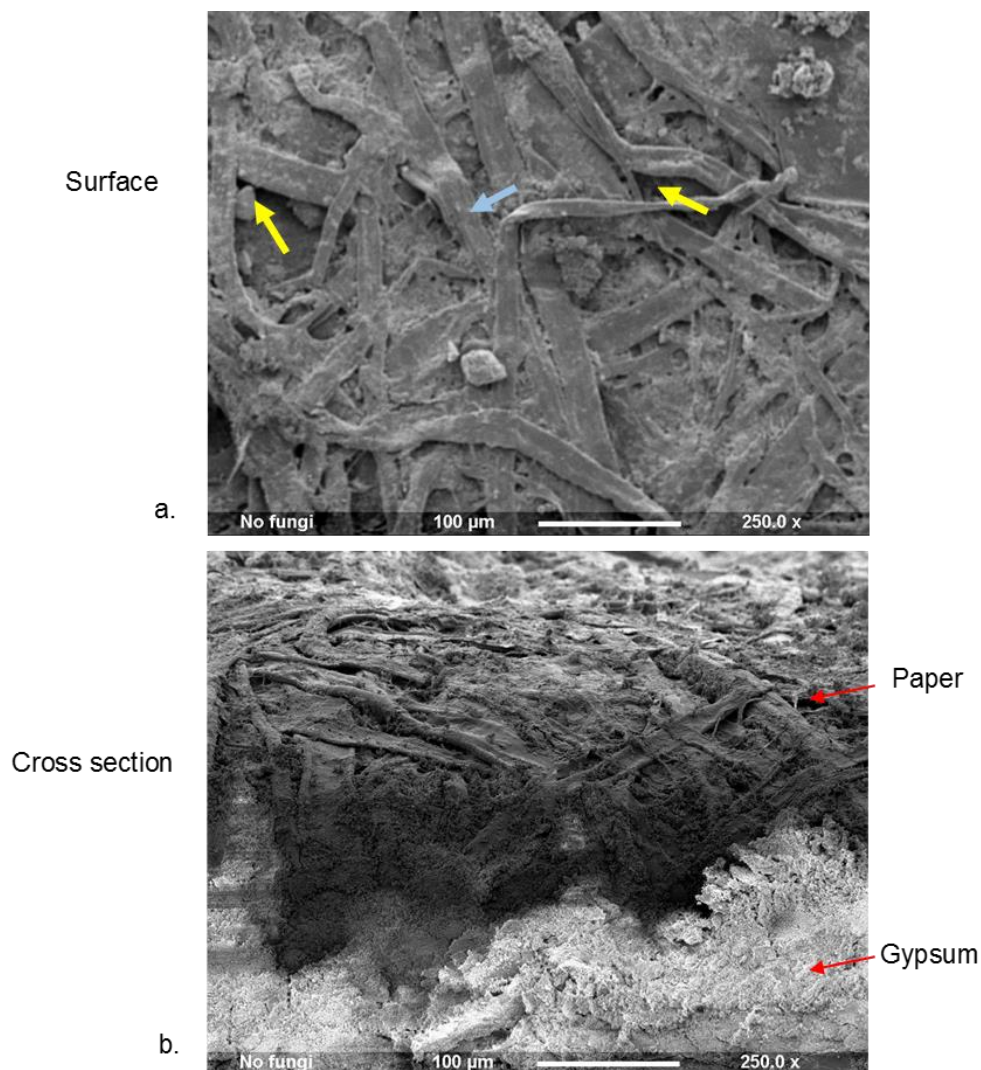


Figure 7-6: Sections of uninoculated gypsum board a. surface and b. cross-sections images at 250x magnification. The coloured arrows mark different areas. Blue: paper fibres with flat exposed surface, and yellow: porous, non-flat surface.

The materials (gypsum board, mosaic grouting, shower curtain, ceramic tiles and wallpaper) were observed for 11 weeks after inoculation until no further sign of growth could be observed within the specified timeframe. The fungal mass was stained with lactophenol blue and observed under light microscopy at 40x magnification. Only gypsum board and wallpaper supported growth during the 11 weeks period (Figure 7-7).

Gypsum board showed more coverage and the fastest growth compared to other materials. Some germination was observed on fungi inoculated on grouting, however

no complete fungal structures were observed even after 11 weeks of growth. The shower curtain was made of polyester coated with water water-repellent compound which might explain why the spore suspension did not adhere to its surface. These results demonstrated that gypsum board was the best substrate to support fungal growth and most feasible to be used in this study.

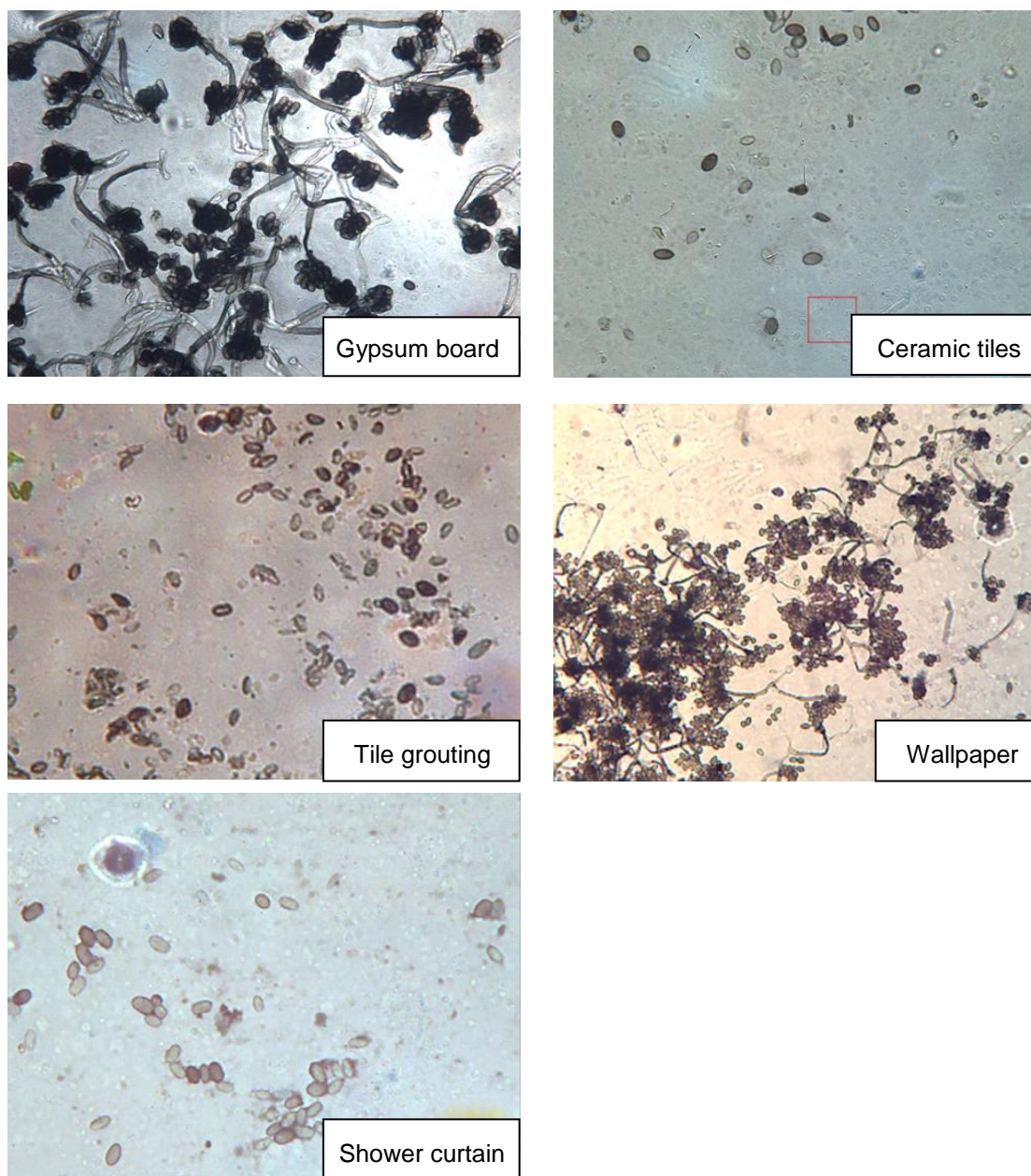


Figure 7-7: Fungal growth on tested materials sampled after 11 weeks growth using tape-mounts, stained with lactophenol blue and observed under light microscopy at 40x magnification.

The behaviour of *S. chartarum* grown on gypsum board was further examined using SEM. The SEM images of the gypsum board with fungal growth showed thick growth

on the surface. Fungus penetrated into the paper surface but it did not reach the gypsum layer (Figure 7-8).

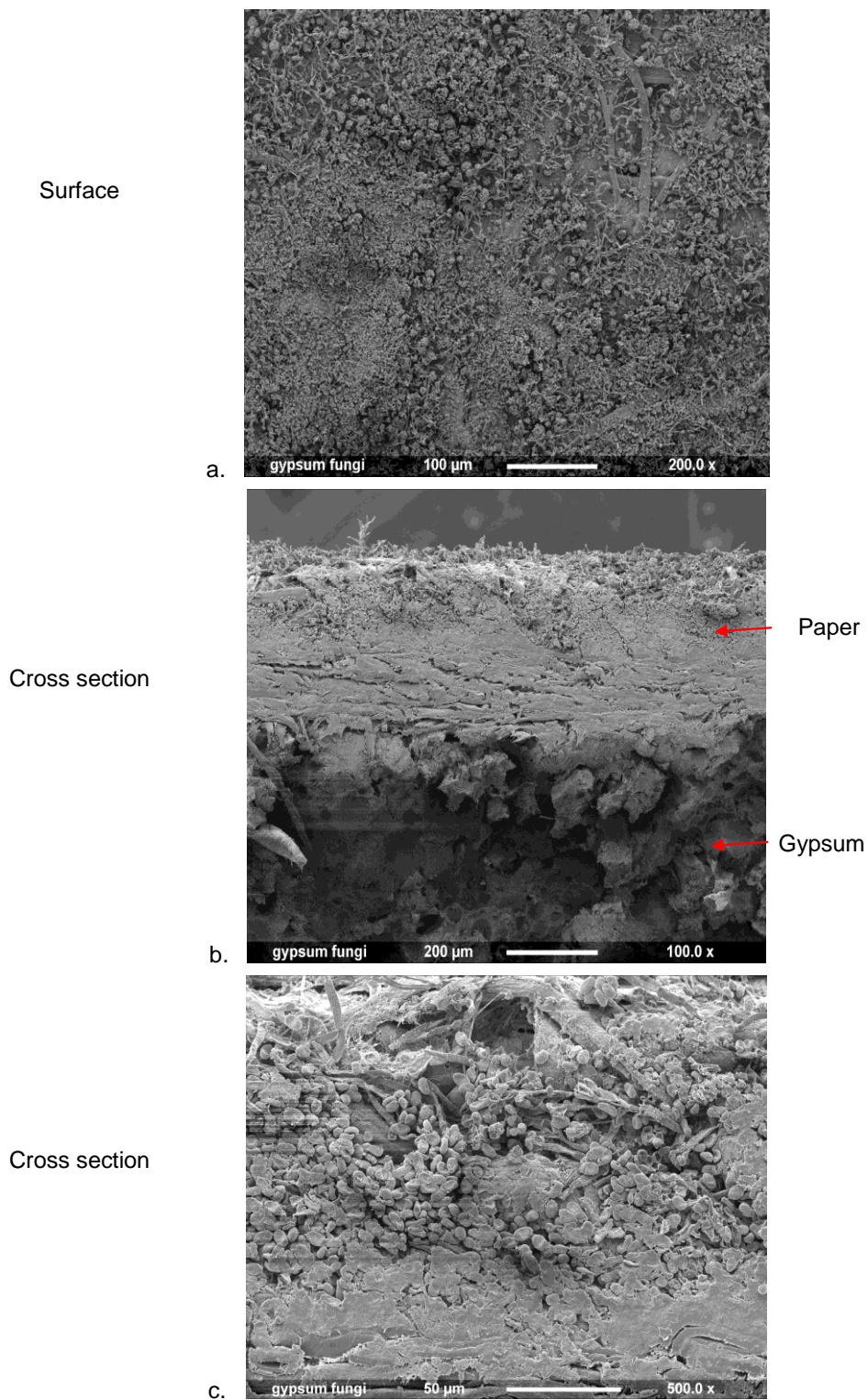


Figure 7-8: The SEM images of *S. chartarum*-infested gypsum board after 11 weeks incubation.

7.3.3 *S. chartarum*-infested gypsum board with or without application of antimicrobial agents

7.3.3.1 Without treatment

To observe the fungal infestation on gypsum board, fungal spores were inoculated on the gypsum board and hung inside the chamber until visible growth was observed approximately after 6 weeks (Figure 7-9). The paper surface was mostly covered with fungal growth, but thick fungal growth was clearly marked by the black coloured area on the surface.

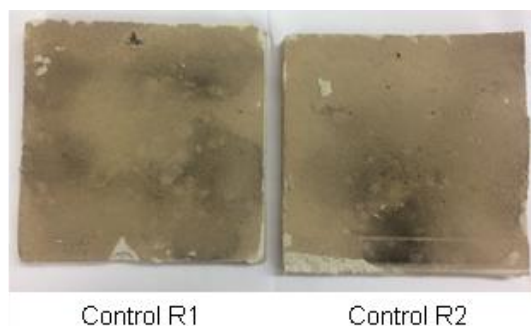


Figure 7-9: Fungal growth on gypsum board without any antimicrobial treatment shown in duplicate.

The materials were then cultured on ESA to determine fungal viability. The plates were examined after 10 days of incubation at 25 °C and showed good growth recovery of *S. chartarum* (Figure 7-10). This showed that the fungal spores were still viable after 6 weeks growth on wetted gypsum board placed in a high humidity environment.

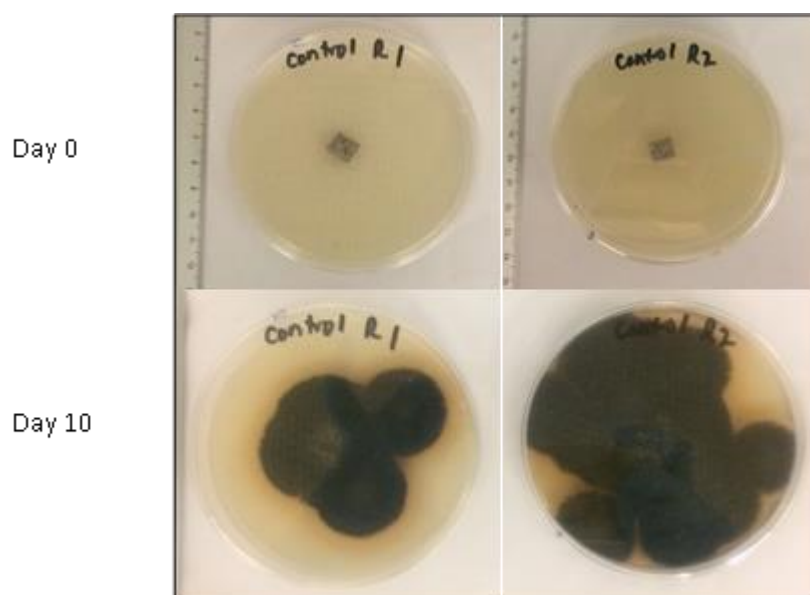


Figure 7-10: Fungal infested gypsum were cut into 1 cm² pieces and placed on ESA for 10 days at 25 °C.

The materials were examined under SEM to assess the fungal growth on the gypsum board and whether the fungus caused any changes in the structure of the material. *S. chartarum* growth was clearly observed using SEM. Despite the lack of colour contrast in SEM, the fungal structures could be distinguished from the substrate as shown at 250x (Figure 7-11) and 1000x magnification (Figure 7-12). The fungal structure was clearly observed at 1000x magnification. Fungal growth penetrated in between the spaces of the paper fibres as shown on the surface and cross section images.

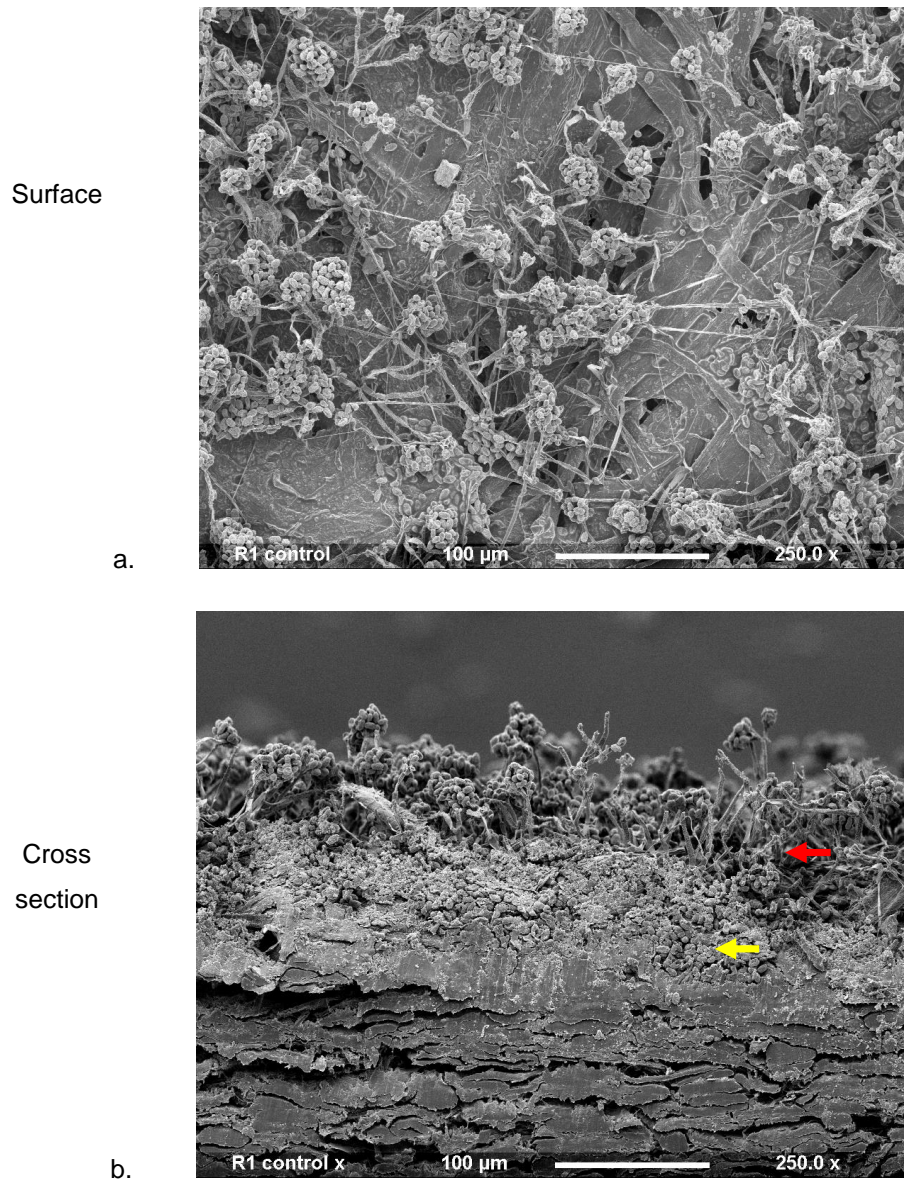


Figure 7-11: Fungal growth on gypsum board without any antimicrobial treatment using SEM images at 250x magnification. a. surface and b. cross-section. The coloured arrows mark different areas. Red: fungal growth on paper surface; Yellow: Fungal growth within the paper layer.

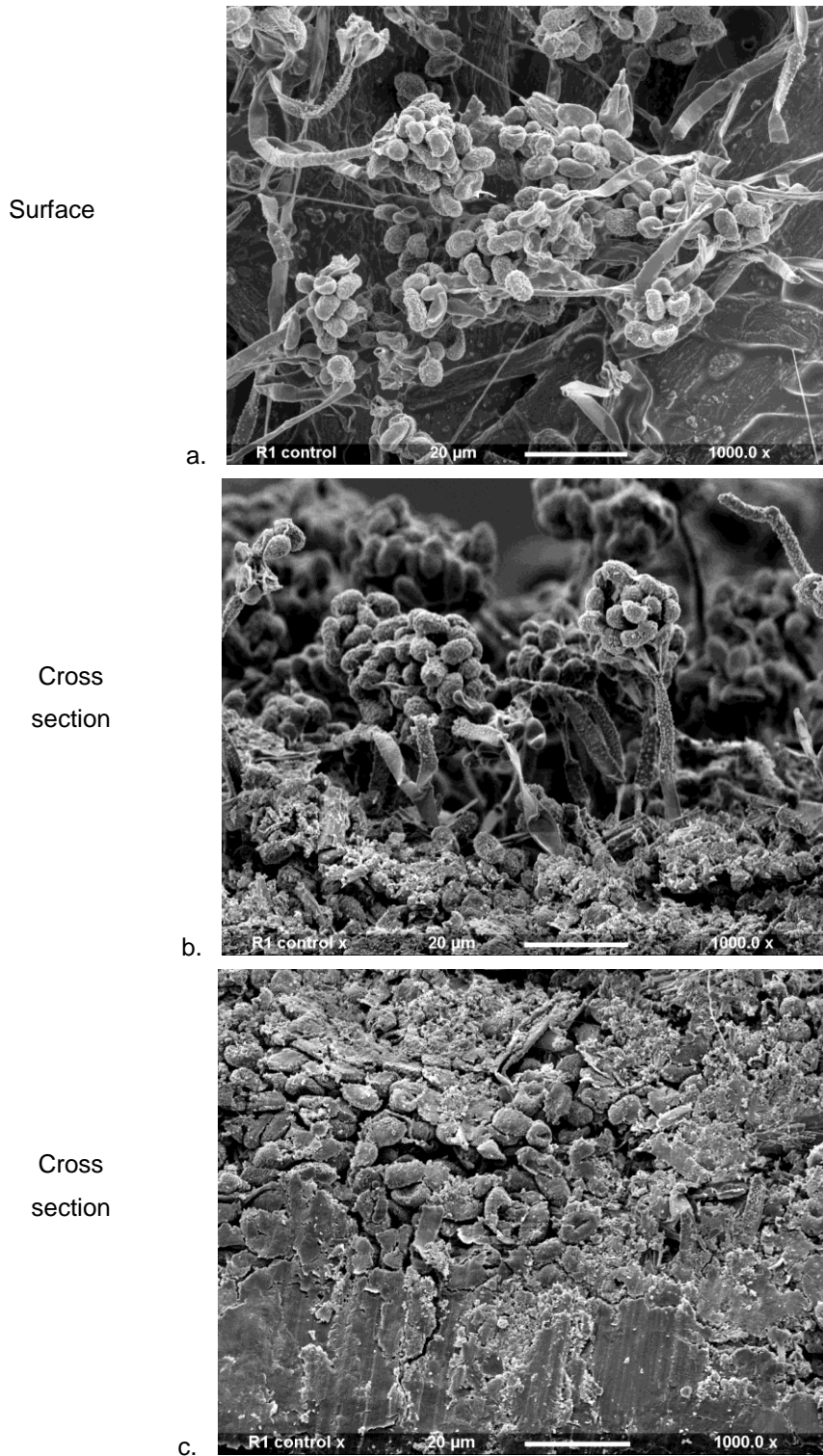


Figure 7-12: Fungal growth on gypsum without any antimicrobial treatment using SEM images at 1000x magnification. a. Surface, b. Cross-section (fungi growth on surface) and c. Cross section (fungal growth penetrating into paper).

7.3.3.2 Effect of sodium hypochlorite (bleach)

Concentrations of 20000 ppm, 25000 ppm and 45000 ppm bleach were applied on the mould-infested gypsum. Concentrations of 20000 ppm and 25000 ppm were tested with 1 application followed by multiple applications at concentrations 25000 ppm and 45000 ppm. From the previous studies (Chapter 6), 25000 ppm bleach was determined as the inhibitory concentration using 1 application, resulting in complete inhibition after 2 applications.

After the single application of bleach at 20000 ppm and 25000 ppm, the black coloured mould had been 'bleached out' from the materials. Some visible growth could be seen as light brown patches in some areas as observed at 20000 ppm (Figure 7-13).

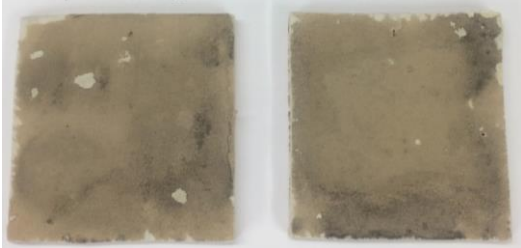

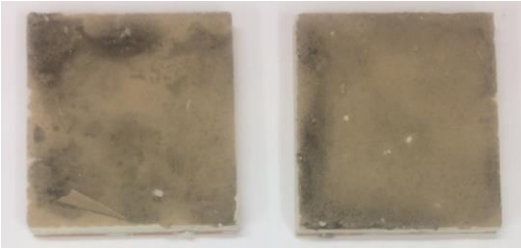

No	Before application	After application
20000 ppm		
25000 ppm		

Figure 7-13: Fungal growth on gypsum before and after treatment with a single application of bleach at concentrations of 20000 ppm and 25000 ppm bleach shown in duplicates.

Fungal growth was recovered from all the treated materials treated with one application of 20000 ppm and 25000 ppm bleach. Fungal growth from gypsum treated with 25000 ppm bleach showed similar diameter size with 20000 ppm bleach (Figure 7-14).

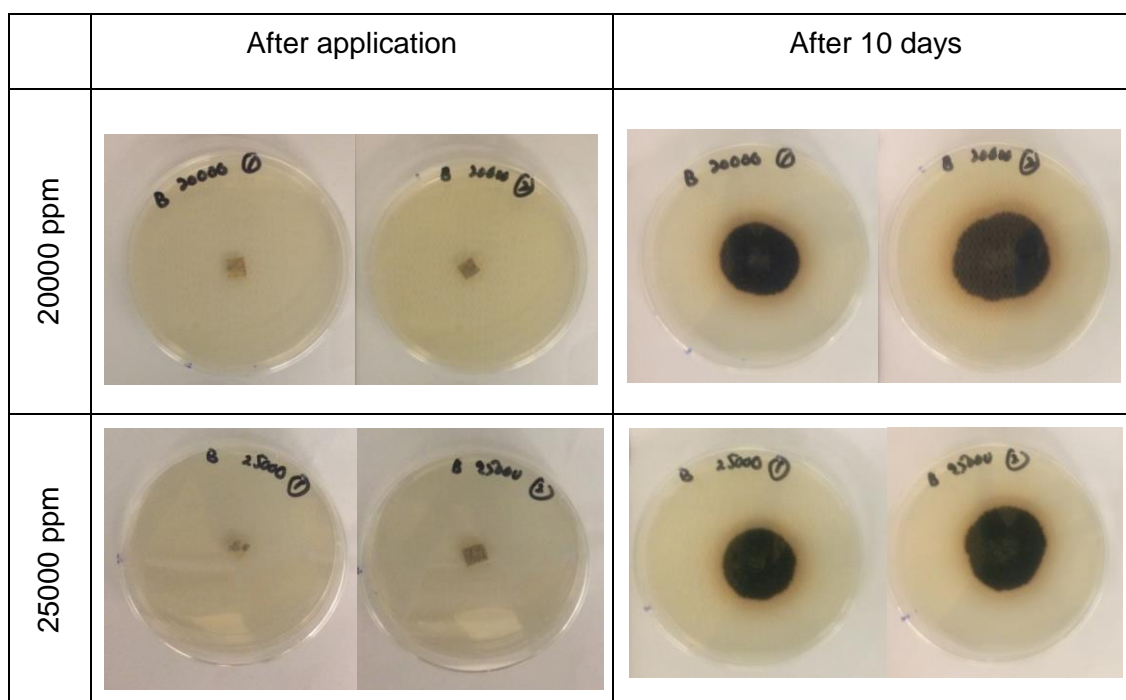


Figure 7-14: The materials were cut into 1 cm² pieces and placed onto ESA on the same day of bleach application. The materials were incubated on ESA where growth recovery was documented after 10 days.

To evaluate the effects of 20000 ppm and 25000 ppm bleach on mould-infested gypsum board, the samples were subjected to SEM. The results show that the fungal structures were collapsed and coated with bleach at both 20000 ppm (Figure 7-15) and 25000 ppm (Figure 7-16). There were also some changes to the material itself as shown by more loose and porous surface (paper) structures seen in the cross-section images.

From the findings, bleach at 20000 ppm and 25000 ppm caused decolourisation of mould, but did not kill *S. chartarum* in the infested gypsum boards. Moreover, bleach also caused a 'bleaching' effect on the material as well as affecting its rigidity due to its known corrosiveness.

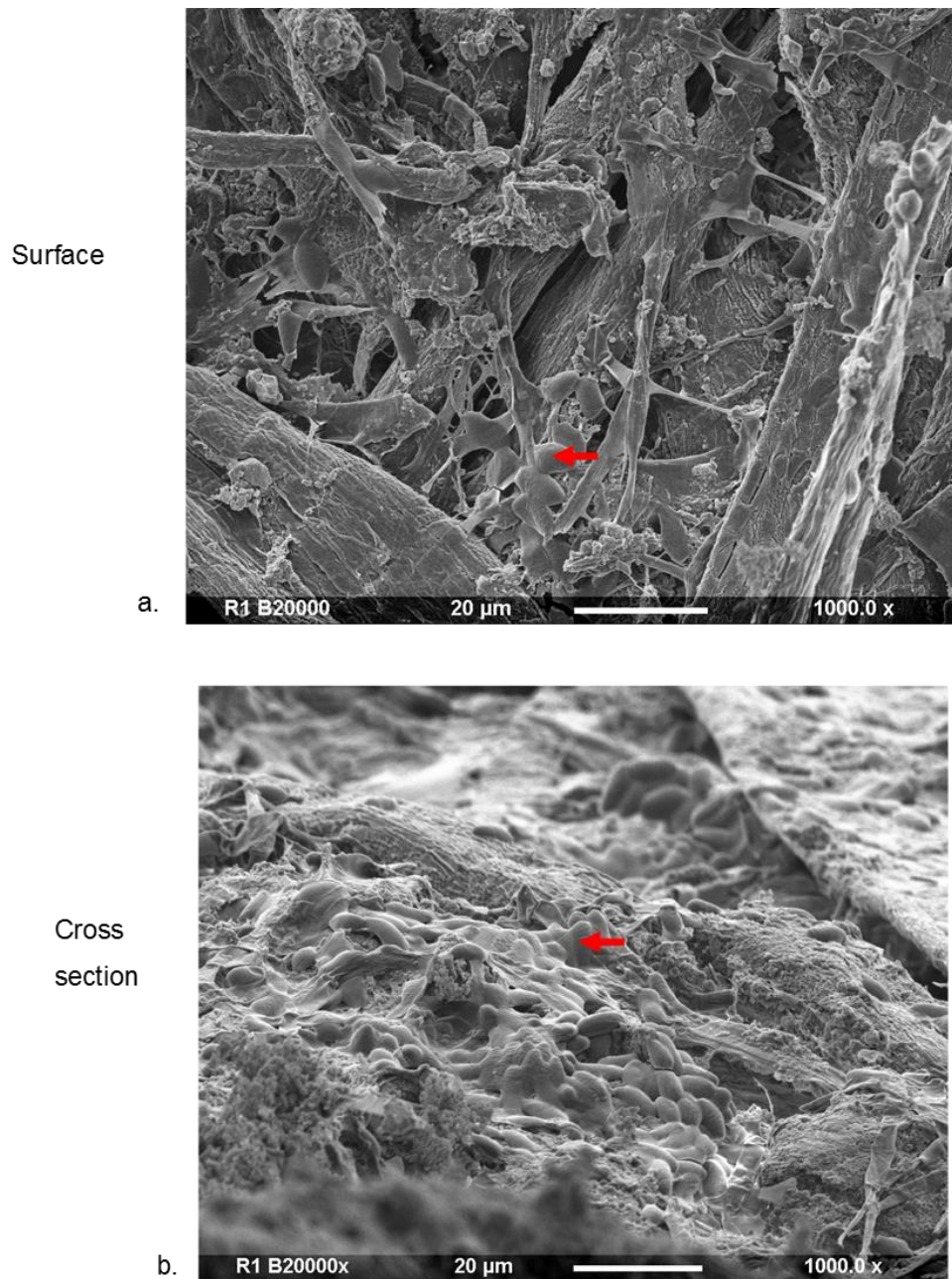


Figure 7-15: Fungal growth on gypsum treated with 20000 ppm bleach. a. Surface; b. Cross-section SEM images at 1000x magnification. The red coloured arrows indicates fungal structures coated with bleach.

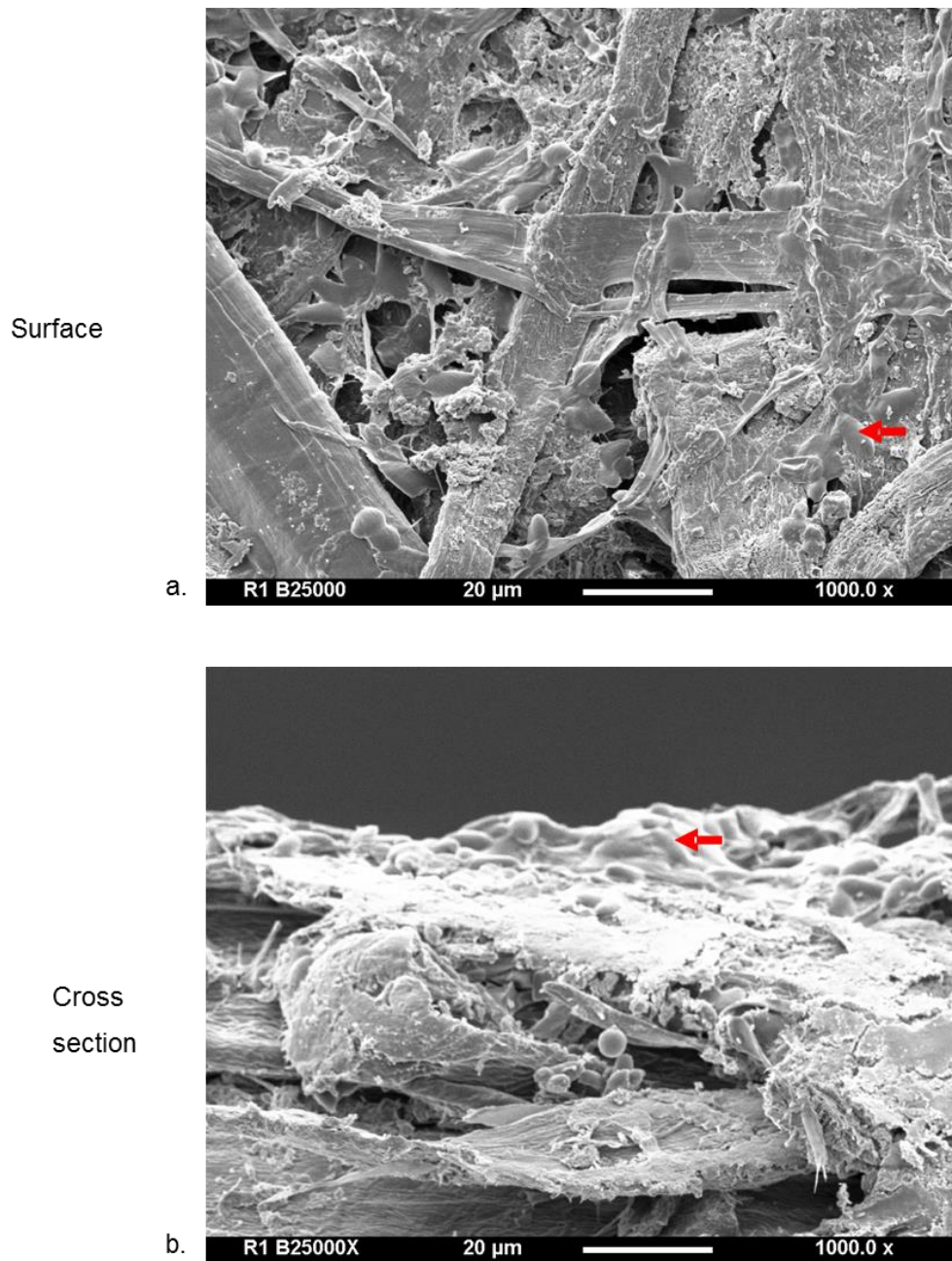


Figure 7-16: Fungal growth on gypsum treated with 25000 ppm bleach. a. Surface, b. Cross-section SEM images at 1000x magnification. The red coloured arrows indicate fungal structure coated with bleach.

The fungicidal effect of bleach on *S. chartarum* was seen at both concentrations after multiple applications at 24-hours interval using the agar-based *in-vitro* method (Chapter 6). To determine the frequency of application required to remediate fungal growth on gypsum board, multiple applications of concentrations of 25000 ppm and 45000 ppm bleach were applied.

The *S. chartarum*-infested gypsum blocks showed fungal growth before and after application of bleach at 25000 ppm (Figure 7-17) and 45000 ppm (Figure 7-18). From the results, mould growth became less visible as it became gradually decolourised with increasing number of applications at both concentrations. Some visible brown spots were clearly observed after 1 application of 25000 ppm. Complete decolourisation of mould was observed after 3 applications at 25000 ppm and 2 applications at 45000 ppm. Bleach also caused decolourisation of the paper surface.

To test whether bleach was capable of inhibiting or killing the mould, approximately 1 cm² of the mould- infested gypsum was cultured on ESA for 10 days after completion of each application. From the result, no fungal growth was recovered after 3 applications at both concentrations (Figure 7-19). There was slightly smaller fungal diameter growth at 45000 ppm compared to 25000 ppm after one and two applications.

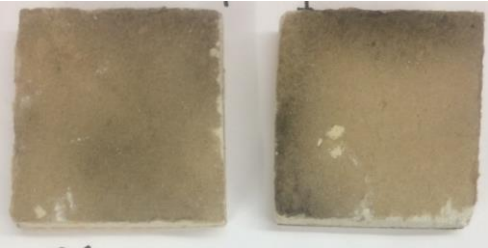
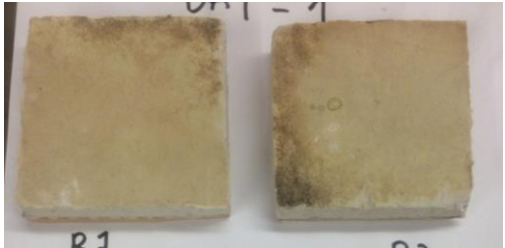
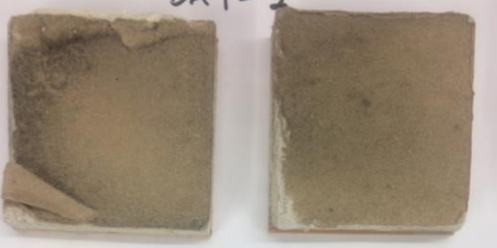

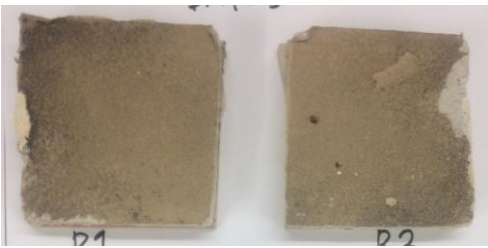

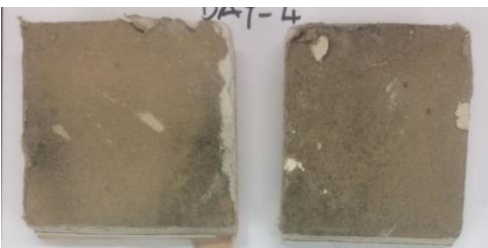

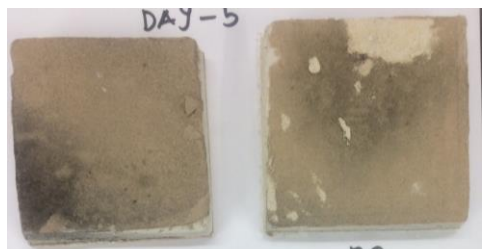

	Before application	After application
1 application		
2 applications		
3 applications		
4 applications		
5 applications		

Figure 7-17: Mould-infested gypsum boards before and after 1 to 5 applications of 25000 ppm bleach at 24-hours interval.

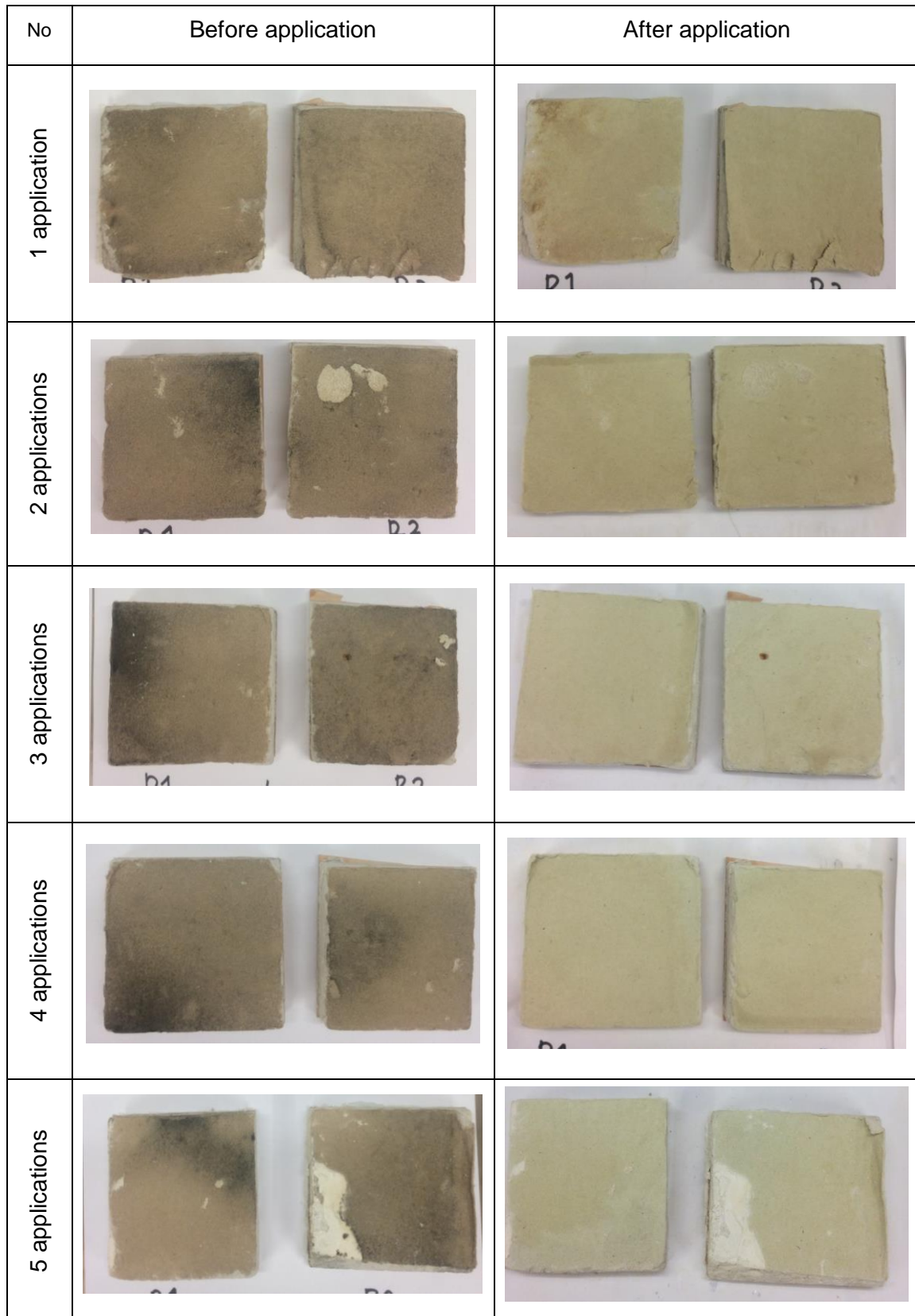


Figure 7-18: Mould-infested gypsum boards before and after 1 to 5 applications of 45000 ppm bleach at 24-hours interval.

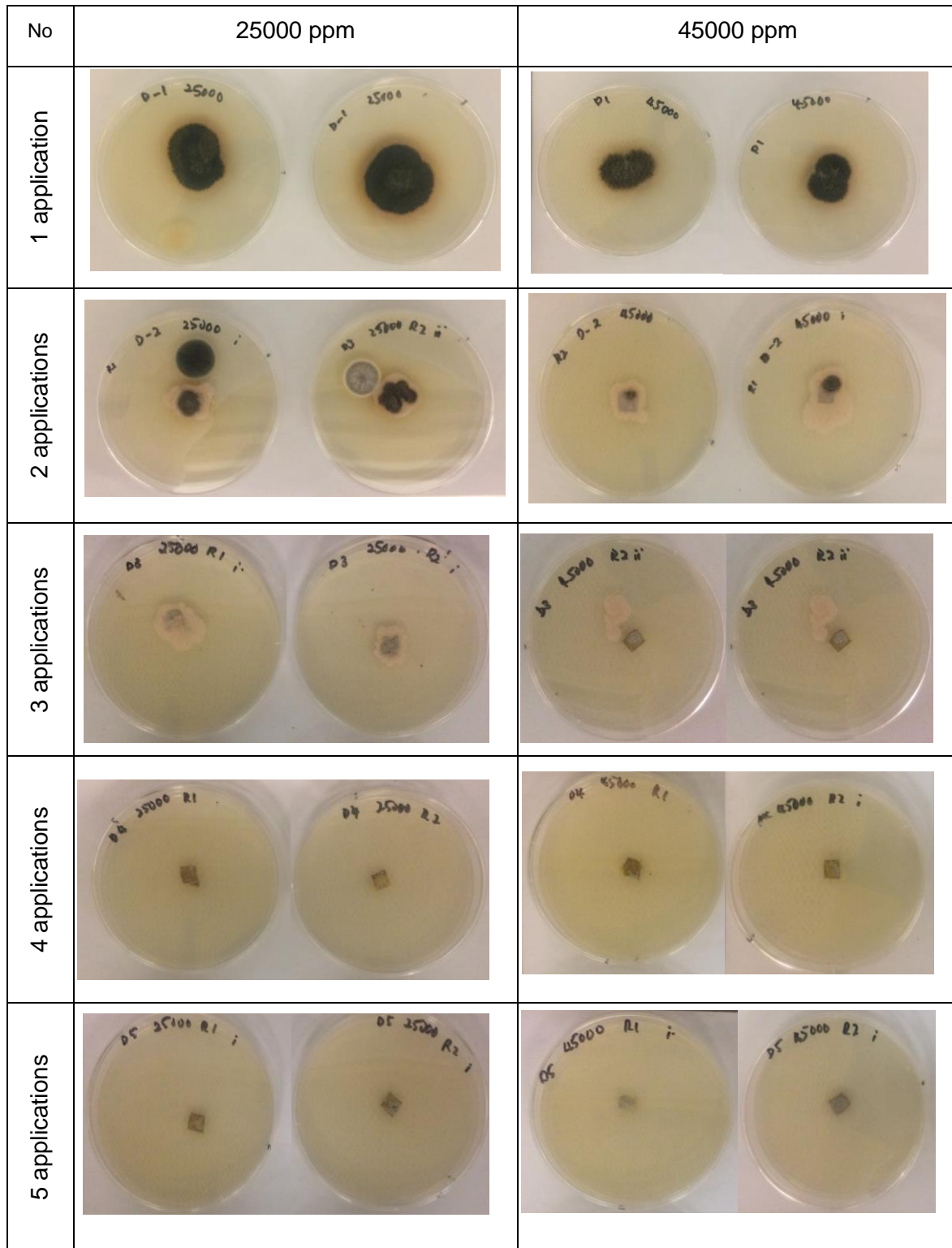


Figure 7-19: Fungal recovery after 10 days from mould-infested gypsum treated with 1 to 5 applications of 25000 ppm and 45000 ppm bleach at 24-hour interval grown on ESA at 25 °C.

The mould infested material treated with 45000 ppm bleach also showed similar white coatings of bleach covering the fungal structures and the material (Figure 7-20). The coatings became thicker as the concentrations increased from 25000 ppm to 45000 ppm making the fungal structures more difficult to visualise.

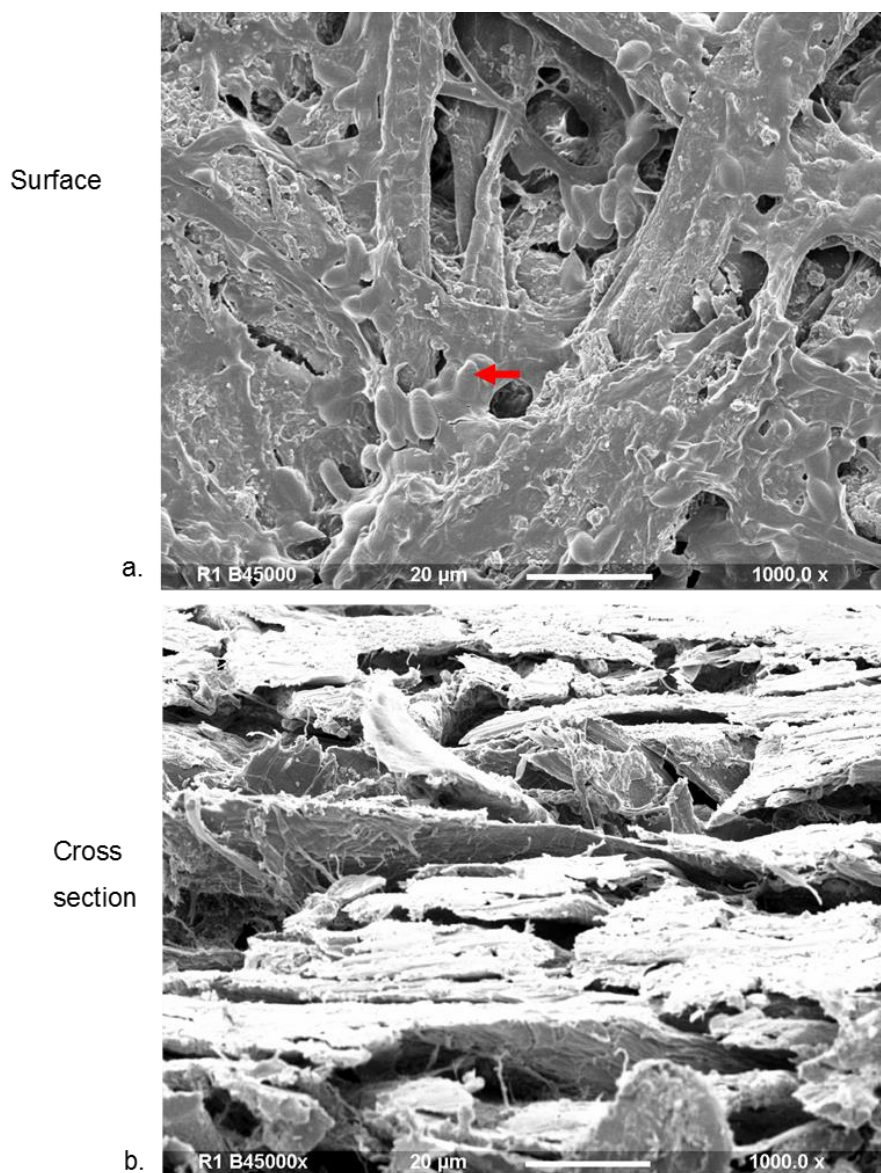


Figure 7-20: Fungal growth on gypsum board following 45000 ppm bleach treatment. a. Surface; b. Cross-section SEM images at 1000x magnification. Fungal structures were hardly observed at 45000 ppm bleach. The red coloured arrow indicates fungal structures coated with thick bleach. No clear fungal structures were observed in the cross section images.

From the findings, bleach was effective in treating mould-infested gypsum board at 3 applications at 25000 ppm and 45000 ppm, although causing bleaching and corrosion of the gypsum board.

7.3.3.3 The effect of aerosolised hydrogen peroxide (AHP)

After 1 cycle AHP application, the chamber was kept closed for a minimum 2 hours contact time for effective decontamination. After 2 hours, the AHP mists settled down as fine white particles in the chamber and on materials. From our observation, there were no significant differences in the appearance of visible mould as well as the surface material before and after 1 cycle of AHP application to the mould-infested gypsum board (Figure 7-21).

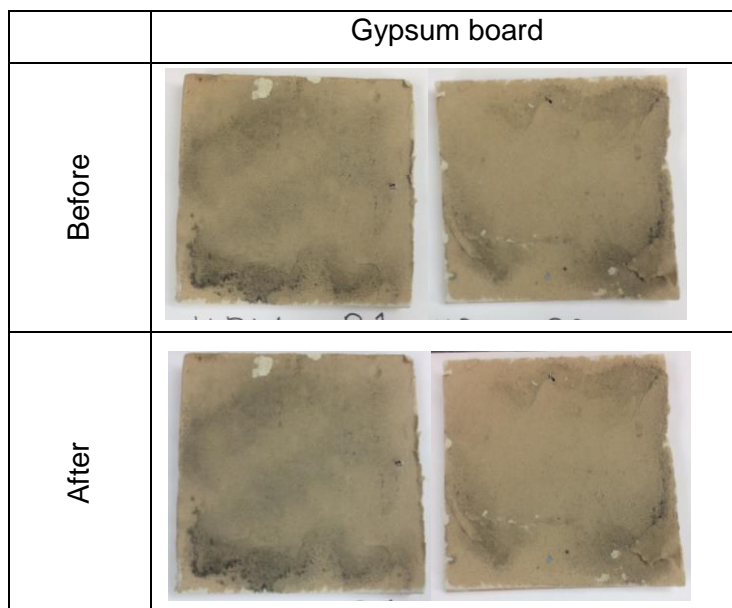


Figure 7-21: Mould-infested gypsum board before and after 1 cycle of AHP treatment.

To determine whether *S. chartarum* was inactivated by AHP, 1 cm² squares of materials were placed on ESA and incubated for 10 days. The result showed fungal recovery from the treated material (Figure 7-22). This indicated that one cycle AHP application did not kill *S. chartarum*.

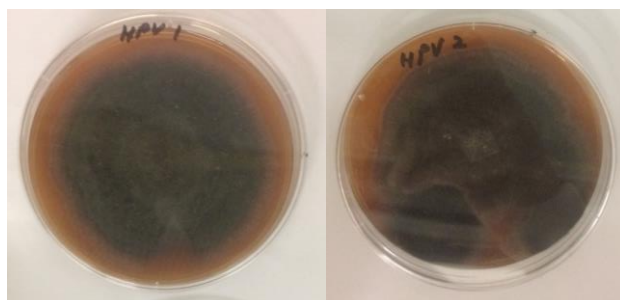


Figure 7-22: Fungal growth recovered from mould-infested gypsum boards after treatment with 1 cycle AHP shown in duplicates incubated at 25 °C on ESA for 10 days.

From the SEM images, there were clear structures of both surface material and fungus as shown at 250x (Figure 7-23) and 1000x (Figure 7-24) magnifications. White particles were seen on both material and fungus as clearly observed at 1000x magnification. Fungal structure on the surface was seen either collapsed or undisturbed.

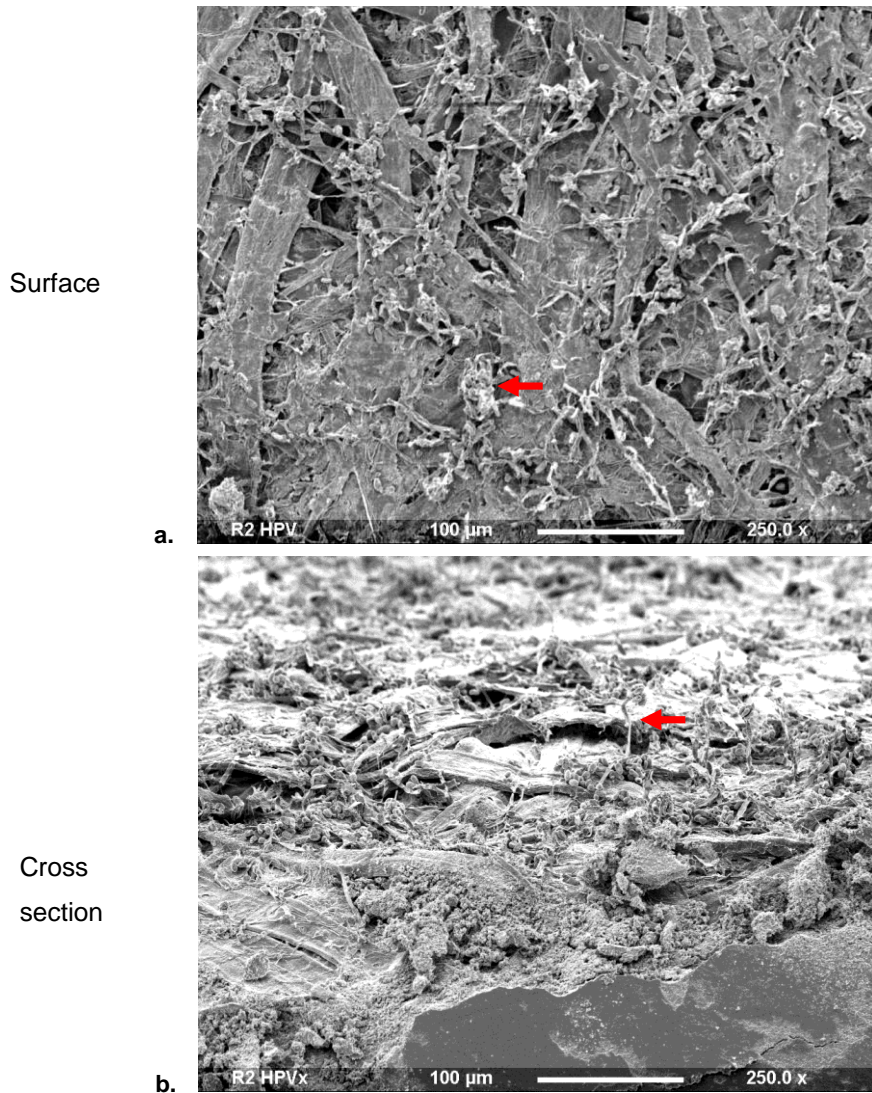


Figure 7-23: Representation of fungal growth on gypsum. a. Surface; b. Cross-section (fungi) with one cycle of AHP treatment using SEM images at 250x magnification. The red coloured arrow indicate 'undisturbed' fungal structures.

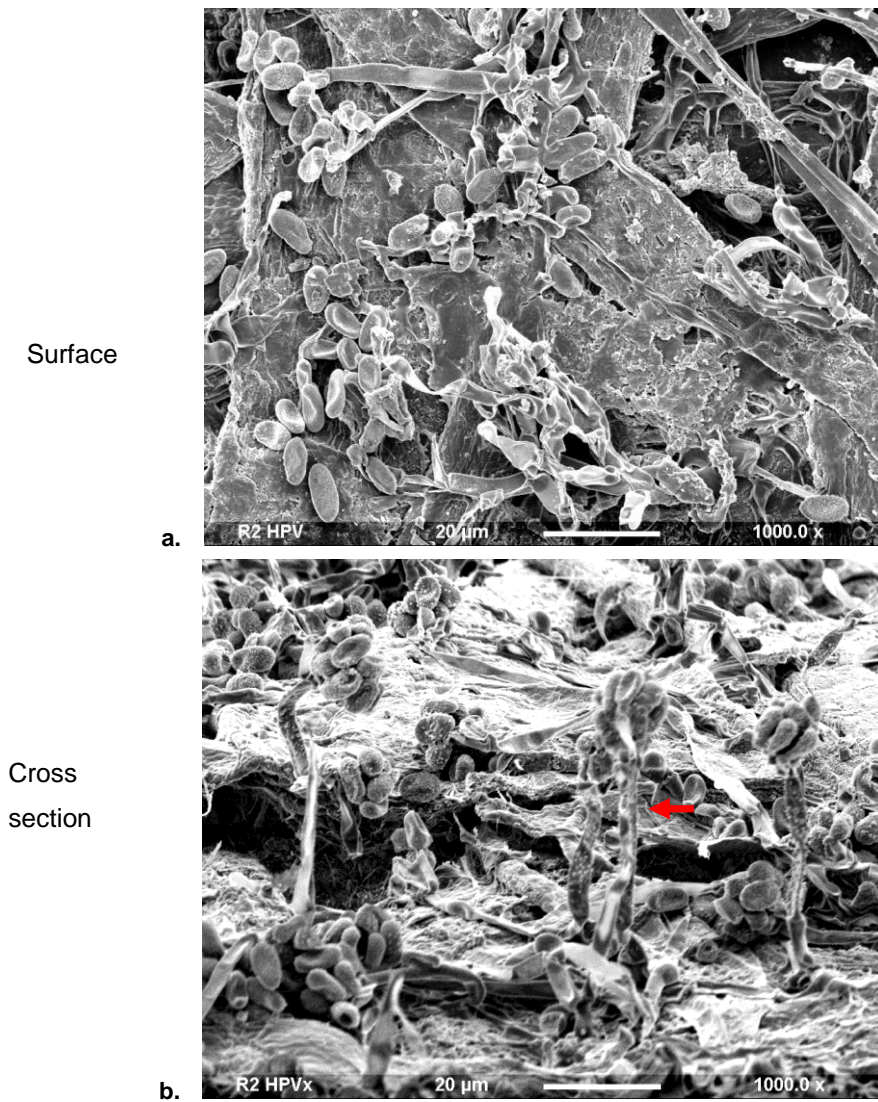


Figure 7-24: Representation of fungal growth on gypsum. a. Surface; b. Cross-section (fungi) with one cycle AHP treatment using SEM images at 1000x magnification. The red coloured arrow indicates 'undisturbed' fungal structure.

From the findings, 1 cycle of AHP was not effective at treating mould-infested gypsum board. The result was in accordance with our previous agar-based observations (Chapter 6). However, there was no significant adverse effect observed on the material structure.

7.3.3.4 The effect of peracetic acid (PAA)

Two concentrations, 4000 ppm (recommended by manufacturer) and 8000 ppm of PAA were sprayed on *S. chartarum*-infested gypsum boards (Figure 7-25). No significant differences were observed before and after application of PAA at 4000 ppm but there was some bleaching of mould at 8000 ppm.

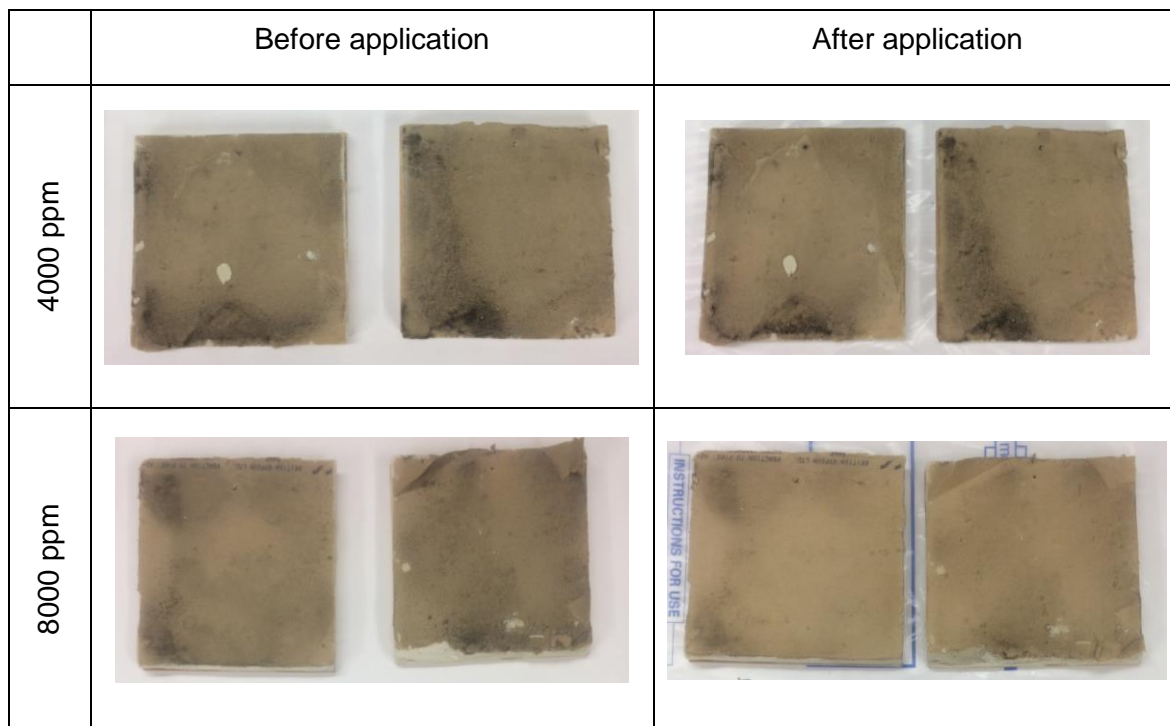


Figure 7-25: Fungal growth on gypsum before and after treatment with PAA at concentrations of 4000 ppm and 8000 ppm shown in duplicate.

The 1 cm² materials from both concentrations showed fungal recovery on ESA after 10 days incubation (Figure 7-26). This indicates that PAA at recommended concentration, 4000 ppm and double the concentration, 8000 ppm were ineffective in killing or inhibiting the growth of *S. chartarum* on gypsum board.

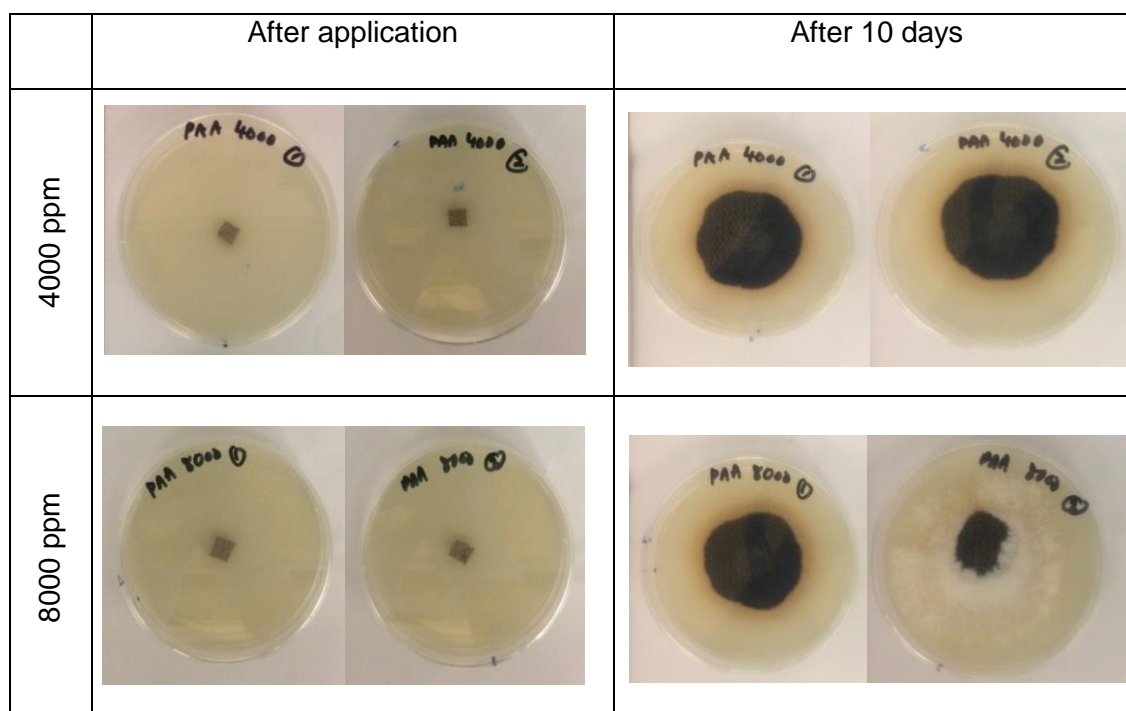


Figure 7-26: The PAA-treated materials were cut into 1 cm² and placed onto ESA on the same day of PAA application. The materials were incubated on ESA at 25 °C where growth recovery was documented after 10 days.

The materials treated with 4000 ppm and 8000 ppm PAA were examined under SEM at 250x magnification (Figure 7-27 and 7-28) and 1000x magnification (Figure 7-29 and Figure 7-30). From the SEM images, it was observed that the fungal structure ‘collapsed’ at both concentration might be due to the spraying application. No other significant abnormality was seen at 4000 ppm at 250x and 1000x magnifications. However, white coloured coating was observed on the mould and materials at 8000 ppm.

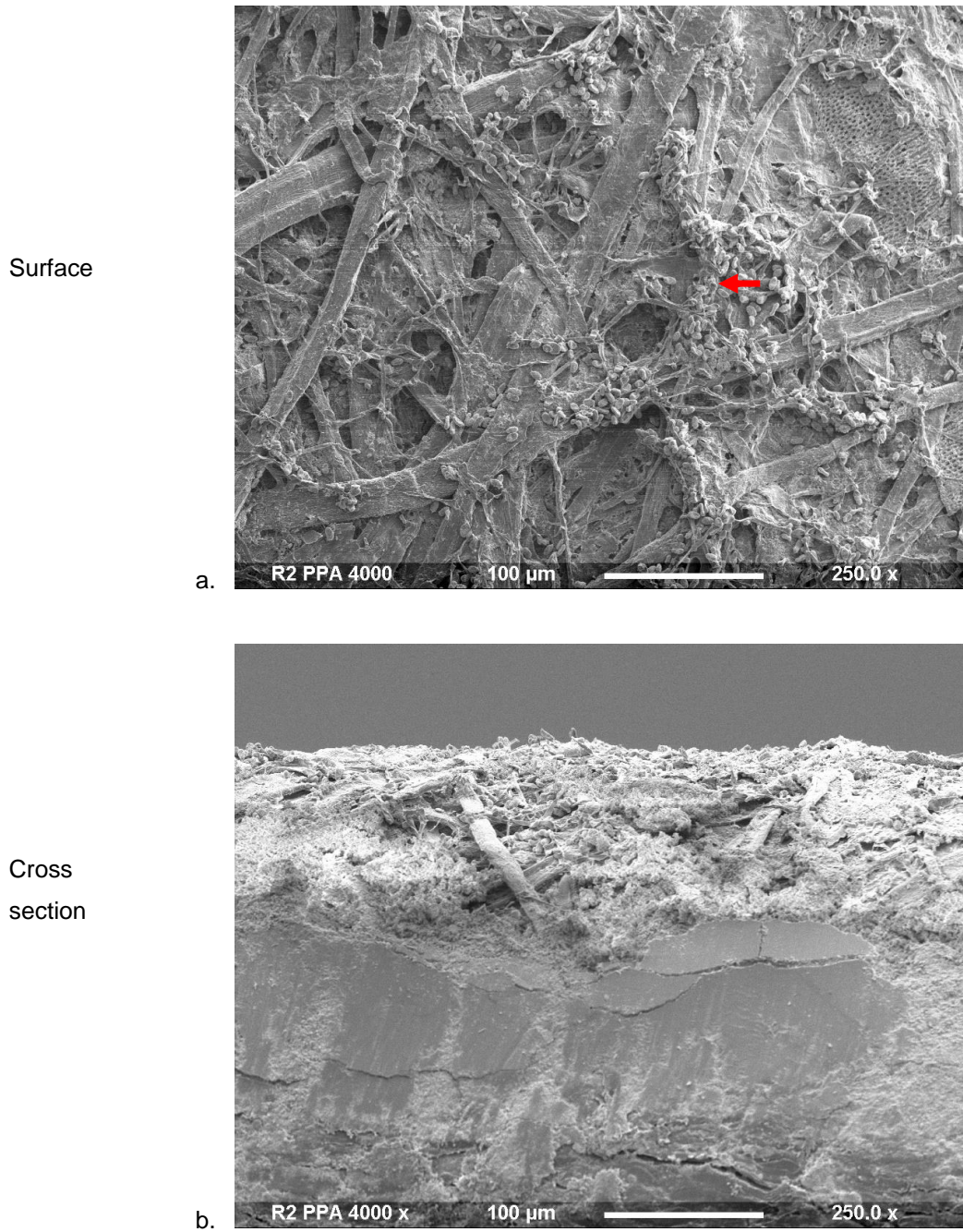


Figure 7-27: Representation of fungal growth on gypsum following PAA treatment at 4000 ppm. a. Surface; b. Cross-section using SEM images at 250x magnification. The red coloured arrow indicates fungal growth.

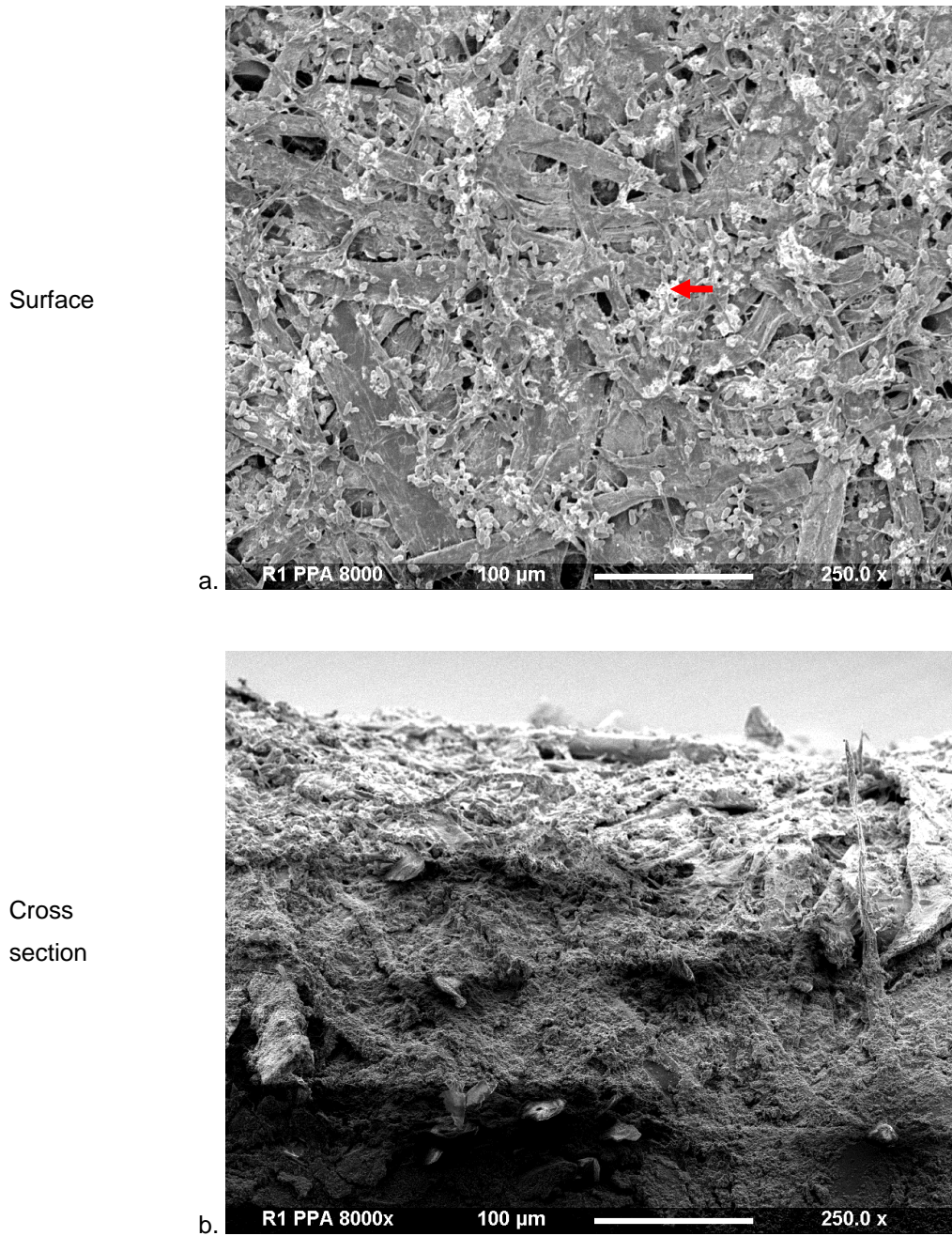


Figure 7-28: Fungal growth on gypsum board following PAA treatment at 8000 ppm. a. Surface; b. cross-section SEM images at 250x magnification. The red coloured arrow indicates white coated fungal structures.

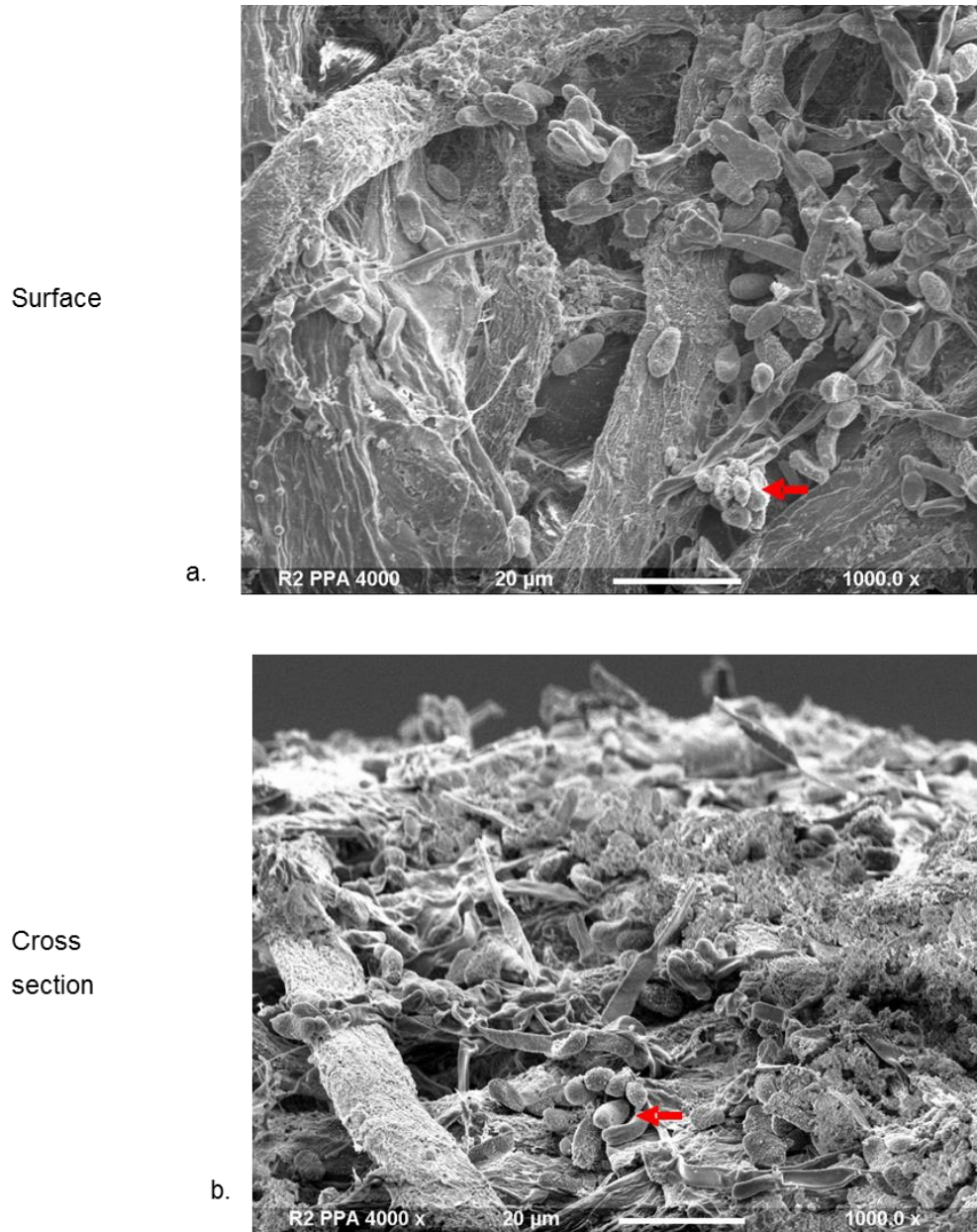


Figure 7-29: Fungal growth on gypsum board following PAA treatment at 4000 ppm. a. Surface; b. Cross-section SEM images at 1000x magnification. The red coloured arrow indicates white coated fungal structures.

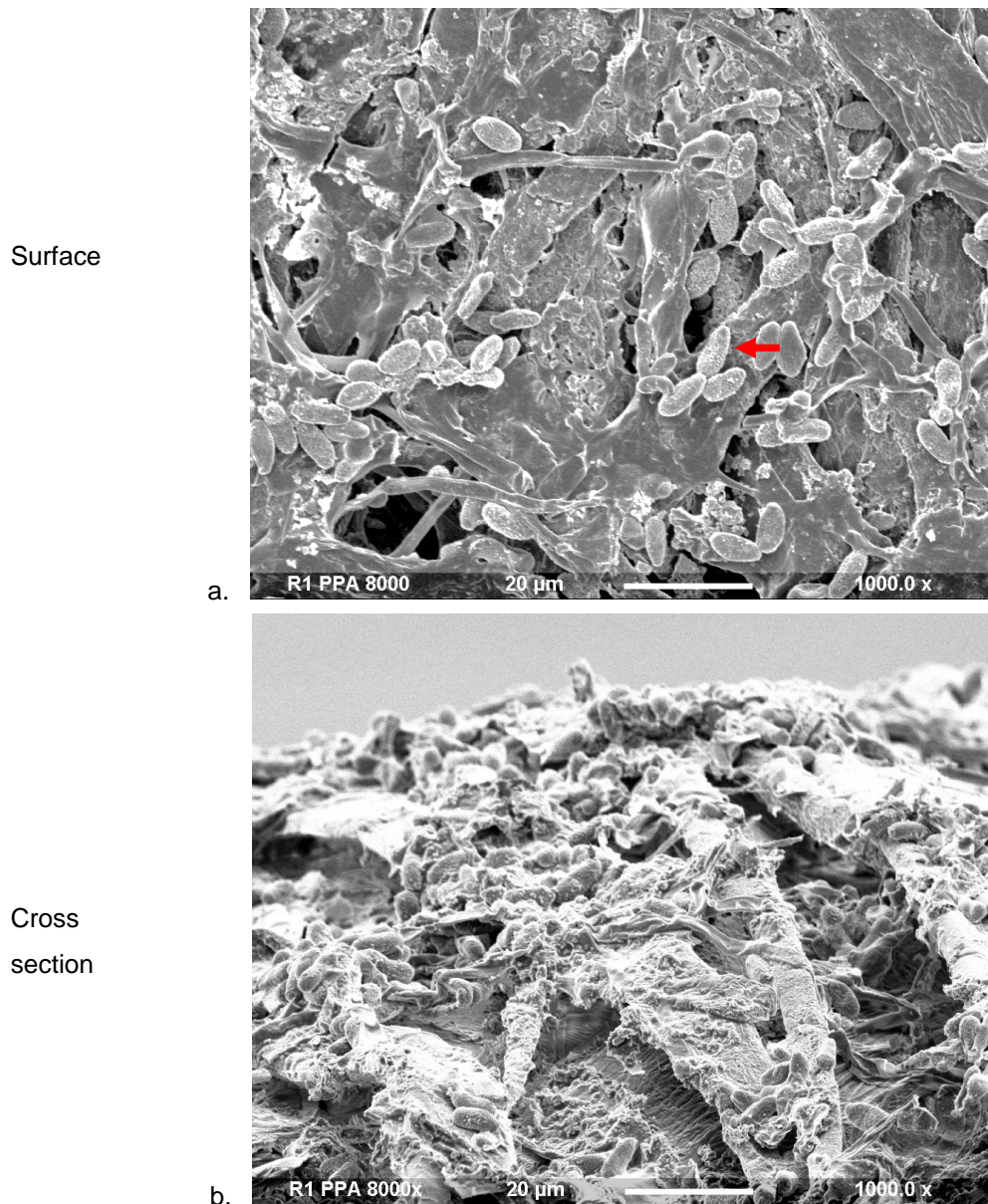


Figure 7-30: Fungal growth on gypsum board following PAA treatment at 8000 ppm. a. Surface; b. Cross-section SEM images at 1000x magnification. The red coloured arrow indicates white coated fungal structures.

From the findings, a concentration of PAA at 4000 ppm (manufacturer's recommendation) and at 8000 ppm were ineffective at treating mould-infested gypsum board. Although there was some discoloration of the mould and material at 8000 ppm, this did not affect the fungal viability. The result was in accordance to our previous observation performed *in vitro* (Chapter 6).

7.3.3.5 The effect of organosilane (OS)

Two concentrations, 2500 ppm and 5000 ppm of OS were applied by spraying to *S. chartarum* - infested gypsum boards (Figure 7-31). The concentrations were derived from the concentration required to inhibit *S. chartarum in vitro* using the agar plate dilution method (Chapter 6). From the results, visible mould was observed with and without application of OS at 2500 ppm and 5000 ppm. This showed that both concentrations did not prevent the growth of *S. chartarum* on gypsum board coated with OS.

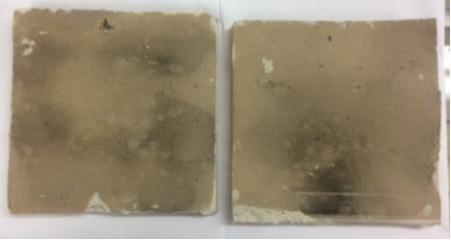
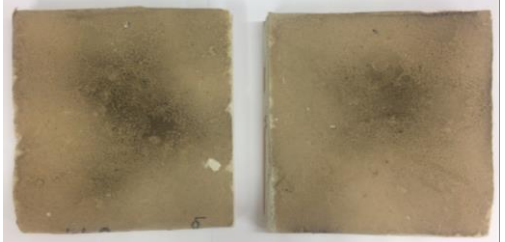
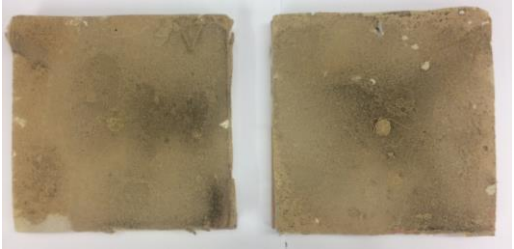
No	Without application	With application
2500 ppm		
5000 ppm		

Figure 7-31: Gypsum board pre-treated with and without OS coating at concentrations 2500 ppm and 5000 ppm prior to inoculation with *S. chartarum* shown in duplicates.

To determine whether *S. chartarum* grown on OS coated gypsum board was viable, 1 cm² materials were cut and placed on ESA. The 1 cm² materials also showed fungal recovery on ESA as documented after 10 days incubation (Figure 7-32).

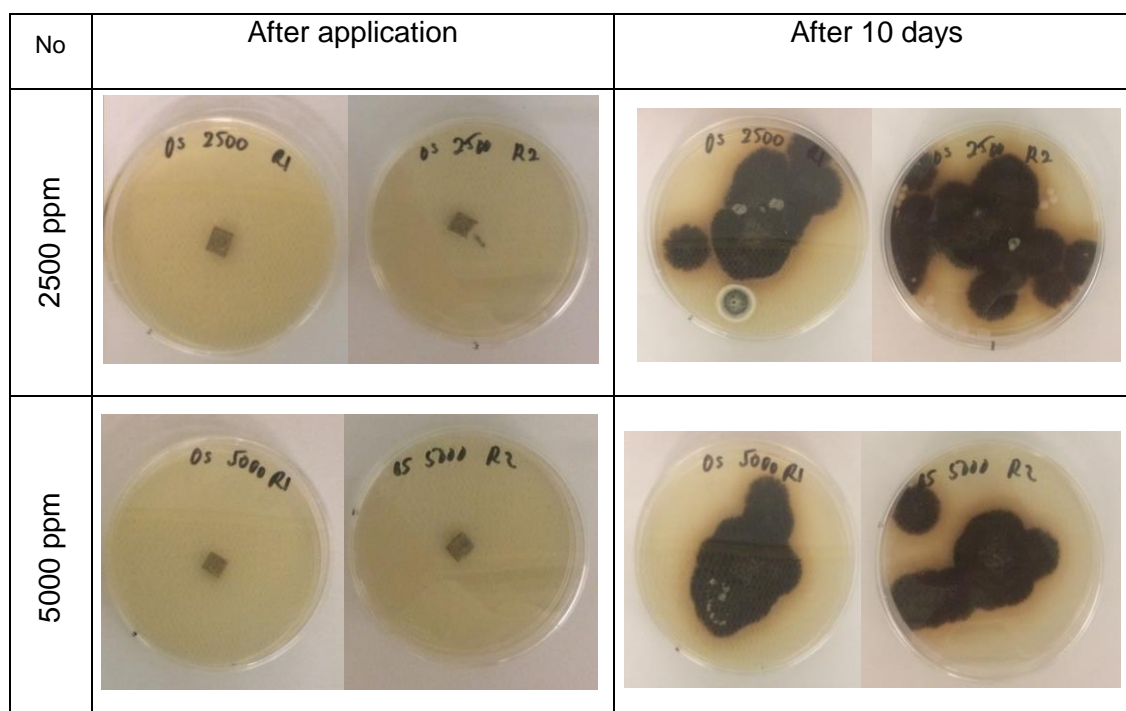


Figure 7-32: The OS-treated materials grown inoculated with *S. chartarum* were cut into 1 cm² after 5 weeks incubation. The materials were grown on ESA and growth recovery was documented after 10 days.

To determine the effects of the OS coating on fungal growth, the materials coated with 2500 ppm and 5000 ppm were subjected to SEM examination at 250x magnification and 1000x magnification.

From the SEM images, the growth was not evenly distributed compared to other treatments as observed at concentrations of 2500 ppm and 5000 ppm. From the 250x magnification, fungal growth were observed only at the porous area of the gypsum board while, no growth on the flat exposed areas of the paper fibres. (Figure 7-33 and Figure 7-34). With closer examination of the fungal growth on the porous area were examined at higher magnification at 1000x, the fungus was seen growing outwards from in between the paper fibres. The surface fibres exposed to the OS coating had no fungal growth (Figure 7-35 and Figure 7-36).

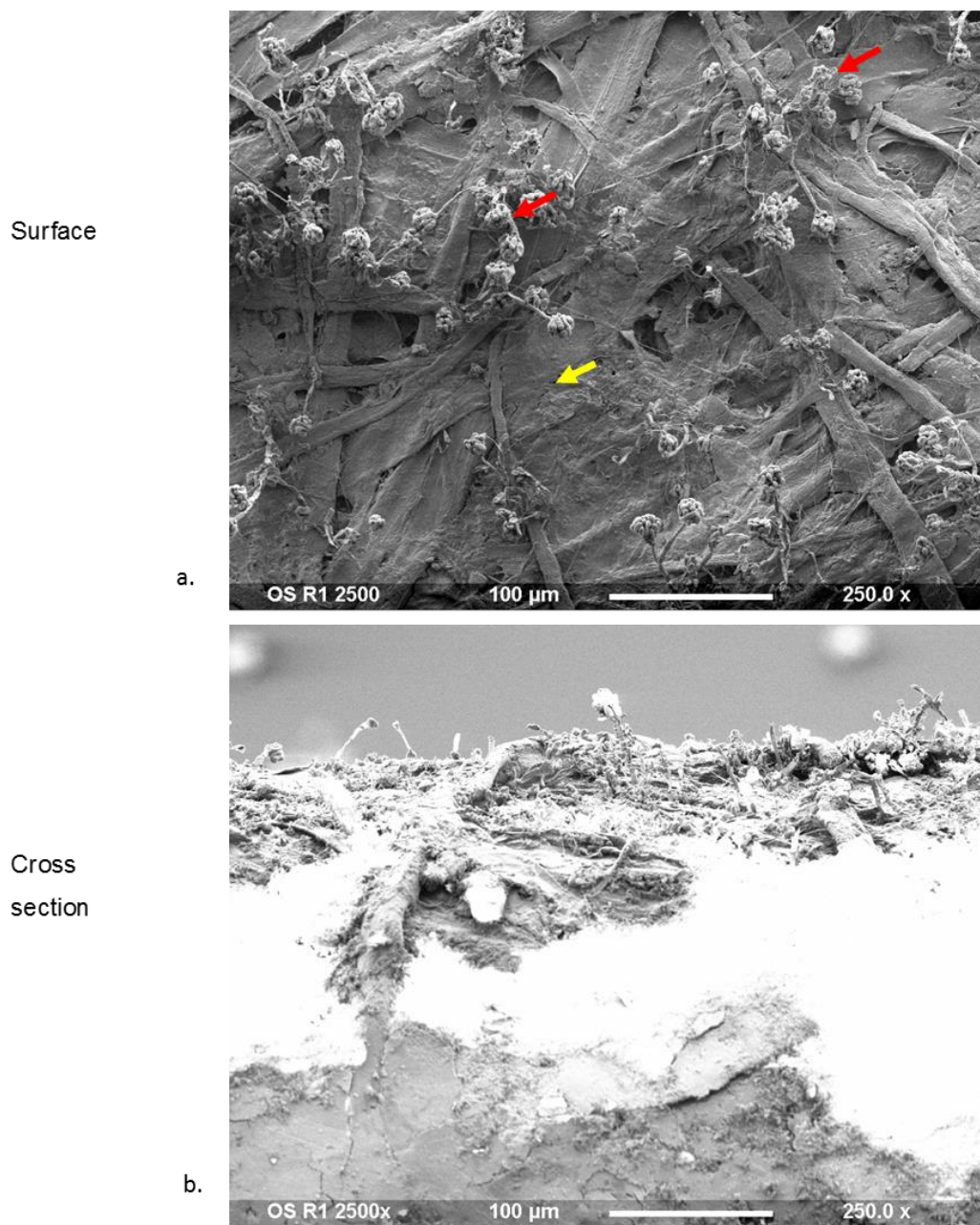


Figure 7-33: Fungal growth on gypsum board following OS pre-inoculation treatment at 2500 ppm. a. Surface; b. Cross-section SEM images at 250x magnification. The arrows marked in red indicate fungal growth from within the porous area and yellow indicates flat exposed surface with no growth.

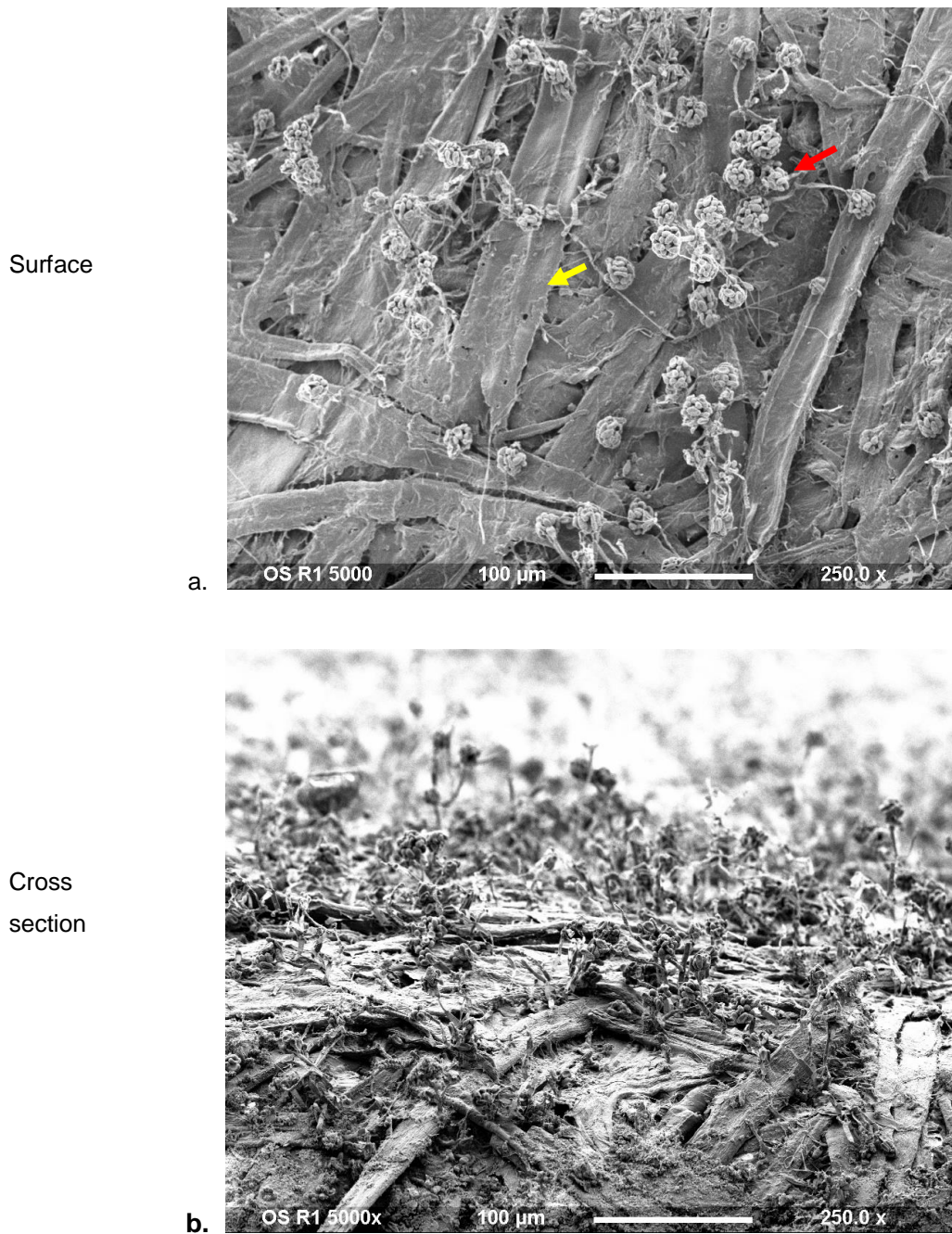
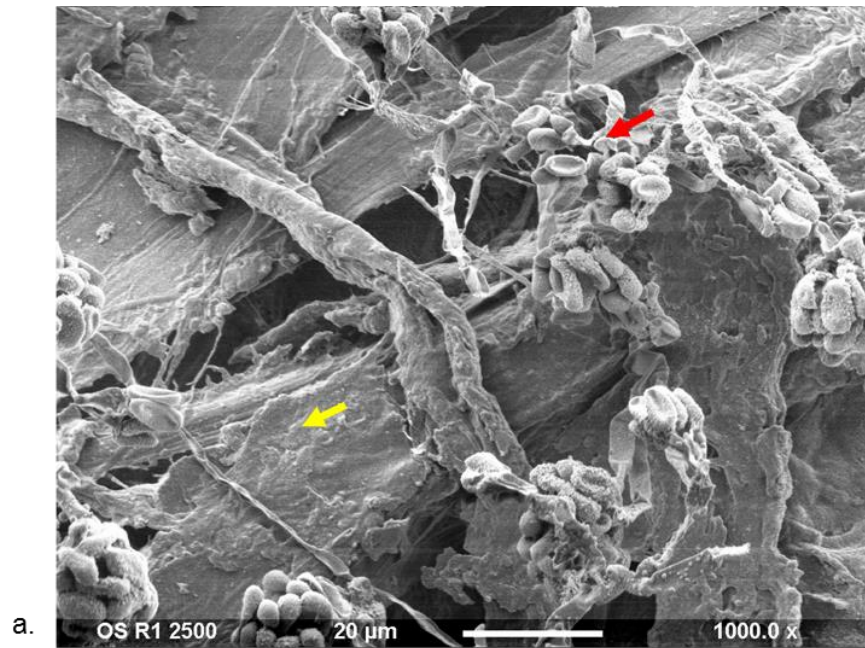


Figure 7-34: Representation of fungal growth on gypsum board following OS treatment at 5000 ppm. a. Surface; b. Cross-section using SEM images at 250x magnification. The arrows marked in red indicate fungal growth from within the porous area and yellow indicates flat exposed surface with no growth.

Surface



Cross section



Figure 7-35: Fungal growth on gypsum board following pre-inoculation OS treatment at 2500 ppm. a. Surface; b. Cross-section using SEM images at 1000x magnification. The arrows marked in red indicate fungal growth from within the porous area and yellow indicates flat exposed surface with no growth.

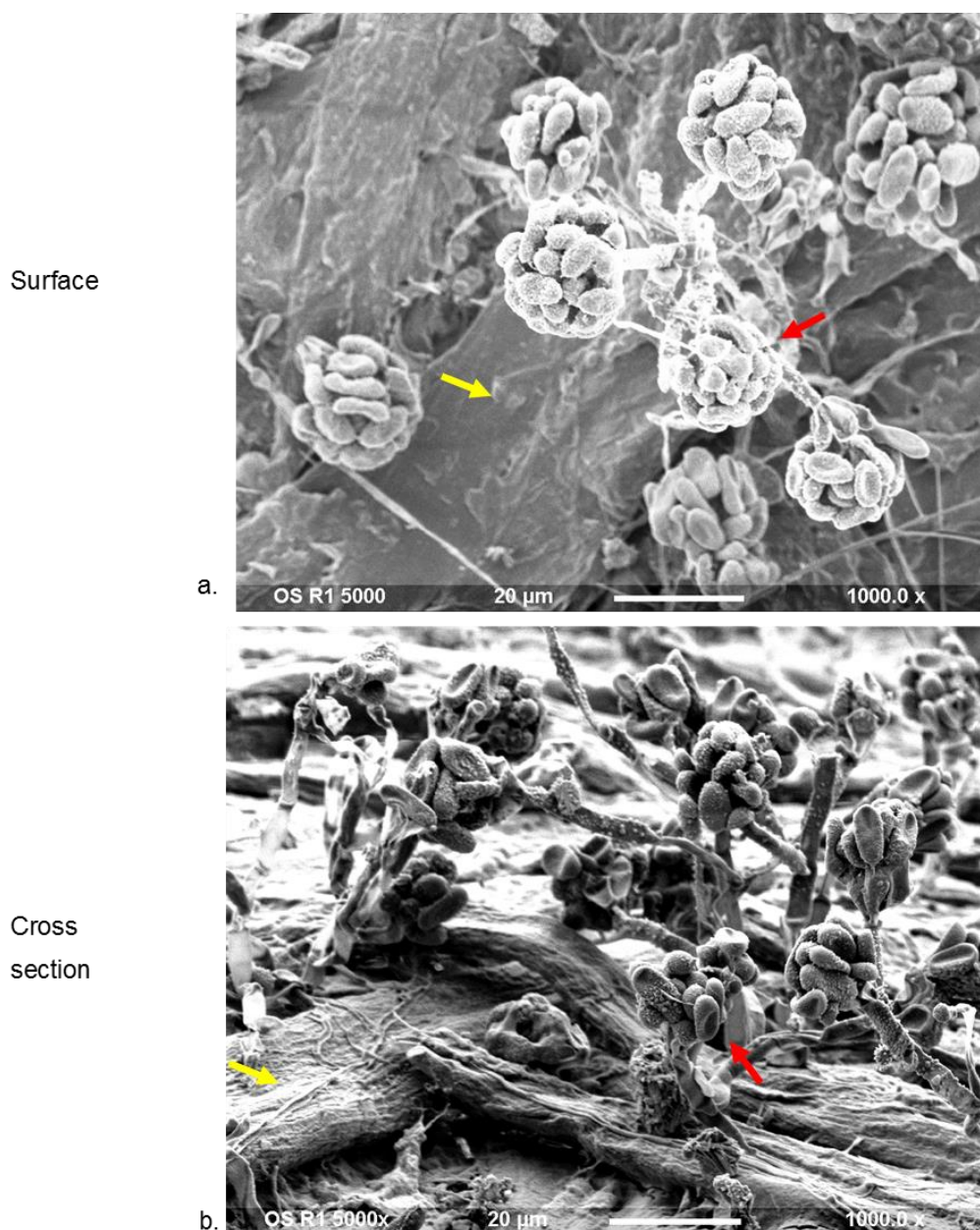


Figure 7-36: Fungal growth on gypsum board following pre-inoculation OS treatment at 5000 ppm. a. Surface; b. Cross-section SEM images at 1000x magnification. The arrow marked in red indicate fungal growth from within the porous area and yellow indicate flat exposed surface with no growth.

The findings showed that fungal growth on the OS-coated gypsum at 2500 ppm and 5000 ppm occurred in the porous area or in between the paper fibres. No fungal growth was detected on the surface readily exposed to OS.

7.4 DISCUSSION

This study demonstrates the effectiveness of antimicrobial agents at killing or preventing the growth of *S. chartarum* on gypsum board.

7.4.1 The effects of environmental condition and building materials on *S. chartarum*.

Moulds need moisture and a suitable substrate to grow^(5, 274). *S. chartarum* is known as one of the hydrophilic moulds which requires a wet substrate with more than 90% relative humidity (RH) for optimal growth^(23, 275, 276). In the indoor environment, it is commonly isolated from cellulose-based materials used in construction, finishing and furnishing^(2, 5, 23). Relative humidity has been proposed as an indicator of *S. chartarum* infestation. It has been isolated from walls of dwellings with a higher RH of 97% compared to an average of 42% RH for other moulds such as *Aspergillus* spp., *Cladosporium* spp., *Penicillium* spp. and *Ulocladium* spp.⁽²⁷⁷⁾. In this study, potassium sulphate dissolved in water was optimised to provide a constant RH of $98 \pm 5\%$ at 25 °C to support the optimal growth of *S. chartarum* (Figure 7-4).

The choice of building materials can greatly affect fungal growth. Porous materials such as grouting between tiles, wood and gypsum board are not only highly susceptible to mould growth, but they are also more difficult to clean^(19, 278). In this study, *S. chartarum* thrived on gypsum board compared to other tested materials (Figure 7-7). Several studies have also utilised gypsum board as a model to study mould infestation and antimicrobial effectiveness in the indoor environment⁽²⁷⁹⁻²⁸¹⁾. Gypsum board (also known as plaster board or dry board) is composed of paper layers and is used as construction material which makes it a good substrate to support mould growth. From our results, *S. chartarum* penetrated into the paper surface layer but did not reach the gypsum layer after 6 weeks growth (Figure 7-11). Lewinska *et al.*⁽²⁸²⁾ has inoculated *S. chartarum* on gypsum board and proposed that the fungus only grew on top of the paper surface of the gypsum board (at the point of inoculation) and had no growth detected on the gypsum layer after 8 weeks. In our study, no conclusion could be made regarding the ability of gypsum to support growth since the fungus did not reach the gypsum layer. This was evident in our SEM images in the preliminary study of 11 weeks of incubation (Figure 7-8).

Fungal infestation in gypsum board appears to depend very much on the paper layer as the source of nutrient. In a moisture-damaged building survey, Hyvarinen *et al.*, (2002) has reported that *Stachybotrys* spp. were frequently found in paper-based material particularly in gypsum board compared to other materials such as wood, ceramic and plastics ⁽²⁷⁴⁾. *S. chartarum* grown on wallpaper and gypsum board also produced toxic macrocyclic trichothecenes, mainly satratoxin G and H at high RH ⁽²⁸³⁾. These suggest that gypsum board held in a high humidity environment is the best material model to study *S. chartarum*-infestation in water damaged buildings.

We have also sterilised and dried the gypsum board prior to these experiments to avoid any pre-existing fungal contamination. This is in accordance with Andersen *et al.* ⁽²⁸⁴⁾ who revealed that gypsum wallboard was already pre-contaminated with *S. chartarum*, *Aspergillus hiratsukae* and *Chaetomium globosum* even before reaching construction sites.

7.4.2 Effectiveness of antimicrobial agents on *S. chartarum*-infested gypsum board

7.4.2.1 Sodium hypochlorite (bleach)

Sodium hypochlorite (NaOCl) or bleach is widely used in cleaning, bleaching or stain removal and disinfection at various settings due to its effectiveness, low cost and commercial availability. The concentration of NaOCl varies according to the manufacturers and intended use. For example, the commercially available household bleach is formulated with 3–8% of NaOCl compared to industrial grade bleach with 10–12% of NaOCl as the active ingredient. It needs to be diluted according to the intended use such as general cleaning, disinfection or decontamination.

In this study, undiluted bleach of approximately 45000 ppm NaOCl was recommended by the manufacturer (Evans Vanodine International PLC) for highly contaminated and soiled environment such as that found in sinks, toilets and drains. In chapter 6, we have reported a fungicidal effect on *S. chartarum*, *in vitro* at more than 2 applications of 25000 ppm NaOCl and 1 application of NaOCl at 45000 ppm. Here, we have tested 20000 ppm and 25000 ppm of NaOCl at 1 application; and 25000 and 45000 ppm at multiple applications on *S. chartarum*-infested gypsum board.

From the findings, both mould and surface materials were ‘bleached out’ after treatment with bleach at tested concentrations. However, mould became non-viable only after 3 applications at 25000 and 45000 ppm for 3 consecutive days. Wagner *et*

al.⁽²⁸¹⁾ has reported inactivation of *S. chartarum* grown on gypsum board after continuous exposure to aerosolised NaOCl for 8 hours. In other fungi, 5000 ppm NaOCl (Clorox Co) significantly reduced the number of cultured conidia of *A. fumigatus* on gypsum board after 24 hours incubation ⁽²⁴⁷⁾.

The SEM images also showed bleach coatings on fungus and material. The coatings might derive from detergent added to form the thickness in the preparation. As implied by the manufacturer, the thick bleach is made to increase the “clinging” capabilities and stays longer when applied to surfaces such as the toilet, where it would not get washed away easily. However, the full listings of chemical composition in the preparation is not disclosed by the manufacturer.

In contrast, Peitzsch *et al.*⁽⁵³⁾ reported treatment of approximately 2.5% (25000 ppm) NaOCl for 30 minutes did not inhibit growth and toxin production on *S. chartarum* infested gypsum board and wood block. Chakravarty *et al.*⁽⁸⁴⁾ also found that *S. chartarum* grown on wood block for 8 weeks remained viable after treatment with bleach (6% NaOCl) for 1 hour.

These findings suggest that multiple or continuous exposure is effective at killing *S. chartarum* on gypsum board. However, this depends on the length and concentration of exposure. This may be due to the penetration of the gypsum board paper layer by the fungus making it more difficult for effective concentrations of NaOCl to reach the deeper cells with a single or brief application. Besides, the “corrosion” of the paper layer might release more nutrients and consequently provide a better niche for fungi to grow. The findings also highlight the difficulty of complete fungal eradication and emphasize the importance of prevention rather than remediation.

Despite its cost-effectiveness and availability, bleach is known to be corrosive to many surfaces as well as polluting the environment and safety precautions are important when dealing with concentrated bleach. As it is also an irritant, it poses hazardous side effects to humans via inhalation, dermal contact and ingestion ⁽²⁸⁵⁻²⁸⁷⁾.

7.4.2.2 Aerosolised hydrogen peroxide (AHP)

Aerosolised hydrogen peroxide (AHP) has been widely used in indoor environments particularly in hospitals and laboratories for infection control measure and to disinfect enclosed areas, laboratory workstations and equipment ^(252, 288-290). Different hydrogen peroxide automated room decontamination systems have been introduced and compared, mainly Bioquell™ (Bioquell, UK), ASP Glosair™ (formerly known as

Sterinis) (Johnson & Johnson, UK), Steris Biogenie™ (STERIS VHP®, USA) and Deprox™ (Hygiene Solutions, UK) (193, 258, 290-292). Compared to other disinfectants, improved hydrogen peroxide was claimed to be bactericidal, viricidal and mycobactericidal but more expensive than other low level disinfectants (258). However, evidence of the effectiveness of AHP on mould-infested building materials is still unknown.

In this study, we have tested the efficacy of ASP Glosair™ to treat *S. chartarum*-infested gypsum board. To our knowledge, this is the only study assessing the effectiveness of AHP on *S. chartarum*. From the findings, one cycle of AHP was ineffective at treating *S. chartarum*-infested gypsum board. Koburger *et al.*(256) has reported reduction of >4 log of *Aspergillus brasiliensis* inoculated on walls and plasters, although complete killing was not achieved after 1 cycle ASP Glosair™. Although the study of AHP on fungi is somewhat limited, fungicidal effects of hydrogen peroxide solution have been documented in various settings such as the food industry and agriculture (259, 262, 293, 294).

Most studies on the efficacy of the AHP systems have investigated other healthcare associated bacteria such as methicillin resistant *Staphylococcus aureus* (MRSA) and *Clostridium difficile*, where significant reductions in airborne microbes and infection cases were documented (193, 289, 290). Rogers *et al.*(295) has reported decreased efficacy of AHP to decontaminate bacterial spores on porous material compared to nonporous surfaces. However, Lemmen *et al.*(296) suggested that AHP was effective in reducing bacterial spores in both porous and non-porous surfaces.

Several factors might have contributed to the ineffectiveness of AHP in treating *S. chartarum*-infested gypsum board. The visible mould on the material indicated a high fungal load and is a worst case scenario. However, such a high fungal biomass is unlikely to occur on a pre-cleaned surface in real environments. Also, in our study the fungus had been left to grow on the board for several weeks and had penetrated into the paper surface and, in addition, porous materials are difficult to clean. These suggest the importance of pre-cleaning prior to disinfection to reduce the initial inoculum. However, there is currently no evidence for the efficacy of AHP at standard concentrations for the remediation of *Stachybotrys* infestation.

7.4.2.3 Peracetic acid (PAA)

Peracetic acid was first registered by the EPA as an antimicrobial agent to be used on surfaces such as those in homes, premises, medical facilities and laboratory animal

rooms ^(196, 253, 297). It has also been used to prevent mould growth in food and agricultural products, as a bleaching agent in textiles as well as to prevent biofilm in cooling tower and wastewater treatment ^(270, 298-301).

In this study, we have tested peracetic acid (Peracide™) in situ to treat *S. chartarum*-infested gypsum board. From our findings, a concentration of PAA at 4000 ppm (manufacturer's recommendation) and double concentration at 8000 ppm were ineffective at treating *S. chartarum*-infested gypsum board.

Although there is no publications available on Peracide™, its effectiveness has been tested by the Environmental Research Group at University College Hospital on hospital-associated pathogens as described by the manufacturer ⁽²⁶⁸⁾. It has been reported to kill *C. difficile* on surfaces in 15 seconds, and also killed MRSA, *Klebsiella pneumonia* and *Pseudomonas aeruginosa in vitro* ⁽²⁶⁷⁾.

Thus far, no evidence is available on the effects of Peracide™ on moulds. Different microorganisms are likely to yield different responses depending on their susceptibility towards biocides. In general, moulds are more resistant to harsh environments than yeast and vegetative bacteria. However, fungal spores may be less resistant than bacterial spores to disinfectants ⁽³⁰²⁾. In a study of peroxygen biocide (27% hydrogen peroxide and 4.5% peracetic acid), Eissa *et al.* ⁽³⁰³⁾ has reported that double the time is required to eliminate bacterial spores (*B. subtilis*) compared to fungal spores (*A. brasiliensis*) from vinyl surface materials. This could serve as evidence that PAA could be effective against fungi at concentrations and exposure times effective against bacterial spores.

The SEM images also showed some white coatings on fungus and material which might come from the chemical composition. As stated by the manufacturer, this preparation contains sodium percarbonate which derived from sodium carbonate (also known as soda ash and soda crystal) and hydrogen peroxide, and TAED (white solid) which is an activator for active oxygen bleaching agent.

This study showed PAA failed to treat *S. chartarum*-infested gypsum at both recommended and twice the recommended concentrations. Apart from the porous surface of gypsum which appears to make fungal infestation harder to treat together with the high fungal load on the surface in our model, lack of effect could be due to the short shelf life of PAA. PAA becomes less stable when diluted and defective PAA has been shown to be associated with an increase in the incidence of hospital infection ⁽³⁰⁴⁾.

7.4.2.4 Organosilane (OS)

An antimicrobial coating is another strategy to inhibit or prevent microbial growth on a material. Failure to attach to a surface should prevent the ability of fungi to colonise and grow. In this study, we have utilised an organosilane coating (Biosafe®) to prevent the growth of *S. chartarum* on gypsum board.

Organosilane (Biosafe®) has been claimed to work on a broad range of materials, both porous and non-porous and on hard or soft surfaces with long term effectiveness. Most organosilane products are claimed to be effective on various surfaces, mainly metals, glass, plastics, rubber, painted surfaces or wood^(305, 306). Gottenbos *et al.*⁽¹⁸⁷⁾ reported a significant reduction of bacterial adherent to silicone rubber, showing reduction of *Staphylococci* from 90% to 0%, and of Gram-negative bacteria from 90% to 25%. In another study, Oosterhof *et al.*⁽¹⁸⁸⁾ reported significant reductions of yeast (12% to 16%) and bacteria (27% to 36%) on coated silicone rubber prostheses.

From the current study, a uneven distribution of fungal growth on the surface at 2500 ppm and 5000 ppm was observed. More fungal growth was observed in some porous areas and a lack of fungal growth was seen on readily exposed surfaces. Higher magnification SEM images showed that fungal growth was in fact growing outwards from within porous areas or between the paper fibres. Our study was in line with Boyce *et al.*⁽¹⁹⁰⁾, who has evaluated 2 organosilane products on high touch surfaces in patient rooms and found no significant reduction in bacterial count. Although most of the surfaces tested were considered non-porous, the authors pointed out the failure might be due to the use of a porous microfibre carrier reducing the efficacy of delivery.

Due to its porous characteristics, the gypsum board might have been coated more evenly with organosilane if it had been covered with a smooth and impermeable substance such as with paint. However, the efficacy of paints to prevent fungal growth depends on the types of paint or surface covering used. Menetrez *et al.*⁽²⁸⁰⁾ have tested 7 different antimicrobial paints and 2 commonly used paints on gypsum board and demonstrated fungal growth in more than half of the samples. In addition to gypsum board, Vacher *et al.*⁽³⁰⁷⁾ has revealed that non-biodegradable material could also become a substrate once covered with acrylic and glycerol-based paints.

The findings suggest that organosilane was partially effective in preventing the growth of *S. chartarum*. However, it appeared that the porous area was not properly coated, even though the materials had been soaked in OS. This also emphasised the

importance of flat non-porous surface materials for the organosilane to be fully efficient and the choice of treatment to be applied prior to the coating.

7.5 CONCLUSIONS

We conclude that porous, cellulose-containing, damp material, as the substrate for fungal growth, significantly influences the efficacy of antimicrobial agents. From our findings, sodium hypochlorite was the best method to eradicate *S. chartarum*-infested gypsum board after several treatments. Although it was the most effective it was also corrosive to the material and may cause irritation to humans. Organosilane was partially effective in preventing the growth on gypsum board, since less fungal growth were observed and only occurred from within the porous areas that might not have been properly covered with organosilane. AHP and peracetic acid were not effective in this study. AHP was relatively easier to use compared to the others. However, it still needed evacuation until short-term exposure limit (STEL) was allowable, taking about 2 hours before it degraded into non harmful products. On the other hand, peracetic acid *in situ* at high concentration bleached the mould, but did not affect its viability. Although both products are claimed to act on soiled surfaces, they have been normally used in combination with pre-cleaned surfaces and we would not consider them suitable for remediating “mouldy” building materials.

CHAPTER 8

PROTEOMIC PROFILES OF *STACHYBOTRYS* *CHARTARUM* IN RESPONSE TO ANTIMICROBIAL AGENTS

This chapter presents the work on the proteomic analysis of *S. chartarum*, NCPF 7587 using gel-free quantitative proteomics consisting of tandem mass spectrometry (TMT) labelling and mass spectrometry techniques. The aim was to provide information on baseline proteins of the fungus and differential protein expression following exposure to antimicrobial agents.

8.1 INTRODUCTION

In the previous chapters, the effects of several antimicrobial agents have been investigated by determining the minimum inhibitory concentration on either solid media or in liquid suspension and their efficacy in controlling fungal growth in a simulated environment. However, these data do not provide any evidence of what is happening inside the fungal cells and how they are affected by antimicrobial treatment or prevention strategies.

Despite the advancement in proteomics, limited information is available on indoor environmental moulds, particularly black moulds such as *S. chartarum*. Nevertheless, there are several proteomic studies on other human pathogenic fungi, such as *Aspergillus* spp. and *Candida* spp. which have been exposed to antifungal agents, which show evident alteration in stress response, cell wall and transport proteins^(179, 180, 308, 309). Subinhibitory concentrations of antimicrobial agents have shown to affect the stress response and enhance the resistance in some bacteria and fungi^(310, 311).

Therefore, this proteomic study on *S. chartarum* is intended to provide a protein database for this species using gel-free shotgun proteomics in order to reveal the changes in protein abundance following exposure to subinhibitory concentrations of selected antimicrobial agents, namely bleach and organosilane (OS).

8.2 MATERIALS AND METHODS

8.2.1 Preparation of fungal samples

Fungal isolates were grown on Sabouraud agar (SDA) and modified Emmons agar (ESA) and were subjected to antifungal agents. Concentrations of 20000 ppm bleach and 1000 ppm organosilane (OS) were chosen based on subinhibitory concentrations determined from the previous experiments (Chapter 6).

Bleach (4.5% sodium hypochlorite) was freshly prepared by mixing in sterile water to make up a final concentration of 20000 ppm. A plug of agar bearing fungal mycelium was removed from a 7 day old culture plate using a 7 mm cork borer and placed carefully at the centre of the media plates, followed by 500 μ l of 20000 ppm bleach dropped onto the inoculum. In total, 12 plates (for each replicate) containing fungal plugs treated with bleach were left to dry under the laminar hood for 30-45 minutes.

Organosilane (0.5% of 3-(trimethoxysilyl)-propyl-di-methyloctadecylammonium chloride) was mixed into ESA to make up a final concentration of 1000 ppm in 20 mL media in each plate. The total of 12 media plates (for each replicate) containing OS were left under the laminar hood until solidified. Fungal conidia (1×10^6 CFU/mL) were prepared in a suspension containing 1:10 PBS-Tween-20 in sterile water. Then, 100 μ l of the suspension were applied to the centre of the plates. Both sets of plates were incubated for 7 days at 25 °C.

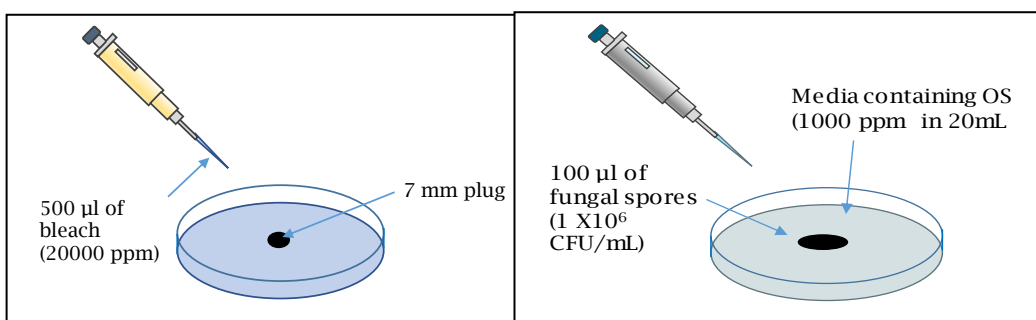


Figure 8-1: Diagram of samples preparation of fungal plugs or suspension with antimicrobial agents' treatment or prevention.

8.2.2 Protein extraction

8.2.2.1 Sample disruption

Two methods of protein extraction from *S. chartarum* were performed as described below, and compared. In the first method, samples were homogenized in buffer containing SDS followed by phenol extraction ⁽³¹²⁾. In the second method, an additional step of trichloroacetic acid (TCA)/acetone precipitation was included prior to homogenization in buffer and phenol extraction as described in the first method ⁽³¹³⁾. Prior to both methods, approximately 400-500 mg biomass was scraped using a sterile scalpel into a microtube. The biomass was then transferred into a clean ceramic mortar and pestle followed by grinding in liquid nitrogen with a circular motion until it turned to a fine powder.

8.2.2.2 TCA/acetone precipitation

Approximately 10 ml of 10% TCA/acetone containing 0.07% dithiothreitol (DDT) was quickly added into the mortar and pestle to maximise the sample recovery. Samples were transferred into several microtubes at this point to facilitate the washing process. Tubes were centrifuged at 14,258 rpm (15,000 x g) for 10 minutes to collect precipitated protein and the supernatant discarded. The obtained pellet was resuspended in 1 to 1.5 ml cold TCA/acetone and centrifuged again for 14,258 rpm (15,000 x g) for 5 minutes and the supernatant was discarded. The pellet was then resuspended in 1.5 ml cold acetone and centrifuged again at 14,258 rpm (15,000 x g) for 5 minutes. The process was repeated until the supernatant became clear. Finally, the pellet was left in a fume cabinet at room temperature until all the acetone had evaporated. Samples were kept at -80 °C until use.

8.2.2.3 Phenol extraction

Next, the tubes containing dried pellet were resuspended in 1.5 ml homogenization buffer containing 50mM Tris-hydrochloric acid (HCl) pH 8.5, 5 mM ethylenediaminetetraacetic acid (EDTA), 100 mM potassium chloride (KCl), 1% polyvinylpyrrolidone (PVPP), 30% sucrose, 2% sodium dodecyl sulfate (SDS) followed by addition of 0.1 M sodium hydroxide (NaOH) in 1:1 ratio (biomass / NaOH) followed by centrifugation at 14,258 rpm (15,000 x g) for 10 minutes. Then, approximately 600 µl supernatant was transferred into new tubes. The samples were added to an equal volume of tris-buffered phenol solution pH 8.0 (Sigma Aldrich), mixed by inversion and centrifuged at 14,258 rpm (15,000 x g) for 5 minutes. The phenolic phase was collected and transferred into new tubes to make up around 300 µl

in each tube. Five volumes of 0.1 M ammonium acetate (w/v) in ice-cold methanol was added followed by incubation at -20 °C overnight. The next day, samples were centrifuged at 14,258 rpm (15,000 x g) for 30 min to obtain precipitated protein pellet. The precipitate was then washed with ice-cold methanol (absolute) followed by ice-cold acetone (80% v/v). The process was repeated twice. At this final washing stage, the samples were pooled into the same tube. The tubes were left to dry at room temperature before adding 100 µL solubilisation buffer of 8 M Urea in 100 mM triethylammonium bicarbonate buffer (TEAB) pH 8.0 to the dried pellet. The samples were kept at -20 °C until use.

8.2.3 Buffer exchange and concentrate

The protein lysates were buffer exchanged using Viva Spin 5kDa spin columns into 0.1 M TEAB to ensure that the final concentration of urea was less than 1 M. An initial concentration of 8 M urea was used, and therefore each sample was added to 450 µL 0.1 M TEAB followed by concentrating the samples to approximately 50 µL by centrifugation at 14,258 rpm (15,000 x g) at 4 °C. Finally, the volume in each tube was determined using a pipette.

8.2.4 Determination of protein concentration using the Bradford assay

Bovine serum albumin (BSA) standard was prepared in 0.1 M TEAB from a 2000 µg/mL stock and diluted into series of standard concentration in order to run a standard curve (Table 8-1). Two microliters of each standard were added in triplicate to 96-well plates. Then, 200 µl of Bradford reagent Coomassie Plus Protein Assay (Cat No 185621, Thermo Scientific) was added into each well and carefully mixed.

To determine the protein concentrations in each sample using the Bradford assay, 2 µL of each sample were diluted 1:5 using 0.1 M TEAB followed by adding 200 µl of Bradford reagent Coomassie Plus Protein Assay.

The absorbance was read at 595 nm.

Table 8-1: BSA standards used in Bradford assay for the quantification of protein concentration.

Vial	Volume of diluent, μl (0.1 M TEAB)	Volume of and source of BSA, μl	Final BSA concentration, $\mu\text{g}/\text{mL}$
A	0	300 of stock	2000
B	125	375 of stock	1500
C	375	325 of stock	1000
D	175	175 of vial B dilution	750
E	325	325 of vial C dilution	500
F	325	325 of vial E dilution	250
G	325	325 of vial F dilution	125
H	400	100 of vial G dilution	25
I	500	0	0 (Blank)

8.2.5 NuPAGE® Bis-Tris Mini Gel electrophoresis

The presence of protein bands was confirmed by gel electrophoresis using NuPAGE® 4 - 12% Bis-Tris Mini Gel electrophoresis (Cat no NP0335, Thermo Fisher Scientific). Fifteen μg of protein were mixed with NuPAGE LDS sample buffer and adjusted to a total volume of 10 μL . The same volume, 10 μL of Novex® Invitrogen pre-stained protein standard was loaded as a protein marker into the first well followed by fungal protein samples, bovine serum albumin (BSA) and 1X sample buffer.

8.2.6 Preparing and labelling peptides for mass spectrometry analysis

8.2.6.1 Protein reduction

Samples were added with tris (2-carboxyethyl) phosphine (TCEP) (Cat No T2556, Thermo Fisher Scientific) to make up a concentration of 1 mM TCEP and incubated for 45 minutes at 37 °C to break up the disulfide bonds (Figure 8-2). The temperature of 37 °C was used instead of 56 °C since the samples contained traces of urea which could lead to protein carbamylation at the N-terminus of lysine, arginine and cysteine at higher temperatures ⁽³¹⁴⁾.

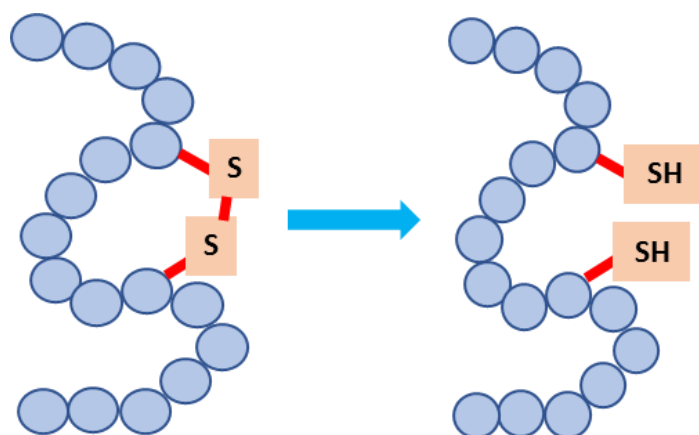


Figure 8-2: Diagram showing the reduction process by TCEP, breaking disulphide bonds to maintain activity and stability and prevent the formation of aggregates.

8.2.6.2 Protein alkylation

The samples were spun down to ensure all liquid was at the bottom of the tube and to cool down the solution. Next, the samples were alkylated by adding iodoacetamide (IAM) (Cat No 90034, Thermo Fisher Scientific) from a 150 mM stock solution to make up a final concentration of 7.5 mM, followed by incubation in the dark for 45 minutes. IAM binds covalently to the thiol group of cysteines to prevent the protein from re-forming disulphide bonds ⁽³¹⁵⁾ (Figure 8-3).

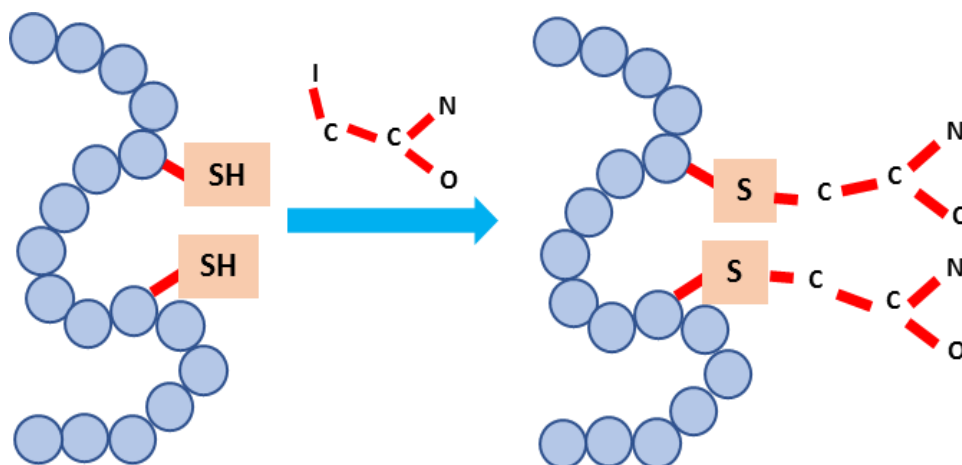


Figure 8-3: Diagram showing the alkylation process by iodoacetamide, adding alkyl groups to cysteine thiol moieties to prevent formation of disulphide bonds.

8.2.6.3 Protein digestion

Sequencing grade modified trypsin (Cat No V511A, Promega) containing 20 µg was resuspended by adding 80 µl of trypsin resuspension buffer (Cat No V542A, Promega) to make up a final concentration of 0.25 µg/ µl trypsin. Trypsin was added into the samples to make up a trypsin-to-protein ratio of 1:100 µg (w/w), followed by overnight incubation at 37 °C. Sample concentrations, previously obtained from the Bradford assay measurements were used to calculate the concentration and volume of trypsin required per sample. The concentration (µg/ µl) for each sample was determined after adding TCEP, IAM, and trypsin. Samples were made up to contain 45 µg of protein digest and added to 0.1 M TEAB to make up a final volume of 100 µl for TMT labelling.

8.2.6.4 Peptide labelling

The TMTsixplex Isobaric label reagent (Cat No 90064, Thermo Fisher Scientific) (Table 8-2) used to label each sample was equilibrated to room temperature before adding 41 µl anhydrous acetonitrile (Cat No 51101, Fisher Scientific) into each of the 0.8 mg TMTsixplex Isobaric label reagent vial. Reagent was carefully mixed by pipetting and spun down briefly to collect all the solution. Then, approximately 100 µl of the digested samples were transferred into each of the TMT reagent vials and labelled accordingly (Figure 8-2), followed by incubation for 1 hour at room temperature. Eight microlitres of 5% hydroxylamine (Cat No 26103, Thermo Fisher Scientific) was added to quench the TMT reaction. All samples were pooled in new microtubes and an equal volume of 4% phosphoric acid was added (to make a final concentration of 2% phosphoric acid) before being subjected to a C18 desalting column.

Table 8-2: TMT reagents of different isobaric mass tags used to label each sample in replicates

Samples	TMTSixplex™ Isobaric Label
Control 1	TMT ⁶ -126
Control 2	TMT ⁶ -127
Bleach 1	TMT ⁶ -128
Bleach 2	TMT ⁶ -129
OS 1	TMT ⁶ -130
OS 2	TMT ⁶ -131

8.2.7 Sample clean-up

Samples were desalted using Oasis HLB 1CC cartridges (Waters) according to the manufacturer's instructions. The cartridge was prepared by adding 1 ml 100% methanol, and 1 ml 2% phosphoric acid. After the column clean-up, the sample was added and the flow through was collected in a new tube. Then, 1 ml 5% methanol was added into the column to wash out contaminants. Finally, 1 ml of 100% methanol was added and the eluate was saved in a new microtube and dried under vacuum.

8.2.8 Sample fractionation

The dried samples were reconstituted in HPLC grade water with 20 mM ammonium formate. It was then fractionated into 30 fractions using high-pH reversed phase separation by collecting aliquots from 1-37 minutes at 1.2 minute intervals at a flow rate of 200 μ l / minute over a gradient of 3.0% to 100% acetonitrile (Cat No 1648, Fisher Scientific), 97% of 20 mM ammonium formate and 100% water pH 8.4 (Cat No 34877, Sigma Aldrich). This was performed on an Agilent 1100 series HPLC with Poroshell, 5 μ m, 300 Extended C18 columns, 2.1 X 75 mm (Agilent). Thirty fractions were combined in concatenation for every 3 fractions to make up 10 fractions in order to improve the protein coverage ⁽³¹⁶⁾, dried, washed by reconstituting in 100 μ l H₂O and drying again with vacuum-centrifugation overnight.

8.2.9 Sample clean- up with Zip-tip® U-18

Fractionated samples were subjected to further clean-up using Zip-tip® U-1, tip size P 10 (Cat no ZTC18M096, Milipore). Firstly, Zip-tip was washed 3 times with 10 μ l of 100% acetonitrile and 3 times with 10 μ l of 0.1% formic acid. This was followed by loading the tip with samples by mixing up and down 10 times. The tip was then washed 6 times with 0.1% formic acid. Next, samples were eluted into tubes pre-filled with 20 μ l 60% acetonitrile / 0.1 % formic acid. This process was performed 6 times by pipetting up and down. Samples were dried under vacuum and resuspended in 20 μ l 0.1% formic acid.

8.2.10 Mass spectrometry and data acquisition

Dried fractionated samples were resuspended in 25 μ l of LCMS water with 0.1 % formic acid (v/v) (Cat No LS118, Thermo Fisher Scientific) followed by vigorous mixing for 10 minutes (PHMT thermoshaker, Grant-Bio) and spun down for 10 minutes at 13,000 rpm (16,060 x g) (Biofuge® Pico® Heraeus). Samples were transferred into 0.2 ml microtubes for mass spectrometry. The MS/MS spectra were processed using

Thermo Proteome Discoverer™ software version 1.4.1.12 (Cat no IQLAAEGABSFAKJMAUH, Thermo Fisher Scientific) by searching against *S. chartarum* using the TrEMBL database.

8.2.10.1 Data analysis and bioinformatic analysis

For the proteins uncharacterised by TrEMBL, homologous protein search was conducted by entering the accession number into the UniProtKB database (<http://www.uniprot.org/blast>) and acquiring all the sequences. The FASTA files containing sequences were then searched for in the NCBI protein database using BLASTp. The homologues were chosen from the most closely related sequences from other fungi whose GO term was available. Protein function for each protein was retrieved from UniProtKB or associated databases such as InterPro and from published literature.

The protein abundance profiles were filtered based on the criteria of having more than 2 peptide matches to differentiate correct identification from random assignment. The parameter of less than 20% variability (CV, ratio of standard deviation to mean), also known as the relative standard deviation, was chosen as an indication of accuracy (precision and repeatability) of the experiment.

Heatmapping was used to summarise protein profile patterns and was coded using RStudio (v 1.0.136 – 2009 - 2016) using hierarchical cluster analysis (HCA). The HCA showed a large set of samples were 'most similar' to each other by calculating a similarity matrix based on distance between samples (Euclidean distance) represented with a colour difference. The proteins that were most similar were grouped in the same limb of a tree and those distinctly different ones were placed in another limb ⁽³¹⁷⁾.

Protein function analysis was performed using the PANTHER classification system PANTHER version 12.0 (released 2017-07-10). The PANTHER (Protein ANalysis THrough Evolutionary Relationships) Classification System classifies proteins (and their genes) to facilitate high-throughput analysis ⁽³¹⁸⁾ (Figure 8-4). Input files were translated into PANTHER scores in PANTHER Generic Mapping files for the gene analysis tools. The PANTHER overrepresentation test was performed against the whole genome set of *Saccharomyces cerevisiae* using Bonferroni correction for multiple testing to generate pie charts and other information on pathway, molecular function, biological process, cellular component and protein class. Since the genome of *S. chartarum* and its homologues were not available in the PANTHER database, we had to first score the sequences against the PANTHER Hidden Markov Models (HMM)

library. Scoring was performed by running the script on the UNIX command line and the output file was referred to as the PANTHER Generic Mapping File consisting of sequence ID, PANTHER accession, family or subfamily name, HMM score and alignment range of the protein ⁽³¹⁹⁾. The output files were used for the gene analysis of *S. chartarum*, with and without antimicrobial exposure.

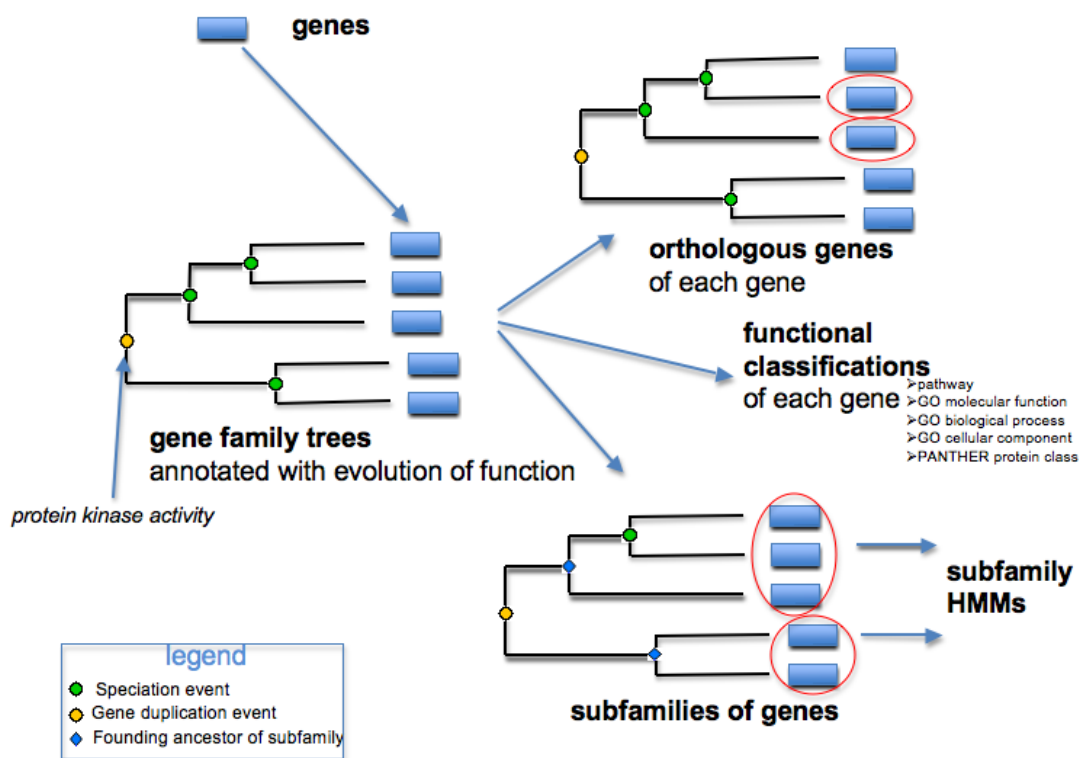


Figure 8-4: The diagram illustrates the relationships between different data types in PANTHER. The PANTHER (Protein ANalysis THrough Evolutionary Relationships) Classification System was designed to classify proteins (and their genes) according to family and subfamily, molecular function of the protein by itself or with directly interacting proteins, biological process and pathway. Orthologous genes are homologous genes gives rise to different species but maintain a similar function to that of the ancestral gene ⁽³¹⁸⁾. Diagram taken from <http://www.pantherdb.org>. Used with permission from ©2018 Paul Thomas.

8.3 RESULTS

8.3.1 Optimization of protein extraction from *S. chartarum*, NCPF 7587

To characterise the protein extract, two methods for protein extraction from *S. chartarum* were performed and compared. The additional steps of TCA/acetone precipitation with 10 minutes' incubation showed the best protein separation as revealed by 1-dimensional gel electrophoresis in comparison to phenol extraction alone or the same treatment with a longer incubation (Figure 8-5).

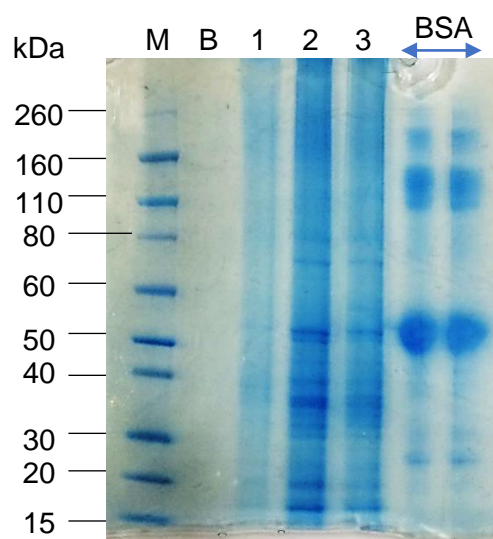


Figure 8-5: Optimisation of protein extraction was performed by comparing phenol extraction alone or in combination with TCA/acetone precipitation in the first step. Fifteen µg protein as determined by the Bradford assay was loaded as follows: M: Marker Novex Sharp pre-stained protein standard, B: 1 time loading buffer, 1: Phenol extraction, 2: TCA/acetone precipitation and phenol extraction (incubation 10 minutes), 3: TCA/acetone precipitation and phenol extraction (incubation 1 hour extraction buffer) and BSA: Bovine serum albumin (control).

8.3.2 Descriptive data and quality control on proteomic analysis of *S. chartarum*, NCPF 7587

Proteomic analysis was performed on *S. chartarum* NCPF 7587 with and without exposure to antimicrobial agents. Initially, a total of 1358 proteins was obtained from the LC MS/MS which was subsequently filtered based on their detection in all samples and number of peptides. From the pie chart shown, 96% of the proteins were identified in all samples, indicating their consistency regardless of their treatment groups (Figure 8-6).

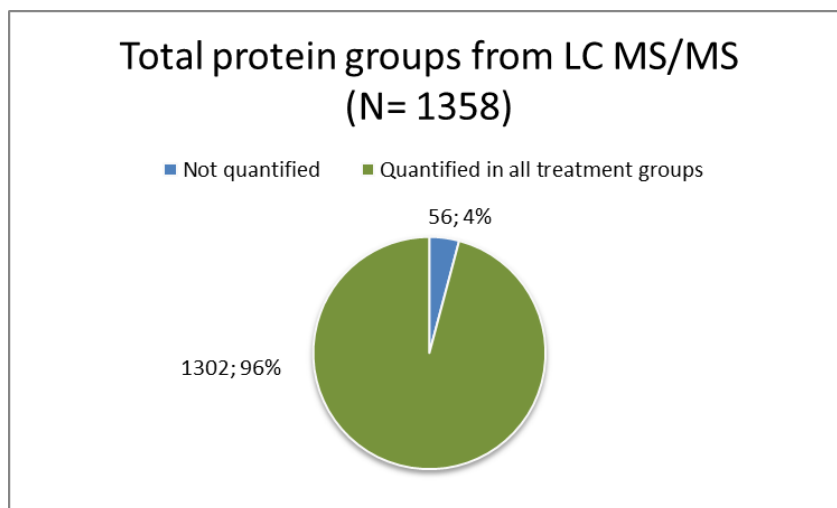


Figure 8-6: Pie chart represents total number and percentage of protein obtained from LC MS/MS and proteins that were quantified in all groups.

Of the 1302 proteins quantified in all samples, 946 proteins (70%) had more than 2 peptides and were therefore included in the following analysis (Figure 8-7). This analysis was also performed using the total of 1358 proteins (including those not quantified in all treatments) which showed 946 proteins with more than 2 peptides (data not shown).

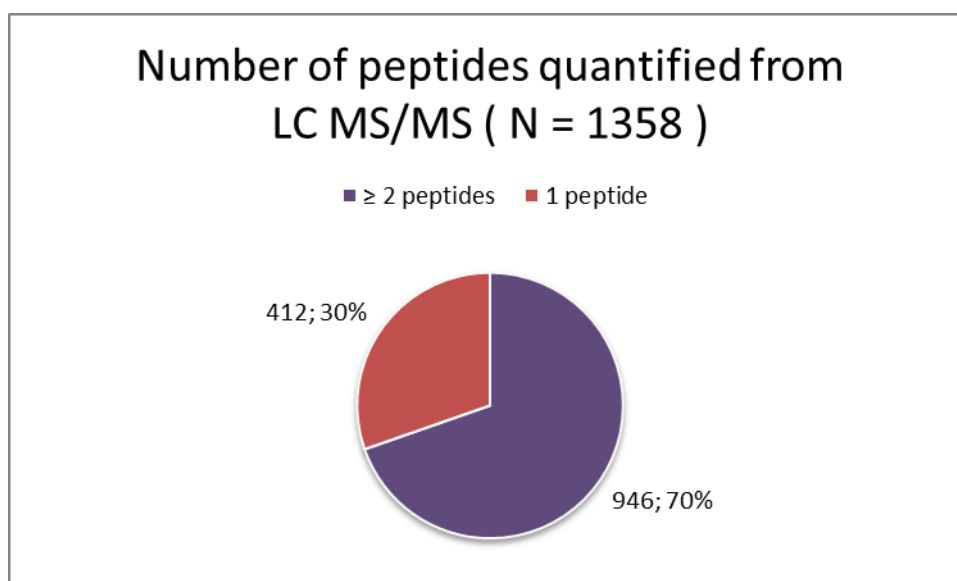


Figure 8-7: Pie chart showing the total number and percentage of proteins obtained from LC MS/MS that were quantified in all groups.

Due to very limited data on *S. chartarum* in the SWISS-PROT database (only 22 entries), proteins were identified from tandem mass spectra by searching the peptides sequences in the TrEMBL database (more than 20 000 entries). Only 199 proteins with more than 2 peptides were identified from TrEMBL database (Figure 8-8).

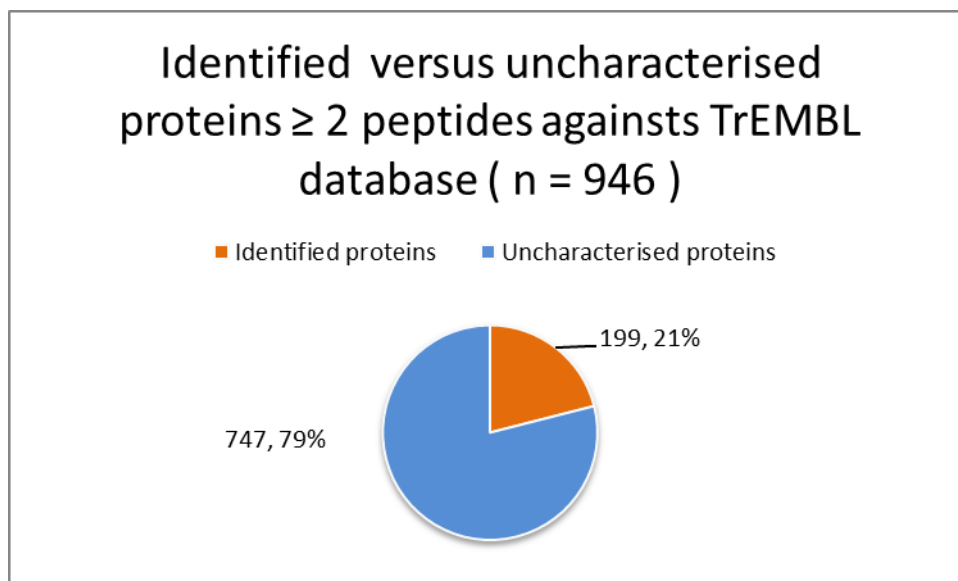


Figure 8-8: Pie chart showing the total number and percentage of identified proteins from the TrEMBL database.

By using the NCBI database, 711 (95%) protein homologues were identified based on the sequence similarities with the highest scores (Figure 8-9). Information on each homologue was compiled and tabulated according to Tesei *et al.*⁽³¹²⁾ (data not shown). The filtering process is summarised in Table 8-3.

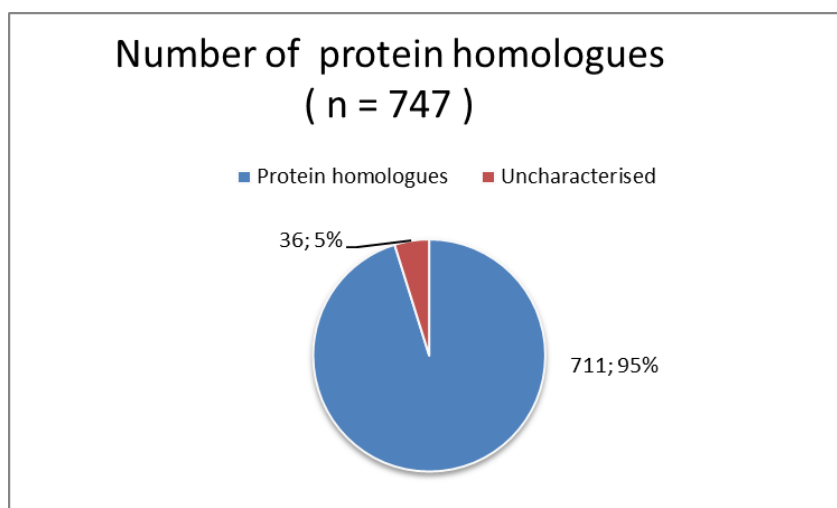


Figure 8-9: Pie chart represents the total number and percentage of homologous proteins obtained from NCBI database.

Table 8-3: Summary of filtering process and number of proteins in each step.

Process	Description	No of proteins (%)
1	Proteins identified from all samples	1358 (100%)
2	Quantified proteins	1302 (96%)
	More than 2 peptides	946 (72%)
3	More than 2 peptides:	946 (100%)
	a. Identified from Uniprot / trEMBL	199 (21%)
	b. Uncharacterised proteins	747 (79%)
4	Proteins with homologues by blastp	711 (95%)

Mean values of both replicates in each treatment were calculated from the protein quantified in all samples with ≥ 2 peptides. Firstly, the data was screened manually for any significant differences of 2-fold or 0.5-fold increase within each group. Then, the mean average and median of each group were determined where mean or median of 1 refers to no significant differences between the replicates and therefore indicates that the results are reliable for further analysis (Table 8-4).

Table 8-4: The differential protein expression of replicates used in each condition measured as mean average and median ratio.

Total protein (N= 943)	Control 1: Control 2	Bleach 1: Bleach 2	OS 1: OS 2
Median	0.998	0.998	0.999
Mean average	1.007	1.010	1.030

8.3.3 PANTHER classification of protein profiles of untreated *S. chartarum*, NCPF 7587

All the proteins with more than 2 peptides and less than 20% variability were subjected to PANTHER analysis. All the sequences were scored with the PANTHER HMM library to obtain sets of Generic Mapping Files. All of the analysis was performed using the PANTHER overrepresentation test. The proteins were searched against the reference list, *Saccharomyces cerevisiae* (all genes in database) in each annotated data set.

From the results, proteins have been classified according to protein classes, molecular functions, biological processes and cellular components using Bonferroni correction for multiple testing. Proteins that were unclassified were not displayed in the pie-charts. The description for each subclass is shown in the appendix (Appendix 8-A, Appendix 8-B, Appendix 8-C and Appendix 8-D). Most of the proteins possessed multiple functions and were therefore categorized in more than one subclass.

8.3.3.1 Protein classes in untreated *S. chartarum*, NCPF 7587

Proteins were classified into 21 classes based on their family (groups that are evolutionarily related) and subfamily (proteins that also have the same function) (Figure 8-10). The protein classes and their functions are summarised in Appendix 8-A.

Most proteins were classified as oxidoreductases which accounted for 16.5% of the total classified proteins in *S. chartarum*, followed by hydrolases (11.1%) and RNA binding proteins (10.8%). Examples of proteins listed under the oxidoreductase class were NADH dehydrogenase [ubiquinone] 1 alpha subcomplex subunit 2 (PTHR12878:SF0, ref|XP_007811183.1) involved in oxidative phosphorylation and the respiratory electron transport chain; superoxide dismutase [Cu-Zn] (Family ID: PTHR10003:SF60, Mapped ID: gb|KPA42379.1) which plays a role in cellular process response to stress; and the peptide methionine sulfoxide reductase (PTHR42799:SF2, ref|XP_018233748.1) which is responsible for cellular protein modification processes and response to stress.

The second largest protein class, the hydrolases, includes the 26S protease regulatory subunit 8 (PTHR23073:SF12, ref|XP_018177538.1) involved in biosynthetic processes, catabolic processes, cellular component organization, cellular processes, nitrogen compound metabolic processes, protein complex assembly, proteolysis, regulation of transcription from the RNA polymerase II promoter and transcription initiation from RNA polymerase II promoter; arginase-2, mitochondrial (PTHR43782:SF3,

tr|A0A084B8F7|A0A084B8F7_STACH) which is involved in cellular amino acid catabolic processes; and the ATPase, H⁺ transporting, V1 subunit G isoform 1 (PTHR12713:SF11, tr|A0A084RP10|A0A084RP10_STACH) which is involved in the nucleobase-containing compound metabolic processes.

The third biggest protein class were the RNA binding proteins which include the 60S ribosomal L22-related protein (PTHR10064:SF0, gb|KND91741.1) which is a structural constituent of ribosome; elongation factor Tu, mitochondrial (PTHR43721:SF12, tr|A0A084RQS9|A0A084RQS9) that plays a role in GTPase activity, pyro phosphatase activity and translation elongation factor activity; and the eukaryotic translation initiation factor 3 subunit I (PTHR19877:SF1, tr|A0A084AXG1|A0A084AXG1_STACH) which possesses translation initiation factor activity.

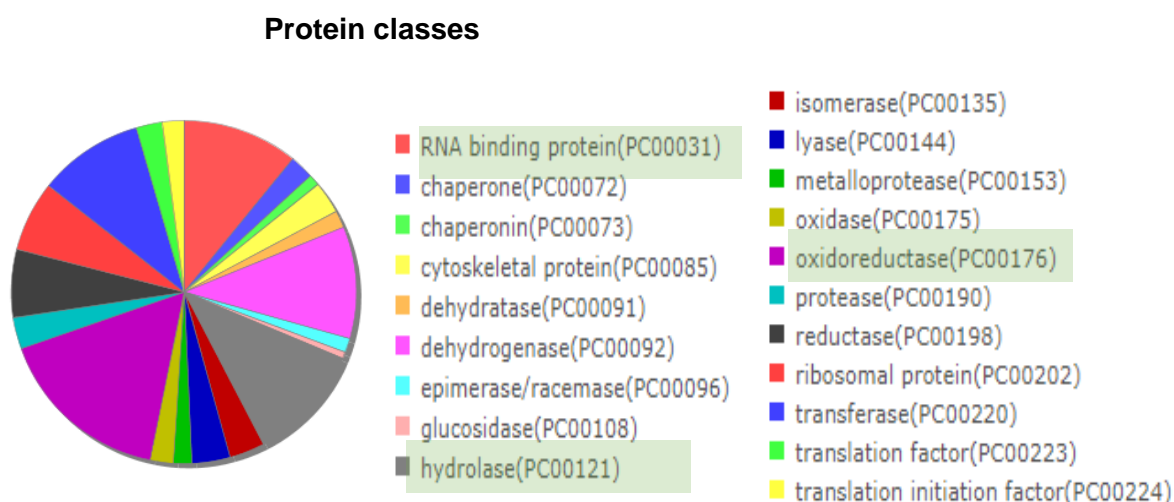


Figure 8-10: PANTHER classification of proteins identified in *S. chartarum*, NCPF 7587 with no contact with antimicrobial agents. Pie chart representing the distribution of identified proteins based on protein class.

8.3.3.2 Molecular functions in untreated *S. chartarum*, NCPF 7587

Proteins were classified into 14 molecular function groups based on the function of the protein by itself or directly interacting proteins at the biochemical level; (eg. protein kinase) (Figure 8-14). The molecular functional classes and their functions are summarised in Appendix 8-B.

The major molecular functions in *S. chartarum* were catalytic activity (44.9%) such as that involving malate and lactate dehydrogenase (Family ID: PTHR11540, Mapped ID: tr|A0A084RHP6|A0A084RHP6_STACH) which are involved in carbohydrate metabolic processes, generation of precursor metabolites and the energy and tricarboxylic acid cycle; saccharopine dehydrogenase [NADP (+), L-glutamate-forming] (Family ID: PTHR11133:SF14 , Mapped ID: ref|XP_007795925.1|) which plays a role in cellular amino acid and catabolic processes; and the 26S proteasome non-ATPase regulatory subunit 2 (Family ID: PTHR10943:SF1, Mapped ID: gb|KHN94209.1|) involved in catabolic processes, cellular processes and proteolysis.

These were followed by proteins with oxidoreductase activity (15.3%) for example, quinone oxidoreductase-related (Family ID: PTHR42975:SF1, Mapped ID: gb|KKP00636.1|) involved in carbohydrate metabolic processes, amino methyltransferase, mitochondrial (Family ID: PTHR43757:SF2, Mapped ID: tr|A0A084RF40|A0A084RF40_STACH) and NAD-specific glutamate dehydrogenase (Family ID: PTHR11606:SF9, Mapped ID: tr|A0A084AJX1|A0A084AJX1_STACH).

The third largest molecular function was structural molecule activity (9.2%), such as actin-related protein 3-related structural constituent of the cytoskeleton (Family ID: PTHR11937:SF175, Mapped ID: ref|XP_018149384.1|), 60S ribosomal protein L18a structural constituent of ribosome (Family ID: PTHR10052:SF1, Mapped ID: tr|A0A084RD17|A0A084RD17_STACH) and actin-related protein 2/3 complex subunit 5 structural constituent of the cytoskeleton (Family ID: PTHR12644:SF0, Mapped ID: tr|A0A084AM96|A0A084AM96_STACH).

Molecular functions

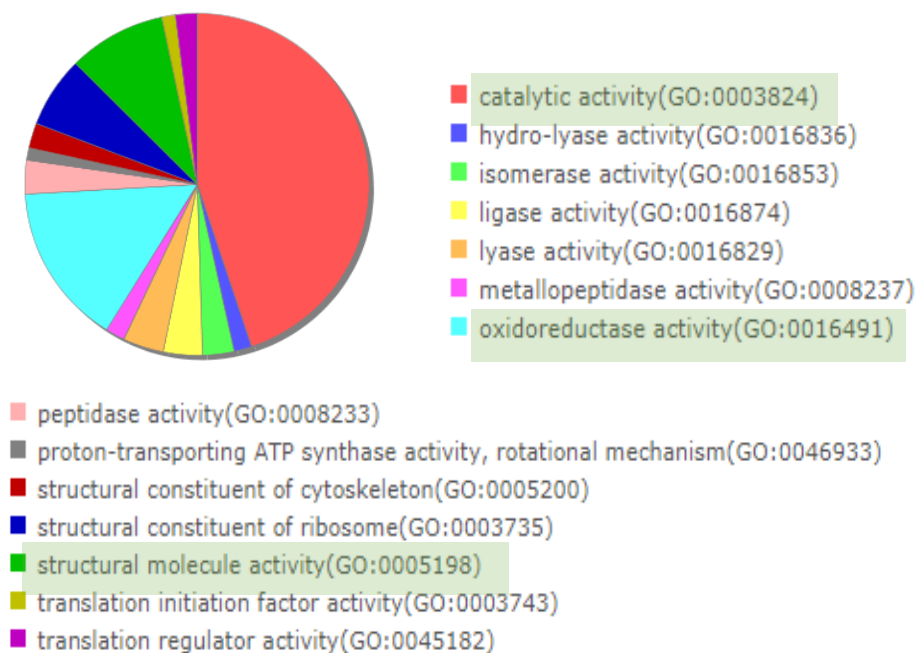


Figure 8-11: PANTHER classification of proteins identified in *S. chartarum*, NCPF 7587 with no contact with antimicrobial agents based on molecular function.

8.3.3.3 Biological processes in untreated *S. chartarum*, NCPF 7587

Proteins were classified into 20 biological process groups according to their functions in the larger network of proteins that interact to accomplish a process at the level of the cell or organism (e.g. mitosis) (Figure 8-15). The biological processes and their functions are summarised in Appendix 8-C.

From the analysis, proteins involved in general metabolic processes accounted for 25.5% of the classified biological process proteins in *S. chartarum*. This was followed by primary metabolic processes (22.4%) and protein metabolic processes (10.0%).

Proteins involved in metabolic / primary metabolic processes included malate and lactate dehydrogenase (Family ID: PTHR11540, Mapped ID: tr|A0A084RHP6|A0A084RHP6_STACH) involved in carbohydrate metabolic processes, generation of precursor metabolites and energy and the tricarboxylic acid cycle; saccharopine dehydrogenase [NADP(+), L-glutamate-forming (Family ID: PTHR11133:SF14, Mapped ID: ref|XP_007795925.1|) involved in cellular amino acid catabolic processes; and threonine synthase-like 2 (Family ID: PTHR42690:SF1,

Mapped ID: gb|EQL02956.1|) which plays a role in biosynthetic processes, cellular amino acid metabolic processes, cellular processes, and nitrogen compound metabolic processes.

Examples of proteins involved in protein metabolic processes are metallopeptidases (Family ID: PTHR12147:SF21, Mapped ID: tr|A0A084B9S7|A0A084B9S7_STACH) involved in proteolysis; heat shock protein HSP 90-alpha-related (Family ID: PTHR11528:SF50, Mapped ID: gb|EXM33465.1|) involved in immune system processes and protein folding response to stress; and 26S proteasome non-ATPase regulatory subunit 2 (Family ID: PTHR10943:SF1, Mapped ID: gb|KHN94209.1|) involved in catabolic processes, cellular processes and proteolysis.

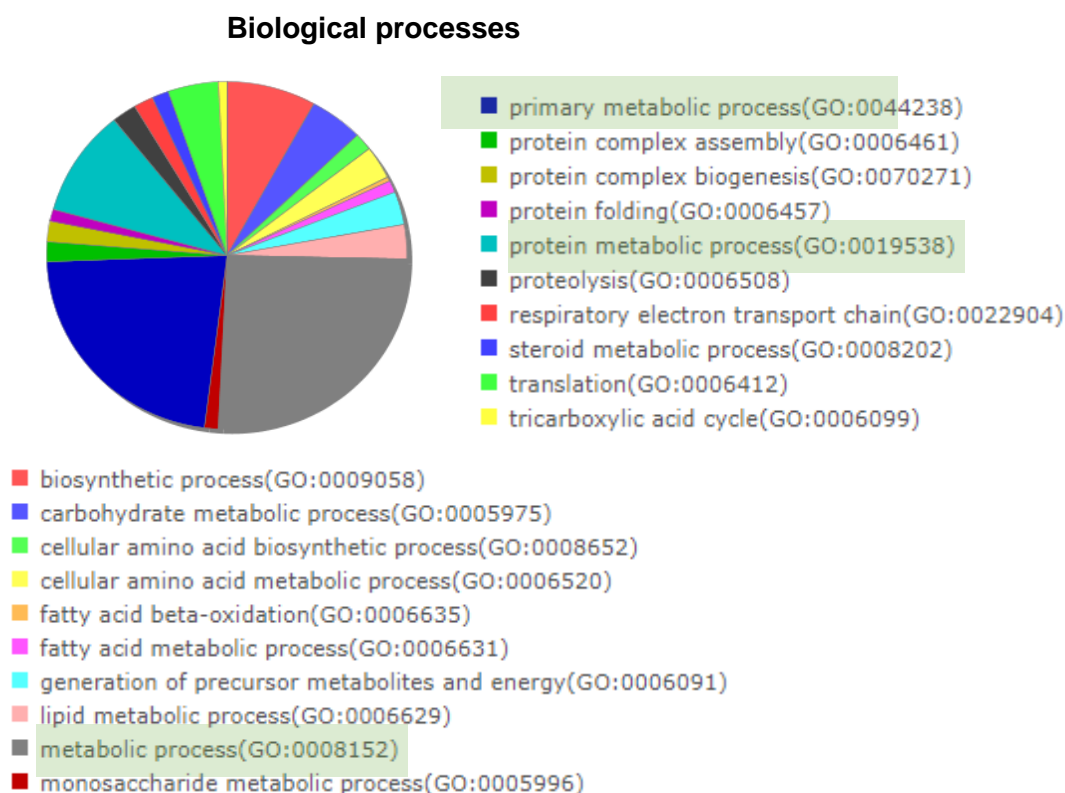


Figure 8-12: PANTHER classification of proteins identified in *S. chartarum*, NCPF 7587 with no contact with antimicrobial agents based on biological processes.

8.3.3.4 Cellular components in *S. chartarum*, NCPF 7587

Proteins were classified into 12 cellular components (Figure 8-16). The cellular components and their functions are summarised in Appendix 8-D.

Proteins in the intracellular compartment accounted for 36.3% of the classified cellular components in *S. chartarum*. This was followed by cytoplasm (28.7 %) and cytosol (13.3%). Examples include actin-related protein 3-related (Family ID: PTHR11937:SF175, Mapped ID: ref|XP_018149384.1| gb|KPA42379.1|) present in the actin cytoskeleton and intracellularly; NADH-cytochrome b5 reductase 2 (Family ID: PTHR19370:SF174, Mapped ID: tr|A0A084AMH8|A0A084AMH8_STACH) present in cytoplasm; and mitochondrion 60S and ribosomal protein L18a (Family ID: PTHR10052:SF1, Mapped ID: tr|A0A084RD17|A0A084RD17_STACH) which is present in cytosol, organelles and ribosomes.

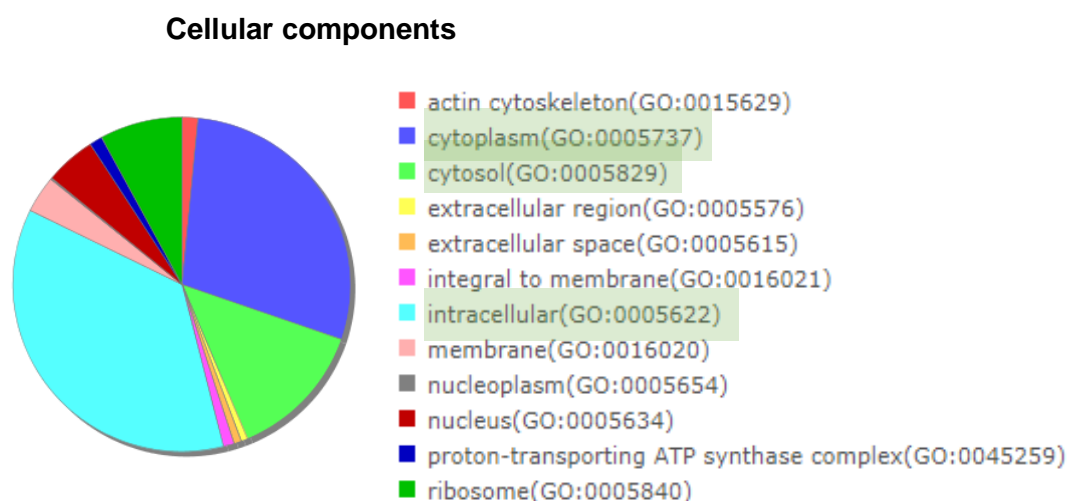


Figure 8-13: PANTHER classification of proteins identified in *S. chartarum*, NCPF 7587 with no contact with antimicrobial agents based on cellular components.

8.3.3.5 PANTHER pathway in *S. chartarum*, NCPF 7587

Four main pathways were identified from the most commonly found proteins in *S. chartarum*, NCPF 7587; valine biosynthesis (Figure 8-14), isoleucine biosynthesis (Figure 8-15), the ubiquitin proteasome pathway (Figure 8-16) and the pathway associated with the pathogenesis of Parkinson's disease (not shown). In *Saccharomyces cerevisiae*, leucine, isoleucine and valine biosynthetic pathways are known as the subpathways for amino acid biosynthesis. The ubiquitin/proteasome-mediated proteolytic pathway is known to play a crucial role in the response of fungi to various stresses.

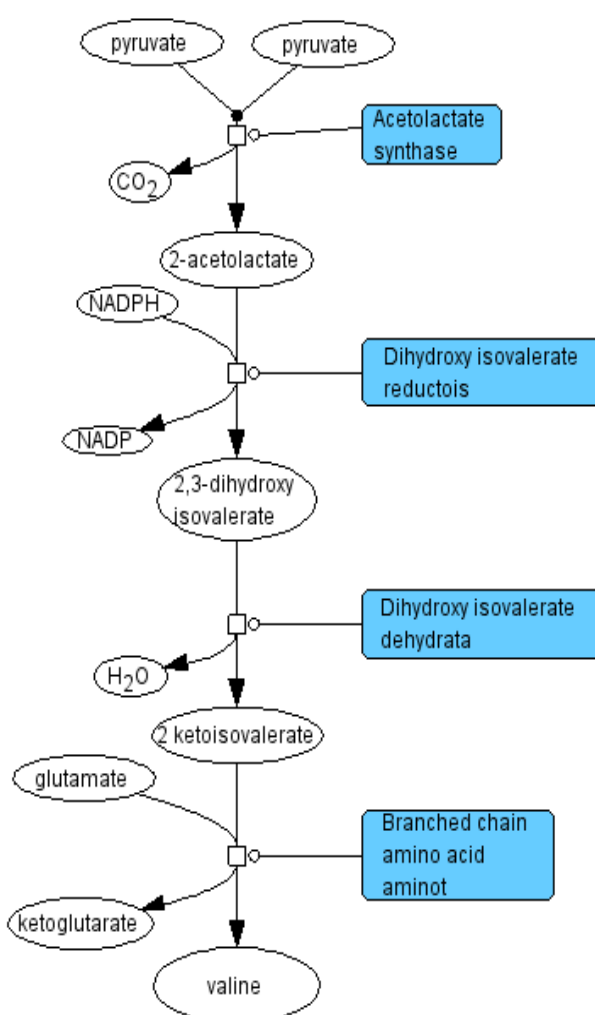


Figure 8-14: The diagram illustrates biosynthesis of the amino acid valine which is critical to protein biosynthesis identified by PANTHER ⁽³²⁰⁾ in *S. chartarum*. Diagram adapted from PANTHER Classification system (www.pantherdb.org). Used with permission from ©2018 Paul Thomas.

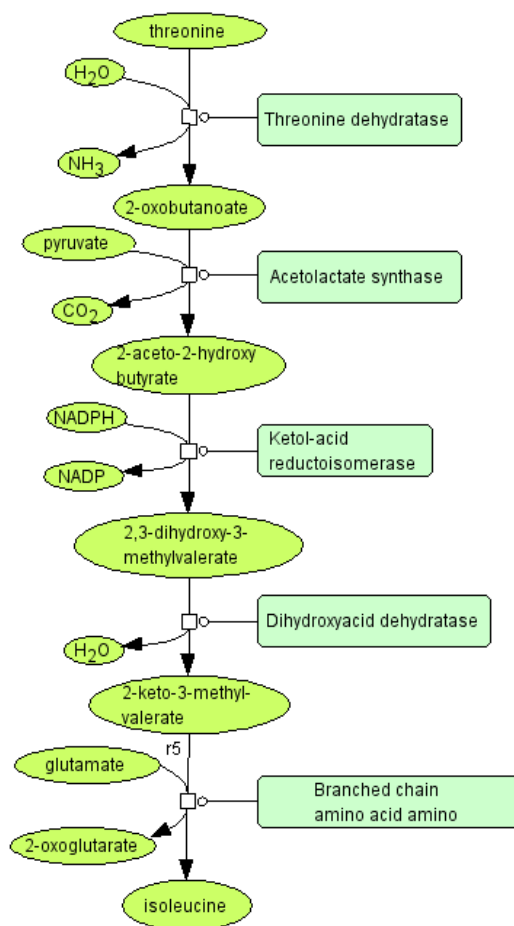


Figure 8-15: The diagram illustrates biosynthesis of the amino acid isoleucine, critical to protein synthesis identified by PANTHER ⁽³²⁰⁾ in *S. chartarum* Diagram adapted from PANTHER Classification system (www.pantherdb.org). Used with permission from ©2018 Paul Thomas.

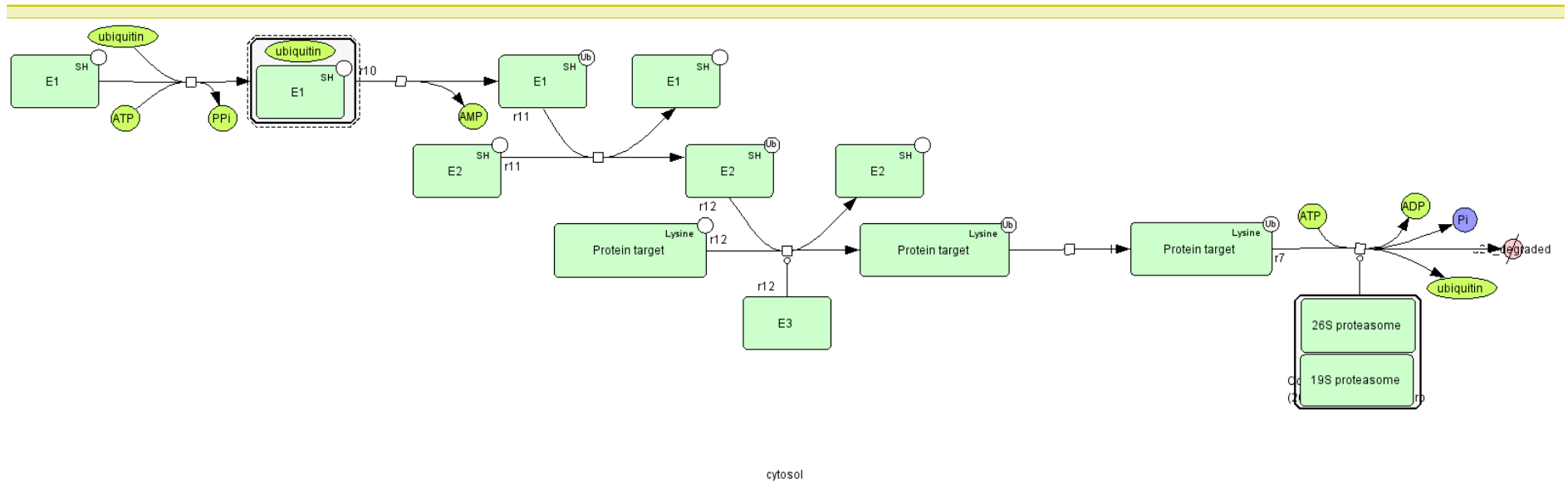


Figure 8-16: The diagram shows the ubiquitin proteasome pathway which can lead to targeting for degradation by the proteasome machinery or can entirely be the basis for regulatory control such as activation of receptor endocytosis identified by PANTHER ⁽³²⁰⁾ in *S. chartarum* Diagram adapted from PANTHER Classification system (www.pantherdb.org). Used with permission from ©2018 Paul Thomas.

From the pie chart, 24 pathways were identified in *S. chartarum* with the major pathways consisting of the pathway associated with the pathogenesis of Parkinson disease, the ubiquitin proteasome, cell cycle, valine biosynthesis, isoleucine biosynthesis and apoptosis signalling pathway. The main difference between *S. cerevisiae* and *S. chartarum* was the abundance of proteins in the wnt signalling pathway. The overall pathways in *S. chartarum* against the reference genome, *S. cerevisiae*, are as shown in Figure 8-17.

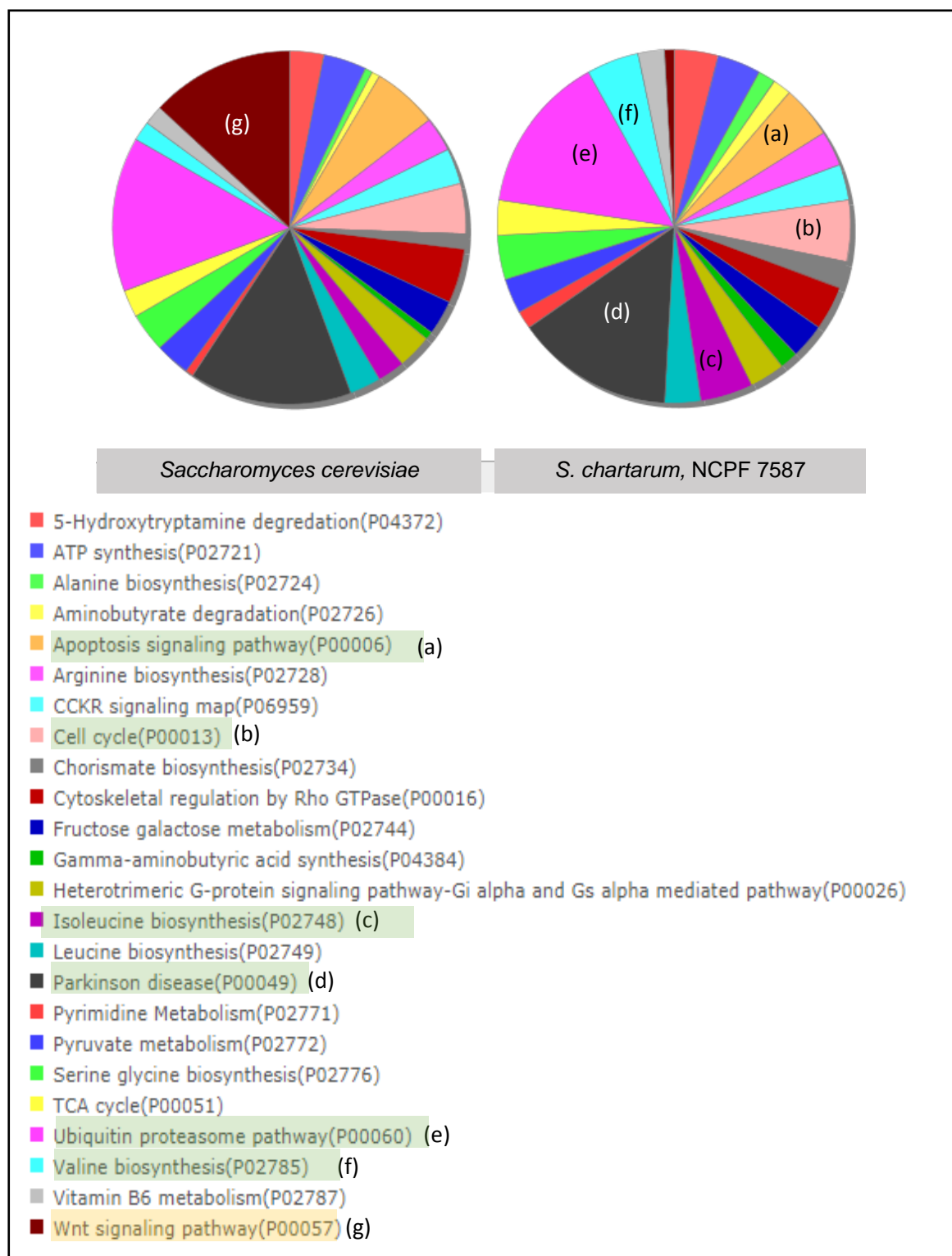


Figure 8-17: PANTHER classification of proteins identified in *S. chartarum*, NCPF 7587 with no contact with antimicrobial agents. Pie chart representing the identified pathways in *S. chartarum* based on reference fungi, *S. cerevisiae* with main pathways consisting of (a) apoptosis signalling pathway, (b) cell cycle, (c) isoleucine biosynthesis, (d) a pathway involved in Parkinson disease, (e). ubiquitin proteasome pathway and (f) valine biosynthesis. The proteins involve in (g) wnt signalling pathway is more abundant in *S. cerevisiae*.

8.3.4 Changes in protein abundance in *S. chartarum*, NCPF 7587, exposed to antimicrobial agents

More than a two-fold increase or decrease (0.5-fold increase) in protein abundance was used as the criterion for a significant change between each of the treated group in comparison to the control group. The protein changes with mean ratios of <20% variability were selected to represent good precision between replicates and reliable measurements. More proteins were reduced following treatment with bleach and increased following exposure to OS, although the total numbers of proteins with changes were almost comparable.

Table 8-5: Number of proteins with changes in abundance in *S. chartarum* treated with bleach and organosilane compared to no exposure to antimicrobial agents.

Antimicrobial Agents	Decreased in abundance	Increased in abundance	Total protein with change in abundance
Bleach	36 (56%)	28 (43%)	64 (100%)
Organosilane	16 (23%)	52 (77%)	68 (100%)

8.3.4.1 Changes in protein abundance in *S. chartarum*, NCPF 7587, exposed to bleach

The full listing of decreased protein levels following exposure to bleach in comparison to no treatment are listed in Appendix 8-E (from TrEMBL) and Appendix 8-F (homologues from NCBI). Levels of 36 proteins were decreased following the treatment with bleach. Out of 36 proteins, six were identified using TrEMBL where three proteins were identified from *Stachybotrys chartarum* IBT 7711 and three proteins from *Stachybotrys chartarum* IBT 40288. Of the 30 uncharacterised proteins, 27 homologous proteins had the most similarities with other filamentous fungal genera such as *Aspergillus* spp., *Fusarium* spp., and *Purpureocillium* spp..

Changes in abundance of significant proteins, particularly the proteins involved in stress response, cell wall and growth recovery were observed. Most of the stress response-related proteins were decreased following treatment with bleach which suggests that the proteins might be depleted or consumed following the treatment (Table 8-6). Other decreased proteins were associated with responses to xenobiotics and adaptive responses such as endoplasmic reticulum transmembrane protein and sphingolipid long chain base-responsive protein Isp1. In addition, cell wall and membrane-associated proteins such as glucanase, the enzyme involved in forming the

main constituent of fungal cell wall ⁽³²¹⁾; and glycerophosphoryl diester phosphodiesterase, involved in glycerophospholipid metabolism as the main component of the cell membrane ⁽³²²⁾, were also decreased.

Table 8-6: Examples of proteins which decreased in abundance in *S. chartarum* treated with bleach and their functions.

Examples of proteins	Functions
Hydroperoxide resistance protein	Detoxification of organic compounds containing the peroxide functional group
Aminoglycoside phosphotransferase	Detoxification of aminoglycosides, plays a role in resistance
S-(hydroxymethyl) glutathione dehydrogenase/alcohol dehydrogenase	As a catalyst for the reaction to form glutathione
Xylitol dehydrogenase	Pentose phosphate pathway for protecting yeast from oxidative stress

In contrast, 28 proteins in *S. chartarum* were increased following exposure to bleach as shown in Appendix 8-G (from TrEMBL) and Appendix 8-H (homologues searched in NCBI). Out of 28 proteins, four proteins were identified using TrEMBL where 2 proteins were identified from *Stachybotrys chartarum* IBT 7711 and 2 proteins from *Stachybotrys chartarum* IBT 40288. Of the 24 uncharacterised proteins, 23 homologous proteins had the most similarities with other filamentous fungal genera such as *Trichoderma* spp., *Fusarium* spp., *Purpureocillium* spp. and *Acremonium* spp.. From the results, it appeared that most of the ribosomal proteins were increased which suggests a focus on fungal growth and recovery following 7 days of the treatment (Table 8-7).

Table 8-7: Examples of proteins which increased in abundance in *S. chartarum* treated with bleach and their functions.

Examples of proteins	Functions
Polyadenylate-binding protein	Multiple roles in the poly(A) tail in mRNA biogenesis, stability and translation
Eukaryotic translation initiation factor 3	Initiates translation of a subset of mRNAs involved in cell proliferation
60S ribosomal protein	Structural constituent of ribosome
Phosphoglycerate mutase family protein	Enzyme involved in glycolysis to form the high-energy molecules ATP and NADH

8.3.4.2 Changes in protein abundance in *S. chartarum*, NCPF 7587, exposed to organosilane

The full list of decreased protein levels following exposure to organosilane in comparison to no treatment are listed in Appendix 8-I (from TrEMBL) and Appendix 8-J (homologues searched in NCBI). Levels of 16 proteins were decreased, with three characterised proteins from *Stachybotrys chartarum* IBT 402883. All the uncharacterised proteins had homologues with other filamentous fungi such as *Acremonium* spp., *Aspergillus* spp., *Purpureocillium* spp. and *Fusarium* spp.. We found that both stress and transport proteins were reduced following treatment with OS. This implies that the proteins might be depleted/consumed or their synthesis down-regulated (Table 8-8).

Table 8-8: Examples of proteins which decreased in abundance in *S. chartarum* treated with organosilane and their functions.

Examples of proteins	Functions
Superoxide dismutase	Antioxidant defence in cells exposed to oxygen
Heat shock protein 30	Produced by cells in response to exposure to stressful conditions
Protein transport protein SEC61 alpha subunit	Intracellular transport
V-type proton ATPase subunit F	Endocytosis and intracellular transport

On the other hand, levels of 52 proteins were increased following exposure to OS as shown in Appendix 8-K (from TrEMBL) and Appendix 8-L (homologues searched in NCBI). Out of the 52 proteins, 12 proteins were characterised from TrEMBL with 8 proteins identified from *Stachybotrys chartarum* IBT 40288 and 4 proteins from *Stachybotrys chartarum* IBT 7711. Of the 40 uncharacterised proteins, 38 homologues had the most similarity with other filamentous fungi such as *Penicillium* spp., *Acremonium* spp., *Fusarium* spp., *Purpureocillium* spp., and *Aspergillus* spp.. From the results, we found that both stress and ribosomal proteins were increased following exposure to OS after 7 days (Table 8-9).

Table 8-9: Examples of proteins which increased in abundance in *S. chartarum* treated with organosilane and their functions.

Examples of proteins	Functions
Eukaryotic translation initiation factor 3	Involved in the initiation phase of eukaryotic translation
40S ribosomal protein	Protein translation
60S ribosomal protein	Protein translation
Superoxide dismutase	Antioxidant defence in cells exposed to oxygen
Hsp90 binding co-chaperone	Chaperone protein that assists other proteins to fold properly, stabilizes proteins against heat stress, and aids in protein degradation

8.3.5 Heatmap of the changes in protein abundance patterns

A heat map is a graphical representation of data where the individual values contained in a similarity matrix are calculated in terms of Euclidean distance and hierarchically clustered ⁽³¹⁷⁾. In molecular biology, heat maps are often used to represent the level of expression of genes/proteins across a number of comparable samples ⁽³²³⁾. A heatmap was used to group the protein response in abundance change following treatment with bleach or OS that are 'most similar' to one another. From the diagram, there were more increased protein levels as indicated in 'red blocks' as well as total protein change in response to OS. On the other hand, more decreased protein levels were observed in response to bleach as indicated in 'green blocks'. The proteins with no significant differences in comparison to control group were seen in 'black blocks' (Figure 8-18).

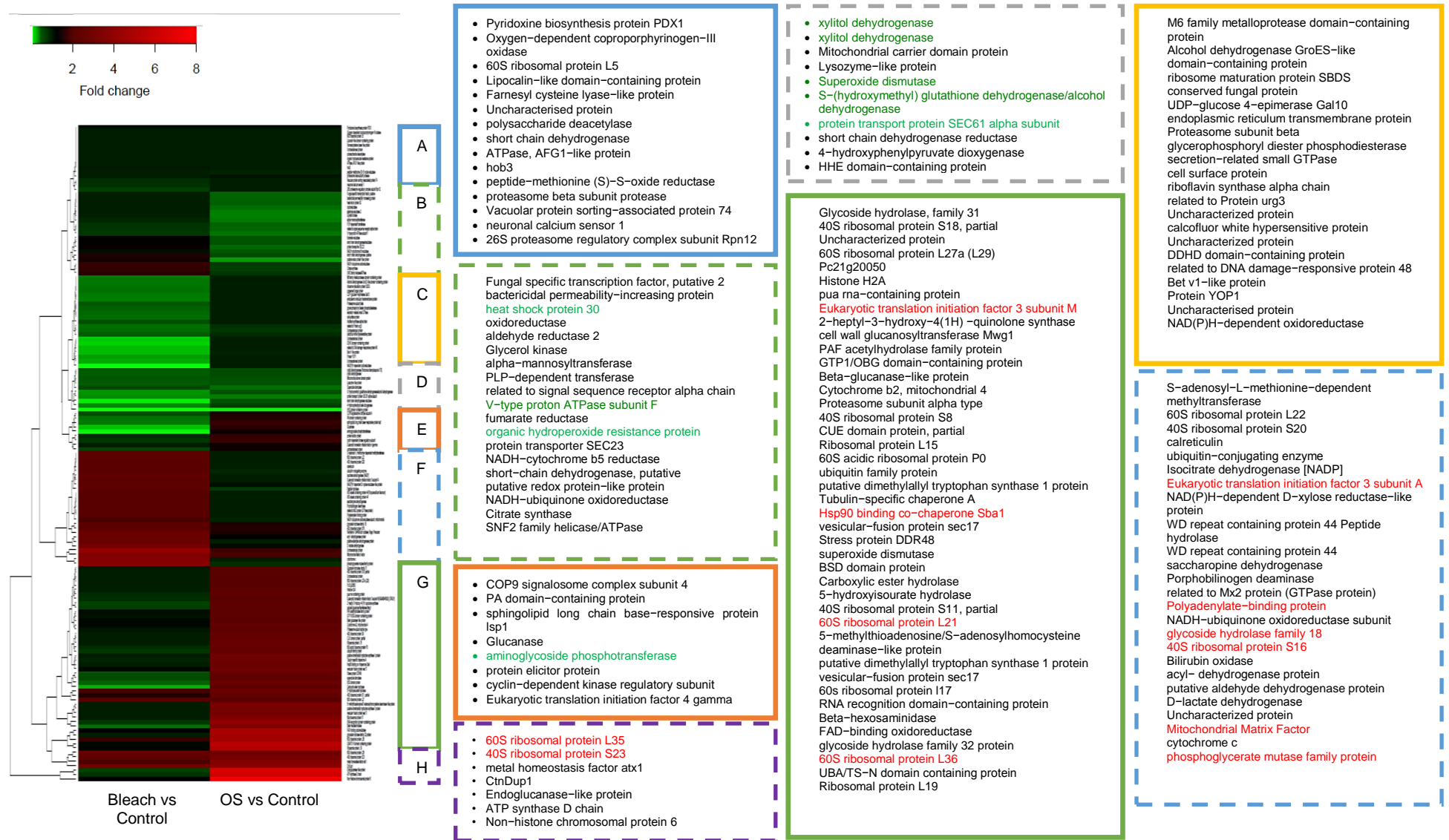


Figure 8-18: Heatmap of significant proteins with changes in abundance in *S. chartarum* after 7 days' growth following the exposure to bleach and OS. Increased protein levels as indicated in 'red blocks' and decreased protein levels as indicated in 'green blocks' of the heatmap. Examples of both stress and ribosomal proteins which changed in abundance are highlighted in red and green.

8.3.6 PANTHER analysis of the different proteomes in response to different chemical treatment methods

To determine the effects of bleach and OS in *S. chartarum*, we performed the PANTHER analysis to systematically classify the proteins with changes in abundance based on protein class, molecular function, biological process and pathway.

8.3.6.1 PANTHER classification based on protein classes

It is clear from figure 8-19 that there are some variations in protein abundance. The same protein classes affected were (a) DNA methyltransferase, (b) RNA binding protein and, (c) ribosomal protein. The major protein class increased in bleach were (i) oxidoreductases (eg. saccharopine dehydrogenase (A0A084B8C5), NADPH-dependent aldose reductase (A0A084RD22) and D-lactate dehydrogenase-related (A0A084RIV2), while in the OS group, (ii) nucleic acid binding (A0A084RPV2 40S ribosomal protein, A0A084R831 Histone H2A and A0A084RAL1 60S ribosomal protein L36) were the most affected.

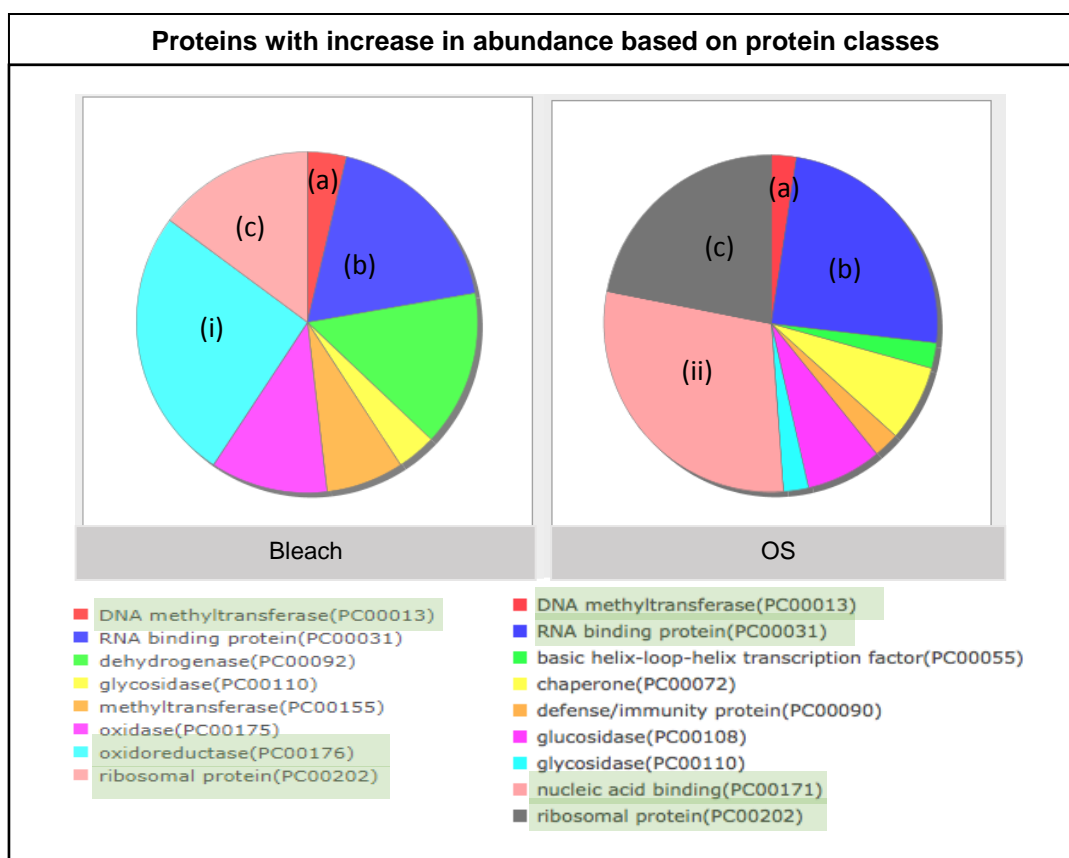


Figure 8-19: PANTHER classification of proteins with increased in abundance based on protein classes of 7 days-old *S. chartarum* following the treatment of bleach and

organosilane on Day-1. The major protein classes affected in each treatment are marked as; i) bleach, and ii) OS.

On the other hand, (a) reductase and, (b) membrane traffic proteins were decreased in both treatment groups (Figure 8-20). In bleach groups, for examples, the protein belonging to the reductase class was A0A084B8Y1 sorbitol dehydrogenase and to the membrane traffic proteins class was A0A084RUH7 Protein transport protein Sec61 subunit alpha isoform 1). The major protein class decreased in bleach were (i) dehydrogenase, while in the OS group, (ii) oxidoreductase were the most affected.

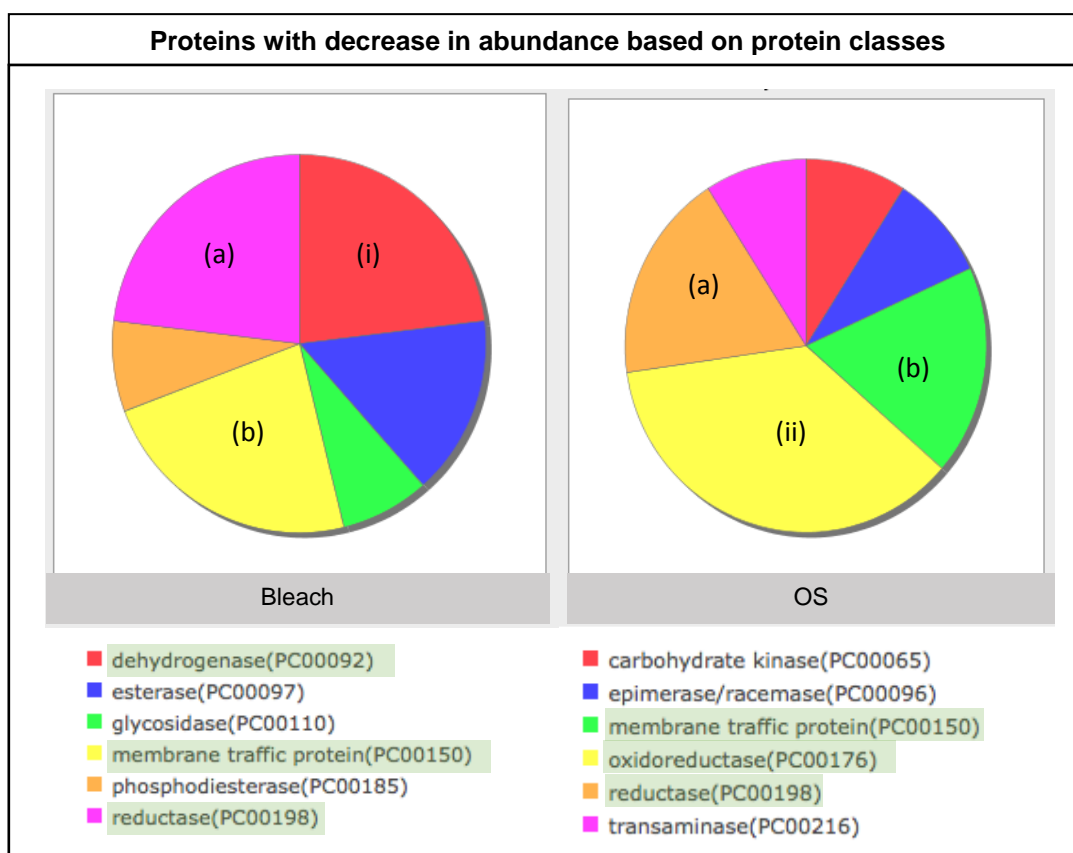


Figure 8-20: PANTHER classification of proteins with decrease in abundance based on protein classes of 7 days-old *S. chartarum* following treatment with bleach and organosilane on Day-1. The major protein classes affected in each treatment group are marked as; i) bleach, and ii) OS.

8.3.6.2 PANTHER classification based on molecular functions

The proteins were then classified based on molecular function. The increased proteins were classified into at least 7 molecular functional classes (Figure 8-21). The molecular activities observed in both groups were acting as (a) structural constituents of ribosomes and those involved in (b) structural molecule activity (eg. A0A084RLH9 60S ribosomal protein L22-related) and, (c) DNA- methyltransferase activity (eg A0A084RYC0 PANTHER Unknown).

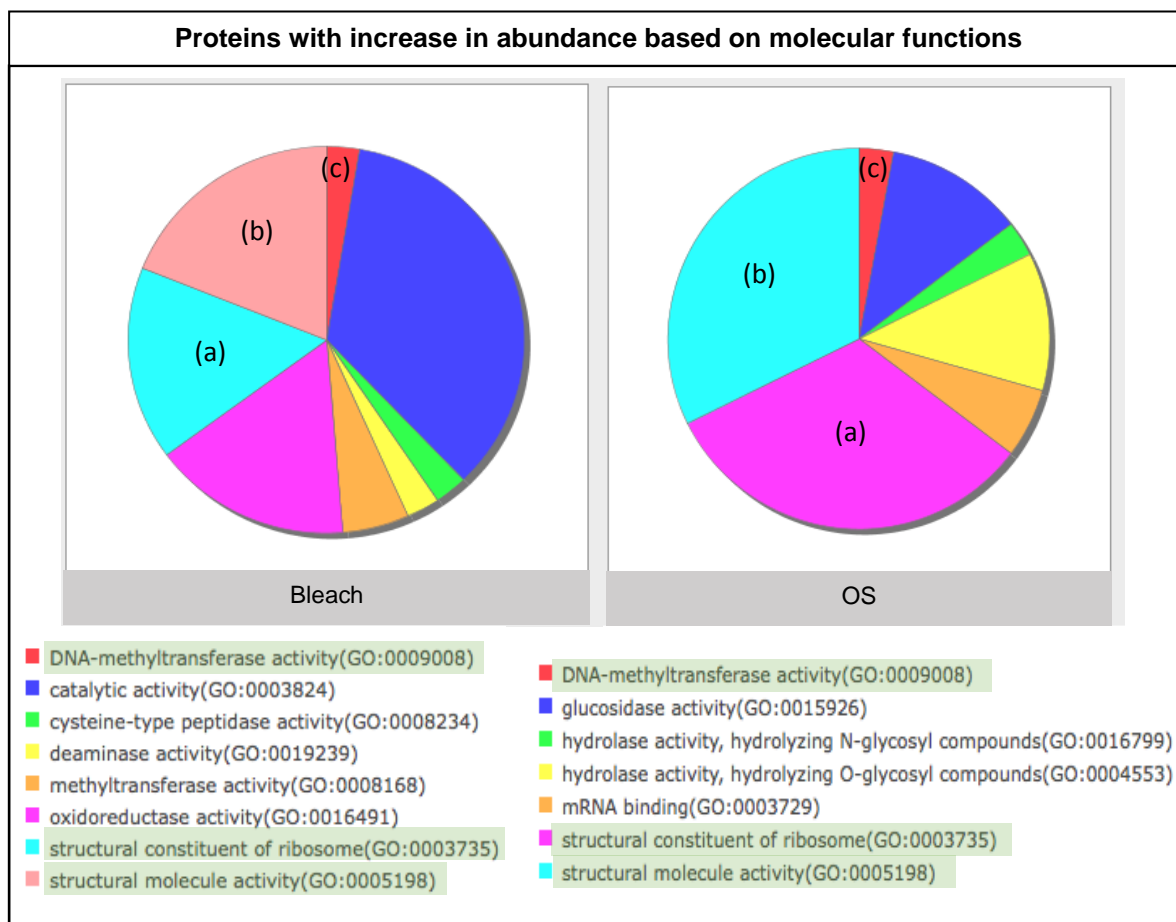


Figure 8-21: PANTHER classification of proteins with increase in abundance based on molecular functions of 7 days-old *S. chartarum* following treatment with bleach and organosilane on Day-1.

Completely different molecular functional classes were observed amongst down-regulated proteins in both groups (Figure 8-22). Furthermore, more molecular functions were observed in the OS compared to the bleach treated groups.

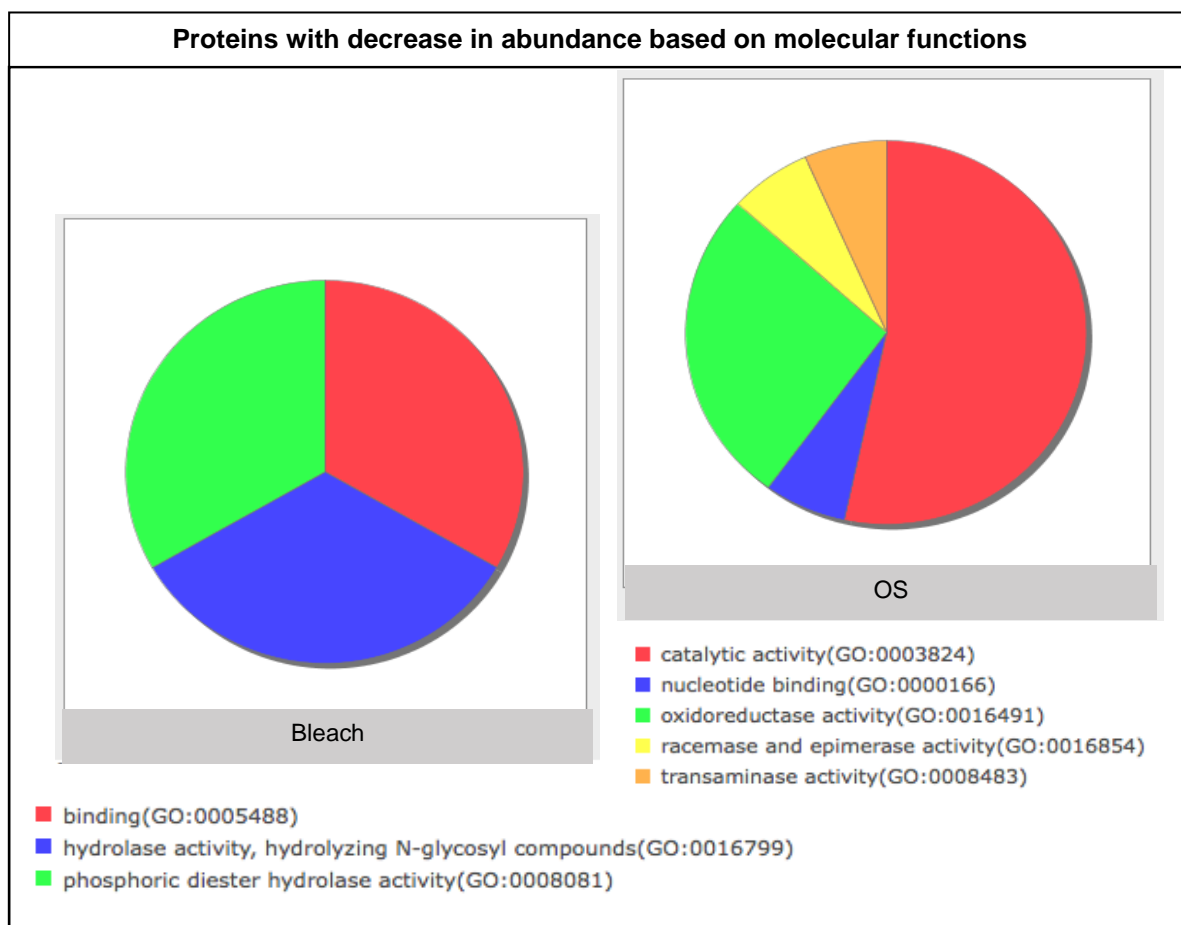


Figure 8-22: PANTHER classification of proteins with decrease in abundance based on molecular functions of 7 days-old *S. chartarum* following treatment with bleach and organosilane on Day-1.

8.3.6.3 PANTHER classification based on biological processes

More biological processes were increased in the bleach treatment group compared to the OS group. However, five biological processes consisting of (a) biosynthetic processes, (b) metabolic processes, (c) primary metabolic processes, (d) protein metabolic processes and (e) translation were affected in both groups (Figure 8-23). We also found some interesting biological processes such as apoptosis, cell-death and fatty-acid beta oxidation following the treatment with bleach but not with OS.

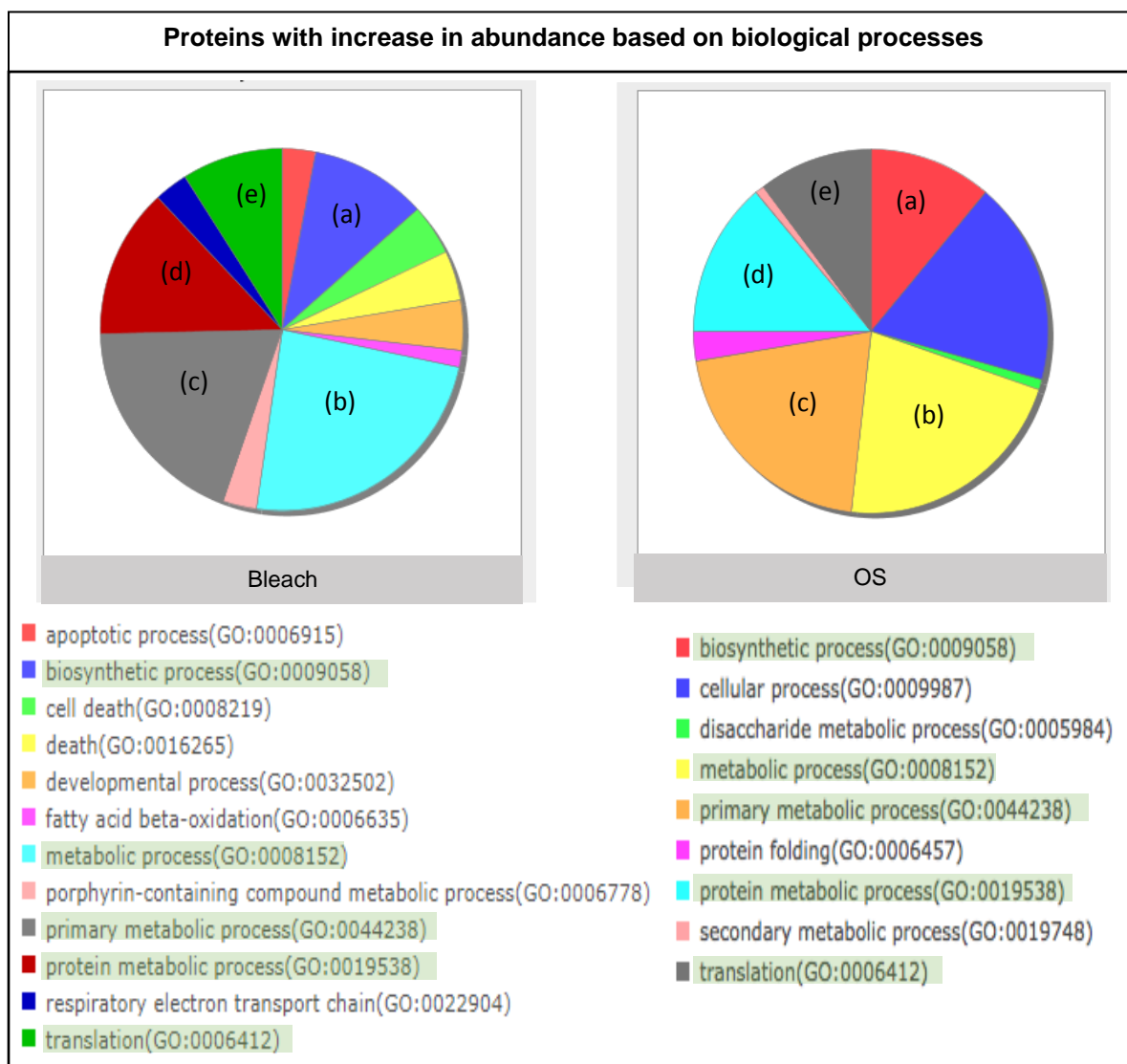


Figure 8-23: PANTHER classification of proteins with increase in abundance based on biological processes of 7 days-old *S. chartarum* following treatment with bleach and organosilane on Day-1.

In contrast, there were no similar processes amongst the down-regulated proteins in the two groups (Figure 8-24). However, more biological processes were affected in the OS group compared to the bleach group with major effects on proteins associated with transport and protein transport.

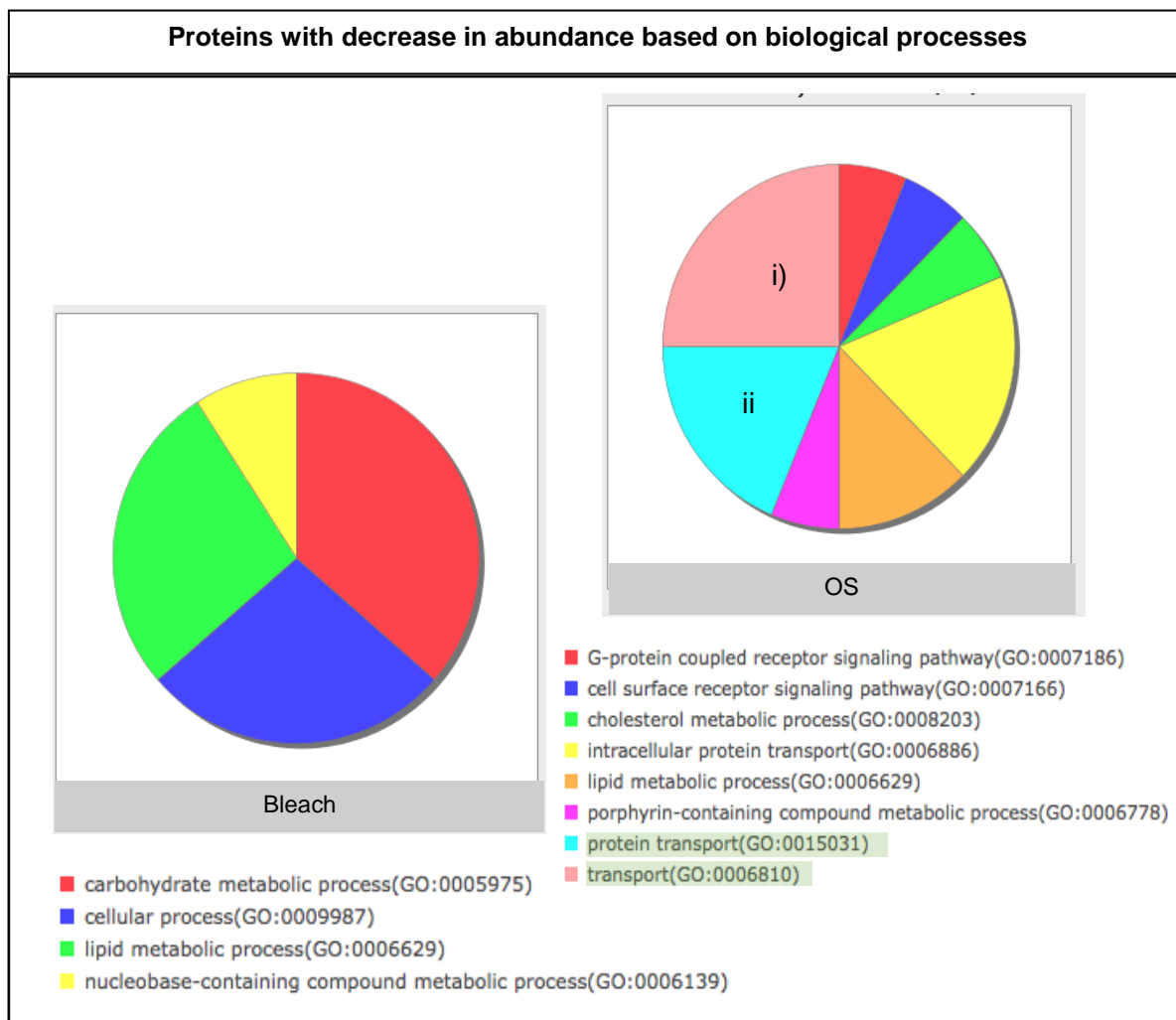


Figure 8-24: PANTHER classification of proteins with decrease in abundance based on biological processes of 7 days-old *S. chartarum* following treatment with bleach and organosilane on Day-1. The major protein classes affected by OS were, i) transport and ii) protein transport.

8.3.6.4 PANTHER classification based on biochemical pathways

In the bleach group, 3 pathways were identified from the decrease in abundance of proteins consisting of the metabotropic glutamate receptor group receptor I and III; GABA-B receptor II signalling (Figure 8-25), and the Hedgehog signalling pathway. Two pathways were affected amongst the increased in abundance of proteins including 5-Hydroxytryptamine degradation and ATP synthesis. In contrast, only 1 pathway was identified from increase in protein abundance in the OS group: the toll receptor signalling pathway (Figure 8-26).

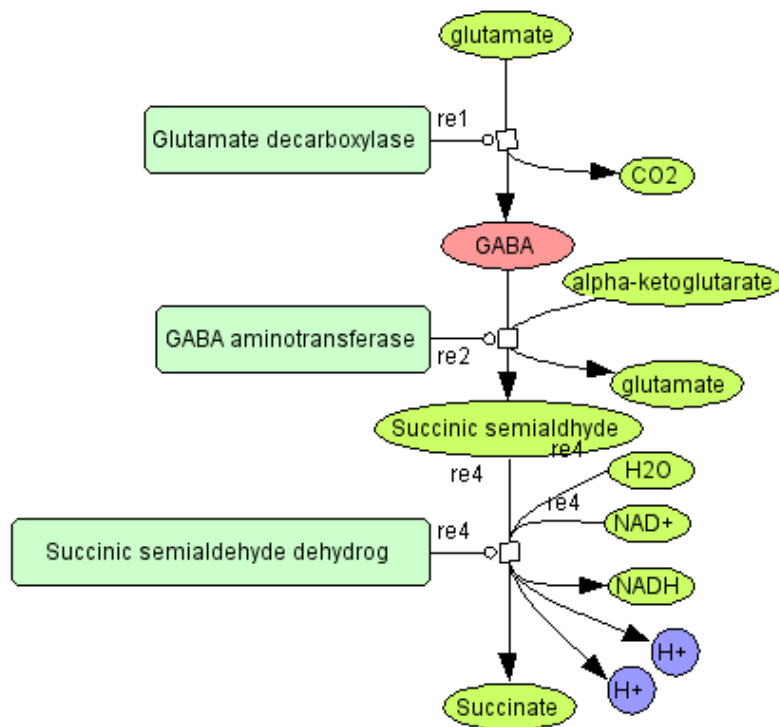


Figure 8-25: The protein levels in the GABA signalling pathway ⁽³²⁰⁾ were decreased following 7 days after exposure to bleach Diagram adapted from PANTHER Classification system (www.pantherdb.org). Used with permission from ©2018 Paul Thomas.

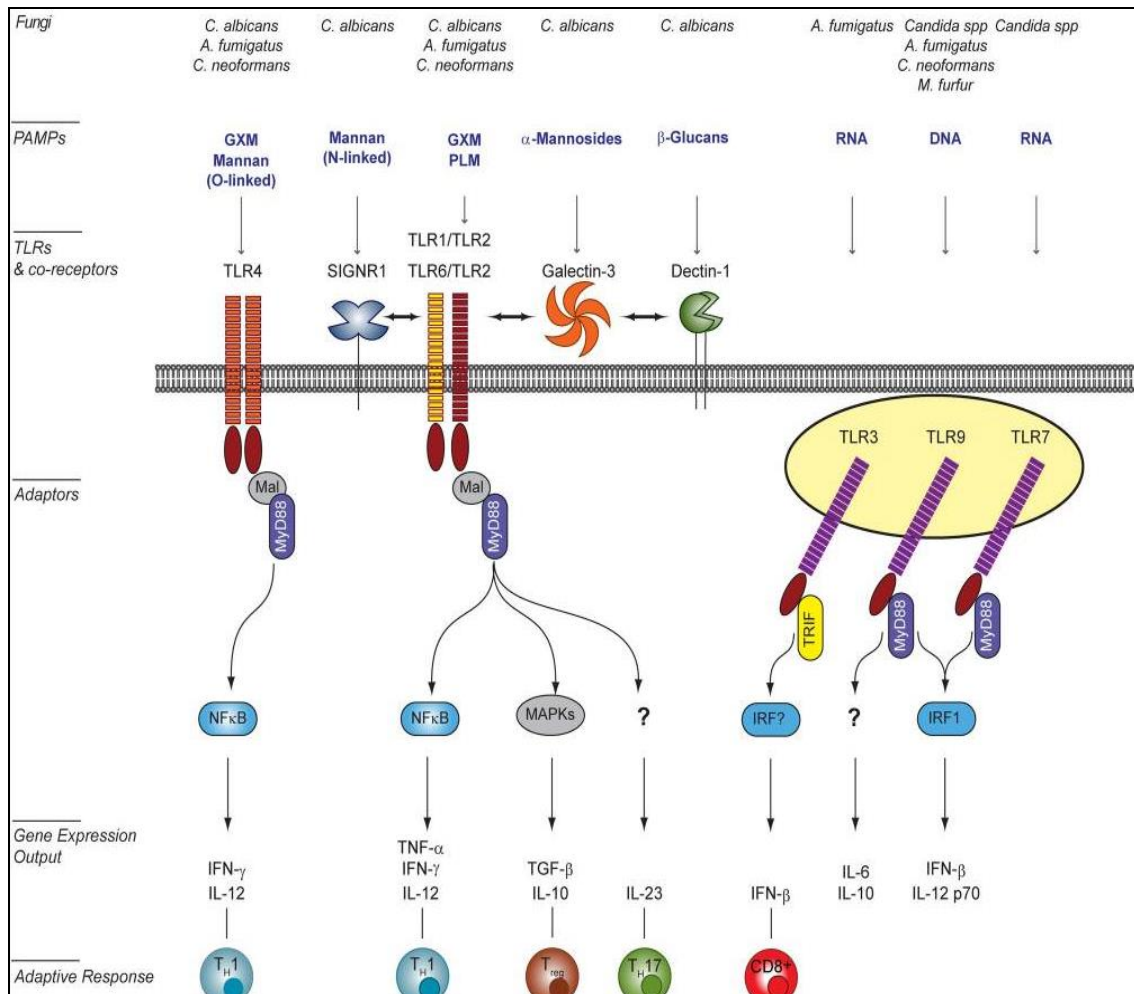


Figure 8-26: The protein levels in the toll receptor signalling pathway were increased in abundance in the OS group. The TLR signalling pathway in a host cell upon recognition of specific pathogen-associated molecular patterns (PAMPs) consisting of fungal polysaccharides, DNA and RNA. Diagram adapted from Bourgeois *et al.*⁽³²⁴⁾. ©2012 Bourgeois and Kuchler. Licensed under Creative Commons Attribution (<http://creativecommons.org/licenses/by/3.0/>).

8.4 DISCUSSION

The present study represents the first proteomic study of *S. chartarum* following treatment with antimicrobial agents commonly used in the built environment. In this study on the differential protein expression in *S. chartarum* in response to antimicrobial agents, we specifically aimed to elucidate the proteins involved in survival following exposure to subinhibitory concentrations. Fungal resilience and survival depends on multiple factors (extrinsic or intrinsic) such as the effectiveness of remediation methods and how the fungus respond to treatment. In the indoor environment, the fungus thrives in high moisture and cellulose-based materials. In addition, its 'anchoring' hyphal network is capable of penetrating the porous space in building materials making it more difficult for complete remediation. Our results have demonstrated what occurred at the protein level following exposure to bleach and organosilane. These results serve as a basis for understanding how *S. chartarum* adapts to different remediation strategies and mechanisms of action.

8.4.1 Method optimisation

Sample preparation is one of the crucial steps in protein studies and often presents a unique set of problems for proteome analysis. It is a challenge for any black fungus due to the thick rigid cell wall and heavy pigmentation⁽³²⁵⁾. The protocol should efficiently remove melanin and any other compounds such as salts and detergents that would cause interference in the downstream process, particularly with LC MS/MS. So far, there is no simple and straightforward protocol for extracting proteins from pigmented, filamentous fungi. Therefore, an optimised protocol is important to ensure maximum disruption of cells and integrity of proteins after disruption to obtain a protein yield sufficient for further steps.

A suitable protein extraction method is the basic yet very crucial step to get rid of the contaminants whether from the fungus itself, reagents used during the process together with the antimicrobial agents prior to LC MS/MS; as well as to obtain enough protein yield for downstream processes. Both mechanical (by grinding under liquid nitrogen) and chemical approaches (TCA/precipitation and phenol extraction) have been used. Although both strategies require safety training, they were shown to be suitable for extracting proteins from a heavily pigmented fungus, such as *S. chartarum*. In addition to the protein extraction method, the protein clean-up is equally important particularly with antimicrobial agents such as organosilane, which is highly hydrophobic, that can bind tightly to the LC MS/MS column.

In this study, we have performed protein extraction according to Tesei *et al.*⁽³¹²⁾ and/ or in combination with Wu *et al.*⁽³¹³⁾ with some modifications. Proteins from *S. chartarum* were successfully extracted using TCA/acetone precipitation followed by phenol extraction combined with methanol/ ammonium acetate precipitation. TCA precipitation is one of the most widely used methods, other than chloroform-methanol or ethyl acetate that can efficiently remove contaminants and detergents before the main extraction and precipitation procedures⁽³²⁶⁾. In many proteomic studies, TCA/acetone precipitation resulted in good protein recovery and protein separation and in 2-dimensional electrophoresis, it generating the highest number of protein spots^(326, 327). This was probably due to the mechanism of TCA which precipitates proteins by forming hydrophobic aggregates even at a low concentration⁽³²⁸⁾. Further washes with acetone removed TCA and allowed solubilisation of the pigments and lipids that are possibly present in the samples⁽³²⁹⁾. Since the samples obtained were still slightly coloured, 1-dimensional electrophoresis was employed to confirm the presence of protein bands following quantification using the Bradford assay.

Other than melanin, interference with LC MS/MS processes could originate from various sources such as solvents, polymers, plasticisers, and additives⁽³³⁰⁾. Antimicrobial agents used in the experiment might also have influenced LC MS/MS. Organosilane, as noted previously, is a highly hydrophobic compound and might bind tightly to the reverse-phase chromatography column causing sample carry-over. This could lead to improper elution and failure of incoming samples to bind properly to the column. To overcome this, we performed a single clean-up step that resulted in signal suppression and chromatographic interference. As a result, we subsequently applied a two-step sample clean-up with cartridges and Zip-tip® U-18 and this additional step improved the mass spectrometry signals significantly.

We also found that it was critical to process the samples in small batches to optimize the disruption and separation of the cell wall and to maximise the removal of pigment and other contaminants. The samples were kept at a low temperature during extraction in order to prevent protein denaturation and fragmentation, especially in the presence of protease in the sample and therefore to promote a better protein yield.

8.4.2 Proteomic searches and databases of *S. chartarum*, NCPF 7587

The MS/MS spectra searches were performed using the TrEMBL database instead of SWISS-PROT. This database was chosen due to the scarcity of information on *S. chartarum* proteomes or the sets of proteins derived from fully sequenced genomes.

To our knowledge, there are only 2 reference proteomes on *Stachybotrys* sp. published in UniProtKB/Swiss-Prot, namely *Stachybotrys chartarum* IBT 40288 (Proteome ID UP000028540) and *Stachybotrys chlorohalonata* IBT 40285 (Proteome ID UP000028524). Another two *S. chartarum* strains deposited in the database were IBT 7711 (Proteome ID UP000028045), which contains part of the *Stachybotrys chartarum* IBT 40288 pan proteome and IBT 40293, which was marked as redundant to IBT 7711 ⁽⁸¹⁾.

Out of these 4 strains, only 22 proteins, e.g. trichodiene synthase (Entry no O59947, protein name TRI5_STACH, gene name TRI5) have been manually annotated and reviewed by UniProtKB/ Swiss-Prot. In contrast, the TrEMBL database contained more than 33 000 EMBL nucleotide entries that have been automatically annotated but have not been reviewed. The high number of uncharacterised proteins (79%) led to protein homologues searches in NCBI that came out with a considerable number of homologues (95%).

In addition to manual screening, we have performed a large scale gene function analysis by using the PANTHER (Protein ANalysis THrough Evolutionary Relationships) classification system ⁽³³¹⁾. The PANTHER classification system is a biological database of gene and protein families and their functionally related subfamilies that can be used to classify and identify the function of gene products according to family, molecular function, biological function and pathway. The most important application of PANTHER is to accurately infer the function of genes and protein function from any organism based on their phylogenetic relationships to model organisms with known functions ⁽³¹⁹⁾.

We observed the distribution patterns of the most abundant protein in each category (Section 8.3.3). In a study by Carberry *et al.* ⁽³³²⁾ using 2-DE and MALDI mass spectrometry, it was found that the major proteins in *A. fumigatus* were involved in energy production with other classes including structural proteins, signalling, heat shock and transcription factors. In this study, we found that proteins involved in metabolic processes and primary metabolic processes were the most abundant in terms of molecular function, followed by those involved in the generation of precursors and metabolites. Although the findings were the same as in the previous study, this study provides more information on *S. chartarum* protein profiles and functions with more confidence as the PANTHER database was used which allows extensive categorisation of all proteins using different annotated databases without restriction to biological classes.

8.4.3 Heatmap of changes in protein abundance patterns in *S. chartarum* following treatment with bleach and organosilane

In this study, we utilised the heatmap to group the protein levels that were ‘most similar’ to one another according to their changes in protein abundance following the treatment with bleach or OS.

From the results, more increased protein levels were observed following exposure to OS as opposed to bleach treatment which resulted in more decreased proteins were seen. Both prevention (OS) and treatment (bleach) methods also produced different protein profile patterns in *S. chartarum*. The variations might be due to different mode of actions or different ways of application (either treatment or prevention) that triggered different biochemical responses towards the agents.

Sodium hypochlorite (bleach) is a powerful oxidising agent which has a germicidal action although it is corrosive. The by-products of bleach consist of the hypochlorite ions (-OCl) and hypochlorous acid (HOCl). The latter being the active compound that can penetrate the lipid bilayer resulting in cidal activity. The mechanism of action of HOCl has been elucidated in several studies in relation to bacteria ^(184, 333) but there is a lack of information about its action on fungi.

We hypothesised the stress response proteins would be increased in accordance with a study by Winter *et al.*⁽³³³⁾ who revealed that the redox-molecular chaperone, Hsp33, played a role in the bacterial survival mechanisms towards bleach by preventing stress-induced protein aggregation. This defence mechanism, however, was restricted to peroxide stress at heat shock temperatures. In this study, we found that the stress response-related proteins such as hydroperoxide resistance protein, aminoglycoside phosphotransferase, S-(hydroxymethyl) glutathione dehydrogenase/alcohol dehydrogenase, and xylitol dehydrogenase were decreased following treatment with bleach. Though the findings contradict the initial hypothesis, this might suggest that the stress proteins might have been “sacrificed” (i.e. degraded, depleted or consumed) as part of the protective mechanism. Since the proteomics showed the changes in protein abundance, this could also be either due to changes in gene expression or physical depletion of proteins.

It has also been proposed that HOCl inactivates bacteria by inhibition of DNA synthesis and consequent inhibition of protein synthesis ⁽³³⁴⁾. Since a subinhibitory concentration of bleach was used, we found that instead of growth inhibition, the fungus started to produce new whitish hyphae. The growth recovery could still be observed after 7 days

of exposure. Our findings showed that most of the ribosomal proteins and developmental proteins, which include polyadenylate-binding protein, eukaryotic translation initiation factor 3, 60S ribosomal protein and phosphoglycerate mutase family protein were increased. Hence bleach does not cause a global inhibition of protein synthesis at a subinhibitory concentration, through a generalised impact on nucleic acid function.

However, we should also take into consideration that incomplete contact with bleach might occur which resulted from the method of application. The direct treatment method on an 'established' fungal mass might contain some proteins derived from the fungal mass underneath with less or no contact with bleach. It is possible that the bleach had no impact on some of the fungal cells deep within the mycelium and so the protein profiles obtained may reflect a mixture of the content of dead, unaffected and stressed cells. However, given that the control plates were processed in the same way, the changes in protein content in the treated samples should represent genuine changes in the viable surviving cells.

Organosilane (OS) is an antimicrobial nanocoating which acts by contact-killing. It consists of a silane base, positively charged nitrogen and a long molecular carbon chain. The silane base acts as antimicrobial anchor, while the positively charged nitrogen attracts the negatively charged microbial membranes. The long molecular chain is thought to mechanically disrupt the cell membrane, penetrating the cytoplasm and leading to membrane leakage and cell death ⁽³³⁵⁾. It has been shown that the antimicrobial surface can prevent the division of cells either during the growth stage or before the onset of growth ⁽³³⁶⁾. The inhibitory effects of silane coatings on bacteria, fungi, and viruses have been reported in several studies to prevent biofilm formation ^(187, 188, 337). OS was found to be effective in preventing microbial attachment ^(187, 337) however its effectiveness was highly dependent on the species, surface material and the method of application ⁽³³⁷⁾. Moreover, Boyce *et al.* ⁽¹⁹⁰⁾ reported inconsistency in the reduction of bacterial colonization when applied to surfaces by touch. However, this may be due to the method of application by wipes instead of spraying onto surfaces.

Studies are still lacking of the effects of OS at the molecular level. In this study, we found that the stress response-related proteins such as the superoxide dismutase and heat shock protein 30 as well as intracellular transport proteins (e.g. protein transporter SEC23, transport protein SEC1 alpha subunit and V-type proton ATPase subunit F) were decreased after 7 days following exposure to OS. This might suggest that OS might penetrate into the cytoplasm to some degree and impact on intracellular

transport mechanisms. On the other hand, both stress-related proteins (e.g. superoxide dismutase and Hsp90 binding co-chaperone) and ribosomal proteins (e.g. eukaryotic translation initiation factor 3, 40S ribosomal protein and 60S ribosomal protein) were increased.

This might suggest that fungal defence against the antimicrobial action of OS, and fungal growth and survival occurred at the same time. This also indicates that organosilane incorporated into the agar was stable after 7 days and was found to continuously affect the growth of fungal cells without inhibiting survival pathways.

8.4.4 PANTHER biological function classification of treated *S. chartarum* proteins

Some differences were demonstrated in the protein changes following the exposure to bleach and OS. However, DNA methyltransferase, RNA binding protein and ribosomal proteins were found to be increased in both groups. These proteins served as key proteins in maintenance or development ^(338, 339). On the other hand, proteins in reductase and membrane traffic proteins were found to be reduced. While reductase is an enzyme with a more general function, membrane traffic proteins play a pivotal role in rapid responses to environmental stress ⁽³⁴⁰⁾. As discussed in the previous section (Discussion, Section 8.4.3), we assumed that the stress response proteins have been degraded, consumed or depleted. Pont ⁽³⁴¹⁾, reported that mycotoxins are a component of stress response in *Fusarium* spp., which is also a trichothecenes producer. The mycotoxins are derived from the isoprenoid pathway which is linked to primary metabolic pathway involve in various cellular processes. On the other hand, developmental proteins were increased as an indication of recovery from stress. Our results were in accordance with Ilyas *et al.* ⁽³⁴²⁾ who found that proteins involved in amino acid metabolism, such as alanine glyoxylate aminotransferase, were increased in *Trichosporon asahii* after 2 days exposure to an environmental stressor, arsenic, while, the proteins related to protein repair and folding such as heat shock protein 70 were reduced.

In the bleach group, 3 pathways were identified from the decreased proteins consisting of metabotropic glutamate receptor group receptor I and III, GABA-B receptor II signalling, and the Hedgehog signalling pathway. Two pathways were affected amongst the increased proteins including 5-Hydroxytryptamine degradation and ATP synthesis. The metabotropic glutamate receptor group was one of the pathways decreased in the bleach group. The metabotropic glutamate receptor is a member of

the G-protein couple receptors (GPCRs) family. In eukaryotes, GPCRs respond to external stimuli by receiving and transducing signals in networks ⁽³⁴³⁾. Mycotoxin production and sporulation were shown to be regulated by the G-protein signalling pathways which also regulate fungal development, stress response and expression of virulence ⁽³⁴⁴⁾. The signal transduction occurs via the binding of a ligand to a GPCR, which resides in the cell membrane, to downstream cascade linking sporulation and secondary metabolism ⁽³⁴⁴⁾. In addition to GPCRs, GABA-B receptor also plays an important role in development and response to environmental stress ⁽³⁴⁵⁾. GABA provides carbon and nitrogen source to fungi and is associated with increase sporulation ^(346, 347).

In contrast, only one altered pathway was identified in the OS group which was the toll-receptor signalling pathway, found to be increased. This pathway in fungi is commonly associated with TLR signalling pathway in host cells upon interaction with fungal pathogens. Several components in the cell wall or surface of the fungi have been identified as ligands/recognition site for toll-like receptor (TLR) in host cells ⁽³²⁴⁾. The ligands also known as pathogen-associated molecular patterns (PAMPs) were consists of fungal polysaccharides with most of them are glucose polymers and constituents of the cell wall, DNA and RNA.

8.5 CONCLUSIONS

In this study, we have documented baseline proteins of *S. chartarum* and its responses to antimicrobial treatment with bleach and prevention with OS at subinhibitory concentrations. *S. chartarum* responded differently to bleach and OS with more increased protein levels observed following exposure to OS as opposed to bleach treatment which resulted in more decreased protein levels. Stress response-related proteins might have been depleted or consumed as a process of recovery following treatment with bleach. On the other hand, both stress-related proteins and ribosomal proteins were increased following exposure to OS. These differences in protein changes towards bleach (used as treatment) and OS (used as prevention), suggest that a combination of antimicrobial agents with different modes of action might provide a more effective way to eliminate fungal growth.

CHAPTER 9

GENERAL DISCUSSION AND FUTURE DIRECTION

9.1 LIMITATIONS OF THE STUDY

Although we have met our aims in this study, several limitations are worth noting. These include:

1. Identity of isolates: Prior to the commencement of this study, isolates were obtained either from other researchers or purchased from culture collections. A few isolates showed different identities when subjected to our laboratory analysis which introduced some uncertainties during the study. However, we have communicated via email with the sources by providing evidence to support our claims. Isolates such as CBS 182.80 and CBS 328.37 have been re-identified by others and their new identities were published in 2016. Stachy CU was identified as *S. chartarum* using conventional methods and has never been characterised by molecular methods. Moreover, sequences obtained using ITS1/4 primers known to be a universal primer set did not give the correct identification which led us to use mycotoxin specific primers. Therefore, during the study the number of isolates representing *S. chartarum* decreased from the initial five isolates to three isolates. However, CBS 182.80 obtained as *S. dichroa* was later identified as *S. chartarum*, resulting in a total of four isolates. Accurate identification also depends on the input of sequences by many researchers which vary in their primer selection and length.

2. Mycotoxin classes: Based on the sequences derived from tri5 primers, all our *S. chartarum* isolates were phylogenetically classified as chemotype S. More diverse samples would give us more information on different chemotypes, a more distinct distribution of mycotoxin classes and increase the confidence of our results. Other direct methods to detect mycotoxins (such as mass spectrometry or ELISA) could be used to complement the findings.

3. Melanin and other contaminants: Most of the isolates were heavily pigmented which greatly affects DNA and protein extraction. Extended or modified methods were performed to eradicate possible inhibitors as well as to obtain sufficient yields for downstream processes. Only small amount of biomass could be used in each tubes to maximise the clean-up process. The additional steps also affected the final yield of DNA or protein and, therefore, several tubes needed to be pooled together to obtain sufficient yield for analysis. Although the methods performed in this study were successful, they required more time and increased the cost compared to those used for non-dematiaceous fungi.

4. Antimicrobial agents: Not all methods were suitable for each antimicrobial agent, thus comparison could not be made for every method. For example, aerosolised hydrogen peroxide application differs to the other antimicrobial agents tested by producing a mist and could be tested only using the direct treatment method. Organosilane (OS) coagulates in RPMI and is not suitable for the microdilution plate method. However, bleach could be tested using all methods and was used as standard comparator.

5. Fungal growth in the real-life setting: We found that *S. chartarum* grown on gypsum board is less susceptible to the antimicrobial agents compared to the *in vitro* studies. Although this study aimed to simulate a real life, the real environment is more complicated with the presence of other microbes and the contaminated surface. The interactions of *S. chartarum* within a more complex fungal communities might impact on growth and the organism might even be outcompeted by other faster growing fungi. We did not obtained satisfactory fungal growth on the shower curtain material in this study. This suggests that, in real life, fungi might not grow directly on water-repellent surfaces such as shower curtains, but grow on organic materials or dirt on the surface. The growth was also relatively slow on wallpaper which made it very difficult for antimicrobial impact to be studied within feasible a time frame.

6. Protein databases: Most of the proteins are not well-annotated in the databases which limits the searches, only 22 proteins have been manually annotated and reviewed by UniProtKB/ Swiss-Prot. Although we have performed automatic searches using the TrEMBL database, there was still a high number of uncharacterised proteins (79%, n= 744) which necessitated manual searches for protein homologues in Blastp. Searching programs such as BLAST provides statistical estimates to infer homology based on sequence similarity. However, the relationship between homology and

function is complex which means that an understanding of the functional impact of these agents requires much more extensive protein annotation than at present.

9.2 SUMMARY OF THE MAIN FINDINGS

Despite of all the limitations, this study has achieved its objectives and contributed to the knowledge of *S. chartarum*, as summarised in table 9-1 and table 9-2.

Table 9-1: Contribution to the identification of *Stachybotrys chartarum*.

Year	Descriptions	References
1837	The first characterisation as <i>Stachybotrys atra</i> Corda as septate, branched hyphae, conidiophore terminate in a whirl of phialide and two-celled conidia	Corda, 1837 ⁽⁹⁸⁾
1943	Total of 20 <i>Stachybotrys</i> spp. (12 new taxa, unispore), revised into 2 species: <i>S. atra</i> Corda and <i>S. subsimplex</i>	Bisby, 1943 ⁽⁹⁸⁾
1958	<i>Stilbospora chartarum</i> Ehrenb. 1818, <i>Oidium chartarum</i> Ehrenb. Ex Link 1824, <i>Oospora chartarum</i> (Ehrenb. ex Link) Wallr. 1833. all classified as <i>S. chartarum</i> (Ehrenb) Hughes	Hughes, 1958 ^(95, 99)
1962	<i>Memnoniella echinata</i> classified as <i>Stachybotrys</i> spp.	Smith, 1962 ⁽⁹⁹⁾
1945-1971	<i>Memnoniella</i> described as distinctive from <i>Stachybotrys</i> spp.	Padwick (1945), Deighton (1960), Matsushima (1971) and Ellis (1971) ⁽⁹⁹⁾
1966	Proposed new variant of <i>S. atra</i> with smaller conidia (6-8 x 4-5 µm), elliptical to globose named <i>S. atra</i> Corda var. <i>microspora</i> Mathur and Sankhla	Manthur and Sankhla, 1966 ⁽⁹⁵⁾
1976	All <i>Stachybotrys</i> spp. described as having unicellular conidia Proposed a standardised and proper nomenclature as <i>S. chartarum</i> (Ehrenberg ex Link) Hughes Re-examined <i>S. atra microspora</i> and found the deposit mixed with <i>S. chartarum</i> . Renamed <i>S. atra microspora</i> into <i>S. microspora</i> (Mathur & Sankhla) Jong & Davis <i>Stachybotrys</i> spp. and <i>Memnoniella</i> spp. were considered as physiologically and morphologically closely related but the main difference is in the conidia	Jong and Davis, 1976 ⁽⁹⁹⁾

1980	No valid generic distinction between <i>Stachybotrys</i> spp. and <i>Memnoniella</i> spp. as proposed by Jong & Davis, 1976 Suggested both genera to be classified under <i>Stachybotrys</i> spp.	Carmichael, 1980 ⁽¹⁰¹⁾
1997	<i>S. yunanensis</i> as a new species (but no new report since 1997), most likely to have been <i>S. chartarum</i>	Kong, 1997 ⁽⁹⁵⁾
2001	<i>Memnoniella echinata</i> (Rivolta) Galloway renamed as <i>Stachybotrys echinata</i> (Rivolta) G. Sm and <i>M. subsimplex</i> (Cooke) Deighton as <i>S. subsimplex</i> Cooke following phylogenetic and morphological analysis using 18S, 28S, 5.8S rDNA genes and ITS1 and ITS2 regions	Haugland, 2001 ⁽¹⁰⁰⁾
2002	Examined 30 isolates of <i>S. chartarum</i> using three genetic markers (chitin-synthase 1, beta tubulin 2 and trichodiene synthase 5), and found two distinct cryptic species exist within the single morphological species	Cruse, 2002 ⁽¹²⁾
2002	Found 2 chemotypes produced by <i>S. chartarum</i> : atronones producing isolates and macrocyclic trichothecenes isolates and one undescribed taxon. Identification was based on morphology, colony characteristics on culture media and metabolite production using LC-MS	Anderson, 2002 ⁽⁹⁴⁾
2003	Examined 25 isolates of <i>Stachybotrys</i> spp. using morphological, chemical and phylogenetic methods. The isolates could be segregated into two chemotypes of <i>S. chartarum</i> , and a novel species, <i>S. chlorohalonata</i> . The new species showed some morphological differences from <i>S. chartarum</i> and possessed different <i>tri5</i> , <i>chs1</i> and <i>tub1</i> gene sequences. There was no difference between the two chemotypes of <i>S. chartarum</i> in the <i>tub1</i> gene, and only a single nucleotide difference in each of the <i>tri5</i> and <i>chs1</i> genes.	Anderson, 2003 ⁽¹¹⁾
2018	Identified 13 <i>Stachybotrys</i> strains representing 5 different species using PCR technique and protein-based method, MALDI-TOF. The universal primers, ITS1/ITS4 primers and <i>HaeIII</i> restriction fragment length polymerase polymorphism (RFLP) patterns were unable to properly distinguish between <i>S. chartarum</i> and <i>S. chlorohalonata</i> . However, sequence alignments with SC1 primers (this study) produced the nucleotide the	This study

	<p>lowest consensus (90.8% identity) for <i>S. chartarum</i> and <i>S. chlorohalonata</i>, compared to other primers (Cruse primers: 94.3% identity; and Black primers: 92.6% identity). Another primer sets, SC3 tri5 amplified all <i>S. chartarum</i> strains but not <i>S. chlorohalonata</i> as shown on the agarose gel and in silico PCR.</p> <p>Clearer cut-off points were obtained using MALDI-TOF for both <i>S. chartarum</i> (2.3 to 2.7) , <i>S. chlorohalonata</i> (1.8 to 2.1) and other <i>Stachybotrys</i> spp. (below 1.6) compared to previous studies by Gruenwald <i>et al.</i>⁽¹⁰⁶⁾ and Ulrich <i>et al.</i>⁽¹⁰⁷⁾ (refer to Table 5-6).</p>	
--	--	--

Table 9-2: The effects of antimicrobial agents used for treatment and prevention on the growth and the changes in protein abundance of *S. chartarum*.

	<i>In vitro</i>	Building material	Proteomics
Bleach	Direct application: No growth after two applications at 25000 and 45000 ppm. Agar dilution plate: No growth at 1500 ppm	Effective, no growth recovery on media after three applications at 25000 and 45000 ppm	36 (56%) proteins (mainly involved in stress response, cell wall and growth recovery) decreased in abundance. Mainly ribosomal proteins increased in abundance.
OS	Agar dilution plate: No growth at 5000 ppm using agar dilution plate	Partially effective, no fungal growth observed flat surface (readily exposed to OS) at 2500 ppm	16 (23%) proteins (mainly involved in stress and transport) decreased in abundance. Mainly stress and ribosomal proteins increased in abundance.
AHP	Direct application: Growth observed after two cycles	Ineffective	Not tested
PAA	Direct application: Growth observed after two applications at 8000 ppm (twice the manufacturer's recommendation)	Ineffective	Not tested

OS: organosilane, AHP: aerosolised hydrogen peroxide, PAA: peracetic acid.

9.3 DISCUSSION OF THE MAIN FINDINGS

Mould infestation has led to numerous health concerns particularly in the indoor environment, as well as having an aesthetic impact due to the visible, black pigmentation of some moulds. Among the 'black moulds', the presence of *Stachybotrys* spp. are mostly associated with severe water intrusion problems. *Stachybotrys* spp. produce either trichothecenes or less toxic atronones mycotoxins which can result in potential negative health effects associated with the indoor environment. *S. chartarum* is known as a species complex fungus and it can often be misidentified with its closely related-species, *S. chlorohalonata*. *Stachybotrys chartarum* produces either atronones (chemotypes A) or macrocyclic trichothecenes (chemotypes S), while *S. chlorohalonata* produces only atronones. Although both species could be distinguished by morphological characteristics⁽¹¹⁾, differentiation has proved challenging using either morphological or DNA-based methods⁽⁹⁵⁾. Therefore, a standardised methodology is vital in order to identify *Stachybotrys* spp. faster, less laboriously and with more confidence.

Although moulds such as *A. niger* appear to be black on the surface, they are not necessarily categorised as a dematiaceous fungus. The term dematiaceous refers to fungal colonies with both a dark surface and reverse appearance, such as *S. chartarum*. In general, dematiaceous fungi form a group of melanised, normally slow to moderately growing filamentous fungi or yeast-like fungi. They share several universal characteristics such as being heavily melanised with thick and multi-layered walls resulting in an extraordinary ability to tolerate chemical and physical stresses from harsh surroundings^(213, 348). Melanin also plays a role in fungal pathogenesis and is considered an important virulence factor that protects against host immune mechanisms by neutralising oxygen radicals⁽³⁴⁹⁻³⁵¹⁾. These characteristics have often led to difficulties in many laboratory methods such as DNA and protein extraction and mass spectrometry which require extensive modified protocols^(163, 164, 172, 218).

Mould remediation is a challenging problem in the indoor environment which demands effective strategies⁽⁵⁾. The Environmental Protection Agency⁽³⁵²⁾ has outlined the key steps for mould remediation which includes action on the source of the water problem, removal of hard to clean mouldy items, and drying or cleaning of the site of contamination. Although moisture has been identified as the key to mould infestation, it is quite difficult to intervene as it is also influenced by the natural environment. Fungal resilience continues to be a problem particularly on building materials where various

remediation strategies have been developed and studied through the years including the use of antimicrobial agents. Although they have been tested by the manufacturers, several studies have documented their ineffectiveness when applied in real-life settings. This has been associated with many factors such as different levels of susceptibility among microbes, mode of application of the antimicrobial agent and types of surface being treated ^(87, 190, 302) .

Therefore, this study was designed to fill gaps in current knowledge by aiming:

1. To evaluate various fungal identification methods to characterise *Stachybotrys* species with confidence and be able to distinguish between its closely-related species based on; a) Culture characteristics and microscopy, b) DNA-based PCR and, c) Protein-based MALDI TOF mass spectrometry.
2. To determine the effects of different antimicrobial agents on *S. chartarum* by evaluating their effectiveness to inhibit or prevent growth of *S. chartarum*; a) *In vitro* and; b) On building material and; c) By quantifying the changes in protein expression profiles following exposure to subinhibitory concentrations.

9.3.1 To evaluate various fungal identification methods to characterise *Stachybotrys* species with confidence (and be able to distinguish between its closely-related species)

Due to developments in identification methodology, prior work has documented continuous revision in the identification of *Stachybotrys* spp. since the genus was proposed by Corda in 1837 ⁽⁹⁸⁾. Morphologically, *Stachybotrys* spp. have a distinct feature of conidia aggregated on phialides. *S. chartarum*, which is the most cited *Stachybotrys* spp., has been referred to as 'black mould', and appears as a greenish to black colony when matured ⁽⁹¹⁾.

At the genus level, *Stachybotrys* spp. closely resemble *Memnoniella* spp., morphologically and physiologically ⁽⁹⁹⁾. Although *Stachybotrys* spp. and *Memnoniella* spp. could be distinguished by the arrangement of conidia and differences in the principal toxic metabolites produced ^(99, 137), *Memnoniella* spp. are now considered synonymous with *Stachybotrys* spp. based on the 28S large subunit sequence (LSU) analysis ^(100, 101, 137). At the family level, *Stachybotrys* was classified under *Dematiaceae* until the new family, *Stachybotriaceae* was established by Crous *et al.*⁽³⁵³⁾. The latest report by Lombard *et al.*⁽²²⁹⁾.has revised the family of *Stachybotriaceae* by using multi-locus phylogenetic analysis of the 28S large subunit (LSU), internal transcribed spacer

regions (ITS), RNA polymerase II second largest subunit (*rpb2*), calmodulin (*cmdA*), translation elongation factor 1-alpha (*tef1*) and β -tubulin (*tub2*) genes complemented with morphological characteristics which has resulted in the revision of the identity of a number of isolates used in this study, including CBS 182.80, the strain used in this study (previously known as *S. dichroa*) to *S. chartarum* ⁽²²⁹⁾.

In addition to the taxonomical revision at the family level, *S. chartarum* is closely-related to another species, *S. chlorohalonata*. Previous studies have identified species by using specific primer sets developed from various regions such as the ITS region, protein coding regions of chitin synthase 1 (*chs1*), beta-tubulin 2 (*tub-2*), and trichodiene synthase 5 (*tri5*) ^(12, 102). Haugland *et al.* ⁽¹⁰²⁾ were the first to develop specific primers only for *S. chartarum* based on the ITS region. However, Cruse *et al.* ⁽¹²⁾ then developed *chs1* and *tri5* primers, which could phylogenetically differentiate *S. chartarum* into 2 chemotypes and the newly discovered species, *S. chlorohalonata*, as reported by Andersen *et al.* ⁽¹¹⁾. Subsequently, Black *et al.* ⁽¹⁰⁵⁾ have reported more specificity with *S. chartarum* compared to other common indoor moulds such as *Aspergillus* spp., *Cladosporium* spp. and *Penicillium* spp. using newly developed primers from *tri5* regions. However, the primer specificity at species level could not be assessed since there was no *S. chlorohalonata* or other *Stachybotrys* spp. isolates included in the study.

In chapter 3, we have documented that differences in culture and microscopic characteristics were affected by types of media and incubation temperature. More pigment was produced on ESA compared to PDA, but there was less pigmentation when incubated at 25 °C compared to 30 °C. Characteristics also differed between strains and media, for example, *S. bisbyi* (CBS 363.58) was seen as a white colony on both media, but with a black reverse only on ESA. Whereas, *S. oenantes* (CBS 463.74) grew as white to light brown colonies on PDA but black colonies on both surface and reverse on ESA. These findings show that the differences in culture characteristics of *Stachybotrys* spp. were influenced by media types as well as challenging the concept that *Stachybotrys* spp. are 'black moulds'. Microscopically, it was difficult to differentiate between species since distinctive structures could not be observed in most of the cultures. This highlights the importance of more comprehensive guidelines on the identification of *Stachybotrys* spp. using culture-based methods and the need for more reliable methods to identify *Stachybotrys* spp. with more confidence.

In chapter 4, we employed a DNA-based methods to characterise *Stachybotrys* spp. using ITS/RFLP and mycotoxin specific primers (tri5). The universal primer ITS/RFLP showed the same pattern for both *S. chartarum* and *S. chlorohalonata*. Moreover, sequence analysis of the amplicons did not discriminate between the two species which suggests the choice of primer is not suitable to distinguish between these species. On the other hand, tri5 primers by Black *et al.* and Cruse *et al.* also amplified both species at approximately the same size and with approximately 1-3 bp differences using *in silico* PCR. Therefore, DNA sequencing is required to properly distinguish both species (Cruse primers 94.3% identity; Black primers 92.6% identity). Further analysis of the two published primer sets and our in-house primer set, SC1, showed distinct divergence of both species as shown by the phylogenetic analysis. Sequences of *S. chartarum* chemotypes A and S diverged which is in accordance with Andersen *et al.*⁽¹¹⁾ who found only 1 bp difference between both chemotypes using the Cruse *et al.* primer set. We also found that, one out of five developed primers sets, SC3 could quickly discriminate between *S. chartarum* and *S. chlorohalonata* by giving a product with one and not the other. However, the number of isolates used in this study is quite low and a wide range of isolates is needed to further confirm the reliability of this primer set. The findings conclude that the tri5 gene offers a solution to species misidentification by the ITS1/ITS4 primers and is useful in aiding the specific identification of the *S. chartarum* complex.

Recently, fungal identification has become less laborious, less time-consuming, and with a low operational cost and high specificity by using MALDI-TOF mass spectrometry. In chapter 5, we have developed the MSPs for *S. chartarum* and its related species since they are not available in the current Bruker database. We found that different media for cultivation affects the fungal pigmentation and results in extra peaks at lower molecular weight in mass spectrometry. The standard extraction process was extended with one extra centrifugation step in order to give a more homogeneous extract which eventually led to more reproducible peaks. We have successfully distinguished *S. chartarum* from other species particularly *S. chlorohalonata*, using the Bruker standard method with clearer cut-off points in the scores values for both species compared to previous studies^(106, 107). However, we found that other *Stachybotrys* spp. were in the range below 1.7 (not reliable identification) which is in accordance with a previous study showing the cut-off range of below 1.6⁽¹⁰⁶⁾. The findings conclude that MALDI-TOF can distinguish between *S. chartarum* and *S. chlorohalonata*, but it also requires individual MSPs for other

Stachybotrys species since they were not in the identifiable range against the MSP of *S. chartarum*.

From the findings in chapters 3, 4 and 5, we conclude that each method is useful in identifying *S. chartarum* and its related species. The method of culture and microscopy is useful for early stage screening with the least cost, but it still requires PCR or MALDI-TOF as a confirmatory test. The choice of PCR primers is important for identifying *Stachybotrys* spp.. Since the *tri5* genes are not present in all *Stachybotrys* spp., the universal primer sets are suitable for identification at the genus level. However, the *tri5* primers provides a quick and specific method for identifying *S. chartarum* and *S. chlorohalonata*. On the other hand, MALDI-TOF can differentiate *S. chartarum* and *S. chlorohalonata* but does not give a reliable identification for other *Stachybotrys* species.

9.3.2 To determine the effects of different antimicrobial agents on *S. chartarum*

Various antimicrobial agents have been developed to inhibit microbial growth or kill the microbes. However, several studies have documented the limited efficacies of antimicrobial agents such Cavicide® and 10% Virkon®⁽⁵²⁾, ozone, peroxide, boron-based chemical, ammonium chloride based chemicals, sodium hypochlorite-based chemicals⁽⁵³⁾, gamma irradiation, steam cleaning⁽³⁵⁴⁾, and organosilane⁽¹⁹⁰⁾ on building materials, and have concluded that prevention is always better than cure.

Furthermore, issues of fungal resilience and resistance in the indoor environment are determined by numerous factors, including types of treatment, types of materials and the development of resistance by the fungi. Some building materials are cellulose-based, made up of paper fibres which are not stable and are highly porous and can be easily affected by prolonged exposure to moisture. Moreover, most testing on antimicrobial agents have mostly been carried out *in vitro* which may not be appropriate for real life settings.

Therefore, fungal remediation was investigated by studying the responses of *S. chartarum* to selected antimicrobial agents. In chapters 6 and 7, we have reported the efficacies of 4 types of antimicrobial agents namely Evans Bleach (4-5% sodium hypochlorite), Biosafe® (organosilane), ASP Glosair™ 400 (aerosolised hydrogen peroxide), and Peracide™ (peracetic acid) on *S. chartarum in vitro* and on building material in a simulated environment. In chapter 8, we have reported changes in protein

abundance following the exposure to two different antimicrobial agents used as treatment (sodium hypochlorite) and prevention (organosilane).

In chapter 6, we have assessed the efficacies of antimicrobial agents by observing radial growth on solid media or optical density (absorbance) in liquid media. Higher concentrations than those recommended by the manufacturers' were required to inhibit the growth of *S. chartarum* in the form of established colonies using direct application, whereby only bleach showed fungicidal effects against *S. chartarum* at concentrations of 25000 ppm or 45000 ppm (undiluted) after repeated application. However, lower MICs were obtained from the agar dilution method compared to direct methods for organosilane (OS) and bleach at much lower concentrations of 5000 ppm and 1500 ppm, respectively. This is probably because spores in liquid suspension are more susceptible to antimicrobial agents than established colonies due to higher surface contact with the chemical and lower number of fungal cells. Moreover, OS was effective in completely preventing the growth of *S. chartarum* spores using the agar dilution plate method at a lower concentration than recommended by the manufacturer. From the findings, we conclude that bleach and OS appeared to be effective *in vitro* as treatment and prevention strategies, respectively.

By using the inhibitory concentration derived by the *in vitro* methods, we have assessed the effects of antimicrobial agents on *S. chartarum* grown on gypsum board as described in chapter 7. We found that, bleach applied at least three times in 24 hours intervals was the best method to treat *S. chartarum*-infested gypsum board. Although organosilane was effective at completely preventing fungal growth when assessed with the agar dilution method (chapter 6), it was only partially effective in preventing fungal growth on gypsum board. This may have been due to the uneven porous surface as shown by the electron microscopy images allowing the fungal hyphae to penetrate the board and preventing contact of the OS with some of the fungal mycelium. This indicates the importance of ensuring smooth surfaces in the indoor environment to maximize the effectiveness of antimicrobial coatings. This might be achieved by applying stable antimicrobial paint to avoid exposure of the porous surface. From the findings, we conclude that bleach remains the best method to inhibit fungal growth on gypsum board, but it is also corrosive to the material. Additionally, the use of OS as an antimicrobial coating might be more effective on a smooth and stable surface.

The findings from *in vitro* and environmental studies show that high fungal load reduces the effectiveness of antimicrobial agents. From chapter 6 and 7, we conclude that the

efficacy of antimicrobial agents used is highly dependent on the frequency of treatment, the method of application and the surface area accessible for antimicrobial agents to interact with the fungal spores. Most antimicrobial agents such as AHP are used in combination with physical cleaning to reduce microbial load and increase surface contact which indicates the importance of a cleaning process preceding treatment with antimicrobial agents.

In chapter 8, we have utilised proteomics as a tool to study the response of *S. chartarum* to antimicrobial agents. The proteomic approaches has been used as a tool to understand microbial virulence and resistance mechanisms to abiotic and biotic stresses as it allows large scale analysis of proteins in a whole organism at a given time at specific conditions. However, fungi often present difficulties in protein extraction due to the thick cell wall which is hard to disrupt and the presence of pigments that can interfere with protein separation by electrophoresis and mass spectrometry ⁽¹⁷⁸⁾. Most studies of fungal resistance have applied gel-based proteomics such as 2-dimensional gel electrophoresis (2-DE). Since 2-DE gels separate proteins based on pH and molecular weight, proteins which are too acidic, too basic or too close in sizes may fail to separate adequately which may lead to the presence of multiple proteins in a single spot. Other issues such as low reproducibility and poor representation of lower abundance protein which might play significant roles in the process have also been reported. On the other hand, gel-free proteomics allows multiplexing of several samples at a time which reduces technical biases, and hence increased the reproducibility and reliability of the results ^(355, 356).

By using gel-free proteomics, we have documented the baseline proteins of *S. chartarum* and its responses to antimicrobial treatment with bleach and prevention with OS agents at subinhibitory concentrations. This is the first study, to our knowledge to report baseline proteins of *S. chartarum*, as well as studying its protein changes in response to antimicrobial agents. The method for protein extraction have been optimised due to the presence of melanin by adding precipitation and washing steps followed by a phenol-chloroform extraction. Additional clean-up steps prior to mass spectrometry were included since organosilane is highly hydrophobic causing signal suppression and poor separation.

Since *S. chartarum* has not been well-annotated in UniProtKB/ Swiss-Prot, the TrEMBL database and protein homologues searches in NCBI have been used. Since both antimicrobial agents tested possessed different modes of action, we have observed variations in the protein profiles suggesting different responses towards the agents.

More protein levels were increased following exposure to OS as opposed to bleach treatment which resulted in more decreased protein levels. Stress response-related proteins might have been depleted or consumed as a process of recovery following treatment with bleach. On the other hand, the levels of both stress-related proteins and ribosomal proteins were increased following exposure to OS which suggests the concurrence of defence and growth recovery. From the findings, we conclude that due to differences in protein changes towards bleach (used as treatment) and OS (used as prevention), a combination of antimicrobial agents with different modes of action might provide a more effective way to eliminate fungal growth.

A 'blanket' approach should not just be taken in tackling the problems of failure of remediation strategies. Combination of different agents which inhibit up-regulated enzymes might provide an effective way of eliminating fungus, as these seems crucial in allowing survival of the fungus after exposure to the antimicrobial agents. More research on fungal growth on different substrates and with different antimicrobial agents may provide more understanding on the fungal resilience so that improved remediation action can be taken accordingly.

9.4 RECOMMENDATION AND FUTURE RESEARCH

This study should be a stepping stone for future research in order to improve laboratory techniques and skills as well as to provide knowledge about the application of antimicrobial agents for more effective remediation strategies.

From this study, we have learnt the importance of confirmatory methods to obtain the correct identification especially for less commonly studied moulds such as *S. chartarum*. Although the PCR technique is widely used in most laboratories, it depends very much on the choice of primer sets to meet the specific purpose. In the future, identification of *Stachybotrys* spp. could be performed more systematically using a standardised workflow from the use of universal primers for genus level identification to specific primer for *S. chartarum* and *S. chlorohalonata*.

On the other hand, MALDI-TOF has proven to be a faster and cheaper than PCR, but also gave an accurate identification for *S. chartarum* and *S. chlorohalonata*. However, the reliability and accuracy of the method needs to be improved in the future by expanding the existing manufacturers' databases such as by developing protein

profiles databases for more diverse clinical or environmental isolates from different regions, worldwide.

Moreover, molecular methods such as PCR and MALDI-TOF are still not well established in Asia and therefore, it is timely for them to be applied as soon as possible. Based on a gap analysis survey from 7 Asian countries with 241 participating laboratories conducted in 2016, the Asia Fungal Working Group (2017) has reported only 16.9% and 12.3% laboratories performed DNA sequencing and MALDI-TOF for isolate identification, respectively. The report also highlighted the need for training of manpower in advanced non-culture-based diagnostic tests for fungal diagnosis in Asia ⁽¹⁾.

The ineffectiveness of antimicrobial agents in the indoor environment is quite alarming and the development of newly emerging chemicals might increase range of antifungals suitable for this purpose. More research and development with regard to an effective application strategy or delivery methods are required to complement the antimicrobial agents that are currently available. From this study, we have also learnt that soiled surfaces or high fungal load make antimicrobial agents less effective. We found that fungi were unable to grow on clean water-repellent shower curtains, whereas in real life, fungi can grow on shower curtain contaminated with dirt or soil surface to support its growth. This highlights the importance of surface cleaning by mechanical force prior to application of antimicrobial agents. Furthermore, engineering controls such as improving ventilation and installing dehumidifiers could control indoor humidity and minimise fungal growth.

The choice of building material and its condition are very important right from the beginning. A green building, for instance, uses renewable building material which can also be affected by mould growth, and therefore should be designed to be resistant to fungal infestation ^(357, 358). Prevention of mould growth is equally important. This may be achieved by the application of antimicrobial coating after decontamination of building materials. Materials should be stored in a clean, dry place to avoid from exposure to prolonged moisture which can weaken some building materials. This may impose more cost in the pre-construction phase but could save a lot of money in the long run. Materials that are unstable need to be treated prior to antimicrobial coating to avoid peeling off or non-uniform coverage. Cellulose-based material should be avoided since it provides a substrate for fungal growth and can retain moisture. Damp construction material provides a good reservoir for mould to proliferate and is difficult to treat once the construction has taken place. Application of antimicrobial agents onto materials

normally occurs following mould infestation although construction material is often pre-contaminated with fungi where fungal growth can be initiated once exposed to moisture⁽²⁸⁴⁾. Hence, pre-treatment with a preventative agent would be appropriate.

Since most antimicrobial agents are chemically synthesized and potentially toxic to humans and the environment, it is timely to explore alternative choices which are less toxic and more environmentally-friendly such as using natural products or plant-based antimicrobials in the indoor environment. Bio pesticides such as essential oils have shown to be fungicidal *in vitro*⁽³⁵⁹⁾, and in agriculture⁽³⁶⁰⁾ and these may also be used for fungal remediation in the indoor environment⁽⁵²⁾. The use of air-filtering houseplant such as by National Aeronautics and Space Administration (NASA) has helped to naturally clean up the air from toxic agents such as benzene and formaldehyde. For a more holistic approach in mould remediation and a healthier indoor environment, similar mechanisms could be tested to purify indoor air during or after application of antimicrobial agents⁽³⁶¹⁾.

In conclusion, despite no direct evidence for its pathogenicity in humans, *S. chartarum* plays a significant role in animal husbandry and, if nothing else, has an aesthetic impact on construction materials in damp buildings, rendering its eradication from the indoor environment an important goal. With the development in various techniques in fungal identification, further research would provide more information on the complexity of this fungal species. The application of current antimicrobial agents should be strategized in order to optimise the fungicidal effect and at the same time minimise the harmful effects to humans and the environment.

REFERENCES

1. Chindamporn A, Chakrabarti A, Li R, Sun P-L, Tan B-H, Chua M, et al. Survey of laboratory practices for diagnosis of fungal infection in seven Asian countries: An Asia Fungal Working Group (AFWG) initiative. *Medical Mycology*. 2017;1-10.
2. Andersen B, Frisvad JC, Sondergaard I, Rasmussen IS, Larsen LS. Associations between fungal species and water-damaged building materials. *Applied and Environmental Microbiology*. 2011;77(12):4180-8.
3. Sahlberg B, Gunnbjörnsdóttir M, Soon A, Jogi R, Gislason T, Wieslander G, et al. Airborne molds and bacteria, microbial volatile organic compounds (MVOC), plasticizers and formaldehyde in dwellings in three North European cities in relation to sick building syndrome (SBS). *Sci Total Environ*. 2013;444(Supplement C):433-40.
4. de Carvalho MP, Weich H, Abraham WR. Macrocyclic trichothecenes as antifungal and anticancer compounds. *Curr Med Chem*. 2016;23(1):23-35.
5. WHO. World Health Organisation. Guidelines for indoor air quality: dampness and mould. WHO Regional Office for Europe. Copenhagen, Denmark. 2009. 2009.
6. Centers for Disease Control and Prevention. Indoor environmental quality [Internet]. 2015. Available from: <https://www.cdc.gov/niosh/topics/indoorenv/whatismold.html>.
7. Johanning E, Auger P, Morey PR, Yang CS, Olmsted E. Review of health hazards and prevention measures for response and recovery workers and volunteers after natural disasters, flooding, and water damage: mold and dampness. *Environ Health Prev*. 2014;19(2):93-9.
8. Dumon H, Palot A, Charpin-Kadouch C, Queralt J, Lehtihet K, Garans M, et al. Mold species identified in flooded dwellings. *Aerobiologia*. 2009;25(4):341-4.
9. Bloom E, Grimsley LF, Pehrson C, Lewis J, Larsson L. Molds and mycotoxins in dust from water-damaged homes in New Orleans after hurricane Katrina. *Indoor Air*. 2009;19(2):153-8.
10. Park JH, Cox-Ganser JM, Kreiss K, White SK, Rao CY. Hydrophilic fungi and ergosterol associated with respiratory illness in a water-damaged building. *Environ Health Persp*. 2008;116(1):45-50.
11. Andersen B, Nielsen KF, Thrane U, Szaro T, Taylor JW, Jarvis BB. Molecular and phenotypic descriptions of *Stachybotrys chlorohalonata* sp nov and two chemotypes of *Stachybotrys chartarum* found in water-damaged buildings. *Mycologia*. 2003;95(6):1227-38.
12. Cruse M, Telerant R, Gallagher T, Lee T, Taylor JW. Cryptic species in *Stachybotrys chartarum*. *Mycologia*. 2002;94(5):814-22.
13. Adon MY, Mohamad ZA, Bakon SA, Mohd Fuat Abdul-Razak MF, MA K. Incidence of microbial contamination in a student hostel in Kuala Lumpur: a case study. Poster presented at: Local authority environmental conference. Putrajaya, Malaysia. 2013.
14. Steinemann A, Wargocki P, Rismanchi B. Ten questions concerning green buildings and indoor air quality. *Build Environ*. 2017;112:351-8.

15. Environmental Protection Agency. Why indoor air quality is important to schools [Internet]. 2017. Available from: <https://www.epa.gov/iaq-schools/why-indoor-air-quality-important-schools>.
16. Talbot PHB. Principles of fungal taxonomy. Macmillan Press. London, UK. 1971.
17. Baldauf SL, Palmer JD. Animals and fungi are each others closest relatives - congruent evidence from multiple proteins. P Natl Acad Sci USA. 1993;90(24):11558-62.
18. Deacon JW. Fungal biology, 4 ed: Blackwell Publishing. Oxord, United Kingdom. 2006.
19. Ellringer PJ, Boone K, Hendrickson S. Building materials used in construction can affect indoor fungal levels greatly. AIHAJ - American Industrial Hygiene Association. 2000;61(6):895-9.
20. EPA U. Environmental Protection Agency. Care for your air: a guide to indoor air quality EPA 402/F-08/008. United States. 2008.
21. EPA U. Environmental Protection Agency. Mold remediation in schools and commercial buildings EPA 402-K-01-001. United States. 2008.
22. Hossain MA, Ahmed MS, Ghannoum MA. Attributes of *Stachybotrys chartarum* and its association with human disease. J Allergy Clin Immunol. 2004;113(2):200-8.
23. Gravesen S, Nielsen PA, Iversen R, Nielsen KF. Microfungal contamination of damp buildings-examples of risk constructions and risk materials. Environ Health Persp. 1999;107(Suppl 3):505-8.
24. Haverinen-Shaughnessy U. Prevalence of dampness and mold in European housing stock J Expo Sci Env Epid. 2012;22(6):654-.
25. Mudarri D, Fisk WJ. Public health and economic impact of dampness and mold. Indoor Air. 2007;17(3):226-35.
26. Mendell MJ, Mirer AG, Cheung K, Tong M, Douwes J. Respiratory and allergic health effects of dampness, mold, and dampness-related agents: A review of the epidemiologic evidence. Environ Health Persp. 2011;119(6):748-56.
27. Jaakkola MS, Quansah R, Hugg TT, Heikkinen SAM, Jaakkola JJK. Association of indoor dampness and molds with rhinitis risk: a systematic review and meta-analysis. J Allergy Clin Immun. 2013;132(5):1099-110.e18.
28. Chrystal Palatya, Shum M. Health effects from mould exposure or dampness in indoor environments National Collaborating Centre for Environmental Health; 2012.
29. Borchers AT, Chang C, Eric Gershwin M. Mold and human health: a reality check. Clin Rev Allerg Immu. 2017;52(3):305-22.
30. Miller JD, McMullin DR. Fungal secondary metabolites as harmful indoor air contaminants: 10 years on. Appl Microbiol Biotechnol. 2014;98(24):9953-66.
31. Øya E, Afanou AKJ, Malla N, Uhlig S, Rolen E, Skaar I, et al. Characterization and pro-inflammatory responses of spore and hyphae samples from various mold species. Indoor Air.1-12.
32. Park JH, Cox-Ganser JM. Mold exposure and respiratory health in damp indoor environments. Frontiers in bioscience. 2011;3:757-71.
33. Gunnbjörnsdóttir MI, Franklin KA, Norbäck D, Björnsson E, Gislason D, Lindberg E, et al. Prevalence and incidence of respiratory symptoms in relation to indoor dampness: the RHINE study. Thorax. 2006;61(3):221.
34. Norbäck D, Zock JP, Plana E, Heinrich J, Tischer C, Jacobsen Bertelsen R, et al. Building dampness and mold in European homes in relation to climate, building

characteristics and socio-economic status: The European Community Respiratory Health Survey ECRHS II. *Indoor Air*. 2017;27(5):921-32.

35. Karvala K, Uitti J, Luukkonen R, Nordman H. Quality of life of patients with asthma related to damp and moldy work environments. *Scandinavian Journal of Work, Environment & Health*. 2013;39(1):96-105.

36. Burney PG, Luczynska C, Chinn S, Jarvis D. The European Community Respiratory Health Survey. *Eur Respir J*. 1994;7(5):954-60.

37. Norbäck D, Zock J-P, Plana E, Heinrich J, Svanes C, Sunyer J, et al. Lung function decline in relation to mould and dampness in the home: the longitudinal European Community Respiratory Health Survey ECRHS II. *Thorax*. 2011;66(5):396.

38. Norback D, Zock JP, Plana E, Heinrich J, Svanes C, Sunyer J, et al. Mould and dampness in dwelling places, and onset of asthma: the population-based cohort ECRHS. *Occup Environ Med*. 2013;70(5):325-31.

39. Tham KW, Zuraimi MS, Koh D, Chew FT, Ooi PL. Associations between home dampness and presence of molds with asthma and allergic symptoms among young children in the tropics. *Pediatr Allergy Immu*. 2007;18(5):418-24.

40. Norbäck D, Hashim JH, Cai G-H, Hashim Z, Ali F, Bloom E, et al. Rhinitis, ocular, throat and dermal symptoms, headache and tiredness among students in schools from Johor Bahru, Malaysia: associations with fungal DNA and mycotoxins in classroom dust. *PloS one*. 2016;11(2):e0147996.

41. Karvala K, Uitti J, Luukkonen R, Nordman H. Quality of life of patients with asthma related to damp and moldy work environments. *Scand J Work Env Hea*. 2013;39(1):96-105.

42. Jaakkola JJK, Hwang B-F, Jaakkola N. Home dampness and molds, parental atopy, and asthma in childhood: a six-year population-based cohort study. *Environ Health Persp*. 2005;113(3):357-61.

43. Shorter C, Crane J, Pierse N, Barnes P, Kang J, Wickens K, et al. Indoor visible mold and mold odor are associated with new-onset childhood wheeze in a dose-dependent manner. *Indoor Air*. 1-10.

44. Fisk WJ, Mirer AG, Mendell MJ. Quantitative relationship of sick building syndrome symptoms with ventilation rates. *Indoor Air*. 2009;19(2):159-65.

45. Sahakian N, Park JH, Cox-Ganser J. Respiratory morbidity and medical visits associated with dampness and air-conditioning in offices and homes. *Indoor Air*. 2009;19(1):58-67.

46. Balmes J, Becklake M, Blanc P, Henneberger P, Kreiss K, Mapp C, et al. American Thoracic Society Statement: Occupational contribution to the burden of airway disease. *Am J Resp Crit Care*. 2003;167(5):787-97.

47. Zhang X, Sahlberg B, Wieslander G, Janson C, Gislason T, Norback D. Dampness and moulds in workplace buildings: Associations with incidence and remission of sick building syndrome (SBS) and biomarkers of inflammation in a 10 year follow-up study. *Sci Total Environ*. 2012;430:75-81.

48. Department of Health and Human Services, Centers for Disease Control and Prevention. NIOSH Alert: Preventing occupational respiratory disease from exposures caused by dampness in office buildings, schools, and other nonindustrial buildings publication No. 2013-102. United States of America. 2012.

49. Centers for Disease Control and Prevention. Guidelines for environmental infection control in healthcare facilities. United States of America. 2003.

50. The American Institute of Architects Academy. Guidelines for design and construction of hospitals and healthcare facilities. United States of America. 2001.

51. William A. Rutala, Weber DJ. Guideline for disinfection and sterilization in healthcare facilities. Centers for Disease Control and Prevention. 2017.
52. Rogawansamy S, Gaskin S, Taylor M, Pisaniello D. An Evaluation of Antifungal Agents for the Treatment of Fungal Contamination in Indoor Air Environments. *Int J Env Res Pub He.* 2015;12(6):6319-32.
53. Peitzsch M, Bloom E, Haase R, Must A, Larsson L. Remediation of mould damaged building materials-efficiency of a broad spectrum of treatments. *J Environ Monitor.* 2012;14(3):908-15.
54. Vesper S, Dearborn DG, Yike I, Allan T, Sobolewski J, Hinkley SF, et al. Evaluation of *Stachybotrys chartarum* in the house of an infant with pulmonary hemorrhage: quantitative assessment before, during, and after remediation. *J Urban Health.* 2000;77(1):68-85.
55. Crook B, Burton NC. Indoor moulds, Sick Building Syndrome and building related illness. *British Mycological Society.* 2010;24:8.
56. Joshi SM. The sick building syndrome. *Indian Journal of Occupational and Environmental Medicine.* 2008;12(2):61-4.
57. Vance PH, Weissfeld AS. The controversies surrounding Sick Building Syndrome. *Clinical Microbiology Newsletter* 2007;29(10):4.
58. Morse R, Acker D. Indoor air quality and mold prevention of the building envelope. National Institute of Building Sciences, Washington, DC. United States of America. 2014.
59. Denning DW, O'Driscoll BR, Hogaboam CM, Bowyer P, Niven RM. The link between fungi and severe asthma: a summary of the evidence. *Eur Respir J.* 2006;27(3):615-26.
60. Douwes J. (1→3)-β-D-glucans and respiratory health: a review of the scientific evidence. *Indoor Air.* 2005;15(3):160-9.
61. Rylander R. Indoor air-related effects and airborne (1 → 3)-beta-D-glucan. *Environ Health Persp.* 1999;107(Suppl 3):501-3.
62. Tischer C, Gehring U, Chen C-M, Kerkhof M, Koppelman G, Sausenthaler S, et al. Respiratory health in children, and indoor exposure to (1,3)-β-glucan, EPS mould components and endotoxin. *Eur Respir J.* 2011;37(5):1050-9.
63. Gregory L, Rand TG, Dearborn D, Yike I, Vesper S. Immunocytochemical localization of stachylysin in *Stachybotrys chartarum* spores and spore-impacted mouse and rat lung tissue. *Mycopathologia.* 2003;156(2):109-17.
64. Vesper SJ, Vesper MJ. Stachylysin may be a cause of hemorrhaging in humans exposed to *Stachybotrys chartarum*. *Infect Immun.* 2002;70(4):2065-9.
65. Vesper SJ, Dearborn DG, Yike I, Sorenson WG, Haugland RA. Hemolysis, toxicity, and randomly amplified polymorphic DNA analysis of *Stachybotrys chartarum* strains. *Appl Environ Microbiol.* 1999;65(7):3175-81.
66. Vesper SJ, Magnuson ML, Dearborn DG, Yike I, Haugland RA. Initial characterization of the hemolysin stachylysin from *Stachybotrys chartarum*. *Infection and Immunity.* 2001;69(2):912-6.
67. Gao PF, Korley F, Martin J, Chen BT. Determination of unique microbial volatile organic compounds produced by five *Aspergillus* species commonly found in problem buildings. *Aihaj.* 2002;63(2):135-40.
68. Gao P, Martin J. Volatile metabolites produced by three strains of *Stachybotrys chartarum* cultivated on rice and gypsum board. *Appl Occup Environ Hyg.* 2002;17(6):430-6.
69. Wolkoff P, Nielsen GD. Organic compounds in indoor air - their relevance for perceived indoor air quality? *Atmos Environ.* 2001;35(26):4407-17.

70. Bennett JW, Inamdar AA. Are some fungal volatile organic compounds (VOCs) mycotoxins? *Toxins*. 2015;7(9):3785-804.
71. Haugland RA, Heckman JL, Wymer LJ. Evaluation of different methods for the extraction of DNA from fungal conidia by quantitative competitive PCR analysis. *J Microbiol Meth*. 1999;37(2):165-76.
72. Bennett JW, Klich M. Mycotoxins. *Clinical Microbiology Reviews*. 2003;16(3):497-516.
73. Diener UL, Cole RJ, Sanders TH, Payne GA, Lee LS, Klich MA. Epidemiology of aflatoxin formation by *Aspergillus flavus*. *Ann Rev Phytopathol*. 1987;25:249-70.
74. Spensley PC. Aflatoxin, the active principle in turkey 'X' disease. *Endeavour*. 1963;22:75-9.
75. Kiessling KH. Biochemical mechanism of action of mycotoxins. *Pure Appl Chem* 1986. p. 327.
76. Pestka JJ, Yike I, Dearborn DG, Ward MD, Harkema JR. *Stachybotrys chartarum*, trichothecene mycotoxins, and damp building-related illness: new insights into a public health enigma. *Toxicol Sci*. 2008;104(1):4-26.
77. McCormick SP, Stanley AM, Stover NA, Alexander NJ. Trichothecenes: from simple to complex mycotoxins. *Toxins*. 2011;3(7):802-14.
78. Robbins CA, Swenson LJ, Nealley ML, Gots RE, Kelman BJ. Health effects of mycotoxins in indoor air: a critical review. *Appl Occup Environ Hyg*. 2000;15(10):773-84.
79. Jarvis BB, Miller JD. Mycotoxins as harmful indoor air contaminants. *Appl Microbiol Biot*. 2005;66(4):367-72.
80. Miller JD, Rand TG, Jarvis BB. *Stachybotrys chartarum*: cause of human disease or media darling? *Med Mycol*. 2003;41(4):271-91.
81. Semeiks J, Borek D, Otwinowski Z, Grishin NV. Comparative genome sequencing reveals chemotype-specific gene clusters in the toxigenic black mold *Stachybotrys*. *BMC genomics*. 2014;15:590.
82. Isaac S. How do fungi degrade and obtain nutrients from cellulose? *Mycologist*. 1997;11(2):92-3.
83. Nielsen KF, Hansen MO, Larsen TO, Thrane U. Production of trichothecene mycotoxins on water damaged gypsum boards in Danish buildings. *Int Biodeter Biodegr*. 1998;42(1):1-7.
84. Chakravarty P, Kovar B. Evaluation of five antifungal agents used in remediation practices against six common indoor fungal species. *Journal of Occupational and Environmental Hygiene*. 2013;10(1):D11-D6.
85. Cochrane VW. Dormancy in spores of fungi. *T Am Microsc Soc*. 1974;93(4):599-609.
86. Feofilova EP, Ivashechkin AA, Alekhin AI, Sergeeva YE. Fungal spores: dormancy, germination, chemical composition and role in biotechnology (review). *Appl Biochem Micro+*. 2012;48(1):1-11.
87. Murtoniemi T, Nevalainen A, Hirvonen MR. Effect of plasterboard composition on *Stachybotrys chartarum* growth and biological activity of spores. *Appl Environ Microbiol*. 2003;69(7):3751-7.
88. Snelders E, Veld RAGHI, Rijs AJMM, Kema GHJ, Melchers WJG, Verweij PE. Possible environmental origin of resistance of *Aspergillus fumigatus* to medical triazoles. *Applied and Environmental Microbiology*. 2009;75(12):4053-7.

89. Verweij PE, Snelders E, Kema GHJ, Mellado E, Melchers WJG. Azole resistance in *Aspergillus fumigatus*: a side-effect of environmental fungicide use? *Lancet Infect Dis*. 2009;9(12):789-95.
90. Deising HB, Reimann S, Pascholati SF. Mechanisms and significance of fungicide resistance. *Braz J Microbiol*. 2008;39(2):286-95.
91. Larone D. *Medically important fungi: A guide to identification*, 5 ed. ASM Press. Washington DC, United States of America. 2011.
92. Domsch KH, Gams W, Anderson TH. *Compendium of Soil Fungi*: Academic Press; 1981. 860 p.
93. Izabel TDSS, Barbosa FR, Marques MFO, Da Cruz ACR, Ferreira SML, Gusmão LFP. The genus *Stachybotrys* (anamorphic fungi) in the semi-arid region of Brazil. *Brazilian Journal of Botany*. 2010;33(3):9.
94. Andersen B, Nielsen KF, Jarvis BB. Characterization of *Stachybotrys* from water-damaged buildings based on morphology, growth, and metabolite production. *Mycologia*. 2002;94(3):392-403.
95. Li DW, Yang CS. Taxonomic history and current status of *Stachybotrys chartarum* and related species. *Indoor Air*. 2005;15 Suppl 9:5-10.
96. Koster B, Scott J, Wong B, Malloch D, Straus N. A geographically diverse set of isolates indicates two phylogenetic lineages within *Stachybotrys chartarum*. *Can J Bot*. 2003;81(6):633-43.
97. Brasel TL, Martin JM, Carriker CG, Wilson SC, Straus DC. Detection of airborne *Stachybotrys chartarum* macrocyclic trichothecene mycotoxins in the indoor environment. *Applied and Environmental Microbiology*. 2005;71(11):7376-88.
98. Bisby GR. Mycological nomenclature. *Phytopathology*. 1942;32(7):644-5.
99. Jong SC, Davis EE. Contribution to the knowledge of *Stachybotrys* and *Memmoniella* in culture. *Mycotaxon*. 1976;III(3):77.
100. Haugland RA, Vesper SJ, Harmon SM. Phylogenetic relationships of *Memmoniella* and *Stachybotrys* species and evaluation of morphological features for *Memmoniella* species identification. *Mycologia*. 2001;93(1):54-65.
101. Wang Y, Hyde KD, McKenzie EHC, Jiang YL, Li DW, Zhao DG. Overview of *Stachybotrys* (*Memmoniella*) and current species status. *Fungal Divers*. 2015;71(1):17-83.
102. Haugland RA, Heckman JL. Identification of putative sequence specific PCR primers for detection of the toxigenic fungal species *Stachybotrys chartarum*. *Mol Cell Probes*. 1998;12(6):387-96.
103. Dean TR, Kohan M, Betancourt D, Menetrez MY. A simple polymerase chain reaction/restriction fragment length polymorphism assay capable of identifying medically relevant filamentous fungi. *Molecular biotechnology*. 2005;31(1):21-7.
104. Cruz-Perez P, Buttner MP, Stetzenbach LD. Specific detection of *Stachybotrys chartarum* in pure culture using quantitative polymerase chain reaction. *Mol Cell Probes*. 2001;15(3):129-38.
105. Black JA, Dean TR, Foarde K, Menetrez M. Detection of *Stachybotrys chartarum* using rRNA, tri5, and beta-tubulin primers and determining their relative copy number by real-time PCR. *Mycol Res*. 2008;112(Pt 7):845-51.
106. Gruenwald M, Rabenstein A, Remesch M, Kuever J. MALDI-TOF mass spectrometry fingerprinting: A diagnostic tool to differentiate dematiaceous fungi *Stachybotrys chartarum* and *Stachybotrys chlorohalonata*. *J Microbiol Meth*. 2015;115:83-8.

107. Ulrich S, Biermaier B, Bader O, Wolf G, Straubinger RK, Didier A, et al. Identification of *Stachybotrys* spp. by MALDI-TOF mass spectrometry. *Analytical and Bioanalytical Chemistry*. 2016;408(27):7565-81.
108. Selke SBC. Distribution and occurrence of *Stachybotrys chartarum* in North Central Florida habitats. University of Florida. 2007.
109. Page EH, Trout DB. The role of *Stachybotrys* mycotoxins in building-related illness. *AIHAJ*. 2001;62(5):644-8.
110. Nielsen KF, Holm G, Uttrup LP, Nielsen PA. Mould growth on building materials under low water activities. Influence of humidity and temperature on fungal growth and secondary metabolism. *Int Biodeter Biodegr*. 2004;54(4):325-36.
111. Grant IWB. The sick building syndrome. *Brit Med J*. 1985;290(6464):321.
112. Frazer S, Magan N, Aldred D. The influence of water activity and temperature on germination, growth and sporulation of *Stachybotrys chartarum* strains. *Mycopathologia*. 2011;172(1):17-23.
113. Dosen I, Andersen B, Phippen CBW, Clausen G, Nielsen KF. *Stachybotrys* mycotoxins: from culture extracts to dust samples. *Analytical and Bioanalytical Chemistry*. 2016;408(20):5513-26.
114. Rocchi S, Reboux G, Frossard V, Scherer E, Valot B, Laboissiere A, et al. Microbiological characterization of 3193 French dwellings of Elfe cohort children. *Sci Total Environ*. 2015;505:1026-35.
115. Penttinen P, Pelkonen J, Huttunen K, Toivola M, Hirvonen MR. Interactions between *Streptomyces californicus* and *Stachybotrys chartarum* can induce apoptosis and cell cycle arrest in mouse RAW264.7 macrophages. *Toxicol Appl Pharmacol*. 2005;202(3):278-88.
116. Doggett MS. Characterization of fungal biofilms within a municipal water distribution system. *Applied and Environmental Microbiology*. 2000;66(3):1249-51.
117. Chapman JA. *Stachybotrys chartarum* (*chartarum* = *atra* = *alternans*) and other problems caused by allergenic fungi. *Allergy Asthma Proc*. 2003;24(1):1-7.
118. Koster B, Wong B, Straus N, Malloch D. A multi-gene phylogeny for *Stachybotrys* evidences lack of trichodiene synthase (*tri5*) gene for isolates of one of three intrageneric lineages. *Mycological Research*. 2009;113:877-86.
119. Jarvis BB. *Stachybotrys chartarum*: a fungus for our time. *Phytochemistry*. 2003;64(1):53-60.
120. Drobotko VG. Stachybotryotoxicosis. A new disease of horses and humans. *American Review of Soviet Medicine*. 1945;2(3):238-42.
121. Schumaier G, Creek RD, Devolt HM, Laffer NC. Stachybotryotoxicosis of chicks. *Poultry Sci*. 1963;42(1):70-&.
122. Schneider DJ, Marasas WFO, Dalekuys JC, Kriek NPJ, Vanschalkwyk GC. Field outbreak of suspected stachybotryotoxicosis in sheep. *Journal of the South African Veterinary Association-Tydskrif Van Die Suid-Afrikaanse Veterinere Vereniging*. 1979;50(2):73-81.
123. Harrach B, Danko G, Cseh G, Benko M. Isolation of macrocyclic trichothecenes from straw associated with death of calves (stachybotryotoxicosis). *Magy Allatorvosok*. 1982;37(12):808-9.
124. Szemerédi G. Domestic occurrence of stachybotryotoxicosis in dogs. Case report. *Magy Allatorvosok*. 2005;127(12):727-32.
125. Prigent N, Bailly S, Kammerer M. Stachybotryotoxicosis in cattle - about a case. *J Vet Pharmacol Ther*. 2015;38:39-.

126. Pestka JJ, Yike I, Dearborn DG, Ward MDW, Harkema JR. *Stachybotrys chartarum*, trichothecene mycotoxins, and damp building-related illness: New insights into a public health enigma. *Toxicol Sci.* 2008;104(1):4-26.
127. Yike I, Miller MJ, Sorenson WG, Walenga R, Tomaszewski JF, Jr., Dearborn DG. Infant animal model of pulmonary mycotoxicosis induced by *Stachybotrys chartarum*. *Mycopathologia.* 2002;154(3):139-52.
128. Yike I, Rand TG, Dearborn DG. Acute inflammatory responses to *Stachybotrys chartarum* in the lungs of infant rats: time course and possible mechanisms. *Toxicol Sci.* 2005;84(2):408-17.
129. Ebling PM. Effectiveness of sodium hypochlorite against spores of *Penicillium brevicompactum* in an insect rearing facility. *Natural Resources Canada.* 2007.
130. Islam Z, Harkema JR, Pestka JJ. Satratoxin G from the black mold *Stachybotrys chartarum* evokes olfactory sensory neuron loss and inflammation in the murine nose and brain. *Environ Health Persp.* 2006;114(7):1099-107.
131. Carey SA, Plopper CG, Hyde DM, Islam Z, Pestka JJ, Harkema JR. Satratoxin-G from the black mold *Stachybotrys chartarum* induces rhinitis and apoptosis of olfactory sensory neurons in the nasal airways of rhesus monkeys. *Toxicol Pathol.* 2012;40(6):887-98.
132. Huttunen K, Pelkonen J, Nielsen KF, Nuutinen U, Jussila J, Hirvonen MR. Synergistic interaction in simultaneous exposure to *Streptomyces californicus* and *Stachybotrys chartarum*. *Environ Health Perspect.* 2004;112(6):659-65.
133. Nielsen KF. Mycotoxin production by indoor molds. *Fungal Genetics and Biology.* 2003;39(2):103-17.
134. da Rocha MEB, Freire FDO, Maia FBF, Guedes MIF, Rondina D. Mycotoxins and their effects on human and animal health. *Food Control.* 2014;36(1):159-65.
135. Croft WA, Jarvis BB, Yatawara CS. Airborne outbreak of trichothecene toxicosis. *Atmospheric Environment (1967).* 1986;20(3):549-52.
136. Etzel RA, Montana E, Sorenson WG, Kullman GJ, Allan TM, Dearborn DG. Acute pulmonary hemorrhage in infants associated with exposure to *Stachybotrys atra* and other fungi. *Arch Pediat Adol Med.* 1998;152(8):757-62.
137. Jarvis BB, Sorenson WG, Hintikka EL, Nikulin M, Zhou YH, Jiang J, et al. Study of toxin production by isolates of *Stachybotrys chartarum* and *Memnoniella echinata* isolated during a study of pulmonary hemosiderosis in infants. *Applied and Environmental Microbiology.* 1998;64(10):3620-5.
138. Montaña E, Etzel RA, Allan T, Horgan TE, Dearborn DG. Environmental risk factors associated with pediatric idiopathic pulmonary hemorrhage and hemosiderosis in a Cleveland community. *Pediatrics.* 1997;99(1):e5.
139. Centers for Disease Control and Prevention. Update: pulmonary hemorrhage/hemosiderosis among infants—Cleveland, Ohio, 1993-1996. *JAMA.* 2000;283(15):1951-3.
140. Dearborn DG, Smith PG, Dahms BB, Allan TM, Sorenson WG, Montana E, et al. Clinical profile of 30 infants with acute pulmonary hemorrhage in Cleveland. *Pediatrics.* 2002;110(3):627.
141. Mussalo-Rauhamaa H, Nikulin M, Koukila-Kahkola P, Hintikka EL, Malmberg M, Haahtela T. Health effects of residents exposed to *Stachybotrys* in water-damaged houses in Finland. *Indoor Built Environ.* 2010;19(4):476-85.
142. Thrasher JD, Hooper DH, Taber J. Family of six, their health and the death of a 16 month old male from pulmonary hemorrhage: identification of mycotoxins and mold in the home and lungs, liver and brain of deceased infant. *Global Journal of Medical Research.* 2014;14(5):1-12.

143. Terr AI. Sick Building Syndrome: is mould the cause? *Medical Mycology*. 2009;47:S217-S22.
144. Brandt M, Brown C, Burkhart J, Burton N, Cox-Ganser J, Damon S, et al. Mold Prevention Strategies and Possible Health Effects in the Aftermath of Hurricanes and Major Floods. *Morbidity and Mortality Weekly Report: Recommendations and Reports*. 2006;55(8):1-CE-4.
145. Aleksic B, Draghi M, Ritoux S, Bailly S, Lacroix M, Oswald IP, et al. Aerosolization of Mycotoxins after Growth of Toxinogenic Fungi on Wallpaper. *Applied and Environmental Microbiology*. 2017;83(16).
146. Jarvis B, Hinkley S, Nielsen K. *Stachybotrys*: an unusual mold associated with water-damaged buildings. *Mycotoxin Res*. 2000;16 Suppl 1:105-8.
147. Betancourt DA, Krebs K, Moore SA, Martin SM. Microbial volatile organic compound emissions from *Stachybotrys chartarum* growing on gypsum wallboard and ceiling tile. *BMC Microbiol*. 2013;13:283.
148. Posteraro B, De Carolis E, Vella A, Sanguinetti M. MALDI-TOF mass spectrometry in the clinical mycology laboratory: identification of fungi and beyond. *Expert review of proteomics*. 2013;10(2):151-64.
149. Ellis D, Davis S, Alexious H, Handke R, Bartley R. Descriptions of medical fungi. Published by the Authors. Underdale, South Australia 2007.
150. Watanabe T. Pictorial atlas of soil and seed fungi 2 ed. CRC Press. United States of America. 2002.
151. Leck A. Preparation of lactophenol cotton blue slide mounts. *Community eye health / International Centre for Eye Health*. 1999;12(30):24.
152. Guarín FA, Abril MAQ, Alvarez A, Fonnegra R. Atmospheric pollen and spore content in the urban area of the city of Medellin, Colombia. *Hoehnea*. 2015;42:9-19.
153. Mullis KB, Faloona FA. Specific synthesis of DNA *in vitro* via a polymerase-catalyzed chain reaction. *Methods in Enzymology Academic Press* 1987. 155. p. 335-50.
154. Valones MAA, Guimarães RL, Brandão LAC, de Souza PRE, de Albuquerque Tavares Carvalho A, Crovela S. Principles and applications of polymerase chain reaction in medical diagnostic fields: a review. *Braz J Microbiol*. 2009;40(1):1-11.
155. van Oorschot RA, Ballantyne KN, Mitchell RJ. Forensic trace DNA: a review. *Investigative Genetics*. 2010;1(1):14.
156. Thomsen PF, Willerslev E. Environmental DNA – An emerging tool in conservation for monitoring past and present biodiversity. *Biological Conservation*. 2015;183(Supplement C):4-18.
157. Untergasser A, Nijveen H, Rao X, Bisseling T, Geurts R, Leunissen JAM. Primer3Plus, an enhanced web interface to Primer3. *Nucleic Acids Res*. 2007;35(suppl 2):W71-W4.
158. Carbone I, Kohn LM. A method for designing primer sets for speciation studies in filamentous ascomycetes. *Mycologia*. 1999;91(3):553-6.
159. Abd-Elsalam KA, Aly IN, Abdel-Satar M, Khalil MS, Verreet JA. PCR identification of *Fusarium* genus based on nuclear ribosomal-DNA sequence data *African Journal of Biotechnology*. 2003;2(4):4.
160. Martin KJ, Rygielwicz PT. Fungal-specific PCR primers developed for analysis of the ITS region of environmental DNA extracts. *BMC Microbiology*. 2005;5.
161. Niessen L, Schmidt H, Vogel RF. The use of *tri5* gene sequences for PCR detection and taxonomy of trichothecene-producing species in the *Fusarium* section *Sporotrichiella*. *Int J Food Microbiol*. 2004;95(3):305-19.

162. Bellemain E, Carlsen T, Brochmann C, Coissac E, Taberlet P, Kauserud H. ITS as an environmental DNA barcode for fungi: an *in silico* approach reveals potential PCR biases. *BMC Microbiology*. 2010;10:189-.
163. Black JA, Foarde KK. Comparison of four different methods for extraction of *Stachybotrys chartarum* spore DNA and verification by real-time PCR. *J Microbiol Methods*. 2007;70(1):75-81.
164. Eckhart L, Bach J, Ban J, Tschachler E. Melanin binds reversibly to thermostable DNA polymerase and inhibits its activity. *Biochem Biophys Res Commun*. 2000;271(3):726-30.
165. Leli C, Cenci E, Cardaccia A, Moretti A, D'Alo F, Pagliochini R, et al. Rapid identification of bacterial and fungal pathogens from positive blood cultures by MALDI-TOF MS. *Int J Med Microbiol*. 2013;303(4):205-9.
166. Buchan BW, Ledebor NA. Advances in identification of clinical yeast isolates by use of matrix-assisted laser desorption/ionization–time of flight mass spectrometry. *Journal of clinical microbiology*. 2013;51(5):1359-66.
167. Lau AF, Drake SK, Calhoun LB, Henderson CM, Zelazny AM. Development of a clinically comprehensive database and a simple procedure for identification of molds from solid media by matrix-assisted laser desorption/ionization–time of flight mass spectrometry. *Journal of clinical microbiology*. 2013;51(3):828-34.
168. Sanguinetti M, Posteraro B. Identification of molds by matrix-assisted laser desorption/ionization–time of flight mass spectrometry. *Journal of clinical microbiology*. 2017;55(2):369-79.
169. Kemptner J, Marchetti-Deschmann M, Mach R, Druzhinina IS, Kubicek CP, Allmaier G. Evaluation of matrix-assisted laser desorption/ionization (MALDI) preparation techniques for surface characterization of intact *Fusarium* spores by MALDI linear time-of-flight mass spectrometry. *Rapid communications in mass spectrometry : RCM*. 2009;23(6):877-84.
170. Normand AC, Cassagne C, Ranque S, L'Ollivier C, Fourquet P, Roesems S, et al. Assessment of various parameters to improve MALDI-TOF MS reference spectra libraries constructed for the routine identification of filamentous fungi. *BMC Microbiology*. 2013;13.
171. Hettick JM, Green BJ, Buskirk AD, Slaven JE, Kashon ML, Beezhold DH. Discrimination of fungi by MALDI-TOF mass spectrometry. *ACS Symposium Series*. 2011;1065:35-50.
172. Buskirk AD, Hettick JM, Chipinda I, Law BF, Siegel PD, Slaven JE, et al. Fungal pigments inhibit the matrix-assisted laser desorption/ionization time-of-flight mass spectrometry analysis of darkly pigmented fungi. *Analytical Biochemistry*. 2011;411(1):122-8.
173. Goldstein JE, Zhang L, Borrer CM, Rago JV, Sandrin TR. Culture conditions and sample preparation methods affect spectrum quality and reproducibility during profiling of *Staphylococcus aureus* with matrix-assisted laser desorption/ionization time-of-flight mass spectrometry. *Lett Appl Microbiol*. 2013;57(2):144-50.
174. Bhadauria V, Zhao WS, Wang LX, Zhang Y, Liu JH, Yang J, et al. Advances in fungal proteomics. *Microbiological research*. 2007;162(3):193-200.
175. Kim Y, Nandakumar MP, Marten MR. Proteome map of *Aspergillus nidulans* during osmoadaptation. *Fungal Genet Biol*. 2007;44(9):886-95.
176. Grinyer J, Hunt S, McKay M, Herbert BR, Nevalainen H. Proteomic response of the biological control fungus *Trichoderma atroviride* to growth on the cell walls of *Rhizoctonia solani*. *Current Genetics*. 2005;47(6):381-8.

177. Graves PR, Haystead TAJ. Molecular biologist's guide to proteomics. *Microbiology and Molecular Biology Reviews*. 2002;66(1):39-63.
178. Bianco L, Perrotta G. Methodologies and perspectives of proteomics applied to filamentous fungi: from sample preparation to secretome analysis. *Int J Mol Sci*. 2015;16(3):5803-29.
179. Hooshdaran MZ, Barker KS, Hilliard GM, Kusch H, Morschhauser J, Rogers PD. Proteomic analysis of azole resistance in *Candida albicans* clinical isolates. *Antimicrob Agents Ch*. 2004;48(7):2733-5.
180. Gautam P, Shankar J, Madan T, Sirdeshmukh R, Sundaram CS, Gade WN, et al. Proteomic and transcriptomic analysis of *Aspergillus fumigatus* on exposure to amphotericin b. *Antimicrob Agents Ch*. 2008;52(12):4220-7.
181. Tang J, Liu LX, Huang XL, Li YY, Chen YP, Chen J. Proteomic analysis of *Trichoderma atroviride* mycelia stressed by organophosphate pesticide dichlorvos. *Canadian Journal of Microbiology*. 2010;56(2):121-7.
182. Russell AD. Mechanisms of antimicrobial action of antiseptics and disinfectants: an increasingly important area of investigation. *The Journal of antimicrobial chemotherapy*. 2002;49(4):597-9.
183. McDonnell G, Russell AD. Antiseptics and disinfectants: Activity, action, and resistance. *Clinical Microbiology Reviews*. 1999;12(1):147-79.
184. Fukuzaki S. Mechanisms of actions of sodium hypochlorite in cleaning and disinfection processes. *Biocontrol Science*. 2006;11(4):147-57.
185. World Health Organization. Annex G Use of disinfectants: alcohol and bleach. In: *Infection prevention and control of epidemic- and pandemic-prone acute respiratory infections in healthcare*. WHO Guidelines Approved by the Guidelines Review Committee. Geneva. 2014.
186. Reynolds KA, Boone S, Bright KR, Gerba CP. Occurrence of household mold and efficacy of sodium hypochlorite disinfectant. *Journal of Occupational and Environmental Hygiene*. 2012;9(11):663-9.
187. Gottenbos B, van der Mei HC, Klatter F, Nieuwenhuis P, Busscher HJ. *In vitro* and *in vivo* antimicrobial activity of covalently coupled quaternary ammonium silane coatings on silicone rubber. *Biomaterials*. 2002;23(6):1417-23.
188. Oosterhof JJH, Buijssen KJDA, Busscher HJ, van der Laan BFAM, van der Mei HC. Effects of quaternary ammonium silane coatings on mixed fungal and bacterial biofilms on tracheoesophageal shunt prostheses. *Applied and Environmental Microbiology*. 2006;72(5):3673-7.
189. Murray PR, Niles AC, Heeren RL. Microbial inhibition on hospital garments treated with Dow Corning 5700 antimicrobial agent. *Journal of clinical microbiology*. 1988;26(9):1884-6.
190. Boyce JM, Havill NL, Guercia KA, Schweon SJ, Moore BA. Evaluation of two organosilane products for sustained antimicrobial activity on high-touch surfaces in patient rooms. *American journal of infection control*. 2014;42(3):326-8.
191. Finnegan M, Linley E, Denyer SP, McDonnell G, Simons C, Maillard J-Y. Mode of action of hydrogen peroxide and other oxidizing agents: differences between liquid and gas forms. *J Antimicrob Chemoth*. 2010;65(10):2108-15.
192. Linley E, Denyer SP, McDonnell G, Simons C, Maillard J-Y. Use of hydrogen peroxide as a biocide: new consideration of its mechanisms of biocidal action. *J Antimicrob Chemoth*. 2012;67(7):1589-96.
193. Fu TY, Gent P, Kumar V. Efficacy, efficiency and safety aspects of hydrogen peroxide vapour and aerosolized hydrogen peroxide room disinfection systems. *J Hosp Infect*. 2012;80(3):199-205.

194. Kitis M. Disinfection of wastewater with peracetic acid: a review. *Environ Int.* 2004;30(1):47-55.
195. Wagner M, Brumelis D, Gehr R. Disinfection of wastewater by hydrogen peroxide or peracetic acid: development of procedures for measurement of residual disinfectant and application to a physicochemically treated municipal effluent. *Water Environ Res.* 2002;74(1):33-50.
196. Crow S. Peracetic acid sterilization: A timely development for a busy healthcare industry. *Infection Control* 2016;13(2):111-3.
197. Cristofari-Marquand E, Kacel M, Milhe F, Magnan A, Lehucher-Michel M-P. Asthma caused by peracetic acid-hydrogen peroxide mixture. *J Occup Health.* 2007;49(2):155-8.
198. Azmi OR, Seppelt RD. Fungi of the Windmill islands, continental Antarctica. Effect of temperature, pH and culture media on the growth of selected microfungi. *Polar Biol.* 1997;18(2):128-34.
199. Sharma G, Pandey R. Influence of culture media on growth, colony character and sporulation of fungi isolated from decaying vegetable wastes. *Journal of Yeast and Fungal Research.* 2010;1(8):157-64.
200. Wheeler KA, Hurdman BF, Pitt JI. Influence of pH on the growth of some toxigenic species of *Aspergillus*, *Penicillium* and *Fusarium*. *Int J Food Microbiol.* 1991;12(2-3):141-50.
201. Taner S, Pekey B, Pekey H. Fine particulate matter in the indoor air of barbeque restaurants: Elemental compositions, sources and health risks. *Sci Total Environ.* 2013;454:79-87.
202. Li SX, Hartman GL, Jarvis BB, Tak H. A *Stachybotrys chartarum* isolate from soybean. *Mycopathologia.* 2002;154(1):41-9.
203. Lichtenstein JHR, Molina RM, Donaghey TC, Amuzie CJ, Pestka JJ, Coull BA, et al. Pulmonary responses to *Stachybotrys chartarum* and its toxins: Mouse strain affects clearance and macrophage cytotoxicity. *Toxicol Sci.* 2010;116(1):113-21.
204. Sigma-Aldrich. Sabouraud glucose agar with chloramphenicol. 2013.
205. HealthLink. Sabouraud dextrose agar. . 2007.
206. Becton, Dickinson and Company. Sabouraud Dextrose Agar, Emmons. 2006.
207. Frazer S. Characterisation of *Stachybotrys chartarum* from water damaged buildings. Cranfield Health. Cranfield. 2011.
208. American Type Culture Collection. *Stachybotrys chartarum* (ATCC® 16026™).
209. Biermaier B, Gottschalk C, Schwaiger K, Gareis M. Occurrence of *Stachybotrys chartarum* chemotype S in dried culinary herbs. *Mycotoxin Res.* 2015;31(1):23-32.
210. Foladi S, Hedayati MT, Shokohi T, Mayahi S. Study on fungi in archives of offices, with a particular focus on *Stachybotrys chartarum*. *Journal De Mycologie Medicale.* 2013;23(4):242-6.
211. Andersen B, Nissen AT. Evaluation of media for detection of *Stachybotrys* and *Chaetomium* species associated with water-damaged buildings. *Int Biodeter Biodegr.* 2000;46(2):111-6.
212. Billups R, Warden P, Fallon K, Parent J. Mycologic genera specific selective agar and method of manufacture. US Patent Application Publication. 2002.
213. Eisenman HC, Casadevall A. Synthesis and assembly of fungal melanin. *Appl Microbiol Biot.* 2012;93(3):931-40.

214. Babitha S, Soccol CR, Pandey A. Effect of stress on growth, pigment production and morphology of *Monascus* sp in solid cultures. *J Basic Microb.* 2007;47(2):118-26.
215. Bata A, Harrach B, Ujszászi K, Kis-Tamás A, Lásztity R. Macrocyclic trichothecene toxins produced by *Stachybotrys atra* strains isolated in Middle Europe. *Applied and Environmental Microbiology.* 1985;49(3):678-81.
216. Harrach B, Bata A, Bajmocy E, Benko M. Isolation of Satratoxins from the Bedding Straw of a Sheep Flock with Fatal Stachybotryotoxicosis. *Applied and Environmental Microbiology.* 1983;45(5):1419-22.
217. Straus DC, Wilson SC. Respirable trichothecene mycotoxins can be demonstrated in the air of *Stachybotrys chartarum*-contaminated buildings. *J Allergy Clin Immunol.* 2006;118(3):760; author reply 7-8.
218. Griffin DW, Kellogg CA, Peak KK, Shinn EA. A rapid and efficient assay for extracting DNA from fungi. *Lett Appl Microbiol.* 2002;34(3):210-4.
219. Sunde M, Kwan AHY, Templeton MD, Beaver RE, Mackay JP. Structural analysis of hydrophobins. *Micron.* 2008;39(7):773-84.
220. Fredricks DN, Smith C, Meier A. Comparison of six DNA extraction methods for recovery of fungal DNA as assessed by quantitative PCR. *Journal of clinical microbiology.* 2005;43(10):5122-8.
221. Diguta CF, Vincent B, Guilloux-Benatier M, Alexandre H, Rousseaux S. PCR ITS-RFLP: A useful method for identifying filamentous fungi isolates on grapes. *Food microbiology.* 2011;28(6):1145-54.
222. Vancov T, Keen B. Amplification of soil fungal community DNA using the ITS86F and ITS4 primers. *Fems Microbiol Lett.* 2009;296(1):91-6.
223. Gardes M, Bruns TD. ITS primers with enhanced specificity for basidiomycetes--application to the identification of mycorrhizae and rusts. *Mol Ecol.* 1993;2(2):113-8.
224. Robert V, Vu D, Amor ABH, van de Wiele N, Brouwer C, Jabas B, et al. MycoBank gearing up for new horizons. *IMA Fungus.* 2013;4(2):371-9.
225. Federhen S. The NCBI Taxonomy database. *Nucleic Acids Res.* 2012;40(Database issue):D136-D43.
226. Aleksic B, Bailly S, Draghi M, Pestka JJ, Oswald IP, Robine E, et al. Production of four macrocyclic trichothecenes by *Stachybotrys chartarum* during its development on different building materials as measured by UPLC-MS/MS. *Build Environ.* 2016;106:265-73.
227. Gareis M, Gottschalk C. *Stachybotrys* spp. and the guttation phenomenon. *Mycotoxin Research.* 2014;30(3):151-9.
228. Peltola J, Niessen L, Nielsen KF, Jarvis BB, Andersen B, Salkinoja-Salonen M, et al. Toxigenic diversity of two different RAPD groups of *Stachybotrys chartarum* isolates analyzed by potential for trichothecene production and for boar sperm cell motility inhibition. *Can J Microbiol.* 2002;48(11):1017-29.
229. Lombard L, Houbraken J, Decock C, Samson RA, Meijer M, Reblova M, et al. Generic hyper-diversity in *Stachybotriaceae*. *Persoonia.* 2016;36:156-246.
230. Wieser A, Schneider L, Jung J, Schubert S. MALDI-TOF MS in microbiological diagnostics—identification of microorganisms and beyond (mini review). *Appl Microbiol Biot.* 2012;93(3):965-74.
231. Yu B, Zhang C. *In Silico* PCR analysis. In: Yu B, Hinchcliffe M, editors. *In silico* tools for gene discovery Humana Press Totowa, NJ 2011. p. 91-107.
232. Watal C, Oberoi JK, Goel N, Raveendran R, Khanna S. Matrix-assisted laser desorption ionization time of flight mass spectrometry (MALDI-TOF MS) for rapid

identification of micro-organisms in the routine clinical microbiology laboratory. *Eur J Clin Microbiol.* 2017;36(5):807-12.

233. Bille E, Dauphin B, Leto J, Bougnoux ME, Beretti JL, Lotz A, et al. MALDI-TOF MS Andromas strategy for the routine identification of bacteria, mycobacteria, yeasts, *Aspergillus* spp. and positive blood cultures. *Clinical microbiology and infection : the official publication of the European Society of Clinical Microbiology and Infectious Diseases.* 2012;18(11):1117-25.

234. Clark AE, Kaleta EJ, Arora A, Wolk DM. Matrix-assisted laser desorption ionization–time of flight mass spectrometry: A fundamental shift in the routine practice of clinical microbiology. *Clinical Microbiology Reviews.* 2013;26(3):547-603.

235. Levesque S, Dufresne PJ, Soualhine H, Domingo MC, Bekal S, Lefebvre B, et al. A side by side comparison of Bruker biotyper and VITEK MS: utility of MALDI-TOF MS technology for microorganism identification in a public health reference laboratory. *PloS one.* 2015;10(12):e0144878.

236. Singhal N, Kumar M, Kanaujia PK, Viridi JS. MALDI-TOF mass spectrometry: an emerging technology for microbial identification and diagnosis. *Front Microbiol.* 2015;6:791.

237. Singh A, Singh PK, Kumar A, Chander J, Khanna G, Roy P, et al. Molecular and Matrix-Assisted Laser Desorption Ionization-Time of Flight Mass Spectrometry-Based Characterization of Clinically Significant Melanized Fungi in India. *Journal of clinical microbiology.* 2017;55(4):1090-103.

238. Hettick JM, Green BJ, Buskirk AD, Kashon ML, Slaven JE, Janotka E, et al. Discrimination of *Aspergillus* isolates at the species and strain level by matrix-assisted laser desorption/ionization time-of-flight mass spectrometry fingerprinting. *Analytical Biochemistry.* 2008;380(2):276-81.

239. Ferreira L, Sanchez-Juanes F, Vega M, Gonzalez M, Garcia MI, Rodriguez S, et al. Identification of fungal clinical isolates by matrix-assisted laser desorption ionization-time-of-flight mass spectrometry. *Revista espanola de quimioterapia : publicacion oficial de la Sociedad Espanola de Quimioterapia.* 2013;26(3):193-7.

240. Schulthess B, Ledermann R, Mouttet F, Zbinden A, Bloemberg GV, Böttger EC, et al. Use of the Bruker MALDI biotyper for identification of molds in the clinical mycology laboratory. *Journal of clinical microbiology.* 2014;52(8):2797-803.

241. Normand AC, Cassagne C, Gautier M, Becker P, Ranque S, Hendrickx M, et al. Decision criteria for MALDI-TOF MS-based identification of filamentous fungi using commercial and in-house reference databases. *BMC Microbiology.* 2017;17.

242. Lewis JS, Graybill JR. Fungicidal versus fungistatic: what"s in a word? *Expert Opin Pharmacol.* 2008;9(6):927-35.

243. Graybill JR, Burgess DS, Hardin TC. Key issues concerning fungistatic versus fungicidal drugs. *Eur J Clin Microbiol.* 1997;16(1):42-50.

244. Galvan M, Gonzalez S, Cohen CL, Alonizan FA, Chen CTL, Rich SK, et al. Periodontal effects of 0.25% sodium hypochlorite twice-weekly oral rinse. A pilot study. *J Periodontal Res.* 2014;49(6):696-702.

245. De Nardo R, Chiappe V, Gomez M, Romanelli H, Slots J. Effects of 0.05% sodium hypochlorite oral rinse on supragingival biofilm and gingival inflammation. *Int Dent J.* 2012;62(4):208-12.

246. Stambullian J, Rossotti D, Fridman D, Luchetti P, Cheade Y, Stamboulian D. Efficacy of five disinfectants to reduce bacterial load in the household. *Medicina-Buenos Aire.* 2011;71(3):218-24.

247. Martyny JW, Harbeck RJ, Barker EA, Sills M, Silveira L, Arbuckle S, et al. Aerosolized sodium hypochlorite inhibits viability and allergenicity of mold on building materials. *J Allergy Clin Immunol*. 2005;116(3):630-5.
248. Lantagne DS. Sodium hypochlorite dosage for household and emergency water treatment. *J Am Water Works Ass*. 2008;100(8):106.
249. Advisory Committee on Dangerous Pathogens. Management of Hazard Group 4 viral haemorrhagic fevers and similar human infectious diseases of high consequence. Department of Health, United Kingdom. 2015.
250. Evans Vanodine International. Evans Bleach MSDS. . 2015.
251. Boyce JM. Modern technologies for improving cleaning and disinfection of environmental surfaces in hospitals. *Antimicrob Resist In*. 2016;5.
252. Hall L, Otter JA, Chewins J, Wengenack NL. Use of hydrogen peroxide vapor for deactivation of *Mycobacterium tuberculosis* in a biological safety cabinet and a room. *Journal of clinical microbiology*. 2007;45(3):810-5.
253. Kimura T. Effective decontamination of laboratory animal rooms with vapour-phase ("vaporized") hydrogen peroxide and peracetic acid. *Scand J Lab Anim Sci*. 2012;39(1):17-23.
254. Ukuku DO. Effect of hydrogen peroxide treatment on microbial quality and appearance of whole and fresh-cut melons contaminated with *Salmonella* spp. *Int J Food Microbiol*. 2004;95(2):137-46.
255. Pedahzur R, Lev O, Fattal B, Shuval HI. The interaction of silver ions and hydrogen peroxide in the inactivation of *E. coli*: a preliminary evaluation of a new long acting residual drinking water disinfectant. *Water Sci Technol*. 1995;31(5):123-9.
256. Koburger T, Below H, Dornquast T, Kramer A. Decontamination of room air and adjoining wall surfaces by nebulizing hydrogen peroxide. *GMS Krankenhaushygiene interdisziplinär*. 2011;6(1):9.
257. Davies A, Pottage T, Bennett A, Walker J. Gaseous and air decontamination technologies for *Clostridium difficile* in the healthcare environment. *J Hosp Infect*. 2011;77(3):199-203.
258. Rutala WA, Weber DJ. Disinfectants used for environmental disinfection and new room decontamination technology. *American journal of infection control*. 2013;41(5):S36-S41.
259. Joseph LM, Koon TT, Man WS. Antifungal effects of hydrogen peroxide and peroxidase on spore germination and mycelial growth of *Pseudocercospora* species. *Can J Bot*. 1998;76(12):2119-24.
260. Polo-Lopez MI, Garcia-Fernandez I, Oller I, Fernandez-Ibanez P. Solar disinfection of fungal spores in water aided by low concentrations of hydrogen peroxide. *Photoch Photobio Sci*. 2011;10(3):381-8.
261. Szymanska J. Antifungal efficacy of hydrogen peroxide in dental unit waterline disinfection. *Ann Agr Env Med*. 2006;13(2):313-7.
262. Cerioni L, Rapisarda VA, Hilal M, Prado FE, Rodriguez-Montelongo L. Synergistic antifungal activity of sodium hypochlorite, hydrogen peroxide, and cupric sulfate against *Penicillium digitatum*. *J Food Protect*. 2009;72(8):1660-5.
263. Venturini ME, Blanco D, Oria R. *In vitro* antifungal activity of several antimicrobial compounds against *Penicillium expansum*. *J Food Protect*. 2002;65(5):834-9.
264. Moore A, Nannapaneni R, Kiess A, Sharma CS. Evaluation of USDA approved antimicrobials on the reduction of *Salmonella* and *Campylobacter* in ground chicken frames and their effect on meat quality. *Poultry Sci*. 2017;96(7):2385-92.

265. Kaskova A, Ondrasovicova O, Vargova M, Ondrasovic M, Venglovsky J. Application of peracetic acid and quarternary ammonium disinfectants as a part of sanitary treatment in a poultry house and poultry processing plant. *Zoonoses and public health*. 2007;54(3-4):125-30.
266. Krizman P, Kovac F, Tavcer PF. Bleaching of cotton fabric with peracetic acid in the presence of different activators. *Color Technol*. 2005;121(6):304-9.
267. Sky Chemicals (UK) Ltd. Peracide: A new product effective against *Clostridium difficile* 027 spores. 2012. [Available from: <http://www.skychemicals.co.uk/content/19-peracide-c-difficile-027>].
268. Sky Chemicals (UK) Ltd. Peracide information pack. 2012. [Available from: <http://www.skychemicals.co.uk>].
269. Abd-Alla M.A., M.M. Abd- El- Kader, F. Abd-El-Kareem, ElMohamedy RSR. Evaluation of lemongrass, thyme and peracetic acid against gray mold of strawberry fruits. *Journal of Agricultural Technology* 2011; 7 (6):1775-87.
270. María V. Kyanko, Mara L. Russo, Mariela Fernández, Pose G. Effectiveness of peracetic acid on fungal spores reduction of moulds causing rotting in fruits and vegetables. *Información tecnológica*. 2010;21(4):125-30.
271. Thierry Materne, François de Buyl, Gerald L. Witucki. *Organosilane Technology in Coating Applications: Review and Perspectives*. USA: Dow Corning Corporation; 2012.
272. Torkelson AA, da Silva AK, Love DC, Kim JY, Alper JP, Coox B, et al. Investigation of quaternary ammonium silane-coated sand filter for the removal of bacteria and viruses from drinking water. *J Appl Microbiol*. 2012;113(5):1196-207.
273. Baxa D, Shetron-Rama L, Golembieski M, Golembieski M, Jain S, Gordon M, et al. *In vitro* evaluation of a novel process for reducing bacterial contamination of environmental surfaces. *American journal of infection control*. 2011;39(6):483-7.
274. Hyvarinen A, Meklin T, Vepsalainen A, Nevalainen A. Fungi and actinobacteria in moisture-damaged building materials - concentrations and diversity. *Int Biodeter Biodegr*. 2002;49(1):27-37.
275. Menetrez MY, Foarde KK, Webber TD, Betancourt D, Dean T. Growth response of *Stachybotrys chartarum* to moisture variation on common building materials. *Indoor Built Environ*. 2004;13(3):183-7.
276. Kuhn R, Trimble M, Hofer V, Lee M, Nassof R. Prevalence and airborne spore levels of *Stachybotrys* spp. in 200 houses with water incursions in Houston, Texas. *Canadian Journal of Microbiology*. 2005;51(1):25-8.
277. Charpin D, Boutin-Forzano S, Chabbi S, Dumon H, Charpin-Kadouch C. Wall relative humidity: a simple and reliable index for predicting *Stachybotrys chartarum* infestation in dwellings. *B Acad Nat Med Paris*. 2005;189(1):43-51.
278. Environmental Protection Agency. A brief guide to mold, moisture and your home EPA 402-K-02-003. United States of America. 2012.
279. Menetrez MY, Foarde KK, Webber TD, Dean TR, Betancourt DA. Mold growth on gypsum wallboard-a summary of three techniques. *J Environ Health*. 2009;72(1):24-8.
280. Menetrez MY, Foarde K, Webber TD, Dean R, Betancourt DA. Testing antimicrobial paint efficacy on gypsum wallboard contaminated with *Stachybotrys chartarum*. *Journal of Occupational and Environmental Hygiene*. 2008;5(2):63-6.
281. Wagner A, Hoffman M, Green CF, Barth E, Davidson C, Gibbs SG, et al. Inactivation of *Stachybotrys chartarum* grown on gypsum board using aerosolized chemical agents. *J Environ Eng Sci*. 2006;5(1):75-9.

282. Lewinska AM, Hoof JB, Peuhkuri RH, Rode C, Lilje O, Foley M, et al. Visualization of the structural changes in plywood and gypsum board during the growth of *Chaetomium globosum* and *Stachybotrys chartarum*. *J Microbiol Meth.* 2016;129:28-38.
283. Nikulin M, Pasanen AL, Berg S, Hintikka EL. *Stachybotrys atra* growth and toxin production in some building-materials and fodder under different relative humidities. *Applied and Environmental Microbiology.* 1994;60(9):3421-4.
284. Andersen B, Dosen I, Lewinska AM, Nielsen KF. Pre-contamination of new gypsum wallboard with potentially harmful fungal species. *Indoor Air.* 2017;27(1):6-12.
285. Zock JP, Plana E, Anto JM, Benke G, Blanc PD, Carosso A, et al. Domestic use of hypochlorite bleach, atopic sensitization, and respiratory symptoms in adults. *J Allergy Clin Immun.* 2009;124(4):731-8.
286. Hostynek JJ, Wilhelm KP, Cua AB, Maibach HI. Irritation factors of sodium-hypochlorite solutions in human skin. *Contact Dermatitis.* 1990;23(5):316-24.
287. Jakobsson SW, Rajs J, Jonsson JA, Persson H. Poisoning with sodium-hypochlorite solution - report of a fatal case, supplemented with an experimental and clinico-epidemiologic study. *Am J Foren Med Path.* 1991;12(4):320-7.
288. Benga L, Benten WPM, Engelhardt E, Gougoula C, Schulze-Robbecke R, Sager M. Survival of bacteria of laboratory animal origin on cage bedding and inactivation by hydrogen peroxide vapour. *Lab Anim-Uk.* 2017;51(4):412-21.
289. Horn K, Otter JA. Hydrogen peroxide vapor room disinfection and hand hygiene improvements reduce *Clostridium difficile* infection, methicillin-resistant *Staphylococcus aureus*, vancomycin-resistant *Enterococci*, and extended-spectrum beta-lactamase. 2015;43(12):1354-6.
290. Ali S, Muzslay M, Bruce M, Jeanes A, Moore G, Wilson AP. Efficacy of two hydrogen peroxide vapour aerial decontamination systems for enhanced disinfection of methicillin-resistant *Staphylococcus aureus*, *Klebsiella pneumoniae* and *Clostridium difficile* in single isolation rooms. *J Hosp Infect.* 2016;93(1):70-7.
291. Holmdahl T, Lanbeck P, Wullt M, Walder MH. A head-to-head comparison of hydrogen peroxide vapor and aerosol room decontamination systems. *Infect Control Hosp Epidemiol.* 2011;32(9):831-6.
292. Meszaros JE, Antloga K, Justi C, Plesnicher C, McDonnell G. Area fumigation with hydrogen peroxide vapor. *Applied Biosafety.* 2005;10(2):91-100.
293. Schreier TM, Rach JJ, Howe GE. Efficacy of formalin, hydrogen peroxide, and sodium chloride on fungal-infected rainbow trout eggs. *Aquaculture.* 1996;140(4):323-31.
294. Kitanchaen N, Yamamoto A, Hatai K. Fungicidal effect of hydrogen peroxide on fungal infection of rainbow trout eggs. *Mycoscience.* 1997;38(4):375-8.
295. Rogers JV, Sabourin CL, Choi YW, Richter WR, Rudnicki DC, Riggs KB, et al. Decontamination assessment of *Bacillus anthracis*, *Bacillus subtilis*, and *Geobacillus stearothermophilus* spores on indoor surfaces using a hydrogen peroxide gas generator. *J Appl Microbiol.* 2005;99(4):739-48.
296. Lemmen S, Scheithauer S, Hafner H, Yezli S, Mohr M, Otter JA. Evaluation of hydrogen peroxide vapor for the inactivation of nosocomial pathogens on porous and nonporous surfaces. 2015;43(1):82-5.
297. Environmental Protection Agency. Prevention, pesticides and toxic substance: Peroxy compounds EPA-738-F-93-026. United States of America. 1993.
298. Gursoy NC, Dayioglu H. Evaluating peracetic acid bleaching of cotton as an environmentally safe alternative to hypochlorite bleaching. *Text Res J.* 2000;70(6):475-80.

299. Saby S, Vidal A, Suty H. Resistance of *Legionella* to disinfection in hot water distribution systems. *Water Sci Technol*. 2005;52(8):15.
300. Milne NJ. Oxygen bleaching systems in domestic laundry. *J Surfactants Deterg*. 1998;1(2):253-61.
301. Straus DL, Meinelt T, Farmer BD, Mitchell AJ. Peracetic acid is effective for controlling fungus on channel catfish eggs. *Journal of fish diseases*. 2012;35(7):505-11.
302. Russell AD. Similarities and differences in the responses of microorganisms to biocides. *The Journal of antimicrobial chemotherapy*. 2003;52(5):750-63.
303. Eissa ME, Abd El Naby M, Beshir MM. Bacterial vs. fungal spore resistance to peroxygen biocide on inanimate surfaces. *Bulletin of Faculty of Pharmacy, Cairo University*. 2014;52(2):219-24.
304. Cadnum JL, Jencson AL, O'Donnell MC, Flannery ER, Nerandzic MM, Donskey CJ. An increase in healthcare-associated *Clostridium difficile* infection associated with use of a defective peracetic acid-based surface disinfectant. *Infect Cont Hosp Ep*. 2017;38(3):300-5.
305. Gelest, Inc. Organosilane antimicrobials. United States of America.
306. Howard G Ohlhausen, Ludwig JH, inventors Cleaning and multifunctional coating composition containing an organosilane quaternary compound and hydrogen peroxide. US Patent US 6,994,890 B2. 2006.
307. Vacher S, Hernandez C, Bartschi C, Poussereau N. Impact of paint and wall-paper on mould growth on plasterboards and aluminum. *Build Environ*. 2010;45(4):916-21.
308. Sorgo AG, Heilmann CJ, Dekker HL, Bekker M, Brul S, de Koster CG, et al. Effects of fluconazole on the secretome, the wall proteome, and wall integrity of the clinical fungus *Candida albicans*. *Eukaryot Cell*. 2011;10(8):1071-81.
309. Gautam P, Upadhyay SK, Hassan W, Madan T, Sirdeshmukh R, Sundaram CS, et al. Transcriptomic and proteomic profile of *Aspergillus fumigatus* on exposure to artemisinin. *Mycopathologia*. 2011;172(5):331-46.
310. Knudsen GM, Holch A, Gram L. Subinhibitory concentrations of antibiotics affect stress and virulence gene expression in *Listeria monocytogenes* and cause enhanced stress sensitivity but do not affect Caco-2 cell invasion. *J Appl Microbiol*. 2012;113(5):1273-86.
311. Arana DM, Nombela C, Pla J. Fluconazole at subinhibitory concentrations induces the oxidative- and nitrosative-responsive genes TRR1, GRE2 and YHB1, and enhances the resistance of *Candida albicans* to phagocytes. *The Journal of antimicrobial chemotherapy*. 2010;65(1):54-62.
312. Tesei D, Marzban G, Marchetti-Deschmann M, Tafer H, Arcalis E, Sterflinger K. Proteome of tolerance fine-tuning in the human pathogen black yeast *Exophiala dermatitidis*. *Journal of proteomics*. 2015;128:39-57.
313. Wu X, Xiong E, Wang W, Scali M, Cresti M. Universal sample preparation method integrating trichloroacetic acid/acetone precipitation with phenol extraction for crop proteomic analysis. *Nature protocols*. 2014;9(2):362-74.
314. McCarthy J, Hopwood F, Oxley D, Laver M, Castagna A, Righetti PG, et al. Carbamylation of proteins in 2-D electrophoresis - Myth or reality? *J Proteome Res*. 2003;2(3):239-42.
315. Thermo Scientific. Instructions iodoacetamide, single-use. 2009.
316. Wang Y, Yang F, Gritsenko MA, Wang Y, Clauss T, Liu T, et al. Reversed-phase chromatography with multiple fraction concatenation strategy for proteome profiling of human MCF10A cells. *Proteomics*. 2011;11(10):2019-26.
317. Crawley MJ. *The R Book*: Wiley Publishing; 2012. 1076 p.

318. Mi H, Muruganujan A, Casagrande JT, Thomas PD. Large-scale gene function analysis with the PANTHER classification system. *Nature protocols*. 2013;8:1551.
319. Mi H, Muruganujan A, Thomas PD. PANTHER in 2013: modeling the evolution of gene function, and other gene attributes, in the context of phylogenetic trees. *Nucleic Acids Res*. 2013;41(Database issue):D377-D86.
320. Mi H, Thomas P. PANTHER Pathway: An Ontology-Based Pathway Database Coupled with Data Analysis Tools. In: Nikolsky Y, Bryant J, editors. *Protein Networks and Pathway Analysis*. Totowa, NJ: Humana Press; 2009. p. 123-40.
321. Adams DJ. Fungal cell wall chitinases and glucanases. *Microbiology+*. 2004;150(Pt 7):2029-35.
322. Ikeda M, Kihara A, Igarashi Y. Lipid asymmetry of the eukaryotic plasma membrane: functions and related enzymes. *Biol Pharm Bull*. 2006;29(8):1542-6.
323. Khomtchouk BB, Van Booven DJ, Wahlestedt C. HeatmapGenerator: high performance RNAseq and microarray visualization software suite to examine differential gene expression levels using an R and C++ hybrid computational pipeline. *Source Code for Biology and Medicine*. 2014;9(1):30.
324. Bourgeois C, Kuchler K. Fungal pathogens—a sweet and sour treat for toll-like receptors. *Frontiers in Cellular and Infection Microbiology*. 2012;2:142.
325. Isola D, Marzban G, Selbmann L, Onofri S, Laimer M, Sterflinger K. Sample preparation and 2-DE procedure for protein expression profiling of black microcolonial fungi. *Fungal Biol*. 2011;115(10):971-7.
326. Fic E, Kedracka-Krok S, Jankowska U, Pirog A, Dziedzicka-Wasylewska M. Comparison of protein precipitation methods for various rat brain structures prior to proteomic analysis. *Electrophoresis*. 2010;31(21):3573-9.
327. Lakshman DK, Natarajan SS, Lakshman S, Garrett WM, Dhar AK. Optimized protein extraction methods for proteomic analysis of *Rhizoctonia solani*. *Mycologia*. 2008;100(6):867-75.
328. Rajalingam D, Loftis C, Xu JJ, Kumar TKS. Trichloroacetic acid-induced protein precipitation involves the reversible association of a stable partially structured intermediate. *Protein Sci*. 2009;18(5):980-93.
329. Méchin V, Damerval C, Zivy M. Total protein extraction with TCA-acetone. In: Thiellement H, Zivy M, Damerval C, Méchin V, editors. *Plant Proteomics: Methods and Protocols*. Totowa, NJ: Humana Press; 2007. p. 1-8.
330. Online etymology dictionary. Last accessed 11/02/2014. 2014. [Available from: <http://www.etymonline.com/>].
331. Mi H, Muruganujan A, Casagrande JT, Thomas PD. Large-scale gene function analysis with the PANTHER classification system. *Nat Protocols*. 2013;8(8):1551-66.
332. Carberry S, Neville CM, Kavanagh KA, Doyle S. Analysis of major intracellular proteins of *Aspergillus fumigatus* by MALDI mass spectrometry: identification and characterisation of an elongation factor 1B protein with glutathione transferase activity. *Biochem Biophys Res Commun*. 2006;341(4):1096-104.
333. Winter J, Ilbert M, Graf PCF, Özcelik D, Jakob U. Bleach activates a redox-regulated chaperone by oxidative protein unfolding. *Cell*. 2008;135(4):691-701.
334. McKenna SM, Davies KJ. The inhibition of bacterial growth by hypochlorous acid. Possible role in the bactericidal activity of phagocytes. *Biochemical Journal*. 1988;254(3):685-92.
335. Isquith AJ, Abbott EA, Walters PA. Surface-bonded antimicrobial activity of an organosilicon quaternary ammonium chloride. *Applied Microbiology*. 1972;24(6):859-63.

336. Yamada H, Takahashi N, Okuda S, Tsuchiya Y, Morisaki H. Direct observation and analysis of bacterial growth on an antimicrobial surface. *Appl Environ Microbiol.* 2010;76(16):5409-14.
337. Gkana EN, Doulgeraki AI, Chorianopoulos NG, Nychas G-JE. Anti-adhesion and anti-biofilm potential of organosilane nanoparticles against foodborne pathogens. *Front Microbiol.* 2017;8(1295).
338. Moore LD, Le T, Fan G. DNA methylation and its basic function. *Neuropsychopharmacology.* 2013;38(1):23-38.
339. Glisovic T, Bachorik JL, Yong J, Dreyfuss G. RNA-binding proteins and post-transcriptional gene regulation. *Febs Lett.* 2008;582(14):1977-86.
340. Saloheimo M, Pakula TM. The cargo and the transport system: secreted proteins and protein secretion in *Trichoderma reesei* (*Hypocrea jecorina*). *Microbiology+.* 2012;158(Pt 1):46-57.
341. Ponts N. Mycotoxins are a component of *Fusarium graminearum* stress-response system. *Front Microbiol.* 2015;6:1234.
342. Ilyas S, Rehman A, Varela AC, Sheehan D. Redox proteomics changes in the fungal pathogen *Trichosporon asahii* on arsenic exposure: identification of protein responses to metal-induced oxidative stress in an environmentally-sampled isolate. *PLoS one.* 2014;9(7).
343. Sugiyama K, Niki TP, Inokuchi K, Teranishi Y, Ueda M, Tanaka A. Heterologous expression of metabotropic glutamate receptor subtype 1 in *Saccharomyces cerevisiae*. *Appl Microbiol Biot.* 2004;64(4):531-6.
344. Brodhagen M, Keller NP. Signalling pathways connecting mycotoxin production and sporulation. *Mol Plant Pathol.* 2006;7(4):285-301.
345. Kinnersley AM, Turano FJ. Gamma aminobutyric acid (GABA) and plant responses to stress. *Critical Reviews in Plant Sciences.* 2000;19(6):479-509.
346. Kumar S, Punekar NS. The metabolism of 4-aminobutyrate (GABA) in fungi. *Mycological Research.* 1997;101(4):403-9.
347. Mead O, Thynne E, Winterberg B, Solomon PS. Characterising the role of GABA and its metabolism in the wheat pathogen *Stagonospora nodorum*. *PLoS one.* 2013;8(11).
348. Gow NAR, Latge JP, Munro CA. The fungal cell wall: Structure, biosynthesis, and function. *Microbiology spectrum.* 2017;5(3).
349. Liu GY, Nizet V. Color me bad: microbial pigments as virulence factors. *Trends Microbiol.* 2009;17(9):406-13.
350. Revankar SG. Dematiaceous fungi. *Sem Resp Crit Care M.* 2004;25(2):183-9.
351. Schnitzler N, Peltroche-Llacsahuanga H, Bestier N, Zundorf J, Lutticken R, Haase G. Effect of melanin and carotenoids of *Exophiala (Wangiella) dermatitidis* on phagocytosis, oxidative burst, and killing by human neutrophils. *Infect Immun.* 1999;67(1):94-101.
352. Environmental Protection Agency. Mold Remediation in schools and commercial buildings. EPA 402-K-01-001. United States of America. 2008.
353. Crous PW, Shivas RG, Quaedvlieg W, van der Bank M, Zhang Y, Summerell BA, et al. Fungal planet description sheets: 214-280. *Persoonia.* 2014;32:184-306.
354. Wilson SC, Brasel TL, Carriker CG, Fortenberry GD, Fogle MR, Martin JM, et al. An investigation into techniques for cleaning mold-contaminated home contents. *Journal of Occupational and Environmental Hygiene.* 2004;1(7):442-7.
355. Abdallah C, Dumas-Gaudot E, Renaut J, Sergeant K. Gel-based and gel-free quantitative proteomics approaches at a glance. *International Journal of Plant Genomics.* 2012;2012:17.

356. Thompson A, Schäfer J, Kuhn K, Kienle S, Schwarz J, Schmidt G, et al. Tandem mass tags: a novel quantification strategy for comparative analysis of complex protein mixtures by MS/MS. *Anal Chem.* 2003;75(8):1895-904.
357. Coombs K, Vesper S, Green BJ, Yermakov M, Reponen T. Fungal microbiomes associated with green and non-green building materials. *Int Biodeter Biodegr.* 2017;125(Supplement C):251-7.
358. Hoang CP, Kinney KA, Corsi RL, Szaniszlo PJ. Resistance of green building materials to fungal growth. *Int Biodeter Biodegr.* 2010;64(2):104-13.
359. Hammer KA, Carson CF, Riley TV. *In vitro* activity of *Melaleuca alternifolia* (tea tree) oil against dermatophytes and other filamentous fungi. *J Antimicrob Chemoth.* 2002;50(2):195-9.
360. Yoon M-Y, Cha B, Kim J-C. Recent trends in studies on botanical fungicides in agriculture. *The Plant Pathology Journal.* 2013;29(1):1-9.
361. Claudio L. Planting healthier indoor air. *Environ Health Persp.* 2011;119(10):a426-a7.

APPENDICES

Chapter 4 : Identification of *Stachybotrys* species using DNA-based methods

Appendix 4-A: NCBI search for *tri5* gene sequence used for alignments

Locus	Definition	Length (bp)
AF053926.1	<i>S. chartarum</i> trichodiene synthase (TRI5) gene, complete cds	1514
AF329103.1	<i>S. chartarum</i> trichodiene synthase (TRI5) gene, complete cds	1227
AY095981.1	<i>S. chartarum</i> strain B14 trichodiene synthase (<i>tri5</i>) gene, partial cds	410
AY095982.1	<i>S. chartarum</i> strain J1 trichodiene synthase (<i>tri5</i>) gene, partial cds	410
AY095983.1	<i>S. chartarum</i> strain B18 trichodiene synthase (<i>tri5</i>) gene, partial cds	410
AY095984.1	<i>S. chartarum</i> strain B6 trichodiene synthase (<i>tri5</i>) gene, partial cds	410
AY180274.1	<i>S. chartarum</i> strain ATCC 26303 trichodiene synthase (<i>tri5</i>) gene, partial cds	409
AY180275.1	<i>S. chartarum</i> strain UAMH 6715 trichodiene synthase (<i>tri5</i>) gene, partial cds	409
AY180276.2	<i>S. chartarum</i> strain ATCC 16026 trichodiene synthase (<i>tri5</i>) gene, partial cds	704
EU288799.1	<i>S. chartarum</i> isolate 13 trichodiene synthase (<i>tri5</i>) gene, partial cds	485
EU288800.1	<i>S. chartarum</i> isolate 22 trichodiene synthase (<i>tri5</i>) gene, partial cds	485
EU288801.1	<i>S. chartarum</i> isolate 17 trichodiene synthase (<i>tri5</i>) gene, partial cds	485
EU288802.1	<i>S. chartarum</i> isolate 23 trichodiene synthase (<i>tri5</i>) gene, partial cds	485
EU288803.1	<i>S. chartarum</i> isolate 01 trichodiene synthase (<i>tri5</i>) gene, partial cds	485
EU288805.1	<i>S. chartarum</i> isolate 11 trichodiene synthase (<i>tri5</i>) gene, partial cds	485
EU288804.1	<i>S. chartarum</i> isolate 19 trichodiene synthase (<i>tri5</i>) gene,	485

Appendices

	partial cds	
EU288806.1	<i>S. chartarum</i> isolate 14 trichodiene synthase (tri5) gene, partial cds	485
EU288807.1	<i>S. chartarum</i> isolate 21 trichodiene synthase (tri5) gene, partial cds	485
EU288808.1	<i>S. chartarum</i> isolate 24 trichodiene synthase (tri5) gene, partial cds	485
EU288809.1	<i>S. chartarum</i> isolate 36 trichodiene synthase (tri5) gene, partial cds	485
EU288810.1	<i>S. chartarum</i> isolate 48 trichodiene synthase (tri5) gene, partial cds	485
EU288811.1	<i>S. chartarum</i> isolate 34 trichodiene synthase (tri5) gene, partial cds	485
EU288812.1	<i>S. chartarum</i> isolate 41 trichodiene synthase (tri5) gene, partial cds	485
EU288813.1	<i>S. chartarum</i> isolate 04 trichodiene synthase (tri5) gene, partial cds	485
EU288815.1	<i>S. chartarum</i> isolate 08 trichodiene synthase (tri5) gene, partial cds	485
EU288814.1	<i>S. chartarum</i> isolate 15 trichodiene synthase (tri5) gene, partial cds	485
EU288816.1	<i>S. chartarum</i> isolate 18 trichodiene synthase (tri5) gene, partial cds	485
EU288817.1	<i>S. chartarum</i> isolate 09 trichodiene synthase (tri5) gene, partial cds	485
EU288818.1	<i>S. chartarum</i> isolate 42 trichodiene synthase (tri5) gene, partial cds	485
EU288819.1	<i>S. chartarum</i> isolate 16 trichodiene synthase (tri5) gene, partial cds	485
EU288820.1	<i>S. chartarum</i> isolate 20 trichodiene synthase (tri5) gene, partial cds	485
EU288821.1	<i>S. chartarum</i> isolate 56 trichodiene synthase (tri5) gene, partial cds	485
EU288822.1	<i>S. chartarum</i> isolate 10 trichodiene synthase (tri5) gene, partial cds	485
EU288823.1	<i>S. chartarum</i> isolate 31 trichodiene synthase (tri5) gene, partial cds	485
EU288824.1	<i>S. chartarum</i> isolate 50 trichodiene synthase (tri5) gene, partial cds	485

Appendices

EU288825.1	<i>S. chartarum</i> isolate 47 trichodiene synthase (tri5) gene, partial cds	485
EU288826.1	<i>S. chartarum</i> isolate 25 trichodiene synthase (tri5) gene, partial cds	485
EU288827.1	<i>S. chartarum</i> isolate 49 trichodiene synthase (tri5) gene, partial cds	485
EU288828.1	<i>S. chartarum</i> isolate 27 trichodiene synthase (tri5) gene, partial cds	485
EU288829.1	<i>S. chartarum</i> isolate 33 trichodiene synthase (tri5) gene, partial cds	485
EU288830.1	<i>S. chartarum</i> isolate 28 trichodiene synthase (tri5) gene, partial cds	485
EU288831.1	<i>S. chartarum</i> isolate 32 trichodiene synthase (tri5) gene, partial cds	485
EU288832.1	<i>S. chartarum</i> isolate 35 trichodiene synthase (tri5) gene, partial cds	485
EU288833.1	<i>S. chartarum</i> isolate 29 trichodiene synthase (tri5) gene, partial cds	485
EU288834.1	<i>S. chartarum</i> isolate 12 trichodiene synthase (tri5) gene, partial cds	485
EU288835.1	<i>S. chartarum</i> isolate 52 trichodiene synthase (tri5) gene, partial cds	485
EU288836.1	<i>S. chartarum</i> isolate 46 trichodiene synthase (tri5) gene, partial cds	485

Appendix 4-B: The sequences of *S. chartarum* (AF 329103.1) used to align and standardise the nucleotide position.

>AF329103.1 *Stachybotrys chartarum* trichodiene synthase (TRI5) gene, complete cds
ATGGAGGCATTCCCGACCGAGTACTTCCTGGGCACCGCTGTGCGGCTGCTGGAG
AATGTCAAGTACAGGGACAGTAACTACACCAGGGAGGAGCGTGTGAAAATCTCC
AGTATGCCTACAACAAGGCTGCGGCCCACTTCGCACAAGAGCGGCAGCAACAGA
TTTTGAAGGTCAGCCCCAAGAGACTGGAGGCTTCCCTTCGAACCATTGTGCGCAT
GGTGGTTTACTCCTGGGCCAAGGTTTCCAAGGAGCTCATGGCAGATCTCAGCATC
CACTACACCTACACTCTCATCCTCGATGATAGCGAGGACGACCCTCACCTCAGA
TGTTGACATACTTTGATGATCTTCAGAGTGGCAACCCGCAAAGCATCCCTGGTG
GATGCTGGTCAACGAGCACTTCCCTAATGTGCTGAGACACTTTGGCCCTTTCTGC
TCGCTAAACCTCATTTCGAGCACACTGGACTGTAAGTCTATACTCGACAATAGTCC
CCAAAATATTCCAAGAAAGAGCAAGAAAATAACACGCTTCCACAATAGTCTTTG
AAGGTTGCTGGATTGAGCAATATAACTTCCATGGCTTCCAGGCTCCTTTGACTAT
CCTGGGTTCTTCGTATGAATGGACTAGGACACTGTGTGCGGAGGATCTTTGT
GGCAAAGGAAAACCTCAACGAGCAGGAGCATTCTTGAAATCACCAGCGCCAT
CGCCCAAATGGAAAACCTGGATGGTTTGGGTTAACGACCTCATGTCTTCTACAAG
GAGTTCGACGACCCTCGCGACCAGACCAGCCTCGTCAAGAACTATGTGCTCTCC
GAAGGCATCACCTGAACCAGGCTTTGGAGAAGCTGACCCAAGATACCCTCCAGT
CGTCGGAACAAATGATGGTAGTGTCTCTCAGAAGGATCCCAAGATCATGGACAC
GATTGAGTGTTCATGCACGGCTACATTACCTGGCACCTGTGCGACAACCGGTAC
AGGCTGAAGGAGATCTACGACAGAACCAAGGACATCCAGACCGAGGACGCTATG
AAGTTCCGCAAGTTCTATGAGCAGGCTTTCAAGGTTGGAGCCATCGAGGCTACGG
AATGGGCTTATCCGACTGTAGTGGAGCGATTGGAGCAGCGAAAGGCGGAGGAGC
AGGCCGAAAGGGACGAGCAGGCCGCCCTTGCCAACCCTGAGAAGGCTCAGGTT
GCCAGGTTGTGCTAGCCTGA

Appendix 4-C: The alignment from all 3 primers (Cruse *et al.*, Black *et al.*, and SC1) with *S. chartarum* (AF 329103.1).

	10	20	30	40	50	60	70	80
AF329103.1	ATGGAGGCATTCCCACCGAGTACTTCCTGGGCACCGCTGTGCGGCTGCTGGAGAATGTCAAGTACAGGGACAGTAACTA 80							
ATCC16026_Cruse	-TGGAGGCATTCCCACCGAGTACTTCCTGGGCACCGCTGTGCGGCTGCTGGAGAATGTCAAGTACAGGGACAGTAACTA 79							
NCPF7587_Cruse	-TGGAGGCATTCCCACCGAGTACTTCCTGGGCACCGCTGTGCGGCTGCTGGAGAATGTCAAGTACAGGGACAGTAACTA 79							
CBS324.65_Cruse	-TGGAGGCATTCCCACCGAGTACTTCCTGGGCACCGCTGTGCGGCTGCTGGAGAATGTCAAGTACAGGGACAGTAACTA 79							
CBS182.80_Cruse	-TGGAGGCATTCCCACCGAGTACTTCCTGGGCACCGCTGTGCGGCTGCTGGAGAATGTCAAGTACAGGGACAGTAACTA 79							
CU_Cruse	-TGGAGACATTCCCGACTGAGTACTTCCTGGGCACCGCTGTGCGGCTGCTGGAGAACGTCAAGTACAGAGACAGCAACTA 79							
CBS328.37_Cruse	-TGGAGACATTCCCGACTGAGTACTTCCTGGGCACCGCTGTGCGGCTGCTGGAGAACGTCAAGTACAGAGACAGCAACTA 79							
CBS109286_Cruse	-TGGAGACATTCCCGACTGAGTACTTCCTGGGCACCGCTGTGCGGCTGCTGGAGAACGTCAAGTACAGAGACAGCAACTA 79							
CBS109283_Cruse	-TGGAGACATTCCCGACTGAGTACTTCCTGGGCACCGCTGTGCGGCTGCTGGAGAACGTCAAGTACAGAGACAGCAACTA 79							
ATCC16026_Black	----- 0							
NCPF7587_Black	----- 0							
CBS324.65_Black	----- 0							
CBS182.80_Black	----- 0							
CU_Black	----- 0							
CBS328.37_Black	----- 0							
CBS109286_Black	----- 0							
CBS109283_Black	----- 0							
ATCC16026_SC1	----- 0							
NCPF7587_SC1	----- 0							
CBS324.65_SC1	----- 0							
CBS182.80_SC1	----- 0							
CU_SC1	----- 0							
CBS328.37_SC1	----- 0							
CBS109286_SC1	----- 0							
CBS109283_SC1	----- 0							
Majority	-----							
	90	100	110	120	130	140	150	160
AF329103.1	CACCAGGGAGGAGCGTGTGAAAATCTCCAGTATGCCTACAACAAGGCTGCGGCCCACTTCGCACAAGAGCGGCAGCAAC 160							
ATCC16026_Cruse	CACCAGGGAGGAGCGTGTGAAAATCTCCAGTATGCCTACAACAAGGCTGCGGCCCACTTCGCACAAGAGCGGCAGCAAC 159							
NCPF7587_Cruse	CACCAGGGAGGAGCGTGTGAAAATCTCCAGTATGCCTACAACAAGGCTGCGGCCCACTTCGCACAAGAGCGGCAGCAAC 159							
CBS324.65_Cruse	CACCAGGGAGGAGCGTGTGAAAATCTCCAGTATGCCTACAACAAGGCTGCGGCCCACTTCGCACAAGAGCGGCAGCAAC 159							
CBS182.80_Cruse	CACCAGGGAGGAGCGTGTGAAAATCTCCAGTATGCCTACAACAAGGCTGCGGCCCACTTCGCACAAGAGCGGCAGCAAC 159							
CU_Cruse	CACCAGGGAGGAGCGGTTGAAAATCTTCAGTATGCCTACAACAAGGCTGCGGCTCATTTTCGCACAAGAACGGCAGCAAC 159							
CBS328.37_Cruse	CACCAGGGAGGAGCGGTTGAAAATCTTCAGTATGCCTACAACAAGGCTGCGGCTCATTTTCGCACAAGAACGGCAGCAAC 159							
CBS109286_Cruse	CACCAGGGAGGAGCGGTTGAAAATCTTCAGTATGCCTACAACAAGGCTGCGGCTCATTTTCGCACAAGAACGGCAGCAAC 159							
CBS109283_Cruse	CACCAGGGAGGAGCGGTTGAAAATCTTCAGTATGCCTACAACAAGGCTGCGGCTCATTTTCGCACAAGAACGGCAGCAAC 159							
ATCC16026_Black	----- 0							
NCPF7587_Black	----- 0							
CBS324.65_Black	----- 0							
CBS182.80_Black	----- 0							
CU_Black	----- 0							
CBS328.37_Black	----- 0							
CBS109286_Black	----- 0							
CBS109283_Black	----- 0							
ATCC16026_SC1	----- 0							
NCPF7587_SC1	----- 0							
CBS324.65_SC1	----- 0							
CBS182.80_SC1	----- 0							
CU_SC1	----- 0							
CBS328.37_SC1	----- 0							
CBS109286_SC1	----- 0							
CBS109283_SC1	----- 0							
	10	20	30	40	50	60	70	80
AF329103.1	ATGGAGGCATTCCCACCGAGTACTTCCTGGGCACCGCTGTGCGGCTGCTGGAGAATGTCAAGTACAGGGACAGTAACTA 80							
ATCC16026_Cruse	-TGGAGGCATTCCCACCGAGTACTTCCTGGGCACCGCTGTGCGGCTGCTGGAGAATGTCAAGTACAGGGACAGTAACTA 79							
NCPF7587_Cruse	-TGGAGGCATTCCCACCGAGTACTTCCTGGGCACCGCTGTGCGGCTGCTGGAGAATGTCAAGTACAGGGACAGTAACTA 79							
CBS324.65_Cruse	-TGGAGGCATTCCCACCGAGTACTTCCTGGGCACCGCTGTGCGGCTGCTGGAGAATGTCAAGTACAGGGACAGTAACTA 79							
CBS182.80_Cruse	-TGGAGGCATTCCCACCGAGTACTTCCTGGGCACCGCTGTGCGGCTGCTGGAGAATGTCAAGTACAGGGACAGTAACTA 79							
CU_Cruse	-TGGAGACATTCCCGACTGAGTACTTCCTGGGCACCGCTGTGCGGCTGCTGGAGAACGTCAAGTACAGAGACAGCAACTA 79							
CBS328.37_Cruse	-TGGAGACATTCCCGACTGAGTACTTCCTGGGCACCGCTGTGCGGCTGCTGGAGAACGTCAAGTACAGAGACAGCAACTA 79							
CBS109286_Cruse	-TGGAGACATTCCCGACTGAGTACTTCCTGGGCACCGCTGTGCGGCTGCTGGAGAACGTCAAGTACAGAGACAGCAACTA 79							
CBS109283_Cruse	-TGGAGACATTCCCGACTGAGTACTTCCTGGGCACCGCTGTGCGGCTGCTGGAGAACGTCAAGTACAGAGACAGCAACTA 79							
ATCC16026_Black	----- 0							
NCPF7587_Black	----- 0							
CBS324.65_Black	----- 0							
CBS182.80_Black	----- 0							
CU_Black	----- 0							
CBS328.37_Black	----- 0							
CBS109286_Black	----- 0							
CBS109283_Black	----- 0							
ATCC16026_SC1	----- 0							
NCPF7587_SC1	----- 0							
CBS324.65_SC1	----- 0							
CBS182.80_SC1	----- 0							
CU_SC1	----- 0							
CBS328.37_SC1	----- 0							
CBS109286_SC1	----- 0							
CBS109283_SC1	----- 0							

Appendices

Majority		-----							
		90	100	110	120	130	140	150	160
AF329103.1	CACCAGGGAGGAGCGTGTGAAAAATCTCCAGTATGCCTACAACAAGGCTGCGGCCCACTTCGCACAAGAGCGGCAGCAAC								160
ATCC16026_Cruse	CACCAGGGAGGAGCGTGTGAAAAATCTCCAGTATGCCTACAACAAGGCTGCGGCCCACTTCGCACAAGAGCGGCAGCAAC								159
NCPF7587_Cruse	CACCAGGGAGGAGCGTGTGAAAAATCTCCAGTATGCCTACAACAAGGCTGCGGCCCACTTCGCACAAGAGCGGCAGCAAC								159
CBS324.65_Cruse	CACCAGGGAGGAGCGTGTGAAAAATCTCCAGTATGCCTACAACAAGGCTGCGGCCCACTTCGCACAAGAGCGGCAGCAAC								159
CBS182.80_Cruse	CACCAGGGAGGAGCGTGTGAAAAATCTCCAGTATGCCTACAACAAGGCTGCGGCCCACTTCGCACAAGAGCGGCAGCAAC								159
CU_Cruse	CACCAGGGAGGAGCGTGTGAAAAATCTCCAGTATGCCTACAACAAGGCTGCGGCCCACTTCGCACAAGAGCGGCAGCAAC								159
CBS328.37_Cruse	CACCAGGGAGGAGCGCGTTGAAAAATCTTCCAGTATGCCTACAACAAGGCTGCGGCCCACTTCGCACAAGAGCGGCAGCAAC								159
CBS109286_Cruse	CACCAGGGAGGAGCGCGTTGAAAAATCTTCCAGTATGCCTACAACAAGGCTGCGGCCCACTTCGCACAAGAGCGGCAGCAAC								159
CBS109283_Cruse	CACCAGGGAGGAGCGCGTTGAAAAATCTTCCAGTATGCCTACAACAAGGCTGCGGCCCACTTCGCACAAGAGCGGCAGCAAC								159
ATCC16026_Black	-----								0
NCPF7587_Black	-----								0
CBS324.65_Black	-----								0
CBS182.80_Black	-----								0
CU_Black	-----								0
CBS328.37_Black	-----								0
CBS109286_Black	-----								0
CBS109283_Black	-----								0
ATCC16026_SC1	-----								0
NCPF7587_SC1	-----								0
CBS324.65_SC1	-----								0
CBS182.80_SC1	-----								0
CU_SC1	-----								0
CBS328.37_SC1	-----								0
CBS109286_SC1	-----								0
CBS109283_SC1	-----								0

Majority		-----							
		170	180	190	200	210	220	230	240
AF329103.1	AGATTTTGAAGGTCAGCCCCAAGAGACTGGAGGCTTCCCTTCGAACCATTGTCGGCATGGTGGTTTACTCCTGGGCCAAG								240
ATCC16026_Cruse	AGATTTTGAAGGTCAGCCCCAAGAGACTGGAGGCTTCCCTTCGAACCATTGTCGGCATGGTGGTTTACTCCTGGGCCAAG								239
NCPF7587_Cruse	AGATTTTGAAGGTCAGCCCCAAGAGACTGGAGGCTTCCCTTCGAACCATTGTCGGCATGGTGGTTTACTCCTGGGCCAAG								239
CBS324.65_Cruse	AGATTTTGAAGGTCAGCCCCAAGAGACTGGAGGCTTCCCTTCGAACCATTGTCGGCATGGTGGTTTACTCCTGGGCCAAG								239
CBS182.80_Cruse	AGATTTTGAAGGTCAGCCCCAAGAGACTGGAGGCTTCCCTTCGAACCATTGTCGGCATGGTGGTTTACTCCTGGGCCAAG								239
CU_Cruse	AGATTTTGAAGGTCAGCCCCAAGAGACTGGAGGCTTCCCTTCGAACCATTGTCGGCATGGTGGTTTACTCCTGGGCCAAG								239
CBS328.37_Cruse	AGATCTTGAAGGTCAGCCCCAAGAGACTGGAGGCTTCCCTTCGAACCATTGTCGGCATGGTGGTTTACTCCTGGGCCAAG								239
CBS109286_Cruse	AGATCTTGAAGGTCAGCCCCAAGAGACTGGAGGCTTCCCTTCGAACCATTGTCGGCATGGTGGTTTACTCCTGGGCCAAG								239
CBS109283_Cruse	AGATCTTGAAGGTCAGCCCCAAGAGACTGGAGGCTTCCCTTCGAACCATTGTCGGCATGGTGGTTTACTCCTGGGCCAAG								239
ATCC16026_Black	-----								0
NCPF7587_Black	-----								0
CBS324.65_Black	-----								0
CBS182.80_Black	-----								0
CU_Black	-----								0
CBS328.37_Black	-----								0
CBS109286_Black	-----								0
CBS109283_Black	-----								0
ATCC16026_SC1	-----								0
NCPF7587_SC1	-----								0
CBS324.65_SC1	-----								0
CBS182.80_SC1	-----								0
CU_SC1	-----								0
CBS328.37_SC1	-----								0
CBS109286_SC1	-----								0
CBS109283_SC1	-----								0

Majority		-----							
		250	260	270	280	290	300	310	320
AF329103.1	GTTTCCAAGGAGCTCATGGCAGATCTCAGCATCCACTACACCTACACTCTCATCCTCGATGATAGCGAGGACGACCTCA								320
ATCC16026_Cruse	GTTTCCAAGGAGCTCATGGCAGATCTCAGCATCCACTACACCTACACTCTCATCCTCGATGATAGCGAGGACGACCTCA								319
NCPF7587_Cruse	GTTTCCAAGGAGCTCATGGCAGATCTCAGCATCCACTACACCTACACTCTCATCCTCGATGATAGCGAGGACGACCTCA								319
CBS324.65_Cruse	GTTTCCAAGGAGCTCATGGCAGATCTCAGCATCCACTACACCTACACTCTCATCCTCGATGATAGCGAGGACGACCTCA								319
CBS182.80_Cruse	GTTTCCAAGGAGCTCATGGCAGATCTCAGCATCCACTACACCTACACTCTCATCCTCGATGATAGCGAGGACGACCTCA								319
CU_Cruse	GTTTCCAAGGAGCTCATGGCAGATCTCAGCATCCACTACACCTACACTCTCATCCTCGATGATAGCGAGGACGACCTCA								319
CBS328.37_Cruse	GTTTCCAAGGAGCTCATGGCAGATCTCAGCATCCACTACACCTACACTCTCATCCTCGATGATAGCGAGGACGACCTCA								319
CBS109286_Cruse	GTTTCCAAGGAGCTCATGGCAGATCTCAGCATCCACTACACCTACACTCTCATCCTCGATGATAGCGAGGACGACCTCA								319
CBS109283_Cruse	GTTTCCAAGGAGCTCATGGCAGATCTCAGCATCCACTACACCTACACTCTCATCCTCGATGATAGCGAGGACGACCTCA								319
ATCC16026_Black	-----								0
NCPF7587_Black	-----								0
CBS324.65_Black	-----								0
CBS182.80_Black	-----								0
CU_Black	-----								0
CBS328.37_Black	-----								0
CBS109286_Black	-----								0
CBS109283_Black	-----								0
ATCC16026_SC1	-----								0
NCPF7587_SC1	-----								0
CBS324.65_SC1	-----								0
CBS182.80_SC1	-----								0
CU_SC1	-----								0
CBS328.37_SC1	-----								0
CBS109286_SC1	-----								0
CBS109283_SC1	-----								0

Appendices

Majority	-----CTGACTGTAAGTCTATA-----							
	330	340	350	360	370	380	390	400
AF329103.1	CCCTCAGATGTTGACATACTTTGATGATCTTCAGAGTGGCAACCCGCAAAGCATCCCTGGTGGATGCTGGTCAACGAGC							400
ATCC16026_Cruse	CCCTCAGATGTTGACATACTTTGATGATCTTCAGAGTGGCAACCCGCAAAGCATCCCTGGTGGATGCTGGTCAACGAGC							399
NCPF7587_Cruse	CCCTCAGATGTTGACATACTTTGATGATCTTCAGAGTGGCAACCCGCAAAGCATCCCTGGTGGATGCTGGTCAACGAGC							399
CBS324.65_Cruse	CCCTCAGATGTTGACATACTTTGATGATCTTCAGAGTGGCAACCCGCAAAGCATCCCTGGTGGATGCTGGTCAACGAGC							399
CBS182.80_Cruse	CCCTCAGATGTTGACATACTTTGATGATCTTCAGAGTGGCAACCCGCAAAGCATCCCTGGTGGATGCTGGTCAACGAGC							399
CU_Cruse	CCCTCAGATGTTGACATACTTTGATGATCTTCAGAGTGGCAACCCGCAAAGCATCCCTGGTGGATGCTGGTCAACGAGC							399
CBS328.37_Cruse	CCCTCAGATGTTGACATACTTTGATGATCTTCAGAGTGGCAACCCGCAAAGCATCCCTGGTGGATGCTGGTCAACGAGC							399
CBS109286_Cruse	CCCTCAGATGTTGACATACTTTGATGATCTTCAGAGTGGCAACCCGCAAAGCATCCCTGGTGGATGCTGGTCAACGAGC							399
CBS109283_Cruse	CCCTCAGATGTTGACATACTTTGATGATCTTCAGAGTGGCAACCCGCAAAGCATCCCTGGTGGATGCTGGTCAACGAGC							399
ATCC16026_Black	-----							0
NCPF7587_Black	-----							0
CBS324.65_Black	-----							0
CBS182.80_Black	-----							0
CU_Black	-----							0
CBS328.37_Black	-----							0
CBS109286_Black	-----							0
CBS109283_Black	-----							0
ATCC16026_SC1	-----							0
NCPF7587_SC1	-----							0
CBS324.65_SC1	-----							0
CBS182.80_SC1	-----							0
CU_SC1	-----							0
CBS328.37_SC1	-----							0
CBS109286_SC1	-----							0
CBS109283_SC1	-----							0

Majority	-----CTGACTGTAAGTCTATA-----							
	410	420	430	440	450	460	470	480
AF329103.1	ACTTCCCTAATGTGCTGAGACACTTTGGCCCTTTCTGCTCGCTAAACCTCATTTCGAGCACA							480
ATCC16026_Cruse	ACTTCCCTAATGTGCTGAGACACTTTGGCCCTTTCTGCTCGCTAAACCTCATTTCGAGCACA							479
NCPF7587_Cruse	ACTTCCCTAATGTGCTGAGACACTTTGGCCCTTTCTGCTCGCTAAACCTCATTTCGAGCACA							479
CBS324.65_Cruse	ACTTCCCTAATGTGCTGAGACACTTTGGCCCTTTCTGCTCGCTAAACCTCATTTCGAGCACA							479
CBS182.80_Cruse	ACTTCCCTAATGTGCTGAGACACTTTGGCCCTTTCTGCTCGCTAAACCTCATTTCGAGCACA							479
CU_Cruse	ACTTCCCTAATGTGCTGAGACACTTTGGCCCTTTCTGCTCGCTAAACCTCATTTCGAGCACA							GC. 479
CBS328.37_Cruse	ACTTCCCTAATGTGCTGAGACACTTTGGCCCTTTCTGCTCGCTAAACCTCATTTCGAGCACA							GC. 479
CBS109286_Cruse	ACTTCCCTAATGTGCTGAGACACTTTGGCCCTTTCTGCTCGCTAAACCTCATTTCGAGCACA							GC. 479
CBS109283_Cruse	ACTTCCCTAATGTGCTGAGACACTTTGGCCCTTTCTGCTCGCTAAACCTCATTTCGAGCACA							GC. 479
ATCC16026_Black	-----							0
NCPF7587_Black	-----							0
CBS324.65_Black	-----							0
CBS182.80_Black	-----							0
CU_Black	-----							0
CBS328.37_Black	-----							0
CBS109286_Black	-----							0
CBS109283_Black	-----							0
ATCC16026_SC1	-----							18
NCPF7587_SC1	-----							18
CBS324.65_SC1	-----							18
CBS182.80_SC1	-----							18
CU_SC1	-----							GC. 18
CBS328.37_SC1	-----							GC. 18
CBS109286_SC1	-----							GC. 18
CBS109283_SC1	-----							GC. 18

Majority	CTCGACAATAGTCCCC-AAAATATTCCAAGAAAGAGCAAGAAAACTAACACGCTTCCACAATAGTCTTTGAGGTTGCTG							
	490	500	510	520	530	540	550	560
AF329103.1C.....							560
ATCC16026_CruseC.....							545
NCPF7587_CruseC.....							545
CBS324.65_CruseC.....							545
CBS182.80_CruseC.....							545
CU_Cruse	..GT.A.....A.....GA.....C.....TG.....			544
CBS328.37_Cruse	..GT.A.....A.....GA.....C.....TG.....			544
CBS109286_Cruse	..GT.A.....A.....GA.....C.....TG.....			544
CBS109283_Cruse	..GT.A.....A.....GA.....C.....TG.....			544
ATCC16026_Black	-----							49
NCPF7587_Black	-----							49
CBS324.65_Black	-----							49
CBS182.80_Black	-----							49
CU_Black	-----		GA.....C.....TG.....C.....	49
CBS328.37_Black	-----		GA.....C.....TG.....C.....	49
CBS109286_Black	-----		GA.....C.....TG.....C.....	49
CBS109283_Black	-----		GA.....C.....TG.....C.....	49
ATCC16026_SC1C.....							98
NCPF7587_SC1C.....							98
CBS324.65_SC1C.....							98
CBS182.80_SC1C.....							98
CU_SC1	..GT.A.....A.....GA.....C.....TG.....C.....		97
CBS328.37_SC1	..GT.A.....A.....GA.....C.....TG.....C.....		97
CBS109286_SC1	..GT.A.....A.....GA.....C.....TG.....C.....		97
CBS109283_SC1	..GT.A.....A.....GA.....C.....TG.....C.....		97

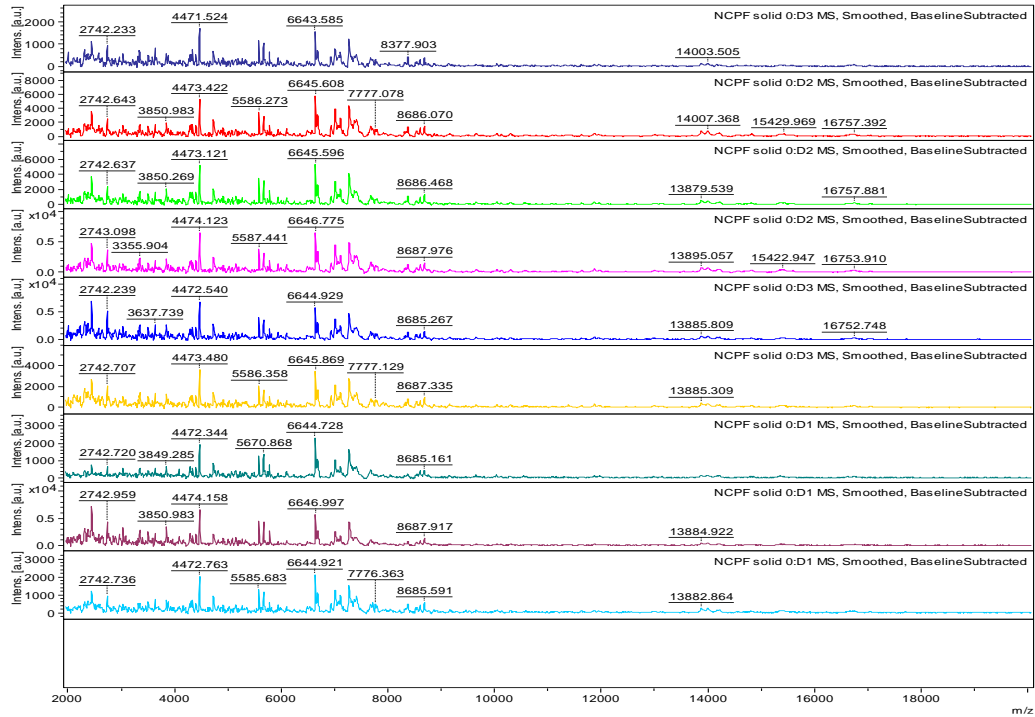
Appendices

Majority	GATTGAGCAATATAACTTCCATGGCTTCCCAGXX										
	570	580	590	600	610	620	630	640			
AF329103.1GCTCCTTTGACTATCCTGGGTTCCTTCGTCGTATGAATGGACTAGGAC										640
ATCC16026_Cruse											545
NCPF7587_Cruse											545
CBS324.65_Cruse											545
CBS182.80_Cruse											545
CU_Cruse											544
CBS328.37_Cruse											544
CBS109286_Cruse											544
CBS109283_Cruse											544
ATCC16026_Black										81
NCPF7587_Black										81
CBS324.65_Black										81
CBS182.80_Black										81
CU_Black										81
CBS328.37_Black										81
CBS109286_Black										81
CBS109283_Black										81
ATCC16026_SC1GCTCCTTTGACTATCCTGGGTTCCTTCGTCGTATGAATGGTTTAGGAC										178
NCPF7587_SC1GCTCCTTTGACTATCCTGGGTTCCTTCGTCGTATGAATGGTTTAGGAC										178
CBS324.65_SC1GCTCCTTTGACTATCCTGGGTTCCTTCGTCGTATGAATGGACTAGGAC										178
CBS182.80_SC1GCTCCTTTGACTATCCTGGGTTCCTTCGTCGTATGAATGGACTAGGAC										178
CU_SC1GGTCCTTTGACTATCCCGGGTTCCTTCGTCGTATGAATGGACTGGGAC										177
CBS328.37_SC1GGTCCTTTGACTATCCCGGGTTCCTTCGTCGTATGAATGGACTGGGAC										177
CBS109286_SC1GGTCCTTTGACTATCCCGGGTTCCTTCGTCGTATGAATGGACTGGGAC										177
CBS109283_SC1GGTCCTTTGACTATCCCGGGTTCCTTCGTCGTATGAATGGACTGGGAC										177
Majority	XX										
	650	660	670	680	690	700	710	720			
AF329103.1	ACTGTGTCGGAGGATCTTTGTGGCCAAAGGAAAACCTCAACGAGCAGGAGCATTCTTGAAATCACCAGCGCCATCGCC										720
ATCC16026_Cruse											545
NCPF7587_Cruse											545
CBS324.65_Cruse											545
CBS182.80_Cruse											545
CU_Cruse											544
CBS328.37_Cruse											544
CBS109286_Cruse											544
CBS109283_Cruse											544
ATCC16026_Black											81
NCPF7587_Black											81
CBS324.65_Black											81
CBS182.80_Black											81
CU_Black											81
CBS328.37_Black											81
CBS109286_Black											81
CBS109283_Black											81
ATCC16026_SC1	ACTGTGTCGGAGGATCTTT										197
NCPF7587_SC1	ACTGTGTCGGAGGATCTTT										197
CBS324.65_SC1	ACTGTGTCGGAGGATCTTT										197
CBS182.80_SC1	ACTGTGTCGGAGGATCTTT										197
CU_SC1	ACTGTGTCGGAGGATCTTT										196
CBS328.37_SC1	ACTGTGTCGGAGGATCTTT										196
CBS109286_SC1	ACTGTGTCGGAGGATCTTT										196
CBS109283_SC1	ACTGTGTCGGAGGATCTTT										196

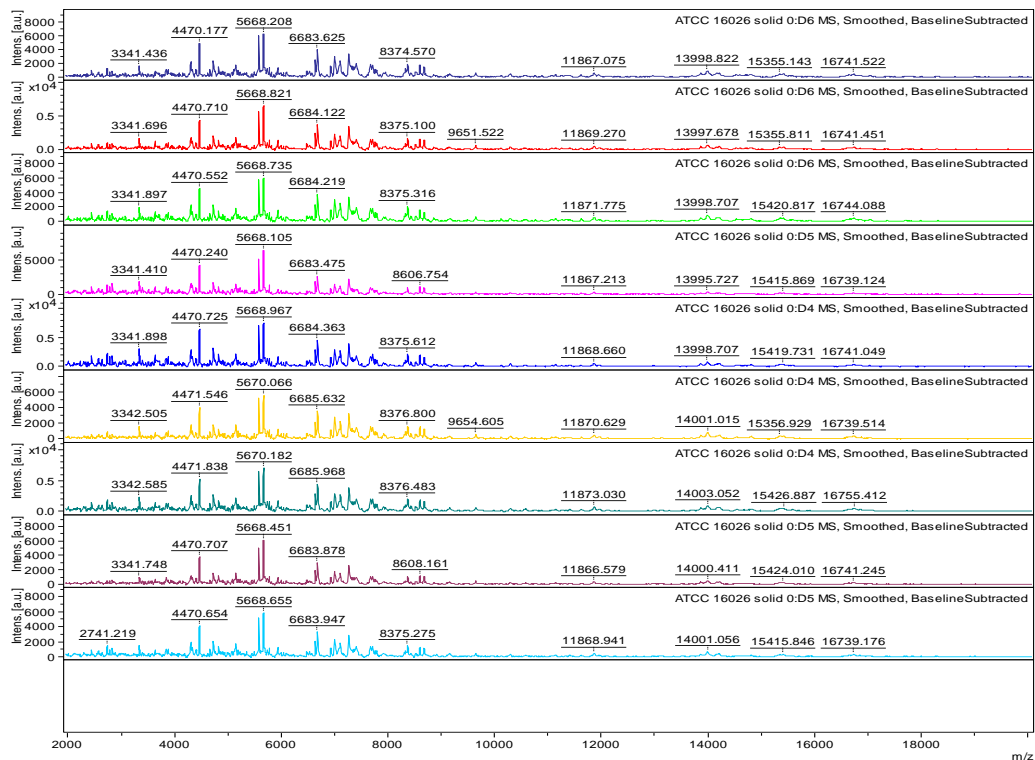
Chapter 5 : Identification of *Stachybotrys chartarum* using Matrix Assisted Laser Desorption Ionisation – Time of Flight (MALDI-TOF)

Appendix 5-A: Protein profiles obtained from *S. chartarum* (NCPF 7587, ATCC 16026 and CBS 182.80) directly extracted from solid media.

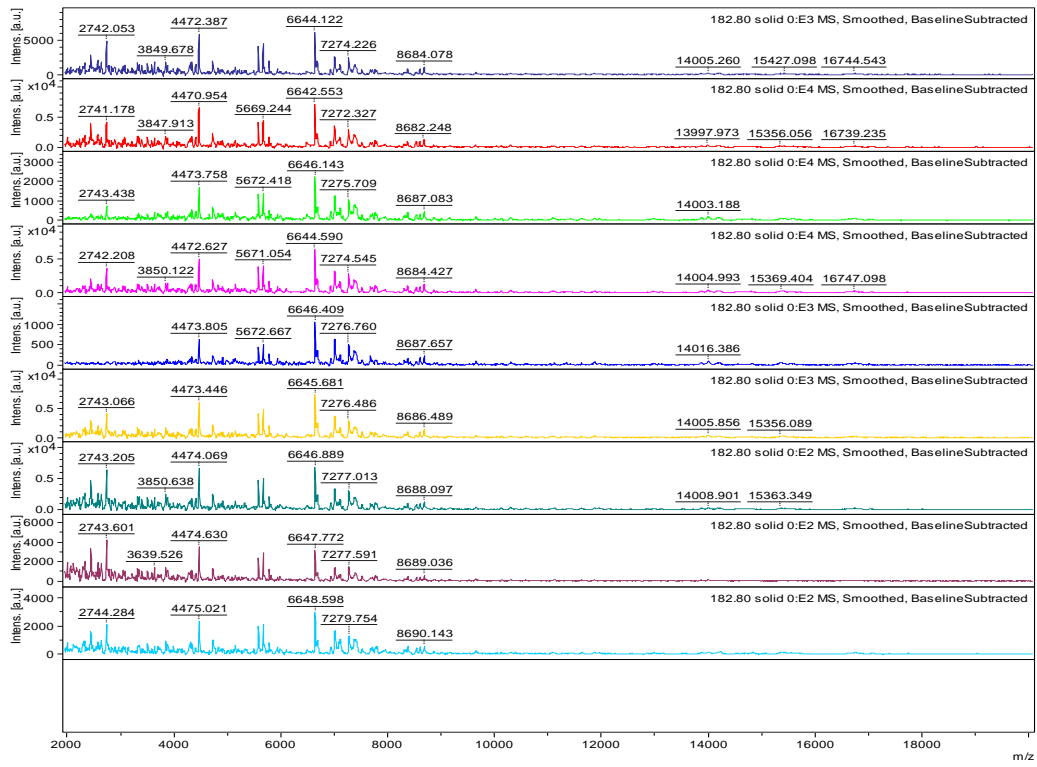
1. *S. chartarum*, NCPF 7587



2. *S. chartarum*, ATCC 16026

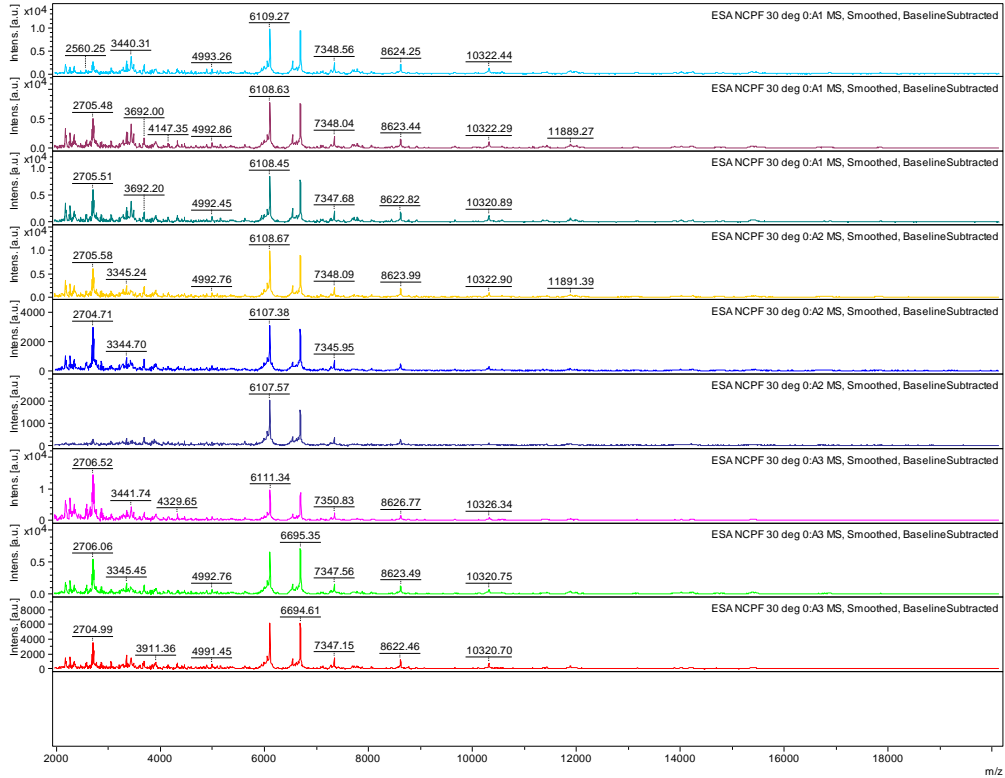


3. *S. chartarum* , CBS 182.80

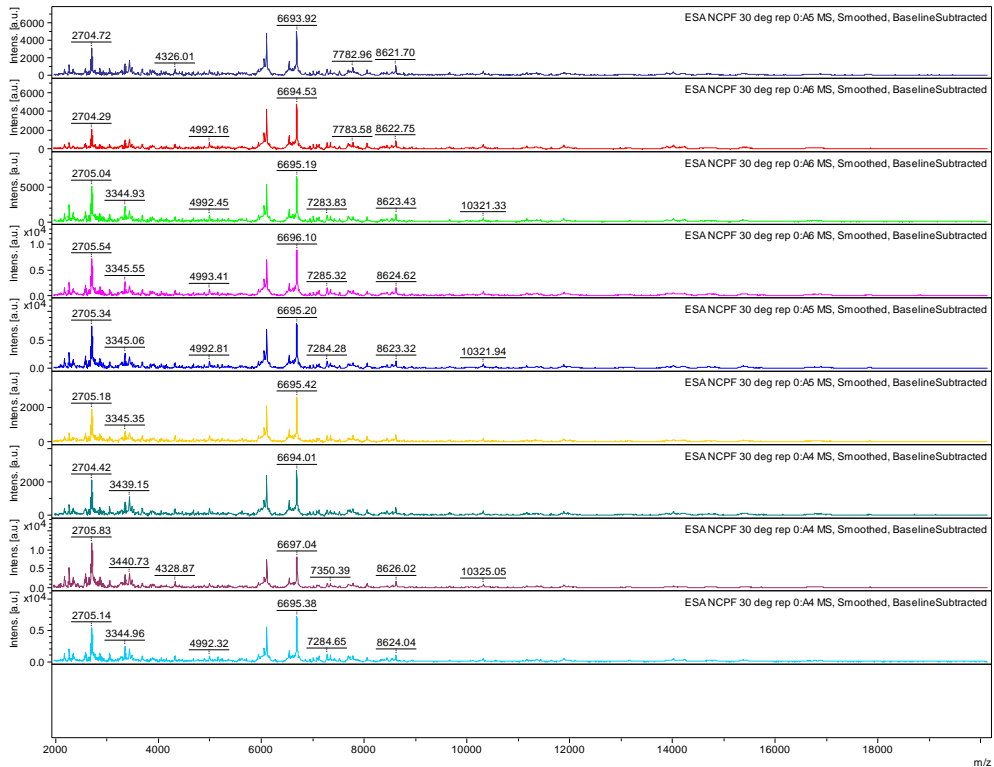


Appendix 5-B: Protein profiles obtained from *S. chartarum*, NCPF 7587 grown in SDB at 30 °C in replicates.

Replicate 1

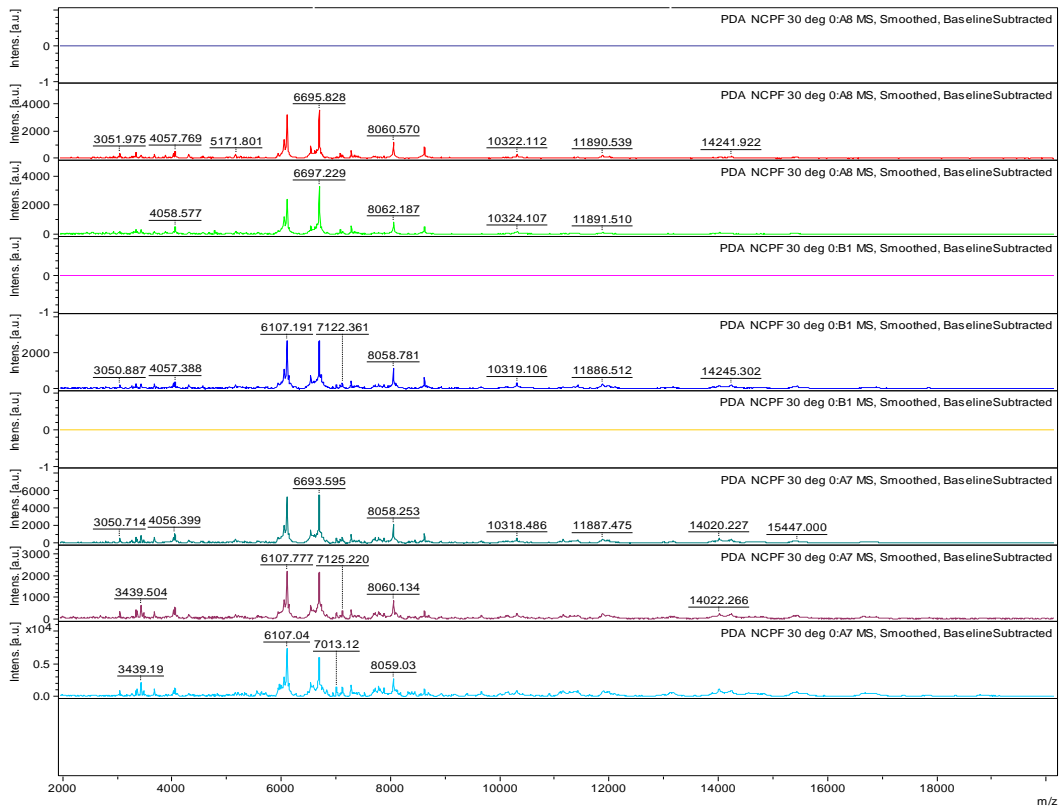


Replicate 2

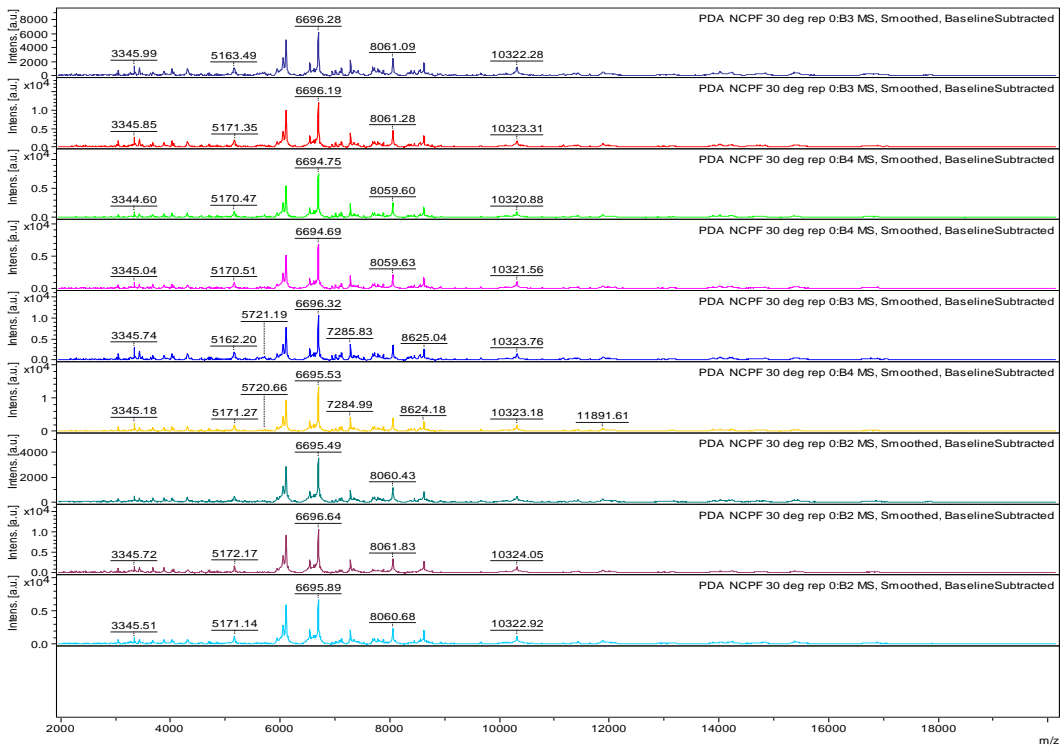


Appendix 5-C: Protein profiles obtained from *S. chartarum*, NCPF 7587 grown in PDB at 30 °C in replicates.

Replicate 1

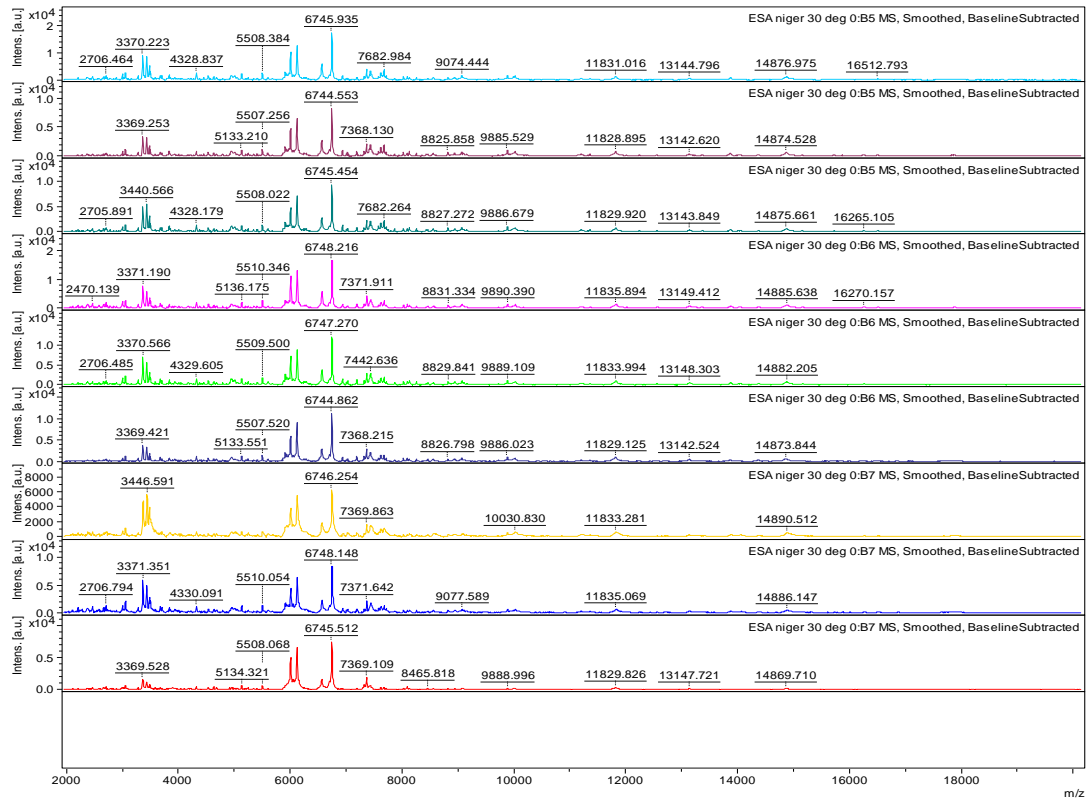


Replicate 2

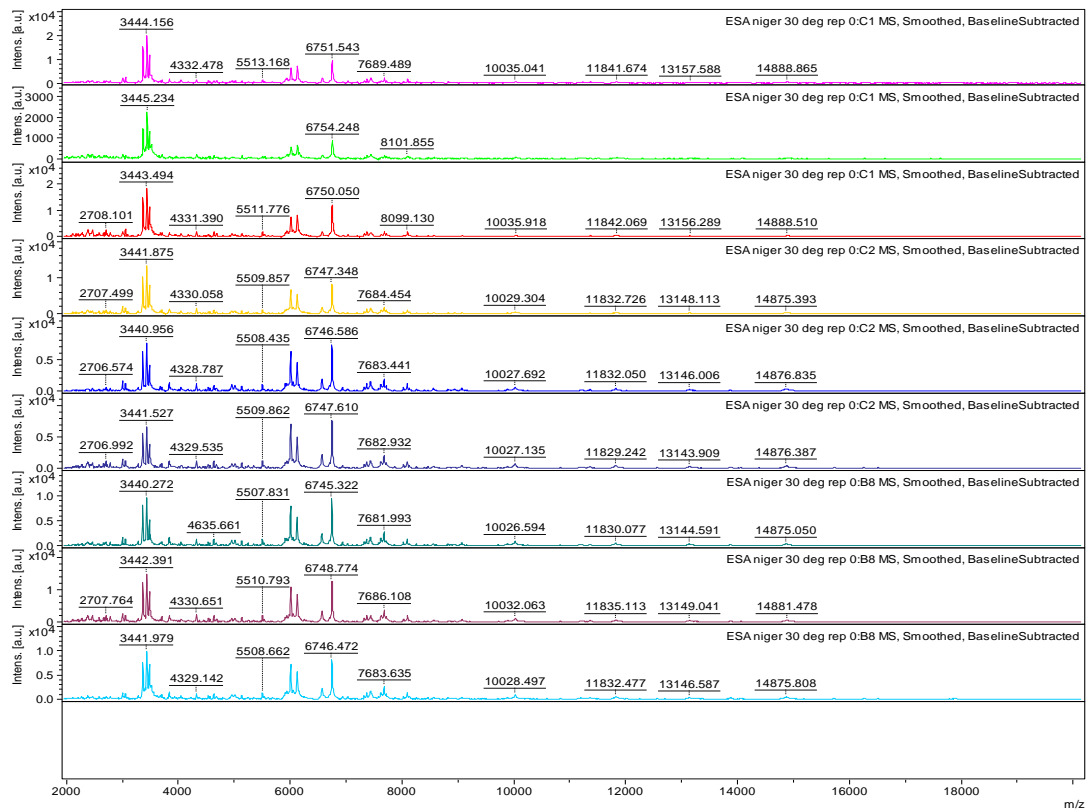


Appendix 5-D: Protein profiles obtained from *A. niger*, ATCC 16888 grown in SDB at 30 °C in replicates.

Replicate 1

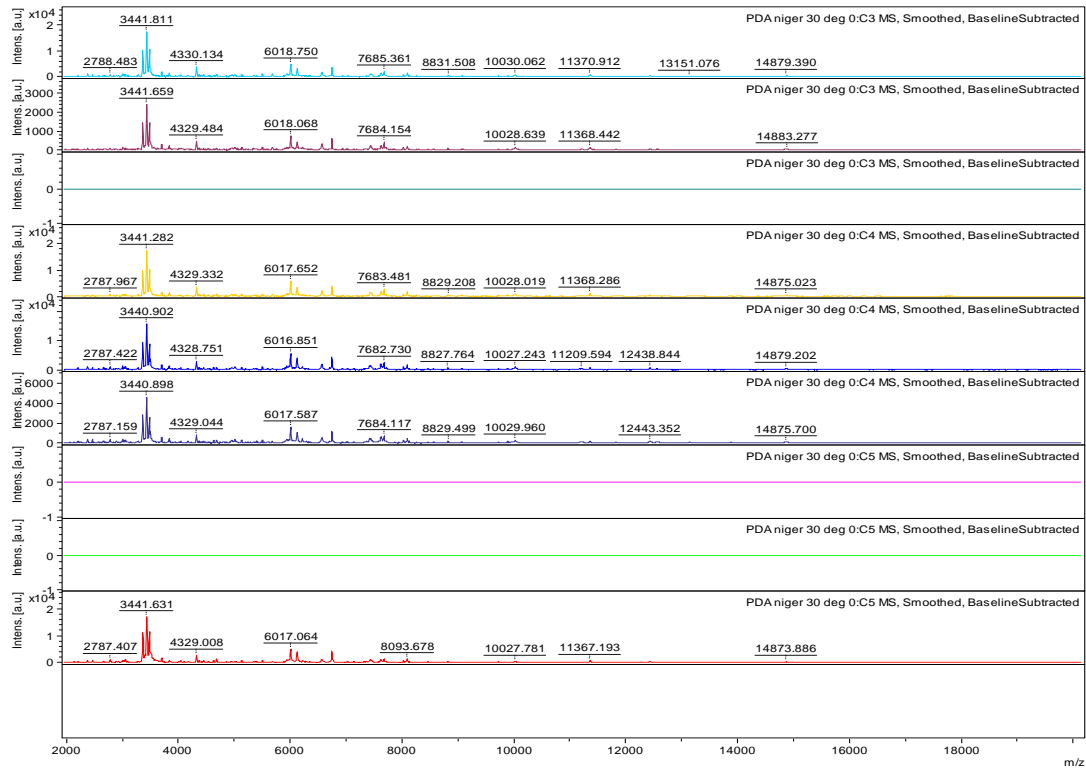


Replicate 2

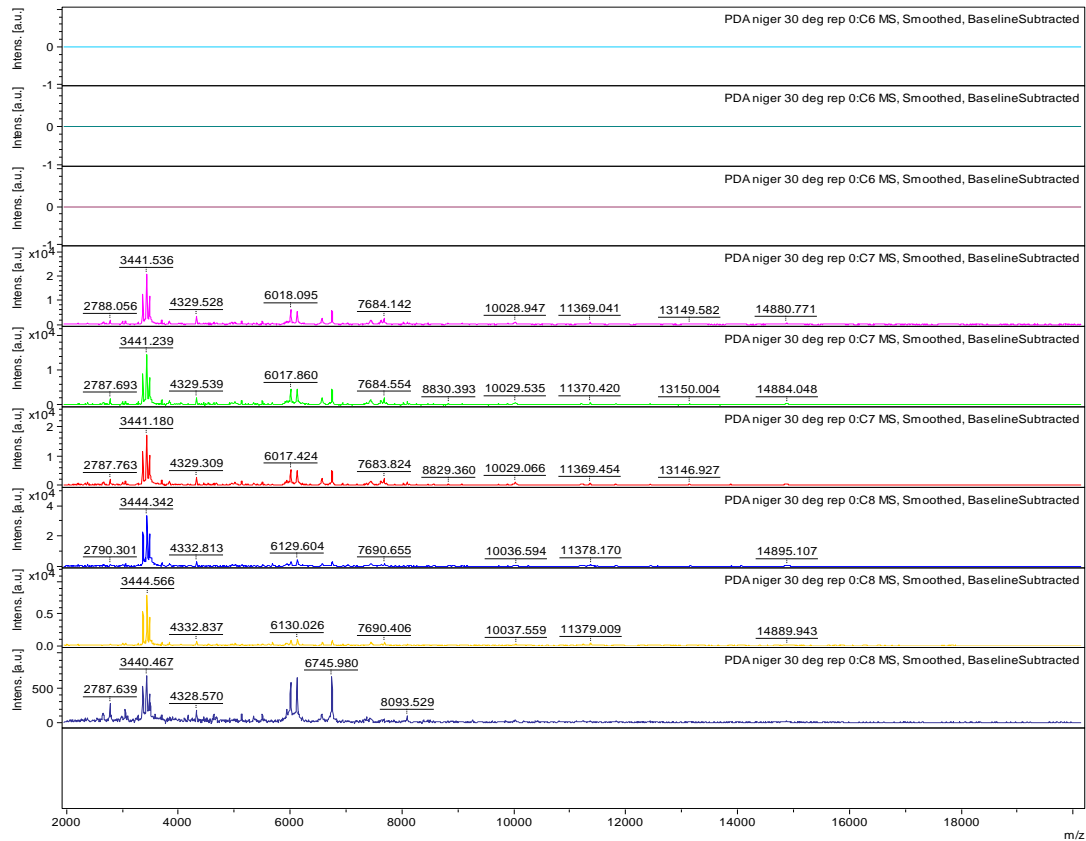


Appendix 5-E: Protein profiles obtained from *A. niger*, ATCC 16888 grown in PDB at 30 °C in replicates.

Replicate 1

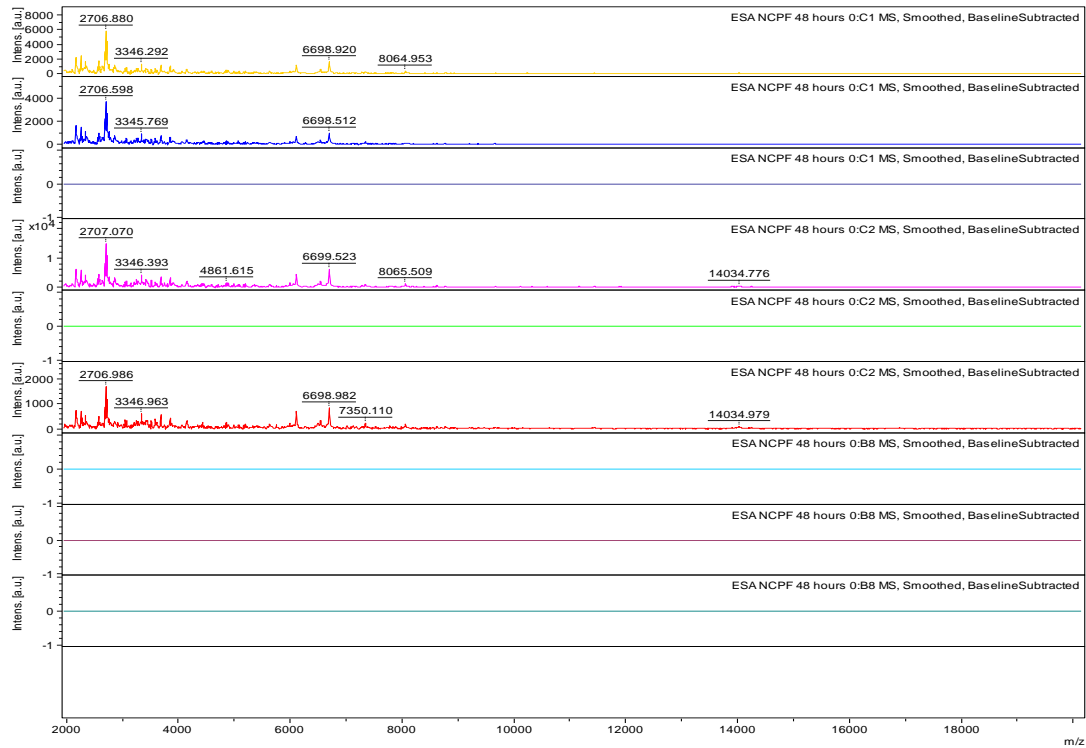


Replicate 2

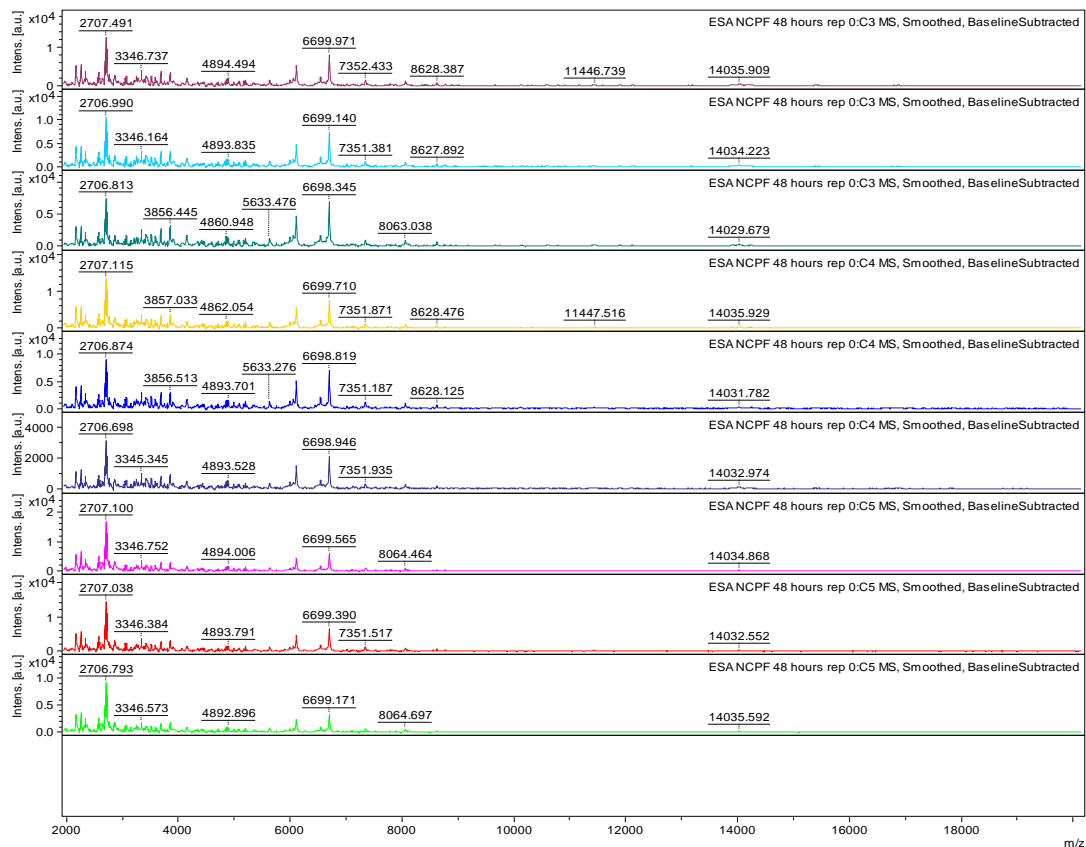


Appendix 5-F: Protein profiles obtained from *S. chartarum*, NCPF 7587 grown in SDB incubated for 48 hours at 25 °C in replicates.

Replicate 1

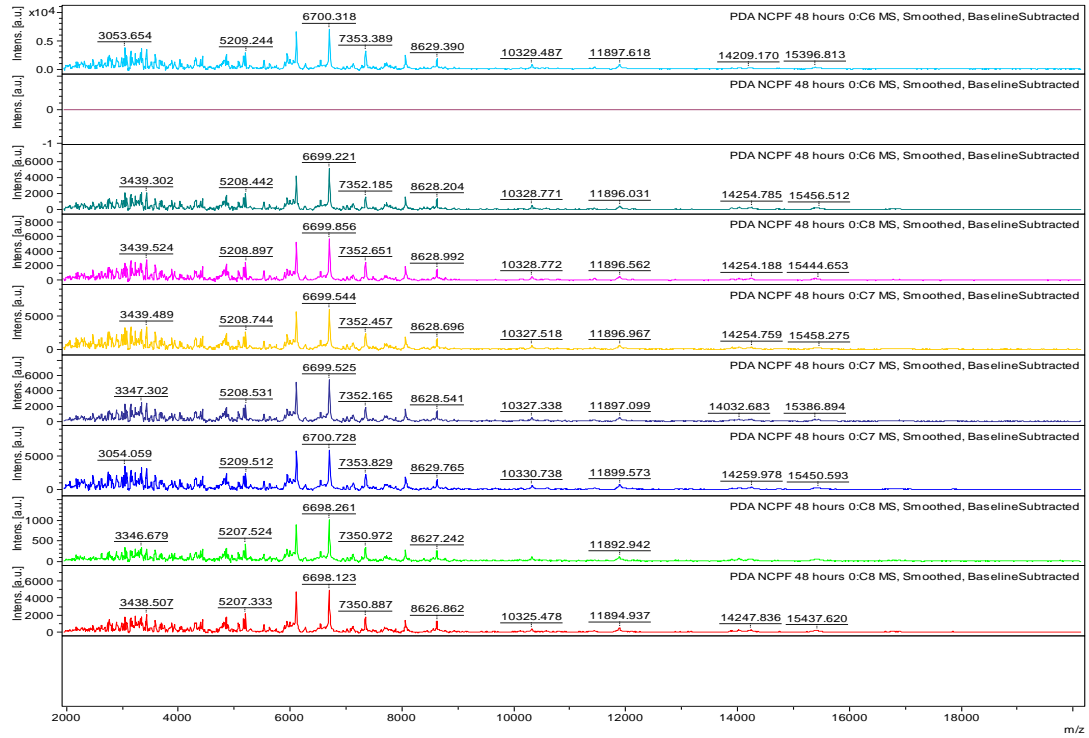


Replicate 2

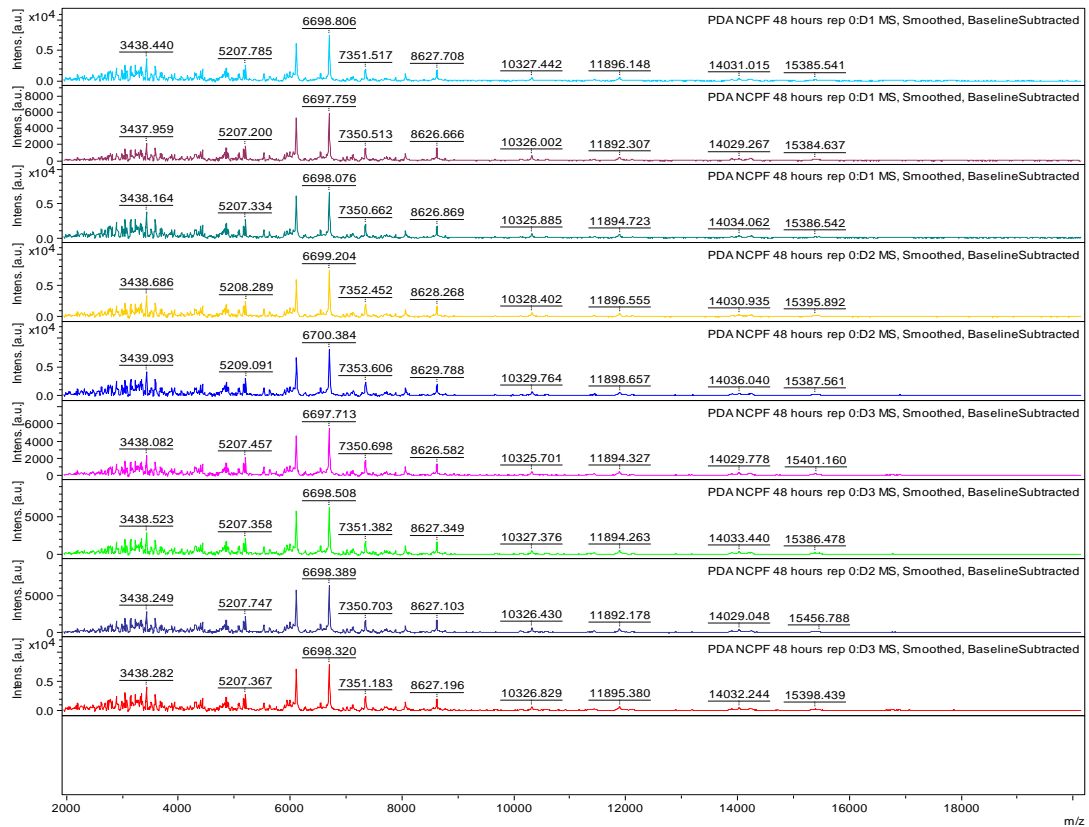


Appendix 5-G: Protein profiles obtained from *S. chartarum*, NCPF 7587 grown in PDB incubated for 48 hours at 25 °C in replicates.

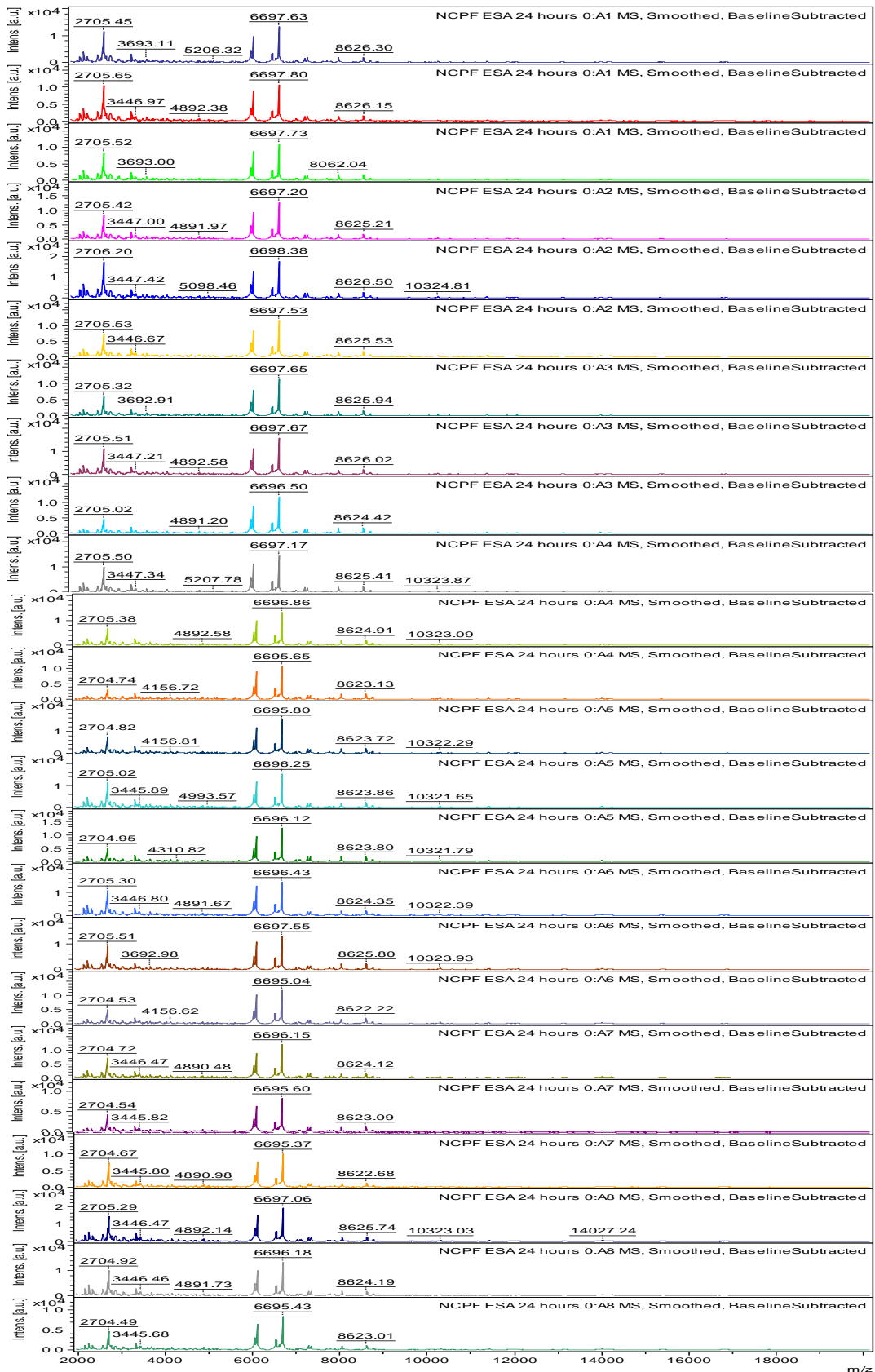
Replicate 1



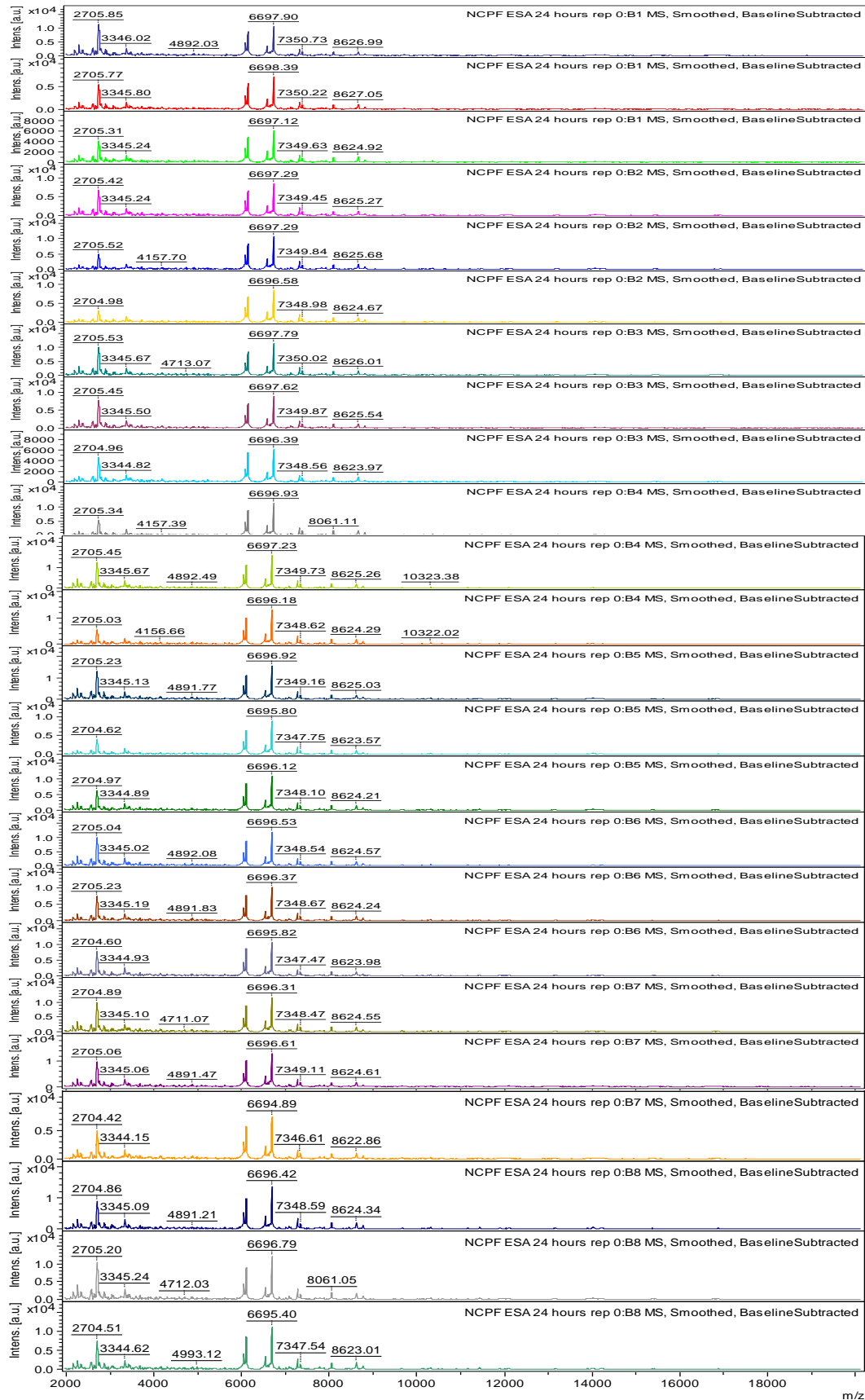
Replicate 2



Appendix 5-H: Protein profiles from *S. chartarum*, NCPF 7587 (replicate 1) grown in SDB at 25 °C spotted 8 times on MALDI target with 3 measurements in each spots gave total of 24 spectra.



Appendix 5-I: Protein profiles from *S. chartarum*, NCPF 7587 (replicate 2)
grown in SDB at 25 °C spotted 8 times on MALDI target with 3 measurements
in each spots gave total of 24 spectra.



Appendix 5-J: Statistical analysis of the mean differences from 2 replicates of *Stachybotrys chartarum*, NCPF 7587 grown in SDB for 24 hours at 25 °C.

Peak range (m/z)	Replicate 1 (n=24)	Replicate 2 (n=24)	p-value
	Mean	Mean	
3000	3345.24	3345.18	0.711021
4000	4157.3	4156.98	0.123644
	4311.37	4311.53	0.460438
5000	5206.89	5207.23	0.274595
6000	6109.74	6109.77	0.886814
	6544.63	6544.61	0.939725
	6696.66	6696.7	0.885932
7000	7088.35	7087.76	0.240706
	7285.97	7286.02	0.83371
	7348.96	7348.86	0.748059
8000	8060.85	8060.89	0.894766
	8624.68	8624.74	0.854441
	8777.11	8777.19	0.815178
10000	10322.72	10322.61	0.788617

Appendix 5-K: The mass peaks for all the 8 spots in triplicates of *Stachybotrys chartarum*, NCPF 7587 (replicate 1) grown in SDB.

Tolerance		1.5	2	2	2.5	3	3	3.5	3.5	3.5	4	4	4
		3000	4000	4000	6000	6000	6000	7000	7000	7000	8000	8000	8000
A1	1	3345.7	4157.39	4312.12	6110.47	6545.45	6697.61	7088.48	7287.07	7350.05	8062.1	8626.3	8778.2
	2	3346.16	4158.84	4312.17	6110.8	6545.47	6697.79	7089.05	7287.16	7350.86	8062.68	8626.28	8779.02
	3	3345.8	4158.13	4312.11	6110.82	6545.86	6697.7	7089.42	7286.86	7350.03	8061.98	8626.15	8778.61
A2	1	3345.24	4157.65	4311.56	6110.15	6544.9	6697.18	7088.24	7286.4	7349.91	8061.64	8625.21	8777.73
	2	3346.6	4158.74	4313.4	6111.21	6546.21	6698.37	7090.05	7287.81	7350.85	8062.75	8626.49	8778.93
	3	3345.78	4157.93	4311.56	6110.43	6545.46	6697.33	7089.29	7286.75	7349.54	8061.64	8625.52	8778.04
A3	1	3345.53	4157.35	4312.17	6110.52	6545.55	6697.45	7088.93	7286.8	7349.96	8062.01	8625.97	8778.14
	2	3345.75	4157.42	4312.16	6110.49	6545.6	6697.66	7088.82	7286.95	7350.01	8062.19	8626.02	8777.78
	3	3345.01	4157.23	4311.56	6109.56	6544.63	6696.5	7088.04	7286.01	7348.78	8060.53	8624.43	8776.59
A4	1	3345.6	4157.04	4311.95	6110.32	6545.1	6697.14	7088.02	7286.39	7349.39	8061.49	8625.41	8778.1
	2	3345.47	4157.35	4311.06	6109.78	6544.83	6696.86	7087.85	7286.7	7349.02	8060.82	8624.93	8777.26
	3	3344.66	4156.78	4310.72	6108.8	6543.49	6695.65	7086.89	7284.89	7347.69	8059.43	8623.12	8775.16
A5	1	3344.77	4156.8	4310.44	6109	6543.97	6695.79	7086.53	7284.85	7347.95	8059.73	8623.71	8776.16
	2	3345.09	4156.98	4311.15	6109.39	6544.23	6696.23	7087.29	7285.42	7348.22	8060.18	8623.85	8776.51
	3	3345	4156.81	4310.83	6109.13	6544	6695.91	7087.12	7285.31	7348.58	8059.89	8623.79	8775.87
A6	1	3345.18	4158.14	4311.17	6109.63	6544.59	6696.43	7087.73	7285.54	7348.66	8060.78	8624.37	8777.09
	2	3345.69	4158.16	4311.79	6110.6	6545.21	6697.48	7088.97	7286.73	7349.73	8061.71	8625.78	8778.5
	3	3344.51	4156.77	4309.72	6108.31	6543.17	6695.04	7097.12	7284.06	7347.16	8058.91	8622.22	8775.12
A7	1	3344.74	4156.41	4311.56	6109.1	6544.1	6696.14	7087.53	7285.59	7348.35	8060.31	8624.12	8777.75
	2	3344.36	4156.35	4310.33	6108.88	6543.41	6695.61	7086.51	7284.76	7347.75	8059.78	8623.07	8775.09
	3	3344.39	4156.07	4310.33	6108.33	6543.26	6695.36	7085.82	7284.85	7347.33	8058.99	8622.69	8775.85
A8	1	3345.58	4157.45	4311.56	6110.14	6545.29	6697.04	7088.87	7286.37	7349.34	8061.53	8625.72	8777.59
	2	3344.99	4156.87	4311.14	6109.26	6544.2	6696.19	7087.31	7285.45	7348.37	8060.29	8624.17	8776.4
	3	3344.19	4156.46	4310.33	6108.52	6543.18	6695.42	7086.51	7284.51	7347.57	8058.96	8623.04	8775.05

Appendix 5-L: The allowed peaks were calculated as the differences between the smallest and the largest mass for each peaks. The masses outside the allowable range were removed and a new set of spectra were used for generating the MSP (highlighted in red).

m/z range	3000	4000	4000	6000	6000	6000	7000	7000	7000	8000	8000	8000	8000
Mass peaks	3344.19	4156.07	4309.72	4890.16	6108.31	6543.17	6695.04	7085.82	7284.06	7347.16	8058.91	8622.22	8775.05
	3344.36	4156.35	4310.33	4890.46	6108.33	6543.18	6695.36	7086.51	7284.51	7347.33	8058.96	8622.69	8775.09
	3344.39	4156.41	4310.33	4890.83	6108.52	6543.26	6695.42	7086.51	7284.76	7347.57	8058.99	8623.04	8775.12
	3344.51	4156.46	4310.33	4890.96	6108.8	6543.41	6695.61	7086.53	7284.85	7347.69	8059.43	8623.07	8775.16
	3344.66	4156.77	4310.44	4890.96	6108.88	6543.49	6695.65	7086.89	7284.85	7347.75	8059.73	8623.12	8775.85
	3344.74	4156.78	4310.72	4891.19	6109	6543.97	6695.79	7087.12	7284.89	7347.95	8059.78	8623.71	8775.87
	3344.77	4156.8	4310.83	4891.26	6109.1	6544	6695.91	7087.29	7285.31	7348.22	8059.89	8623.79	8776.16
	3344.99	4156.81	4311.06	4891.26	6109.13	6544.1	6696.14	7087.31	7285.42	7348.35	8060.18	8623.85	8776.4
	3345	4156.87	4311.14	4891.26	6109.26	6544.2	6696.19	7087.53	7285.45	7348.37	8060.29	8624.12	8776.51
	3345.01	4156.98	4311.15	4891.26	6109.39	6544.23	6696.23	7087.73	7285.54	7348.58	8060.31	8624.17	8776.59
	3345.09	4157.04	4311.17	4891.59	6109.56	6544.59	6696.43	7087.85	7285.59	7348.66	8060.53	8624.37	8777.09
	3345.18	4157.23	4311.56	4891.67	6109.63	6544.63	6696.5	7088.02	7286.01	7348.78	8060.78	8624.43	8777.26
	3345.24	4157.35	4311.56	4891.79	6109.78	6544.83	6696.86	7088.04	7286.37	7349.02	8060.82	8624.93	8777.59
	3345.47	4157.35	4311.56	4891.92	6110.14	6544.9	6697.04	7088.24	7286.39	7349.34	8061.49	8625.21	8777.73
	3345.53	4157.39	4311.56	4891.92	6110.15	6545.1	6697.14	7088.48	7286.4	7349.39	8061.53	8625.41	8777.75
	3345.58	4157.42	4311.56	4891.95	6110.32	6545.21	6697.18	7088.82	7286.7	7349.54	8061.64	8625.52	8777.78
	3345.6	4157.45	4311.79	4892.18	6110.43	6545.29	6697.33	7088.87	7286.73	7349.73	8061.64	8625.72	8778.04
	3345.69	4157.65	4311.95	4892.34	6110.47	6545.45	6697.45	7088.93	7286.75	7349.91	8061.71	8625.78	8778.1
	3345.7	4157.93	4312.11	4892.57	6110.49	6545.46	6697.48	7088.97	7286.8	7349.96	8061.98	8625.97	8778.14
	3345.75	4158.13	4312.12	4892.6	6110.52	6545.47	6697.61	7089.05	7286.86	7350.01	8062.01	8626.02	8778.2
3345.78	4158.14	4312.16	4892.63	6110.6	6545.55	6697.66	7089.29	7286.95	7350.03	8062.1	8626.15	8778.5	
3345.8	4158.16	4312.17	4892.66	6110.8	6545.6	6697.7	7089.42	7287.07	7350.05	8062.19	8626.28	8778.61	
3346.16	4158.74	4312.17	4892.9	6110.82	6545.86	6697.79	7090.05	7287.16	7350.85	8062.68	8626.3	8778.93	
3346.6	4158.84	4313.4	4893.22	6111.21	6546.21	6698.37	7097.12	7287.81	7350.86	8062.75	8626.49	8779.02	
Peak shift	1.44	2.09	1.84	2.44	2.9	2.69	2.75	2.91	3.1	2.89	3.84	3.61	3.97

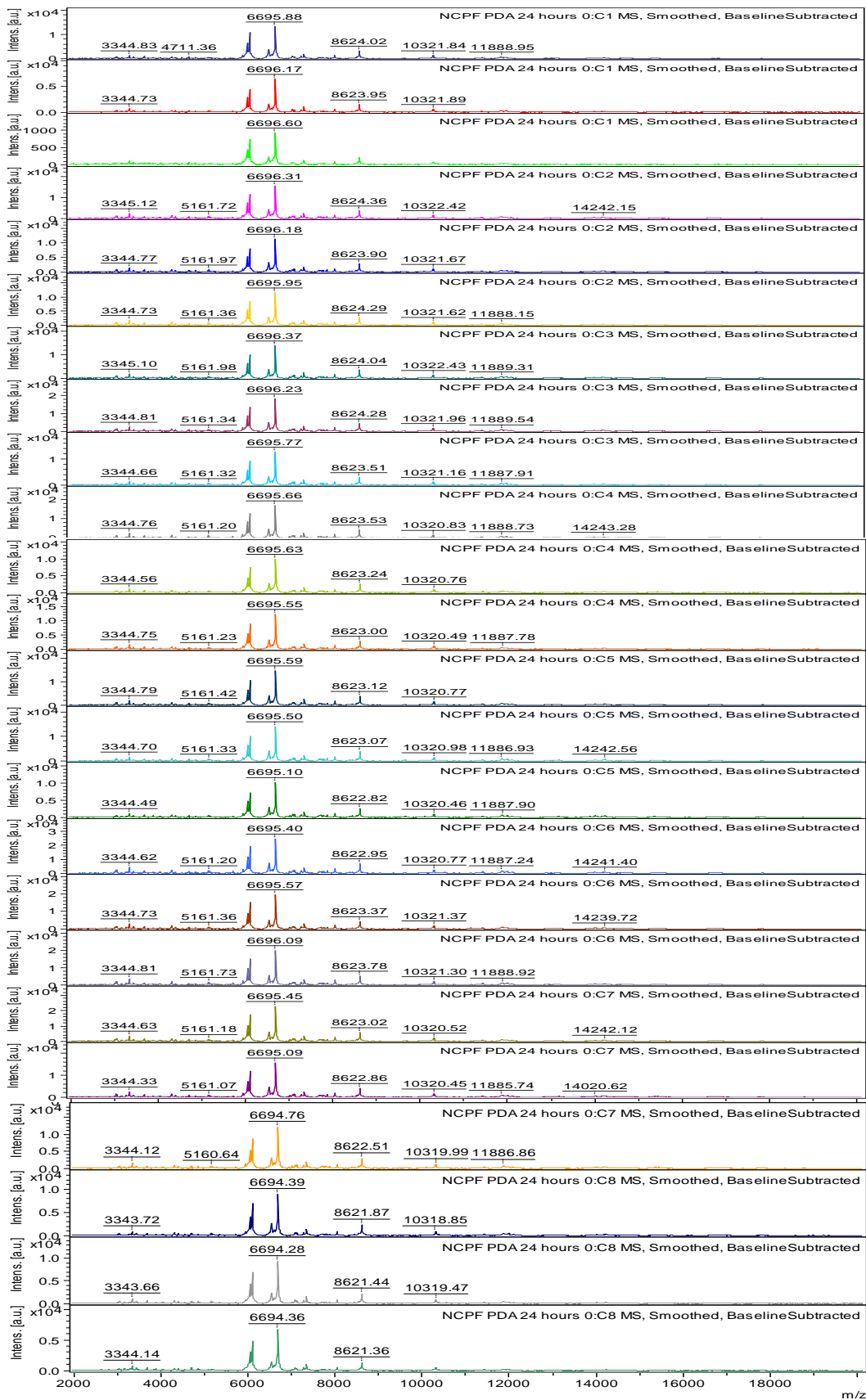
Appendix 5-M: The mass peaks for all the 8 spots in triplicates of *Stachybotrys chartarum*, NCPF 7587 (replicate 2) grown in SDB.

Tolerance		1.5	2	3	3	3	3	3.5	3.5	3.5	4	4	4
Replicates/	mass	3000	4000	4000	6000	6000	6000	7000	7000	7000	8000	8000	8000
B1	1	3346.02	4157.56	4312.17	6110.96	6546.02	6697.9	7089.49	7287.64	7350.73	8062.78	8626.99	8778.52
	2	3345.8	4158.16	4312.17	6111.13	6545.71	6698.39	7089.76	7287.19	7350.22	8062.61	8627.05	8779.44
	3	3345.24	4156.06	4311.56	6110.21	6545.08	6697.12	7088.97	7286.22	7349.63	8061.47	8624.92	8777.68
B2	1	3345.24	4157.46	4311.56	6110.27	6545.41	6697.29	7088.18	7286.81	7349.45	8061.11	8625.27	8777.62
	2	3345.71	4157.7	4311.56	6110.37	6545.3	6697.29	7088.49	7286.89	7349.84	8061.75	8625.68	8778.32
	3	3344.99	4156.96	4312.17	6109.65	6544.48	6696.58	7086.61	7285.98	7348.98	8060.5	8624.67	8777.42
B3	1	3345.67	4156.86	4312.79	6110.93	6545.49	6697.79	7089.32	7287.323	7350.02	8062.25	8626.01	8778.11
	2	3345.5	4157.81	4312.17	6110.51	6544.97	6697.62	7088.88	7286.76	7349.87	8062.07	8625.54	8778.36
	3	3344.82	4156.35	4311.29	6109.42	6544.18	6696.39	7087.39	7286.04	7348.56	8060.26	8623.97	8776.81
B4	1	3345.53	4157.39	4311.56	6110.05	6544.89	6696.93	7087.23	7286.24	7349.04	8061.11	8624.86	8777.24
	2	3345.67	4157.5	4312.17	6110.23	6545.41	6697.23	7088.46	7286.67	7349.73	8061.58	8625.26	8777.69
	3	3345.14	4156.66	4310.91	6109.49	6544.24	6696.18	7087.51	7285.43	7348.62	8060.3	8624.29	8776.33
B5	1	3345.13	4156.83	4311.56	6109.72	6545.03	6696.92	7088.25	7286.33	7349.16	8061.18	8625.03	8777.75
	2	3344.69	4156.06	4312.17	6108.89	6543.67	6695.8	7085.82	7284.98	7347.75	8059.65	8623.57	8775.81
	3	3344.89	4156.22	4310.95	6109.08	6543.88	6696.12	7087.16	7285.26	7348.1	8059.92	8624.21	8775.73
B6	1	3345.02	4157.06	4311.29	6109.61	6544.77	6696.53	7087.84	7285.65	7348.54	8061.02	8624.21	8777.89
	2	3345.19	4157.13	4310.95	6109.59	6544.06	6696.37	7087.34	7285.49	7348.67	8060.43	8624.24	8776.48
	3	3344.93	4156.75	4311.56	6108.93	6543.92	6695.82	7086.59	7285.2	7347.47	8060.01	8623.98	8775.88
B7	1	3345.1	4157.54	4310.95	6109.48	6544.44	6696.37	7087.87	7285.7	7347.47	8060.67	8624.55	8777.26
	2	3345.06	4156.93	4312.17	6109.7	6544.86	6696.61	7087.97	7286.24	7349.11	8061.14	8624.61	8777.43
	3	3344.15	4155.62	4310.33	6108.22	6542.85	6694.89	7085.55	7284.42	7346.61	8058.71	8622.86	8775.05
B8	1	3345.09	4157.33	4310.62	6109.58	6544.23	6696.42	7087.18	7285.57	7348.59	8060.37	8624.34	8776.43
	2	3345.24	4157.56	4311.77	6109.77	6544.63	6696.79	7087.87	7286	7349.05	8061.05	8624.74	8777.71
	3	3344.62	4156.02	4310.32	6108.64	6543.19	6695.4	7086.54	7284.55	7347.54	8059.4	8623.01	8775.52

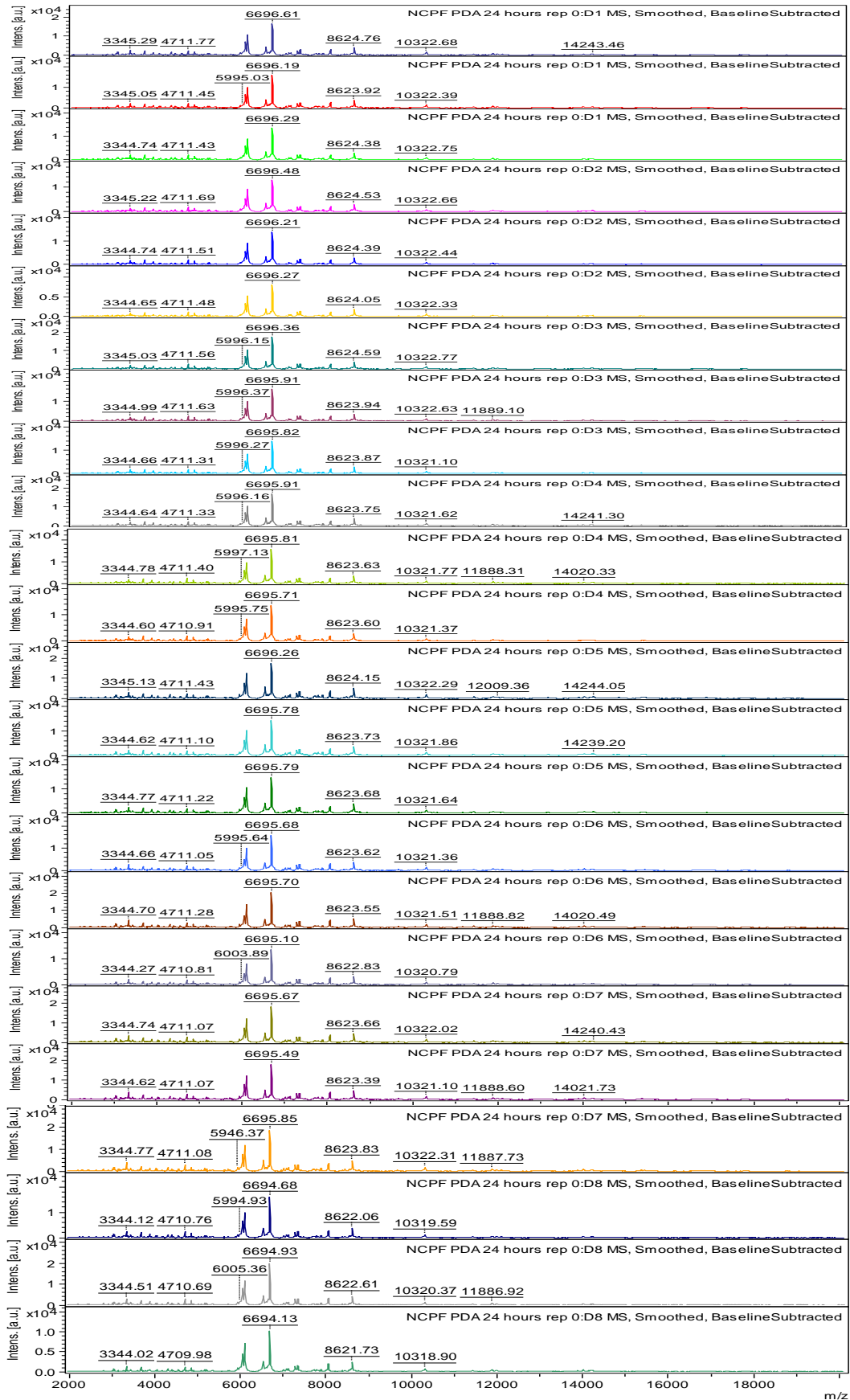
Appendix 5-N: The allowed peaks were calculated as the differences between the smallest and the largest mass for each peaks. The masses outside the allowable range were removed and a new set of spectra were used for generating the MSP (highlighted in red).

Mass range	3000	4000	4000	6000	6000	6000	7000	7000	7000	8000	8000	8000
Mass peaks	3344.15	4155.62	4310.32	6108.22	6542.85	6694.89	7085.55	7284.42	7346.61	8058.71	8622.86	8775.05
	3344.62	4156.02	4310.33	6108.64	6543.19	6695.4	7085.82	7284.55	7347.47	8059.4	8623.01	8775.52
	3344.69	4156.06	4310.62	6108.89	6543.67	6695.8	7086.54	7284.98	7347.47	8059.65	8623.57	8775.73
	3344.82	4156.06	4310.91	6108.93	6543.88	6695.82	7086.59	7285.2	7347.54	8059.92	8623.97	8775.81
	3344.89	4156.22	4310.95	6109.08	6543.92	6696.12	7086.61	7285.26	7347.75	8060.01	8623.98	8775.88
	3344.93	4156.35	4310.95	6109.42	6544.06	6696.18	7087.16	7285.43	7348.1	8060.26	8624.21	8776.33
	3344.99	4156.66	4310.95	6109.48	6544.18	6696.37	7087.18	7285.49	7348.54	8060.3	8624.21	8776.43
	3345.02	4156.75	4311.29	6109.49	6544.23	6696.37	7087.23	7285.57	7348.56	8060.37	8624.24	8776.48
	3345.06	4156.83	4311.29	6109.58	6544.24	6696.39	7087.34	7285.65	7348.59	8060.43	8624.29	8776.81
	3345.09	4156.86	4311.56	6109.59	6544.44	6696.42	7087.39	7285.7	7348.62	8060.5	8624.34	8777.24
	3345.1	4156.93	4311.56	6109.61	6544.48	6696.53	7087.51	7285.98	7348.67	8060.67	8624.55	8777.26
	3345.13	4156.96	4311.56	6109.65	6544.63	6696.58	7087.84	7286	7348.98	8061.02	8624.61	8777.42
	3345.14	4157.06	4311.56	6109.7	6544.77	6696.61	7087.87	7286.04	7349.04	8061.05	8624.67	8777.43
	3345.19	4157.13	4311.56	6109.72	6544.86	6696.79	7087.87	7286.22	7349.05	8061.11	8624.74	8777.62
	3345.24	4157.33	4311.56	6109.77	6544.89	6696.92	7087.97	7286.24	7349.11	8061.11	8624.86	8777.68
	3345.24	4157.39	4311.77	6110.05	6544.97	6696.93	7088.18	7286.24	7349.16	8061.14	8624.92	8777.69
	3345.24	4157.46	4312.17	6110.21	6545.03	6697.12	7088.25	7286.33	7349.45	8061.18	8625.03	8777.71
	3345.5	4157.5	4312.17	6110.23	6545.08	6697.23	7088.46	7286.67	7349.63	8061.47	8625.26	8777.75
	3345.53	4157.54	4312.17	6110.27	6545.3	6697.29	7088.49	7286.76	7349.73	8061.58	8625.27	8777.89
	3345.67	4157.56	4312.17	6110.37	6545.41	6697.29	7088.88	7286.81	7349.84	8061.75	8625.54	8778.11
3345.67	4157.56	4312.17	6110.51	6545.41	6697.62	7088.97	7286.89	7349.87	8062.07	8625.68	8778.32	
3345.71	4157.7	4312.17	6110.93	6545.49	6697.79	7089.32	7287.19	7350.02	8062.25	8626.01	8778.36	
3345.8	4157.81	4312.17	6110.96	6545.71	6697.9	7089.49	7287.323	7350.22	8062.25	8626.01	8778.52	
3346.02	4158.16	4312.79	6111.13	6546.02	6698.39	7089.76	7287.64	7350.73	8062.78	8627.05	8779.44	
Peak shift	1.18	1.79	1.85	2.91	2.86	3.01	3.5	2.773	3.41	3.54	3.15	3.47

Appendix 5-O: Protein profiles obtained from *S. chartarum*, NCPF 7587 (replicate 1) grown in PDB at 25 °C spotted 8 times on MALDI target with 3 measurements in each spots gave total of 24 spectra.



Appendix 5-P: Protein profiles obtained from *S. chartarum*, NCPF 7587 (replicate 2) grown in PDB at 25 °C spotted 8 times on MALDI target with 3 measurements in each spots gave total of 24 spectra.



Appendix 5-Q: Statistical analysis of the mean differences from 2 replicates of *Stachybotrys chartarum*, NCPF 7587 grown in PDB for 24 hours at 25 °C. (*) indicates statistically significant at p-value < 0.05.

Peak range (m/z)	Replicate 1 (n=24)	Replicate 2 (n=24)	p-value
	Mean	Mean	
3000	3344.62	3344.68	0.551042
	3438.84	3438.72	0.37928
	3684.65	3684.67	0.804137
4000	4028.26	4028.27	0.910293
	4310.51	4310.86	0.012953*
5000	5161.46	5161.64	0.43366
6000	6108.65	6108.84	0.245749
	6695.6	6695.78	0.342292
7000	7086.82	7087.08	0.208117
	7348.05	7348.17	0.564472
8000	8060.06	8060.26	0.417871
	8623.24	8623.68	0.077205

Appendix 5-R: The mass peaks for all the 8 spots in triplicates of *Stachybotrys chartarum*, NCPF 7587 (replicate 1) grown in PDB.

Tolerance		1.5	1.5	1.5	2	2	2.5	3	3	3.5	3.5	4	4	4.5
Replicates/ mass		3000	3000	3000	4000	4000	5000	6000	6000	7000	7000	8000	8000	10000
C1	1	3344.83	3439.14	3684.94	4028.4	4310.65	5161.85	6109.06	6695.88	7087.55	7348.51	8060.76	8623.97	10321.84
	2	3344.73	3438.93	3684.51	4028.74	4310.95	5161.85	6109.15	6696.71	7087.39	7348.77	8061.71	8623.96	10322.05
	3	3345.26	3439.48	3685.08	4027.11	4309.1	5165.21	6109.59	6696.6	7088.18	7348.93	8060.87	8624.05	10321.1
C2	1	3345.12	3439.52	3685.12	4028.82	4311.01	5161.75	6109.41	6696.31	7087.81	7349.1	8061.14	8624.4	10322.42
	2	3344.77	3438.93	3685.03	4028.46	4310.72	5161.91	6109.01	6696.18	7087.11	7348.73	8060.85	8623.94	10321.67
	3	3344.73	3439.35	3685	4028.34	4311	5161.56	6109.08	6695.95	7087.57	7348.62	8060.81	8624.29	10321.62
C3	1	3345.1	3438.94	3684.77	4028.38	4311.09	5161.94	6109.16	6696.37	7087.72	7348.76	8061.07	8624.29	10322.43
	2	3344.81	3439.12	3684.93	4028.73	4311.09	5161.36	6109.14	6696.23	7087.48	7348.68	8060.95	8624.3	10321.96
	3	3344.66	3438.87	3684.4	4028.49	4310.38	5161.29	6108.79	6695.77	7087.34	7348.28	8060.02	8623.58	10321.16
C4	1	3344.76	3439.12	3684.76	4028.33	4310.82	5161.21	6108.78	6695.66	7087.04	7348.26	8060.25	8623.56	10320.83
	2	3344.56	3438.93	3684.51	4028.64	4310.23	5160.5	6108.63	6695.63	7086.65	7348.01	8059.91	8623.49	10320.76
	3	3344.75	3438.39	3684.62	4028.65	4310.82	5161.2	6108.68	6695.55	7086.47	7347.77	8059.62	8623.02	10320.49
C5	1	3344.79	3439.11	3685	4028.34	4310.49	5161.59	6108.74	6695.59	7086.71	7347.92	8059.89	8623.12	10320.77
	2	3344.7	3438.73	3684.83	4028.76	4310.37	5161.3	6108.7	6695.5	7086.59	7347.97	8059.87	8623.07	10320.98
	3	3344.49	3438.93	3684.75	4027.87	4310.22	5161.85	6108.29	6695.1	7086.64	7347.7	8059.54	8622.85	10320.46
C6	1	3344.62	3438.62	3684.42	4028.26	4310.69	5161.21	6108.41	6695.4	7086.39	7347.87	8059.95	8622.96	10320.77
	2	3344.73	3439.05	3684.96	4028.61	4310.76	5161.32	6108.72	6695.57	7086.92	7348	8060.34	8623.4	10321.37
	3	3344.81	3438.89	3685.01	4028.65	4310.96	5161.73	6109.04	6696.09	7087.31	7348.62	8060.71	8623.81	10321.3
C7	1	3344.63	3439.14	3684.64	4028.03	4310.69	5161.2	6108.41	6695.45	7086.63	7347.79	8060.24	8621.03	10320.52
	2	3344.33	3438.31	3684.05	4027.72	4310.28	5161.09	6108.22	6695.09	7086.47	7347.63	8059.02	8622.87	10320.45
	3	3344.12	3438.19	3684.52	4027.94	4310.06	5160.66	6107.96	6694.76	7085.75	7347.47	8058.76	8622.53	10319.99
C8	1	3343.72	3437.83	3683.94	4027.53	4310.33	5160.5	6107.61	6694.39	7085.42	7346.82	8058.38	8621.87	10318.85
	2	3343.66	3438.38	3683.76	4027.03	4309.1	5160.5	6107.52	6694.28	7085.58	7346.78	8058.38	8621.67	10319.47
	3	3344.14	3438.38	3683.94	4028.3	4310.33	5160.5	6107.61	6694.36	7085.03	7346.31	8058.35	8621.61	10319.2

Appendix 5-S: The allowed peaks were calculated as the differences between the smallest and the largest mass for each peaks. The masses outside the allowable range were removed and a new set of spectra were used for generating the MSP (highlighted in red).

Mass range	3000	3000	3000	4000	4000	5000	6000	6000	7000	7000	8000	8000	10000
Mass peaks	3343.66	3437.83	3683.76	4027.03	4309.1	5160.5	6107.52	6694.28	7085.03	7346.31	8058.35	8621.03	10318.85
	3343.72	3438.19	3683.94	4027.11	4309.1	5160.5	6107.61	6694.36	7085.42	7346.78	8058.38	8621.61	10319.2
	3344.12	3438.31	3683.94	4027.53	4310.06	5160.5	6107.61	6694.39	7085.58	7346.82	8058.38	8621.67	10319.47
	3344.14	3438.38	3684.05	4027.72	4310.22	5160.5	6107.96	6694.76	7085.75	7347.47	8058.76	8621.87	10319.99
	3344.33	3438.38	3684.4	4027.87	4310.23	5160.66	6108.22	6695.09	7086.39	7347.63	8059.02	8622.53	10320.45
	3344.49	3438.39	3684.42	4027.94	4310.28	5161.09	6108.29	6695.1	7086.47	7347.7	8059.54	8622.85	10320.46
	3344.56	3438.62	3684.51	4028.03	4310.33	5161.2	6108.41	6695.4	7086.47	7347.77	8059.62	8622.87	10320.49
	3344.62	3438.73	3684.51	4028.26	4310.33	5161.2	6108.41	6695.45	7086.59	7347.79	8059.87	8622.96	10320.52
	3344.63	3438.87	3684.52	4028.3	4310.37	5161.21	6108.63	6695.5	7086.63	7347.87	8059.89	8623.02	10320.76
	3344.66	3438.89	3684.62	4028.33	4310.38	5161.21	6108.68	6695.55	7086.64	7347.92	8059.91	8623.07	10320.77
	3344.7	3438.93	3684.64	4028.34	4310.49	5161.29	6108.7	6695.57	7086.65	7347.97	8059.95	8623.12	10320.77
	3344.73	3438.93	3684.75	4028.34	4310.65	5161.3	6108.72	6695.59	7086.71	7348	8060.02	8623.4	10320.83
	3344.73	3438.93	3684.76	4028.38	4310.69	5161.32	6108.74	6695.63	7086.92	7348.01	8060.24	8623.49	10320.98
	3344.73	3438.93	3684.77	4028.4	4310.69	5161.36	6108.78	6695.66	7087.04	7348.26	8060.25	8623.56	10321.1
	3344.75	3438.94	3684.83	4028.46	4310.72	5161.56	6108.79	6695.77	7087.11	7348.28	8060.34	8623.58	10321.16
	3344.76	3439.05	3684.93	4028.49	4310.76	5161.59	6109.01	6695.88	7087.31	7348.51	8060.71	8623.81	10321.3
	3344.77	3439.11	3684.94	4028.61	4310.82	5161.73	6109.04	6695.95	7087.34	7348.62	8060.76	8623.94	10321.37
	3344.79	3439.12	3684.96	4028.64	4310.82	5161.75	6109.06	6696.09	7087.39	7348.62	8060.81	8623.96	10321.62
	3344.81	3439.12	3685	4028.65	4310.95	5161.85	6109.08	6696.18	7087.48	7348.68	8060.85	8623.97	10321.67
	3344.81	3439.14	3685	4028.65	4310.96	5161.85	6109.14	6696.23	7087.55	7348.73	8060.87	8624.05	10321.84
3344.83	3439.14	3685.01	4028.73	4311	5161.85	6109.15	6696.31	7087.57	7348.76	8060.95	8624.29	10321.96	
3345.1	3439.35	3685.03	4028.74	4311.01	5161.91	6109.16	6696.37	7087.72	7348.77	8061.07	8624.29	10322.05	
3345.12	3439.48	3685.08	4028.76	4311.09	5161.94	6109.41	6696.6	7087.81	7348.93	8061.14	8624.3	10322.42	
3345.26	3439.52	3685.12	4028.82	4311.09	5165.21	6109.59	6696.71	7088.18	7349.1	8061.71	8624.4	10322.43	
Peak shift	1.46	1.52	1.36	1.79	1.99	1.44	1.89	2.43	3.15	2.79	3.36	3.37	3.58

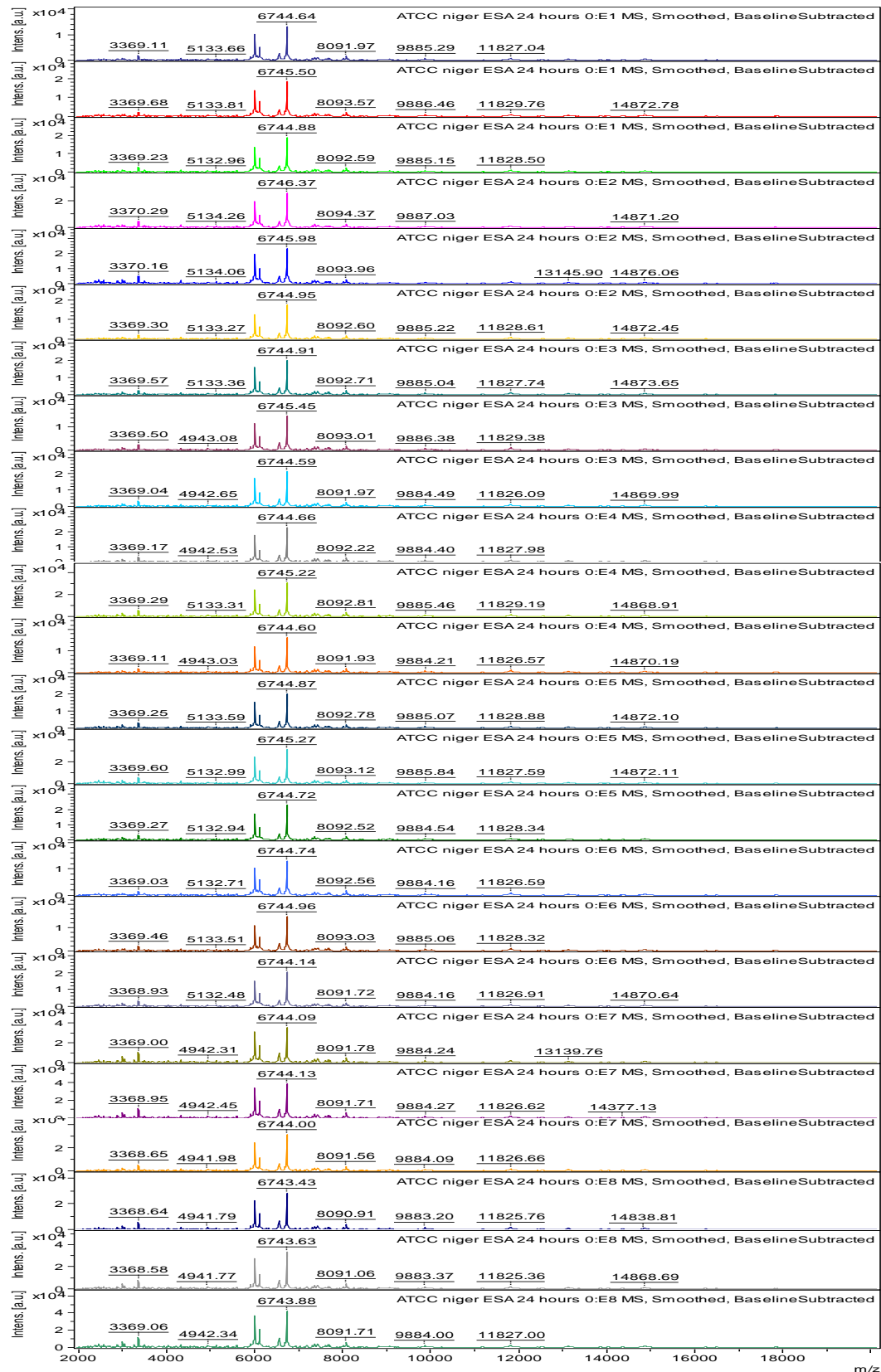
Appendix 5-T: The mass peaks for all the 8 spots in triplicates of *Stachybotrys chartarum*, NCPF 7587 (replicate 2) grown in PDB.

Tolerance		1.5	1.5	1.5	2.0	2.0	2.5	3	3	3.5	3.5	4	4	4.5
Replicates/ mass		3000	3000	3000	4000	4000	5000	6000	6000	7000	7000	8000	8000	10000
D1	1	3345.29	3438.85	3685.15	4028.84	4311.44	5162.02	6109.71	6696.61	7087.86	7349.2	8061.26	8624.76	10322.68
	2	3345.05	3438.92	3684.94	4028.95	4311.17	5161.76	6109.11	6696.19	7087.4	7348.58	8060.62	8623.92	10322.39
	3	3344.74	3439.02	3684.82	4028.9	4311.34	5162.22	6109.13	6696.29	7087.44	7348.56	8060.81	8624.38	10322.75
D2	1	3345.22	3439.56	3684.99	4028.3	4311.21	5162.52	6109.47	6696.48	7088.04	7348.72	8061.29	8624.53	10322.66
	2	3344.74	3438.97	3684.9	4028.9	4310.6	5161.17	6109.11	6696.21	7087.82	7348.73	8060.59	8624.39	10322.44
	3	3344.65	3438.38	3684.52	4028.3	4310.98	5162.85	6109.14	6696.27	7087.39	7348.51	8060.75	8624.05	10322.33
D3	1	3344.03	3439.35	3684.66	4028.66	4311.13	5162.01	6109.13	6696.36	7087.32	7348.78	8060.82	8624.59	10322.77
	2	3344.99	3438.93	3684.86	4028	4311.11	5162.28	6109.08	6695.91	7087.18	7348.52	8060.71	8623.94	10322.63
	3	3344.66	3439.51	3684.65	4028.3	4310.79	5162.85	6108.89	6695.82	7086.84	7348.29	8060.37	8623.87	10321.1
D4	1	3344.64	3439.38	3684.89	4027.99	4311.15	5161.33	6109.02	6695.91	7087.08	7348.3	8060.62	8623.75	10321.62
	2	3344.78	3438.97	3684.85	4028.12	4310.98	5161.59	6108.89	6695.81	7087.12	7348.05	8060.34	8623.63	10321.77
	3	3344.6	3438.47	3684.57	4028.33	4311.03	5161.83	6108.74	6695.71	7087.78	7348.19	8060.07	8623.6	10321.37
D5	1	3345.13	3438.87	3684.96	4028.86	4311.12	5161.97	6109.13	6696.26	7087.38	7348.6	8060.68	8624.15	10322.29
	2	3344.62	3438.38	3684.92	4027.74	4311.29	5161.61	6108.89	6695.78	7086.92	7348.05	8060.34	8623.73	10321.86
	3	3344.77	3438.65	3684.92	4028.14	4311.12	5161.26	6108.96	6695.79	7087.47	7348.3	8060.45	8623.68	10321.64
D6	1	3344.66	3438.3	3684.54	4028.35	4310.61	5161.27	6108.78	6695.68	7086.93	7348	8060.31	8623.62	10321.36
	2	3344.7	3439.26	3684.86	4028.36	4310.59	5161.73	6108.83	6695.7	7086.96	7348.21	8059.91	8623.55	10321.51
	3	3344.27	3438.83	3684.32	4028.16	4310.38	5161.11	6108.3	6695.1	7086.45	7347.6	8059.49	8622.83	10320.79
D7	1	3344.74	3438.52	3684.59	4028.42	4310.78	5161.75	6108.83	6695.67	7086.99	7348.19	8060.35	8623.66	10322.02
	2	3344.62	3438.44	3684.47	4027.98	4310.73	5161.27	6108.66	6695.49	7086.93	7347.74	8059.81	8623.39	10321.1
	3	3344.77	3438.64	3684.81	4028.38	4310.87	5161.48	6109	6695.85	7087.14	7348.57	8060.53	8623.83	10322.31
D8	1	3344.12	3437.7	3683.92	4027.34	4310.14	5160.61	6107.71	6694.68	7086.19	7346.83	8058.92	8622.06	10319.59
	2	3344.51	3438.1	3684.02	4027.47	4310.4	5160.48	6108.1	6694.93	7085.96	7347.15	8059.15	8622.61	10320.37
	3	3344.02	3437.28	3683.99	4027.71	4309.69	5160.5	6107.45	6694.13	7085.43	7346.37	8058.02	8621.73	10318.9

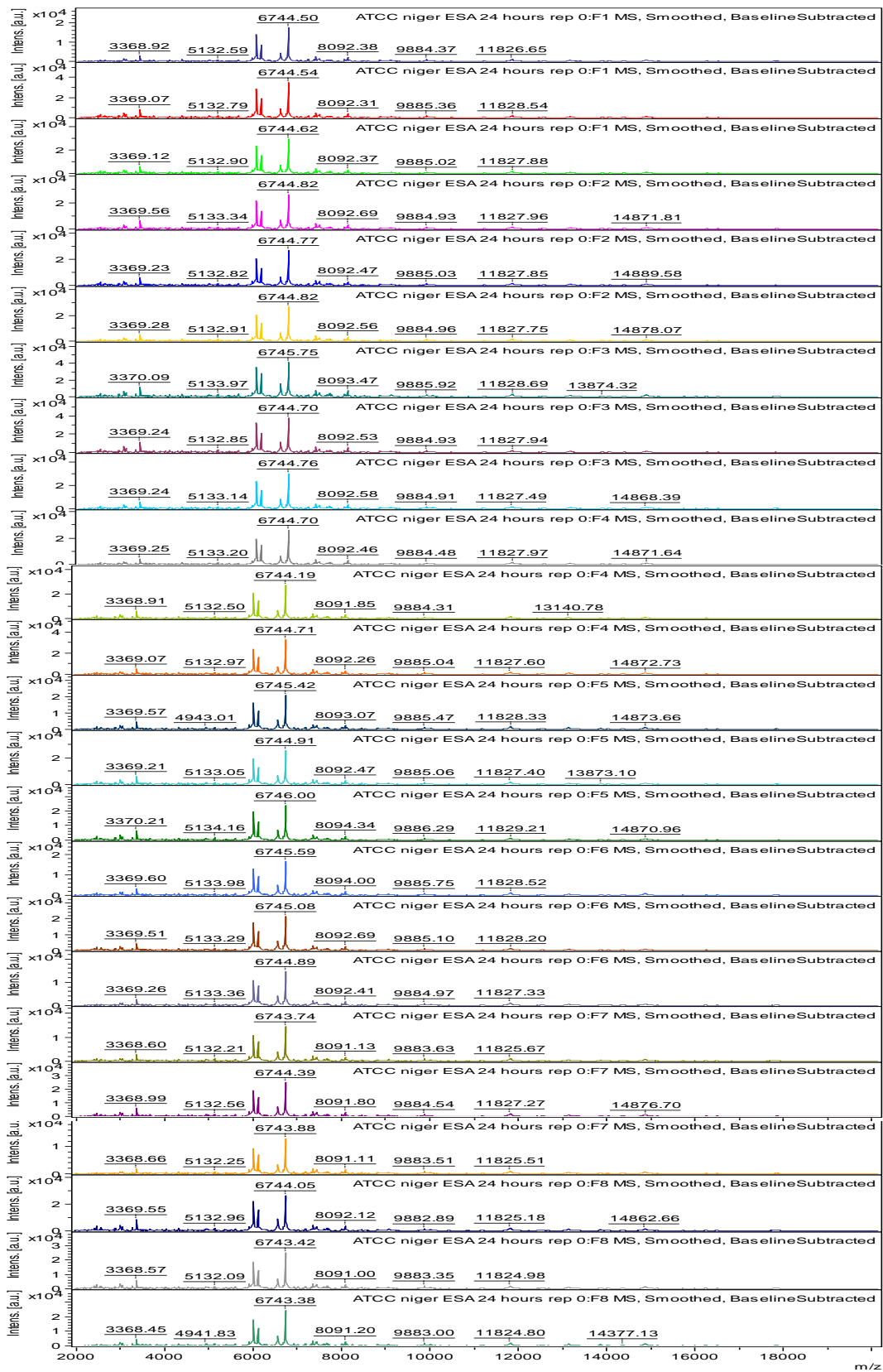
Appendix 5-U: The allowed peaks were calculated as the differences between the smallest and the largest mass for each peaks. The masses outside the allowable range were removed and a new set of spectra were used for generating the MSP (highlighted in red).

Mass range	3000	3000	3000	4000	4000	5000	6000	6000	7000	7000	8000	8000	10000
Mass peaks	3344.02	3437.28	3683.92	4027.34	4309.69	5160.48	6107.45	6694.13	7085.43	7346.37	8058.02	8621.73	10318.9
	3344.03	3437.7	3683.99	4027.47	4310.14	5160.5	6107.71	6694.68	7085.96	7346.83	8058.92	8622.06	10319.59
	3344.12	3438.1	3684.02	4027.71	4310.38	5160.61	6108.1	6694.93	7086.19	7347.15	8059.15	8622.61	10320.37
	3344.27	3438.3	3684.32	4027.74	4310.4	5161.11	6108.3	6695.1	7086.45	7347.6	8059.49	8622.83	10320.79
	3344.51	3438.38	3684.47	4027.98	4310.59	5161.17	6108.66	6695.49	7086.84	7347.74	8059.81	8623.39	10321.1
	3344.6	3438.38	3684.52	4027.99	4310.6	5161.26	6108.74	6695.67	7086.92	7348	8059.91	8623.55	10321.1
	3344.62	3438.44	3684.54	4028	4310.61	5161.27	6108.78	6695.68	7086.93	7348.05	8060.07	8623.6	10321.36
	3344.62	3438.47	3684.57	4028.12	4310.73	5161.27	6108.83	6695.7	7086.93	7348.05	8060.31	8623.62	10321.37
	3344.64	3438.52	3684.59	4028.14	4310.78	5161.33	6108.83	6695.71	7086.96	7348.19	8060.34	8623.63	10321.51
	3344.65	3438.64	3684.65	4028.16	4310.79	5161.48	6108.89	6695.78	7086.99	7348.19	8060.34	8623.66	10321.62
	3344.66	3438.65	3684.66	4028.3	4310.87	5161.59	6108.89	6695.79	7087.08	7348.21	8060.35	8623.68	10321.64
	3344.66	3438.83	3684.81	4028.3	4310.98	5161.61	6108.89	6695.81	7087.12	7348.29	8060.37	8623.73	10321.77
	3344.7	3438.85	3684.82	4028.3	4310.98	5161.73	6108.96	6695.82	7087.14	7348.3	8060.45	8623.75	10321.86
	3344.74	3438.87	3684.85	4028.33	4311.03	5161.75	6109	6695.85	7087.18	7348.3	8060.53	8623.83	10322.02
	3344.74	3438.92	3684.86	4028.35	4311.11	5161.76	6109.02	6695.91	7087.32	7348.51	8060.59	8623.87	10322.29
	3344.74	3438.93	3684.86	4028.36	4311.12	5161.83	6109.08	6695.91	7087.38	7348.52	8060.62	8623.92	10322.31
	3344.77	3438.97	3684.89	4028.38	4311.12	5161.97	6109.11	6696.19	7087.39	7348.56	8060.62	8623.94	10322.33
	3344.77	3438.97	3684.9	4028.42	4311.13	5162.01	6109.11	6696.21	7087.4	7348.57	8060.68	8624.05	10322.39
	3344.78	3439.02	3684.92	4028.66	4311.15	5162.02	6109.13	6696.26	7087.44	7348.58	8060.71	8624.15	10322.44
	3344.99	3439.26	3684.92	4028.84	4311.17	5162.22	6109.13	6696.27	7087.47	7348.6	8060.75	8624.38	10322.63
3345.05	3439.35	3684.94	4028.86	4311.21	5162.28	6109.13	6696.29	7087.78	7348.72	8060.81	8624.39	10322.66	
3345.13	3439.38	3684.96	4028.9	4311.29	5162.52	6109.14	6696.36	7087.82	7348.73	8060.82	8624.53	10322.68	
3345.22	3439.51	3684.99	4028.9	4311.34	5162.85	6109.47	6696.48	7087.86	7348.78	8061.26	8624.59	10322.75	
3345.29	3439.56	3685.15	4028.95	4311.44	5162.85	6109.71	6696.61	7088.04	7349.2	8061.29	8624.76	10322.77	
Peak shift	1.27	1.46	1.23	1.61	1.75	2.37	2.26	2.48	2.61	2.83	3.27	3.03	3.87

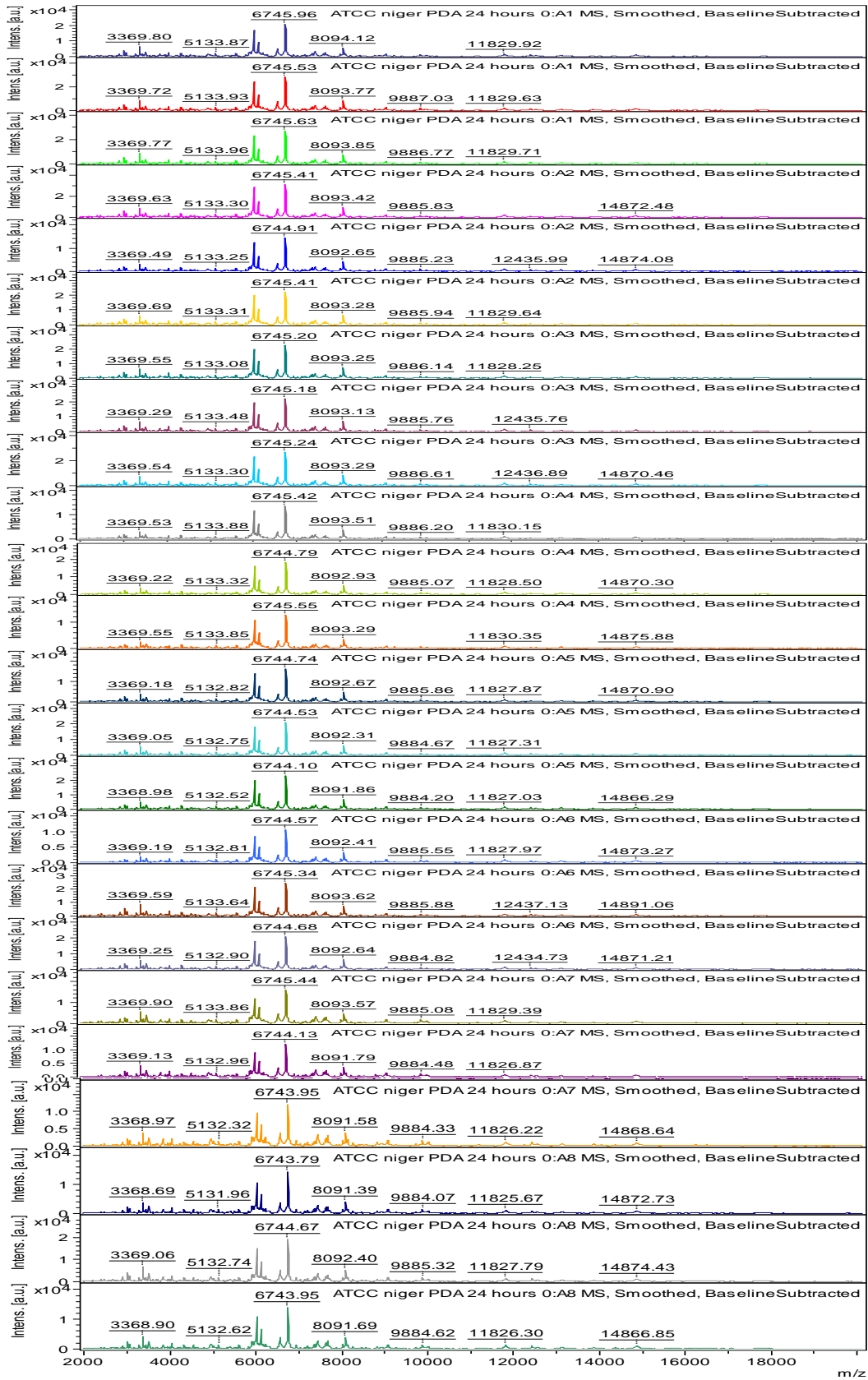
Appendix 5-V: Protein profiles obtained from *A. niger*, ATCC 16888 (replicate 1) grown in SDB at 25 °C spotted 8 times on MALDI target with 3 measurements in each spots to give total of 24 spectra.



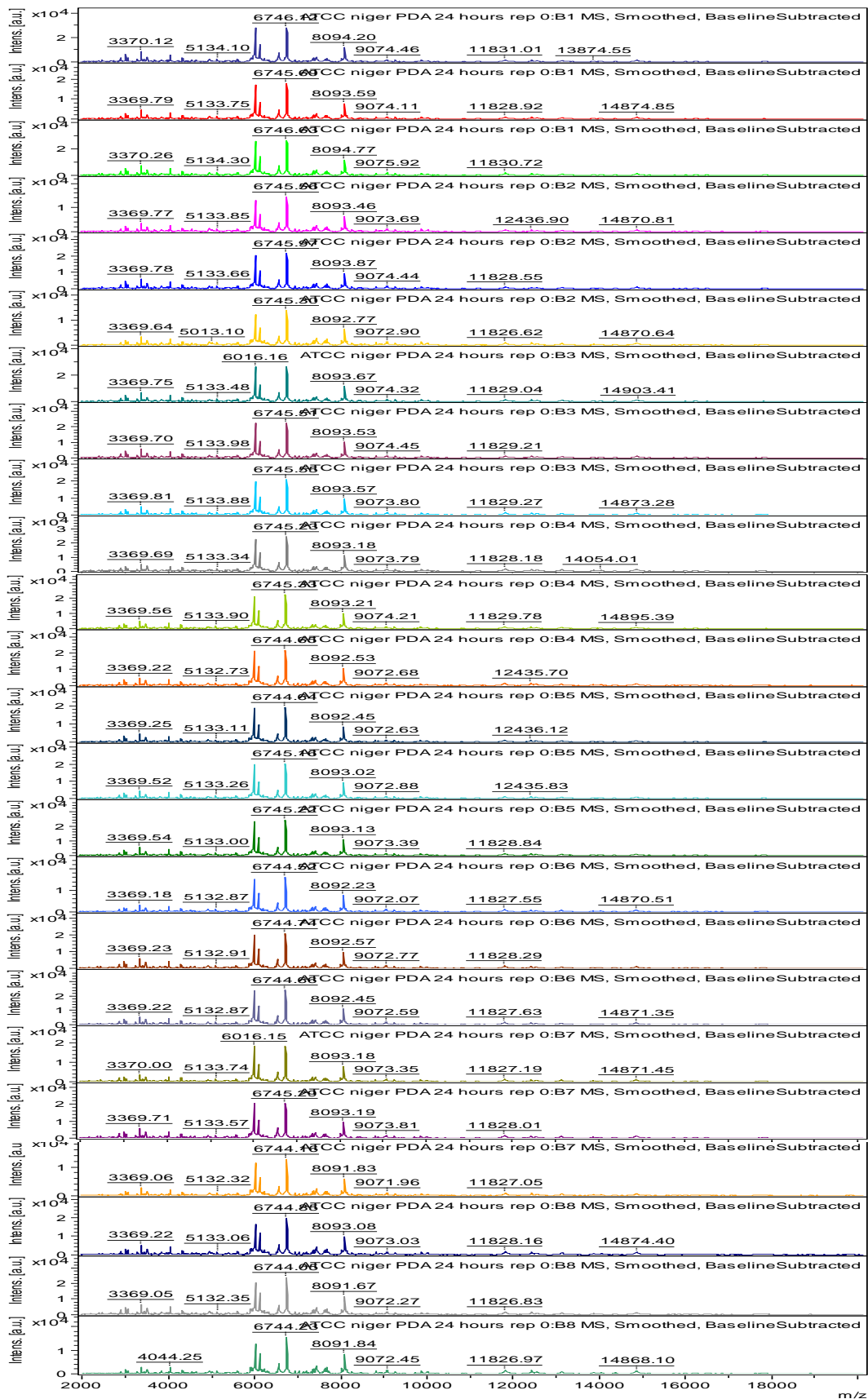
Appendix 5-W: Protein profiles obtained from *A. niger*, ATCC 16888 (replicate 2) grown in SDB at 25 °C spotted 8 times on MALDI target with 3 measurements in each spots to give total of 24 spectra.



Appendix 5-X: Protein profiles obtained from *A. niger*, ATCC 16888 (replicate 1) grown in PDB at 25 °C spotted 8 times on MALDI target with 3 measurements in each spots to give total of 24 spectra.

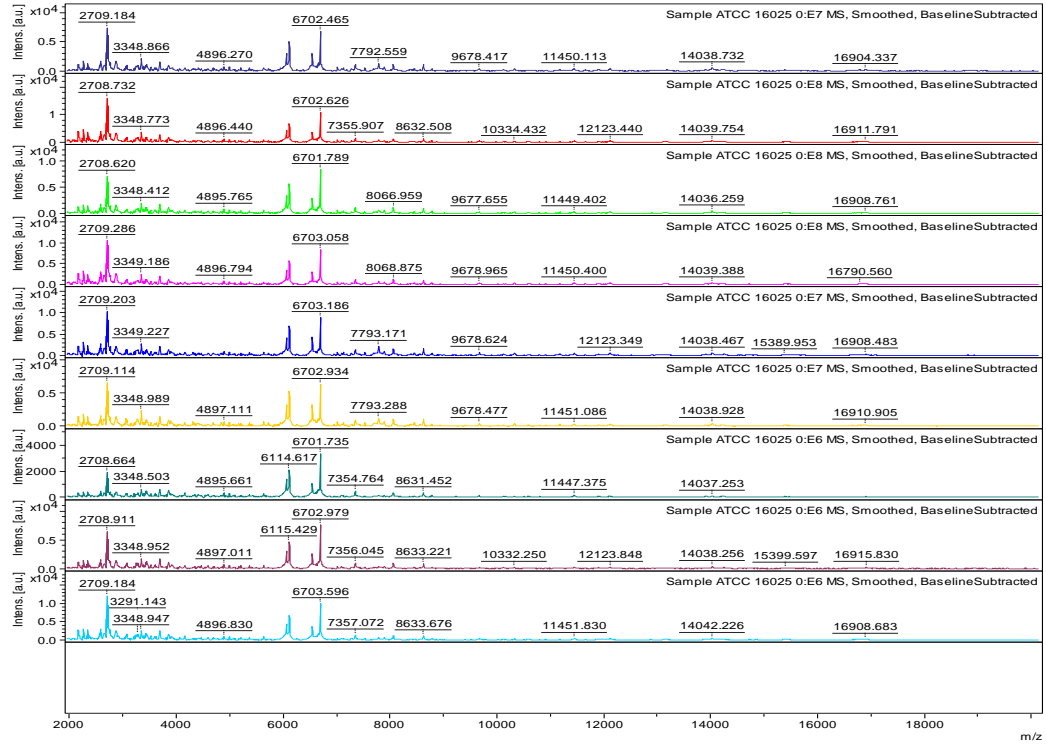


Appendix 5-Y: Protein profiles obtained from *A. niger*, ATCC 16888 (replicate 2) grown in PDB at 25 °C spotted 8 times on MALDI target with 3 measurements in each spots to give total of 24 spectra.

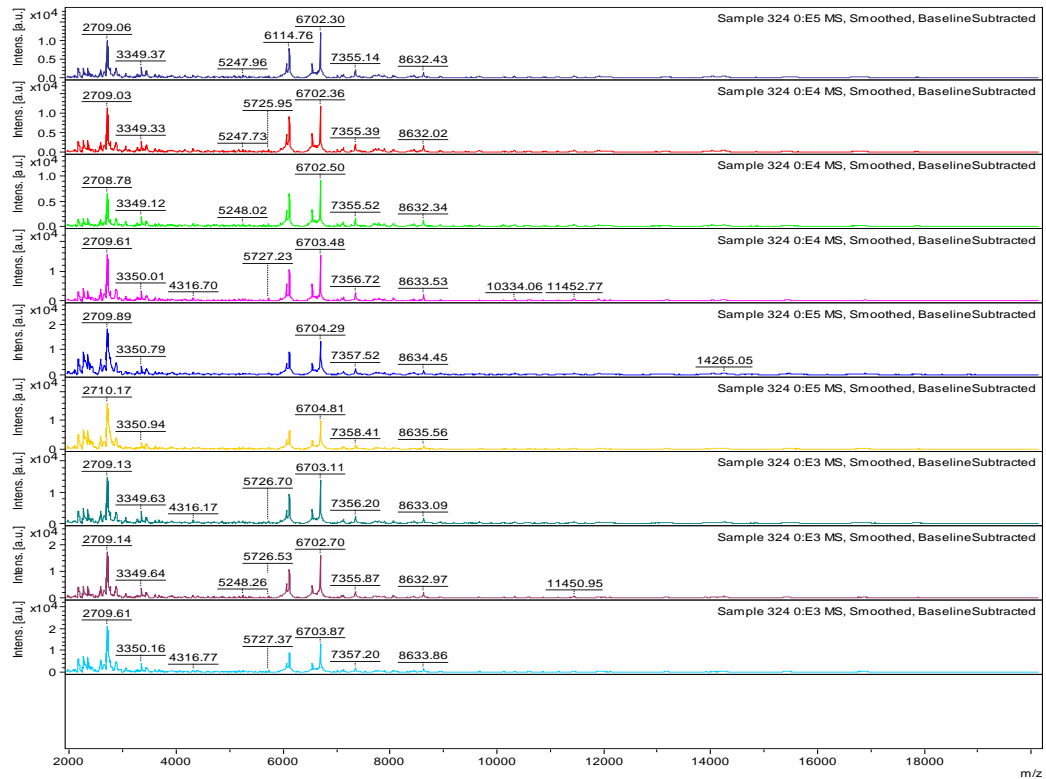


Appendix 5-Z: Protein profiles obtained from other *Stachybotrys spp* grown in SDB at 25 °C spotted 3 times on MALDI target with 3 measurements in each spots to give total of 9 spectra.

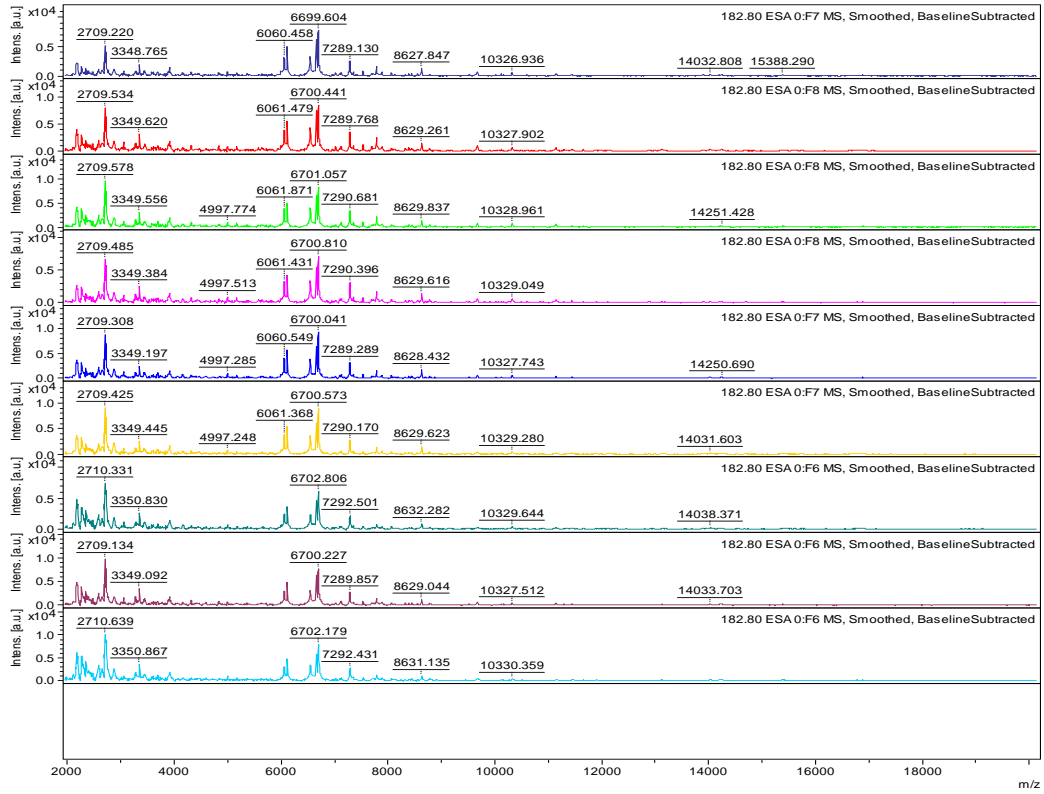
1. *S. chartarum*, ATCC 16026



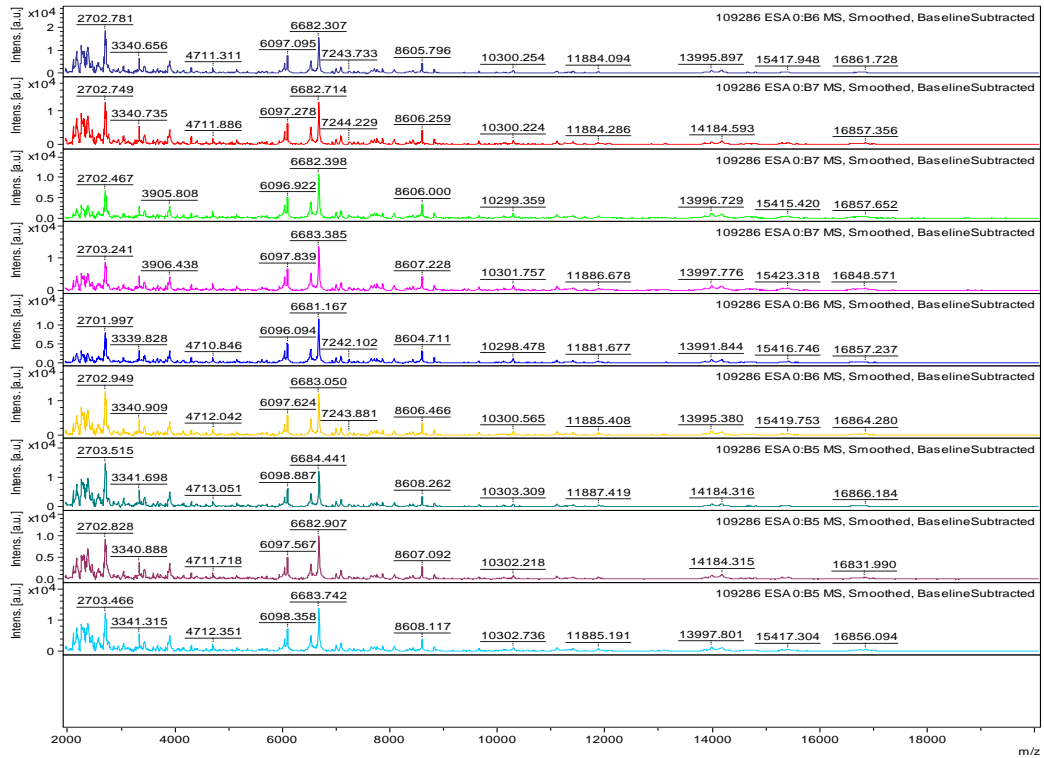
2. *S. chartarum*, CBS 324.65



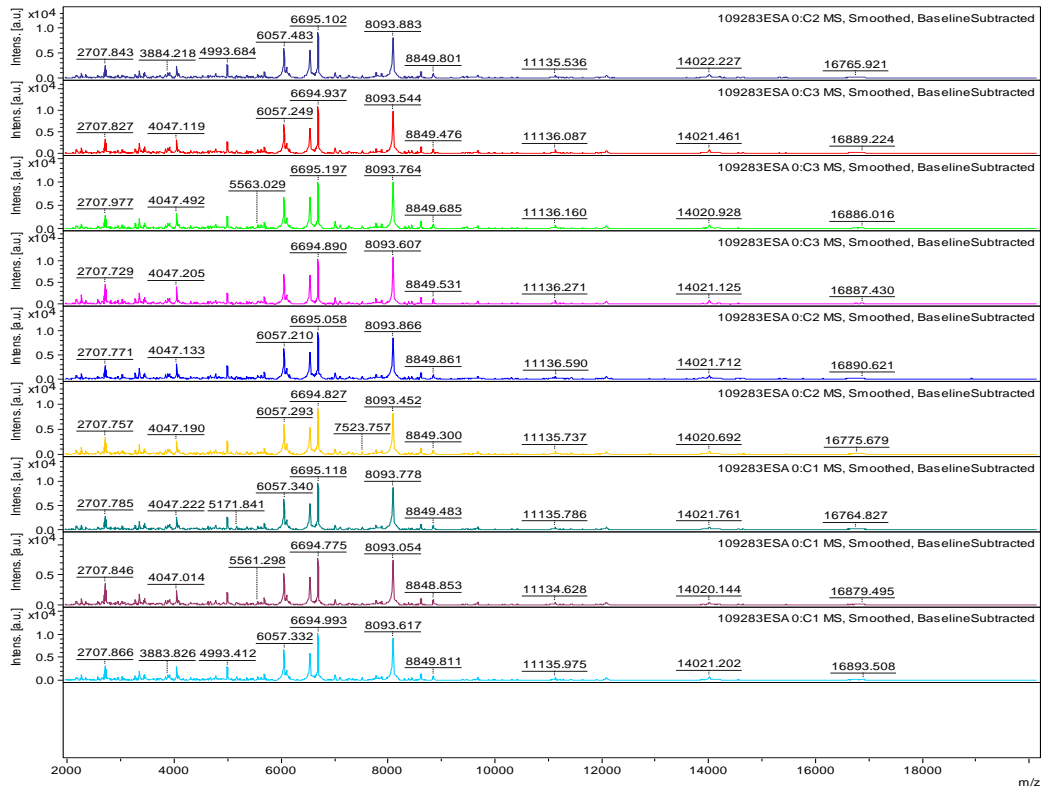
3. *S. chartarum*, CBS 182.80



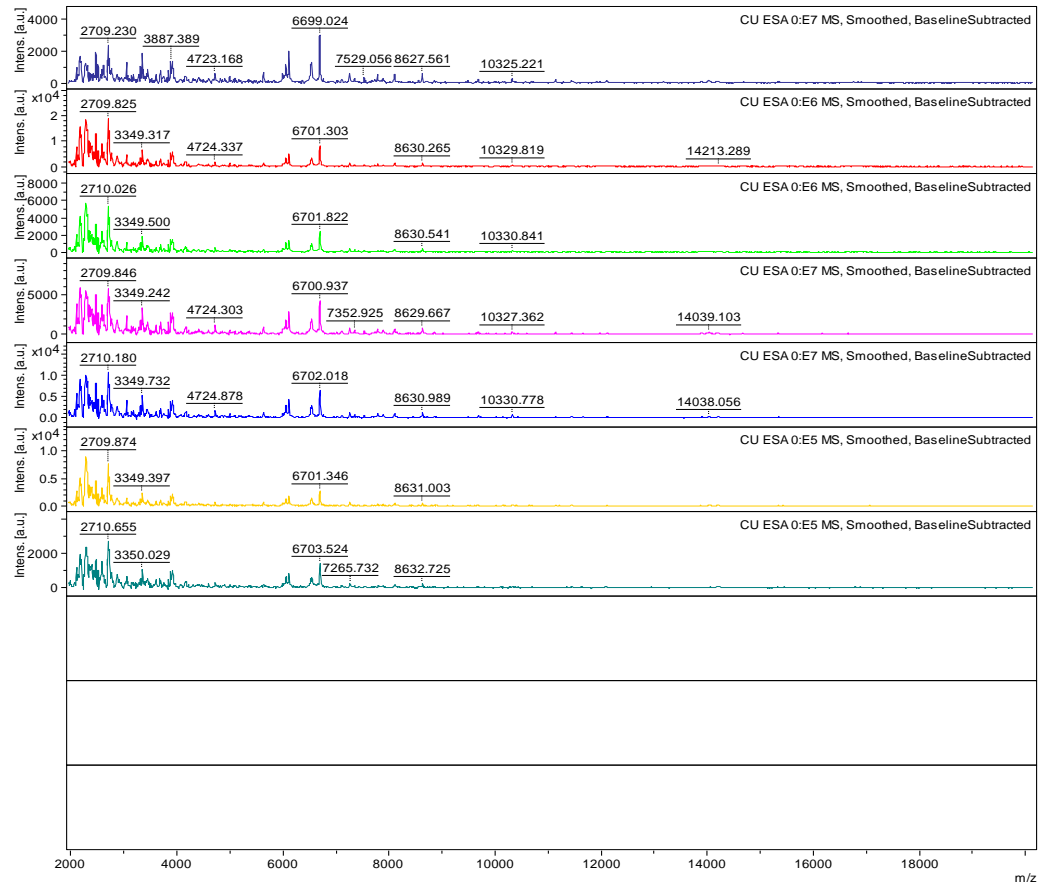
4. *S. chlorohalonata*, CBS 109286



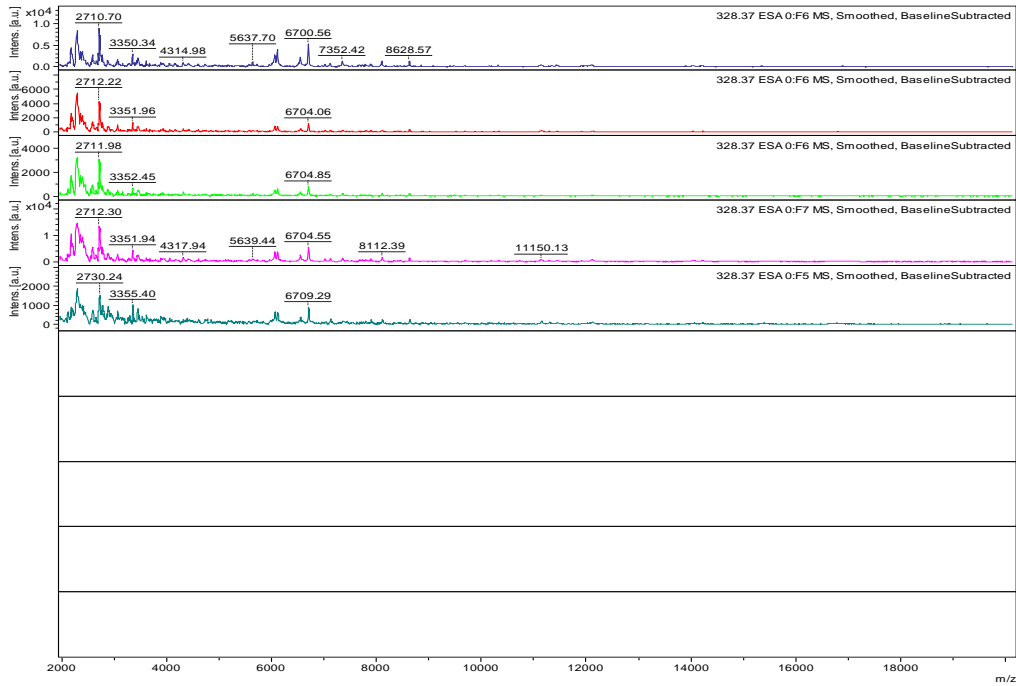
5. *S. chlorohalonata*, CBS 109283



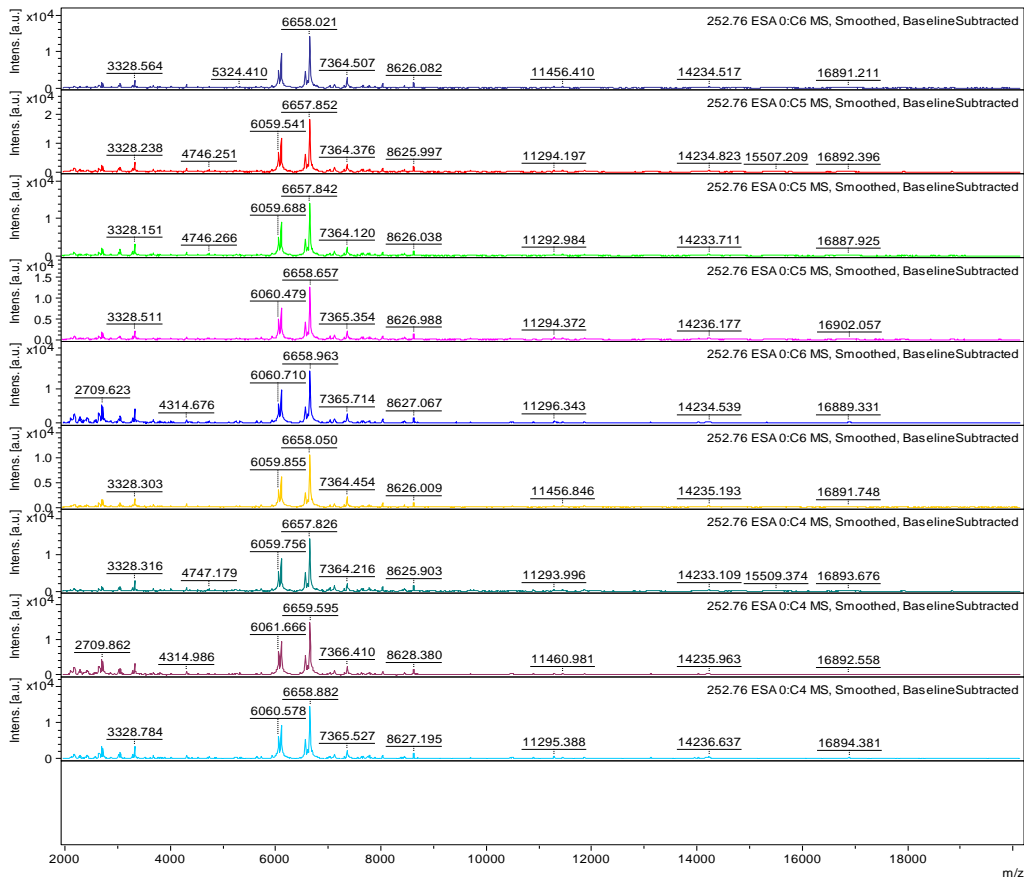
6. *S. chlorohalonata*, Stachy CU



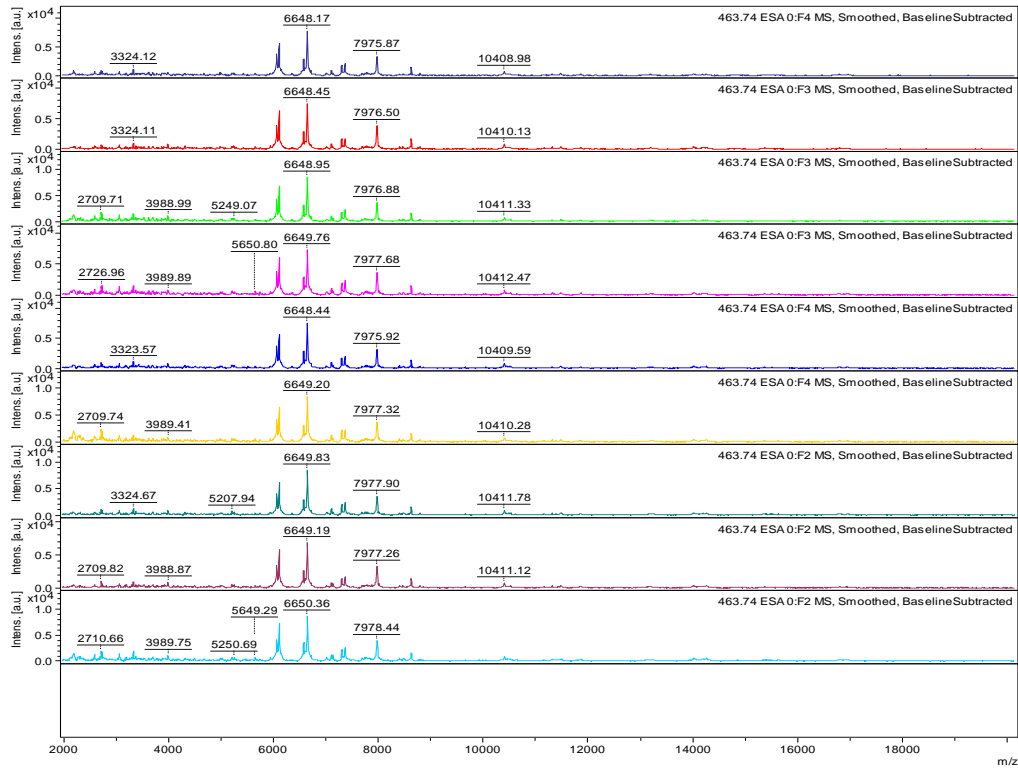
7. *S. chartarum* (*S. chlorohalonata*), CBS 328.37



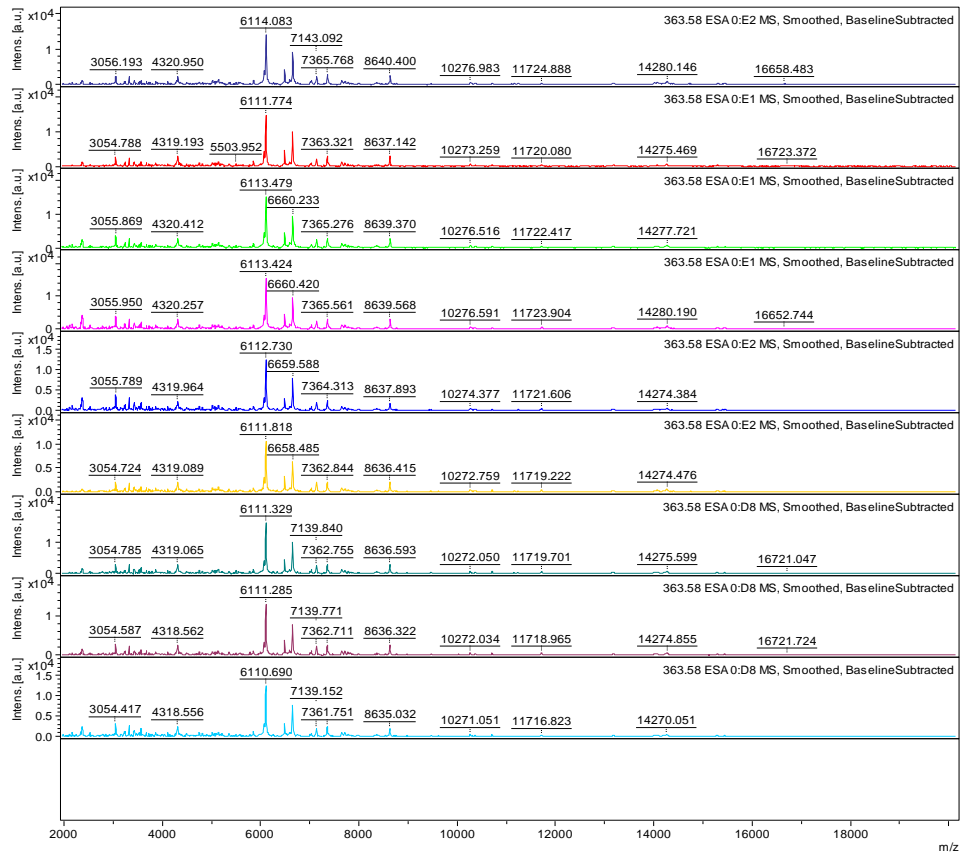
8. *S. oenantes*, CBS 252.76



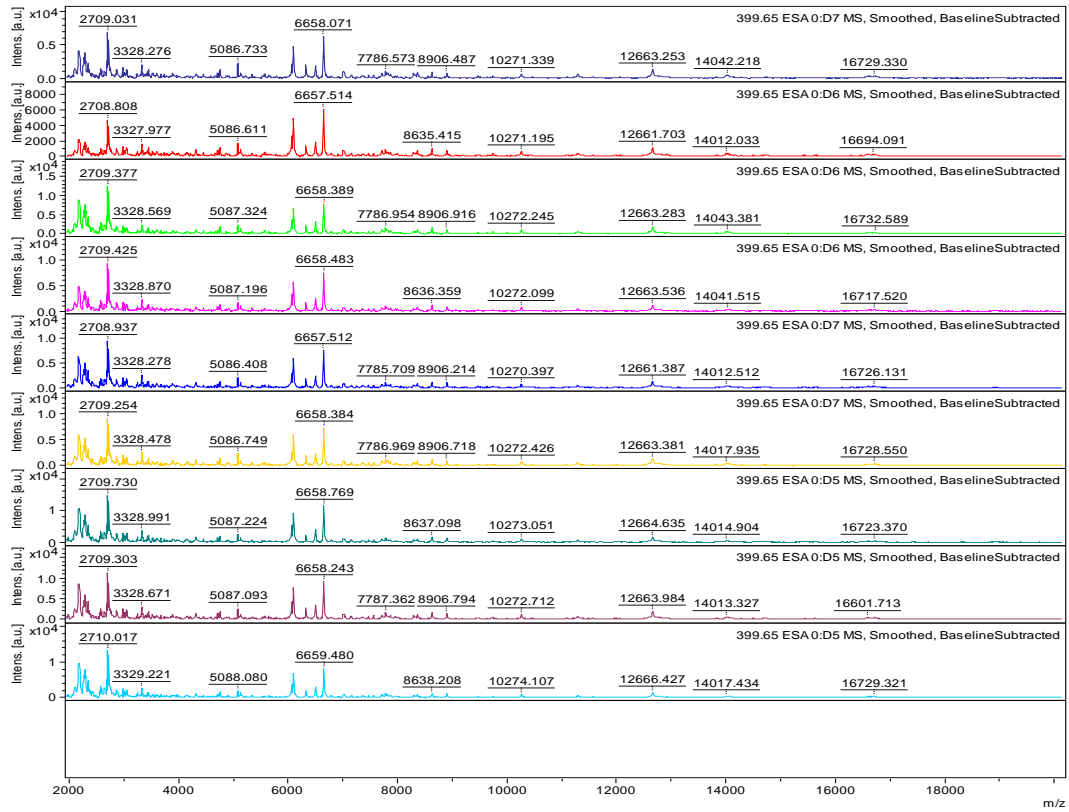
9. *S. oenanthes*, CBS 463.74



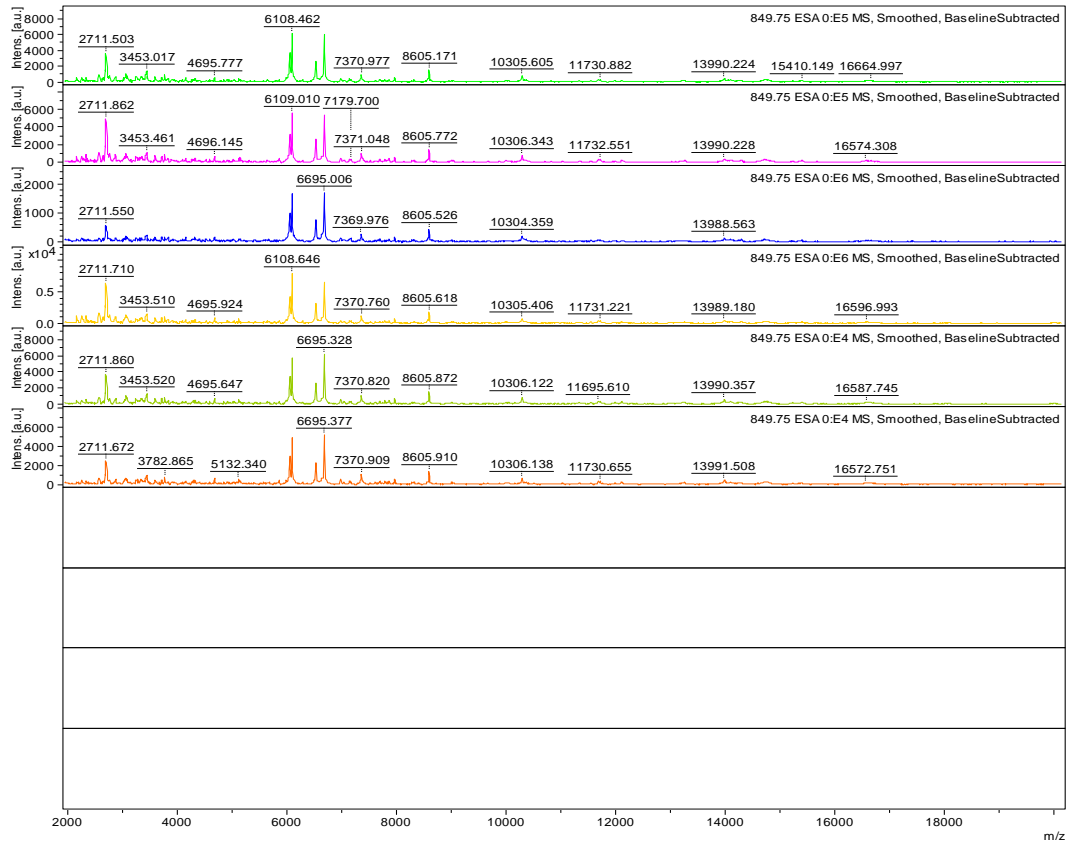
10. *S. bisbyi*, CBS 363.58



11. *S. bisbyi*, CBS 399.65

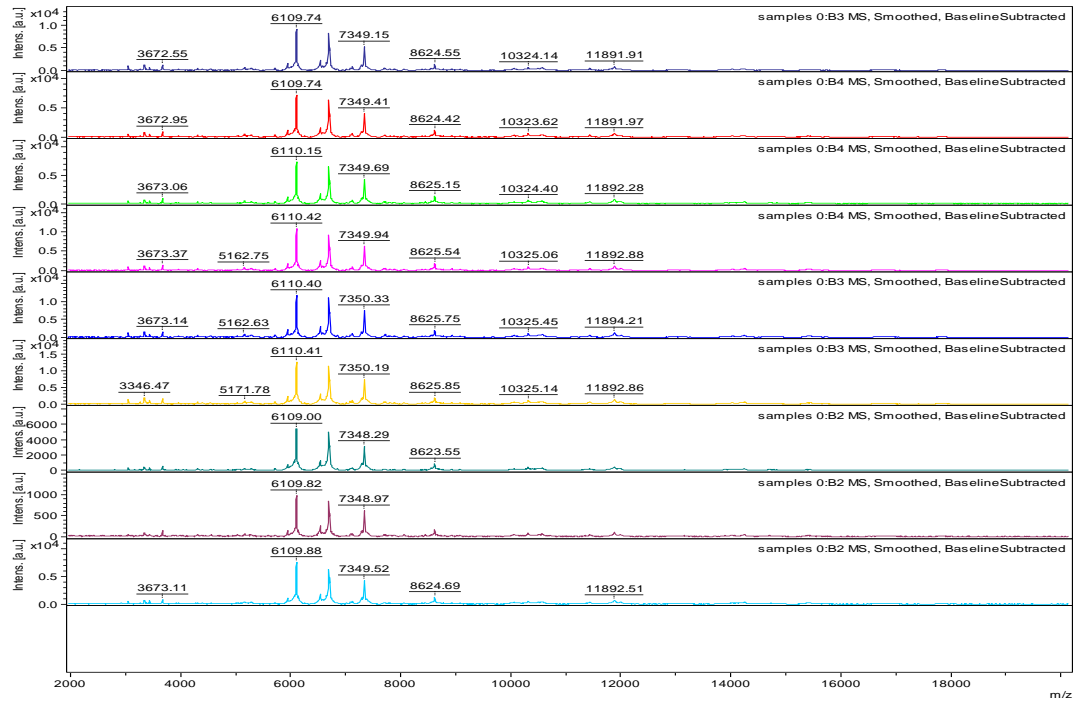


12. *S. dichroa*, CBS 949.72

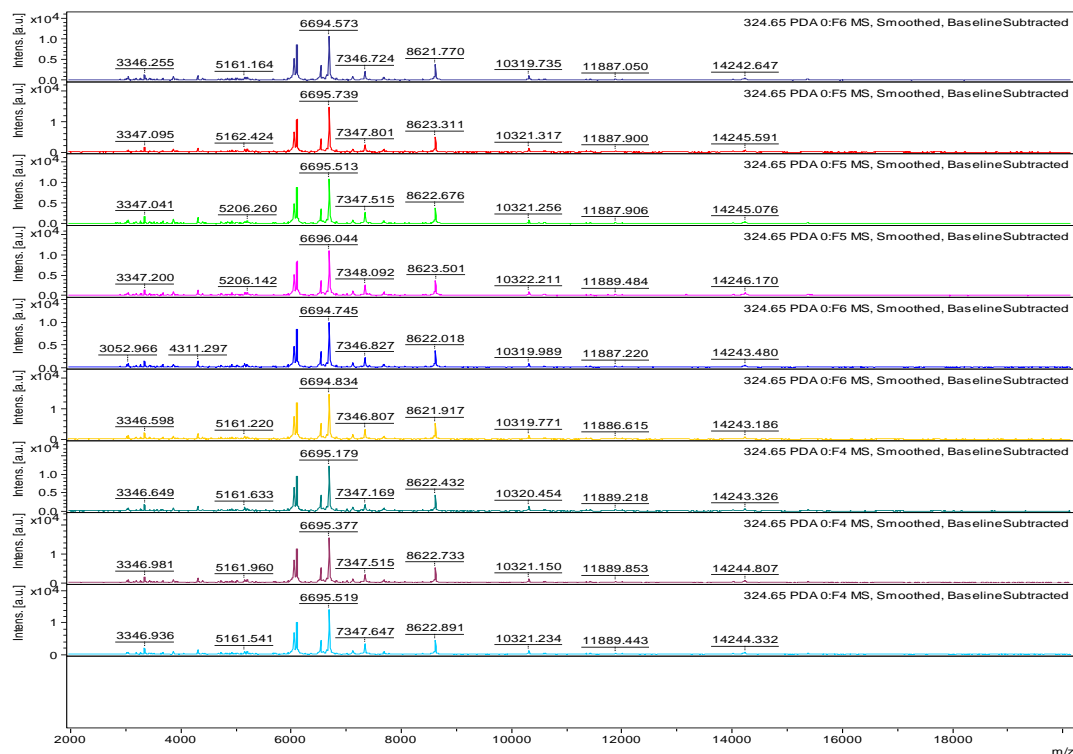


Appendix 5-AA: Protein profiles obtained from *Stachybotrys spp* grown in PDB at 25 °C spotted 3 times on MALDI target with 3 measurements in each spots to give total of 9 spectra.

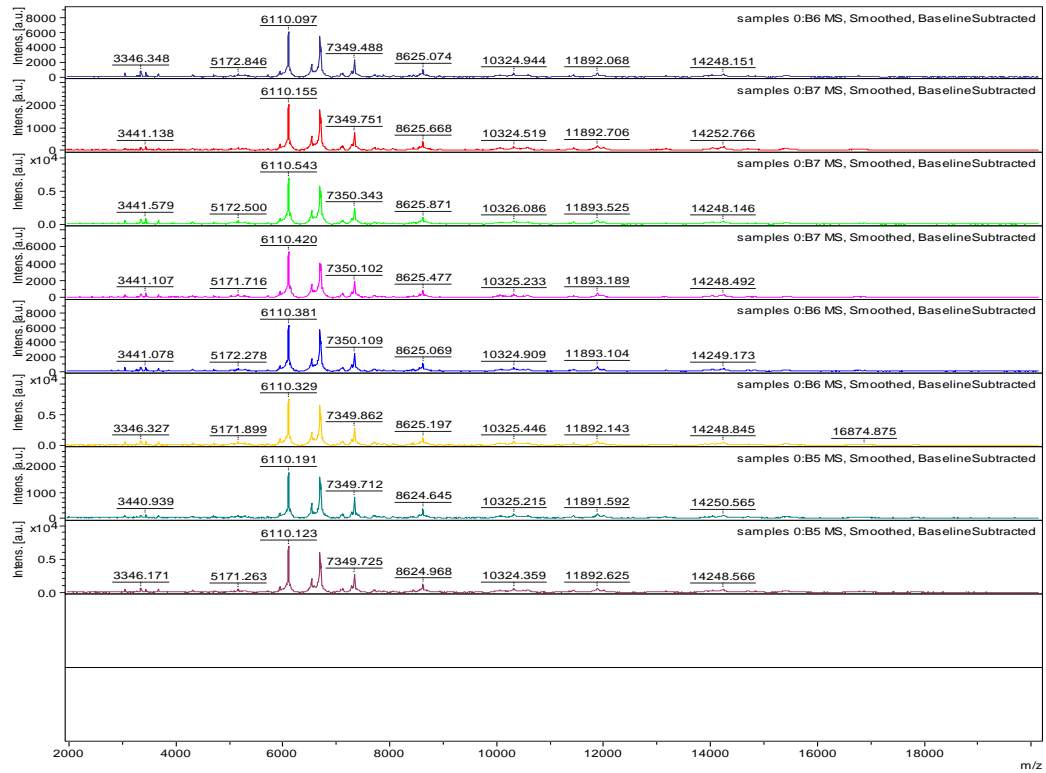
1. *S. chartarum*, ATCC 16026



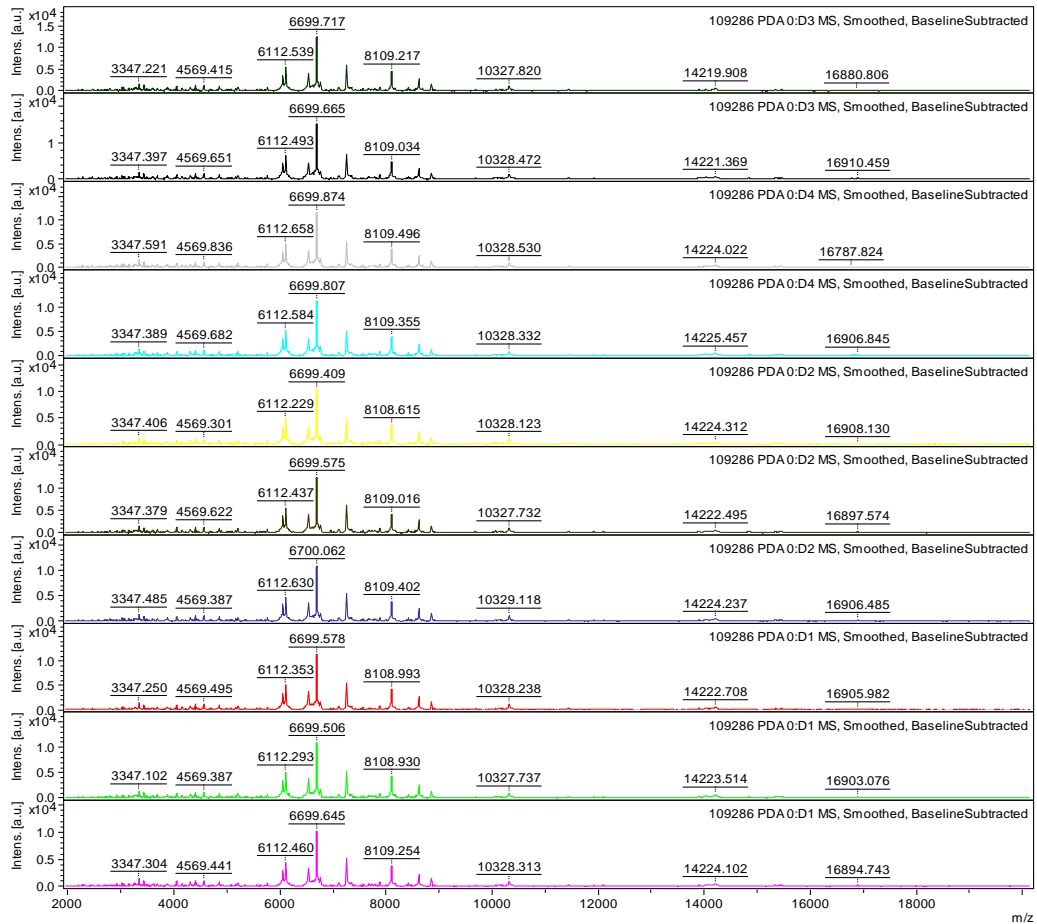
2. *S. chartarum*, CBS 324.65



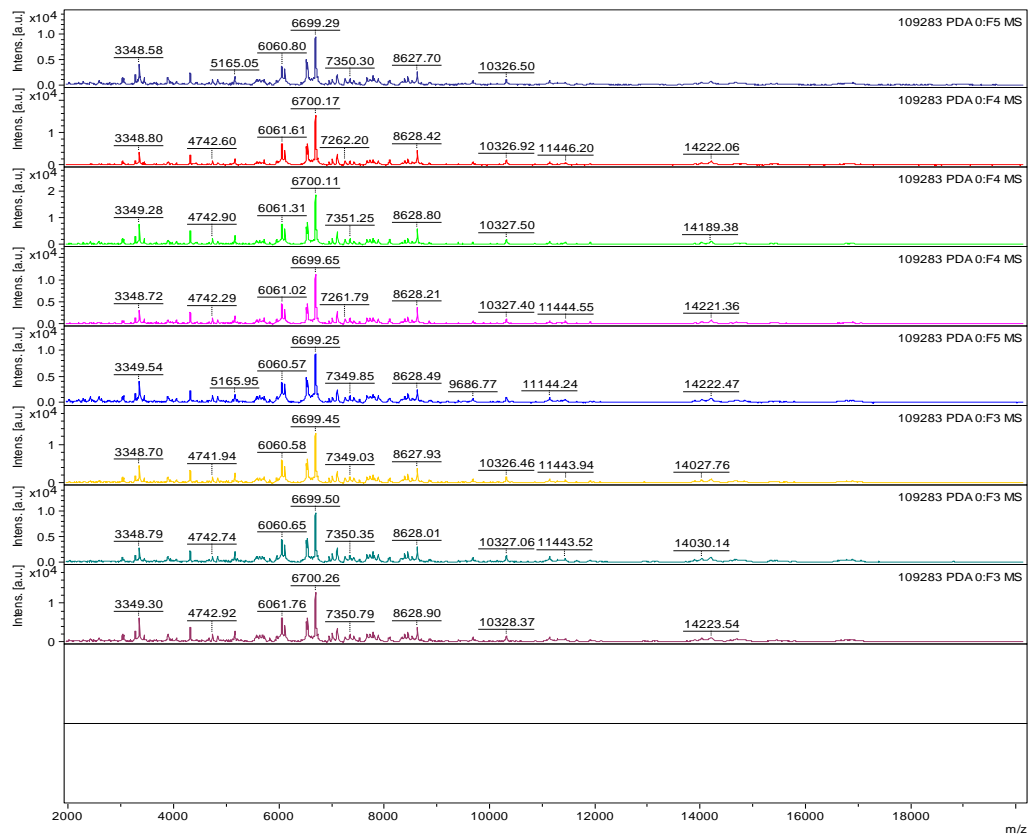
3. *S. chartarum*, CBS 182.80



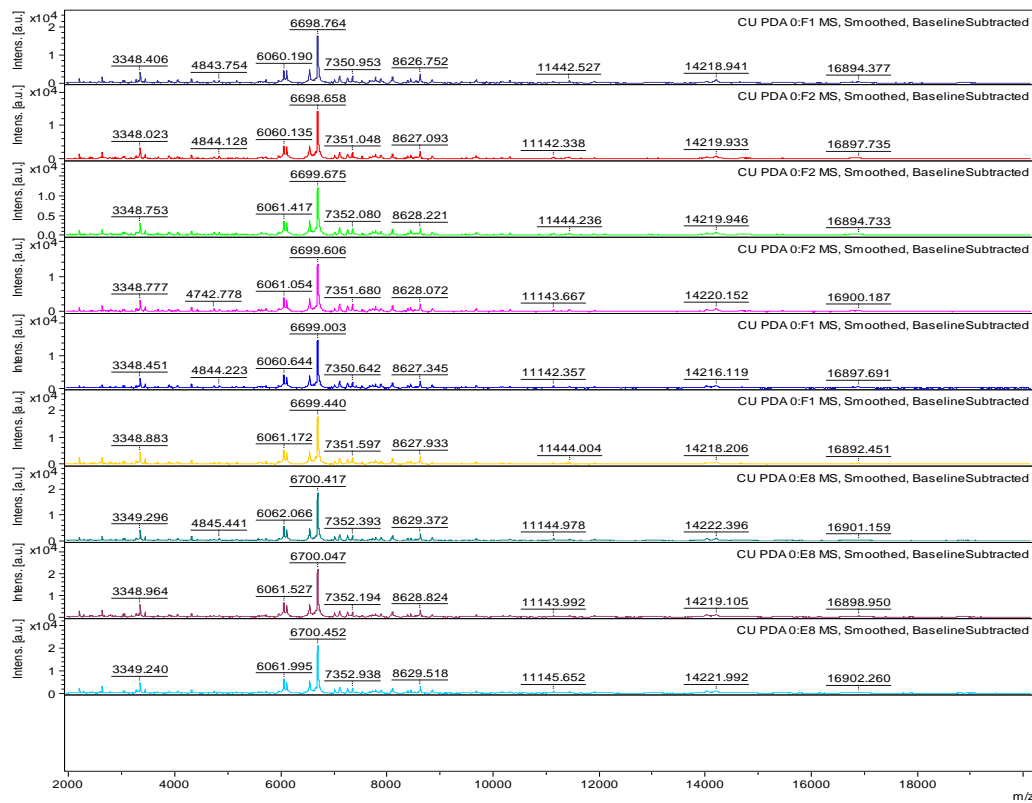
4. *S. chlorohalonata*, CBS 109286



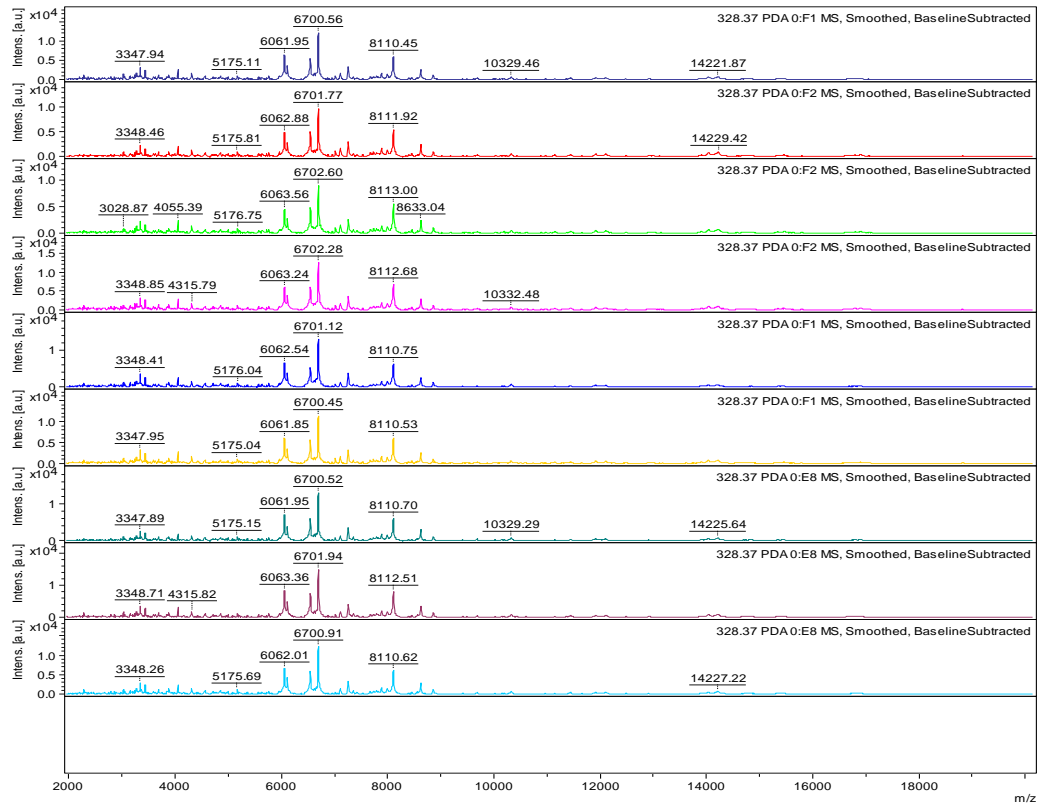
5. *S. chlorohalonata*, CBS 109283



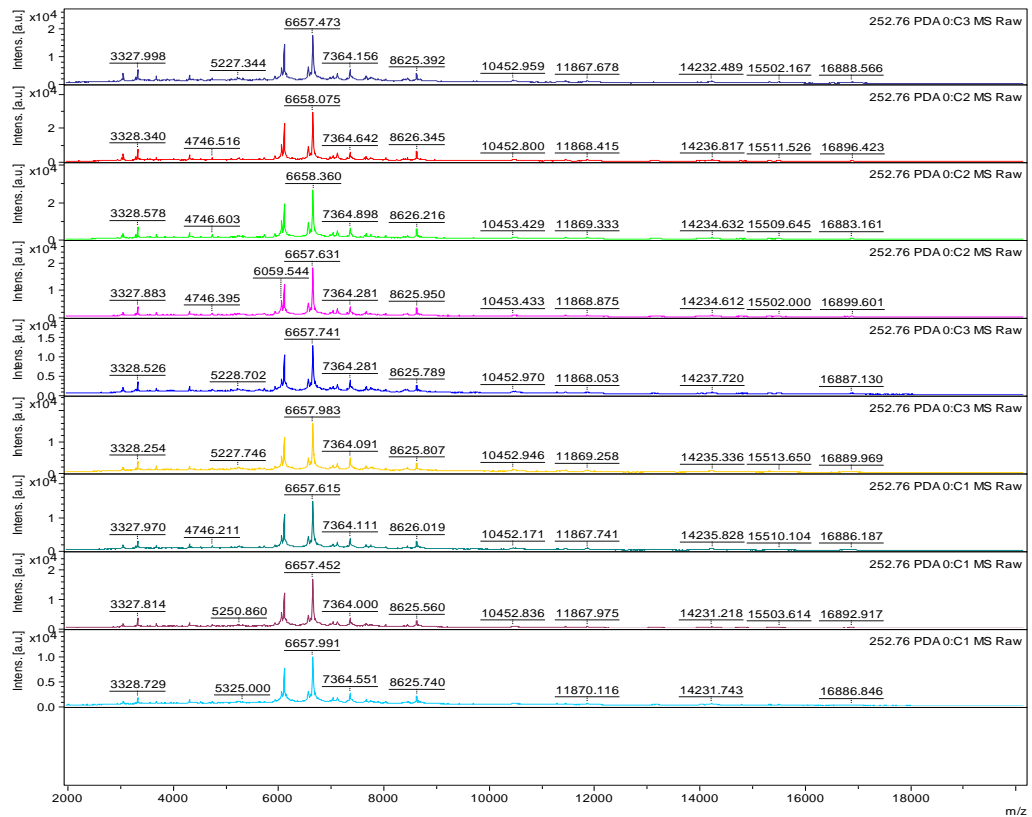
6. *S. chlorohalonata*, Stachy CU



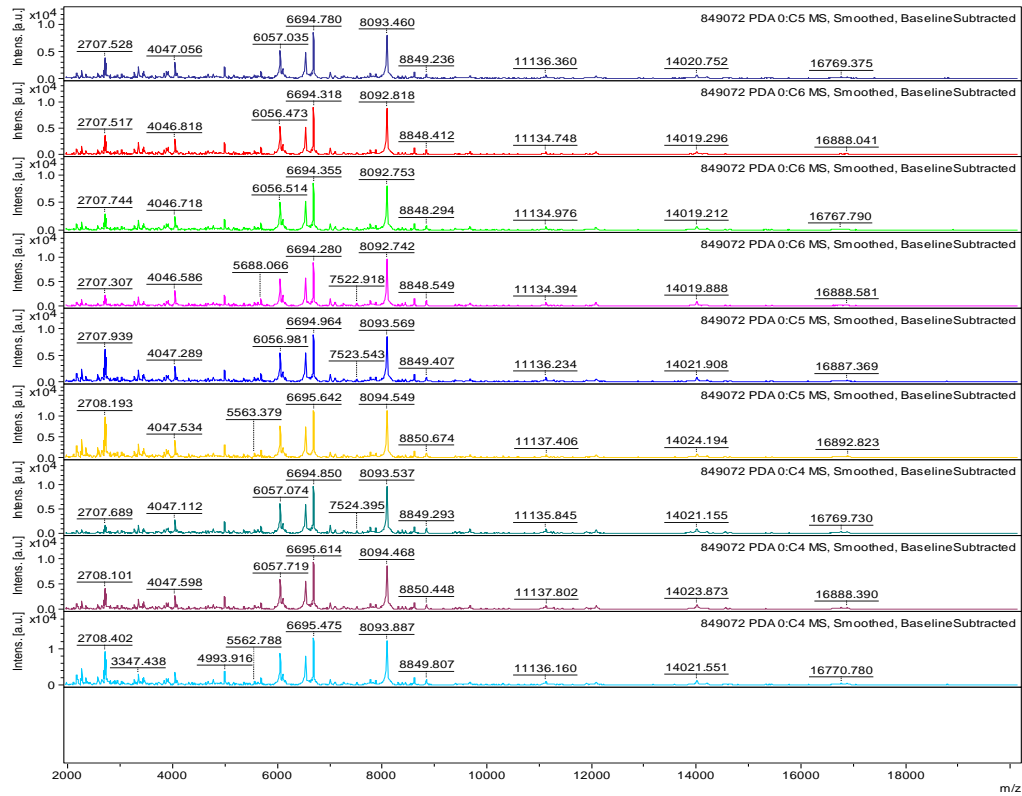
7. *S. chartarum* (*S. chlorohalonata*), CBS 328.37



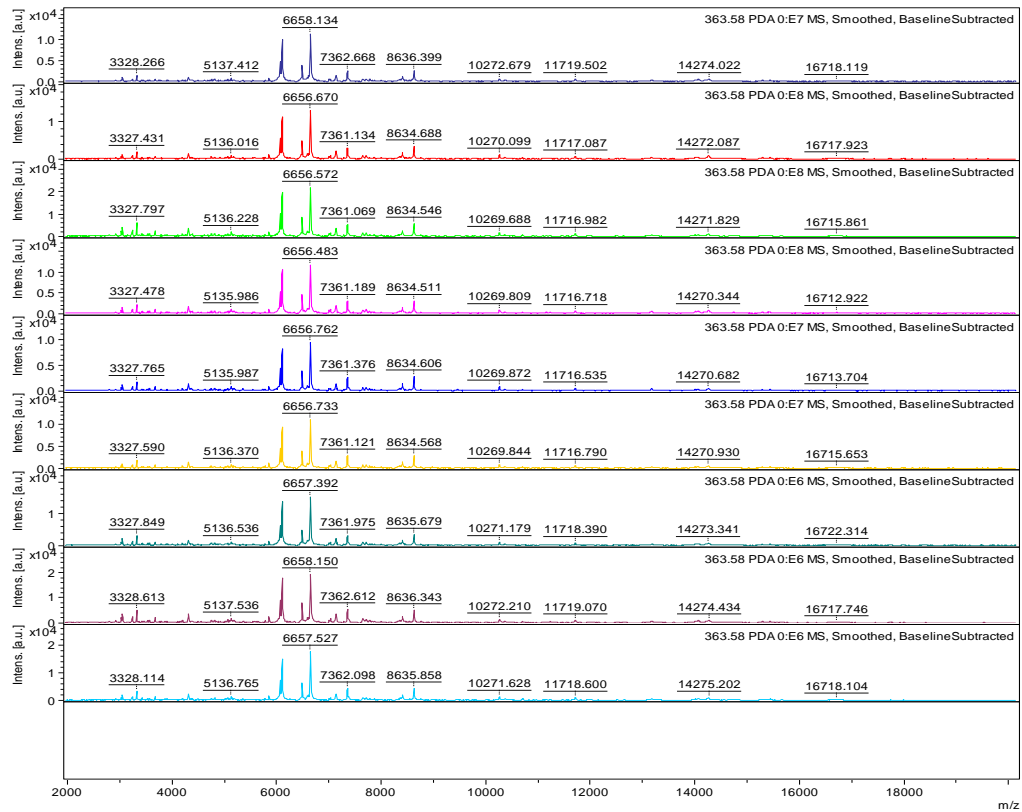
8. *S. oenantes*, CBS 252.76



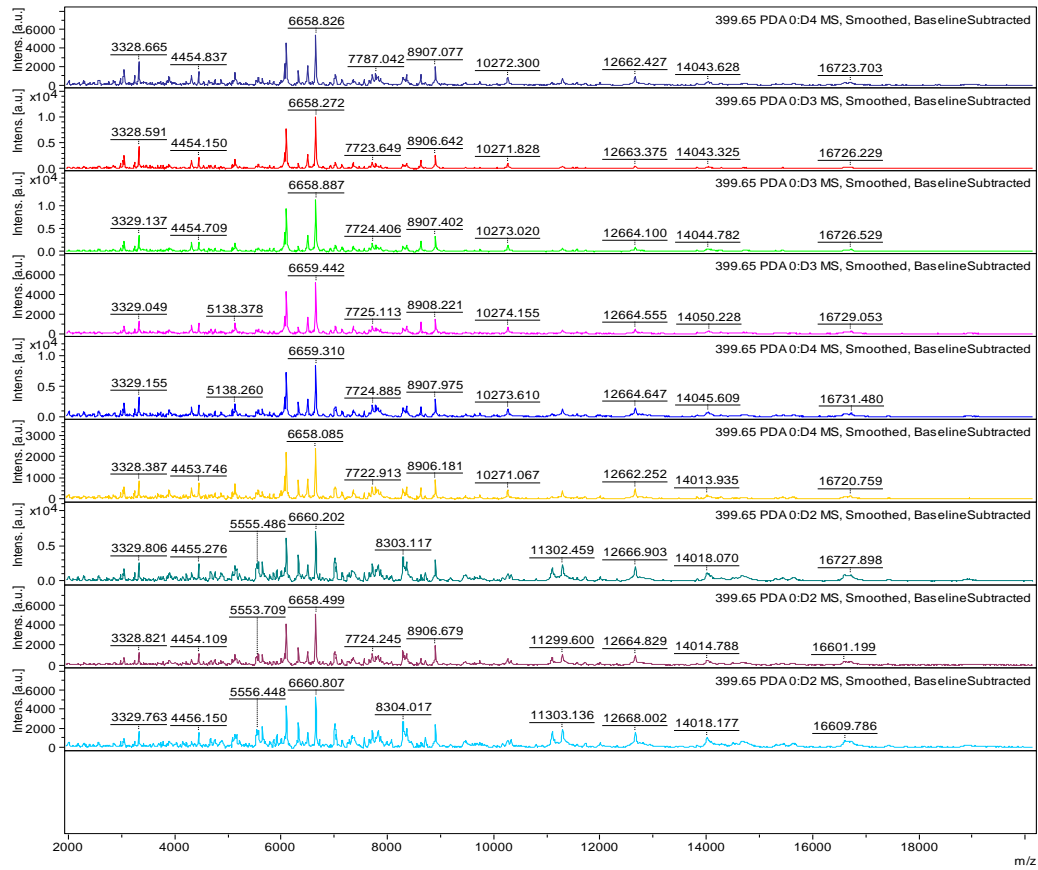
9. *S. oenanthes*, CBS 463.74



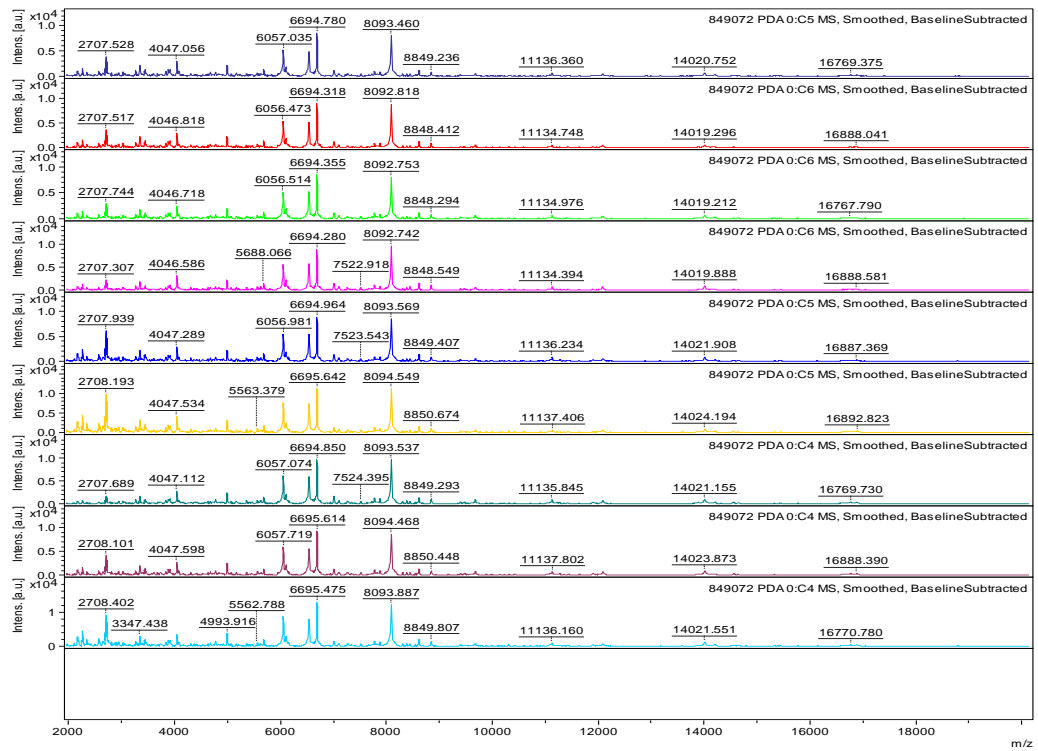
10. *S. bisbyi*, CBS 363.58



11. *S. bisbyi*, CBS 399.65



12. *S. dichroa*, CBS 949.72



Chapter 6 :Inhibitory effects of selected antimicrobial agents on *Stachybotrys chartarum*

Appendix 6-A: Preparation of 500 ml of RPMI 1640 plus 2% glucose – buffered with MOPS.

Component	Double strength
dH2O	400 ml ^a
RPMI 1640	10.40 g
3- (N-morpholino) propanesulfonic acid (MOPS) (M1254, Sigma Aldrich)	34.53 g
Glucose (G8270, Sigma Aldrich)	18.0 g

^a Mix the solution carefully with magnetic stirrer, and adjust the pH to 7.0 at 25°C using 1M NaOH. Make up the solution to final volume and filter sterilize before use.

Appendix 6-B: Calculation of cell density using haemocytometer.

Spore density (CFU/mL) = Average number of spores X dilution factor X 10⁴

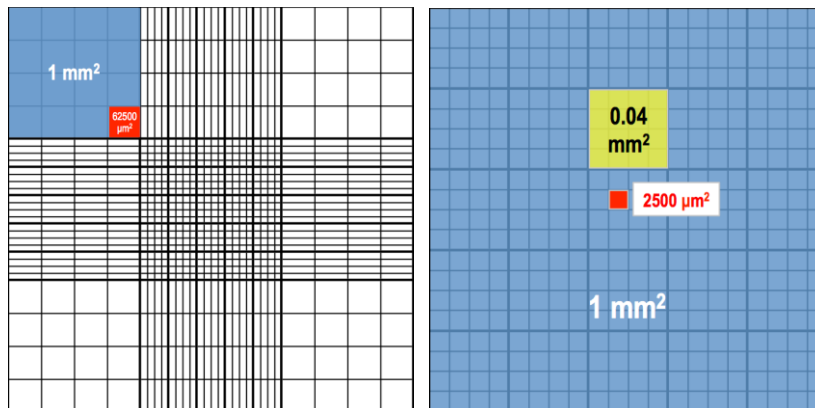
Depth: 0.001 mm

Area of each main square : 1 mm²

Therefore, volume of each main square :

1 mm² area x 0.1 mm depth = 0.1 mm³ = 0.0001 mL

Dilution factor = 2 (100 µl cell suspension diluted in 100 µl dye)



Depiction of a haemocytometer (adopted from Haemocytometer.org) showing area 1 mm² of each main square area

Example:

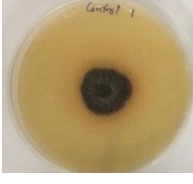
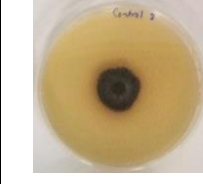
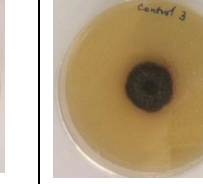
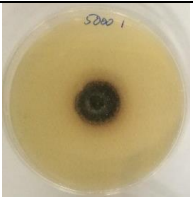
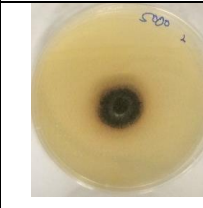
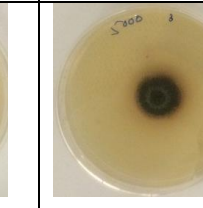
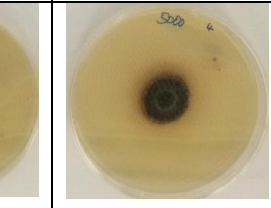
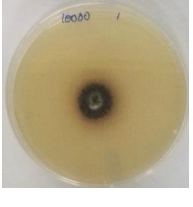
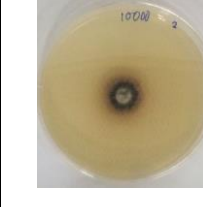
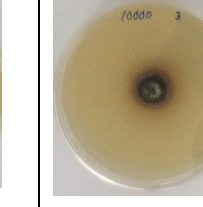
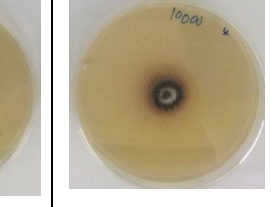
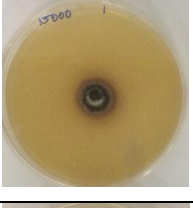

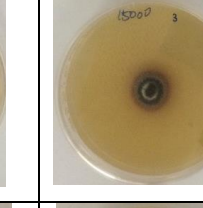
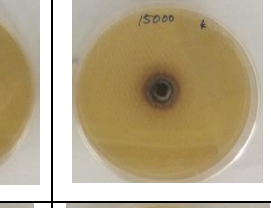
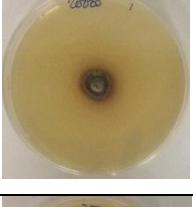

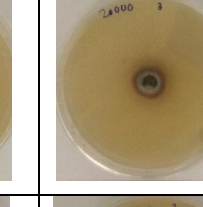
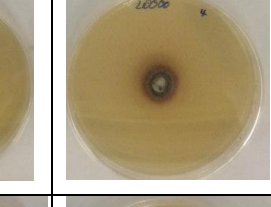
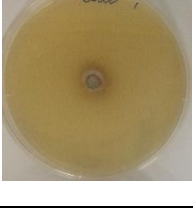

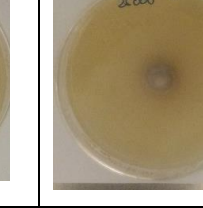
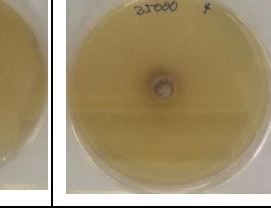
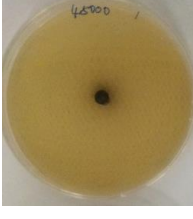
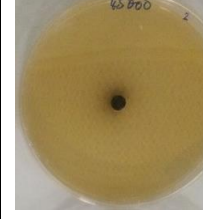
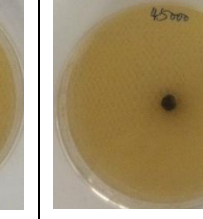
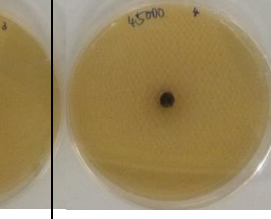
No of spores: 107

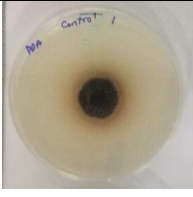
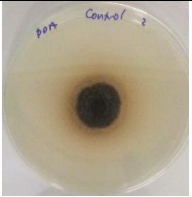
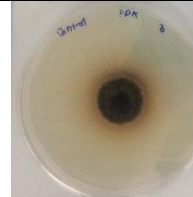
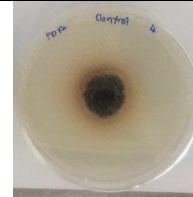
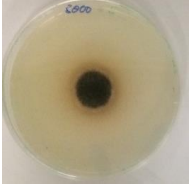
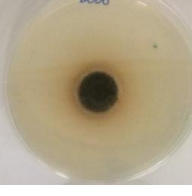
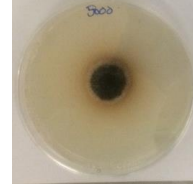
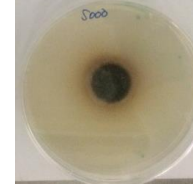
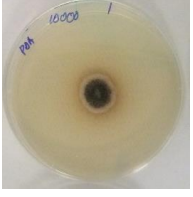
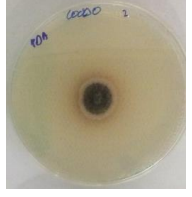

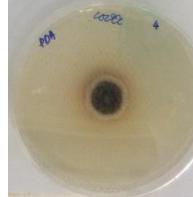
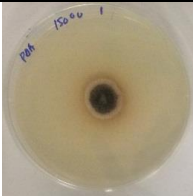
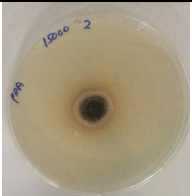
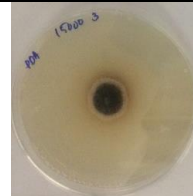
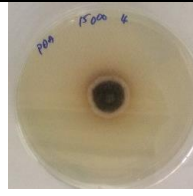
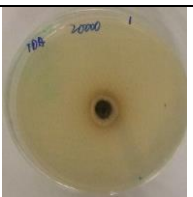
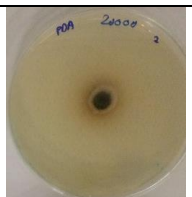
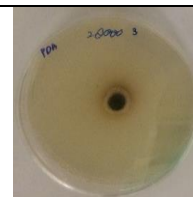
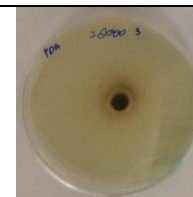
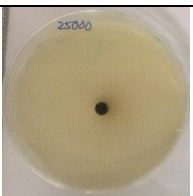
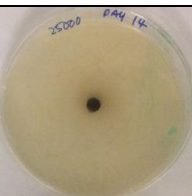
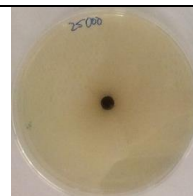
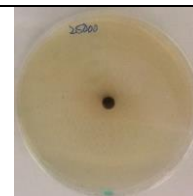
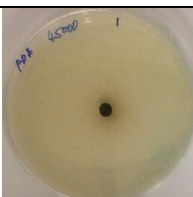
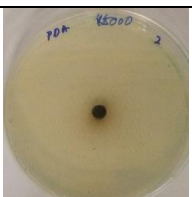
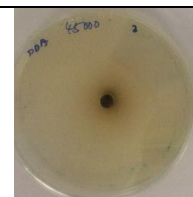
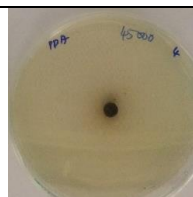
Average :21.4

No of spores: 21.4 X 2 X 10 000

= 4.28 x 10⁵ cells/mL

Appendix 6-C: Growth and colony diameter of *S. chartarum* grown on ESA and PDA treated with single application of bleach (500 µl), in replicates.

Concentration	Growth of <i>S. chartarum</i> grown on ESA treated with 1 application of bleach			
Control				Nil (plate excluded to due growth deformity)
5000				
10000				
15000				
20000				
25000				
45000				

Concentration	Growth of <i>S. chartarum</i> grown on PDA treated with 1 application of bleach			
Control				
5000				
10000				
15000				
20000				
25000				
45000				

Colony diameter of <i>S. chartarum</i> grown on ESA treated with single application of bleach					
Concentration	Means	SD	SE	Mean difference 95% CI	p-value
Control	2.8670	0.058	0.033	-	-
5000	2.775	0.050	0.025	0.092 (-0.003 to 0.230)	0.0738
*10000	2.575	0.050	0.025	0.258 (0.154 to 0.363)	*0.0014
*15000	2.400	0.000	0.000	0.467 (0.395 to 0.538)	*0.0001
*20000	2.325	0.096	0.048	0.542 (0.379 to 0.704)	*0.0004
*25000	1.725	0.171	0.085	1.142 (0.872 to 1.411)	*0.0001
*45000	0.700	0.000	0.000	2.167 (2.095 to 2.238)	*0.0001


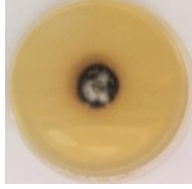
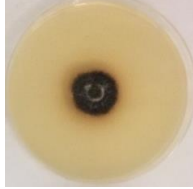

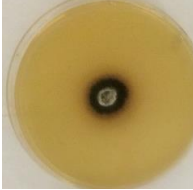
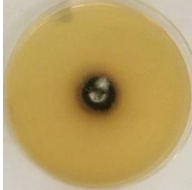
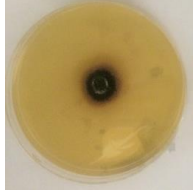
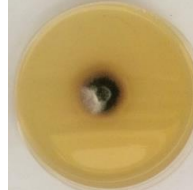
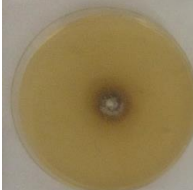
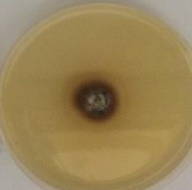
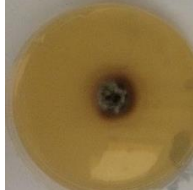
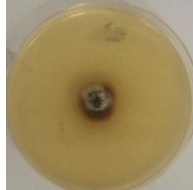
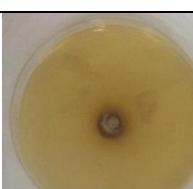
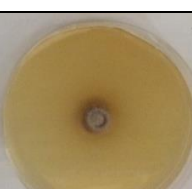
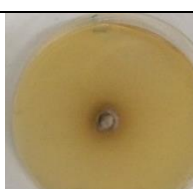

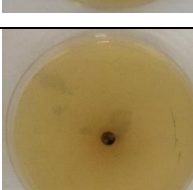
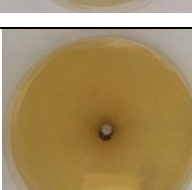
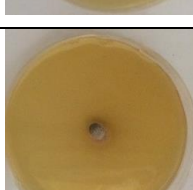
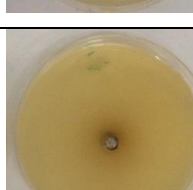
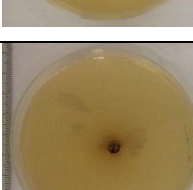
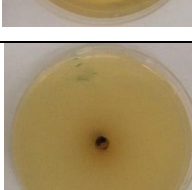
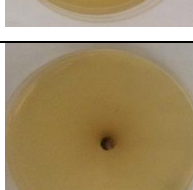
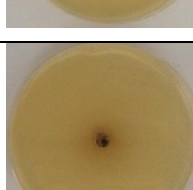
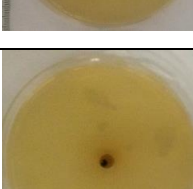
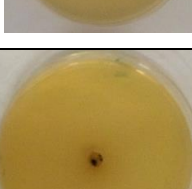
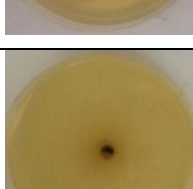
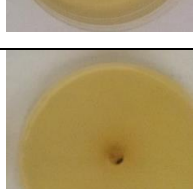
Colony diameter of <i>S. chartarum</i> grown on PDA treated with single application of bleach					
Concentration	Means	SD	SE	Mean difference 95% CI	p-value
Control	2.650	0.058	0.029	-	-
5000	2.575	0.050	0.025	0.075 (-0.018 to 0.168)	0.0972
*10000	2.175	0.050	0.025	0.475 (0.382 to 0.568)	*0.0001
*15000	2.075	0.050	0.025	0.575 (0.482 to 0.668)	*0.0001
*20000	1.300	0.400	0.200	1.350 (0.856 to 1.844)	*0.0005
*25000	0.700	0.000	0.000	1.950 (1.879 to 2.021)	*0.0001
*45000	0.700	0.000	0.000	1.950 (1.879 to 2.021)	*0.0001

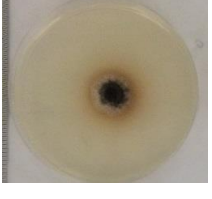
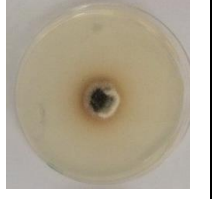
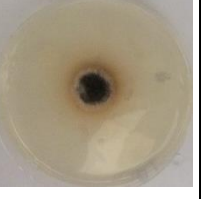
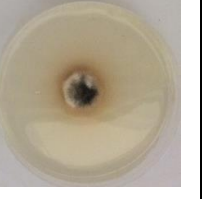
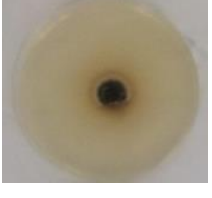


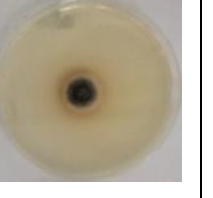
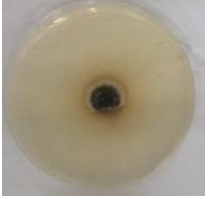
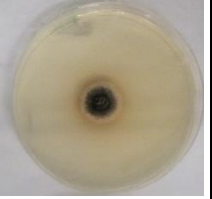
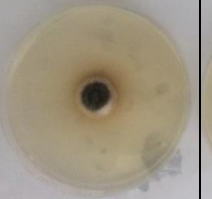
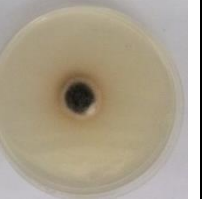
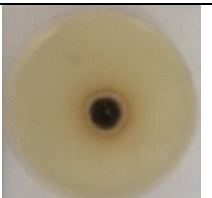
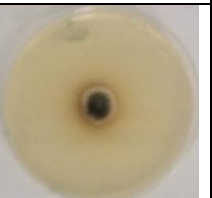
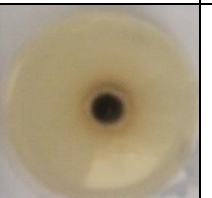
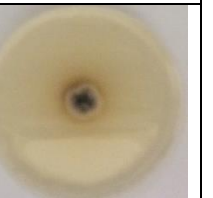


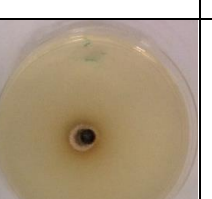
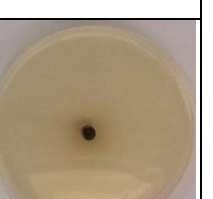
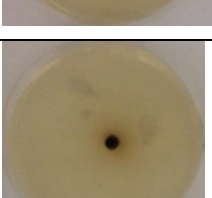
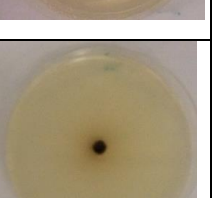
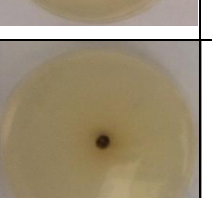
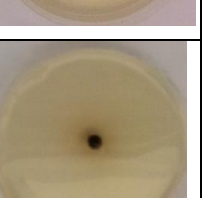
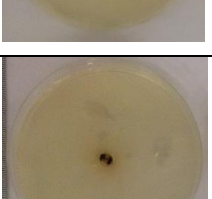
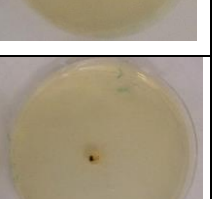

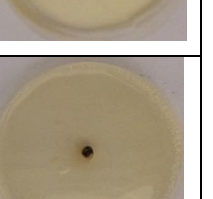
*Significant differences, p value < 0.05

Significant differences starting from 10000 ppm

No change in colony diameter on ESA: 45000ppm; and on PDA: 25000 ppm

Appendix 6-D: Growth and colony diameter of *S. chartarum* grown on ESA and PDA treated with 2 applications of bleach (500 µl), in replicates.

Concentration	Growth of <i>S. chartarum</i> grown on ESA treated with 2 application of bleach			
Control				
5000				
10000				
15000				
20000				
25000				
45000				

Concentration	Growth of <i>S. chartarum</i> grown on PDA treated with 2 application of bleach			
Control				
5000				
10000				
15000				
20000				
25000				
45000				

Colony diameter of <i>S. chartarum</i> grown on ESA treated with two applications of bleach					
Concentration	Means	SD	SE	Mean difference 95% CI	p-value
Control	2.775	0.096	0.048	-	-
5000	2.650	0.058	0.029	0.125 (-0.012 to 0.262)	0.0667
*10000	2.550	0.100	0.050	0.225 (0.056 to 0.394)	*0.0175
*15000	1.625	0.096	0.048	1.150 (0.984 to 1.316)	*0.0001
*20000	0.950	0.129	0.065	1.825 (1.628 to 2.022)	*0.0001
*25000	0.700	0.000	0.000	2.075 (1.958 to 2.192)	*0.0001
*45000	0.700	0.000	0.000	2.075 (1.958 to 2.192)	*0.0001

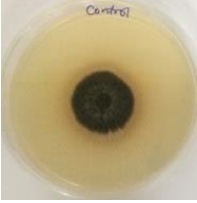
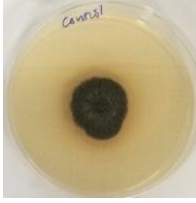
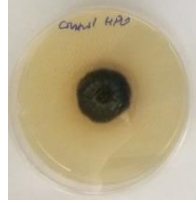
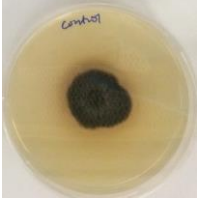
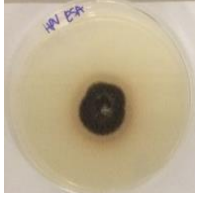
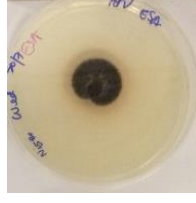
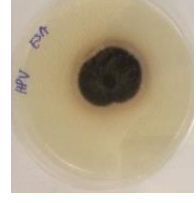
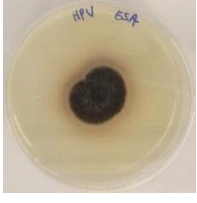
Colony diameter of <i>S. chartarum</i> grown on PDA treated with two applications of bleach					
Concentration	Means	SD	SE	Mean difference 95% CI	p-value
Control	2.100	0.082	0.041	-	-
5000	2.025	0.050	0.025	0.075 (-0.042 to 0.192)	0.1682
*10000	1.900	0.141	0.071	0.200 (0.000 to 0.400)	*0.0498
*15000	1.450	0.173	0.087	0.650 (0.416 to 0.884)	*0.0005
*20000	1.100	0.316	0.158	1.000 (0.600 to 1.400)	*0.0009
*25000	0.700	0.000	0.000	1.400 (1.300 to 1.500)	*0.0001
*45000	0.700	0.000	0.000	1.400 (1.300 to 1.500)	*0.0001

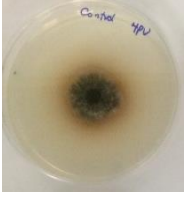
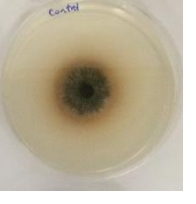
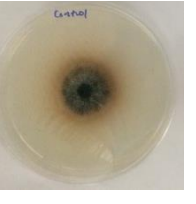
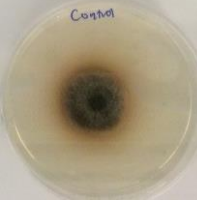
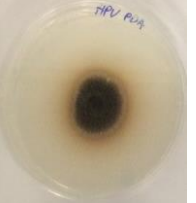
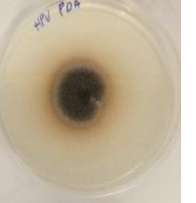
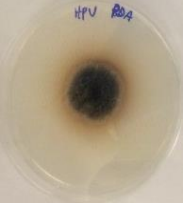
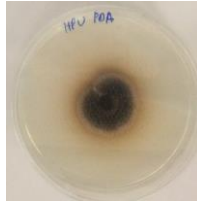
*Significant differences, p value < 0.05

Significant differences starting from 10000 ppm

No change in colony diameter on ESA: 25000ppm; and on PDA: 25000 ppm

Appendix 6-E: Growth and colony diameter of *S. chartarum* grown on ESA and PDA treated with one cycle of AHP, in replicates.

Growth of <i>S. chartarum</i> grown on ESA treated with one cycle of AHP				
Treatment	Replicate 1	Replicate 2	Replicate 3	Replicate 4
Control				
AHP				

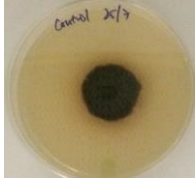
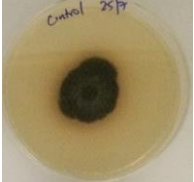


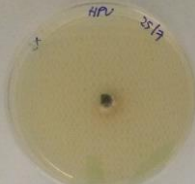
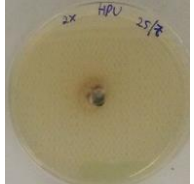

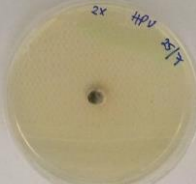
Growth of <i>S. chartarum</i> grown on PDA treated with one cycle of AHP				
Treatment	Replicate 1	Replicate 2	Replicate 3	Replicate 4
Control				
AHP				

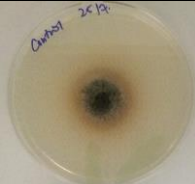
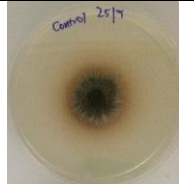
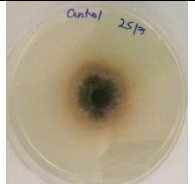
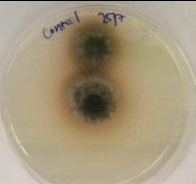



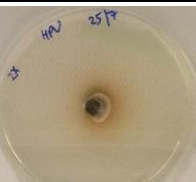
Colony diameter of <i>S. chartarum</i> grown on ESA treated with one cycle AHP					
Media	Means	SD	SE	Mean difference 95% CI	p-value
ESA Control	3.475	0.050	0.025	-	-
ESA AHP	3.275	0.189	0.095	0.200 (-0.040 to 0.440)	0.0871

Colony diameter of <i>S. chartarum</i> grown on PDA treated with one cycle AHP					
Media	Means	SD	SE	Mean difference 95% CI	p-value
PDA Control	3.175	0.126	0.063	-	-
PDA AHP	3.250	0.058	0.029	-0.075 (-0.244 to 0.094)	0.3202

*Significant differences, p value < 0.05

Appendix 6-F: Growth and colony diameter of *S. chartarum* grown on ESA and PDA treated with two cycles of AHP, in replicates.

Growth of <i>S. chartarum</i> grown on ESA treated with two cycles of AHP				
Treatment	Replicate 1	Replicate 2	Replicate 3	Replicate 4
Control				
AHP				

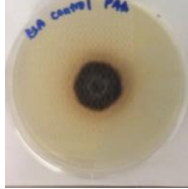
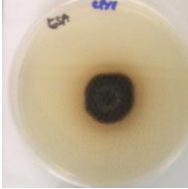
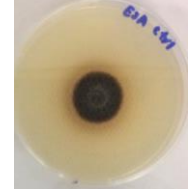


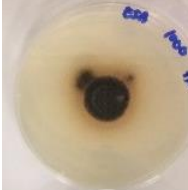
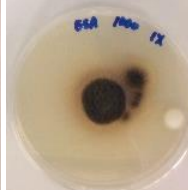

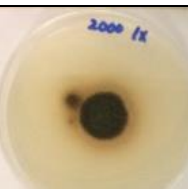
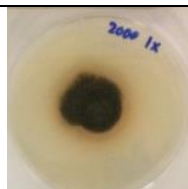

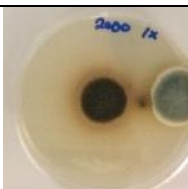
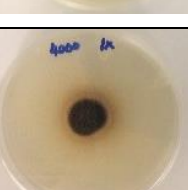


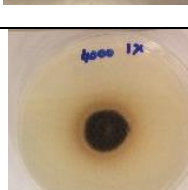
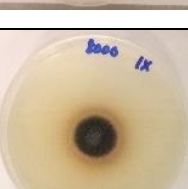

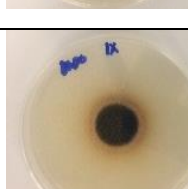
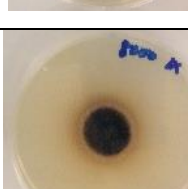
Growth of <i>S. chartarum</i> grown on PDA treated with two cycles of AHP				
Treatment	Replicate 1	Replicate 2	Replicate 3	Replicate 4
Control				
AHP				


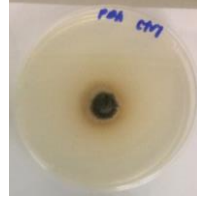
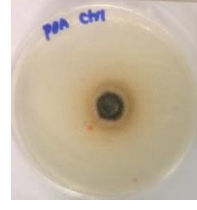

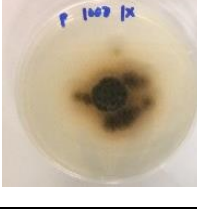
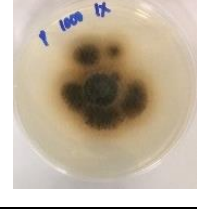

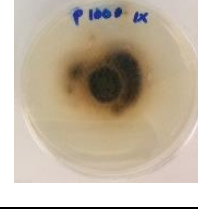
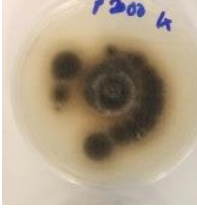

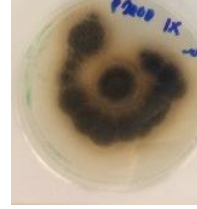
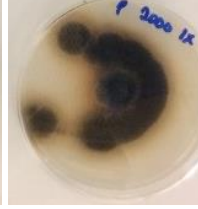
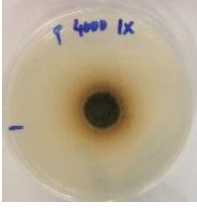

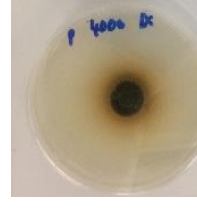
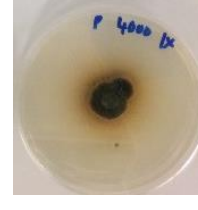
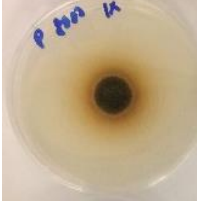
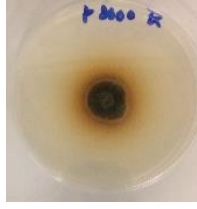
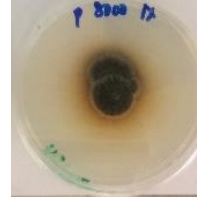

Colony diameter of <i>S. chartarum</i> grown on ESA treated with two cycles AHP					
Media	Means	SD	SE	Mean difference 95% CI	p-value
ESA Control	3.475	0.050	0.025	-	-
ESA AHP	1.000	0.115	0.058	2.475 (2.321 to 2.629)	*0.0001

Colony diameter of <i>S. chartarum</i> grown on PDA treated with two cycles AHP					
Media	Means	SD	SE	Mean difference 95% CI	p-value
PDA Control	3.200	0.141	0.071	-	-
PDA AHP	1.825	0.171	0.085	1.375 (1.104 to 1.646)	*0.0001

*Significant differences, p value < 0.05

Appendix 6-G: Growth and colony diameter of *S. chartarum* grown on ESA and PDA treated with single application of PAA (500 µl), in replicates.

Concentration	Growth of <i>S. chartarum</i> grown on ESA treated with 1 application of PAA			
Control				
1000				
2000				
4000				
8000				

Concentration	Growth of <i>S. chartarum</i> grown on PDA treated with 1 application of PAA			
Control	 PAA ctrl	 PAA ctrl	 PAA ctrl	 PAA ctrl
1000	 P 1000 1x	 P 1000 1x	 P 1000 1x	 P 1000 1x
2000	 P 2000 1x	 P 2000 1x	 P 2000 1x	 P 2000 1x
4000	 P 4000 1x	 P 4000 1x	 P 4000 1x	 P 4000 1x
8000	 P 8000 1x	 P 8000 1x	 P 8000 1x	 P 8000 1x

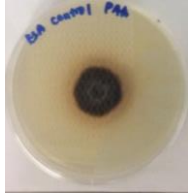
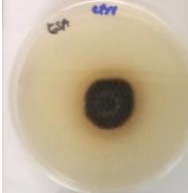
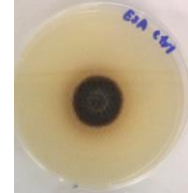

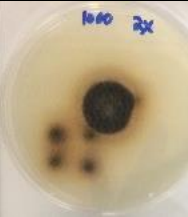
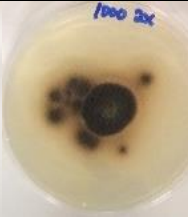
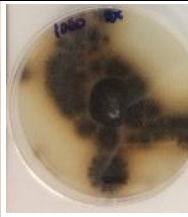
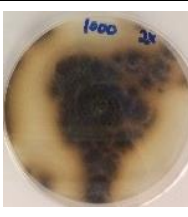

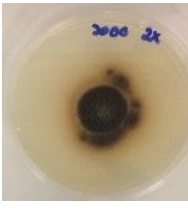
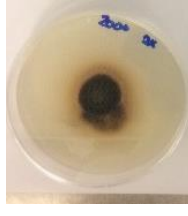
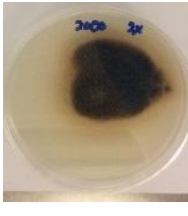

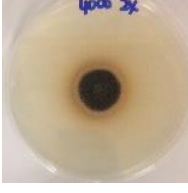


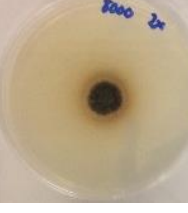
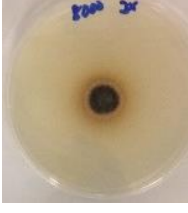
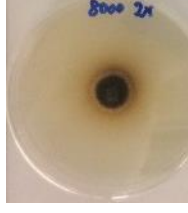

Colony diameter of <i>S. chartarum</i> grown on ESA treated with one application of PAA					
Concentration	Means	SD	SE	Mean difference 95% CI	p-value
Control	3.033	0.058	0.033	-	-
1000	2.875	0.050	0.025	0.158	*0.0115
2000	2.733	0.058	0.033	(0.054 to 0.263)	*0.0031
4000	2.775	0.050	0.025	0.300	*0.0014
8000	2.550	0.058	0.029	(0.169 to 0.431)	*0.0001

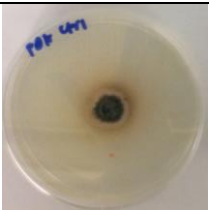
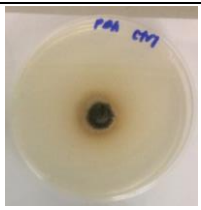
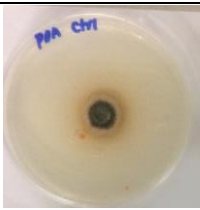
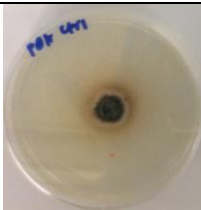
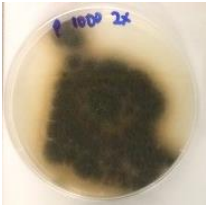

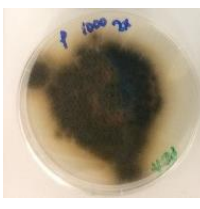
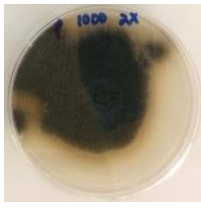
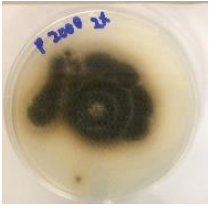
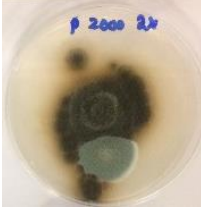
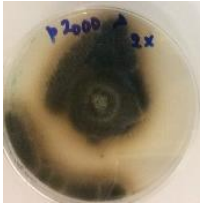
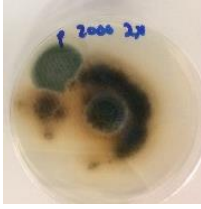
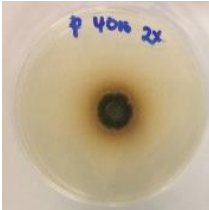


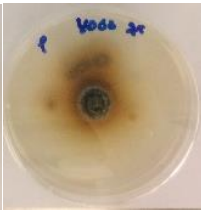
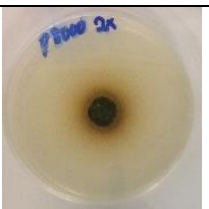
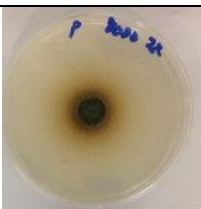

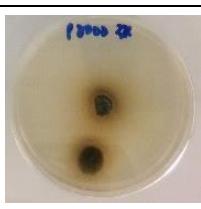
Colony diameter of <i>S. chartarum</i> grown on PDA treated with one application of PAA					
Concentration	Means	SD	SE	Mean difference 95% CI	p-value
Control	2.175	0.050	0.025	-	-
1000	undetermined				
2000	undetermined				
4000	2.175	0.050	0.025	0.000	
8000	2.200	0.000	0.000	(-0.087 to 0.087)	1.0000

*Significant differences, p value < 0.05

Undetermined colony diameter refers to colony diameter with lack of single colony formation.

Appendix 6-H: Growth and colony diameter of *S. chartarum* grown on ESA and PDA treated with two applications of PAA (500 µl), in replicates.

Concentration	Growth of <i>S. chartarum</i> grown on ESA treated with 2 applications of PAA			
Control				
1000				
2000				
4000				
8000				

Concentration	Growth of <i>S. chartarum</i> grown on PDA treated with 2 applications of PAA			
Control				
1000				
2000				
4000				
8000				

Notes: Grey coloured colonies on plates at 2000 ppm are contamination from other fungi.

Colony diameter of <i>S. chartarum</i> grown on ESA treated with two applications of PAA					
Concentration	Means	SD	SE	Mean difference 95% CI	p-value
Control	3.033	0.058	0.033	-	-
1000	2.750	0.071	0.050	0.283	0.0156
2000	2.575	0.050	0.0253	(0.102 to 0.465)	0.0001
4000	2.575	0.050	0.025	0.458	0.0001
8000	2.033	0.058	0.033	(0.354 to 0.563)	0.0001

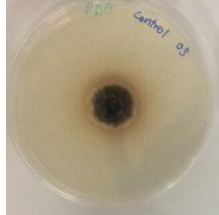
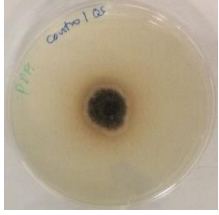
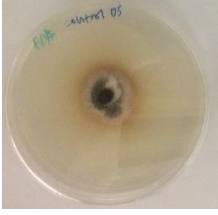

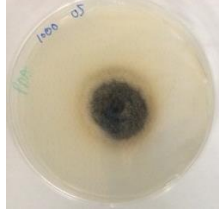
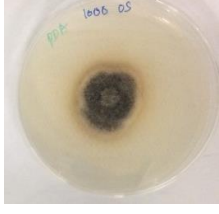
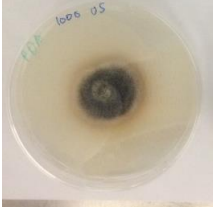

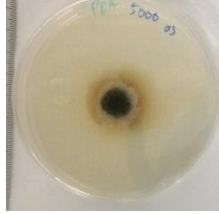
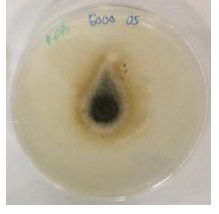
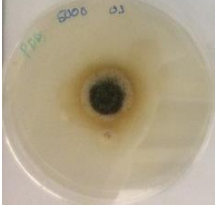
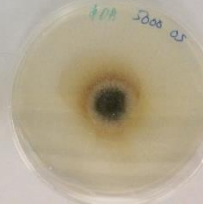
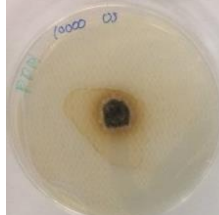
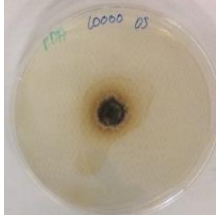


Colony diameter of <i>S. chartarum</i> grown on PDA treated with two applications of PAA					
Concentration	Means	SD	SE	Mean difference 95% CI	p-value
Control	2.175			-	-
1000	undetermined				
2000	undetermined				
4000	2.075	0.126	0.063	0.100 (-0.066 to 0.266)	0.1901
8000	1.925	0.222	0.111	0.250 (-0.028 to 0.528)	0.0701

*Significant differences, p value < 0.05

Undetermined colony diameter refers to colony diameter with lack of single colony formation.

Appendix 6-I: Growth and colony diameter of *S. chartarum* grown on ESA and PDA treated with single application of OS (500 µl), in replicates.

Concentration	Growth of <i>S. chartarum</i> grown on ESA treated with 1 application of OS			
Control				
1000				
5000				
10000				

Concentration	Growth of <i>S. chartarum</i> grown on PDA treated with 1 application of OS			
Control				
1000				
5000				
10000				

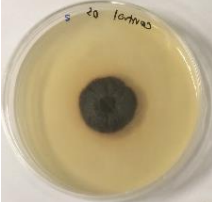

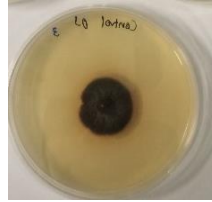




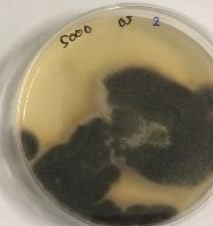


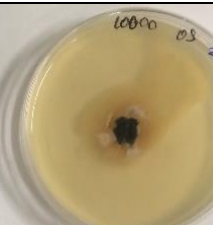
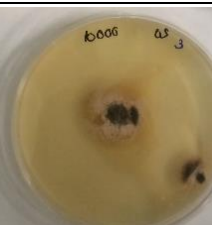
Colony diameter of <i>S. chartarum</i> grown on ESA treated with one application of OS					
Concentration	Means	SD	SE	Mean difference 95% CI	p-value
Control	2.925	0.050	0.025	-	-
1000	undetermined				
*5000	1.200	0.163	0.082	1.725 (1.516 to 1.934)	*0.0001
*10000	1.050	0.058	0.029	1.875 (1.782 to 1.968)	0.0001

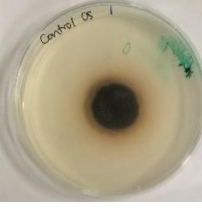
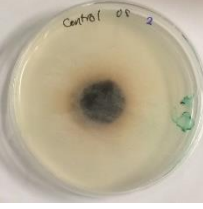
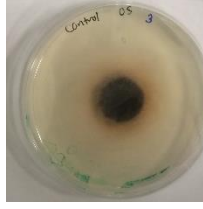
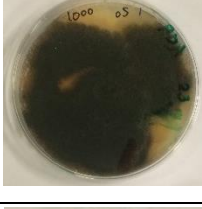
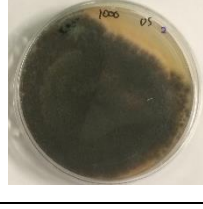
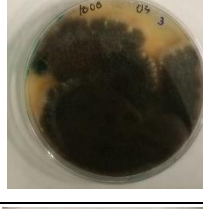

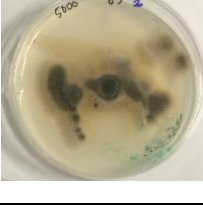

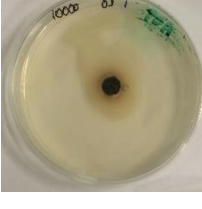
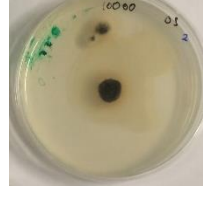
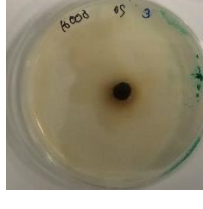
Colony diameter of <i>S. chartarum</i> grown on PDA treated with one application of OS					
Concentration	Means	SD	SE	Mean difference 95% CI	p-value
Control	2.375	0.150	0.075	-	-
1000	3.167	0.058	0.033	-0.792 (-1.031 to - 0.553)	0.0004 (increased in diameter due to spreading of OS solution)
5000	2.375	0.126	0.063	0.000 (-0.240 to 0.240)	1.0000
*10000	1.550	0.058	0.029	0.825 (0.628 to 1.022)	*0.0001

*Significant differences, p value < 0.05

Undetermined colony diameter refers to colony diameter with lack of single colony formation.

Appendix 6-J: Growth and colony diameter of *S. chartarum* grown on ESA and PDA treated with two applications of OS (500 µl), in replicates.

Concentration	Growth of <i>S. chartarum</i> grown on ESA treated with 2 applications of OS		
Control			
1000			
5000			
10000			

Concentration	Growth of <i>S. chartarum</i> grown on PDA treated with 2 applications of OS		
Control	 Petri dish showing a small, dark, circular growth on a light-colored agar surface. The dish is labeled "Control OS 1".	 Petri dish showing a small, dark, circular growth on a light-colored agar surface. The dish is labeled "Control OS 2".	 Petri dish showing a small, dark, circular growth on a light-colored agar surface. The dish is labeled "Control OS 3".
1000	 Petri dish showing a large, dark, irregular growth covering most of the agar surface. The dish is labeled "1000 OS 1".	 Petri dish showing a large, dark, irregular growth covering most of the agar surface. The dish is labeled "1000 OS 2".	 Petri dish showing a large, dark, irregular growth covering most of the agar surface. The dish is labeled "1000 OS 3".
5000	 Petri dish showing a large, dark, irregular growth covering most of the agar surface. The dish is labeled "5000 OS 1".	 Petri dish showing a large, dark, irregular growth covering most of the agar surface. The dish is labeled "5000 OS 2".	 Petri dish showing a large, dark, irregular growth covering most of the agar surface. The dish is labeled "5000 OS 3".
10000	 Petri dish showing a small, dark, circular growth on a light-colored agar surface. The dish is labeled "10000 OS 1".	 Petri dish showing a small, dark, circular growth on a light-colored agar surface. The dish is labeled "10000 OS 2".	 Petri dish showing a small, dark, circular growth on a light-colored agar surface. The dish is labeled "10000 OS 3".

Colony diameter of <i>S. chartarum</i> grown on ESA treated with two applications of OS					
Concentration	Means	SD	SE	Mean difference 95% CI	p-value
Control	2.933	0.058	0.033	-	-
1000	undetermined				
5000	undetermined				
1000	1.233	0.058	0.033	1.700 (1.569 to 1.831)	0.0001

Colony diameter of <i>S. chartarum</i> grown on PDA treated with two applications of OS					
Concentration	Means	SD	SE	Mean difference 95% CI	p-value
Control	2.567	0.058	0.033	-	-
1000	undetermined				
5000	undetermined				
10000	1.033	0.153	0.088	1.533 (1.272 to 1.795)	0.0001

*Significant differences, p value < 0.05

Undetermined colony diameter refers to colony diameter with lack of single colony formation.

Appendix 6-K: The absorbance OD_{650nm} of RPMI 1640 - 2% G- buffered with MOPS with and without spores containing various concentrations of bleach.

Without spores (background)

Conc.	2250	20000	15000	10000	5000	2500	1500	1250	1000	500	250	200	100	RPMI and water	
	0.038	0.042	0.042	0.042	0.052	0.049	0.046	0.05	0.049	0.046	0.046	0.047	0.04	0.04	0.043
	0.038	0.04	0.041	0.041	0.052	0.05	0.046	0.051	0.049	0.043	0.044	0.043	0.04	0.04	0.041
	0.038	0.043	0.041	0.042	0.053	0.049	0.045	0.05	0.048	0.044	0.046	0.043	0.04	0.04	0.041
Mean	0.038	0.041	0.041	0.041	0.052	0.049	0.045	0.050	0.048	0.044	0.045	0.044	0.04	0.04	0.041
s		7	3	7	3	3	7	3	7	3	3	3	1	5	7

With spores

Conc.	22500	20000	15000	10000	5000	2500	1500	1250	1000	500	250	200	100	Pos	Blank
R1	0.048	0.092	0.259	0.28	0.292	0.303	0.291	0.306	0.478	0.336	0.327	0.359	0.366	0.492	0.042
R2	0.044	0.091	0.253	0.287	0.291	0.286	0.3	0.319	0.349	0.407	0.406	0.389	0.432	0.415	0.042
R3	0.057	0.079	0.25	0.281	0.285	0.306	0.296	0.303	0.447	0.461	0.499	0.502	0.487	0.492	0.041

The mean of the background reading was subtracted from each replicate was to obtain the final reading used to plot the graph in Figure 6.13

Appendix 6-L: Statistical analysis of the ODs produced by different concentrations of bleach on *S. chartarum* grown in liquid media – ANOVA.

Table Analyzed	Bleach 24hrs		
One-way analysis of variance			
P value	< 0.0001		
P value summary	***		
Are means signif. different? (P < 0.05)	Yes		
Number of groups	15		
F	62.13		
R square	0.9508		
ANOVA Table	SS	df	MS
Treatment (between columns)	1.066	14	0.07612
Residual (within columns)	0.05513	45	0.001225
Total	1.121	59	

Dunnett's Multiple Comparison Test	Mean Diff.	q	Significant? P < 0.05?	Summary	95% CI of diff
+ve control vs 22500	0.4097	16.55	Yes	***	0.3371 to 0.4822
+ve control vs 20000	0.3757	15.18	Yes	***	0.3031 to 0.4483
+ve control vs 15000	0.2086	8.429	Yes	***	0.1360 to 0.2812
+ve control vs 10000	0.1804	7.287	Yes	***	0.1078 to 0.2529
+ve control vs 5000	0.1843	7.446	Yes	***	0.1117 to 0.2569
+ve control vs 2500	0.1723	6.962	Yes	***	0.09972 to 0.2449
+ve control vs 1500	0.1714	6.923	Yes	***	0.09877 to 0.2439
+ve control vs 1250	0.1623	6.558	Yes	***	0.08972 to 0.2349
+ve control vs 1000	0.04535	1.832	No	ns	-0.02723 to 0.1179
+ve control vs 500	0.0643	2.598	No	ns	-0.008284 to 0.1369
+ve control vs 250	0.05595	2.261	No	ns	-0.01663 to 0.1285
+ve control vs 200	0.04895	1.978	No	ns	-0.02363 to 0.1215
+ve control vs 100	0.03400	1.374	No	ns	-0.03858 to 0.1066
+ve control vs Blank	0.4211	17.02	Yes	***	0.3485 to 0.4937

Appendix 6-M: The absorbance OD650nm of RPMI 1640 - 2% G- buffered with MOPS with and without spores containing various concentrations of PAA.

Without spores (background)

Conc.	8000	4000	2000	1000	RPMI and water
	0.091	0.052	0.026	0.012	0.042
	0.093	0.053	0.024	0.011	0.041
	0.087	0.051	0.024	0.011	0.041
Means	0.0903	0.052	0.0247	0.0113	0.0413

With spores

Conc.	8000	4000	2000	1000	Positive control	Blank
R1	0.095	0.069	0.045	0.032	0.149	0.042
R2	0.094	0.067	0.045	0.032	0.135	0.041
R3	0.094	0.07	0.05	0.034	0.139	0.042

The mean of the background reading was subtracted from each replicate to obtain the final reading used to plot the graph in Figure 6.14

Appendix 6-N: Statistical analysis of the ODs produced by different concentrations of PAA on *S. chartarum* grown in liquid media – ANOVA.

Table Analyzed Peracetic acid 24hrs

One-way analysis of variance

P value < 0.0001

P value summary ***

Are means signif. different? (P < 0.05) Yes

Number of groups 6

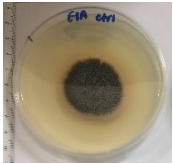
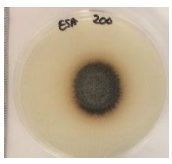
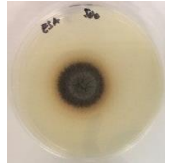
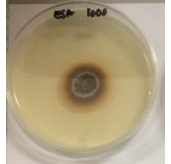
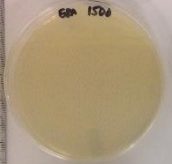
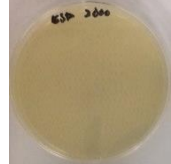
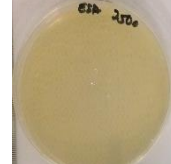
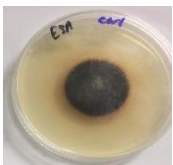
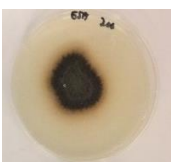

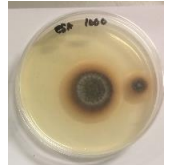


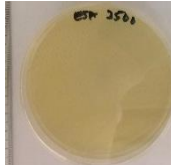
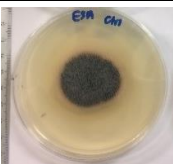
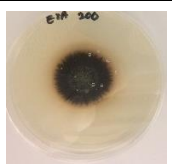

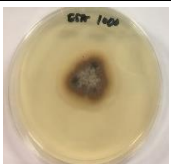


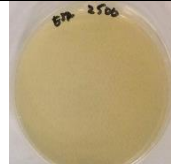
F 373.1

R square 0.9936

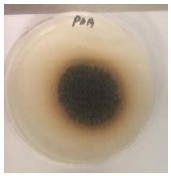
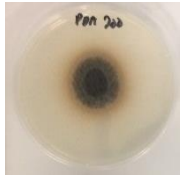
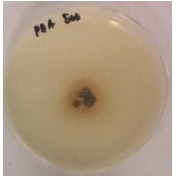
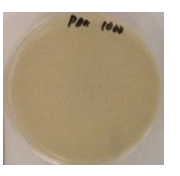

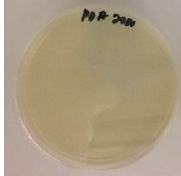
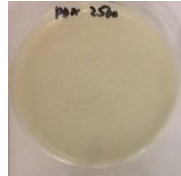
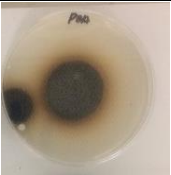
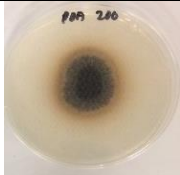
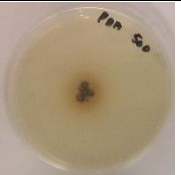
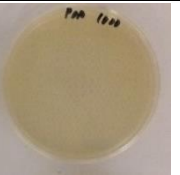

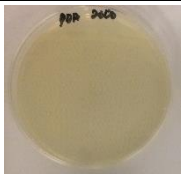

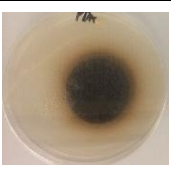
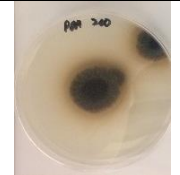

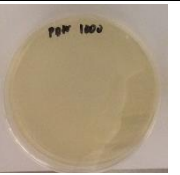
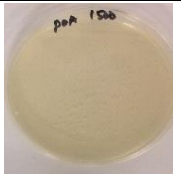
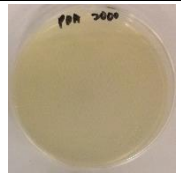
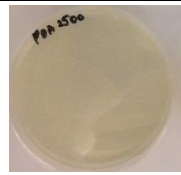
ANOVA Table	SS	df	MS
Treatment (between columns)	0.02002	5	0.004003
Residual (within columns)	0.0001287	12	1.073e-005
Total	0.02014	17	

Dunnett's Multiple Comparison Test	Mean Diff.	q	Significant? P < 0.05?	Summary	95% CI of diff
+ve control vs 8000	0.09567	35.77	Yes	***	0.08791 to 0.1034
+ve control vs 4000	0.08300	31.04	Yes	***	0.07524 to 0.09076
+ve control vs 2000	0.07767	29.04	Yes	***	0.06991 to 0.08543
+ve control vs 1000	0.07833	29.29	Yes	***	0.07057 to 0.08609
+ve control vs Blank	0.09911	37.06	Yes	***	0.09135 to 0.1069

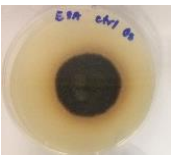

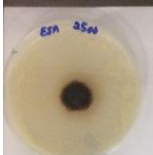



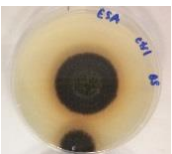




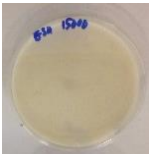

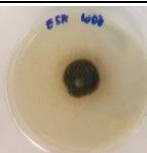

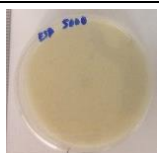
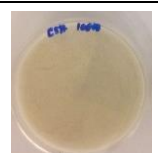

Appendix 6-O: Agar dilution method performed to determine the lowest concentration of bleach where no fungal growth was visible on ESA after 7 days incubation at 25 °C.

Media	Replicates	Control	200 ppm	500 ppm	1000 ppm	1500 ppm	2000 ppm	2500 ppm	
ESA	R1								
	R2								
	R2								
	Means		4.133	3.867	3.533	3.467	No growth	No growth	No growth
	SD		0.115 /	0.153	0.058	0.321			
	SE		0.067	0.088	0.033	0.186			
	95% CI		-	0.267 (-0.040 to 0.574)	0.600 (0.393 to 0.807)	0.667 (0.119 to 1.214)			
p-value		-	0.0734	*0.0013	*0.0278				

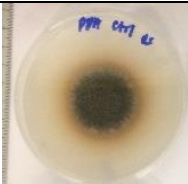




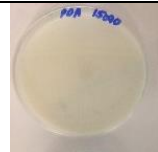
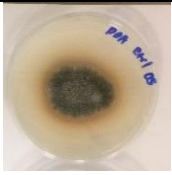


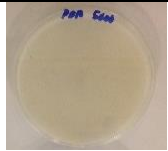
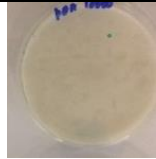

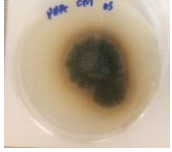



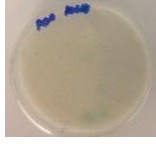

Appendix 6-P: Agar dilution method performed to determine the lowest concentration of bleach where no fungal growth was visible on PDA after 7 days incubation at 25 °C.

Media	Replicates	Control	200 ppm	500 ppm	1000 ppm	1500 ppm	2000 ppm	2500 ppm
PDA	R1							
	R2							
	R2							
	Means	4.367	3.733	2.100	No growth	No growth	No growth	No growth
	SD	0.058	0.231	0.265				
	SE	0.033	0.133	0.153				
	95% CI		0.633 (0.252 to 1.015)	2.267 (1.833 to 2.701)				
	p-value		*0.0100	*0.0001				

Appendix 6-Q: Agar dilution method performed to determine the lowest concentration of OS where no fungal growth was visible on ESA after 7 days incubation at 25 °C.

Media	Replicates	Control	1000 ppm	2500 ppm	5000 ppm	10000 ppm	15000 ppm
ESA	R1						
	R2						
	R2						
	Means	4.267	3.233	2.367	No growth	No growth	No growth
	SD	0.058	0.115	0.153			
	SE	0.033	0.067	0.088			
	95% CI		1.033 (0.826 to 1.240)	1.900 (1.638 to 2.162)			
	p-value		*0.0002	*0.0001			

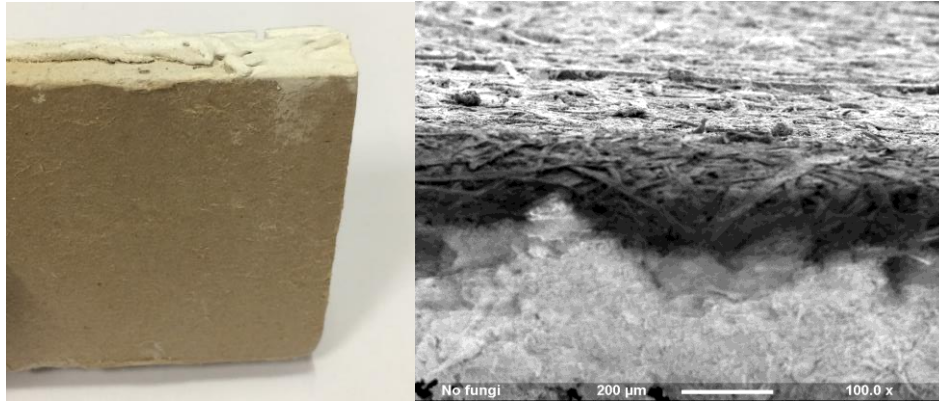
Appendix 6-R: Agar dilution method performed to determine the lowest concentration of OS where no fungal growth was visible on PDA after 7 days incubation at 25 °C.

Media	Replicates	Control	1000 ppm	2500 ppm	5000 ppm	10000 ppm	15000 ppm
PDA	R1						
	R2						
	R2						
	Means	4.100	2.900	No growth	No growth	No growth	No growth
	SD	0.100	0.436				
	SE	0.058	0.252				
	95% CI		1.200 (0.483 to 1.917)				
	p-value		*0.0097				

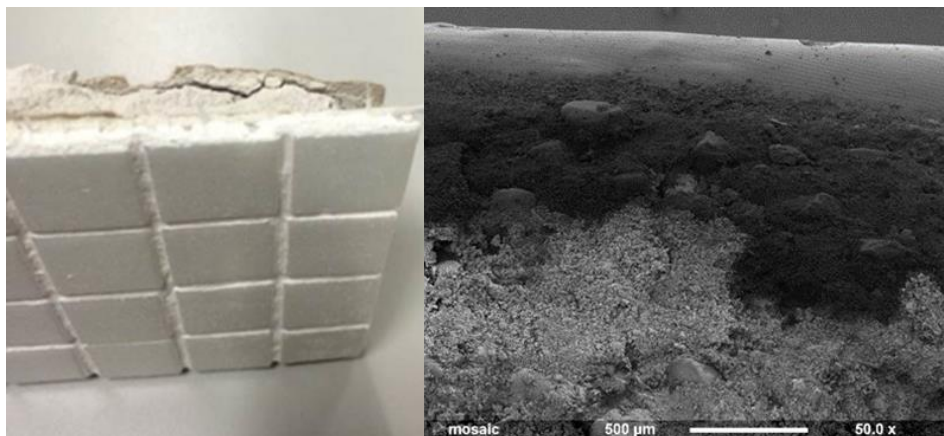
Chapter 7 : Efficacy of antimicrobial treatment and prevention on *S. chartarum* infested building material

Appendix 7-A: Materials tested for fungal growth and their microscopic features as observed under electron microscope.

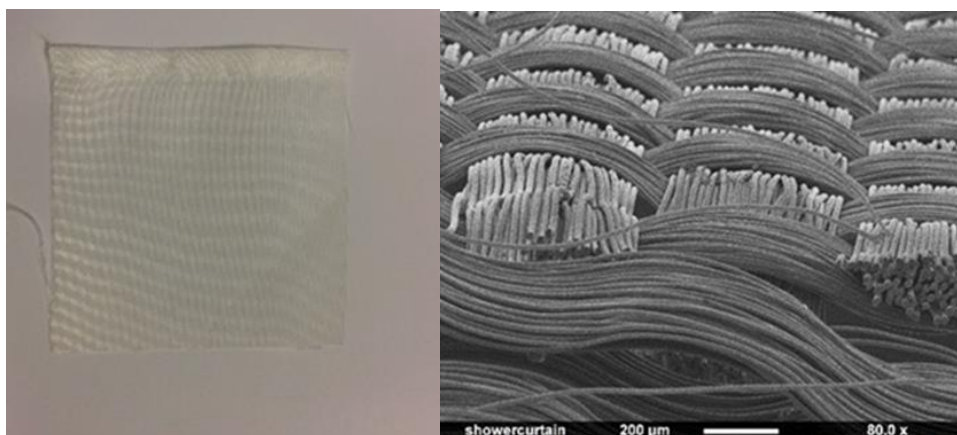
1. Gypsum board



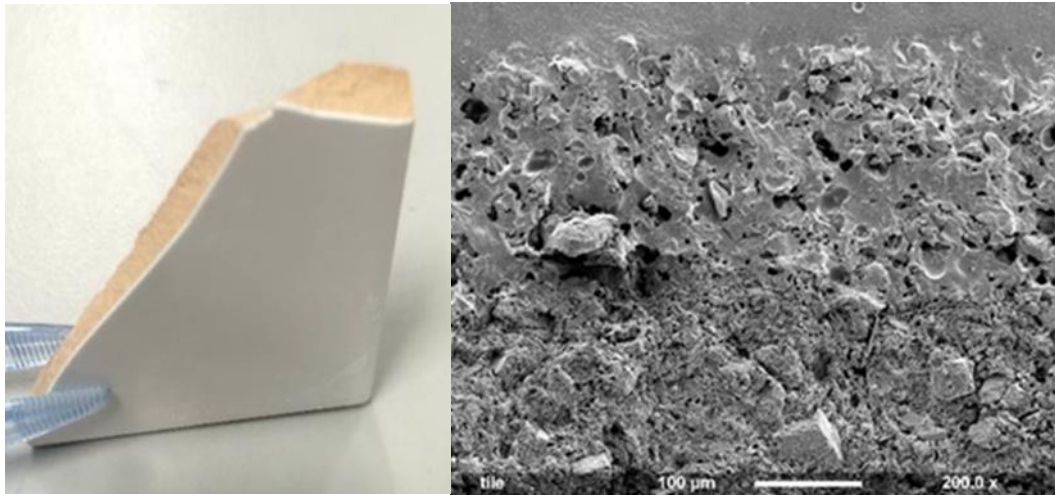
2. Mosaic and grouting



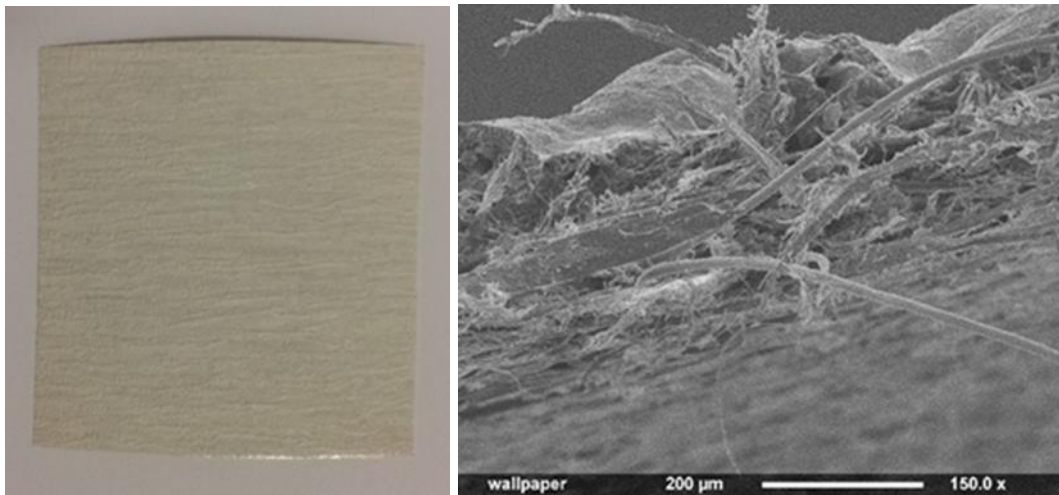
3. Shower curtain



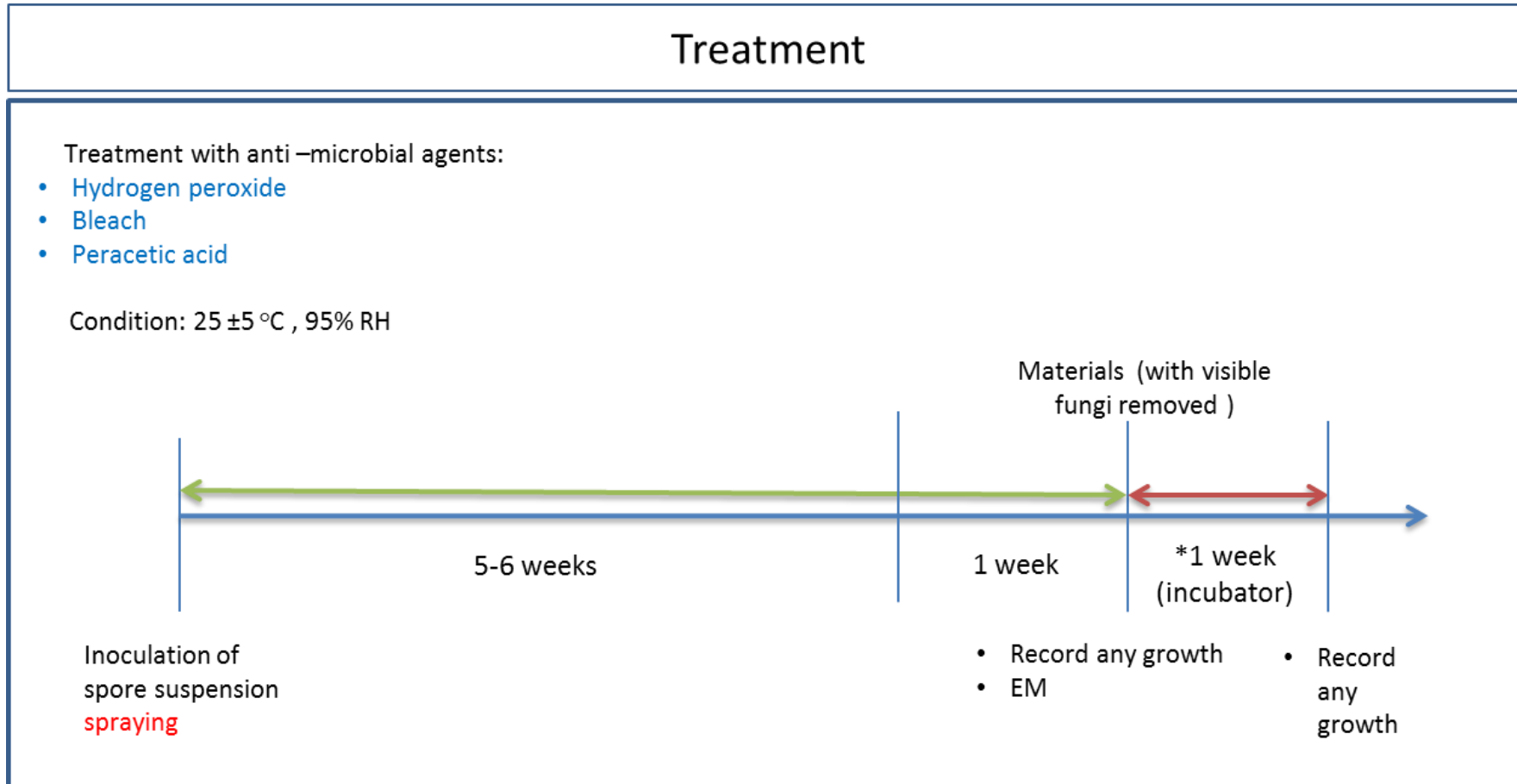
4. Ceramic tile



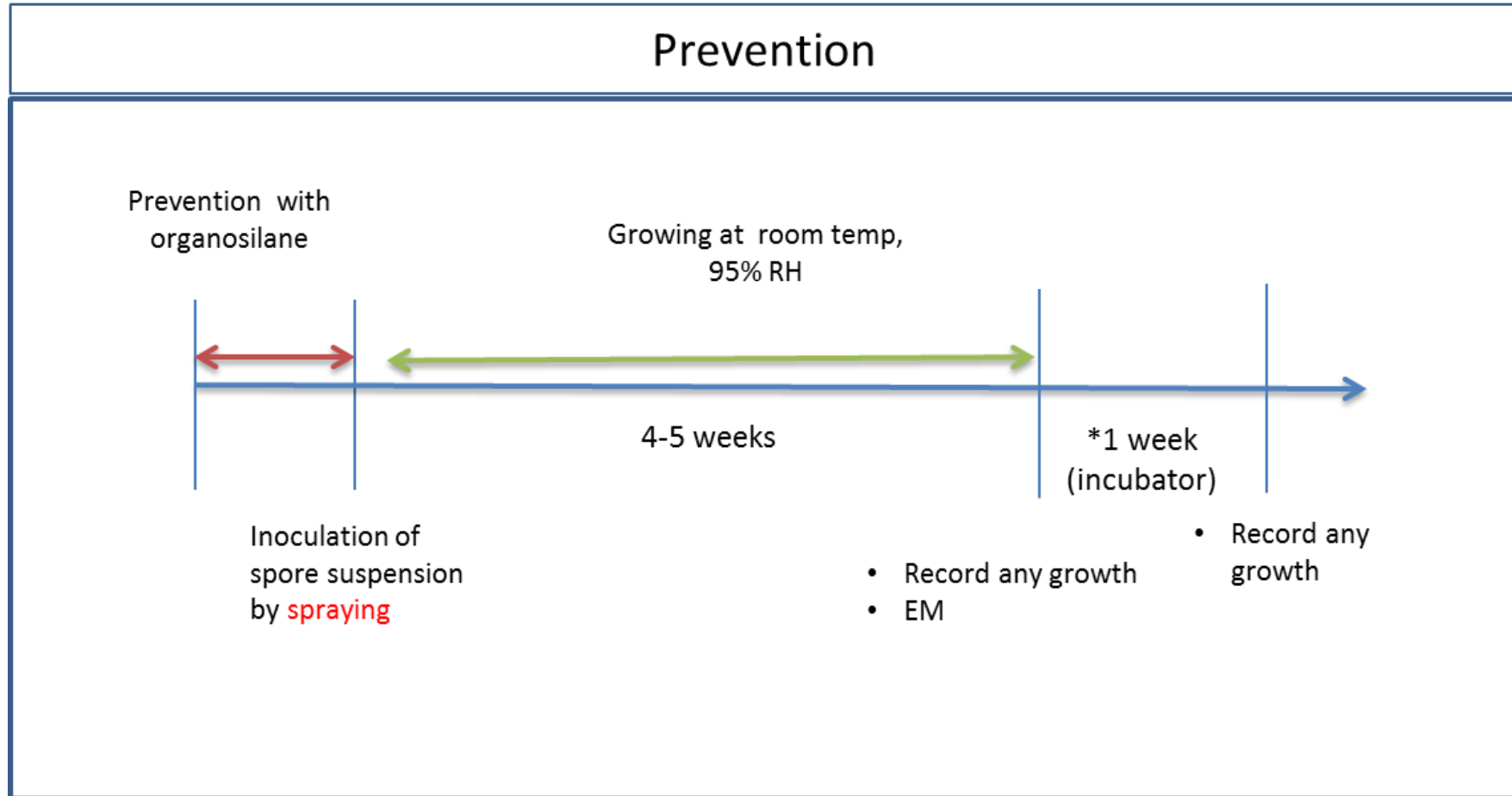
5. Wallpaper



Appendix 7-B: Schematic diagram of fungal growth and application of antimicrobial treatment.



Appendix 7-C: Schematic diagram of antimicrobial prevention and inoculation of spores suspension.



Chapter 8 : Proteomic profiles of *Stachybotrys chartarum* in response to antimicrobial agents

Appendix 8-A: Protein classes identified in *S. chartarum* and their functions

(331)

Protein classes	Functions
Glucosidase	Enzymes that hydrolyse o-glucosyl-compounds.
Hydrolase	Enzymes catalysing hydrolysis of a variety of bonds, such as esters, glycosides, or peptides
Chaperonin	Subset of chaperone proteins found in prokaryotes, mitochondria and plastids
Chaperone	A cytoplasmic protein that binds to nascent or unfolded polypeptides and ensures correct folding or transport
Dehydrogenase	An enzyme that oxidizes a substrate by transferring hydrogen to an acceptor that is either NAD/NADP or a flavin enzyme
Oxidoreductase	An enzyme that catalyses a redox reaction
Reductase	An enzyme that introduces an electron into its substrate from an electron donor. The reaction is usually coupled with an oxidation reaction
Epimerase/ racemase	Enzymes that catalyse inversion of the configuration around an asymmetric carbon in a substrate having one (racemase) or more (epimerase) centre(s) of asymmetry (EC5.1)
Isomerase	A class of enzymes that catalyse geometric or structural changes within a molecule to form a single product. The reactions do not involve a net change in the concentrations of compounds other than the substrate and the product
Dehydratase	Enzymes that remove hydroxyl groups from compounds, producing water in the process.
Lyase	Enzymes that either strip a group from a molecule to form a double bond or add a group to a double bond.
Metalloprotease	A protease whose catalytic activity requires a transition metal.
Protease	Enzymes that hydrolyse peptide bonds.
Translation initiation factor	A non-ribosomal protein involved in translation initiation.
Translation factor	A non-ribosomal protein involved in translation initiation, elongation or termination
RNA binding protein	A protein that binds RNA and is involved in RNA processing or metabolism.
Oxidase	An enzyme that removes an electron from its substrate to an electron acceptor. The reaction is usually coupled with a reduction reaction.
Cytoskeletal proteins	Major constituent of the cytoskeleton found in the cytoplasm of eukaryotic cells. They form a flexible framework for the cell, provide attachment points for organelles and formed bodies, and make communication between parts of the cell possible.
Ribosomal protein	A protein that comprises part of the ribosome.
Transferase	Enzymes transferring a group from one compound (donor) to another compound (acceptor). Kinase is a separate category, so it is not included here.

Appendix 8-B: Molecular functional groups identified in *S. chartarum* and their functions ⁽³³¹⁾.

Molecular functions	Functions
Proton-transporting ATP synthase activity, rotational mechanism	Catalysis of the transfer of protons from one side of a membrane to the other according to the reaction: $ADP + H_2O + H^+(in) = ATP + \text{phosphate} + H^+(out)$, by a rotational mechanism
Hydro-lyase activity	Catalysis of the cleavage of a carbon-oxygen bond by elimination of water
Lyase activity	Catalysis of the cleavage of C-C, C-O, C-N and other bonds by other means than by hydrolysis or oxidation, or conversely adding a group to a double bond. They differ from other enzymes in that two substrates are involved in one reaction direction, but only one in the other direction. When acting on the single substrate, a molecule is eliminated and this generates either a new double bond or a new ring
Catalytic activity	Catalysis of a biochemical reaction at physiological temperatures. In biologically catalysed reactions, the reactants are known as substrates, and the catalysts are naturally occurring macromolecular substances known as enzymes. Enzymes possess specific binding sites for substrates, and are usually composed wholly or largely of protein, but RNA that has catalytic activity (ribozyme) is often also regarded as enzymatic
Metallopeptidase activity	Catalysis of the hydrolysis of peptide bonds by a mechanism in which water acts as a nucleophile, one or two metal ions hold the water molecule in place, and charged amino acid side chains are ligands for the metal ions
Peptidase activity	Catalysis of the hydrolysis of a peptide bond. A peptide bond is a covalent bond formed when the carbon atom from the carboxyl group of one amino acid shares electrons with the nitrogen atom from the amino group of a second amino acid
Translation initiation factor activity	Functions in the initiation of ribosome-mediated translation of mRNA into a polypeptide
Translation regulator activity	Any molecular function involved in the initiation, activation, perpetuation, repression or termination of polypeptide synthesis at the ribosome
Oxidoreductase activity	Catalysis of an oxidation-reduction (redox) reaction, a reversible chemical reaction in which the oxidation state of an atom or atoms within a molecule is altered. One substrate acts as a hydrogen or electron donor and becomes oxidized, while the other acts as hydrogen or electron acceptor and becomes reduced
Isomerase activity	Catalysis of the geometric or structural changes within one molecule. Isomerase is the systematic name for any enzyme of EC class 5
Structural constituent of cytoskeleton	The action of a molecule that contributes to the structural integrity of a cytoskeletal structure
Structural molecule activity	The action of a molecule that contributes to the structural integrity of a complex or assembly within or outside a cell
Structural constituent of ribosome	The action of a molecule that contributes to the structural integrity of the ribosome
Ligase activity	Catalysis of the joining of two substances, or two groups within a single molecule, with the concomitant hydrolysis of the diphosphate bond in ATP or a similar triphosphate

Appendix 8-C: Biological processes identified in *S. chartarum* and their functions ⁽³³¹⁾.

Biological process	Functions
Fatty acid beta-oxidation	A fatty acid oxidation process that results in the complete oxidation of a long-chain fatty acid. Fatty acid beta-oxidation begins with the addition of coenzyme A to a fatty acid, and occurs by successive cycles of reactions during each of which the fatty acid is shortened by a two-carbon fragment removed as acetyl coenzyme A; the cycle continues until only two or three carbons remain (as acetyl-CoA or propionyl-CoA respectively)
Fatty acid metabolic process	The chemical reactions and pathways involving fatty acids, aliphatic monocarboxylic acids liberated from naturally occurring fats and oils by hydrolysis
Lipid metabolic process	The chemical reactions and pathways involving lipids, compounds soluble in an organic solvent but not, or sparingly, in an aqueous solvent. Includes fatty acids; neutral fats, other fatty-acid esters, and soaps; long-chain (fatty) alcohols and waxes; sphingoids and other long-chain bases; glycolipids, phospholipids and sphingolipids; and carotenes, polyprenols, sterols, terpenes and other isoprenoids
Primary metabolic process	The chemical reactions and pathways involving those compounds which are formed as a part of the normal anabolic and catabolic processes. These processes take place in most, if not all, cells of the organism
Metabolic process	The chemical reactions and pathways, including anabolism and catabolism, by which living organisms transform chemical substances. Metabolic processes typically transform small molecules, but also include macromolecular processes such as DNA repair and replication, and protein synthesis and degradation
Tricarboxylic acid cycle	A nearly universal metabolic pathway in which the acetyl group of acetyl coenzyme A is effectively oxidized to two CO ₂ and four pairs of electrons are transferred to coenzymes. The acetyl group combines with oxaloacetate to form citrate, which undergoes successive transformations to isocitrate, 2-oxoglutarate, succinyl-CoA, succinate, fumarate, malate, and oxaloacetate again, thus completing the cycle. In eukaryotes, the tricarboxylic acid is confined to the mitochondria
Steroid metabolic process	The chemical reactions and pathways involving steroids, compounds with a 1,2, cyclopentanoperhydrophenanthrene nucleus.
Respiratory electron transport chain	A process in which a series of electron carriers operate together to transfer electrons from donors such as NADH and FADH ₂ to any of several different terminal electron acceptors to generate a transmembrane electrochemical gradient
Generation of precursor metabolites and energy	The chemical reactions and pathways resulting in the formation of precursor metabolites, substances from which energy is derived, and any process involved in the liberation of energy from these substances
Protein folding	The process of assisting in the covalent and noncovalent assembly of single chain polypeptides or multisubunit complexes into the correct tertiary structure
Protein metabolic process	The chemical reactions and pathways involving a specific protein, rather than of proteins in general. Includes protein modification
Monosaccharide metabolic process	The chemical reactions and pathways involving monosaccharides, the simplest carbohydrates. They are polyhydric alcohols containing either an aldehyde or a keto group and between three to ten or more carbon atoms. They form the constitutional repeating units of oligo- and polysaccharides
Carbohydrate metabolic process	The chemical reactions and pathways involving carbohydrates, any of a group of organic compounds based of the general formula C _x (H ₂ O) _y . Includes the formation of carbohydrate derivatives by the addition of a carbohydrate residue to another molecule
Proteolysis	The hydrolysis of proteins into smaller polypeptides and/or amino acids by cleavage of their peptide bonds
Translation	The cellular metabolic process in which a protein is formed, using the sequence of a mature mRNA molecule to specify the sequence of amino acids in a polypeptide chain. Translation is mediated by the ribosome, and begins with the formation of a ternary complex between amino acylated initiator methionine tRNA, GTP, and initiation factor 2, which subsequently associates with the small subunit of the ribosome and an mRNA. Translation ends with the release of a polypeptide chain from the ribosome
Protein complex assembly	The aggregation, arrangement and bonding together of a set of components to form a protein complex
Protein complex biogenesis	A cellular process that results in the biosynthesis of constituent macromolecules, assembly, and arrangement of constituent parts of a protein complex. Includes the synthesis of the constituent protein molecules, and those protein modifications that are involved in synthesis or assembly of the complex

Cellular amino acid biosynthetic process	The chemical reactions and pathways resulting in the formation of amino acids, organic acids containing one or more amino substituents
Biosynthetic process	The chemical reactions and pathways resulting in the formation of substances; typically, the energy-requiring part of metabolism in which simpler substances are transformed into more complex ones

Appendix 8-D: Cellular components identified in *S. chartarum* and their functions ⁽³³¹⁾.

Cellular component	Functions
Extracellular space	That part of a multicellular organism outside the cells proper, usually taken to be outside the plasma membranes, and occupied by fluid
Extracellular region	The space external to the outermost structure of a cell. For cells without external protective or external encapsulating structures this refers to space outside of the plasma membrane
Proton-transporting ATP synthase complex	A proton-transporting two-sector ATPase complex that catalyses the phosphorylation of ADP to ATP during oxidative phosphorylation. The complex comprises a membrane sector (F ₀) that carries out proton transport and a cytoplasmic compartment sector (F ₁) that catalyses ATP synthesis by a rotational mechanism; the extramembrane sector (containing 3 a and 3 b subunits) is connected via the d-subunit to the membrane sector by several smaller subunits. Within this complex, the g and e subunits and the 9-12 c subunits rotate by consecutive 120 degree angles and perform parts of ATP synthesis. This movement is driven by the hydrogen ion electrochemical potential gradient
Actin cytoskeleton	The part of the cytoskeleton (the internal framework of a cell) composed of actin and associated proteins. Includes actin cytoskeleton-associated complexes
Cytosol	The part of the cytoplasm that does not contain organelles but which does contain other particulate matter, such as protein complexes
Cytoplasm	All the contents of a cell excluding the plasma membrane and nucleus, but including other subcellular structures
Intracellular	The living contents of a cell; the matter contained within (but not including) the plasma membrane, usually taken to exclude large vacuoles and masses of secretory or ingested material. In eukaryotes, it includes the nucleus and cytoplasm
Ribosome	An intracellular organelle, about 200 Å in diameter, consisting of RNA and protein. It is the site of protein biosynthesis resulting from translation of messenger RNA (mRNA). It consists of two subunits, one large and one small, each containing only protein and RNA. Both the ribosome and its subunits are characterized by their sedimentation coefficients, expressed in Svedberg units (symbol: S). Hence, the prokaryotic ribosome (70S) comprises a large (50S) subunit and a small (30S) subunit, while the eukaryotic ribosome (80S) comprises a large (60S) subunit and a small (40S) subunit. Two sites on the ribosomal large subunit are involved in translation, namely the aminoacyl site (A site) and peptidyl site (P site). Ribosomes from prokaryotes, eukaryotes, mitochondria, and chloroplasts have characteristically distinct ribosomal proteins
Integral to membrane	Penetrating at least one phospholipid bilayer of a membrane. May also refer to the state of being buried in the bilayer with no exposure outside the bilayer. When used to describe a protein, indicates that all or part of the peptide sequence is embedded in the membrane

Membrane	Double layer of lipid molecules that encloses all cells, and, in eukaryotes, many organelles; may be a single or double lipid bilayer; also includes associated proteins
Nucleoplasm	That part of the nuclear content other than the chromosomes or the nucleolus
Nucleus	A membrane-bounded organelle of eukaryotic cells in which chromosomes are housed and replicated. In most cells, the nucleus contains all the cell's chromosomes except the organellar chromosomes, and is the site of RNA synthesis and processing. In some species, or in specialized cell types, RNA metabolism or DNA replication may be absent

Appendix 8-E: Decreased protein levels of *S. chartarum* treated with bleach versus control (<20% variability, < 0.5-fold change, n = 36).

Accession	Proteins	Fold change	Coverage	# peptide	MW (kDa)	pI
A0A084AUC3	Uncharacterized protein OS= <i>Stachybotrys chartarum</i> IBT 7711 GN=S7711_03834 PE=4 SV=1 - [A0A084AUC3_STACH]	0.110	11.87	3	25.1	6.54
A0A084RAP9	Uncharacterized protein OS= <i>Stachybotrys chartarum</i> IBT 40288 GN=S40288_07240 PE=3 SV=1 - [A0A084RAP9_STACH]	0.118	10.54	3	31.9	6.30
A0A084AMZ1	Uncharacterized protein OS= <i>Stachybotrys chartarum</i> IBT 7711 GN=S7711_01960 PE=4 SV=1 - [A0A084AMZ1_STACH]	0.148	5.62	3	50.8	4.84
A0A084B5L7	Uncharacterized protein OS= <i>Stachybotrys chartarum</i> IBT 7711 GN=S7711_04427 PE=4 SV=1 - [A0A084B5L7_STACH]	0.162	18.86	3	18.8	9.01
A0A084REZ0	Uncharacterized protein OS= <i>Stachybotrys chartarum</i> IBT 40288 GN=S40288_06605 PE=4 SV=1 - [A0A084REZ0_STACH]	0.208	14.84	2	16.4	9.52
A0A084RMI1	Uncharacterized protein OS= <i>Stachybotrys chartarum</i> IBT 40288 GN=S40288_03106 PE=4 SV=1 - [A0A084RMI1_STACH]	0.229	25.27	2	9.9	4.82
A0A084ALH7	Glucanase OS= <i>Stachybotrys chartarum</i> IBT 7711 GN=S7711_05326 PE=3 SV=1 - [A0A084ALH7_STACH]	0.242	13.00	4	47.9	4.18
A0A084BBL6	Uncharacterized protein OS= <i>Stachybotrys chartarum</i> IBT 7711 GN=S7711_01294 PE=4 SV=1 - [A0A084BBL6_STACH]	0.258	20.61	4	18.5	6.73
A0A084RKB2	Uncharacterized protein OS= <i>Stachybotrys chartarum</i> IBT 40288 GN=S40288_05974 PE=4 SV=1 - [A0A084RKB2_STACH]	0.259	37.50	5	12.0	4.59
A0A084B8F5	Uncharacterized protein OS= <i>Stachybotrys chartarum</i> IBT 7711 GN=S7711_03129 PE=4 SV=1 - [A0A084B8F5_STACH]	0.295	45.12	5	8.7	6.73
A0A084B7D6	Carboxylic ester hydrolase OS= <i>Stachybotrys chartarum</i> IBT 7711 GN=S7711_07491 PE=3 SV=1 - [A0A084B7D6_STACH]	0.310	3.00	2	58.4	6.16
A0A084RGX9	Protein YOP1 OS= <i>Stachybotrys chartarum</i> IBT 40288 GN=S40288_01175 PE=3 SV=1 - [A0A084RGX9_STACH]	0.328	11.18	2	19.0	8.91
A0A084ASD5	Uncharacterized protein OS= <i>Stachybotrys chartarum</i> IBT 7711 GN=S7711_04750 PE=4 SV=1 -	0.355	8.87	3	49.3	6.21

Appendices

	[A0A084ASD5_STACH]						
A0A084RUH7	Uncharacterized protein OS= <i>Stachybotrys chartarum</i> IBT 40288 GN=S40288_03757 PE=3 SV=1 - [A0A084RUH7_STACH]	0.359	9.45	4	52.4	7.85	
A0A084S0E2	4-hydroxyphenylpyruvate dioxygenase OS= <i>Stachybotrys chartarum</i> IBT 40288 GN=S40288_06899 PE=3 SV=1 - [A0A084S0E2_STACH]	0.364	9.65	5	47.4	5.50	
A0A084RA55	Uncharacterized protein OS= <i>Stachybotrys chartarum</i> IBT 40288 GN=S40288_02751 PE=4 SV=1 - [A0A084RA55_STACH]	0.408	13.62	3	24.7	9.42	
A0A084R8I5	Uncharacterized protein OS= <i>Stachybotrys chartarum</i> IBT 40288 GN=S40288_07869 PE=4 SV=1 - [A0A084R8I5_STACH]	0.411	14.69	5	38.6	5.66	
A0A084RR81	Uncharacterized protein OS= <i>Stachybotrys chartarum</i> IBT 40288 GN=S40288_01625 PE=4 SV=1 - [A0A084RR81_STACH]	0.413	36.67	4	12.2	5.49	
A0A084ASM0	Uncharacterized protein OS= <i>Stachybotrys chartarum</i> IBT 7711 GN=S7711_07047 PE=4 SV=1 - [A0A084ASM0_STACH]	0.423	19.77	6	37.8	6.48	
A0A084B4B3	Uncharacterized protein OS= <i>Stachybotrys chartarum</i> IBT 7711 GN=S7711_01061 PE=4 SV=1 - [A0A084B4B3_STACH]	0.425	4.77	3	79.7	4.81	
A0A084RAK3	Uncharacterized protein OS= <i>Stachybotrys chartarum</i> IBT 40288 GN=S40288_05389 PE=4 SV=1 - [A0A084RAK3_STACH]	0.428	59.83	10	13.1	6.38	
A0A084RXL1	Uncharacterized protein OS= <i>Stachybotrys chartarum</i> IBT 40288 GN=S40288_09722 PE=4 SV=1 - [A0A084RXL1_STACH]	0.432	6.21	4	77.9	4.79	
A0A084AUP2	Uncharacterized protein OS= <i>Stachybotrys chartarum</i> IBT 7711 GN=S7711_03322 PE=4 SV=1 - [A0A084AUP2_STACH]	0.436	6.21	6	99.5	8.76	
A0A084AP10	Uncharacterized protein OS= <i>Stachybotrys chartarum</i> IBT 7711 GN=S7711_04720 PE=4 SV=1 - [A0A084AP10_STACH]	0.439	8.08	3	47.7	5.83	
A0A084RPR6	Uncharacterized protein OS= <i>Stachybotrys chartarum</i> IBT 40288 GN=S40288_01420 PE=3 SV=1 - [A0A084RPR6_STACH]	0.446	8.82	3	23.2	6.44	
A0A084ALQ4	Uncharacterized protein OS= <i>Stachybotrys chartarum</i> IBT 7711 GN=S7711_09259 PE=3 SV=1 - [A0A084ALQ4_STACH]	0.448	7.28	3	50.5	5.85	
A0A084RBZ7	Uncharacterized protein OS= <i>Stachybotrys chartarum</i> IBT 40288 GN=S40288_06255 PE=4 SV=1 -	0.456	40.57	9	23.4	6.13	

Appendices

	[A0A084RBZ7_STACH]					
A0A084AQC0	Beta-hexosaminidase OS= <i>Stachybotrys chartarum</i> IBT 7711 GN=S7711_02419 PE=3 SV=1 - [A0A084AQC0_STACH]	0.461	3.45	2	69.4	4.97
A0A084ANH1	Uncharacterized protein OS= <i>Stachybotrys chartarum</i> IBT 7711 GN=S7711_05204 PE=4 SV=1 - [A0A084ANH1_STACH]	0.464	7.04	2	43.6	4.77
A0A084BCD4	Uncharacterized protein OS= <i>Stachybotrys chartarum</i> IBT 7711 GN=S7711_07129 PE=4 SV=1 - [A0A084BCD4_STACH]	0.474	6.87	3	45.5	4.61
A0A084RCA0	Uncharacterized protein OS= <i>Stachybotrys chartarum</i> IBT 40288 GN=S40288_07852 PE=4 SV=1 - [A0A084RCA0_STACH]	0.476	34.85	5	13.7	9.45
A0A084B8Y1	Uncharacterized protein OS= <i>Stachybotrys chartarum</i> IBT 7711 GN=S7711_02604 PE=3 SV=1 - [A0A084B8Y1_STACH]	0.487	5.23	2	38.6	6.98
A0A084B7C5	Uncharacterized protein OS= <i>Stachybotrys chartarum</i> IBT 7711 GN=S7711_07483 PE=4 SV=1 - [A0A084B7C5_STACH]	0.488	21.39	4	19.5	8.02
A0A084AN16	Uncharacterized protein OS= <i>Stachybotrys chartarum</i> IBT 7711 GN=S7711_01982 PE=4 SV=1 - [A0A084AN16_STACH]	0.493	16.48	2	20.2	4.28

Appendix 8-F: Homologues of the decreased protein levels of *S. chartarum* treated with bleach versus control searched by using BLASTP within the NCBI protein database.

Accession	Proteins	NCBI accession	Max score	ID (%)	Positives (%)	Gap (%)	Expected value (%)
A0A084AUC3	HHE domain-containing protein [Pochonia chlamydosporia 170]	XP_018144970.1	313	142/184(77%)	168/184(91%)	0/184(0%)	3.00E-106
A0A084RAP9	NAD(P)H-dependent oxidoreductase [Fusarium fujikuroi]	KLO94417.1	420	196/291(67%)	238/291(81%)	2/291(0%)	9.00E-146
A0A084AMZ1	aminoglycoside phosphotransferase [Aspergillus oryzae]	OOO07243.1	114	62/141(44%)	82/141(58%)	8/141(5%)	1.00E-23
A0A084B5L7	organic hydroperoxide resistance protein [Fusarium langsethiae]	KPA36532.1	271	136/177(77%)	152/177(85%)	4/177(2%)	7.00E-91
A0A084REZ0	DDHD domain-containing protein [Purpureocillium lilacinum]	XP_018179064.1	241	116/150(77%)	130/150(86%)	0/150(0%)	1.00E-79
A0A084RMI1	Uncharacterized protein	-	-	-	-	-	-
A0A084BBL6	Bet v1-like protein [Glonium stellatum]	OCL03481.1	232	117/163(72%)	131/163(80%)	15/163(9%)	7.00E-76
A0A084RKB2	related to DNA damage-responsive protein 48 [Fusarium proliferatum]	CVL10842.1	142	78/111(70%)	84/111(75%)	3/111(2%)	5.00E-42
A0A084B8F5	Uncharacterized protein	-	-	-	-	-	-
A0A084ASD5	S-(hydroxymethyl) glutathione dehydrogenase/alcohol dehydrogenase [Fusarium oxysporum f. sp. lycopersici 4287]	XP_018248504.1	777	365/453(81%)	404/453(89%)	2/453(0%)	0
A0A084RUH7	protein transport protein SEC61 alpha subunit [Purpureocillium lilacinum]	XP_018173590.1	939	458/476(96%)	467/476(98%)	0/476(0%)	0
A0A084RA55	endoplasmic reticulum transmembrane protein [Purpureocillium lilacinum]	OAQ76120.1	387	187/213(88%)	202/213(94%)	2/213(0%)	2.00E-135
A0A084R8I5	sphingolipid long chain base-responsive protein lsp1 [Fusarium langsethiae]	KPA45284.1	434	223/314(71%)	259/314(82%)	13/314(4%)	1.00E-149

Appendices

A0A084RR81	UDP-glucose 4-epimerase Gal10 [Trichoderma reesei]	AAN16350.1	700	334/370(90%)	351/370(94%)	0/370(0%)	0
A0A084ASMO	Alcohol dehydrogenase GroES-like domain-containing protein [Cladophialophora immunda]	OQV01736.1	407	204/351(58%)	254/351(72%)	6/351(1%)	1.00E-138
A0A084B4B3	M6 family metalloprotease domain-containing protein [Purpureocillium lilacinum]	OAQ78920.1	950	455/663(69%)	527/663(79%)	3/663(0%)	0
A0A084RAK3	ribosome maturation protein SBDS [Purpureocillium lilacinum]	XP_018180307.1	160	74/117(63%)	96/117(82%)	3/117(2%)	1.00E-48
A0A084RXL1	PA domain-containing protein [Colletotrichum higginsianum IMI 349063]	XP_018154961.1	1083	527/710(74%)	590/710(83%)	590/710(83%)	0
A0A084AUP2	conserved fungal protein [Pochonia chlamyosporia 170]	XP_018140119.1	1178	565/818(69%)	680/818(83%)	16/818(1%)	0
A0A084AP10	related to Protein urg3 [Fusarium fujikuroi IMI 58289]	CCT75034.1	550	275/438(63%)	334/438(76%)	11/438(2%)	0
A0A084RPR6	cell surface protein [Ustilagoidea virens]	KDB14955.1	198	184/426(43%)	225/426(52%)	62/426(14%)	1.00E-54
A0A084ALQ4	Alpha-L-rhamnosidase-like protein [Acremonium chrysogenum ATCC 11550]	KFH41239.1	520	249/395(63%)	305/395(77%)	3/395(0%)	4.00E-180
A0A084RBZ7	secretion-related small GTPase [Pochonia chlamyosporia 170]	XP_018147663.1	423	205/212(97%)	208/212(98%)	0/212(0%)	6.00E-150
A0A084ANH1	BSD domain protein [Metarhizium rileyi RCEF 4871]	OAA51902.1	579	287/400(72%)	337/400(84%)	3/400(0%)	0
A0A084BCD4	glycerophosphoryl diester phosphodiesterase [Colletotrichum salicis]	KXH61015.1	577	272/421(65%)	326/421(77%)	8/421(1%)	0
A0A084RCA0	calcofluor white hypersensitive protein [Purpureocillium lilacinum]	XP_018175314.1	180	99/129(77%)	112/129(86%)	0/129(0%)	4.00E-56
A0A084B8Y1	xylitol dehydrogenase [Pochonia chlamyosporia 170]	XP_018140411.1	640	297/362(82%)	340/362(93%)	0/362(0%)	0
A0A084B7C5	Lysozyme-like protein [Acremonium chrysogenum ATCC 11550]	KFH40740.1	251	126/189(67%)	145/189(76%)	4/189(2%)	9.00E-83
A0A084AN16	Uncharacterized protein	-	-	-	-	-	-
A0A084RHJ8	Mitochondrial carrier domain protein [Aschersonia aleyrodii RCEF 2490]	KZZ92979.1	587	283/333(85%)	304/333(91%)	0/333(0%)	0

Appendix 8-G: Increased protein levels of *S. chartarum* treated with bleach versus control (<20% variability, > 2-fold change, n = 28).

Accession	Proteins	Fold change	Coverage	# peptide	MW (kDa)	pI
A0A084AXU4	Uncharacterized protein OS= <i>Stachybotrys chartarum</i> IBT 7711 GN=S7711_08653 PE=3 SV=1 - [A0A084AXU4_STACH]	2.039	10.36	2	36.9	5.91
A0A084RX31	Uncharacterized protein OS= <i>Stachybotrys chartarum</i> IBT 40288 GN=S40288_05576 PE=4 SV=1 - [A0A084RX31_STACH]	2.065	44.94	10	19.6	8.68
A0A084RGR1	Uncharacterized protein OS= <i>Stachybotrys chartarum</i> IBT 40288 GN=S40288_02000 PE=4 SV=1 - [A0A084RGR1_STACH]	2.071	16.25	3	18.2	10.37
A0A084B8C5	Uncharacterized protein OS= <i>Stachybotrys chartarum</i> IBT 7711 GN=S7711_03104 PE=4 SV=1 - [A0A084B8C5_STACH]	2.075	20.37	9	47.6	6.14
A0A084RE37	Polyadenylate-binding protein OS= <i>Stachybotrys chartarum</i> IBT 40288 GN=S40288_06423 PE=3 SV=1 - [A0A084RE37_STACH]	2.102	5.47	5	80.8	6.25
A0A084R3D6	Uncharacterized protein OS= <i>Stachybotrys chartarum</i> IBT 40288 GN=S40288_07608 PE=3 SV=1 - [A0A084R3D6_STACH]	2.112	3.70	3	85.0	5.17
A0A084RLE3	Uncharacterized protein OS= <i>Stachybotrys chartarum</i> IBT 40288 GN=S40288_04729 PE=3 SV=1 - [A0A084RLE3_STACH]	2.119	24.48	5	16.0	10.26
A0A084RIY8	Uncharacterized protein OS= <i>Stachybotrys chartarum</i> IBT 40288 GN=S40288_04131 PE=3 SV=1 - [A0A084RIY8_STACH]	2.181	12.24	2	16.5	6.92
A0A084RI52	Uncharacterized protein OS= <i>Stachybotrys chartarum</i> IBT 40288 GN=S40288_01916 PE=3 SV=1 - [A0A084RI52_STACH]	2.186	23.28	4	13.0	9.55
A0A084RLH9	Uncharacterized protein OS= <i>Stachybotrys chartarum</i> IBT 40288 GN=S40288_07470 PE=4 SV=1 - [A0A084RLH9_STACH]	2.200	25.60	3	14.3	9.42
A0A084RBR7	Uncharacterized protein OS= <i>Stachybotrys chartarum</i> IBT 40288 GN=S40288_10012 PE=4 SV=1 - [A0A084RBR7_STACH]	2.206	9.19	3	40.9	4.97
A0A084RD22	Uncharacterized protein OS= <i>Stachybotrys chartarum</i> IBT 40288 GN=S40288_03819 PE=4 SV=1 - [A0A084RD22_STACH]	2.242	14.86	4	36.5	5.71
A0A084AHZ9	Uncharacterized protein OS= <i>Stachybotrys chartarum</i> IBT 7711 GN=S7711_08927 PE=3 SV=1 -	2.244	13.17	8	62.1	4.92

Appendices

	[A0A084AHZ9_STACH]					
A0A084RPV2	Uncharacterized protein OS= <i>Stachybotrys chartarum</i> IBT 40288 GN=S40288_02638 PE=3 SV=1 - [A0A084RPV2_STACH]	2.283	17.24	4	15.7	10.45
A0A084RP82	Eukaryotic translation initiation factor 3 subunit A OS= <i>Stachybotrys chartarum</i> IBT 40288 GN=TIF32 PE=3 SV=1 - [A0A084RP82_STACH]	2.312	1.50	2	121.1	9.48
A0A084B8C7	Uncharacterized protein OS= <i>Stachybotrys chartarum</i> IBT 7711 GN=S7711_03106 PE=3 SV=1 - [A0A084B8C7_STACH]	2.315	10.25	6	44.1	5.44
A0A084AVM3	Peptide hydrolase OS= <i>Stachybotrys chartarum</i> IBT 7711 GN=S7711_09744 PE=3 SV=1 - [A0A084AVM3_STACH]	2.371	5.08	3	53.0	5.16
A0A084B3G1	Isocitrate dehydrogenase [NADP] OS= <i>Stachybotrys chartarum</i> IBT 7711 GN=S7711_00106 PE=3 SV=1 - [A0A084B3G1_STACH]	2.378	7.37	3	50.2	8.35
A0A084RPL3	Uncharacterized protein OS= <i>Stachybotrys chartarum</i> IBT 40288 GN=S40288_01429 PE=3 SV=1 - [A0A084RPL3_STACH]	2.601	19.59	4	16.8	10.86
A0A084AWD2	Uncharacterized protein OS= <i>Stachybotrys chartarum</i> IBT 7711 GN=S7711_06238 PE=3 SV=1 - [A0A084AWD2_STACH]	2.615	6.03	2	52.3	5.66
A0A084AJP6	Uncharacterized protein OS= <i>Stachybotrys chartarum</i> IBT 7711 GN=S7711_08758 PE=4 SV=1 - [A0A084AJP6_STACH]	2.630	8.41	3	63.7	4.93
A0A084AXA6	Uncharacterized protein OS= <i>Stachybotrys chartarum</i> IBT 7711 GN=S7711_06468 PE=4 SV=1 - [A0A084AXA6_STACH]	2.703	13.29	4	45.0	5.74
A0A084RYC0	Uncharacterized protein OS= <i>Stachybotrys chartarum</i> IBT 40288 GN=S40288_07524 PE=4 SV=1 - [A0A084RYC0_STACH]	3.009	4.68	2	52.3	6.65
A0A084RIV2	Uncharacterized protein OS= <i>Stachybotrys chartarum</i> IBT 40288 GN=S40288_00345 PE=3 SV=1 - [A0A084RIV2_STACH]	3.041	22.64	6	38.0	6.54
A0A084RPM3	Uncharacterized protein OS= <i>Stachybotrys chartarum</i> IBT 40288 GN=S40288_01366 PE=4 SV=1 - [A0A084RPM3_STACH]	3.464	20.00	2	13.6	5.91
A0A084RS34	Uncharacterized protein OS= <i>Stachybotrys chartarum</i> IBT 40288 GN=S40288_00557 PE=3 SV=1 - [A0A084RS34_STACH]	3.656	33.96	6	11.6	9.31
A0A084RJ95	Uncharacterized protein OS= <i>Stachybotrys chartarum</i> IBT 40288 GN=S40288_03599 PE=4 SV=1 - [A0A084RJ95_STACH]	3.779	10.16	2	27.7	6.01

Appendices

A0A084R6G6	Uncharacterized protein OS= <i>Stachybotrys chartarum</i> IBT 40288 GN=S40288_11261 PE=4 SV=1 - [A0A084R6G6_STACH]	4.292	32.97	3	8.9	8.62
-------------------	--	-------	-------	---	-----	------

Appendix 8-H: Homologues of the increased protein levels of *S. chartarum* treated with bleach versus control searched by using BLASTP within the NCBI protein database.

Accession	Proteins	NCBI accession	Max score	ID (%)	Positives (%)	Gap (%)	Expected value (%)
A0A084AXU4	Porphobilinogen deaminase [Hirsutella minnesotensis 3608]	KJZ71276.1	500	237/337(70%)	290/337(86%)	4/337(1%)	4.00E-176
A0A084RX31	WD repeat containing protein 44 [Purpureocillium lilacinum]	XP_018182189.1	267	130/156(83%)	142/156(91%)	2/156(1%)	3.00E-89
A0A084RGR1	60S ribosomal protein L21 [Nectria haematococca mpVI 77-13-4]	XP_003053295.1	302	145/160(91%)	154/160(96%)	0/160(0%)	1.00E-103
A0A084B8C5	saccharopine dehydrogenase [Trichoderma gamsii]	XP_018661771.1	673	322/390(83%)	353/390(90%)	1/390(0%)	0
A0A084R3D6	related to Mx2 protein (GTPase protein) [Fusarium proliferatum ET1]	CZR39150.1	729	370/686(54%)	479/686(69%)	12/686(1%)	0
A0A084RLE3	40S ribosomal protein S16 [Trichoderma harzianum]	KKO98101.1	285	136/143(95%)	141/143(98%)	0/143(0%)	3.00E-97
A0A084RIY8	ubiquitin-conjugating enzyme [Purpureocillium lilacinum]	XP_018181535.1	307	147/147(100%)	147/147(100%)	0/147(0%)	5.00E-106
A0A084RI52	40S ribosomal protein S20 [Isaria fumosorosea ARSEF 2679]	XP_018701577.1	225	110/116(95%)	114/116(98%)	0/116(0%)	1.00E-74
A0A084RLH9	60S ribosomal protein L22 [Tolypocladium ophioglossoides CBS 100239]	KND91741.1	237	116/126(92%)	121/126(96%)	1/126(0%)	2.00E-78
A0A084RBR7	S-adenosyl-L-methionine-dependent methyltransferase [Trichoderma reesei RUT C-30]	ETR98844.1	385	181/344(53%)	237/344(68%)	8/344(2%)	1.00E-129
A0A084RD22	NAD(P)H-dependent D-xylose reductase-like protein [Acremonium chrysogenum ATCC 11550]	KFH46419.1	583	265/323(82%)	299/323(92%)	0/323(0%)	0
A0A084AHZ9	calreticulin [Metarhizium anisopliae]	KFG87612.1	905	456/563(81%)	505/563(89%)	1/563(0%)	0

Appendices

A0A084RPV2	40S ribosomal protein S23 [Nectria haematococca mpVI 77-13-4]	XP_003048047.1	288	145/145(100%)	145/145(100%)	0/145(0%)	1.00E-98
A0A084B8C7	glycoside hydrolase family 18 [Purpureocillium lilacinum]	XP_018181629.1	657	312/400(78%)	349/400(87%)	0/400(0%)	0
A0A084RPL3	60S ribosomal protein L35 [Aschersonia aleyrodis RCEF 2490]	KZZ98796.1	234	115/127(91%)	122/127(96%)	0/127(0%)	3.00E-77
A0A084AWD2	putative aldehyde dehydrogenase protein [Eutypa lata UCREL1]	XP_007789151.1	756	362/481(75%)	406/481(84%)	0/481(0%)	0
A0A084AJP6	RecName: Full=Bilirubin oxidase; Flags: Precursor	Q12737.1	926	433/572(76%)	498/572(87%)	3/572(0%)	0
A0A084AXA6	acyl- dehydrogenase protein [Fusarium langsethiae]	KPA38083.1	743	351/429(82%)	389/429(90%)	0/429(0%)	0
A0A084RYC0	CtnDup1 [Monascus ruber]	AIY68803.1	442	230/455(51%)	299/455(65%)	12/455(2%)	3.00E-149
A0A084RIV2	D-lactate dehydrogenase [Fusarium graminearum PH-1]	XP_011328009.1	524	245/349(70%)	296/349(84%)	1/349(0%)	0
A0A084RPM3	Mitochondrial Matrix Factor [Trichoderma parareesei]	OTA06950.1	234	108/125(86%)	120/125(96%)	0/125(0%)	9.00E-78
A0A084RS34	cytochrome c [Metarhizium album ARSEF 1941]	KHN99232.1	211	102/106(96%)	104/106(98%)	0/106(0%)	4.00E-69
A0A084RJ95	phosphoglycerate mutase family protein [Drechmeria coniospora]	KYK55004.1	328	157/244(64%)	186/244(76%)	1/244(0%)	4.00E-111
A0A084R6G6	Uncharacterized protein	-	-	-	-	-	-

Appendix 8-I: Decreased protein levels of *S. chartarum* treated with organosilane versus control (<20% variability, < 0.5-fold change, n = 16).

Accession	Proteins	Fold change	Coverage	# peptide	MW (kDa)	pI
A0A084AUC3	Uncharacterized protein OS= <i>Stachybotrys chartarum</i> IBT 7711 GN=S7711_03834 PE=4 SV=1 - [A0A084AUC3_STACH]	0.185	11.87	3	25.1	6.54
A0A084AU26	Uncharacterized protein OS= <i>Stachybotrys chartarum</i> IBT 7711 GN=S7711_00673 PE=4 SV=1 - [A0A084AU26_STACH]	0.351	15.83	2	15.2	8.43
A0A084AK76	Uncharacterized protein OS= <i>Stachybotrys chartarum</i> IBT 7711 GN=S7711_07532 PE=3 SV=1 - [A0A084AK76_STACH]	0.402	6.41	3	56.2	6.13
A0A084RB15	Uncharacterized protein OS= <i>Stachybotrys chartarum</i> IBT 40288 GN=S40288_04214 PE=4 SV=1 - [A0A084RB15_STACH]	0.404	8.48	2	37.3	4.91
A0A084RUH7	Uncharacterized protein OS= <i>Stachybotrys chartarum</i> IBT 40288 GN=S40288_03757 PE=3 SV=1 - [A0A084RUH7_STACH]	0.412	9.45	4	52.4	7.85
A0A084AVC1	Uncharacterized protein OS= <i>Stachybotrys chartarum</i> IBT 7711 GN=S7711_01704 PE=4 SV=1 - [A0A084AVC1_STACH]	0.418	9.48	6	75.5	6.98
A0A084R8H2	V-type proton ATPase subunit F OS= <i>Stachybotrys chartarum</i> IBT 40288 GN=S40288_06661 PE=3 SV=1 - [A0A084R8H2_STACH]	0.430	32.52	4	13.7	6.01
A0A084AH83	Uncharacterized protein OS= <i>Stachybotrys chartarum</i> IBT 7711 GN=S7711_02862 PE=4 SV=1 - [A0A084AH83_STACH]	0.445	3.13	2	72.2	6.24
A0A084RK37	Superoxide dismutase OS= <i>Stachybotrys chartarum</i> IBT 40288 GN=S40288_01534 PE=3 SV=1 - [A0A084RK37_STACH]	0.446	10.04	2	26.0	6.13
A0A084RBF4	Uncharacterized protein OS= <i>Stachybotrys</i>	0.456	3.49	2	86.0	6.19

Appendices

	<i>chartarum</i> IBT 40288 GN=S40288_07701 PE=4 SV=1 - [A0A084RBF4_STACH]					
A0A084RH44	Uncharacterized protein OS= <i>Stachybotrys chartarum</i> IBT 40288 GN=S40288_01183 PE=4 SV=1 - [A0A084RH44_STACH]	0.461	21.29	5	28.2	7.06
A0A084RWB1	Uncharacterized protein OS= <i>Stachybotrys chartarum</i> IBT 40288 GN=S40288_02063 PE=4 SV=1 - [A0A084RWB1_STACH]	0.469	6.60	2	47.3	5.55
A0A084B4B8	Uncharacterized protein OS= <i>Stachybotrys chartarum</i> IBT 7711 GN=S7711_01066 PE=4 SV=1 - [A0A084B4B8_STACH]	0.469	4.14	3	83.8	6.33
A0A084AY80	Uncharacterized protein OS= <i>Stachybotrys chartarum</i> IBT 7711 GN=S7711_10827 PE=4 SV=1 - [A0A084AY80_STACH]	0.472	23.65	4	17.1	6.10
A0A084RF12	Uncharacterized protein OS= <i>Stachybotrys chartarum</i> IBT 40288 GN=S40288_03485 PE=3 SV=1 - [A0A084RF12_STACH]	0.479	9.80	2	22.8	6.83
A0A084RKH6	NADH-cytochrome b5 reductase OS= <i>Stachybotrys chartarum</i> IBT 40288 GN=S40288_08111 PE=3 SV=1 - [A0A084RKH6_STACH]	0.497	7.21	2	36.6	8.68

Appendix 8-J: Homologues of the decreased proteins of *S. chartarum* treated with organosilane versus control searched by using BLASTP within the NCBI protein database.

Accession	Proteins	NCBI accession	Max score	ID (%)	Positives (%)	Gap (%)	Expected value (%)
A0A084AUC3	HHE domain-containing protein [Pochonia chlamydosporia 170]	XP_018144970.1	313	142/184(77%)	168/184(91%)	0/184(0%)	3.00E-106
A0A084AU26	putative redox protein-like protein [Acremonium chrysogenum ATCC 11550]	KFH47021.1	226	112/139(81%)	118/139(84%)	0/139(0%)	3.00E-74
A0A084AK76	Glycerol kinase [Colletotrichum chlorophyti]	OLN95273.1	928	439/509(86%)	474/509(93%)	0/509(0%)	0
A0A084RB15	aldehyde reductase 2 [Aspergillus udagawae]	GAO86291.1	503	239/339(71%)	281/339(82%)	0/339(0%)	3.00E-177
A0A084RUH7	protein transport protein SEC61 alpha subunit [Purpureocillium lilacinum]	XP_018173590.1	939	458/476(96%)	467/476(98%)	0/476(0%)	0
A0A084AVC1	alpha-mannosyltransferase [Colletotrichum incanum]	OHW95224.1	596	284/463(61%)	349/463(75%)	11/463(2%)	0
A0A084AH83	oxidoreductase [Fusarium verticillioides 7600]	XP_018751056.1	412	198/328(60%)	251/328(76%)	8/328(2%)	1.00E-136
A0A084RBF4	protein transporter SEC23 [Fusarium oxysporum f. sp. lycopersici 4287]	XP_018238815.1	1549	739/773(96%)	755/773(97%)	2/773(0%)	0
A0A084RH44	related to signal sequence receptor alpha chain [Fusarium mangiferae]	CVK89781.1	316	156/263(59%)	197/263(74%)	4/263(1%)	9.00E-106
A0A084RWB1	PLP-dependent transferase [Trichoderma reesei RUT C-30]	ETS02194.1	795	371/423(88%)	402/423(95%)	0/423(0%)	0
A0A084B4B8	bactericidal permeability-increasing protein [Ophiocordyceps sinensis CO18]	EQL01225.1	847	409/740(55%)	559/740(75%)	8/740(1%)	0
A0A084AY80	Fungal specific transcription factor, putative [Beauveria bassiana ARSEF 2860]	XP_008599277.1	176	88/155(57%)	103/155(66%)	12/155(7%)	4.00E-54
A0A084RF12	heat shock protein 30 [Fusarium lichenicola]	ACP18866.1	251	123/214(57%)	153/214(71%)	14/214(6%)	5.00E-82

Appendix 8-K: Increased protein levels of *S. chartarum* treated with organosilane versus control (<20% variability, > 2-fold change, n = 52).

Accession	Proteins	Fold change	Coverage	# peptide	MW (kDa)	pI
A0A084AQM4	Uncharacterized protein OS= <i>Stachybotrys chartarum</i> IBT 7711 GN=S7711_11233 PE=4 SV=1 - [A0A084AQM4_STACH]	2.025	36.78	13	37.8	5.45
A0A084RGR1	Uncharacterized protein OS= <i>Stachybotrys chartarum</i> IBT 40288 GN=S40288_02000 PE=4 SV=1 - [A0A084RGR1_STACH]	2.090	16.25	3	18.2	10.37
A0A084BAV4	Uncharacterized protein (Fragment) OS= <i>Stachybotrys chartarum</i> IBT 7711 GN=S7711_05436 PE=3 SV=1 - [A0A084BAV4_STACH]	2.095	80.56	7	7.9	9.52
A0A084R633	Uncharacterized protein OS= <i>Stachybotrys chartarum</i> IBT 40288 GN=S40288_08065 PE=4 SV=1 - [A0A084R633_STACH]	2.121	37.50	4	17.5	4.68
A0A084RFI7	Uncharacterized protein OS= <i>Stachybotrys chartarum</i> IBT 40288 GN=S40288_02203 PE=3 SV=1 - [A0A084RFI7_STACH]	2.147	33.33	6	17.8	10.55
A0A084R8Q8	Eukaryotic translation initiation factor 3 subunit M OS= <i>Stachybotrys chartarum</i> IBT 40288 GN=S40288_09372 PE=3 SV=1 - [A0A084R8Q8_STACH]	2.156	37.19	15	49.6	5.02
A0A084RVF2	Uncharacterized protein OS= <i>Stachybotrys chartarum</i> IBT 40288 GN=S40288_07329 PE=4 SV=1 - [A0A084RVF2_STACH]	2.162	3.90	2	54.3	5.08
A0A084AJ57	Uncharacterized protein (Fragment) OS= <i>Stachybotrys chartarum</i> IBT 7711 GN=S7711_01847 PE=4 SV=1 - [A0A084AJ57_STACH]	2.177	12.31	4	29.5	8.31
A0A084BBL2	Uncharacterized protein OS= <i>Stachybotrys chartarum</i> IBT 7711 GN=S7711_01290 PE=3 SV=1 - [A0A084BBL2_STACH]	2.184	2.50	3	107.9	4.63
A0A084AZK4	Uncharacterized protein OS= <i>Stachybotrys chartarum</i> IBT 7711 GN=S7711_03229 PE=4 SV=1 - [A0A084AZK4_STACH]	2.206	21.64	7	42.1	4.31
A0A084B7D6	Carboxylic ester hydrolase OS= <i>Stachybotrys chartarum</i> IBT 7711 GN=S7711_07491 PE=3 SV=1 - [A0A084B7D6_STACH]	2.230	3.00	2	58.4	6.16
A0A084RF32	Uncharacterized protein OS= <i>Stachybotrys chartarum</i> IBT 40288 GN=S40288_03519 PE=4 SV=1 - [A0A084RF32_STACH]	2.232	37.01	3	13.0	6.52
A0A084R831	Histone H2A OS= <i>Stachybotrys chartarum</i> IBT 40288 GN=S40288_05619 PE=3 SV=1 - [A0A084R831_STACH]	2.253	11.94	2	14.1	10.55
A0A084B320	Uncharacterized protein OS= <i>Stachybotrys chartarum</i> IBT 7711 GN=S7711_07098 PE=4 SV=1 - [A0A084B320_STACH]	2.280	6.70	2	50.5	6.54
A0A084RT98	Uncharacterized protein OS= <i>Stachybotrys chartarum</i> IBT 40288 GN=S40288_09231 PE=4 SV=1 - [A0A084RT98_STACH]	2.284	10.21	3	42.0	4.40
A0A084RCQ3	Uncharacterized protein OS= <i>Stachybotrys chartarum</i> IBT 40288 GN=S40288_07097 PE=4 SV=1 - [A0A084RCQ3_STACH]	2.290	51.85	4	9.1	5.15
A0A084RNL9	Proteasome subunit alpha type OS= <i>Stachybotrys chartarum</i> IBT 40288 GN=S40288_00483 PE=3 SV=1 - [A0A084RNL9_STACH]	2.373	13.91	3	28.9	5.20
A0A084RN05	Uncharacterized protein OS= <i>Stachybotrys chartarum</i> IBT 40288 GN=S40288_05721 PE=4 SV=1 - [A0A084RN05_STACH]	2.397	53.37	9	17.1	6.95
A0A084RYS7	Uncharacterized protein OS= <i>Stachybotrys chartarum</i> IBT 40288	2.413	17.00	6	44.3	5.62

Appendices

	GN=S40288_06050 PE=3 SV=1 - [A0A084RYS7_STACH]					
A0A084RJ12	Uncharacterized protein OS= <i>Stachybotrys chartarum</i> IBT 40288 GN=S40288_07277 PE=3 SV=1 - [A0A084RJ12_STACH]	2.449	8.85	3	21.8	10.21
A0A084RW98	Uncharacterized protein OS= <i>Stachybotrys chartarum</i> IBT 40288 GN=S40288_02079 PE=4 SV=1 - [A0A084RW98_STACH]	2.456	14.02	4	47.9	4.79
A0A084RTX7	Uncharacterized protein OS= <i>Stachybotrys chartarum</i> IBT 40288 GN=S40288_04101 PE=4 SV=1 - [A0A084RTX7_STACH]	2.461	18.18	2	11.1	4.91
A0A084REL3	40S ribosomal protein S8 OS= <i>Stachybotrys chartarum</i> IBT 40288 GN=S40288_03207 PE=3 SV=1 - [A0A084REL3_STACH]	2.487	24.51	4	22.9	10.73
A0A084AKJ3	Uncharacterized protein OS= <i>Stachybotrys chartarum</i> IBT 7711 GN=S7711_07203 PE=4 SV=1 - [A0A084AKJ3_STACH]	2.542	74.62	20	27.9	4.75
A0A084REM1	Ribosomal protein L15 OS= <i>Stachybotrys chartarum</i> IBT 40288 GN=S40288_03233 PE=3 SV=1 - [A0A084REM1_STACH]	2.567	21.18	5	24.0	11.41
A0A084AZ60	60S acidic ribosomal protein P0 OS= <i>Stachybotrys chartarum</i> IBT 7711 GN=S7711_02193 PE=3 SV=1 - [A0A084AZ60_STACH]	2.615	25.71	7	34.7	4.88
A0A084RRX6	Uncharacterized protein OS= <i>Stachybotrys chartarum</i> IBT 40288 GN=S40288_00602 PE=4 SV=1 - [A0A084RRX6_STACH]	2.685	31.16	5	23.3	4.51
A0A084RBG8	5-hydroxyisourate hydrolase OS= <i>Stachybotrys chartarum</i> IBT 40288 GN=S40288_09405 PE=3 SV=1 - [A0A084RBG8_STACH]	2.714	16.06	2	15.1	5.81
A0A084ANH1	Uncharacterized protein OS= <i>Stachybotrys chartarum</i> IBT 7711 GN=S7711_05204 PE=4 SV=1 - [A0A084ANH1_STACH]	2.724	7.04	2	43.6	4.77
A0A084RQ66	Uncharacterized protein OS= <i>Stachybotrys chartarum</i> IBT 40288 GN=S40288_05001 PE=4 SV=1 - [A0A084RQ66_STACH]	2.808	9.59	2	32.6	5.15
A0A084B411	Uncharacterized protein OS= <i>Stachybotrys chartarum</i> IBT 7711 GN=S7711_00288 PE=4 SV=1 - [A0A084B411_STACH]	2.813	9.72	3	54.8	6.02
A0A084R8J5	Tubulin-specific chaperone A OS= <i>Stachybotrys chartarum</i> IBT 40288 GN=S40288_07859 PE=3 SV=1 - [A0A084R8J5_STACH]	2.823	13.11	2	13.5	5.19
A0A084RPL3	Uncharacterized protein OS= <i>Stachybotrys chartarum</i> IBT 40288 GN=S40288_01429 PE=3 SV=1 - [A0A084RPL3_STACH]	2.932	19.59	4	16.8	10.86
A0A084AN16	Uncharacterized protein OS= <i>Stachybotrys chartarum</i> IBT 7711 GN=S7711_01982 PE=4 SV=1 - [A0A084AN16_STACH]	3.056	16.48	2	20.2	4.28
A0A084RY47	Uncharacterized protein OS= <i>Stachybotrys chartarum</i> IBT 40288 GN=S40288_00963 PE=4 SV=1 - [A0A084RY47_STACH]	3.168	9.77	4	49.9	5.01
A0A084RPV2	Uncharacterized protein OS= <i>Stachybotrys chartarum</i> IBT 40288 GN=S40288_02638 PE=3 SV=1 - [A0A084RPV2_STACH]	3.181	17.24	4	15.7	10.45
A0A084AYJ7	Uncharacterized protein OS= <i>Stachybotrys chartarum</i> IBT 7711 GN=S7711_09351 PE=4 SV=1 - [A0A084AYJ7_STACH]	3.279	7.95	3	55.1	5.20
A0A084RPH1	Uncharacterized protein OS= <i>Stachybotrys chartarum</i> IBT 40288 GN=S40288_05681 PE=3 SV=1 - [A0A084RPH1_STACH]	3.493	21.08	4	20.7	10.73
A0A084AQC0	Beta-hexosaminidase OS= <i>Stachybotrys chartarum</i> IBT 7711 GN=S7711_02419 PE=3 SV=1 - [A0A084AQC0_STACH]	3.505	3.45	2	69.4	4.97
A0A084AI54	Uncharacterized protein OS= <i>Stachybotrys chartarum</i> IBT 7711	3.594	36.90	2	8.9	5.41

Appendices

	GN=S7711_09544 PE=4 SV=1 - [A0A084AI54_STACH]					
A0A084RYC0	Uncharacterized protein OS= <i>Stachybotrys chartarum</i> IBT 40288 GN=S40288_07524 PE=4 SV=1 - [A0A084RYC0_STACH]	3.877	4.68	2	52.3	6.65
A0A084RBE9	Uncharacterized protein OS= <i>Stachybotrys chartarum</i> IBT 40288 GN=S40288_07694 PE=4 SV=1 - [A0A084RBE9_STACH]	4.086	5.52	3	38.3	8.03
A0A084RAL1	60S ribosomal protein L36 OS= <i>Stachybotrys chartarum</i> IBT 40288 GN=S40288_05394 PE=3 SV=1 - [A0A084RAL1_STACH]	4.656	17.92	3	12.0	11.77
A0A084RH96	Uncharacterized protein OS= <i>Stachybotrys chartarum</i> IBT 40288 GN=S40288_04468 PE=4 SV=1 - [A0A084RH96_STACH]	4.734	5.52	4	63.7	4.51
A0A084R4I9	Uncharacterized protein OS= <i>Stachybotrys chartarum</i> IBT 40288 GN=S40288_04531 PE=3 SV=1 - [A0A084R4I9_STACH]	4.869	6.83	5	54.4	5.38
A0A084AN58	Ribosomal protein L19 OS= <i>Stachybotrys chartarum</i> IBT 7711 GN=S7711_06783 PE=3 SV=1 - [A0A084AN58_STACH]	5.236	0.35	2	312.9	6.93
A0A084B3K6	Uncharacterized protein OS= <i>Stachybotrys chartarum</i> IBT 7711 GN=S7711_00146 PE=4 SV=1 - [A0A084B3K6_STACH]	5.570	7.89	2	35.1	6.11
A0A084AU23	Uncharacterized protein OS= <i>Stachybotrys chartarum</i> IBT 7711 GN=S7711_00670 PE=4 SV=1 - [A0A084AU23_STACH]	6.331	17.24	3	22.1	4.63
A0A084AVZ9	Uncharacterized protein OS= <i>Stachybotrys chartarum</i> IBT 7711 GN=S7711_02016 PE=4 SV=1 - [A0A084AVZ9_STACH]	6.599	5.63	2	36.2	5.44
A0A084ALQ4	Uncharacterized protein OS= <i>Stachybotrys chartarum</i> IBT 7711 GN=S7711_09259 PE=3 SV=1 - [A0A084ALQ4_STACH]	6.964	7.28	3	50.5	5.85
A0A084R5L6	Uncharacterized protein OS= <i>Stachybotrys chartarum</i> IBT 40288 GN=S40288_08316 PE=4 SV=1 - [A0A084R5L6_STACH]	8.281	16.67	2	11.5	9.42
A0A084AUP5	Uncharacterized protein OS= <i>Stachybotrys chartarum</i> IBT 7711 GN=S7711_03325 PE=4 SV=1 - [A0A084AUP5_STACH]	12.531	18.42	3	16.9	8.41

Appendix 8-L: Homologues of the increased protein levels of *S. chartarum* treated with organosilane versus control searched by using BLASTP within the NCBI protein database.

Accession	Proteins	NCBI accession	Max score	ID (%)	Positives (%)	Gap (%)	Expected value (%)
A0A084AQM4	Pc21g20050 [<i>Penicillium rubens</i> Wisconsin 54-1255]	XP_002568995.1	295	141/284(50%)	180/284(63%)	1/284(0%)	4.00E-94
A0A084RGR1	60S ribosomal protein L21 [<i>Nectria haematococca</i> mpVI 77-13-4]	XP_003053295.1	302	145/160(91%)	154/160(96%)	0/160(0%)	1.00E-103
A0A084BAV4	60S ribosomal protein L27a (L29) [<i>Cordyceps militaris</i> CM01]	XP_006666371.1	139	69/72(96%)	72/72(100%)	0/72(0%)	1.00E-40
A0A084R633	-	-	-	-	-	-	-
A0A084RFI7	40S ribosomal protein S18, partial [<i>Metarhizium majus</i> ARSEF 297]	XP_014578934.1	315	155/156(99%)	156/156(100%)	0/156(0%)	6.00E-109
A0A084RVF2	Hsp90 co-chaperone Cdc37 [<i>Fusarium oxysporum</i> f. sp. cubense race 4]	EMT63923.1	712	345/477(72%)	404/477(84%)	8/477(1%)	0
A0A084AJ57	Beta-glucanase-like protein [<i>Acremonium chrysogenum</i> ATCC 11550]	KFH42632.1	336	151/267(57%)	196/267(73%)	1/267(0%)	2.00E-113
A0A084BBL2	Glycoside hydrolase, family 31 [<i>Penicillium camemberti</i>]	CRL28636.1	1573	749/960(78%)	833/960(86%)	9/960(0%)	0
A0A084AZK4	cell wall glucanosyltransferase Mwg1 [<i>Purpureocillium lilacinum</i>]	XP_018181026.1	410	219/410(53%)	278/410(67%)	24/410(5%)	8.00E-139
A0A084RF32	GTP1/OBG domain-containing protein [<i>Purpureocillium lilacinum</i>]	XP_018180368.1	163	84/131(64%)	98/131(74%)	5/131(3%)	2.00E-49
A0A084B320	2-heptyl-3-hydroxy-4(1H)-quinolone synthase [<i>Valsa mali</i> var. pyri]	KUI52937.1	439	225/450(50%)	306/450(68%)	11/450(2%)	1.00E-148
A0A084RT98	PAF acetylhydrolase family protein [<i>Aspergillus kawachii</i> IFO 4308]	GAA90235.1	189	123/350(35%)	185/350(52%)	24/350(6%)	5.00E-53
A0A084RCQ3	pua rna-containing protein [<i>Fusarium langsethiae</i>]	KPA45079.1	130	63/82(77%)	69/82(84%)	1/82(1%)	5.00E-38
A0A084RN05	superoxide dismutase [<i>Fusarium langsethiae</i>]	KPA42379.1	269	130/148(88%)	140/148(94%)	0/148(0%)	2.00E-90
A0A084RYS7	Cytochrome b2, mitochondrial 4 [<i>Colletotrichum chlorophyti</i>]	OLN83334.1	551	264/390(68%)	316/390(81%)	18/390(4%)	0
A0A084RJ12	40S ribosomal protein S11, partial [<i>Trichoderma harzianum</i>]	KKP02404.1	323	157/161(98%)	160/161(99%)	0/161(0%)	2.00E-111
A0A084RW98	CUE domain protein, partial [<i>Metarhizium anisopliae</i> ARSEF 549]	KID67118.1	475	284/444(64%)	333/444(75%)	27/444(6%)	8.00E-163
A0A084RTX7	ubiquitin family protein [<i>Colletotrichum gloeosporioides</i> Cg-14]	EQB59011.1	177	87/98(89%)	90/98(91%)	1/98(1%)	5.00E-56
A0A084AKJ3	Stress protein DDR48 [<i>Penicillium subrubescens</i>]	OKO89669.1	123	133/279(48%)	163/279(58%)	64/279(22%)	4.00E-30
A0A084RRX6	Hsp90 binding co-chaperone Sba1 [<i>Purpureocillium lilacinum</i>]	XP_018177014.1	279	171/199(86%)	178/199(89%)	2/199(1%)	5.00E-93
A0A084ANH1	BSD domain protein [<i>Metarhizium rileyi</i> RCEF	OAA51902.1	579	287/400(72%)	337/400(84%)	3/400(0%)	0

Appendices

	4871]							
A0A084RQ66	vesicular-fusion protein sec17 [Purpureocillium lilacinum]	XP_018177230.1	536	254/292(87%)	279/292(95%)	0/292(0%)	0	
A0A084B411	putative dimethylallyl tryptophan synthase 1 protein [Eutypa lata UCREL1]	XP_007788006.1	418	218/417(52%)	275/417(65%)	58/417(13%)	1.00E-140	
A0A084RPL3	60S ribosomal protein L35 [Aschersonia aleyrodis RCEF 2490]	KZZ98796.1	234	115/127(91%)	122/127(96%)	0/127(0%)	3.00E-77	
A0A084AN16	-	-	-	-	-	-	-	
A0A084RY47	Plasmodium exported protein, unknown function [Plasmodium ovale]	SBT84176.1	54.3	35/61(57%)	45/61(73%)	0/61(0%)	4.00E-04	
A0A084RPV2	40S ribosomal protein S23 [Nectria haematococca mpVI 77-13-4]	XP_003048047.1	288	145/145(100%)	145/145(100%)	0/145(0%)	1.00E-98	
A0A084AYJ7	5-methylthioadenosine/S-adenosylhomocysteine deaminase-like protein [Acremonium chrysogenum ATCC 11550]	KFH47541.1	665	325/504(64%)	390/504(77%)	4/504(0%)	0	
A0A084RPH1	60s ribosomal protein l17 [Fusarium langsethiae]	KPA42578.1	367	176/185(95%)	181/185(97%)	0/185(0%)	2.00E-128	
A0A084AI54	metal homeostasis factor atx1 [Fusarium avenaceum]	KIL89907.1	156	73/82(89%)	80/82(97%)	0/82(0%)	2.00E-48	
A0A084RYC0	CtnDup1 [Monascus ruber]	AIY68803.1	442	230/455(51%)	299/455(65%)	12/455(2%)	3.00E-149	
A0A084RBE9	RNA recognition domain-containing protein [Purpureocillium lilacinum]	XP_018183210.1	372	247/351(70%)	264/351(75%)	34/351(9%)	7.00E-126	
A0A084RH96	glycoside hydrolase family 32 protein [Beauveria bassiana ARSEF 2860]	XP_008596554.1	840	397/567(70%)	469/567(82%)	10/567(1%)	0	
A0A084R4I9	FAD-binding oxidoreductase [Bradyrhizobium sp. WSM1743]	WP_027575620.1	100	117/417(28%)	179/417(42%)	34/417(8%)	3.00E-19	
A0A084B3K6	UBA/TS-N domain containing protein [Ophiocordyceps sinensis CO18]	EQL03473.1	464	245/317(77%)	275/317(86%)	3/317(0%)	2.00E-162	
A0A084AU23	ATP synthase D chain [Ophiocordyceps sinensis CO18]	EQL00895.1	307	178/204(87%)	188/204(92%)	1/204(0%)	3.00E-104	
A0A084AVZ9	Endoglucanase-like protein [Acremonium chrysogenum ATCC 11550]	KFH40812.1	384	202/359(56%)	241/359(67%)	21/359(5%)	2.00E-129	
A0A084ALQ4	Alpha-L-rhamnosidase-like protein [Acremonium chrysogenum ATCC 11550]	KFH41239.1	520	249/395(63%)	305/395(77%)	3/395(0%)	4.00E-180	
A0A084R5L6	Non-histone chromosomal protein 6 [Colletotrichum chlorophyti]	OLN97136.	187	98/104(94%)	99/104(95%)	3/104(2%)	8.00E-60	
A0A084AUP5	40S ribosomal protein S19 [Neurospora crassa OR74A]	XP_962947.1	273	131/149(88%)	138/149(92%)	0/149(0%)	1.00E-92	

